University of HUDDERSFIELD
Inspiring tomorrow's professionals

Exploration of the Synthesis, Reactivity and Applications of 1,2-Oxathiine 2,2-Dioxides

A thesis submitted to the University of Huddersfield in partial fulfilment of the requirements for the degree of Doctor of Philosophy

Dimitrios Zonidis

The University of Huddersfield

December 2020

Declaration Concerning Published Work Contained Within This Thesis

In compliance with The University of Huddersfield Research Degree Guidance I can confirm that work contained within this thesis has featured in three publications. The relevant chapters of this thesis which may appear in part in each of the publications are: Chapter 1 (INTRODUCTION); Chapter 2 (SYNTHESIS OF ENAMINONES AND 1,2-OXATHIINE 2,2-DIOXIDE TARGET SYSTEMS) and Chapter 3 (APPLICATION OF 1,2-OXATHIINE 2,2-DIOXIDE SYSTEMS AS PHOTOCHROMIC MATERIALS). A footnote on each relevant chapter title page has been added to indicate that work contained within the chapter has appeared in a publication and which also directs the reader to the appendices (Appendix 2), where I have indicated my contribution to each publication along and attached a copy of the publication.

ABSTRACT

This thesis constitutes an investigation of the synthesis, reactivity and photochromic applications of the 1,2-oxathiine 2,2-dioxide heterocyclic ring system.

An extensive series of substituted 1,2-oxathiine 2,2-dioxides was obtained using a two-step synthetic route comprising of a sulfene addition to the enaminone substrates **I** to afford the 4-dimethylamino-3,4-dihydro-1,2-oxathiine 2,2-dioxide intermediates **II** (Scheme A1). A mild and highly efficient Cope elimination reaction was employed to introduce the C3-C4 oxathiine ring double bond leading to the unsaturated 1,2-oxathiine 2,2-dioxides **III** with full chemo- and regio- selectivity.

The preparation of the enaminone precursors was accomplished in generally high yields through the reaction of α-methylene-containing ketones **IV** with DMFDMA. The crystal structures of two unique, stable, organic salts (**Va**,**b**) resulting from the action of DMFDMA on benzoylacetonitrile were obtained. The subsequent addition of sulfene derivatives, derived from the action of Et_3N on methanesulfonyl chlorides, proceeded in fair to very good yields and the main structural features of the 3,4-dihydro-1,2-oxathiine 2,2-dioxides **II** were mapped out using extensive NMR experiments and X-ray crystallography. The mechanism, regioselectivity and stereoselectivity of the sulfene additions were also explored, with the enaminone motif found to direct the addition of the sulfene fragment through a concerted process that afforded a thermodynamic and a kinetic product which constitute a pair of *anti*/*syn* diastereomers. The foregoing two step transformation to afford the 1,2-oxathiine 2,2-dioxides **III** was further developed into a convenient "one-pot" method.

The efficient synthesis of α-methylene ketones with either phenyl or 2,5-dimethylthienyl groups appended on their structure allowed access to the 1,2-oxathiine 2,2-dioxide analogues **VI** which exhibited photochemically reversible photochromism as a consequence of the thiophene rings adopting an antiparallel conformation which was established by X-ray crystallography (Scheme A2). The ring-closed photo-isomers **VII**, established by NMR spectroscopy, afforded yellow → red coloured species with λ_{max} at *circa* 410 - 510 nm. UV-Vis spectroscopic studies revealed that, at a photostationary state, the 3,4-dihydro-1,2-oxathiine 2,2-dioxides exhibited less intensely coloured, hypsochromically shifted absorption maxima than their unsaturated derivatives.

The reactivity of the 1,2-oxathiine 2,2-dioxide system was probed by their use as substrates in various transformations (Scheme A3). Ring bromination (structures **VIII**) revealed a clear bias towards bromination at the 3-position of the heterocycle, whereas the 5-position reacted much more slowly and the 4-position was completely inactive towards Br_2. Lithium-bromine exchange of the foregoing brominated products led to their degradation, thus Pd-catalysed methods were explored as means of functionalisation.

The Suzuki cross-coupling reaction of the brominated 1,2-oxathiines **VIII** with a selection of boronic acids afforded the target coupled products **IX** in moderate yields with the concomitant formation of homo-coupled, bis-1,2-oxathiine 2,2,2',2'-tetraoxide, side-products **X**. Homo-coupling of was found to be the exclusive result of a Miyaura borylation protocol. The requirement for brominated 1,2-oxathiine 2,2-dioxides **VIII** was avoided by the use of an efficient C-H activated cross-coupling protocol which afforded a small library of diversely substituted 1,2-oxathiine 2,2-dioxides **IX**.

Cycloaddition reactions of 6-styryl substituted 1,2-oxathiine 2,2-dioxides with PTAD afforded novel tricyclic adducts, 1*H*-[1,2]oxathiino[5,6-*c*][1,2,4]triazolo[1,2-*a*]pyridazine-1,3(2*H*)-dione 8,8-dioxides **XI**, that rearranged upon contact with silica to afford more stable regioisomers (**XII**). Benzyne addition to mono-, di- and tri- substituted 1,2-oxathiine 2,2-dioxides afforded low yields of substituted naphthalenes **XIII** as a consequence of cycloaddition across the fixed diene unit of the 1,2-oxathiine 2,2-dioxide ring with concomitant retro-Diels Alder elimination of SO_3 leading to the aromatised product.

Scheme A1

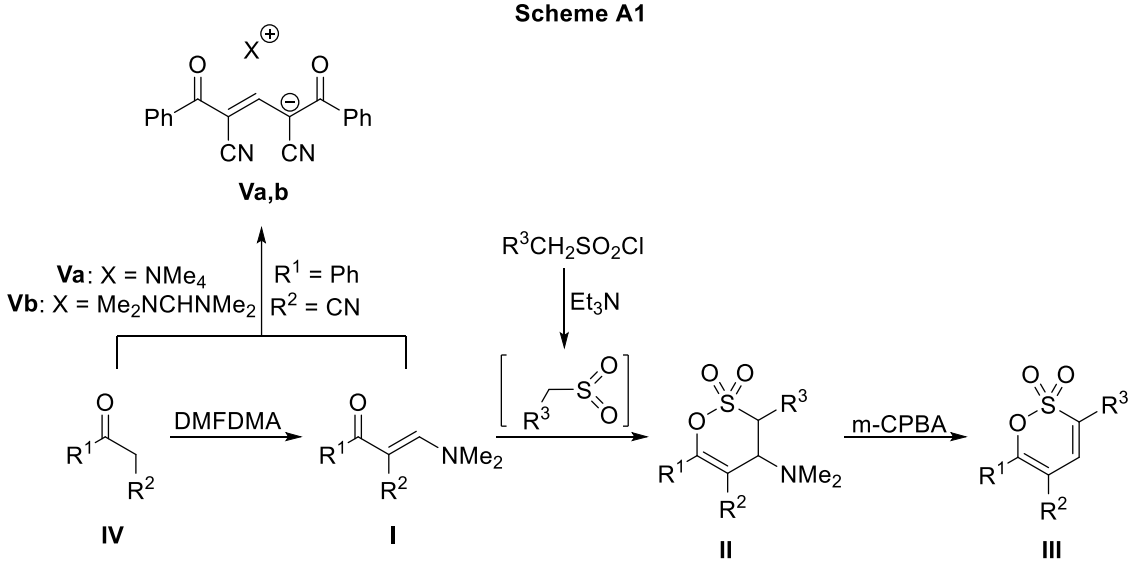

Scheme A2

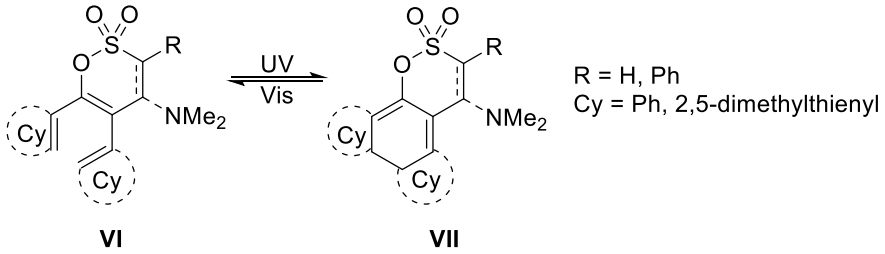

Scheme A3

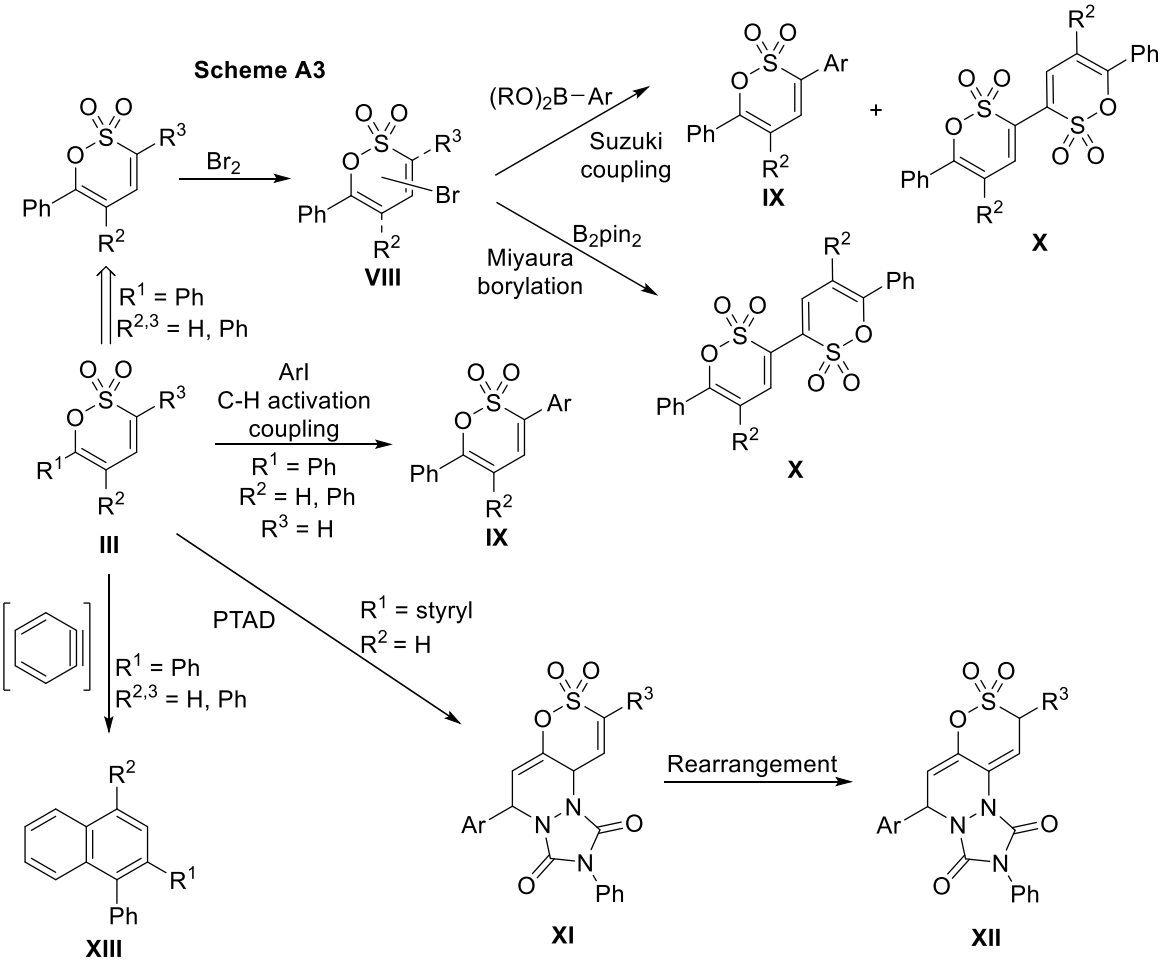

Contents

ABSTRACT 2
List of Figures 6
List of Tables 9
List of abbreviations 10
CHAPTER 1: INTRODUCTION 12
1.1 Enaminones and Sulfenes 12
1.1.1 Preface 12
1.1.2 Enaminones 12
1.1.2.1 General information 12
1.1.2.2 Synthesis of mono- and di- substituted enaminones 14
1.1.2.3 Enaminone reactions leading to heterocyclic systems 20
1.1.3 Sulfenes 26
1.1.3.1 General properties 26
1.1.3.2 Generation of sulfenes 27
1.1.3.3 Reaction overview 30
1.2. 1,2-Oxathiine 2,2-dioxide ring systems 34
1.2.1 1,2-Oxathiine 2,2-dioxides 34
1.2.1.1 General properties 34
1.2.1.2 Synthetic routes 36
1.2.1.3 Reactions with 1,2-oxathiine 2,2-dioxides 39
1.2.2 3,4-Dihydro 1,2-oxathiine 2,2-dioxides 44
1.2.2.1 Overview 44
1.2.2.2 Preparation strategies and reported reactions 45
1.2.3 Applications 49
1.3 Aims of present study 50
CHAPTER 2: SYNTHESIS OF ENAMINONES AND 1,2-OXATHIINE 2,2-DIOXIDE TARGET SYSTEMS 51
2.1 Preparation of Enaminone Precursors 51
2.1.1 Analogue library and structural features 51
2.1.2 Attempts at double substitution using DMFDMA 68
2.2 Sulfene addition to enaminones towards 3,4-dihydro 1,2-oxathiine 2,2-dioxides 74
2.2.1 Analogue library and reaction overview 74
2.2.2 Exploration of the sulfene addition mechanism 86
2.3 Elimination towards 1,2-oxathiine 2,2-dioxides 97
2.3.1 Acid-catalysed elimination attempts 97
2.3.2 Cope elimination: Reaction overview and substituent study 98
2.3.3 One-pot synthesis of 6-substituted 1,2-oxathiine 2,2-dioxides 104
CHAPTER 3: APPLICATION OF 1,2-OXATHIINE 2,2-DIOXIDE SYSTEMS AS PHOTOCHROMIC MATERIALS 107
3.1 Preface 107
3.2 Literature precedent 107
3.2.1 Photochromism and photochromic compounds 107
3.2.2 Diarylethene photochromic systems 110
3.3 Explorations on photochromic activity of 1,2-oxathiine 2,2-dioxide systems 119
3.3.1 Synthesis of diarylethene photochrome candidates based upon a 1,2-oxathiine 2,2-dioxide core 119
3.3.2 UV-Vis spectrophotometric studies 145
CHAPTER 4: REACTIVITY OF 1,2-OXATHIINE 2,2-DIOXIDES 152
4.1 Preface 152
4.2 Bromination of mono-, di- and tri- phenyl-substituted 1,2-oxathiine 2,2-dioxides 154
4.3 Reactions with brominated 1,2-oxathiine 2,2-dioxides 160
4.3.1 Bromine-lithium exchange attempts 160

4.3.2 Suzuki coupling reactions 161
4.3.3 Suzuki-Miyaura borylation 166
4.4 Reactions with unsaturated 1,2-oxathiine 2,2-dioxides 171
4.4.1 C-H activation coupling reactions 171
4.4.2 Exploration of cycloaddition reactions 177
4.4.3 Attempted benzyne addition to 1,2-oxathiine 2,2-dioxides 195
CHAPTER 5: CONCLUSIONS 199
5.1 General comments 199
5.2 Conclusions Pertaining to Chapter 2 199
5.3 Conclusions Pertaining to Chapter 3 201
5.4 Conclusions Pertaining to Chapter 4 202
CHAPTER 6: EXPERIMENTAL SECTION 205
6.1 Equipment and Reagents 205
6.2 Chapter 2 Compounds 206
6.2.1 Preparation of enaminoketones 206
6.2.1.1 Preparation of 3-(dimethylamino)-1-(aryl)prop-2-en-1-ones 206
6.2.1.2 Preparation of 1-(dimethylamino)-5-(aryl)penta-1,4-dien-3-ones and 1-(dimethylamino)-5-phenylpent-1-en-4-yn-3-one 208
6.2.1.3 Preparation of 1,2-disubstituted 3-(dimethylamino)prop-2-en-1-ones 211
6.2.1.4 Preparation of enaminones from amides and carboxylic acids 214
6.2.2 Preparation of 3,4-Dihydro-1,2-oxathiine 2,2-dioxides 216
6.2.2.1 Sulfene additions to 1,2-disubstituted enaminone precursors 216
6.2.2.2 Sulfene additions to 1-aryl enaminone precursors 219
6.2.2.3 Sulfene additions to 1-styryl enaminone precursors 221
6.2.2.4 Preparation of 4-(Dimethylamino)-3-phenyl-6-(phenylethynyl)-3,4-dihydro-1,2-oxathiine 2,2-dioxide **2.51** 224
6.2.2.5 Preparation of (*E*,*Z*)-1,2-diphenylethene **2.60a**/**b** 224
6.2.3 Preparation of 1,2-oxathiine 2,2-dioxides 225
6.2.3.1 Preparation of 3,5,6-trisubstituted 1,2-oxathiine 2,2-dioxides 225
6.2.3.2 Preparation of (*E*)-*N'*-(2,2-dioxido-3,5-diphenyl-1,2-oxathiin-6-yl)-*N,N*-dimethylformimidamide **2.58** 226
6.2.3.3 Preparation of 5,6-disubstituted 1,2-oxathiine 2,2-dioxides 227
6.2.3.4 Preparation of 3,6-disubstituted 1,2-oxathiine 2,2-dioxides 228
6.2.3.5 Preparation of 6-phenyl-1,2-oxathiine 2,2-dioxide **2.76** 232
6.2.4 “One-pot”-synthesis route to 1,2-oxathiine 2,2-dioxides 233
6.3 Chapter 3 compounds 237
6.3.1 α-Methylene ketone precursors and their precursors 237
6.3.2 Enaminone precursors 241
6.3.3 Preparation of 3,4-Dihydro 1,2-oxathiine 2,2-dioxide targets 242
6.3.4 1,2-Oxathiine 2,2-dioxide targets 244
6.4 Chapter 4 compounds 247
6.4.1 Preparation of bromo-1,2-oxathiine 2,2-dioxides 247
6.4.2 Suzuki Coupling/ Miyaura Borylation products 248
6.4.3 C-H Activation Coupling Products 251
6.4.4 Cycloaddition Products 254
6.4.4.1 PTAD addition reactions 254
6.4.4.2 PTAD addition reactions to 6-Styryl-1,2-oxathiine 2,2-dioxides for purpose of characterization of the silica sensitive initial adducts 257
6.4.5 DMAD addition reaction 258
6.4.6 Benzyne addition products 259
REFERENCES 261

APPENDIX 1: Crystal structure information/ CIF files……268
APPENDIX 2: Publications arising from work contained within this thesis……277

List of Figures

Figure 1.1: Different enaminone derivatives with their respective crystal structures (dotted bonds in structure (c) regard the simulated conformation of the analogue) 13
Figure 1.2: a) ORTEP plot of the crystal structure of a stabilised sulfene derivative with bond lengths and angles of interest, b) Atomic charges calculated for sulfene and its methyl counterpart 27
Figure 1.3: Crystal structures of 1,2-oxathiine 2,2-dioxide analogues, highlighting their planar but non-aromatic structure 35
Figure 1.4: Crystal structure of a 3,4-dihydro analogue highlighting its "envelope" conformation 45
Figure 1.5: Anti-tumour activity of a 3,4-dihydro 1,2-oxathiine derivative when screened against murine sarcoma (cyclophosphamide (CTX) used as a control) 50
Figure 2.1a/b: ^{1}H-NMR/ ^{13}C-NMR spectra of enaminone **2.1** 51
Figure 2.2: Selected ^{1}H-NMR spectra examples of enaminone products **2.4** (above) and **2.14** (below) 54
Figure 2.3: ^{1}H-NMR (above) and ^{13}C-NMR (below) spectra of **2.4** and **2.14** 55
Figure 2.4: ^{1}H-NMR spectrum of **2.8** 56
Figure 2.5: ^{13}C-NMR spectrum of **2.8** 56
Figure 2.6: Overlaid spectra of VT-^{1}H-NMR run on analogue **2.8** from 25 °to 70 °C at a 10 ° temperature increase pace (5 ° increase to reach 70 °C) 57
Figure 2.7: ^{1}H-NMR spectra of **2.8** and **2.13** 59
Figure 2.8: ^{13}C-NMR spectrum of **2.13** 59
Figure 2.9: NOE NMR of **2.2** showing key correlations that denote a *cis* geometry 60
Figure 2.10: X-ray crystallography structure of analogue **2.5**, showing the adopted *E*- geometry (thermal ellipsoids shown at 50 % probability level) 61
Figure 2.11: ^{1}H-NMR of the cyano analogue **2.5** and the two side-products **2.5a** and **2.5b** 63
Figure 2.12: Top: Crystal structure of dimer species obtained *via* the initial reaction protocol (**2.5a**), Bottom: Crystal structure of dimer species obtained by using PhMe as solvent (**2.5b**) 62
Figure 2.13: Effects of organocatalysis towards selected enaminones 67
Figure 2.14: a) ^{1}H-NMR spectrum of the mono-substituted analogue **2.21**, b) ^{1}H-NMR of the final crude mixture towards **2.30**, showing potential signals for the bis-enaminone analogue, c) ^{1}H-NMR of pyran-4-one (**2.33**) side-product, d) ^{13}C-NMR spectrum of **2.33** 69
Figure 2.15a/b: ^{1}H-NMR/ ^{13}C-NMR spectra of the bis-enaminone **2.31** 71
Figure 2.16: ^{1}H-NMR spectrum of the bis-enaminone **2.32** juxtaposed with the spectra of analogues **2.2** and **2.14** 73
Figure 2.17: Failure of sulfene addition on enaminones with imine-like moieties hinting at a concerted mechanistic process with the enone as a diene requisite 76
Figure 2.18: Representative examples of 3,4-dihydro-1,2-oxathiine-2,2-dioxide ^{1}H-NMR spectra (spectrum for **2.41** (c) was obtained from a d^{6}-AcMe sample) 77
Figure 2.19: Appearance of starting material signals of a $CDCl_3$ sample of **2.43** after 5 days in solution 79
Figure 2.20: Typical ^{13}C-NMR spectrum of a 3,4-dihydro-1,2-oxathiine 2,2-dioxide system (**2.41**) 81
Figure 2.21: IR spectrum of **2.41** 81
Figure 2.22: Mass spectra of **2.36** showing a molecular ion for **2.54** 82
Figure 2.23: ^{1}H-NMR of isomer mixture for the triphenyl derivative **2.36** 83
Figure 2.24: ^{1}H-NMR spectrum of the unsaturated derivative **2.58** 84
Figure 2.25: ^{1}H-NMR spectrum of the sulfene dimerization reaction mixture 85

Figure 2.26: *Trans*/*Cis* isomers of stilbene (**2.60a/b**) isolated from the dimerization of phenylsulfene ...85
Figure 2.27: Co-elution of the *anti*/*syn* isomers of analogue **2.40** ...87
Figure 2.28: ^{1}H-NMR spectra of the *anti*- (**2.40a**, above) and *syn*- (**2.40b**, below) isomers of derivative **2.40** ...88
Figure 2.29: Developing signals of the major isomer in a $CDCl_3$ solution of the *syn*- isomer **2.40b** over 6 days ...88
Figure 2.30: Full epimerisation of **2.40b** to **2.40a** in the solid state (1 year old stored sample)...89
Figure 2.31: Acid-catalysed elimination attempts of the *syn*- isomer **2.40b**...92
Figure 2.32: Representative examples of ^{1}H-NMR spectra for 1,2-oxathiine 2,2-dioxides (Insert in (d) shows the flow of electron density towards the EW SO_2 group causing deshielding of 4-H) ...101
Figure 2.33: ^{13}C-NMR spectra of indicative 1,2-oxathiine 2,2-dioxide examples ...101
Figure 2.34: MS spectra of the benzyl analogue **2.62**...102
Figure 2.35: Crystal structure of analogue **2.63** (thermal ellipsoids shown at 50 % probability level) ...103
Figure 2.36: MS spectra of **2.68**, wherein no *m/z* peaks of a potential N-oxide can be observed...103
Figure 2.37: ^{1}H-NMR spectrum of **2.78**...105
Figure 3.1: Stilbene photocyclization its parallel in triphenyl substituted 1,2-oxathiine 2,2-dioxide systems ...107
Figure 3.2: UV-Vis spectrum of a photochromic compound before (pale yellow) and after irradiation (red)...108
Figure 3.3: Typical examples of different types of di(hetero)aryl ethene photochromes ...112
Figure 3.4: Performance of 2,3-bis-(2,4,5-trimethylthien-3-yl)maleic anhydride (**3.26**) during a high number of irradiation/photoreversion cycles, where fatigue occurs only after *circa* 5000 repeats (original picture taken from Irie et al., *J. Org. Chem*., 1988, **53**, 803-808 and modified) ...114
Figure 3.5: Target structures of the 1,2-oxathiine 2,2-dioxide photochrome candidates ...119
Figure 3.6: Target thiophene containing α-methylene ketones...119
Figure 3.7: ^{1}H-NMR (above) and ^{13}C-NMR spectra (below) of methyleneketone **3.52** ...121
Figure 3.8: Long-range (^{4}J) coupling between thienyl proton and proximal methyl group protons on **3.52** ...121
Figure 3.9a/b: ^{1}H-NMR/ ^{13}C-NMR spectra of glyoxylate ester **3.60**...124
Figure 3.10: ^{1}H-NMR (above) and ^{13}C-NMR (below) spectra of carboxylic acid **3.61** ...125
Figure 3.11: ^{1}H-NMR (above) and ^{13}C-NMR (below) spectra of ketone **3.53**...127
Figure 3.12a/b: ^{1}H-NMR/^{13}C-NMR spectrum of the thienopyranone **3.62** ...129
Figure 3.13: NOESY spectrum of **3.62**...131
Figure 3.14: ^{1}H-NMR (above) and ^{13}C-NMR (below) spectra of the Weinreb amide species **3.65**...132
Figure 3.15a/b: ^{1}H-NMR/^{13}C-NMR spectrum of ketone **3.54** ...134
Figure 3.16: ^{1}H-NMR and ^{13}C-NMR spectra of enaminone system **3.67**...136
Figure 3.17: Key ^{1}H-^{13}C correlation between the protons and carbons of the NMe_2 terminus on **3.67** ..137
Figure 3.18: NOE NMR deployed to ascertain the *E* geometry of analogue **3.67** parallel to its bis-phenyl counterpart **3.69**...137
Figure 3.19: Overlaid ^{1}H-NMR spectra for **3.66** (blue), **3.67** (red), **3.68** (green) and **3.69** (purple), presenting the key singlets at δ 2.6 – 2.8 for the NMe_2 protons...138
Figure 3.20: Overlaid VT-NMR spectra of **3.68** between 25 ^{o} and 70 ^{o}C, illustrating the increasing C-N bond rotation rate ...139
Figure 3.21: 1H-NMR spectra of the bis-thienyl analogue **3.45**...140
Figure 3.22: ^{1}H-NMR spectra of **3.46** (insert shows the deconvolution of peaks *via* a Gaussian multiplication of the ^{1}H-NMR spectrum) ...140
Figure 3.23: ^{13}C-NMR spectrum of the bis-thienyl analogue **3.45**...141

Figure 3.24: MS spectrum of **3.45**, illustrating the presence of the *in situ* formed furan derivative **3.70** 142
Figure 3.25: Crystal structure of **3.45** (various viewpoints, thermal ellipsoids shown at 50 % probability level) 142
Figure 3.26: ^{1}H-NMR (above) and ^{13}C-NMR (below) spectra of the unsaturated analogue **3.48** 144
Figure 3.27: ^{1}H-NMR spectrum of **3.51** showing the characteristic doublets for 3-H and 4-H 144
Figure 3.28: Absorption spectra (in hexane) of 3,4-dihydro-1,2-oxathiine 2,2-dioxides **3.43** – **3.46** before irradiation and at the photostationary state (PSS) 146
Figure 3.29: Absorption spectra (in hexane) of the unsaturated 1,2-oxathiine 2,2-dioxides **3.48** – **3.51** before irradiation and at photostationary state 148
Figure 3.30: Absorption spectra of **3.50** (initial, after UV activation and after visible light bleaching), insert (a): recyclability after 10 UV activation and visible light bleaching cycles, insert (b): **3.50** hexane solution before (right) and after (left) UV irradiation 149
Figure 3.31: Stacked ^{1}H-NMR spectra (δ 5.5 – 7.7, $CDCl_3$) after increasing UV irradiation intervals (10 min to 2.5 h) showing the gradual emergence of signals for **3.50-closed** upon irradiation of a solution of **3.50** 150
Figure 3.32: ^{1}H-NMR of analogue **3.51** after 30 min of UV irradiation, illustrating the protons of the ring-closed form 150
Figure 4.1: Stacked ^{1}H-NMR spectra after 1.5 h and 72h of reaction time, illustrating the doublet signals of the 3-H and 4-H on the 3,4-dibromo intermediate **4.9a** and pinpointing the vinyl proton of **4.9** in a d_6-AcMe solution 156
Figure 4.2: Mass spectrum of **4.9**, showing the key pair of *m/z* peaks hinting at the two bromine isotopes 156
Figure 4.3: ^{1}H-NMR spectrum of **4.10** with the characteristic ~7 Hz coupling between 4-H and 5-H 157
Figure 4.4: Overlaid ^{13}C-NMR spectrum of **4.11** (bottom) and **4.7** (top), illustrating the upfield shift of C5 and downfield shift of C4 due to bromine substitution 158
Figure 4.5: a) HMBC spectrum of **4.11**, showing the long-range correlation between C6 and the *ortho* protons on the 6-phenyl group, b) NOESY spectrum of **4.11**, bearing the key correlation between the aromatic protons at δ 7.64 and 4-H at δ 7.02 159
Figure 4.6: Order of decreasing reactivity between different sites of a 1,2-oxathiine 2,2-dioxide system 160
Figure 4.7: ^{1}H-NMR spectrum of **4.29** 165
Figure 4.8: a) ^{1}H-NMR spectrum of **4.32**, b) Mass spectrum of **4.32** 166
Figure 4.9: ^{1}H-NMR spectrum of the crude mixture from the C-H activated coupling attempt on **4.5** 172
Figure 4.10: Correlation between yields and 3-aryl substituents across Suzuki and C-H activation coupling protocols 174
Figure 4.11: ^{1}H-NMR spectrum of the 3-pyridyl-5,6-dianisyl 1,2-oxathiine analogue **4.38** 176
Figure 4.12: Library of starting materials for cycloaddition reactions 178
Figure 4.13: ^{1}H-NMR of the crude mixture from the addition of PTAD to the styryl analogue **4.45** 183
Figure 4.14: ^{1}H-NMR spectrum of the compound of **4.63b**, as obtained from chromatographic treatment (blue), compared with the foregoing spectrum of the respective crude mixture (red) 183
Figure 4.15: Spectroscopic features of post-purification product **4.63b** 184
Figure 4.16: Locating the *C* atom of the pivotal proton at 5.48 ppm by HSQC-NMR (above) and placing it on the 9- position by observing two long-range correlations on the HMBC-NMR, as well as noticing the absence of such correlations with the other two distanced protons (5-H and 6-H) 185
Figure 4.17: ^{1}H-NMR of the crude mixture from the addition of PTAD to the nitrophenyl analogue **4.46** 187

Figure 4.18: Differences in the COSY correlations between **4.64a** and **4.64b** highlighting the silica-enabled migration of the aliphatic 10a-H 188
Figure 4.19: Spatial proximity of pivotal protons on **4.64a** and **4.64b** supporting their suggested structures (Note: red boxe on the 2D spectra indicate absence of correlation and green boxes show presence of correlations) 189
Figure 4.20: ^{1}H-NMR spectrum of **4.70** depicting the spin pattern seen for previous PTAD adducts (inserts show regions of the same spectrum after Gaussian multiplication) 190
Figure 4.21: (Below) ^{13}C-NMR spectrum of **4.70**, (above) DEPT90 ^{13}C-NMR spectrum of **4.70**, showing the negatively phased CH_2 signal 191
Figure 4.22: ^{1}H-NMR (above) and ^{13}C-NMR (below) spectra of side-product **4.76** 194
Figure 4.23: ^{1}H-NMR spectrum of **4.80** 195
Figure 4.24: Effect of different substitution patterns in the success of benzyne addition 197

List of Tables

Table 2.1: Enaminones prepared by reflux in neat DMFDMA 53
Table 2.2: Enaminones prepared using PhMe as solvent 65
Table 2.3: Enaminone systems obtained *via* L-proline organocatalysis 66
Table 2.4: Attempts at double DMFDMA substitution 68
Table 2.5a/b: Library of 3,4-dihydro 1,2-oxathiine 2,2-dioxides with varying 3-, 5- and 6- substituents .. 75
Table 2.6: Vicinal coupling constants of various 3,4-dihydro 1,2-oxathiine 2,2-dioxides 78
Table 2.7: Table of reversion yields between 3 analogous 3,4-dihydro 1,2-oxathiine 2,2-dioxides 79
Table 2.8: Varying reaction conditions with the respective ratios of observed isomers (**2.40a** : **2.40b**) ... 90
Table 2.9a/b: Library of unsaturated 1,2-oxathiine 2,2-dioxide products of a Cope elimination 100
Table 2.10: Analogue library of mono-substituted 1,2-oxathiine 2,2-dioxides prepared *via* the one-pot, two-step synthetic route 105
Table 3.1: Main classes of photochromic compounds 109
Table 3.2: High longevity and favourable thermal properties as driving factors of thiophene photochrome efficiency 111
Table 3.3: DMFDMA addition on the 3 α-methylene ketones **3.52 – 3.54** 135
Table 3.4: Sulfene addition towards the 3,4-dihydro-1,2-oxathiine 2,2-dioxides **3.43 – 3.46** 139
Table 3.5: Cope elimination runs towards analogues **3.48** – **3.51** 143
Table 3.6: Key UV-Vis values of the saturated 1,2-oxathiine 2,2-dioxide analogues (**3.43** – **3.46**) 146
Table 3.7: Key UV-Vis values of the unsaturated 1,2-oxathiine 2,2-dioxide analogues (**3.48** – **3.51**) 147
Table 4.1: Bromination attempts on different phenyl-substituted 1,2-oxathiine 2,2-dioxides 155
Table 4.2: Suzuki coupling attempts towards various 1,2-oxathiine 2,2-dioxides 163
Table 4.3: Variation of reaction conditions for a Suzuki-Miyaura catalysed homo-coupling of **4.9** 167
Table 4.4: C-H activated coupling of 1,2-oxathiine 2,2-dioxides with varying aryl iodides 173
Table 4.5: Attempts towards the formation of variously substituted tricyclic 1,2-oxathiine 2,2-dioxides 186
Table 4.6: Diels-Alder attempts using the styryl analogues **4.46** and **4.47** 193
Table 4.7: Attempts at the cycloaddition of benzyne to 1,2-oxathiine 2,2-dioxide analogues 196

List of abbreviations

b.p.: Boiling point
m-CPBA: *m*-Chloroperoxybenzoic Acid
COSY: Correlation Spectroscopy
1,2-DCE: 1,2-Dichloroethane
DCM: Dichloromethane
DEPT90: Distortionless Enhancement by Polarization Transfer (90^{o})
DMA: Dimethylacetamide
DMAD: Dimethyl Acetylenedicarboxylate
DMFDMA: *N,N*-Dimethylformamide dimethyl acetal
DMF: Dimethylformamide
DBU: 1,8-Diazabicyclo[5.4. 0]undec-7-ene
DBN: 1,5-Diazabicyclo[4.3.0]non-5-ene
DDQ: 2,3-Dichloro-5,6-dicyano-1,4-benzoquinone
DMSO: Dimethylsulfoxide
ED: Electron-donating
EM: Electromagnetic (radiation)
EW: Electron-withdrawing
e.g.: Exampli gratia
i.e.: In es
HOMO: Highest Occupied Molecular Orbital
HMBC: Homonuclear Multiple Bond Correlation
HRMS: High Resolution Mass Spectrometry
HSQC: Heteronuclear Single Quantum Correlation
IPOS: Innovative Physical Organic Solutions
IR: Infrared
LUMO: Lowest Unoccupied Molecular Orbital
m.p.: Melting Point
MS: Mass spectrometry
NBS: N-Bromosuccinimide
NMR: Nuclear Magnetic Resonance
NOE: Nuclear Overhauser Effect
NOESY: Nuclear Overhauser Effect Spectroscopy
P.E.: Petroleum Ether
PSS: Photostationary State
PTAD: 4-Phenyl-1,2,4-triazoline-3,5-dione
SOIs: Secondary Orbital Interactions
S.M.: Starting material
THF: Tetrahydrofuran
TLC: Thin Layer Chromatography
TMS: Tetramethylsilane
UV: Ultraviolet
UV-Vis: Ultraviolet-Visible
VT NMR: Variable Temperature NMR

DEDICATIONS AND ACKNOWLEDGEMENTS

This thesis is dedicated to my parents (Christos and Villy), who never wavered in their support for me and stubbornly held on to their faith that I could carry on through and bring this project to fruition.

I feel deeply grateful to my family, friends and special one for truly believing in me, even in times when I did not believe in myself.

I express my deepest gratitude to Prof. Mark Heron and Dr Chris Gabbutt, under whose guidance I was able to successfully undertake the experimental work required in order to compile this thesis. I would also like to thank my academic colleagues Dr Orlando Azevedo, Dr Stuart Aiken, Dr Georgina Armitage, Dr Ross Edgar, Dr Daniel Crossley and Dr Julien Doulcet for their invaluable help and input.

I would further like to express my gratitude to Prof. Craig Rice for his contributions in the X-ray crystallography data presented in this thesis, as well as Dr Neil McLay for his help and contributions in VT-NMR and 2D-NMR spectroscopy. I also note my appreciation for the research work of final year students Ochola W. Ogwang and Kelechi Anozie, which facilitated the research detailed in this thesis.

I finally owe my gratitude to the University of Huddersfield and Essilor International S.A. for the funding that accompanied this project, as well as the extension of this funding due to the unprecedented COVID-19 pandemic circumstances.

"There is only one good, knowledge, and one evil, ignorance."

Socrates, 469-399 BC

CHAPTER 1: INTRODUCTION[a]

1.1 Enaminones and Sulfenes

1.1.1 Preface

The following introductory literature review concerns the synthesis and reactivity of the 1,2-oxathiine 2,2-dioxide ring systems. Such 6-membered *O*,*S*-containing heterocycles have been described in the scientific literature and result from a broad range of transformations on a variety of substrates. Within the framework of this PhD project, the addition of sulfenes to enaminoketone derivatives was selected as the ring synthesis route of choice to 3,4-dihydro-1,2-oxathiine 2,2-dioxide analogues due to its efficiency and simplicity; hence, it was deemed necessary that the main features and chemical behaviour of both enaminoketones and sulfenes be discussed, before any aspect of their 3,4-dihydro-1,2-oxathiine 2,2-dioxide addition products is touched upon. The versatility of both sulfenes and enaminoketones is paramount to the creation of a sizeable library of 3,4-dihydro- and 1,2-oxathiine 2,2-dioxides (δ-sultone) analogues, thus their use in heterocyclic synthesis must be mapped out to a satisfactory extent in order to support the rationale behind the selected synthetic route. Several complementary aspects of this route, *e.g.* rate of the reactions, side-product formation and reproducibility, can also be traced back to the reactivity of these interesting starting materials.

1.1.2 Enaminones

1.1.2.1 General information

Enaminones (or enaminoketones or vinylogous amides) are molecules that contain, as their name suggests, a carbonyl group that neighbours an enamine moiety, thus having the general molecular formula $R^1COCR^2{=}CR^3NR^4R^5$ (R^1= alkyl, aryl or heteroaryl, $R^{2\text{-}5}$= alkyl, aryl, heteroaryl or H). Their unique structure results in nucleophilic as well as electrophilic sites, with the oxygen, C-2 and nitrogen atoms capable of nucleophilic attack and the carbonyl carbon and C-3 posing as an electron-deficient character[1]. This versatile reactivity is brought about *via* resonance forms that allow for the delocalisation of electron density between the terminal O and N atoms (Scheme 1.1)[2].

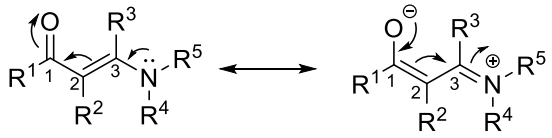

Scheme 1.1: Delocalisation of electron density in an enaminone

The alternation of double and single bonds in the enaminone structure dictates their conformation in space, as the conjugated system of the carbon, nitrogen and oxygen atoms requires for a planar arrangement to reach its ground energy state. It should also be added that, depending on the substitution pattern of the enaminone, either the *E*- or the *Z*- conformation may be adopted, as evidenced by the crystal structures in figure 1.1;[3,4,5] the cyano derivative **1.1** is observed as the *trans* isomer (Fig. 1.1a),

[a] Work contained within this chapter has contributed to the following publication (Appendix 2, p. 277): *Targets in Heterocyclic Systems*, 2020, **24**, pending; DOI: http://dx.medra.org/10.17374/targets.2021.24.33

whereas the di-*tert*-butyl and ester-containing analogues **1.2** and **1.3** (Fig. 1.1b and Fig. 1.1c respectively) adopt the *cis* conformation, thus allowing for optimal space between all substituents in each case.

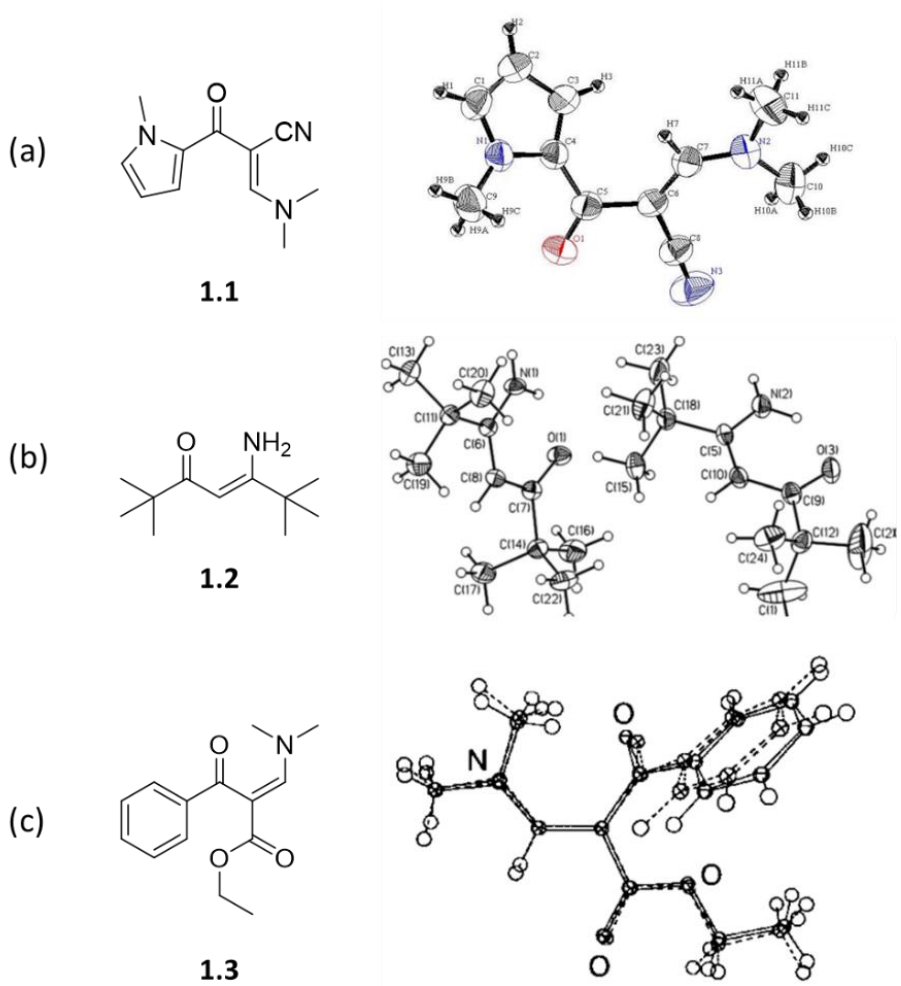

Figure 1.1: Different enaminone derivatives with their respective crystal structures (dotted bonds in structure (c) regard the simulated conformation of the analogue) (Permissions applied for)

The different reactive sites found on enaminone systems (**1.4**) render them quite versatile in organic synthesis, with a significant amount of their activity having been investigated in research papers and reviews.[1,6] In the scope of the current research project, only the 1-substituted and 1,2-di-substituted enaminoketone analogues with a dimethylamino terminus (**1.5**) are of interest, since such substrates are used as precursors in this thesis; hence, the following discussion will focus specifically on these systems (Scheme 1.2).

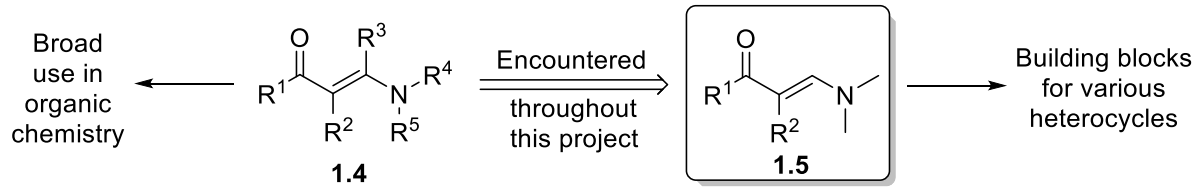

Scheme 1.2: Targeting the scope of reported literature towards mono- and di-substituted enaminones

1.1.2.2 Synthesis of mono- and di- substituted enaminones

When regarding the structure of enaminoketones with substituents on either the 1- and /or the 2-positions, it becomes apparent that the dimethylaminomethylene moiety is common amongst them, thus they can be conveniently obtained from a group of analogous precursor molecules. Indeed, α-methylene containing ketones can be converted to their respective enaminones simply and efficiently by using *N,N*-dimethylformamide dimethyl acetal (DMFDMA, **1.6**, Scheme 1.3) as a source of the dimethylaminomethylene fragment. Obtained by treatment of dimethylformamide (DMF) with dimethyl sulfate and sodium methoxide (Scheme 1.3)[7], DMFDMA is a versatile reagent that can afford a variety of addition products, depending on the precursors and conditions used. In this case, the acidity of the protons adjacent to the carbonyl unit of the starting material is utilised to bring about an attack on the electrophilic central *C* atom of DMFDMA, with concomitant loss of MeOH, and the resulting methoxy iminium intermediate undergoes further elimination of MeOH towards the final, olefinic product (**1.5**, Scheme 1.4)[8].

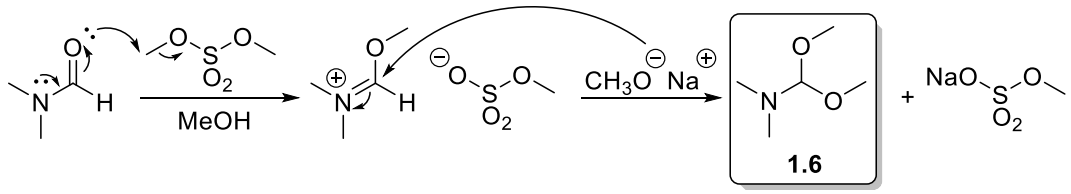

Scheme 1.3: Formation of DMFDMA by methylation and consecutive methoxylation of DMF

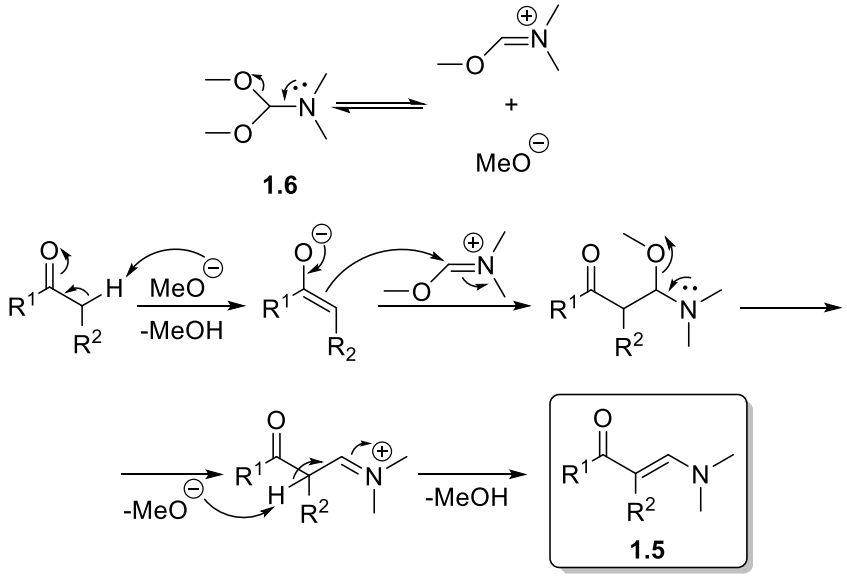

Scheme 1.4: Mechanism of dimethylaminomethylene addition to an α-methylene containing ketone

A wide range of acyclic (**1.7** - **1.10**) and cyclic (**1.11** - **1.12**) ketones have been converted to their derived enaminoketones **1.13** - **1.18** in the same manner[9,10,11] (Scheme 1.5), with DMFDMA being used either neat or in an appropriate high boiling point solvent (commonly PhMe, DMF or xylene). The reaction is always carried out at an elevated temperature which indicates an energy barrier, potentially during the formation of the addition intermediate as this is entropically unfavourable. In most cases, the solid products can be efficiently purified *via* recrystallization or simply by washing with an appropriate solvent. Interestingly, although various substituents on the starting ketone can be tolerated and remain unaltered during the transformation, phenolic groups (-C_6H_4OH) have been reported to be *O*-alkylated and yield the corresponding anisyl moieties (-C_6H_4OMe)[12,13] (Scheme 1.6).

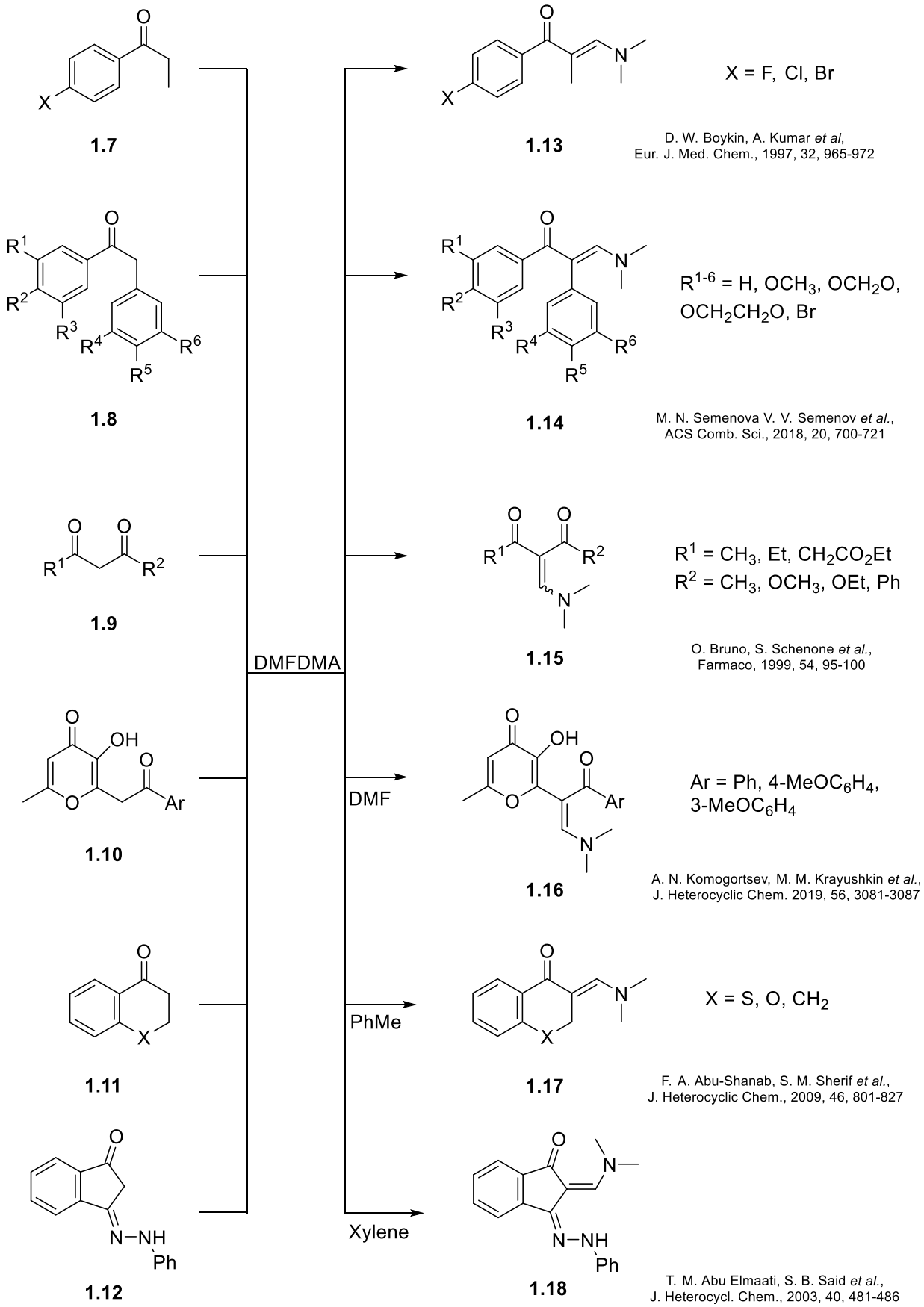

Scheme 1.5: Various methylene containing ketone systems as precursors to their enaminone counterparts

A similar conversion was not observed, albeit anticipated, in the case of the enol-containing compound **1.10**, which retained the enol group upon its enaminone derivatisation.[14] The hydrazine fragment of the starting ketone **1.12** also remained intact, even upon reflux in a high boiling solvent.[15] Regarding -NH_2 groups in general, it has been reported that they react with DMFDMA towards the formation of amidine products (**1.19**, Scheme 1.7); for that reason, -NH_2 moieties have the potential to allow for side-reactions and thus need to be protected during DMFDMA treatment. Protection of an amino group has been exemplified by reacting a halide precursor (**1.20**) with phthalimide and treating the phthaloyl derivative **1.21** with DMFDMA to afford the enaminone **1.22**, which can be subsequently furnished into a variety of heterocyclic systems **1.23** with preservation of the "masked" amino group. An excess of hydrazine can then be utilised to cleave the phthaloyl moiety and afford the amino-substituted products (**1.24**, Scheme 1.8).[16,17,18] It should be noted that no examples have been found where the amino group is deprotected prior to conversion of the enaminone backbone into a heterocycle product.

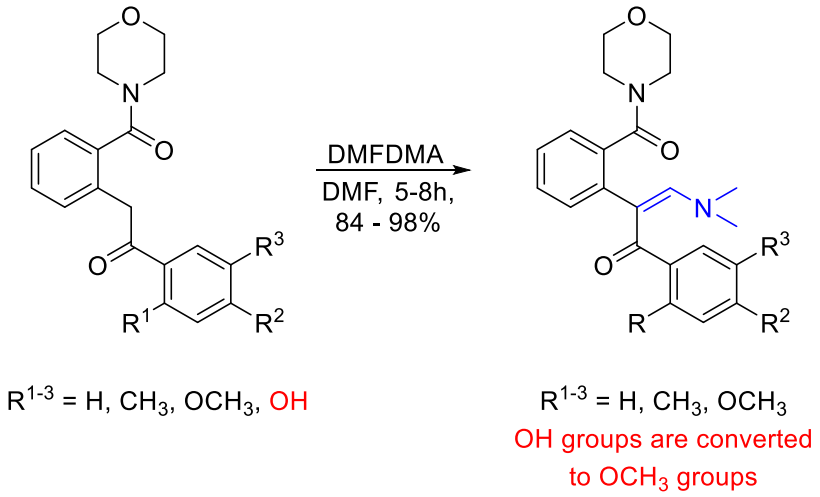

Scheme 1.6: Enaminone formation with concomitant methylation of reactive OH groups

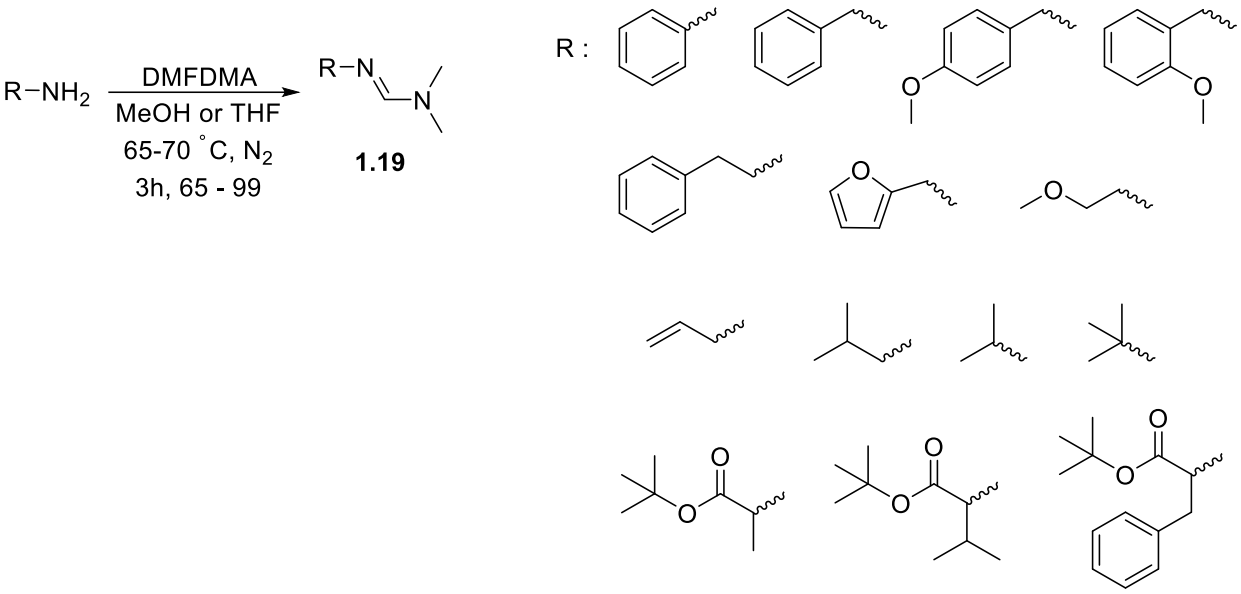

Scheme 1.7: Use of DMFDMA towards amidine species

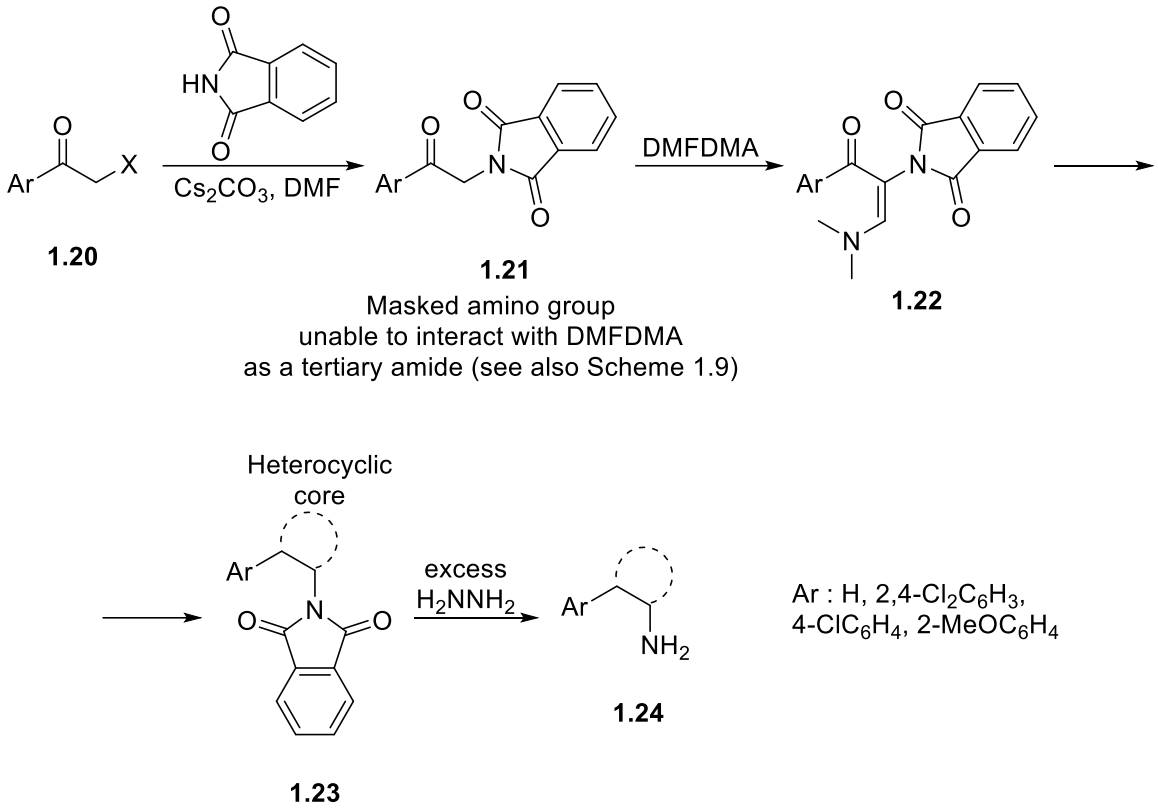

Scheme 1.8: "Masking" of amino groups during DMFDMA treatment and conversion into heterocyclic products

'Enaminone' formation can also be accomplished using amides (**1.25**) as pseudo-α-methylene ketones. Despite the well-known stability of this class of compounds due to resonance, treatment with DMFDMA at elevated temperatures utilises the two protons of the *N* atom in the same manner as the α-protons of the corresponding ketone. These aza-enaminones (**1.26**), thus obtained quantitatively, are quite useful intermediates towards heterocycles with increased heteroatom load.[19]

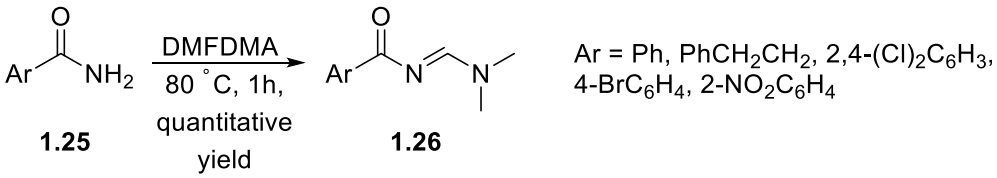

Scheme 1.9: Aza-enaminones from amide starting materials

Regarding mono-substituted enaminoketones (**1.5** R^2 = H), the absence of a substituent on the 2-position of the ketone allows for further activation of this site through organocatalysis.[20,21] As it can be seen in the example of the anisyl derivative **1.27** (Scheme 1.10), (L)-proline is able to ameliorate the reaction rate and afford the desired enaminone system in 82% yield, as compared with the significantly lower yield (20%) reported when no catalyst is used. Although the scope of use for this catalyst is limited to α-methyl ketones, as any substituent on the 2-position induces steric crowding and prevent contact with proline.

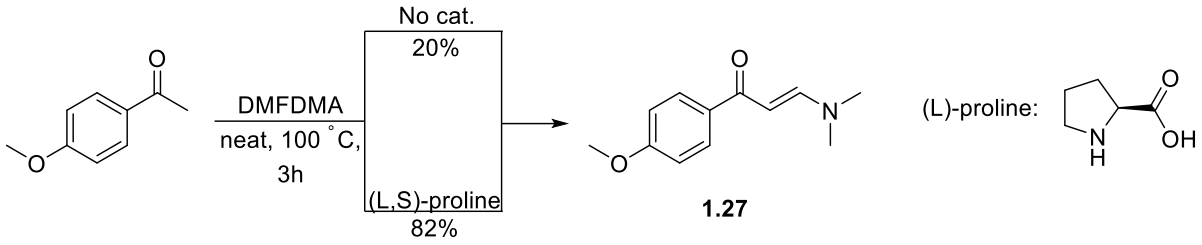

Scheme 1.10: Catalysis of dimethylaminomethylene addition by proline

Ketones with α-methylene groups on each side of the carbonyl unit (**1.28**) have been found to react twice, using an excess of DMFDMA to afford bis-enaminone systems **1.29** with extended conjugation between the two double bonds and the carbonyl (Scheme 1.11a).[22,23] Additionally, it has been reported that the diphenyl analogue can be further transformed into the amide **1.30** at higher temperatures (150-200 °C instead of 110 °C).[24] Structurally similar products can be furnished from α,β-unsaturated ketones (**1.31** - **1.32**), in which case DMFDMA interacts with the terminal methyl group in the usual fashion while the double or triple bond remains intact throughout the transformation (Scheme 1.11b).[25,26]

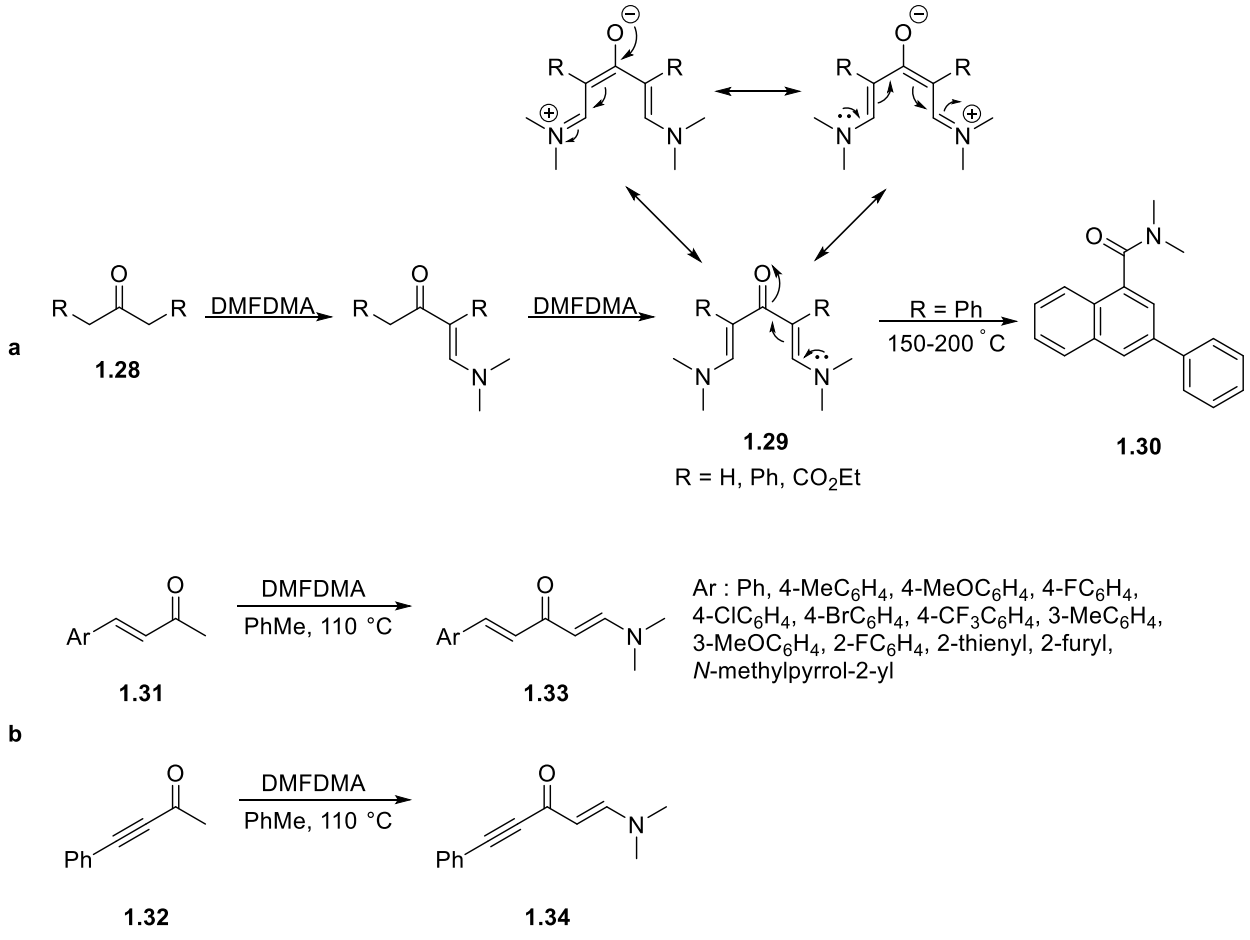

Scheme 1.11: a) Double addition of the dimethylaminomethylidene fragment towards di-enaminones, b) α,β-Unsaturated ketones as starting materials in DMFDMA additions

Parallel to α-methylene containing ketones, unsaturated compounds have been observed to behave in the same fashion as their saturated counterparts (Scheme 1.12). The enol **1.35**, being used as a sodium salt, can be processed with DMFDMA under a set of conditions that differ from the routes seen so far to

afford its enaminone analogue (**1.36**).[27] The aza-enone **1.37** can be converted likewise, owing to the presence of the neighbouring, electron-donating *N* atom.[28] This specific compound also presents an interesting example of different *N*- containing groups that stay intact during DMFMA treatment, allowing for selectivity on the enone site.

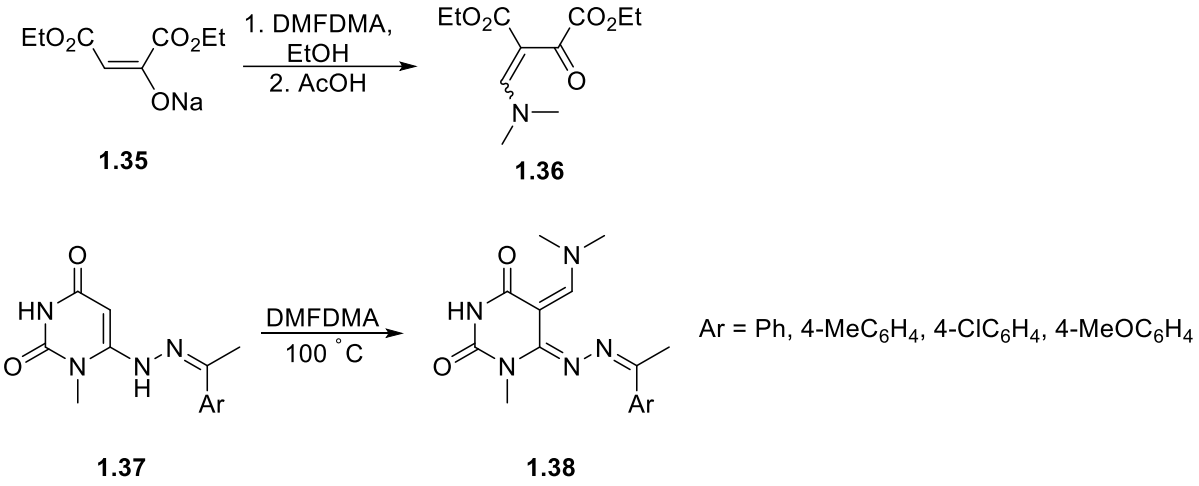

Scheme 1.12: Reaction with DMFDMA on ketones with similar groups to α-methylenes

Although DMFDMA is the reagent used predominantly in the preparation of these enaminone systems, compounds of a similar structure can also effect the same transformation.[29] Specifically, bis(dimethylamino)methoxymethane (**1.40**, colloquially known as Bredereck's reagent[30]) along with its *tert*-butoxy analogue **1.41**, both readily obtainable by alkoxylation of bis(dimethylamino)acetonitrile (**1.39**, Scheme 1.13a), have the ability to "donate" their dimethylaminomethine moiety under similar conditions with DMFDMA (Scheme 1.13b).

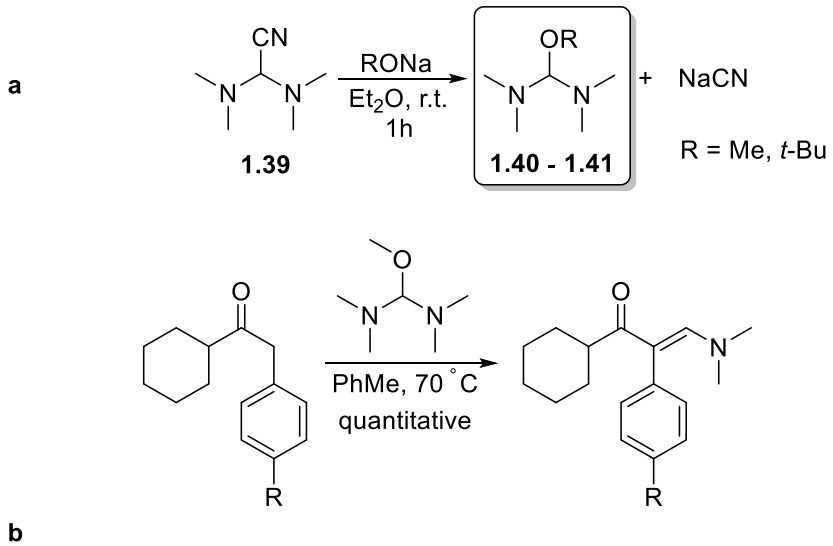

Scheme 1.13a: Alternative methods of enaminone preparation

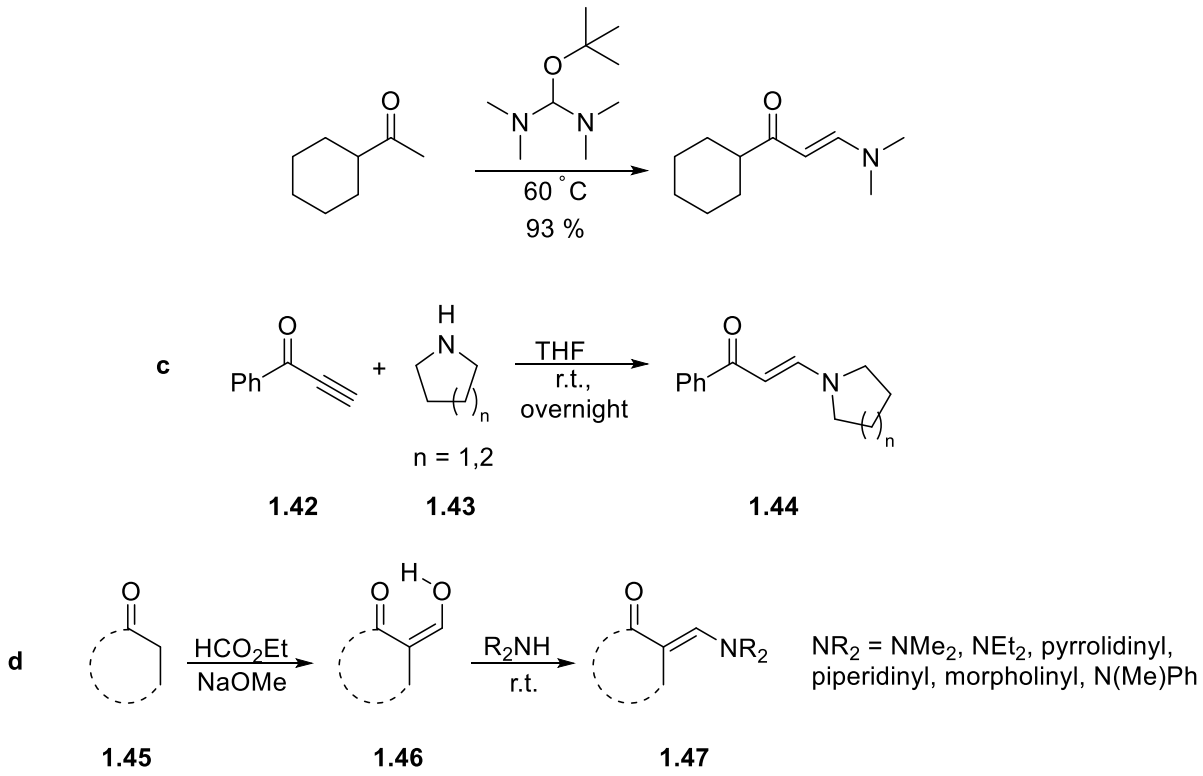

Scheme 1.13b: Alternative methods of enaminone preparation

Jiang *et al*.,[26] have also presented an alternative route towards enaminones with functionalised amino moieties without the use of an acetal-containing reagent. In their work, a terminal alkyne (**1.42**) was treated with secondary, cyclic amines **1.43** in a quite different set of conditions (THF, r.t.) to yield the enaminone adducts (**1.44**, Scheme 1.13c). In another variation (Scheme 1.13d), the hydroxymethylene derivative of a cyclic ketone **1.45**, obtained *via* treatment of the α-methylene containing ketone precursor **1.46** with ethyl formate and sodium methoxide, can be condensed with a 2° amine to furnish the target enaminone **1.47**.[31,32]

1.1.2.3 Enaminone reactions leading to heterocyclic systems

The reactivity of the 1,2-substituted enaminone systems can be thoroughly mapped out, due to the extended spectrum of transformations that have been reported. Various research works describe the use of the two active electron deficient sites on the enaminoketone system, *i.e.* the *C* atoms at the 1- and 3-positions, when these compounds are reacted with nucleophilic reagents. Conversely, the O atom possess nucleophilic properties, as discussed earlier (Section **1.1.2.1**), and is able to attack electrophilic sites of ambient reagents. The ability of the terminal dimethylamino group to be protonated and cleaved *via* an E1cB mechanism is also utilised to complete conversions that lead to eliminated, heterocyclic and, in most cases, heteroaromatic systems. A multitude of pyrroles, oxazoles, pyrazoles, furans and pyrimidines have been prepared, based on the aforementioned reactivity, using a range of different nucleophilic reagents, as shown in scheme 1.14.[1,6,33,14,10,34,35] The reactions are commonly carried out in polar, protic solvents and at elevated temperatures to afford the desired heterocycles. In the case of the fused furan systems **1.51**, the formation of the heterocycle is affected intramolecularly *via* the enol hydroxyl group, similarly to the pyrroles **1.53**, where the initial enaminone is first converted to an *N*-substituted derivative **1.52** which possesses a reactive methylene group utilised to bring forth the ring-closing reaction.

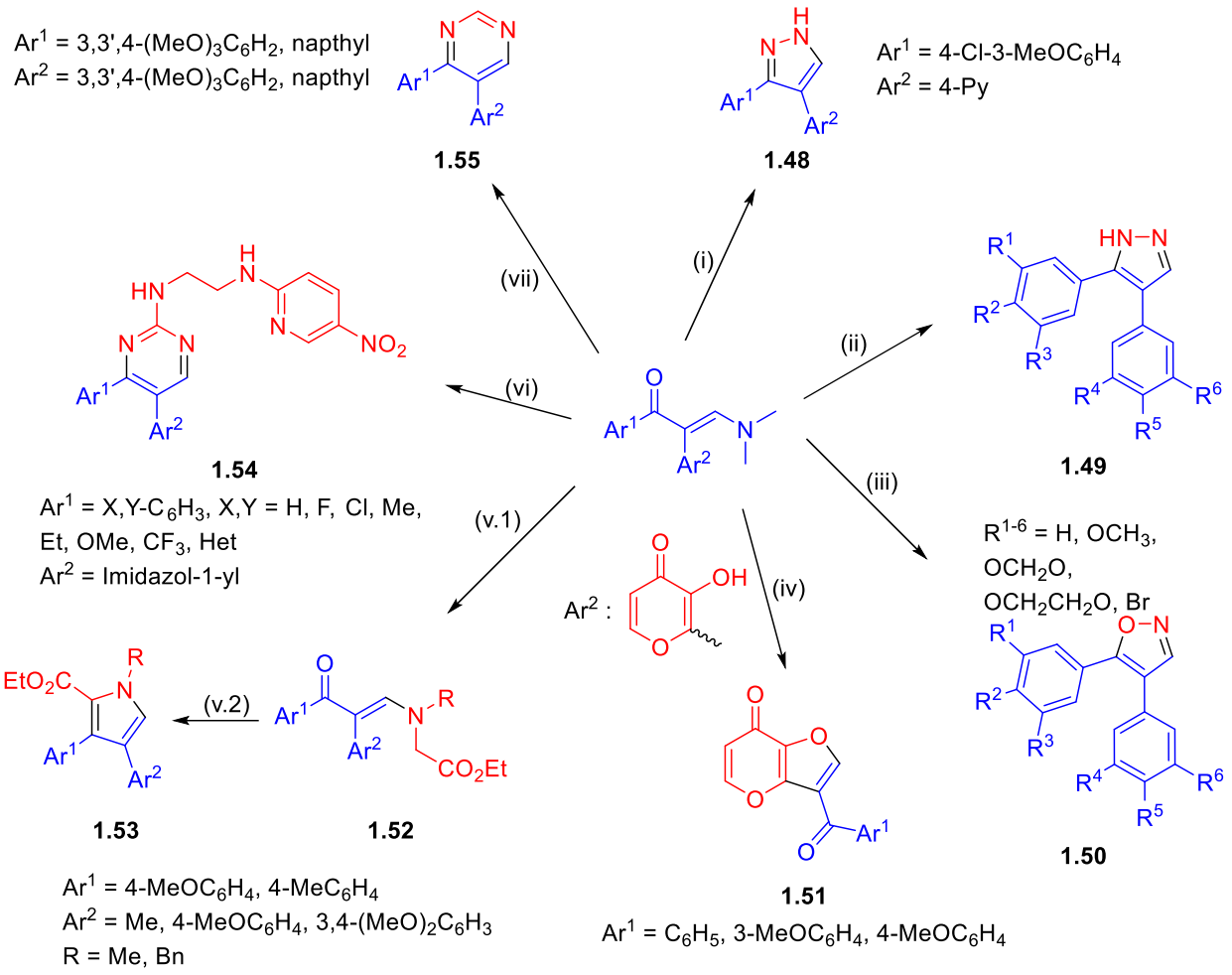

Reagents & Conditions: (i) $H_2NNH_2•H_2O$, EtOH, r.t. o/n, (ii) $H_2NNH_2•2HCl$, MeOH, reflux, 1h, (iii) $NH_2OH•HCl$, MeOH, reflux, 2h, (iv) AcOH, reflux, 8h, (v) 1. $RNHCH_2CO_2Et$, EtOH, reflux, 2. AcOH, reflux, (vi) $(H_2N)HN{=}CNHCH_2CH_2NH$-(5-NO_2)-2-Py, Cs_2CO_3, THF or DMF, 80 °C, 8h, (vii) $NH_4^+HCO_2^-$, $HCONH_2$, AcOH, reflux

Scheme 1.14: Range of transformation of enaminoketones into heterocyclic systems

Moreover, pyrazole formation reactions present an additional point of interest, as different regioisomers can be obtained depending on the substitution level of the reacting hydrazine, as well as the solvents and conditions used (Scheme 1.15). By examining the relevant literature[36], it can be suggested that aqueous conditions favour the formation of the 3,4-substituted isomers (*e.g.* compounds **1.56**), whereas the 4,5-subtituted analogues (*e.g.* products **1.57**) are the favoured products under anhydrous conditions. Huang *et al.*,[16] have provided additional insight on the regioselectivity of this conversion by highlighting that the complexing molecule of the hydrazine reagent also affects which isomer will be formed. *N*-substituted hydrazine sulfate affords predominantly the 3,4-substituted isomers **1.58** as a mixture with their 4,5-substituted counterparts **1.59**, whilst changing the complexing agent to hydrochloride, along with the absence of *N*-substituents, allows for the selective formation of the former upon R-substitution of the NH moiety. Absence of a complexing compound on the hydrazine seems to result in the cyclisation towards a 4,5-substituted pyrazole system (**1.60**).

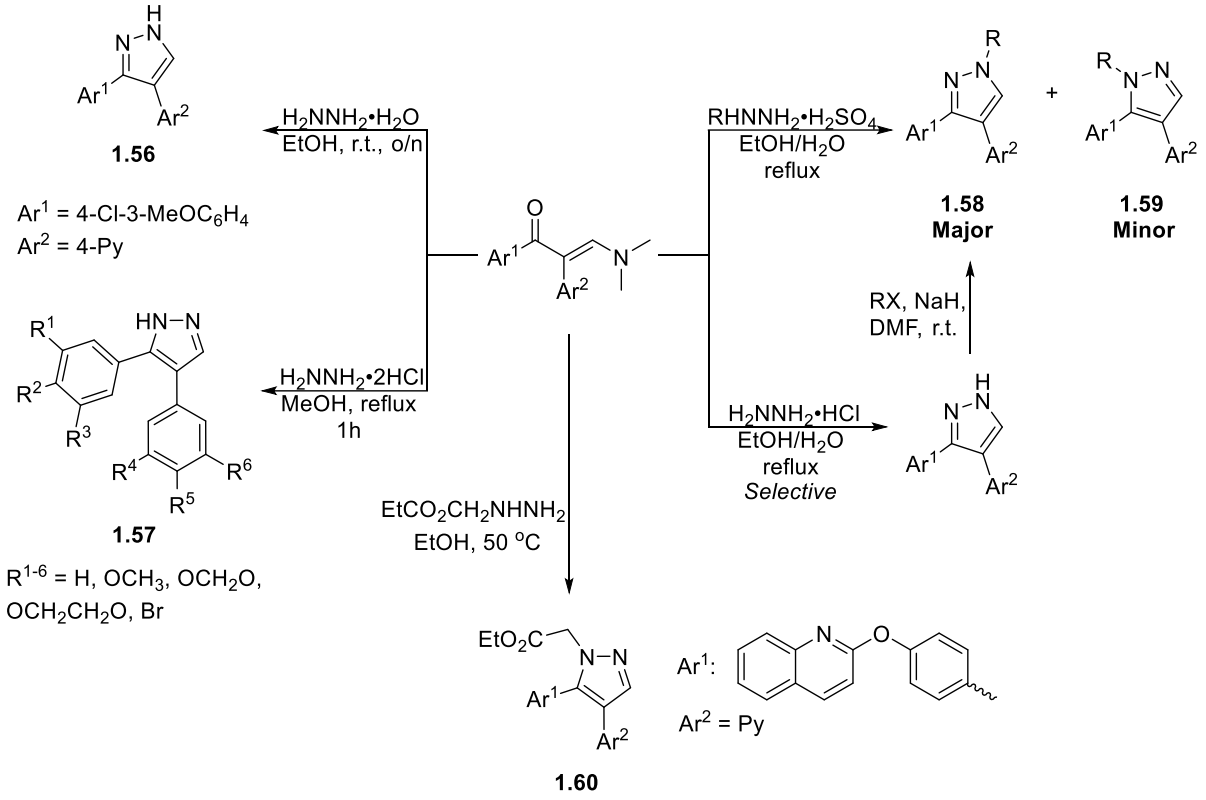

Scheme 1.15: Effect of solvents, conditions and stabilising agents on the regioselectivity of the pyrazole formation

An interesting case of indole formation *via* the use of a neighbouring *N* atom is presented in the work by Shahrisa *et al.*,[37] wherein the starting enaminone **1.62** is prepared by acylation of an aromatic enamine **1.61**. Subsequent treatment with elemental iron in acetic acid to reduce the NO_2 moiety of the phenyl ring eventually yields the ring-closed product **1.63** with the acyl groups intact (Scheme 1.16).

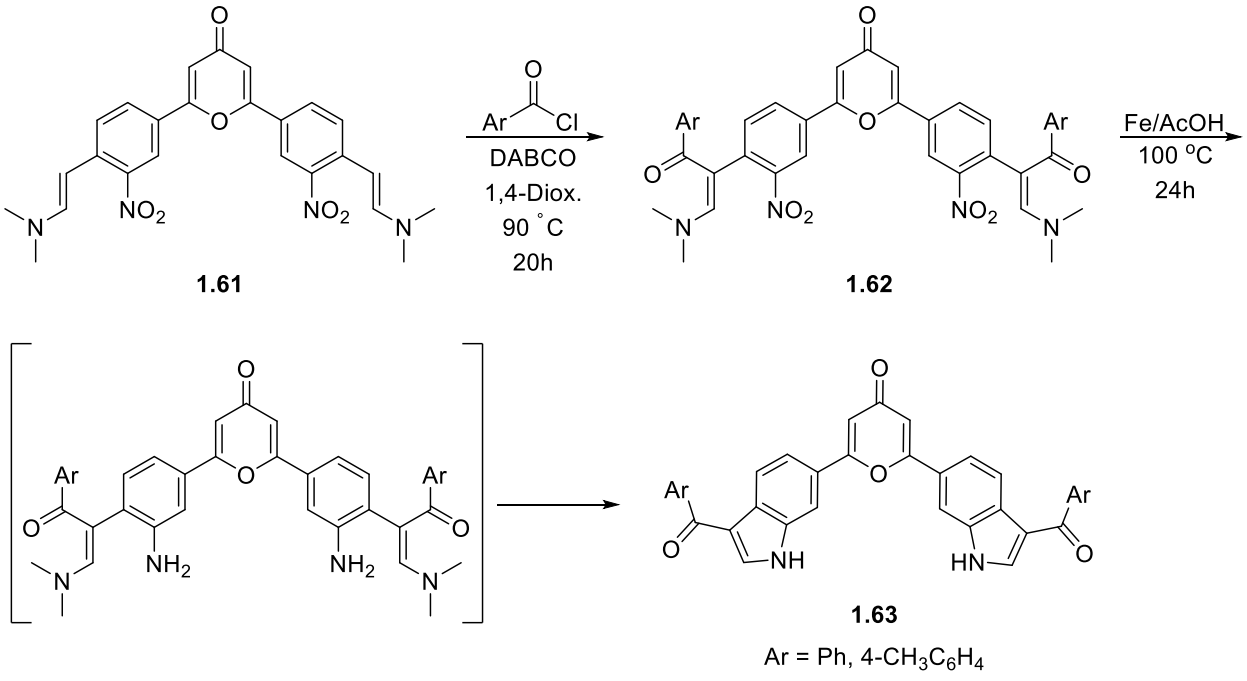

Scheme 1.16: Reaction of an enaminone with an adjacent NH_2 group towards a substituted indole system

As can be expected, the range of heterocyclic products can be expanded into more complex 6-membered ring systems *via* utilisation of the ambient substituents on the enaminoketone. In the case of the ring-open precursors **1.64** (Scheme 1.17), this cyclisation occurs intramolecularly under acidic conditions, wherein the O atom of the enaminone moiety acts as a nucleophile towards the formation of the lactone ring. Subsequent cleavage of the amidic bond and hydrolysis of the NMe_2 moiety afford the isocoumarin systems **1.65**.[12]

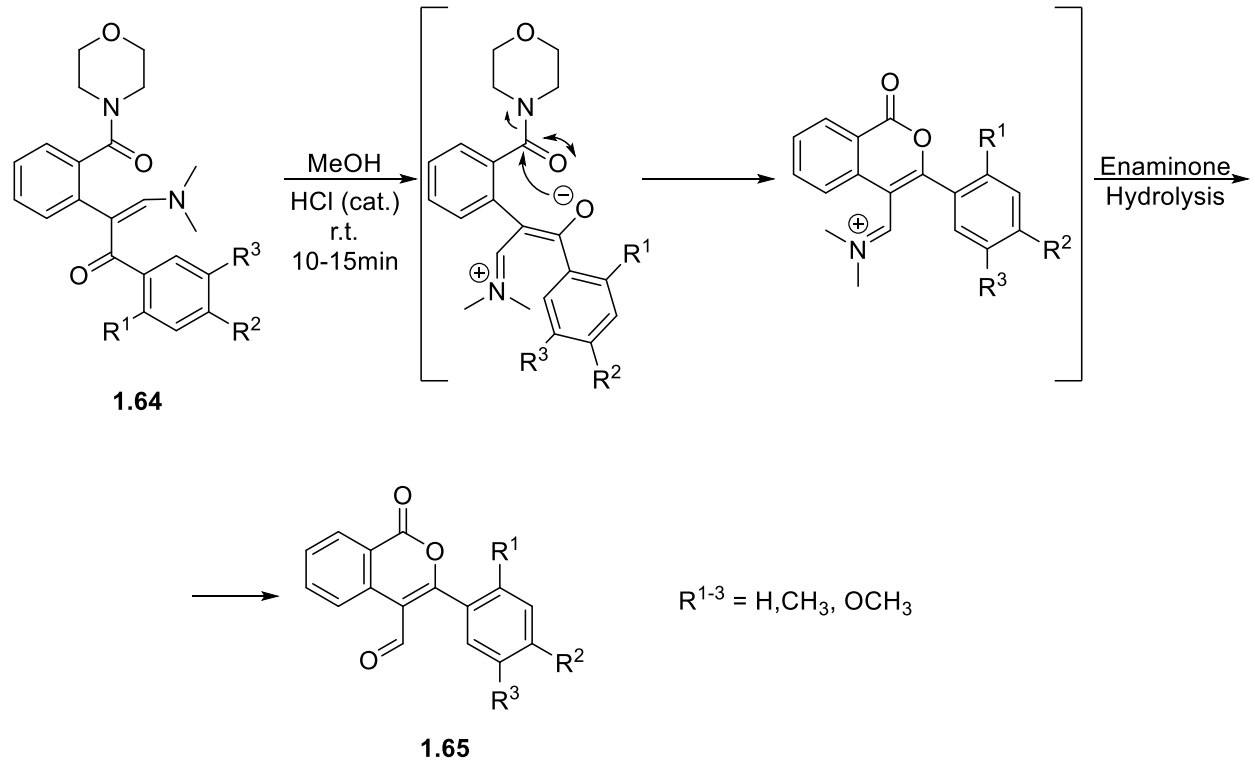

1.64 **1.65**

Scheme 1.17: Fused lactone formation by acid-catalysed activation of the enaminone *O* atom

The addition of amide derivatives has been another point of recent research, since it provides access to novel heterocyclic scaffolds. 2-Cyanoacetamide was found to react with 1,2-di-substituted enaminones using sodium hydride, although there seems to be a conflict in the reported data from different research groups. Wang *et al*.,[38] claim to have isolated the unsaturated pyridine-2(3*H*)-one isomer **1.67**, whereas Meurer *et al*.,[39] as well as Z. Wu and coworkers[40], suggest that the 1*H* tautomers **1.69** and **1.71** are formed instead.

An additional facet of enaminone annulations has been presented by Schenone *et al*. in consecutive pieces of research[41,42], in which enaminones are combined with either sulfenes or ketenes to afford 3,4-dihydro-1,2-oxathiine 2,2-dioxides or 3,4-dihydro-pyran-2-ones, respectively (Scheme 1.19 and Scheme 1.20). In contrast to the reactions reported thus far, these particular conversions were thoroughly explored by the research group, with respect to the substitution pattern of the starting enaminone. Absence of a substituent on the 2-position of the enaminones **1.72** was proven to be detrimental for this addition, due to unfavourable enaminone conformation, with the exception of the 1-phenyl analogues **1.74** – **1.75**, whereas phenyl and alkyl groups on positions 1- and 2- provide suitable steric and electronic properties to the substrate, so that it can react with the sulfene and yield the heterocycle products **1.85** – **1.92**. The *N*-substituents on the amino terminus were also explored; aliphatic groups were found to activate the substrate *via* positive inductive effect, whereas weakly activating, aromatic groups hinder the conversion, potentially due to steric hindrance overcoming electron donation, as seen for the attempted analogues **1.93**.

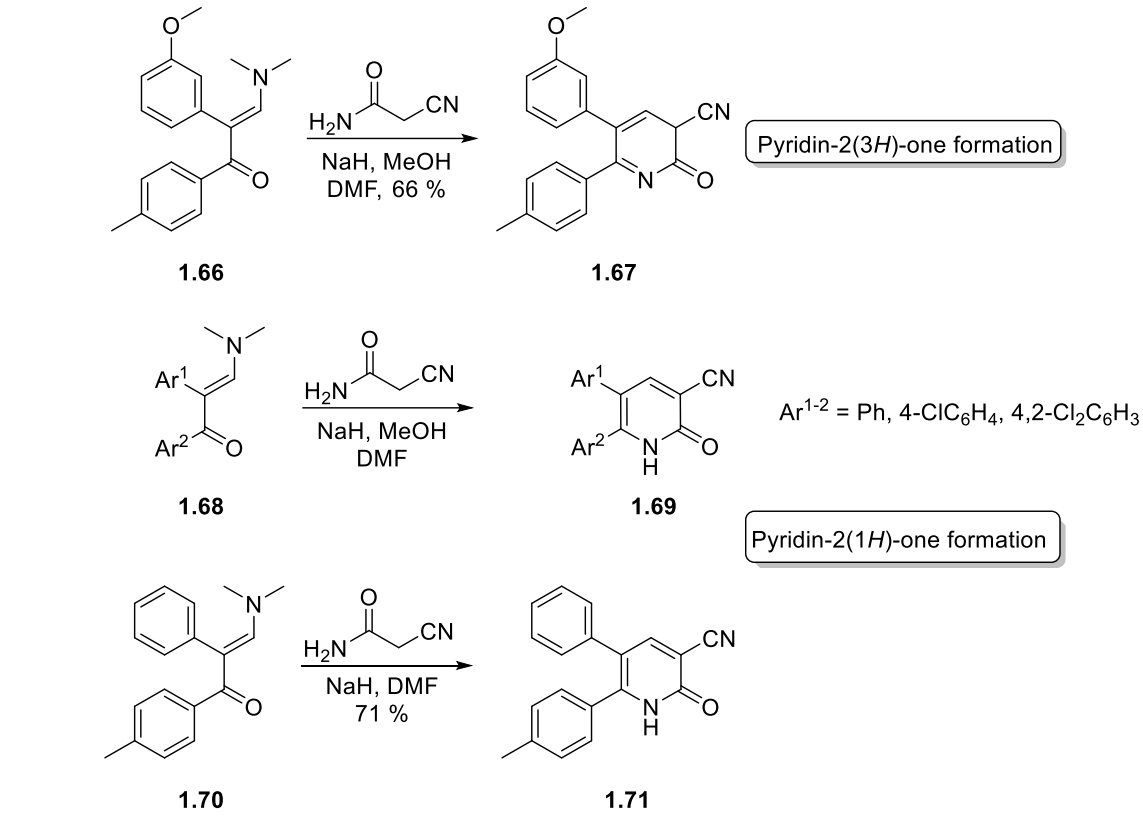

Scheme 1.18: Ring-closing of enaminones with 2-cyanoacetamide into a pyridine-2(3*H*)-one or a pyridine-2(1*H*)-one system

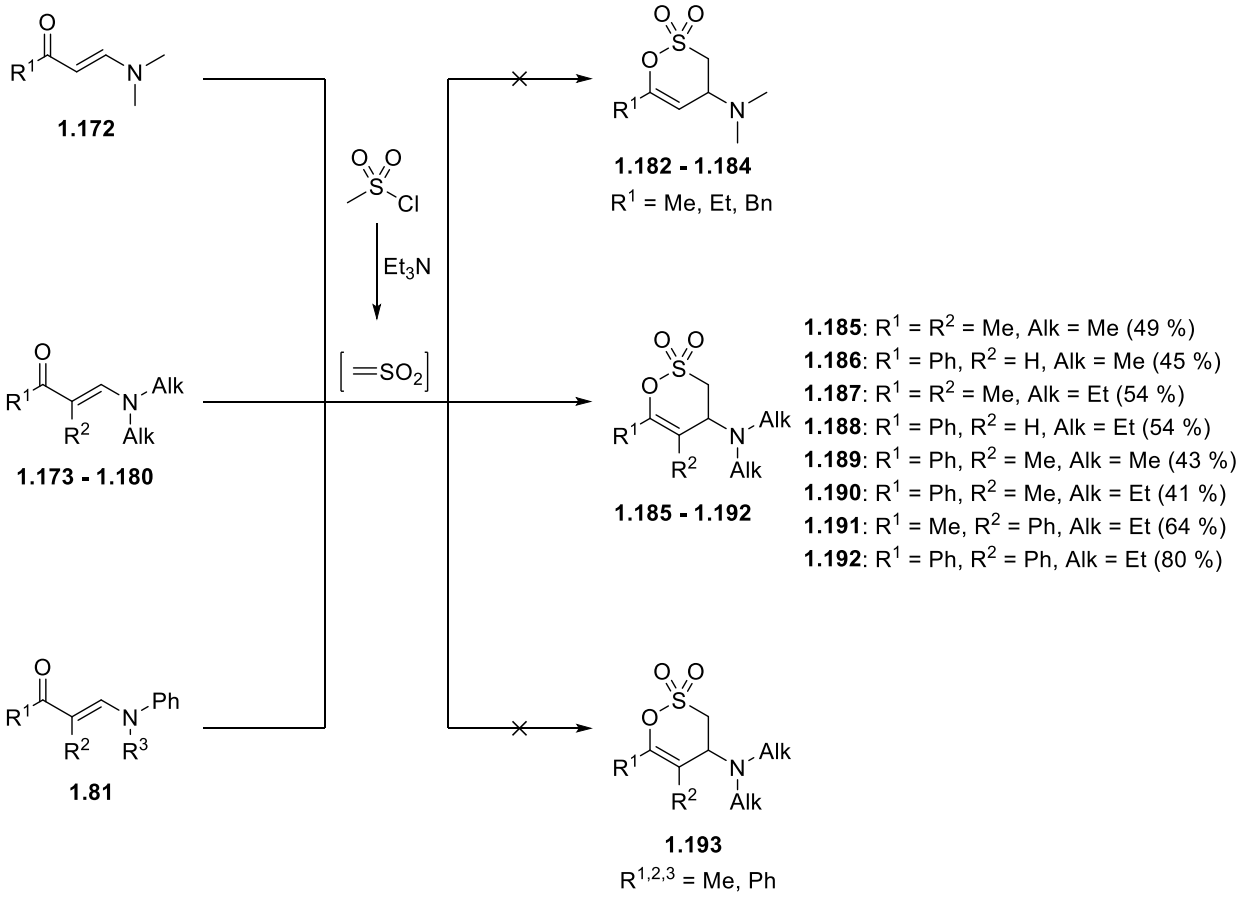

Scheme 1.19: Transformations of enaminoketones into sultone systems

The addition of ketene presented a point of further interest, as here the alkyl *N*-substituents opposed the heterocycle formation (attempted derivatives **1.97**), while enaminones with phenyl groups (**1.95**) proved to be beneficial for the reaction rate, with the exception of the morpholinyl analogues **1.96** which unexpectedly afforded the target compounds **1.99** (Scheme 1.20).[43]

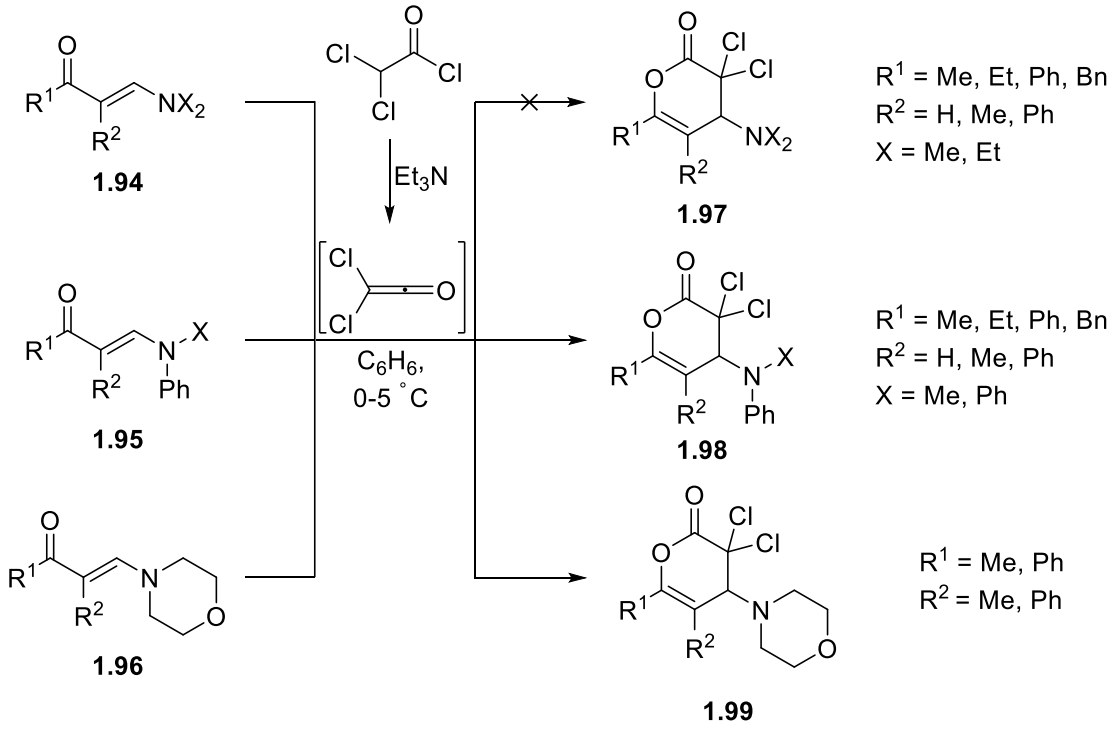

Scheme 1.20: Ketene additions to enaminoketone substrates

In one instance, Schenone *et al*., have also managed to serendipitously isolate the intermediate of one such ketene addition to enaminone **1.100**.[44] IR and NMR spectroscopic data led them to the conclusion that this zwitterion, **1.101**, has the structure shown below (Scheme 1.21). This finding was confirmed when the aforementioned compound afforded the lactone product **1.102** upon reflux in hexane. This result may indicate that these conversions proceed through a step-wise mechanism, although no such intermediate was obtained in the case of sulfene additions. In later chapters regarding the synthesis of 3,4-dihydro-1,2-oxathiine 2,2-dioxide analogues, the sulfene addition work by Schenone will be revisited in order to elaborate on the precepts of the formation of these compounds.

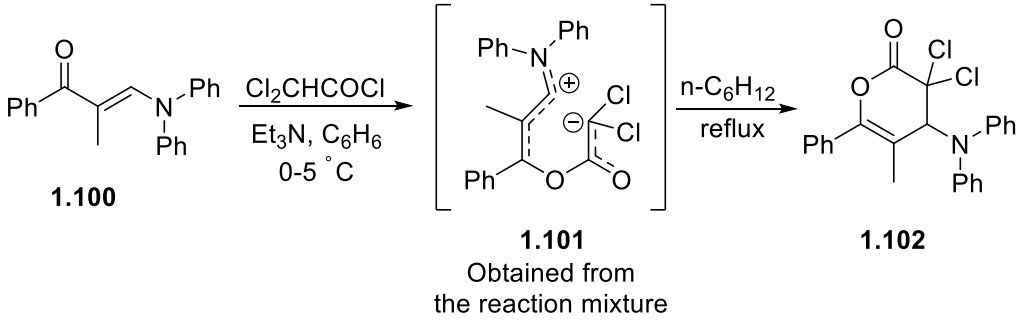

Scheme 1.21: Dipolar intermediate during a ketene addition

1.1.3 Sulfenes

1.1.3.1 General properties

The class of molecules described as *sulfenes* consists of the 2,2-dioxides of thiocarbonyl compounds, *i.e.* thioketones (thiones) **1.103** and thioaldehydes (thials) **1.104**, following the general molecular formula $R^1R^2C=SO_2$ (**1.106**). They belong to a wider group of sulfur derivatives of carbonyl compounds, along with sulfines (**1.105**), thiones (**1.103**) and thials (**1.104**) (Scheme 1.22)[45,46]. With regards to their name, the term "sulfenes" was first used by Wedekind and Schenk in 1911[46], as a reference to the already known ketenes ($R^1R^2C=C=O$, **1.107**), with respect to their structural similarity.

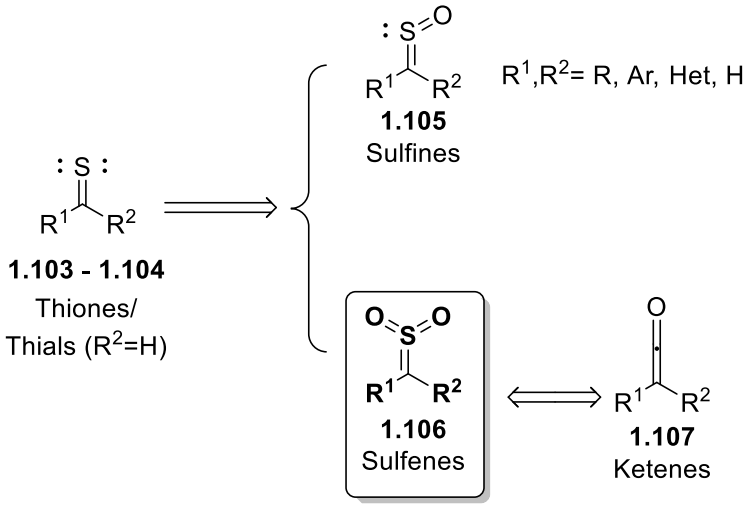

Scheme 1.22: Derivation of sulfenes and their reduced analogues, sulfines, from thiocarbonyl compounds

In spite of their reactivity, the crystal structure of a sulfene analogue (**1.108**), stabilised with quinuclidine *via* coordination, has been reported.[47] Comparing the bond angles of the sulfene centre reveals a trigonal-planar geometry for the olefinic C atom, along with a near trigonal-planar geometry for the adjacent S atom. Additionally, the length of the bond between the aforementioned atoms appear to be smaller than the one computed for the single bond between S2 and C1 (Figure 1.2a); these data suggest the presence of a double bond between C1 and S1, as well as a planar conformation for the sulfene unit, in accordance with their general structure in Scheme 1.22. Examination of the atomic charges of the same atoms in different sulfene analogues (**1.109** and **1.110**, Figure 1.2b) reveals a concentration of electron density towards the C atom, which can also be cemented theoretically.[48]

In contrast to a carbonyl compound where the bond is polarised due to the *O* atom, the sulfur atom is the one bearing a partial positive charge on a sulfene, seeing as it is placed between two electronegative *O* termini. This reversal in charge is established through resonance between the *S* and *O* atoms, stabilising the positive charge of the sulfur atom and establishing its electrophilic character (Scheme 1.23)[46]. Inevitably, the sp^2 carbon atom has nucleophilic potency, on account of its complimentary negative charge; this significant charge polarisation is the key element that dictates the chemical behaviour of these compounds.

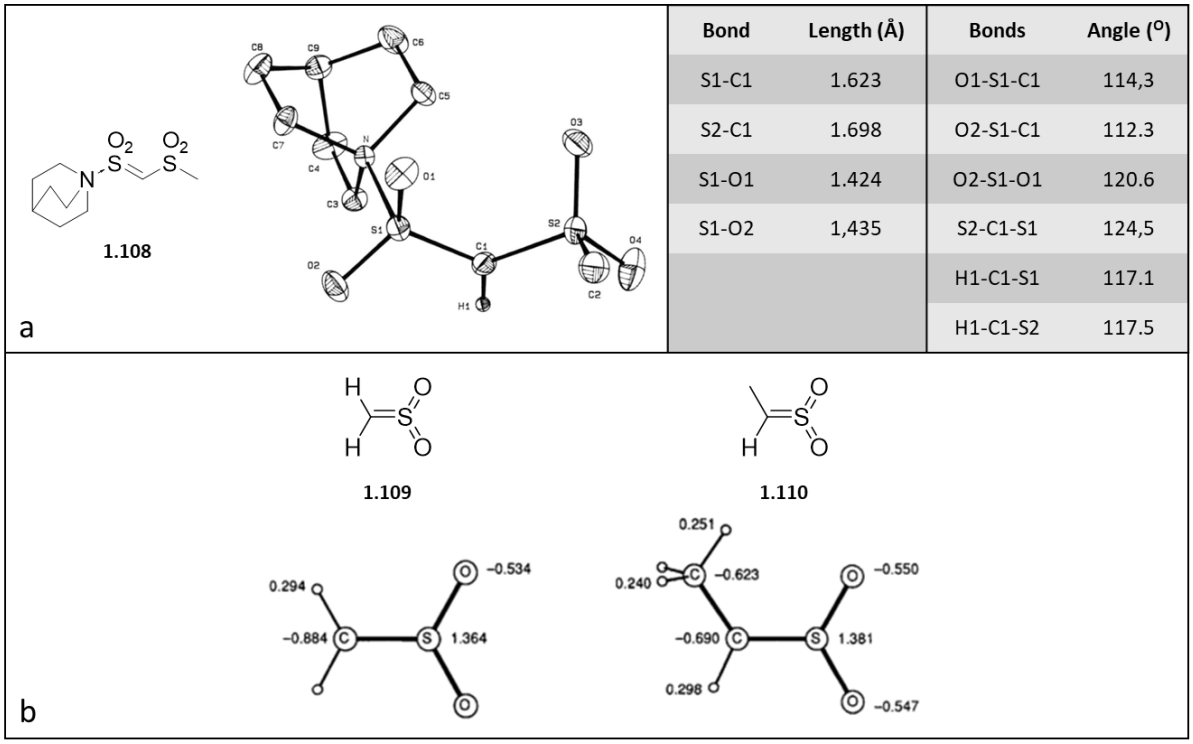

Bond	Length (Å)	Bonds	Angle (°)
S1-C1	1.623	O1-S1-C1	114,3
S2-C1	1.698	O2-S1-C1	112.3
S1-O1	1.424	O2-S1-O1	120.6
S1-O2	1,435	S2-C1-S1	124,5
		H1-C1-S1	117.1
		H1-C1-S2	117.5

Figure 1.2: a) ORTEP plot of the crystal structure of a stabilised sulfene derivative with bond lengths and angles of interest, b) Atomic charges calculated for sulfene and its methyl counterpart (Permissions applied for)[47,48]

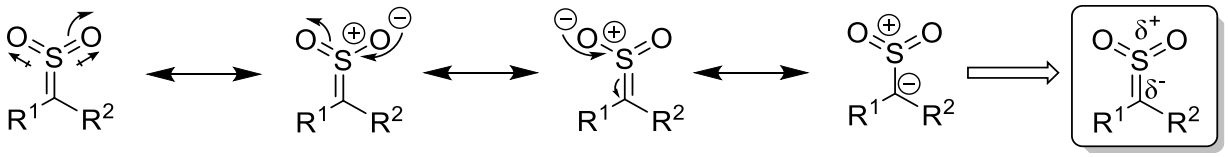

Scheme 1.23: Stabilisation of the sulfur positive charge through resonance forms

1.1.3.2 Generation of sulfenes

The most common precursors for the generation of sulfenes are the corresponding alkylsulfonyl chlorides ($R^1R^2CHSO_2Cl$) (**1.111**), which generate the sulfenes (**1.106**) upon treatment with a moderate base (*e.g.* trimethylamine) *via* elimination of HCl (Scheme 1.24)[45,46]. This is a representative example of the predominant strategy towards preparing sulfenes, involving the *in situ* "revelation" of these compounds from larger precursor molecules (**1.112**). The main problem that encumbers the preparation of these molecules is their low stability once formed, as they proceed to react with either themselves or their precursors towards 'dimerization' derivatives (**1.115** and **1.116**), as seen in the case of monosubstituted methanesulfonyl chlorides (**1.113**)[46,49] (Scheme 1.25). As predicted from scheme 1.25, the dimeric ionic species (**1.116**) can react further with sulfene monomers to yield a range of oligomers, thus further increasing the number of different by-products.

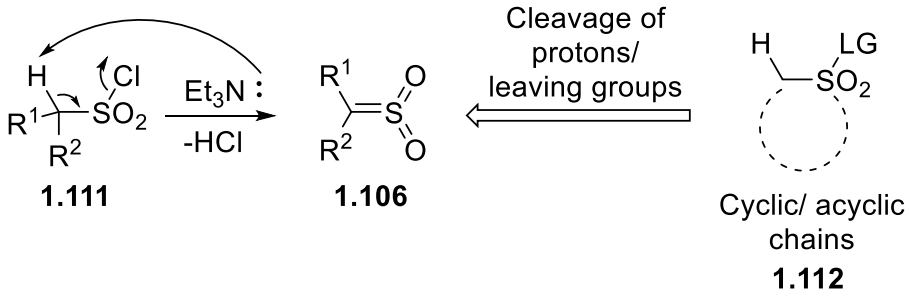

Scheme 1.24: Elimination of HCl on a sulfonyl chloride to afford the sulfene as part of a greater synthetic route niche

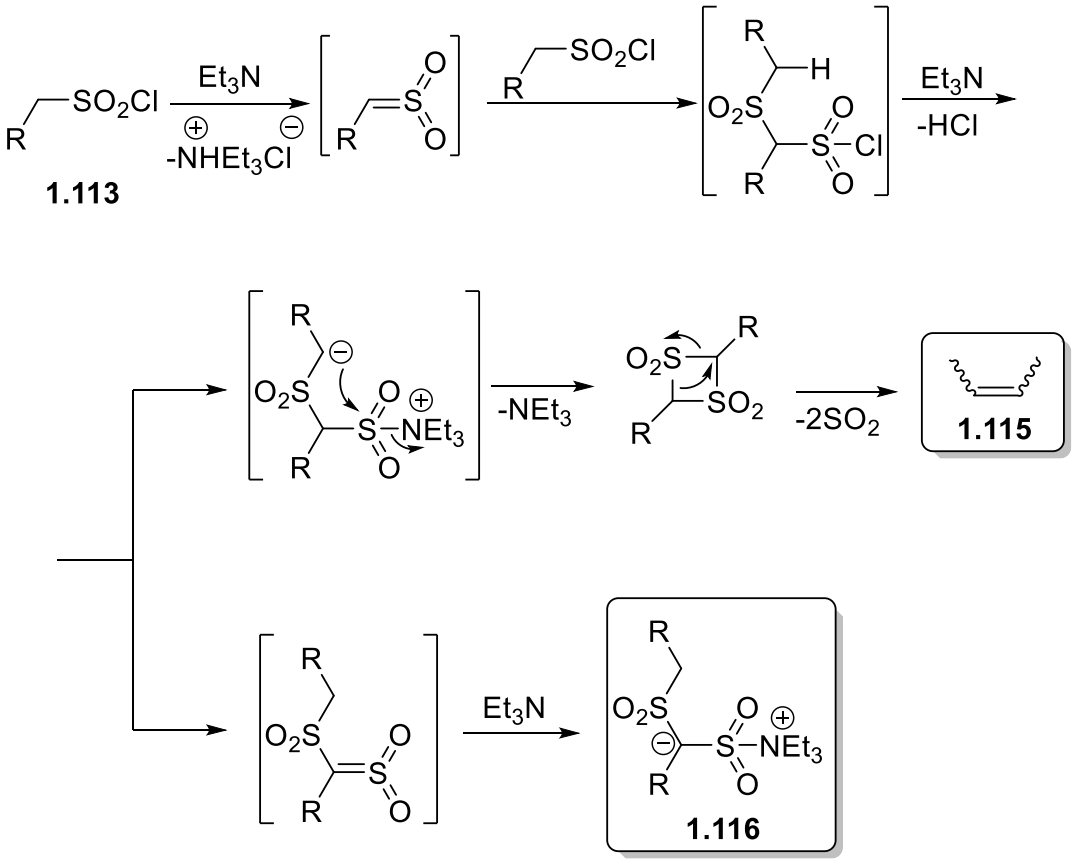

Scheme 1.25: Further transformations of nascent sulfenes towards different side-products

The unstable behaviour of sulfenes explains why the formation of these compounds is invariably combined with their immediate addition to receptor molecules that essentially "trap" the sulfenes *via* the formation of adducts that can be further developed, all while containing the 'reduced sulfene' as part of their structure. Most of the preparations shown below as indicative examples (Scheme 1.26) are performed in the presence of such trapping agents *in situ*.[50,51,52,53] The sulfene targets can be obtained by cyclic or acyclic precursors (**1.117** – **1.119**), which include but are not limited to sulfonyl chlorides, through various elimination reactions, as well as thermal or photochemical rearrangements. Notably, strong bases and reducing agents can bring about the sulfene formation when acting on less active substrates than sulfonyl chlorides, *i.e.* sulfonate esters (**1.120**) and sulfonic acids (**1.121**).[54,55]

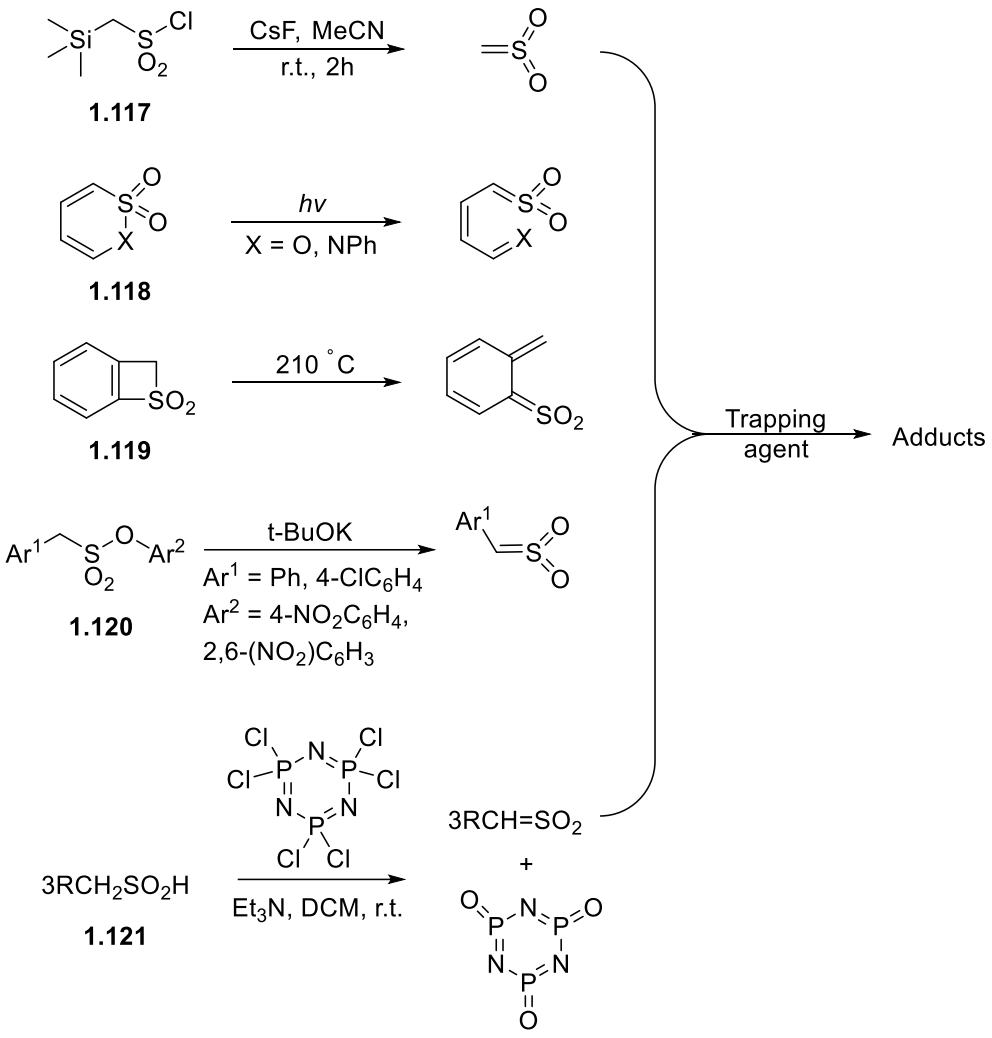

Scheme 1.26: Representative examples of sulfene formation reactions

It is evident from the findings above (Scheme 1.26) that the precursor of a sulfene is required to be structurally similar to the prepared sulfene, since the prevalent formation mechanism involves the cleavage of a labile proton and a leaving group. An iteration that breaks away from this norm can be seen in the work by Smart and Middleton[56], where a 1,3-dithietane 1,1,-dioxide derivative (**1.122**) is processed with tris-(dimethylamino)-sulfonium trimethyldifluorosiliconate (**1.123**) to afford the stable carbanion **1.124**, which in turn can be converted to di-trifluoromethyl-sulfene (**1.125**) *in situ* using silicon tetrafluorate (Scheme 1.27).

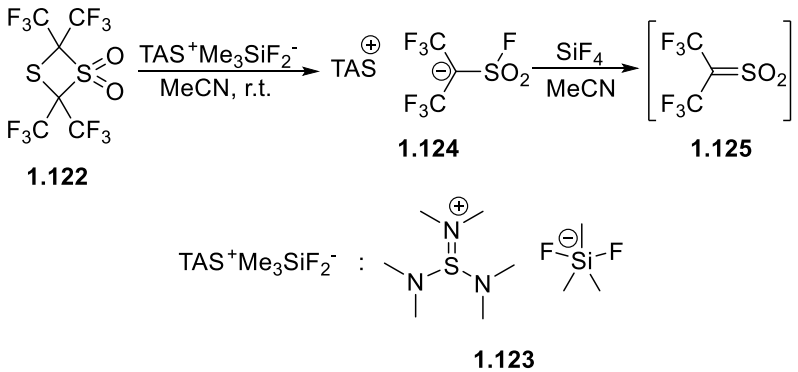

Scheme 1.27: Preparation of a di-substituted sulfene from a dithietane precursor

1.1.3.3 Reaction overview

Trapping the sulfenes *in situ* with receptor compounds constitutes the basic concept that underlies the range of sulfene reactions. Different trapping agents can be used on each occasion to afford predominantly heterocyclic adducts.

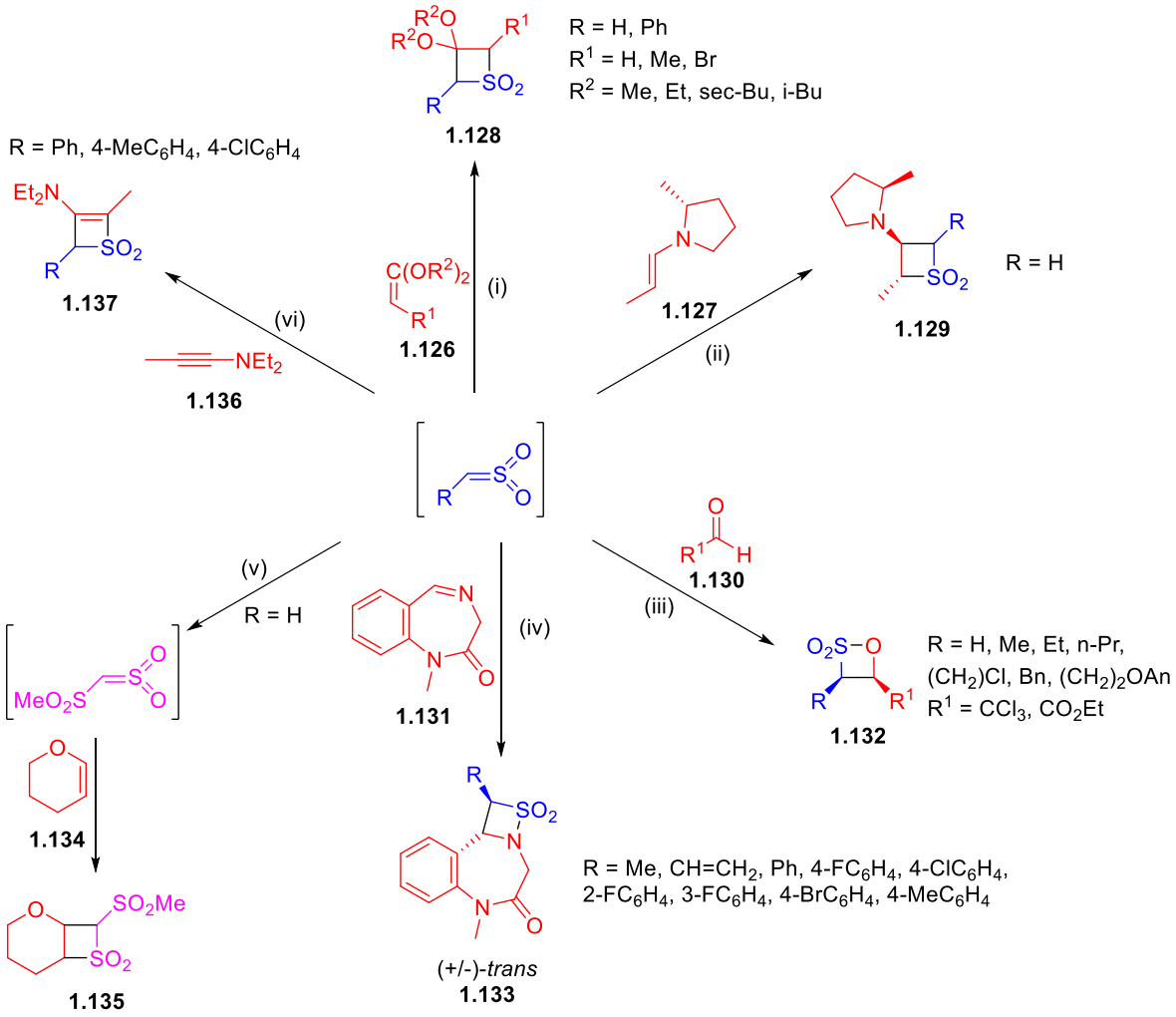

Reagents & Conditions: (i) Et_2O, o/n, (ii) 1. Et_2O, r.t., 2. $HCl_{(g)}$,H_2O, 0 °C, (iii) $(DHQ)_2PYR$ (9%-mol), $Bi(OTf)_3$ or $In(OTf)_3$ (36%-mol), PMP (1.32 eq), DCM, -15 °C, (iv) THF, r.t., 48h, 10 - 44 %, (v) Et_3N, MeCN, -40 °C, (vi) t-BuOK,THF, 0 °C, 72 - 83 %

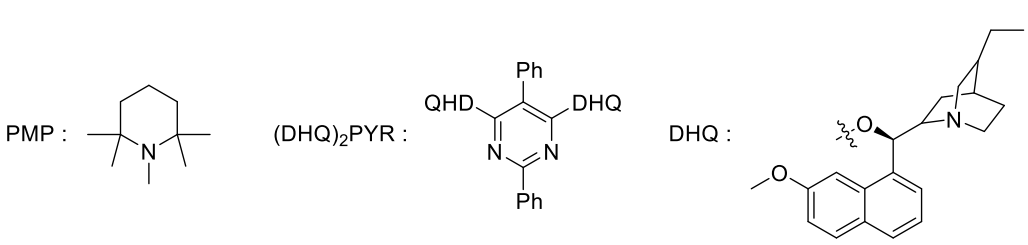

Scheme 1.28: Spectrum of sulfene additions to various compounds aiming at 4-membered heterocycles

A significant amount of research has been undertaken regarding [2+2] additions to sulfenes (Scheme 1.28); vinyl acetals (**1.126**) and enamines (**1.127**) bind them in thietane 1,1-dioxide systems (**1.128** – **1.129**)[57,58,59], while aldehydes (**1.130**) and imines (**1.131**) act in a similar manner towards β-sultones and

β-sultams respectively (**1.132** – **1.133**)[60]. It has also been reported that, in the case of addition to aldehydes, such transformations can occur stereoselectively *via* use of an appropriate catalyst.[61] Moreover, treatment with 3,4-dihydro-2*H*-pyran (**1.134**), a vinyl ether, can yield the fused thietane 1,1-dioxide **1.135**, although a dimerization of the sulfene precedes this addition, thus broadening the range of possible products from this addition.[46] Should an ynamine (**1.136**) be used instead of an enamine, the obtained system is a thiete 1,1-dioxide (**1.137**).[54]

Specific research on the use of dienes along with a sulfene analogue has been undertaken by Smart and Middleton[56], whose work was also discussed in the previous section (**1.1.3.2**). The derivative **1.125** (Scheme 1.27) can effectively form 4-membered thietane 1,1-dioxide ring adducts (**1.138** – **1.140**) with butadiene analogues. These additions were found to occur in a stereoselective manner, which appears to be influenced by the *trans*/*cis* geometry of the participating alkene (Scheme 1.29).

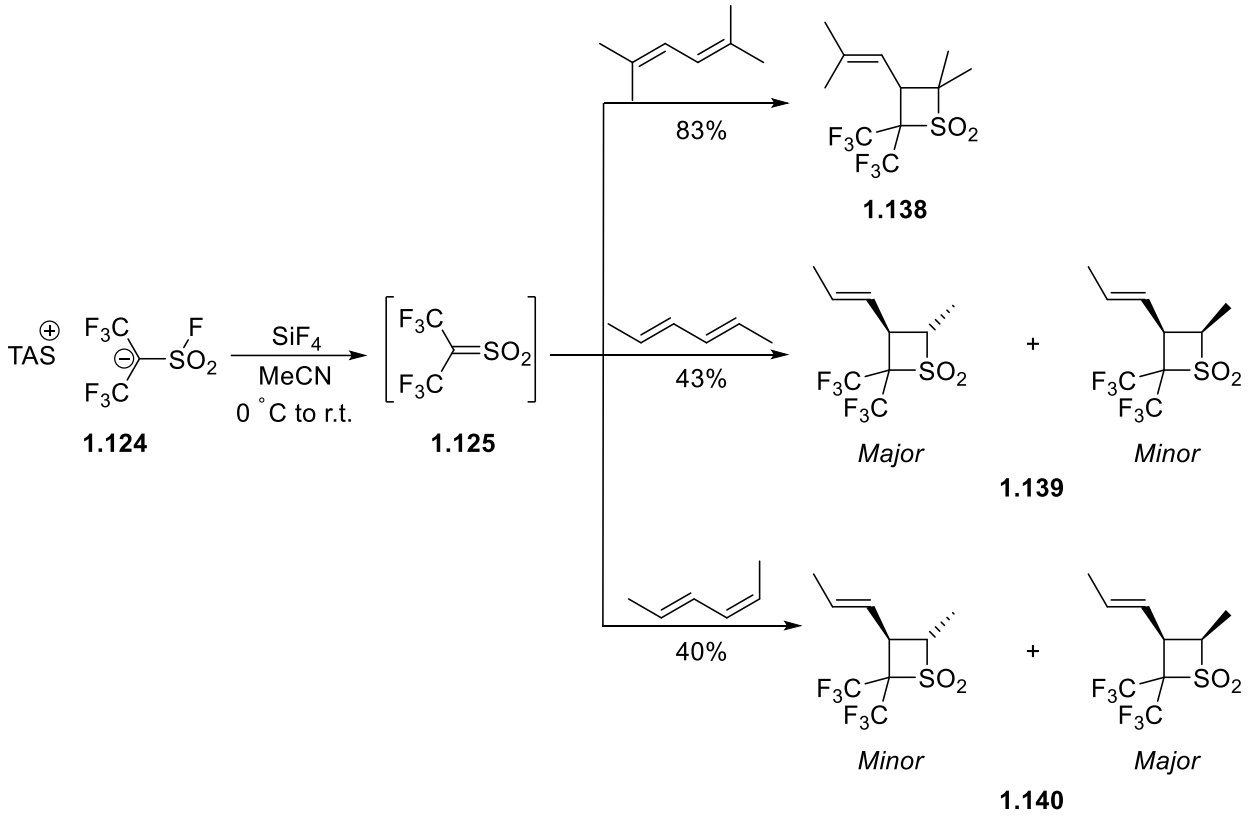

Scheme 1.29: Reactions of di-trifluoromethyl-sulfene with s-*trans* dienes

It should be noted that the relative efficiency of a sulfene to react with olefinic compounds towards 4-membered rings is a very useful synthetic tool for preparing heterocyclic systems with high bond strain that are difficult to obtain otherwise.

Yu, Yang and Xu[62] have provided further insight on the mechanism of such additions by examining the addition of mesylsulfene (**1.141**) to imine systems (**1.142**). Aiming at establishing a mechanistic explanation of the temperature-dependent formation of either a 4- or a 6-membered ring adduct, they concluded that a higher temperature allows for conrotatory movement of the 4-membered intermediate **1.143**, which leads to annulation into a 4-membered β-sultam (**1.144**), whereas low temperatures will mitigate the reactivity of the intermediate and effect the addition of a second imine molecule towards a 6-membered, sulfa-Staudinger product (**1.145**) (Scheme 1.30).

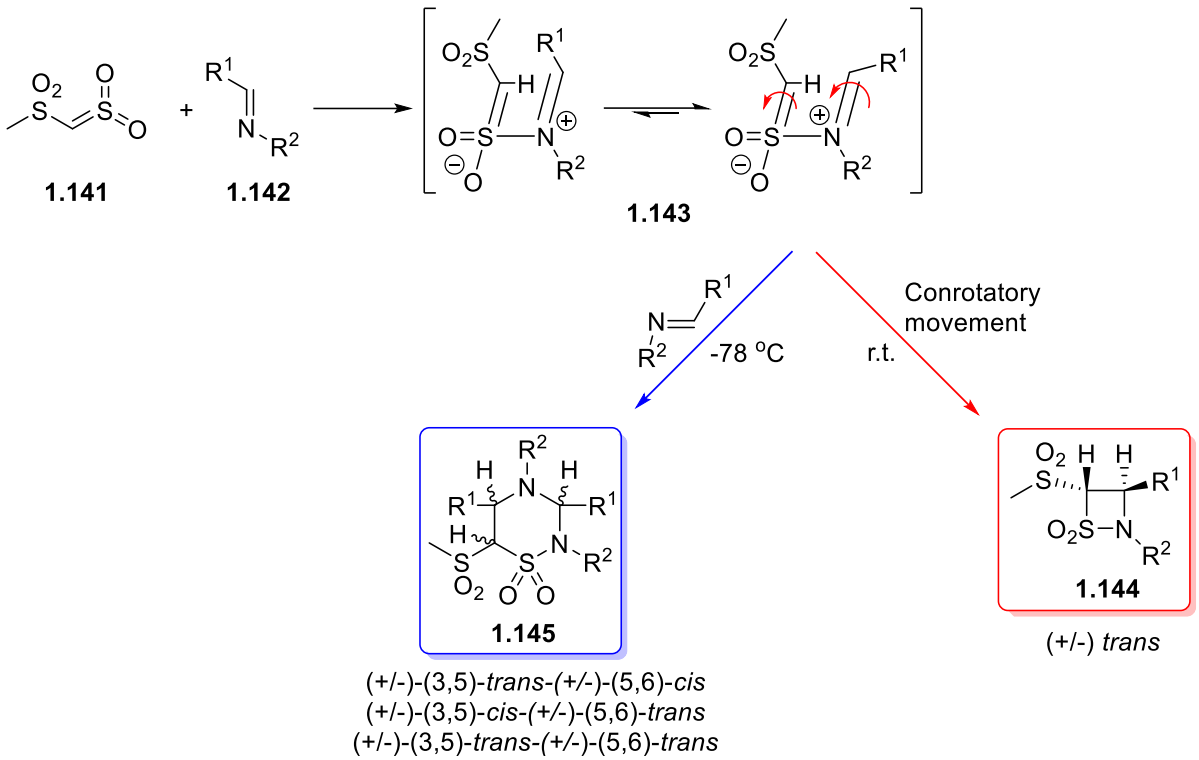

Scheme 1.30: Temperature-dependence for the formation selectivity between a β-sultam and a 4-aza-sultam product

Similar behaviour to that described earlier (Scheme 1.28) would be expected of sulfenes when treated with diene-like molecules. Indeed, a variety of starting olefin materials with consecutive double bonds can undergo hetero Diels-Alder additions with sulfene analogues and yield the expected 6-membered heterocycles (Scheme 1.31). Interestingly, specific ketene dimethylacetals have been found to interact with sulfene in different fashions, affording either the 1,2-oxathiine 2,2-dioxide **1.147**, in the case of the phenyl analogue **1.146**, or a thiopyranone 1,1-dioxide adduct (**1.149**), when the acetyl derivative **1.148** is used.[57] It can be suggested that the reactivity of the α-protons on the acetyl enone is the driving force behind the thiopyran formation, hinting that any other reactive species on that terminus will have priority over the carbonyl *O* atom. The high proclivity of sulfene towards additions is further established in the case of the thiadiazepine 1,1-dioxide derivatives **1.150**, where the cycloaddition proceeds with disruption of the aromaticity of the thiazole ring.[63] Enaminones (**1.73** – **1.80**) have been also reported to afford 1,2-oxathiine 2,2-dioxides (**1.85** – **1.92**) upon reacting with sulfenes, as discussed in section **1.1.2.3**, albeit having limitations on the substitution of the starting materials.[41,42,43,44] The previously mentioned bis-trifluoromethyl sulfene (**1.125**) is also met with interest in this niche, as it can produce thiopyran systems (**1.151**), in addition to the 4-membered adducts shown above (Scheme 1.29), by using dienes with the appropriate conformation and substitution patterns.[56]

Concluding this overview of sulfene reactivity, two cases of acyclic products obtained from sulfene reactions are presented below (Scheme 1.32).[46,57] During the first case, the sulfene **1.152** is initially attacked by an electron-rich olefin (**1.153**) and upon subsequent protonation of the α-carbon, a tetrasubstituted alkene (**1.154**) is formed. In the latter case, a [2+2] addition to an enamine (**1.155**) can bring forth a 4-membered intermediate (**1.156**), which isomerises to the sulfonenamines **1.157** and **1.158**.

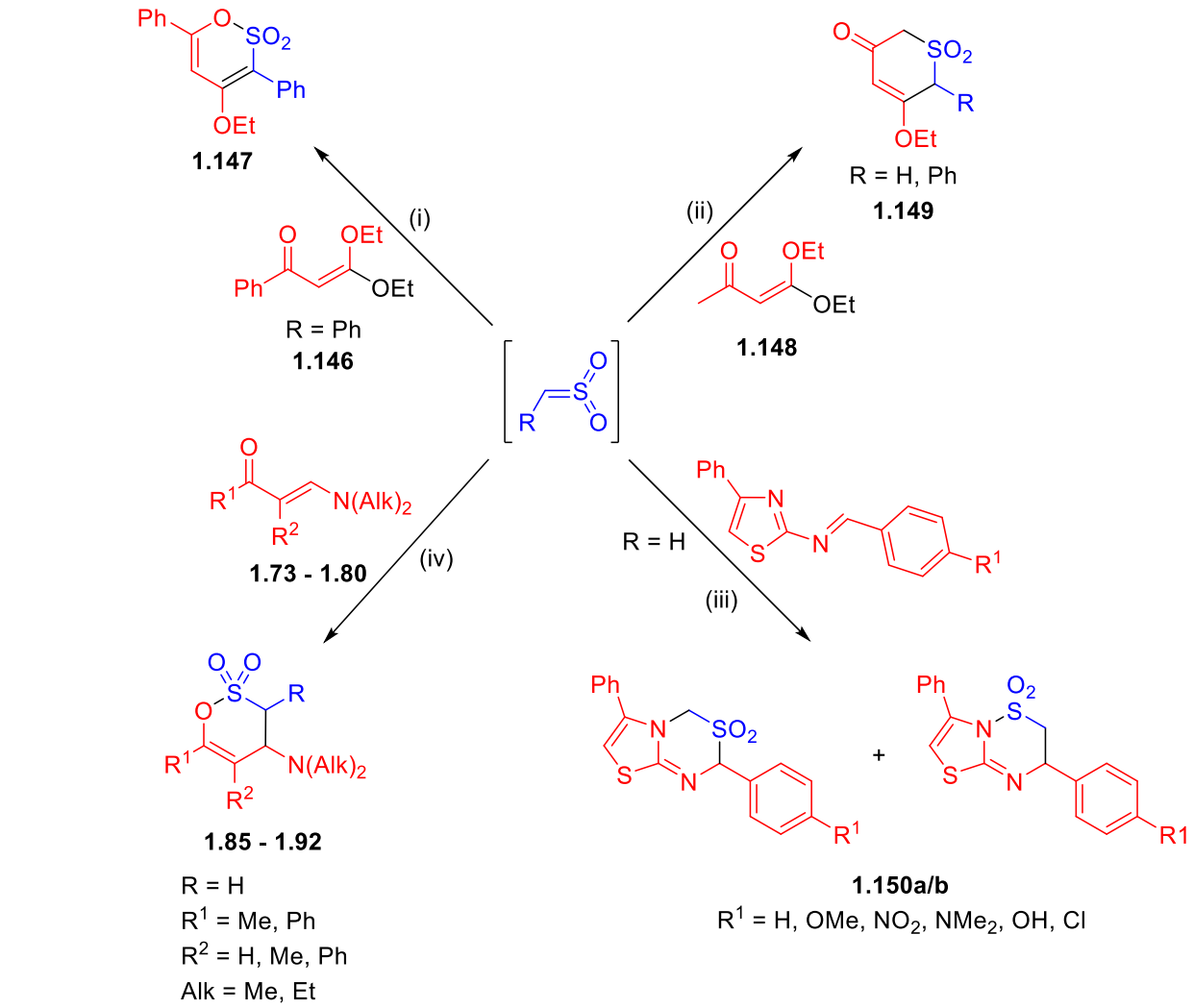

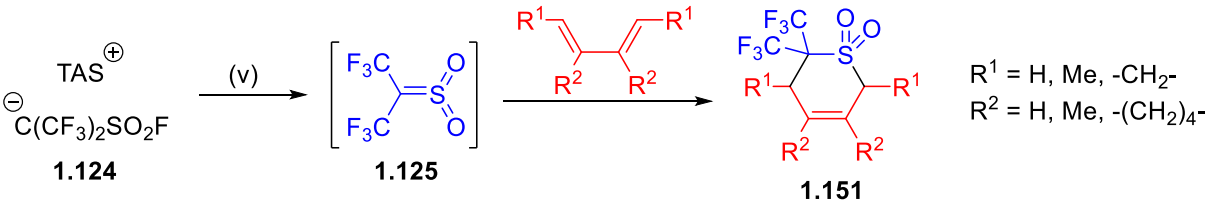

Reagents & conditions: (i) Me_3N, THF/Et_2O, 0 °C to r.t., 20 %, (ii) Et_3N, Et_2O or C_6H_6, 0 °C, 16 - 41 %, (iii) Et_3N, 1,4-Dioxane, 0-5 °C, 3-4 h, 53 - 70 % (**1.150a**)/ 17 - 29 % (**1.150b**), (iv) Et_3N, THF or C_6H_6, 0 °C or r.t. (v) SiF_4, MeCN, 0 °C to r.t., 41 - 81 %,

Scheme 1.31: 6-Membered heterocyclic systems as products of sulfene additions

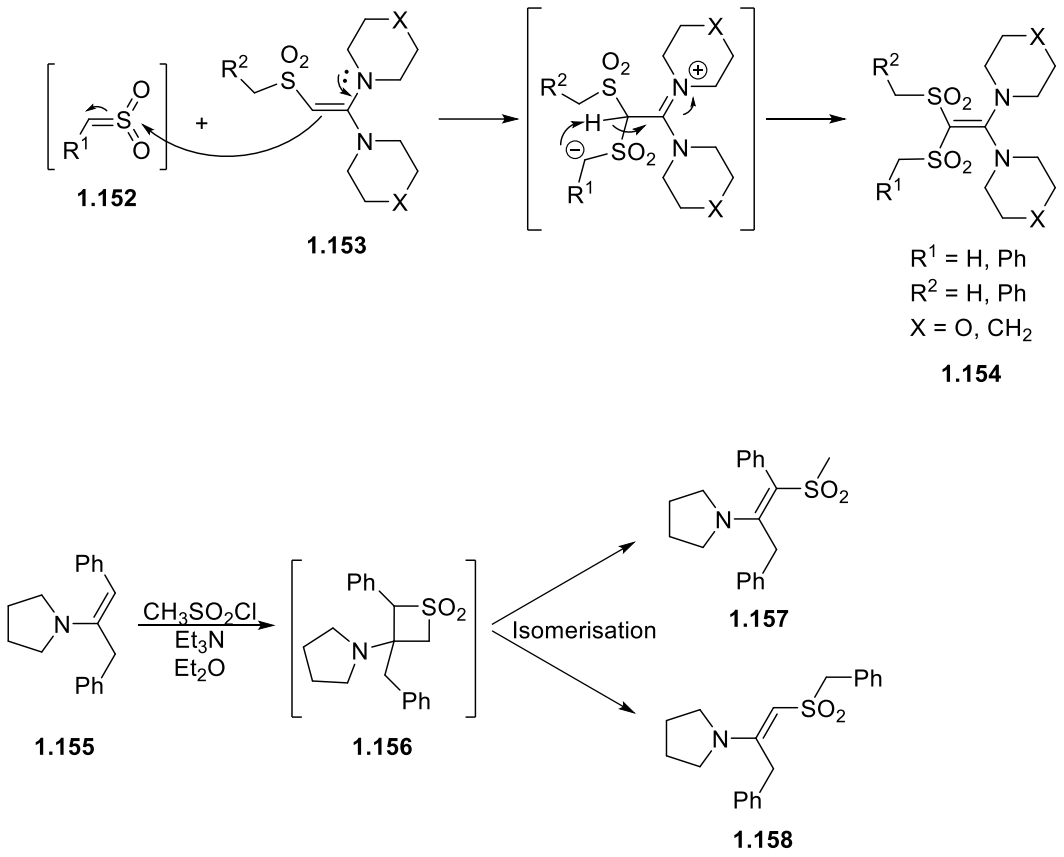

Scheme 1.32: Examples of sulfene additions yielding acyclic adducts

1.2. 1,2-Oxathiine 2,2-dioxide ring systems

1.2.1 1,2-Oxathiine 2,2-dioxides

1.2.1.1 General properties

These relatively unexplored ring systems are a sub-group of the heterocyclic family of molecules collectively called *1,2-oxathiines* and can be essentially characterised as cyclic δ-sultone systems, wherein a 4 carbon chain is tethered to both ends of a sultone (-O-SO_2-) moiety (Scheme 1.33).[64] The first group of 1,2-oxathiine 2,2-dioxide systems that will be discussed consists of the fully unsaturated analogues which possess two neighbouring double bonds that constitute a butadiene chain. It differs from the other 1,2-oxathiine systems presented in scheme 1.33 in the absence of aliphatic character, which has a profound effect in the structure and chemical behaviour of these species.

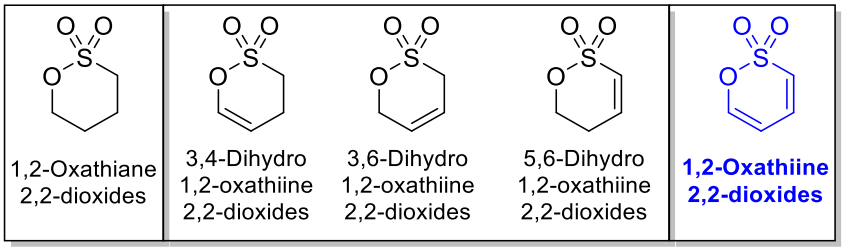

Scheme 1.33: 1,2-Oxathiine 2,2-dioxides as the 5th group of 6-membered ring sultones

The fully unsaturated carbon chain on this analogue is a strong indicator of a planar conformation for these molecules, owing to the stability attained through conjugation of the adjacent π orbitals. Even though the carbon backbone chain has been confirmed to be planar by crystallographic data of derivative **1.159** obtained by Barnett *et al.*[65] (Figure 1.3), as well as by the crystal structures of analogues **1.160** and **1.161**,[66,67] it is evident that the 6-membered ring system is not planar, with the SO_2 moiety escaping the plane of C3-C4-C5-C5-O, while there are distinct bond length differences between the single and the two double bonds. These findings suggest that, although 1,2-oxathiine 2,2-dioxides are 6-membered ring systems with 6 π electrons, they manifest no aromaticity.

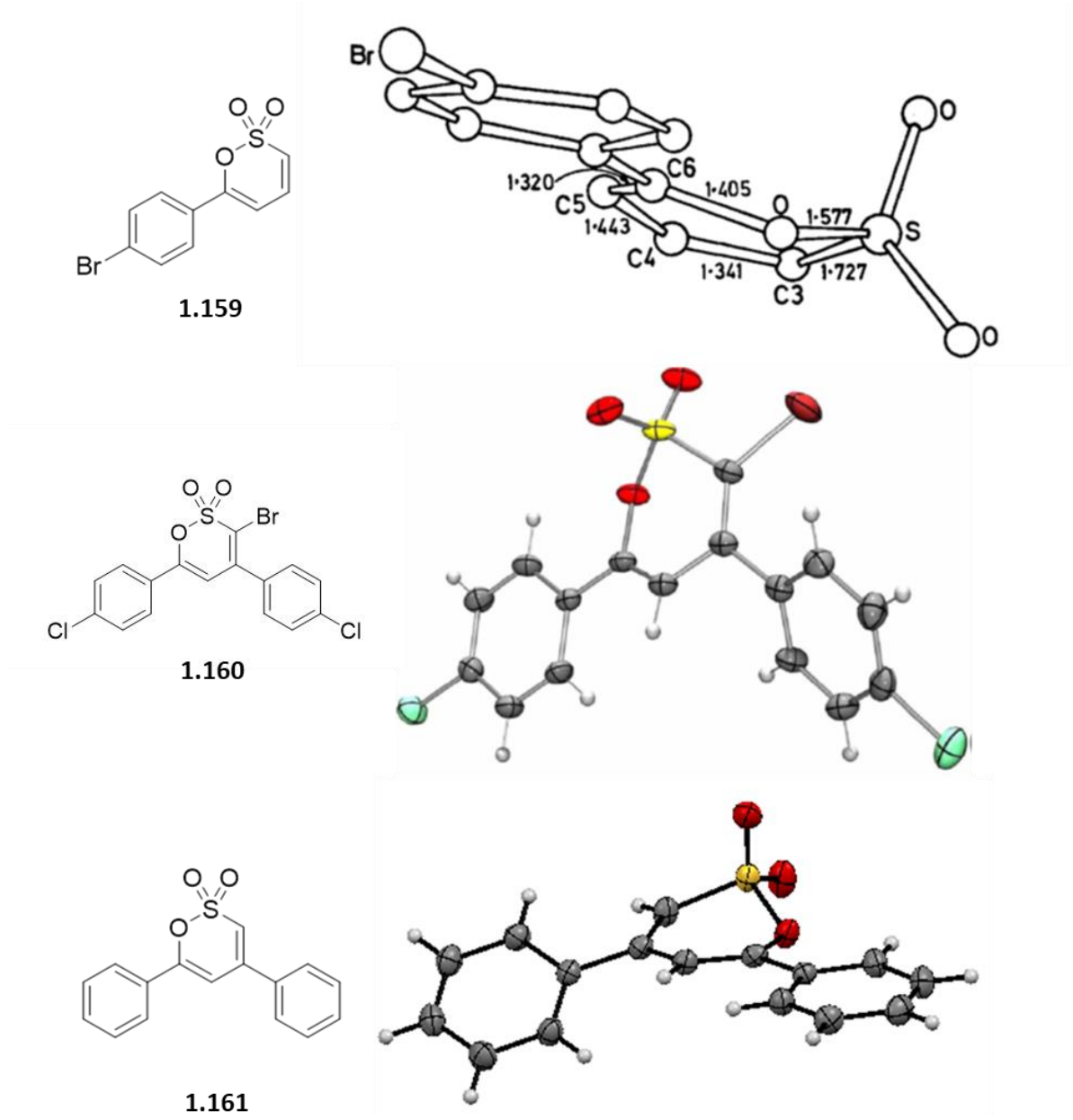

Figure 1.3: Crystal structures of 1,2-oxathiine 2,2-dioxide analogues, highlighting their planar but non-aromatic structure (Permissions applied for)

The presence of two adjacent double bonds on these analogues indicates that they may possess diene properties, in contrast to other, mono-unsaturated analogues which could pose as dienophiles. This can effectively create a versatile spectrum of potential Diels-Alder reaction strategies, depending on the type of analogue that is used as a starting material. Furthermore, the SO_3 unit constitutes another important

factor that determines their behaviour by polarising bonds and positions, thus giving rise to specific reactive sites on the ring.

1.2.1.2 Synthetic routes

Historically, the unsaturated 1,2-oxathiine systems were first prepared by Morel and Verkade[68], whose work regards processing α,β- or β,γ- unsaturated ketones (**1.162**) with concentrated sulfuric acid in acetic anhydride. The conversion of various substrates was met with moderate to good yields and provided the first small library of 1,2-oxathiine 2,2-dioxide derivatives (**1.163**, Scheme 1.34).

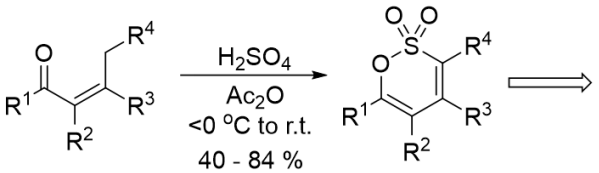

R^1	R^2	R^3	R^4	Yield (%)
Me	H	Me	H	40
Et	H	Me	H	43
t-Bu	H	Me	H	60
Me	H	Ph	H	40
Ph	H	Me	H	84
Me	Me	Me	H	54
Me	H	Me	Me	41

Scheme 1.34: Conversion of unsaturated ketones to the corresponding 1,2-oxathiine 2,2-dioxides

Parallel to the original Morel and Verkade synthesis of δ-sultones, a variation of this reaction using chlorosulfonic acid instead of sulfuric acid brought about the same result with a slightly improved yield (41% over 40% by Morel and Verkade[68]), as reported by Eastman and Gallup[69]. Although other enone substrates were tested, only mesityl oxide **1.164** was found to react cleanly to afford the heterocyclic target **1.165** (Scheme 1.35).

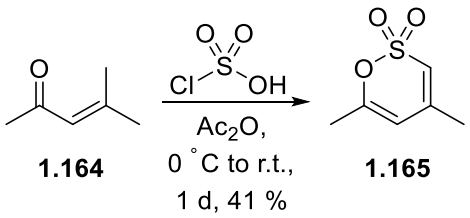

Scheme 1.35: Chlorosulfonic acid as an alternative reagent for the formation of the dimethyl unsaturated analogue

After these initial explorations, different rationales were sought out towards unsaturated analogues with novel substitution patterns (Scheme 1.36). Rad-Moghadam *et al*. have presented several pieces of research on the subject, where a task specific ionic liquid, such as methylsulfonylimidazolium triflate hydrochloride ([MSIm]TfO·HCl), is utilised to effect the sulfonylation and concomitant ring-closing of the starting materials **1.166** and **1.168** into 1,2-oxathiine products comprising of two equivalents of acetophenone (**1.167** and **1.169**).[70,71,72] An interesting aspect of the reaction is that the presence of a solvent is detrimental to the yield and that the best results are obtained when the reagents are mixed neat. Moreover, albeit producing 1,2-oxathiine systems in fairly good yields, the scope of derivatives is limited to patterns of identical substituents exclusively on the 4- and 6- positions of the 6-membered ring. In one iteration[73], the presence of a chlorosulfonyl moiety on the ionic moiety leads to the sulfonyl chloride derivatives of the foregoing dimerisation products (**1.171**).

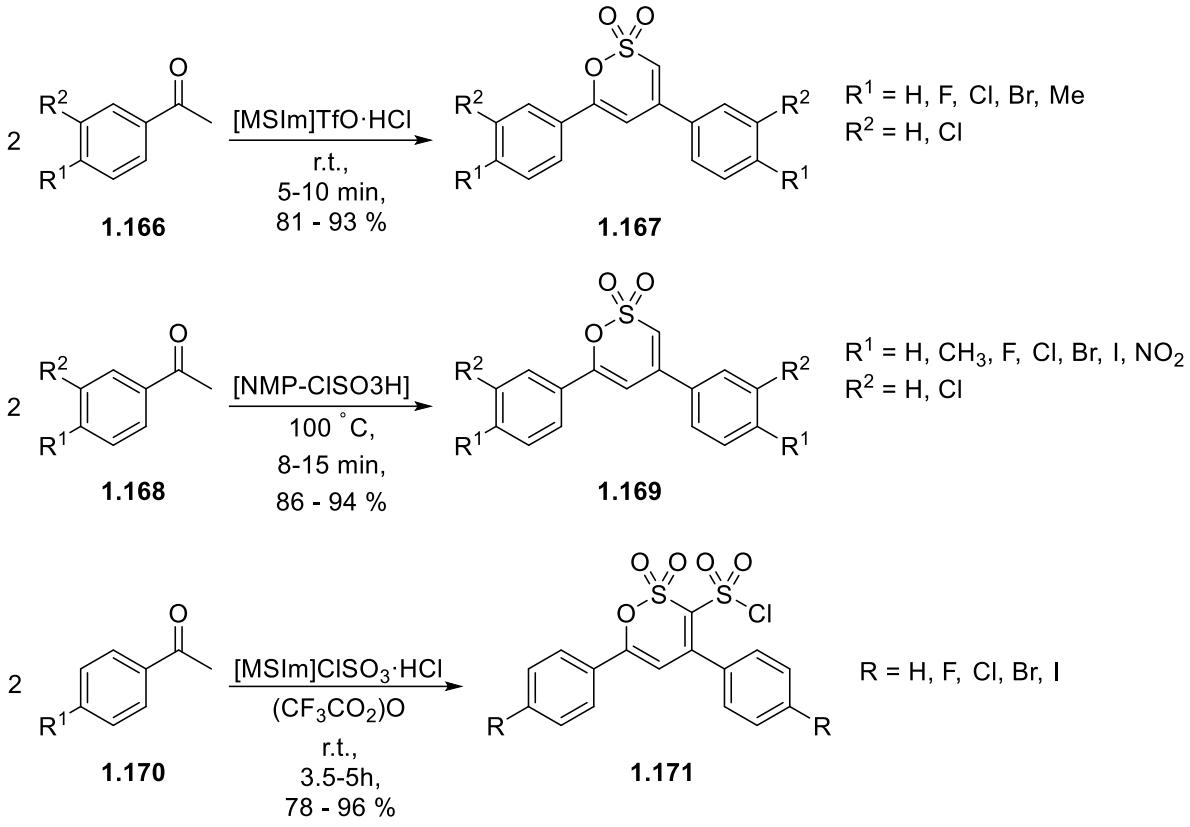

Scheme 1.36: Dimerisation/sulfonylation of substituted acetophenones with ionic liquids to afford 4,6-aryl 1,2-oxathiine systems

The strategy of dimerising/sulfonylating an aryl precursor molecule was further explored by Gaitzsch *et al.*,[66] whose work presents a different route towards 4,6-diaryl 1,2-oxathiine 2,2-dioxides. In this approach, a terminal arylalkyne (**1.172**) is reacted with two different sources of sulfur trioxide to yield the desired heterocyclic system (**1.173**, Scheme 1.37).

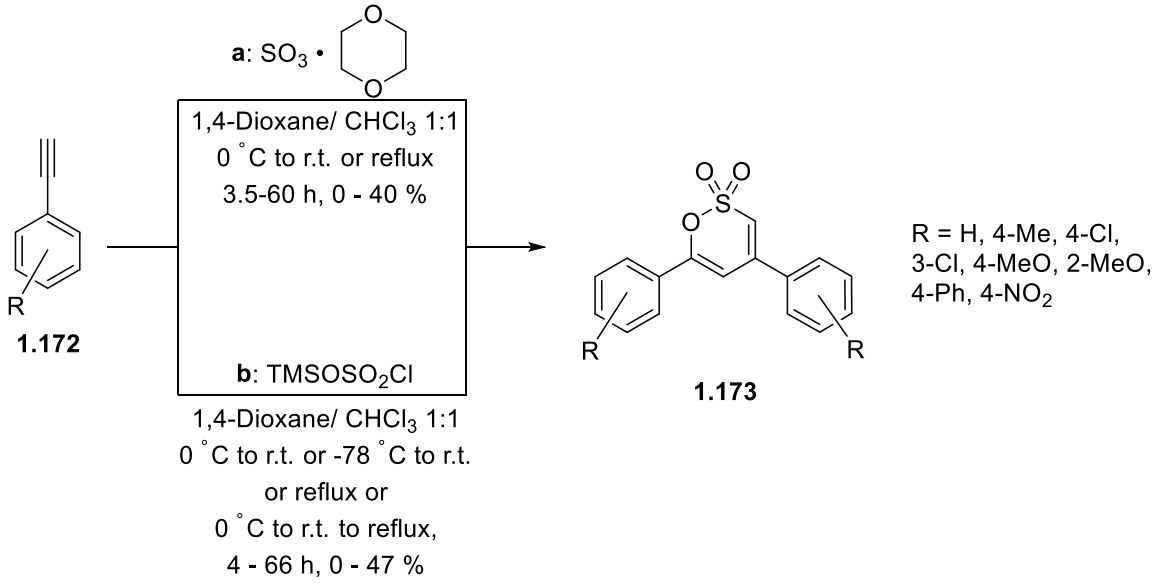

Scheme 1.37: Sulfonylating conditions prompting consequent dimerisation of terminal alkynes into 4,6-aryl-1,2-oxathiine 2,2-dioxides

The yields range from low to moderate due to a proclivity of the activated starting alkynes for side-reactions, while deactivated substrates failed to afford a 1,2-oxathiine product. A small library of derivatives was nonetheless obtained, allowing the reaction to be thoroughly explored.

An unusual but interesting route towards the 4,6-dimethyl derivative of the unsaturated analogue has also been reported by Heilmann *et al.*[73] Specifically, heating a solution 2-acrylamido-2-methylpropanesulfonic acid (**1.174**) in acetic anhydride causes a cascade of rearrangements and additions, as well as a retro-Ritter cleavage, which eventually yields the sultone heterocycle **1.165** *via* the suggested mechanism shown below (Scheme 1.38). This route constitutes one of the two cases of an unsaturated 1,2-oxathiine 2,2-dioxide being serendipitously synthesised.

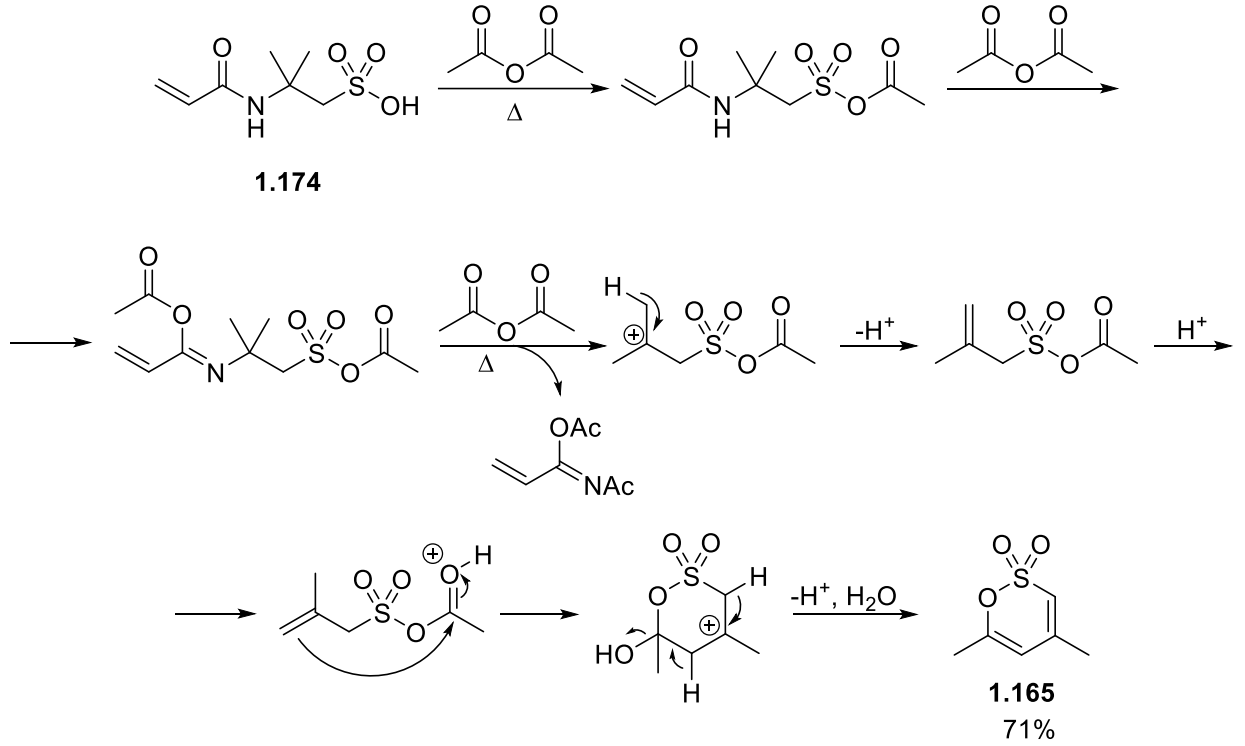

Scheme 1.38: Unexpected formation of the 4,6-dimethyl unsaturated analogue from sulfonic acid precursor

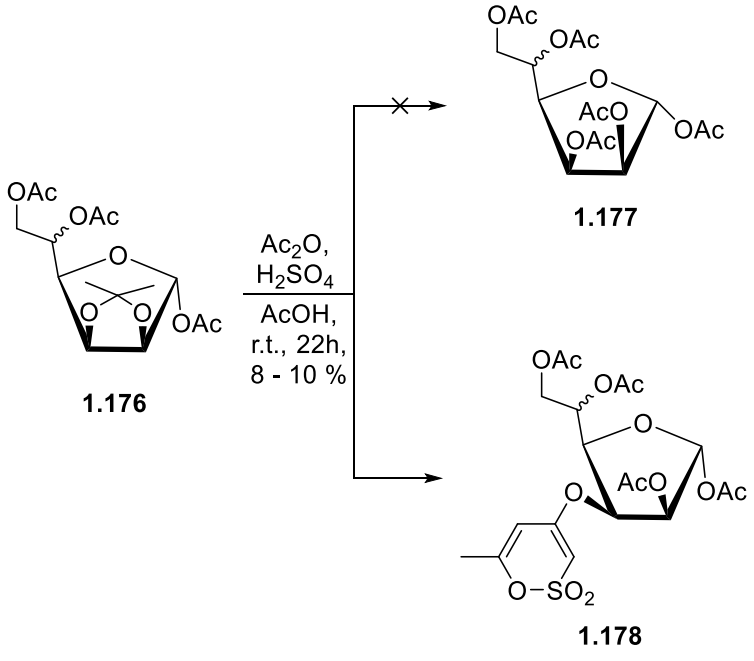

Scheme 1.39: Second case of serendipitous 1,2-oxathiine 2,2-dioxide formation

The second incident of accidental 1,2-oxathiine 2,2-dioxide formation was reported by Craig and Stevens[74], who produced a furanosyl derivative of the heterocycle (**1.178**) in their effort to deprotect the acetal protection group on a furanose ring (**1.176**). Instead of the expected penta-acetate product **1.177**, they obtained its 1,2-oxathiine-substituted counterpart in low yields (Scheme 1.39).
Initially touched upon in section **1.1.3.3**, the hetero Diels-Alder iteration between a ketene acetal (**1.146**) and a sulfene has been explored by Truce *et al.*[57]. The 3,4-dihydro-1,2-oxathiine 2,2-dioxide **1.179** that results from the sulfene addition losses an EtOH fragment *via* a subsequent elimination and is isolated as the 4-ethoxy-3,6-diphenyl-1,2-oxathiine derivative **1.147** (Scheme 1.40).

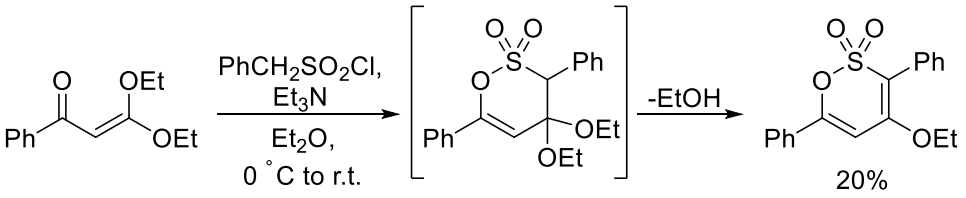

Scheme 1.40: Addition of a sulfene to a ketene acetal, followed by elimination of EtOH

1.2.1.3 Reactions with 1,2-oxathiine 2,2-dioxides

Of all the reactions that have been reported for these unsaturated systems, the most exhaustively explored in the literature is the substitution of the *O* atom of the 6-membered ring with a *N* atom and the formation of a sultam in the place of the initial sultone. Various research groups have carried out this transformation with different substituted amines and varying conditions, thus proving the applicability of the reaction towards a broad range of sultam derivatives.
Zeid, Ismail and Helferich[75,76] used the 4,6-dimethyl unsaturated analogue (**1.165**) as a starting material, which was processed with various substituted anilines to create a small library of sultam heterocycles with aryl substituents (**1.180**, Scheme 1.41).

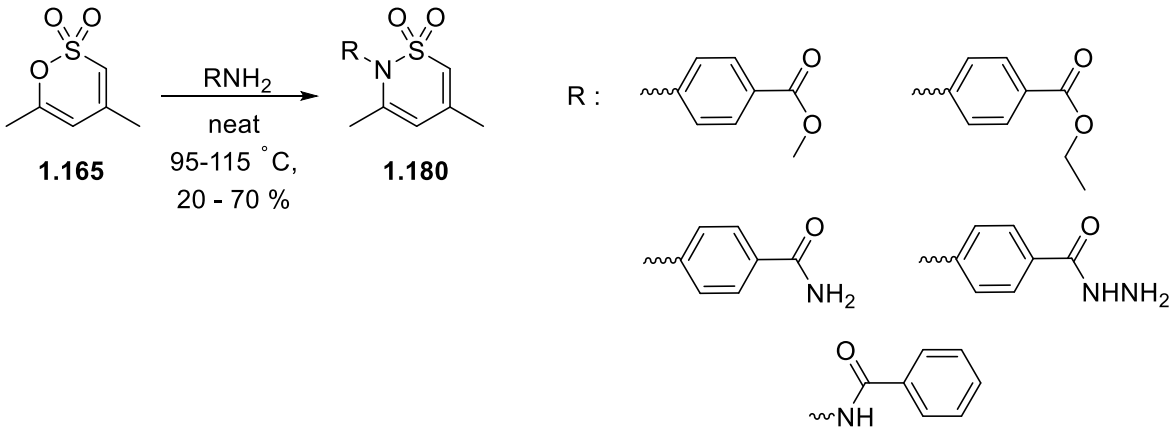

Scheme 1.41: Initial explorations of sultam formation from the corresponding amines acting on 4,6-dimethyl-1,2-oxathiine 2,2-dioxide

Further research by Zeid, Badawi and Ismail[77] introduced more derivatives (**1.181**), including a linked analogue (**1.183**), which was obtained along with the mono-substituted product **1.182** through the use of benzidine ($H_2N(C_6H_4)_2NH_2$) as the reacting amine. Additionally, a brominated analogue of the starting 1,2-oxathiine system (**1.184**) was processed similarly to yield the brominated sultam heterocycle **1.185** (Scheme 1.42).

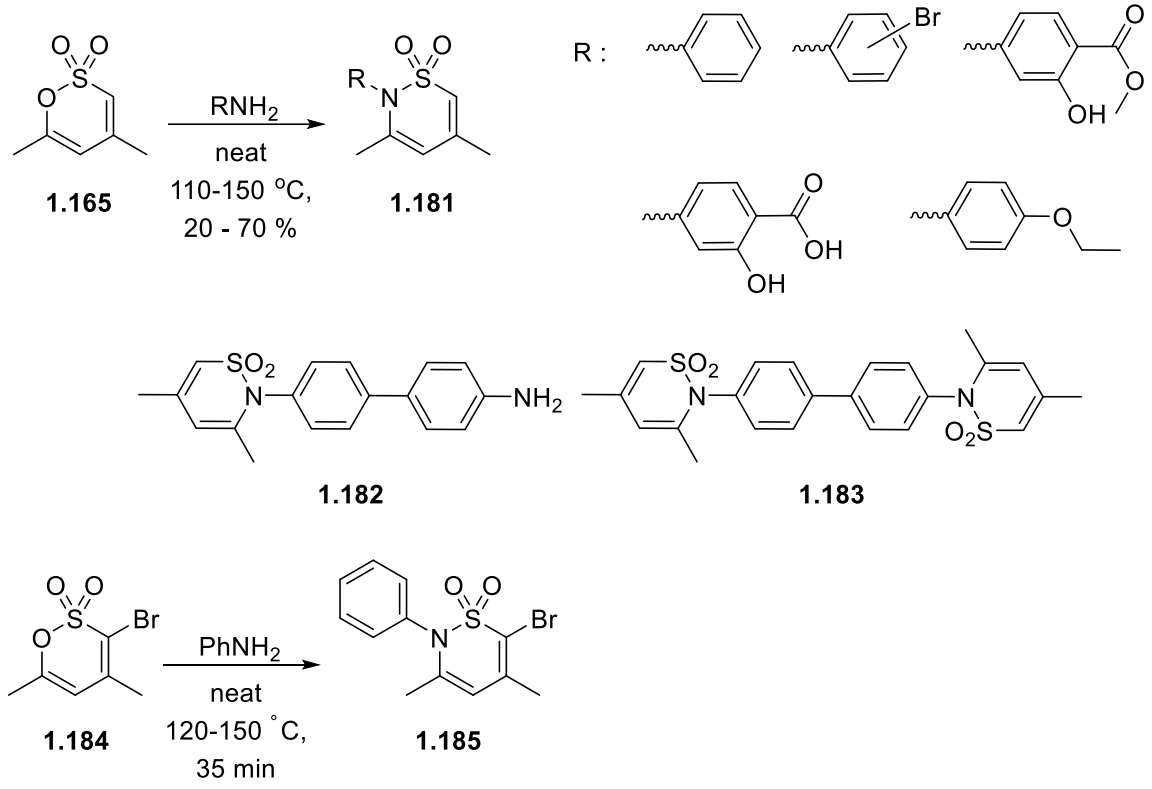

Scheme 1.42: Expansion of the sultam product spectrum, including dimeric and brominated derivatives

The absence of solvent, which had been an established feature of the reaction, was first altered in favour of using a high boiling point solvent in 1997 by Fanghanel *et al.*,[78] who constructed a small library of sultams (**1.186**) *via* the aforementioned process with anisole as a solvent (Scheme 1.43).

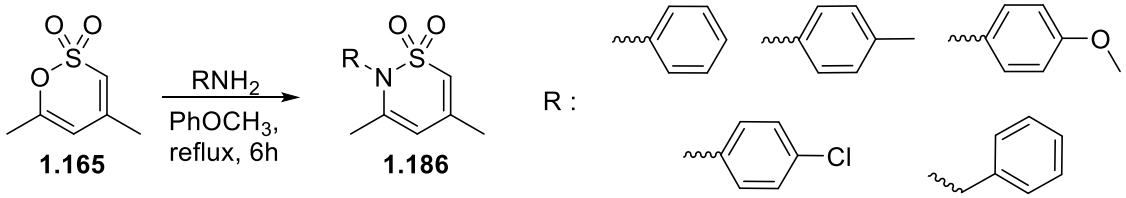

Scheme 1.43: Iteration of the sultam formation using anisole as solvent

The type of solvent that is used to furnish the reaction may have an effect on the type of product that is obtained. This was made apparent by Zeid, Ismail and Helferich[79], who brought about this variation using *n*-BuOH as a solvent and discovered that it may facilitate the addition of H_2O that forms as a by-product during the formation of the sultam ring, leading to ring-opening towards open-chain enaminosulfonic acids (**1.187**) (Scheme 1.44).

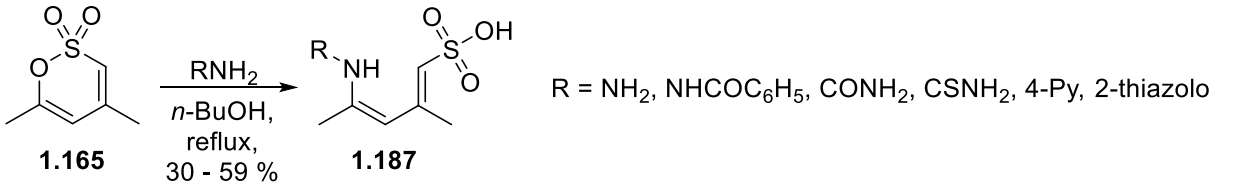

Scheme 1.44: Ring opening of the sultam ring towards an aminosulfonic acid due to potential solvent interference

Elaborating on the reactivity of 4,6-substituted 1,2-oxathiine 2,2-dioxides with amines and hydrazines, Ali, Jäger and Metz[80] presented a range of different addition reactions where *N*-containing nucleophiles ring-

open and rearrange the δ-sultone ring into more complex heterocyclic systems in moderate yields (Scheme 1.45). Various reagents, solvents and conditions have been applied to bring about the formation of pyrrole (**1.189**) and pyridazine (**1.190**) rings, as well as thiadiazine fused systems (**1.191 – 1.192**).

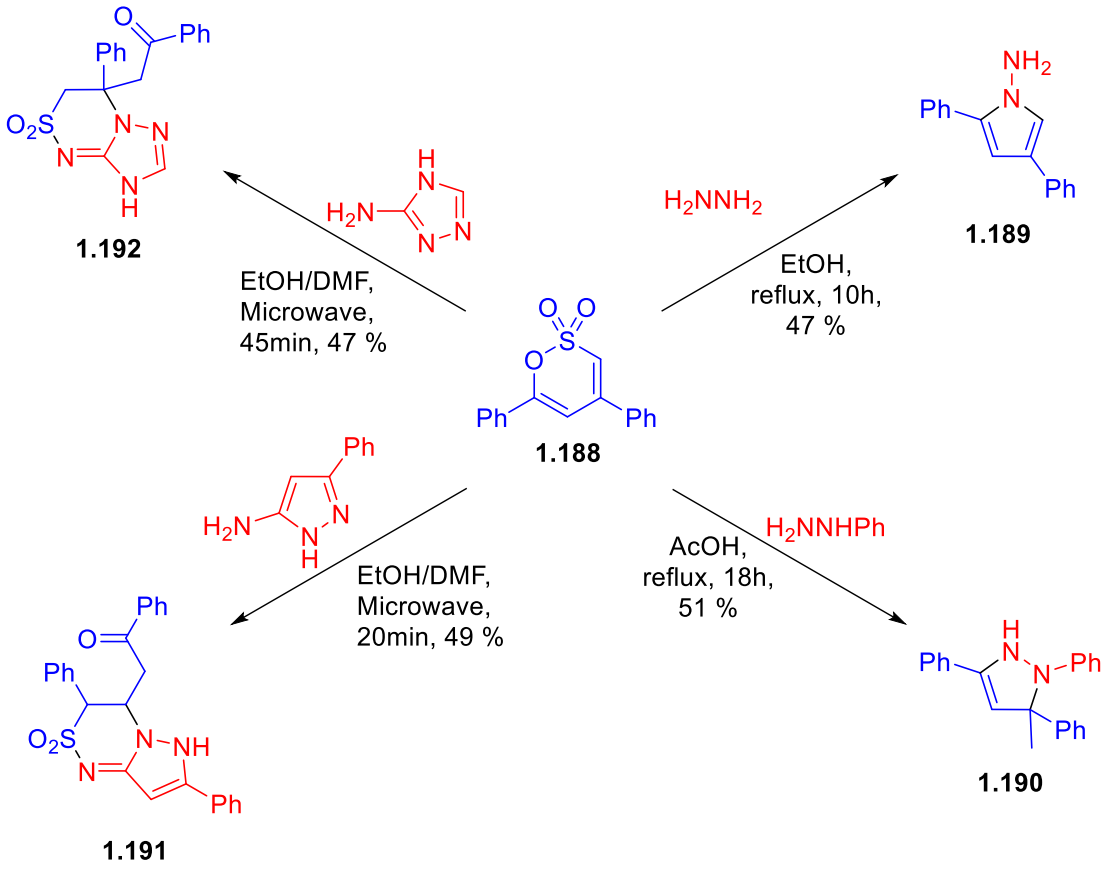

Scheme 1.45: Reactions of the 4,6-diphenyl unsaturated analogue with amines and hydrazines in various conditions

The bromination of unsaturated 1,2-oxathiines is also of significant interest, as it provides brominated precursors for coupling reactions, as seen in scheme 1.46. Eastman and Gallup[69] first attempted a bromination of the 4,6-dimethyl derivative (**1.165**) obtained by the chlorosulfonic acid iteration (Section **1.2.1.2**) and claimed the product to be the 5-bromo analogue **1.193**. This finding was disputed by Barnett and McCormack[81], who postulated that it was in fact the 3-bromo analogue **1.194** that is obtained from the reaction of Br_2 with 4,6-dimethyl 1,2-oxathiine 2,2-dioxide. In order to unequivocally validate this claim, the researchers pressed on to synthesise the 5-bromo derivative **1.193** *via* treatment of bromomesityl oxide (**1.195**) with Ac_2O/H_2SO_4 in order to ensure bromide substitution on the 5-position. H-NMR data comparison between this product and the derivative obtained by Br_2 bromination (**1.194**) confirmed the 5-bromo structure for the former and the 3-bromo structure for the latter compound. This allegation can be theoretically supported as well, since the double bond next to the electron-withdrawing SO_2 moiety is much more polarised and reactive than its 5,6- counterpart, thus an attack on molecular bromine would be largely favoured by the 3,4- double bond towards the 3-bromo analogue. Further research on sultone bromination by Gaitzsch *et al.*[67] cemented this claim, wherein the diaryl counterparts of the initial 4,6-dimethyl 1,2-oxathiine 2,2-dioxide (**1.196**) were found to afford the 3-brominated products **1.197** under different brominating conditions. Additionally, these products were processed under Sonogashira conditions, leading to the functionalisation of the 3-position with an alkyne substituent (derivatives **1.198**, scheme 1.46).

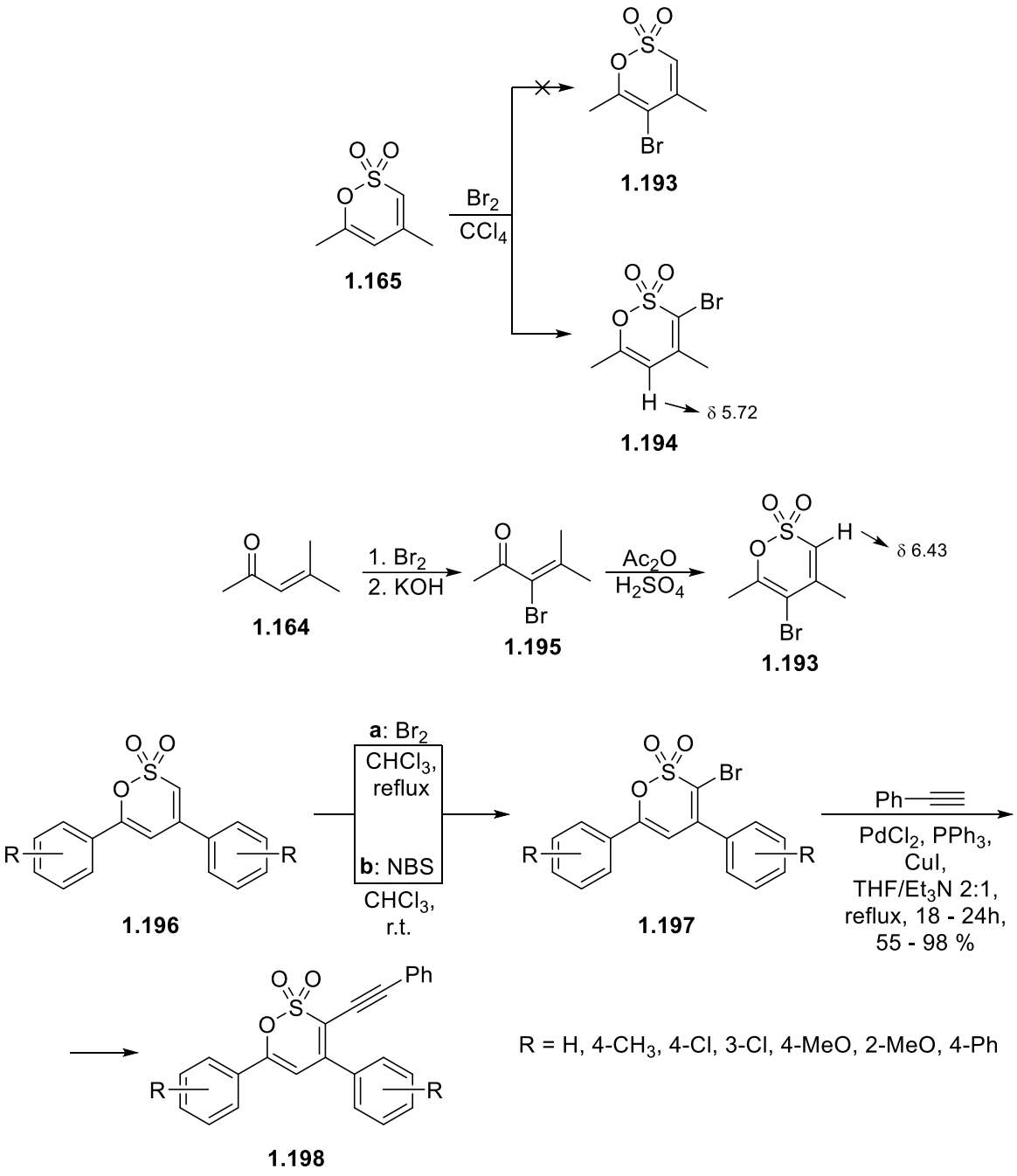

Scheme 1.46: Overview of sultone bromination, with the addition of a Sonogashira coupling on the brominated derivative

Moving away from the reactivity of sultones in substitution/addition reactions, their role as diene has also been examined (Scheme 1.47). Gaitzsch *et al.*[66] first described the Diels-Alder reaction between the 4,6-diphenyl δ-sultone **1.188** with DMAD (**1.199**) as the dienophile. The reaction produced a benzene *m*-terphenyl (**1.200**) and a phthalic anhydride (**1.201**) in different proportions depending on the conditions used, as products of a Diels-Alder/retro Diels-Alder tandem reaction. This conversion requires fairly forcing conditions in order to occur; refluxing the reagents in toluene fails to afford any products, whereas successful results were obtained only under high temperature or pressure with long reaction times and an absence of solvent. The same group explored this conversion further by trying different dienophiles (**1.202**) and conditions to arrive at these tri-substituted systems (**1.203**).[82]

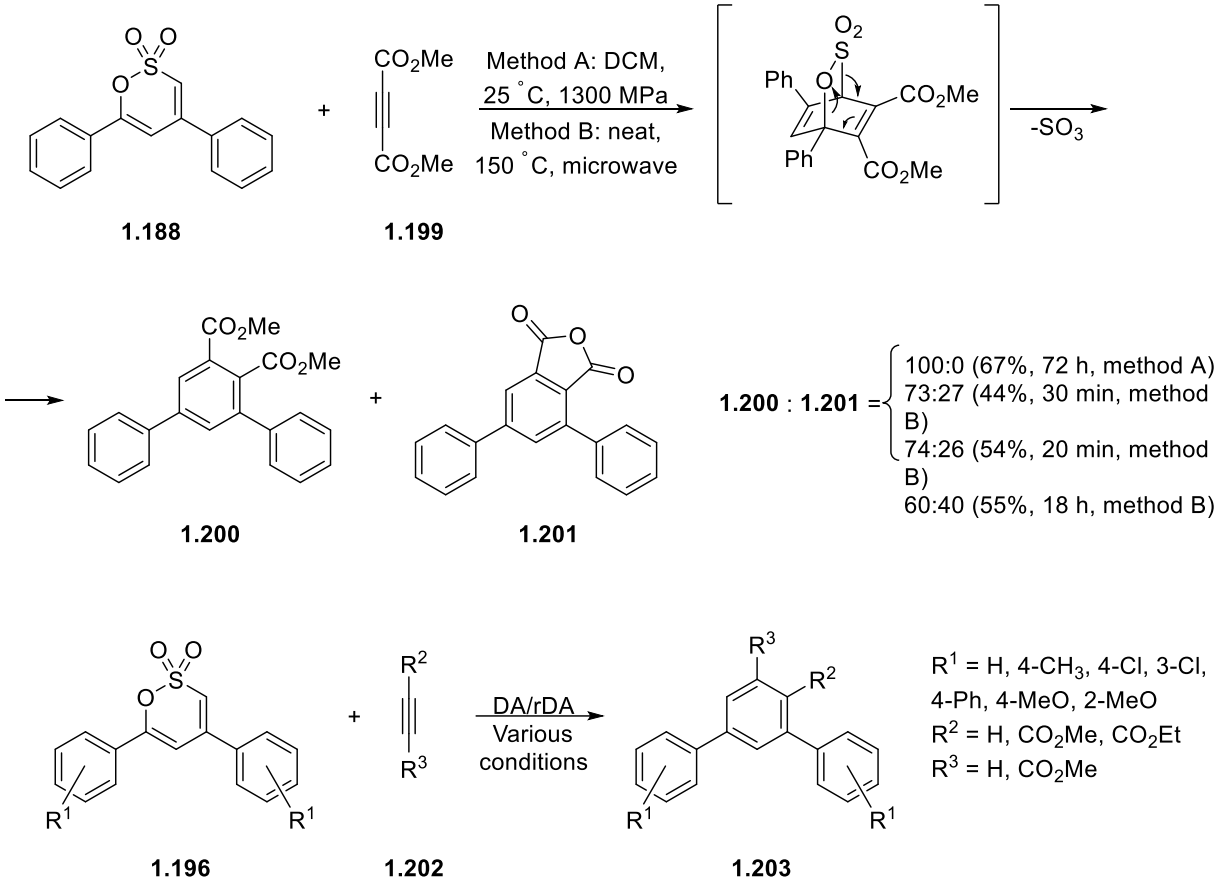

Scheme 1.47: Diels-Alder/retro Diels-Alder transformations of unsaturated 1,2-oxathiine 2,2-dioxides into tri-aryl benzenes

Reflecting on the reactivity of the sulfonyl moiety of the sultone ring, ring contraction reactions have been attempted under either thermal or photochemical conditions (Scheme 1.48). Ancerewicz and Vogel[83] have shown that treatment of the 4,6-dimethyl unsaturated analogue **1.165** with calcium oxide and quinoline yields the desulfonated furan derivative **1.204** in moderate yield.

Gorewit and Rosenblum[84] further illustrated that ether solutions of 4,6-di-substituted 1,2-oxathiine systems (**1.205**) can lose a sulfur monoxide fragment and turn into the corresponding 5-membered lactones (**1.208**) when irradiated. This interesting conversion involves an initial photochemical cleavage of a SO fragment, which affords the γ-ketoaldehyde **1.206**; subsequent photochemical abstraction of the γ-hydrogen leads to an enol-containing ketene intermediate (**1.207**) that ring-closes towards the final lactone system. An iteration of this reaction by the same research group where the photosensitizer benzophenone was also added to the reaction mixture afforded 3,4-dimers of the starting δ-sultones (**1.209**), thus better illustrating the behaviour of these molecules in various photochemical conditions.

Cleavage of sulfur/oxygen fragments can be avoided as established by King *et al.*[85], whose work includes the irradiation of a methanol solution of the 1,2-oxathiine 2,2-dioxide **1.165**, which results in the acyclic sulfone methyl ester **1.210** as the MeOH adduct of the ring-open intermediate **1.211**.

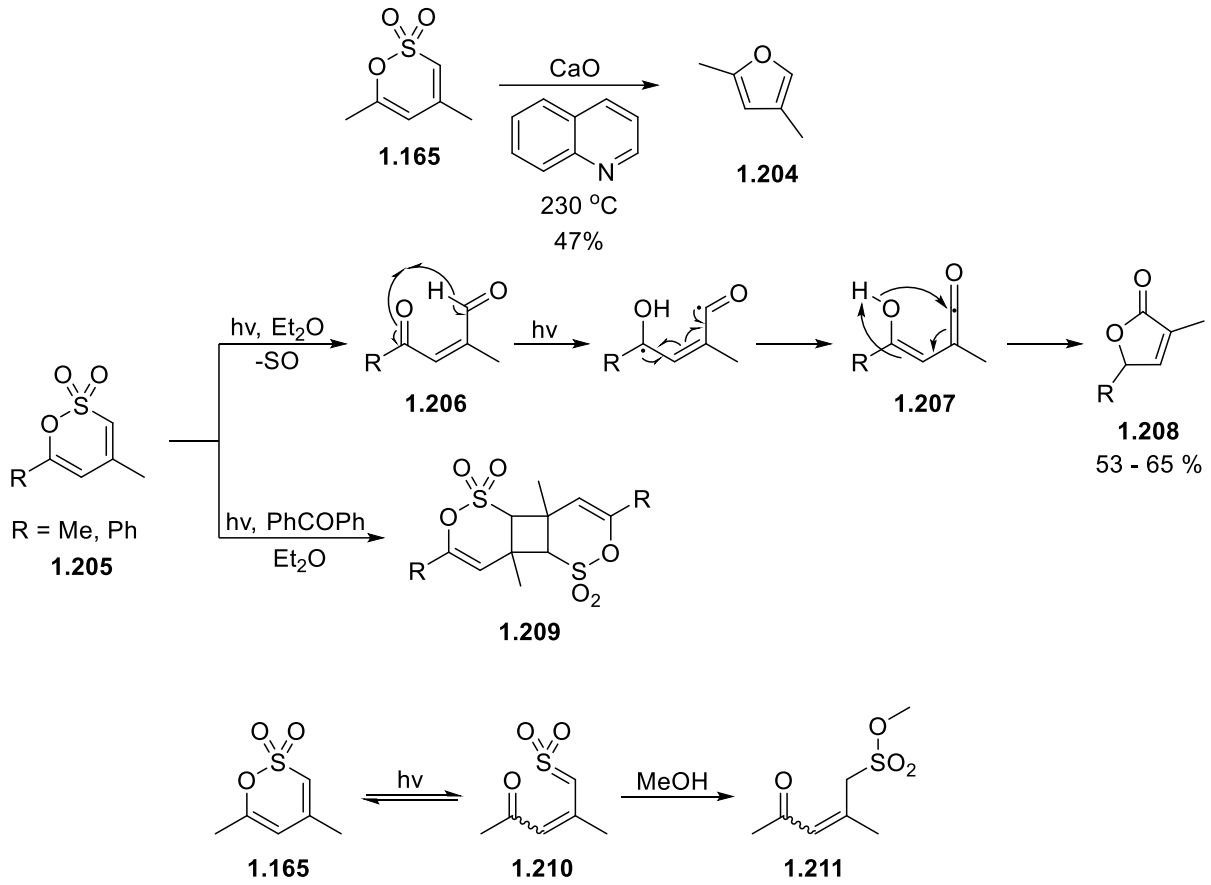

Scheme 1.48: Rearrangement reactions of 1,2-oxathiine 2,2-dioxides under thermal and photochemical conditions

1.2.2 3,4-Dihydro 1,2-oxathiine 2,2-dioxides

1.2.2.1 Overview

The semi-saturated counterparts of 1,2-oxathiine 2,2-dioxides that possess one double bond between C5 and C6 form the 3,4-dihydro analogue sub-family of 1,2-oxathiine systems. This group of compounds, along with their 3,6- and 5,6-dihydro counterparts, constitute the family of dihydro-1,2-oxathiine 2,2-dioxides (Scheme 1.49).

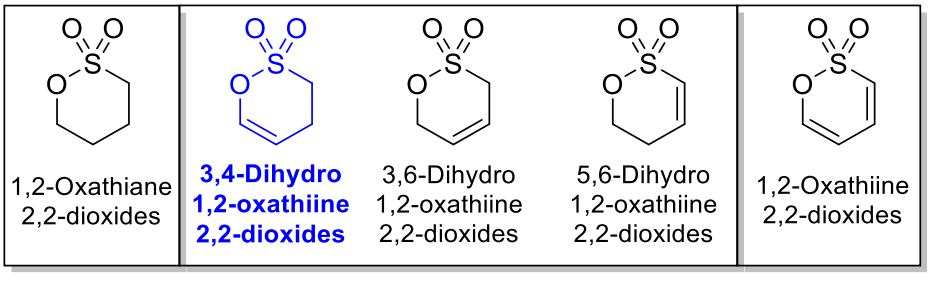

Scheme 1.49: 3,4-Dihydro 1,2-oxathiine 2,2-dioxides as one of the three sub-families of semi-saturated sultone heterocycles

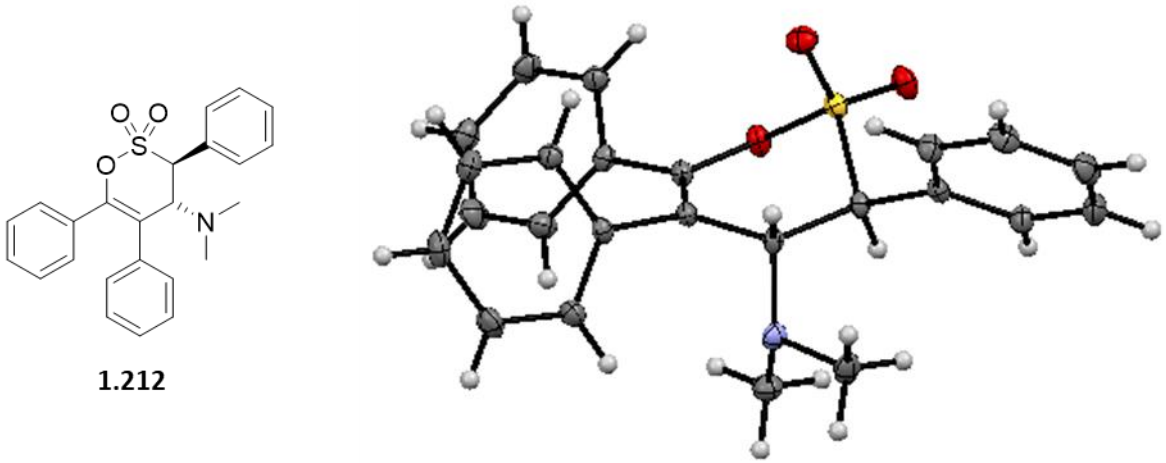

1.212

Figure 1.4: Crystal structure of a 3,4-dihydro analogue highlighting its "envelope" conformation

The crystallographic data obtained for 3,5,6-triphenyl-4-dimethylamino-3,4-dihydro 1,2-oxathiine 2,2-dioxide, **1.212**, present an "envelope" conformation analogous to the one observed for the unsaturated analogues, with the SO_2 fragment is again outside of the plane of the O-C6-C5-C4-C3 backbone (Figure 1.4)[86].

From the above structure, it can be theorised that, although the absence of a second double bond may reduce the number of reactive sites on the sultone ring, the presence of fully saturated carbons permits more complex substitution patterns on these systems, thus broadening the range of potential derivatives and target compounds that can be afforded through them.

1.2.2.2 Preparation strategies and reported reactions

In contrast to their unsaturated counterparts, 3,4-dihydro-1,2-oxathiine 2,2-dioxides have not been explored thoroughly in the established literature, thus only a few methods for their synthesis have been found. The first one bears a resemblance to the Morel and Verkade route towards δ-sultones[68], as sulfuric acid, along with acetic anhydride, is again utilised to annulate a hydroxy-enone (**1.213**) towards a 4-keto-3,4-dihydro 1,2-oxathiine adduct (**1.214**, Scheme 1.50).[87]

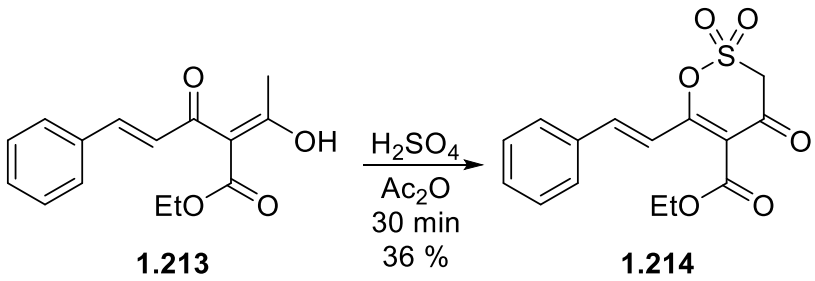

Scheme 1.50: Sulfonylation and consequent ring-closing of an enone with the use of sulphuric acid

Organocatalysis has also been employed as a means of facilitating pericyclic transformations towards the desired 3,4-dihydro 1,2-oxathiine heterocycles *via* activation of the starting materials. In the work by Lupton *et al.*, a carbene catalyst (IMes, **1.224**) effects the addition of a sulfonyl fluoride (**1.215**) to a keto-enol ether (**1.216**) towards a 4,5,6-tri-substituted 3,4-dihydro 1,2-oxathiine target system (**1.223**, Scheme

1.51).[88] Other research groups have opted for 1,8-diazabicyclo[5.4. 0]undec-7-ene (DBU, **1.225**) as a catalyst base able to effect the addition of sulfonyl fluorides (**1.217**, **1.219**) to different carbonyl-containing substrates (**1.218**, **1.220**)[89,90]. Further explorations of these synthetic routes showcase that nickel-based catalysis can be utilised as another alternative towards 3,4-dihydro-1,2-oxathiine target systems[91] from methyl ketone precursors (**1.221**).

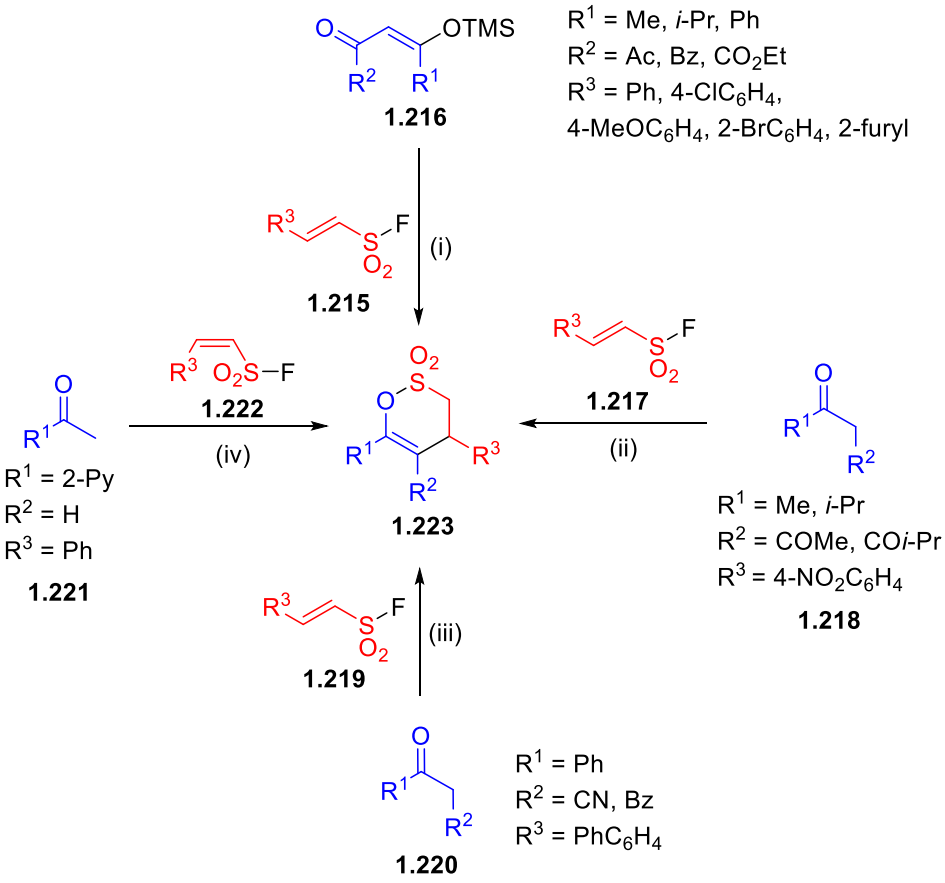

Reagents & Conditions: (i) IMes (10%-mol), 4 Å mol. sieves, THF, 66 °C, 6h, 40 - 88 %, (ii) DBU (20%-mol), $NaHCO_3$ (1.0 equiv), DCM, rt, 44 - 77 %, (iii) DBU (5 mol%), K_2HPO_4 (1.2 equiv), DMF, 50 °C, 69 - 77%, (iv) $Ni(acac)_2$ (20 mol%), K_2CO_3 (2.0 equiv), MeCN, rt, 69 %

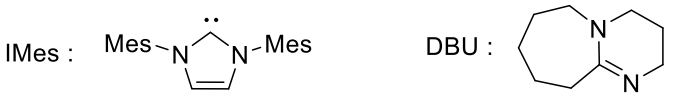

1.224 **1.225**

Scheme 1.51: Various catalytic routes towards the formation of 3,4-dihydro-1,2-oxathiine derivatives

It should be noted that the amount of base used to bring about the annulations in scheme 1.51 may also have the opposite effect, as was the case for the nitrophenyl analogue **1.226**. The foregoing 1,2-oxathiine system was reported to ring-open with concomitant loss of the SO_2 moiety towards a keto-enol derivative (**1.227**) upon treatment with a stoichiometric amount of DBU (Scheme 1.52).

As discussed earlier (Sections **1.1.2.3** and **1.1.3.3**), Schenone *et al.*[41,42,43,44] provided a robust synthetic route to substituted 3,4-dihydro-1,2-oxaxthiine 2,2-dioxides *via* addition of sulfenes to enaminone derivatives (Scheme 1.53).

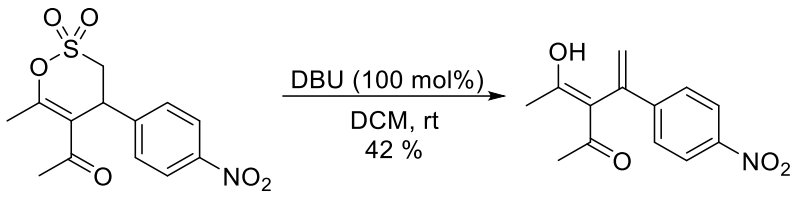

Scheme 1.52: Base-catalysed ring-opening of a 3,4-dihydro 1,2-oxathiine analogue under basic conditions

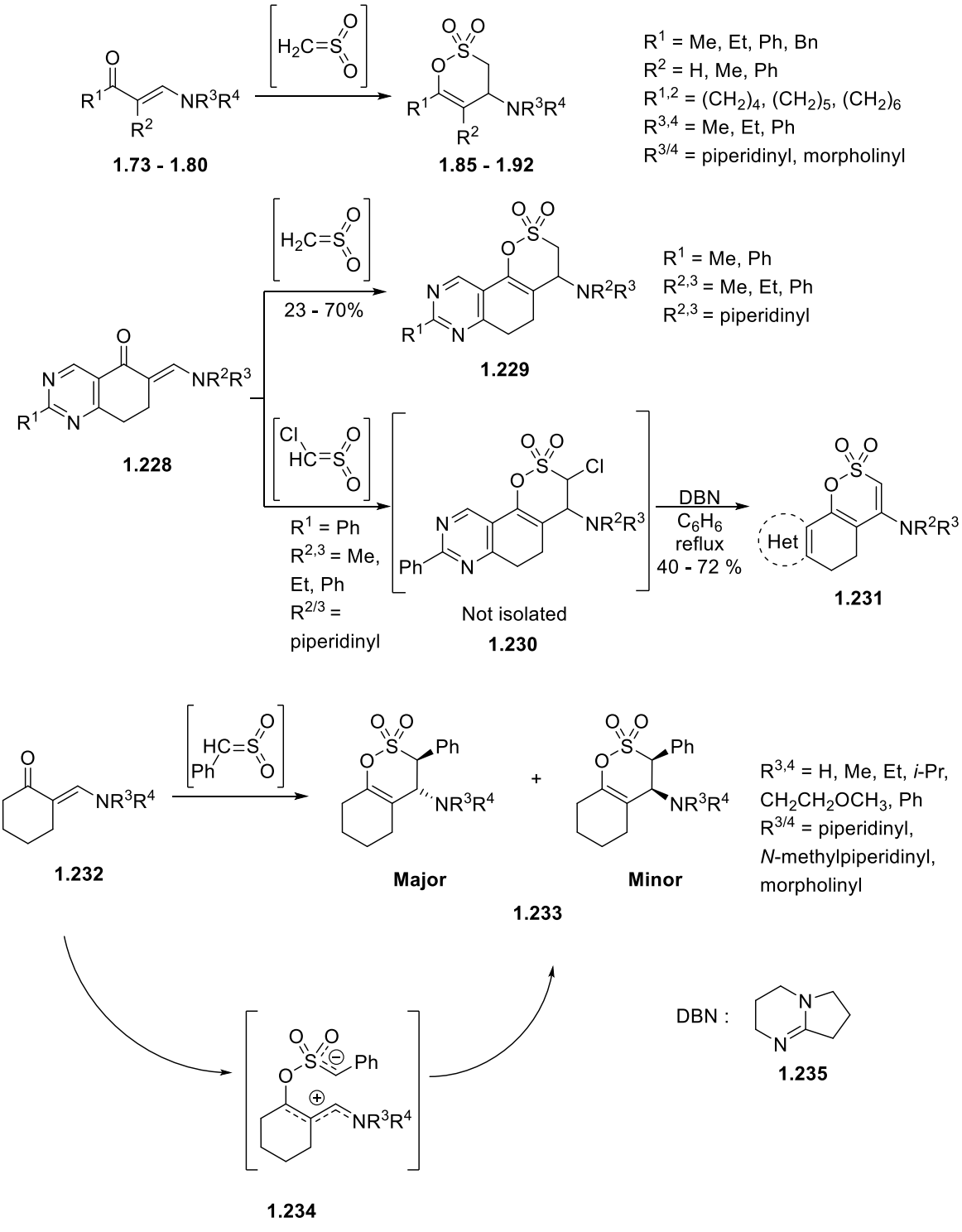

Scheme 1.53: Explorations on the addition of sulfenes to enaminones towards 3,4-dihydro 1,2-oxathiine derivatives

The substitution patterns on the enaminone were found to have an important effect on the yield of this conversion, but once their impact was thoroughly explored, more complex systems, *e.g.* the tricyclic derivatives **1.229** – **1.230**, were synthesised (Scheme 1.53).[92] The presence of a chlorine substituent on the sulfene was singled out, as no adducts of these additions could be isolated; instead, the eliminated counterparts of these compounds (**1.231**) were afforded *via* treatment of the sulfene addition crude product mixtures with 1,5-diazabicyclo(4.3.0)non-5-ene (DBN, **1.235**), thus confirming the addition of the chlorosulfene fragment to the enaminone substrates. Additionally, when phenylsulfene was employed with enaminones derived from cyclohexanone, the afforded 1,2-oxathiine adducts were obtained as pairs of *anti*/*syn* isomers (**1.233**), this time without any detrimental effect by the *N*-substituents of the starting enaminoketones **1.232**. The *anti*- isomer was always obtained as the major isomer, although the lack of stereoselectivity led the research team to the conclusion that the reaction proceeds through a step-wise mechanism involving the intermediate **1.234** shown below.[93]

Mosti *et al.* further expanded the range of 1,2-oxathiine-containing heterocyclic systems, obtaining the indole-fused analogues **1.237** (Scheme 1.54).[32] Two of these compounds were selected to assess the proclivity of these species for oxidation reactions *via* treatment with 2,3-dichloro-5,6-dicyano-1,4-benzoquinone (DDQ, **1.240**). The dimethylamino derivative (R = Me) proceeded to eliminate the Me_2N moiety, as well as an H_2 fragment towards the aromatised product **1.238**. Interestingly, its morpholino counterpart (NR^1R^2 = morpholinyl) was found to aromatise and eliminate on the 3,4-position without loss of the morpholine leaving group, yielding the indole derivative **1.239**.

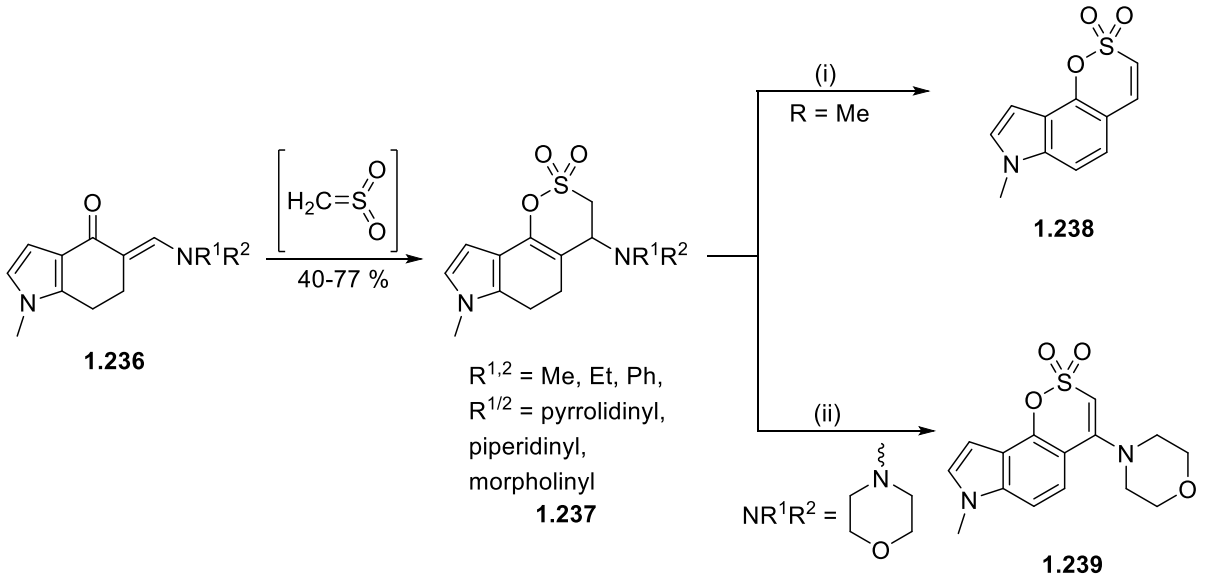

Reagents & Conditions: (i) DDQ, C_6H_6, 10 h, 27 %, (ii) DDQ (exc.), C_6H_6, 1 d, 17 %

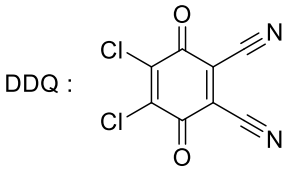

1.240

Scheme 1.54: Indole analogues of 3,4-dihydro-1,2-oxathiine 2,2-dioxides and mapping of their elimination potential

Singh *et al*. have also presented a similar case of sulfene addition to α,β-unsaturated enaminone precursors **1.241**, highlighting the preference of the sulfene fragment towards the more polarised double bond adjacent to the dimethylamino group, rather than the styryl moiety (Scheme 1.55). Furthermore,

the 1,2-oxathiine adducts **1.241** were found to undergo an elimination reaction towards the unsaturated derivatives **1.243**, in a similar fashion to the conversions reported earlier (Schemes 1.53-2.54) *via* cleavage of the dimethylamino group under an excess of base at room temperature, although it seems an absence of 3-substituents is vital for this elimination to take place.[94]

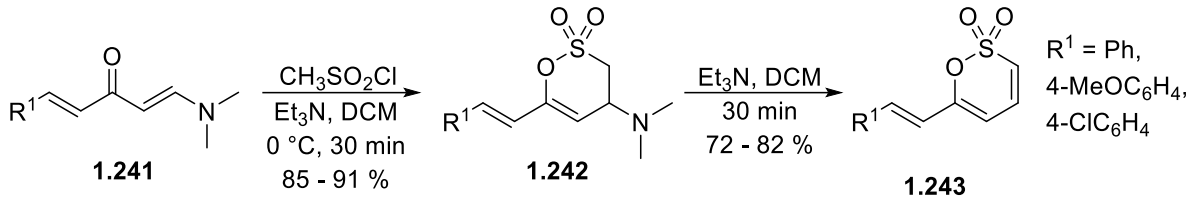

Scheme 1.55: Addition of a sulfene to an α,β-unsaturated enaminoketone starting material with subsequent base-catalysed elimination

1.2.3 Applications

Apart from being useful scaffolds for more complex systems in heterocyclic synthesis as established in sections **1.2.1.3** and **1.2.2.2**, 1,2-oxathiine 2,2-dioxide systems have also been met with interest in the field of lithium battery development, lithography, photoresist systems, as well as bioactive agents (albeit to a limited extent). Specifically, the unsaturated analogues **1.244** have found use in lithium secondary battery technologies (Scheme 1.56). Different patents have exemplified their use as thermo-stabilising agents in the non-aqueous electrolyte solution of the battery[95,96], as well as an additive to enhance the performance of the positive electrode of the device[97].

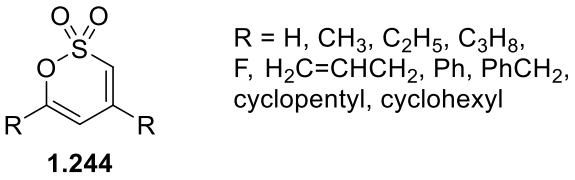

Scheme 1.56: Derivatives of 1,2-oxathiine 2,2-dioxide used in lithium secondary battery systems

Further derivatives (**1.245** – **1.246**) have also been utilised in lithographic printing, as components in the IR photosensitive mixtures that are applied to the plate so as to develop the image forming layer (Scheme 1.57).[98]

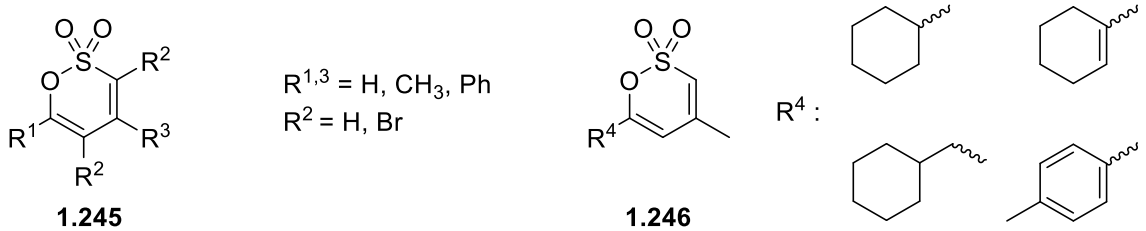

Scheme 1.57: Lithography as another niche for 1,2-oxathiine analogue applications

Finally, the ability of these heterocyclic systems to ring-open when irradiated has been utilised in the development of photosensitive materials (**1.247**) to be used in photoresist (photo-acid generating) systems (Scheme 1.58).[99]

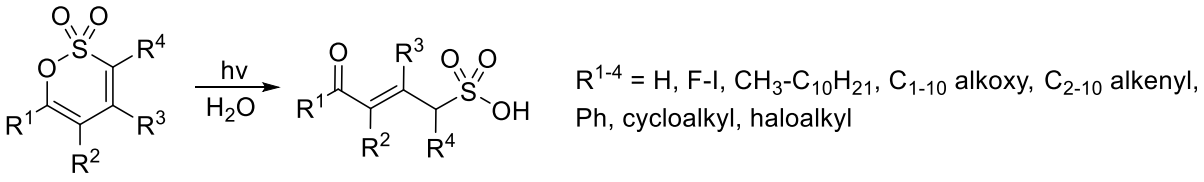

1.247 **1.248**

Scheme 1.58: Formation of a ring-open sulfonic acid as a relay of the presence of irradiation in photoresist systems

The application changes drastically when the 3,4-dihydro derivatives are concerned. Wang *et al.,*[87] have reported that the styryl derivative **1.214** (Section **1.2.2.1**) performed efficiently when tested for antiangiogenetic properties, although no specific mode of action was ascertained. This finding led to further screening of this compound for anti-tumour activity again murine sarcoma, wherein it effected a reduction on the growth of tumour weight without causing serious damage on liver and spleen tissues (Figure 1.5).

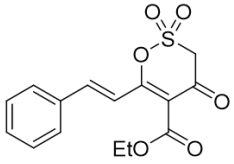

1.214

Group of mice	mg/kg	Tumour weight (g)	Inhibition rate (%)
Blank	-	-	-
Model	-	0.684	-
CTX	20	0.249	63.5%
S-CA	**10**	**0.342**	**44.7%**

Figure 1.5: Anti-tumour activity of a 3,4-dihydro 1,2-oxathiine derivative when screened against murine sarcoma (cyclophosphamide (CTX) used as a control)

1.3 Aims of present study

The aim of the present work is to explore the structure, synthesis and reactivity of the relatively scarcely studied class of 6-membered heterocycles known as 1,2-oxathiine 2,2-dioxides and their 3,4-dihydro-derivatives.

Sulfene addition to a diverse range of enaminoketones, obtained from reacting α-methylene ketones with DMFDMA, will be studied to extend access to the 3,4-dihydro-1,2-oxathiine 2,2-dioxide ring system.

The hitherto unexplored ring transformation of the 4-amino-3,4-dihydro-1,2-oxathiine 2,2-dioxide to the fully unsaturated 1,2-oxathiine 2,2-dioxide system will be subsequently examined under different sets of conditions.

The 3,4-dihydro-1,2-oxathiine 2,2-dioxide and the 1,2-oxathiine 2,2-dioxide units will be utilised as the central scaffold in a photochromic dithienyl ethene. Attempts towards the preparation of an electrochromic 1,2-oxathiine 2,2-dioxide separated viologen will be explored.

The reactivity of the 1,2-oxathiine 2,2-dioxides will be studied by C-H activated coupling, bromination/transition metal mediated chemistry (Suzuki, Suzuki-Miyaura, Heck) and metalation to afford a diverse library of 1,2-oxathiine 2,2-dioxides thus mapping out the reactivity of these ring systems.

Finally, the behaviour of the fixed diene moiety of the 1,2-oxathiine 2,2-dioxides towards various dienophiles, as well as benzyne, will be interrogated to afford new routes to substituted aromatic compounds.

CHAPTER 2: SYNTHESIS OF ENAMINONES AND 1,2-OXATHIINE 2,2-DIOXIDE TARGET SYSTEMS[b]

2.1 Preparation of Enaminone Precursors

2.1.1 Analogue library and structural features

In order to gain access to the desired 1,2-oxathiine 2,2-dioxides *via* the sulfene addition protocol, a series of enaminones were prepared by the reaction of various α-methyleneketones with dimethylformamide dimethyl acetal (DMFDMA) guided by established literature procedures. During the first example, heating acetophenone in neat DMFDMA overnight gave, after evaporation of the volatiles and trituration with Et_2O, the enaminoketone **2.1**[20] as yellow/orange crystals in 69.0 % yield. The formation of **2.1** was initially ascertained by ^{1}H-NMR spectroscopy with the doublets at δ 5.71 and at δ 7.80 with J = 13.4 Hz confirming the presence of two olefin protons with a *trans* configuration, while the broadened singlet at δ 2.92 and at δ 3.13 refer to the NMe_2 terminus (Figure 2.1). The latter signals are broadened as a consequence of the differential shielding experienced by each NMe group due to the restricted rotation about the partial C-N double bond arising from the extended delocalisation of the N-atom lone pair electrons; this behaviour may be linked to that of amides such as *N*,*N*-dimethyl formamide.[100] The ^{13}C-NMR spectrum, with a characteristic carbonyl peak at δ 188.7, also exhibits signals for the olefinic C-atoms at δ 92.2 and at δ 154.2 and weak signals at δ 37.2 and δ 45.0, which are assigned to the different NMe units. IR spectroscopy further confirmed the enaminone structural scaffold with a characteristic sharp peak observed at 1537 cm^{-1} evidencing the C=O stretching, although this value deviates from the values that are common for unsaturated ketone systems (1666-1685 cm^{-1}) as a consequence of the conjugation with the electron donating NMe_2 unit. The anticipated *m/z* peak for the molecular ion at 176.1072 for $[M+H]^+$ ($C_{11}H_{13}NO$ required *m/z* 176.1070 for $[M+H]^+$) was observed in the mass spectrum of **2.1**, thus further attesting to the successful formation of **2.1**.

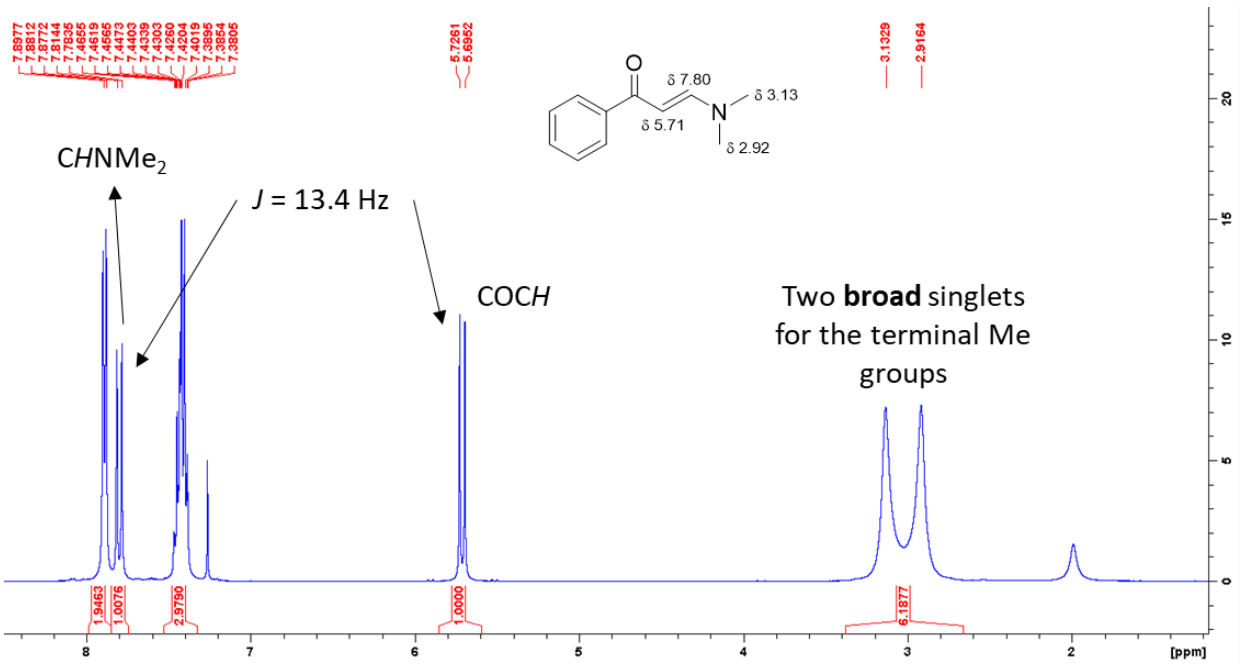

Figure 2.1a: ^{1}H-NMR spectrum of enaminone **2.1**

[b] Work contained within this chapter has contributed to the following publication (Appendix 2, p. 306): *Org. Biomol. Chem.*, **2019**, *17*, 9585-9604; DOI: https://doi.org/10.1039/C9OB01657K

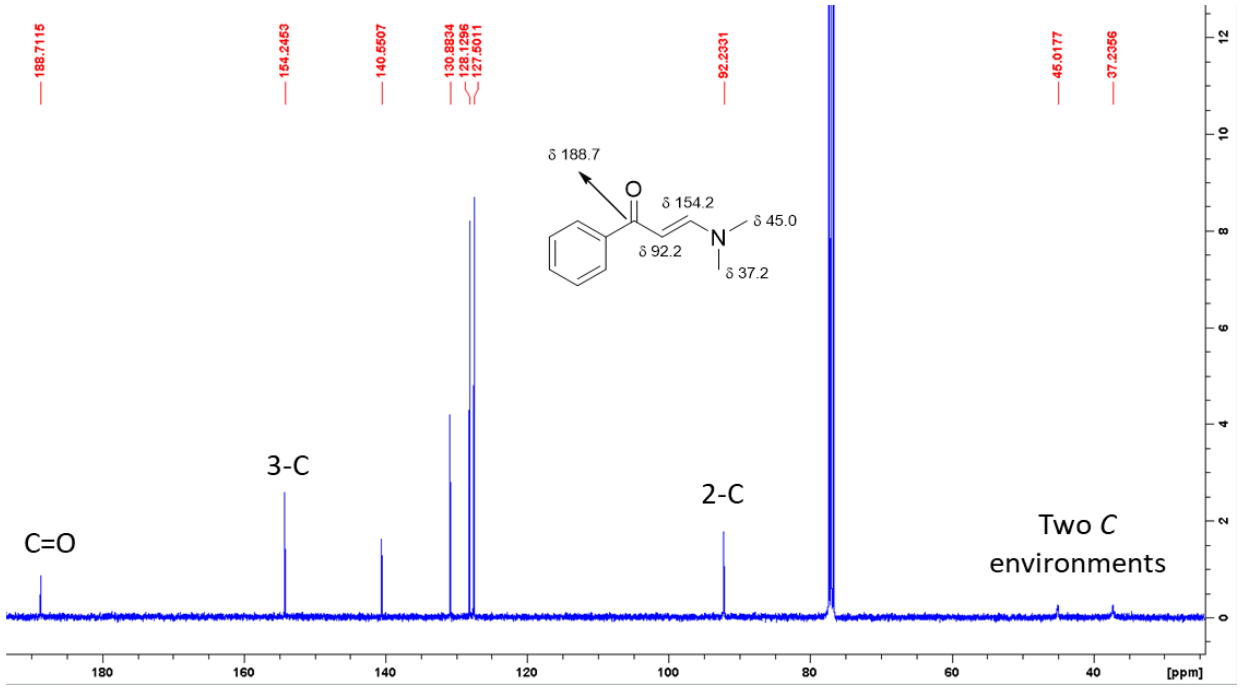

Figure 2.1b: ^{13}C-NMR spectrum of enaminone **2.1**

As discussed in section **1.1.2.2**, the mechanism of this conversion likely involves the formation of an enolate ion from the deprotonation of the starting material by the methoxy fragment of DMFDMA. Subsequent attack of the enolate on the methylene centre of methoxy substituted iminium fragment produces a hemiaminal type intermediate, which undergoes an E1cB elimination towards **2.1** (Scheme 2.1). Various other α-methyleneketones with substituents on the 1- and /or 2- positions were processed through the same protocol to afford their enaminone counterparts in good to excellent yields (Table 2.1).

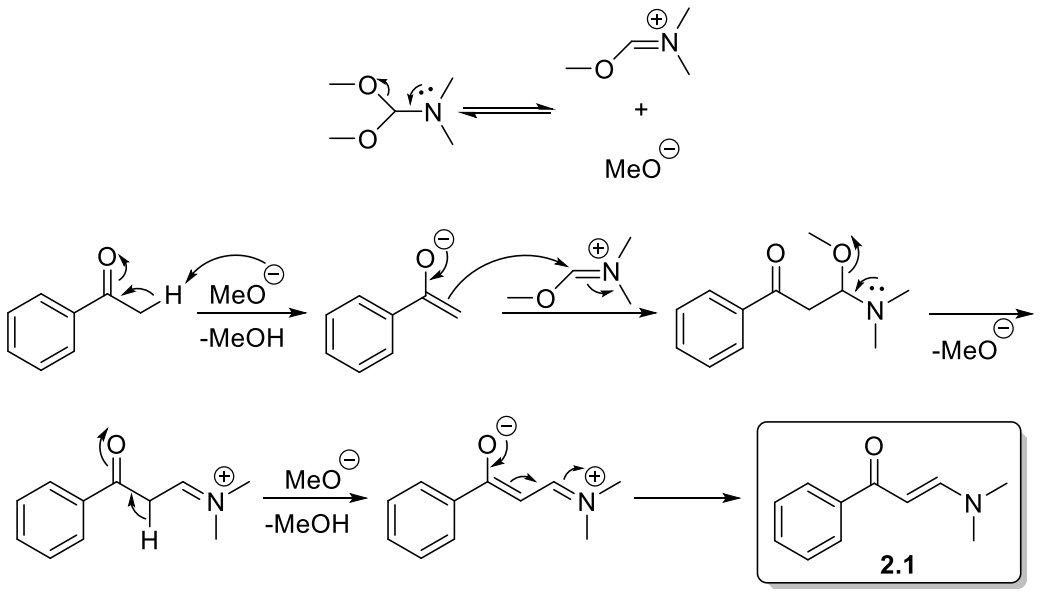

Scheme 2.1: Mechanism of dimethylaminomethylene addition through reaction with DMFDMA

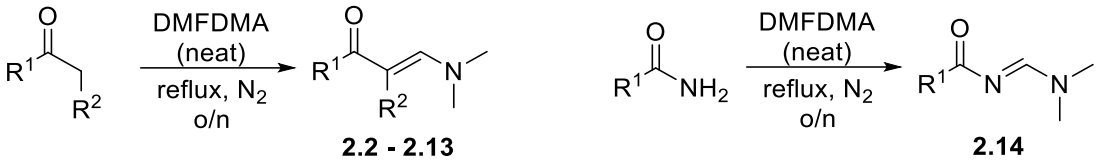

2.2 - 2.13 **2.14**

Entry	Compound No.	R^1	R^2	Yield (%)
1	**2.2**	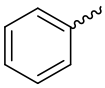	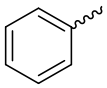	98.4
2	**2.3**	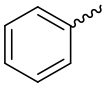	CO_2Et	57.0
3	**2.4**	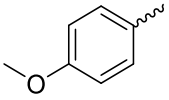	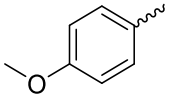	97.2
4	**2.5**	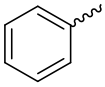	CN	56.7
5	**2.6**	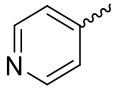	H	84.9
6	**2.7**	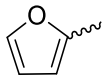	H	84.4
7	**2.8**	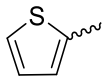	H	98.6
8	**2.9**	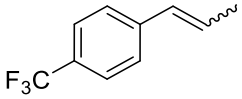	H	50.6
9	**2.10**	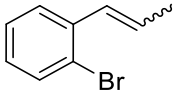	H	92.8
10	**2.11**	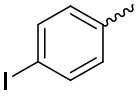	H	85.8
11	**2.12**	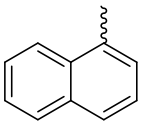	H	78.6
12	**2.13**	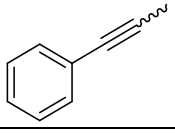	H	76.8
13	**2.14**	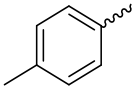	n/a	79.1

Table 2.1: Enaminones prepared by reflux in neat DMFDMA

It is apparent from table 2.1 that a wide variety of substituents are tolerated on the 1-position of the ketone substrate, including *para*-substituted aryl groups (**2.11**), both electron-rich (**2.7**, **2.8**) and electron-deficient (**2.6**) heterocycles, as well as styryl (**2.9**, **2.10**) and phenylethynyl (**2.13**) groups. Additionally, the α-methylene group (R^2 in table 2.1) may be substituted with aryl groups (**2.2** and **2.4**), as well as with an ester or a nitrile function (**2.3**, **2.5**). Finally, the use of toluamide (α-carbon is replaced with an *N* atom)

with DMFDMA results in an 'aza' enaminoketone analogue (**2.14**). As it was the case with analogue **2.1**, the significant structural differences between the ketone starting materials and the enaminone products proved to be quite useful in ascertaining the success of this conversion *via* ^{1}H-NMR spectroscopy. As it can be seen in the examples below (Figure 2.2), the presence of one (for di-substituted derivatives) or two (for mono-substituted derivatives) olefin signals between δ 5 – 8, in conjunction with either one or two signals at *circa* δ 3, unequivocally confirms the formation of the target compounds. Moreover, the nature of the substituents on the enaminoketones in table 2.1 has an apparent influence on the appearance of their ^{1}H-NMR spectra, as it is illustrated by the ^{1}H-NMR spectra for **2.4** and **2.14** (Figure 2.2). For the 1,2-bis(4-methoxyphenyl) substituted example **2.4**, the olefinic proton (3-H) is relatively deshielded and appears as a singlet at δ 7.35 due to of conjugation with the adjacent C=O group.

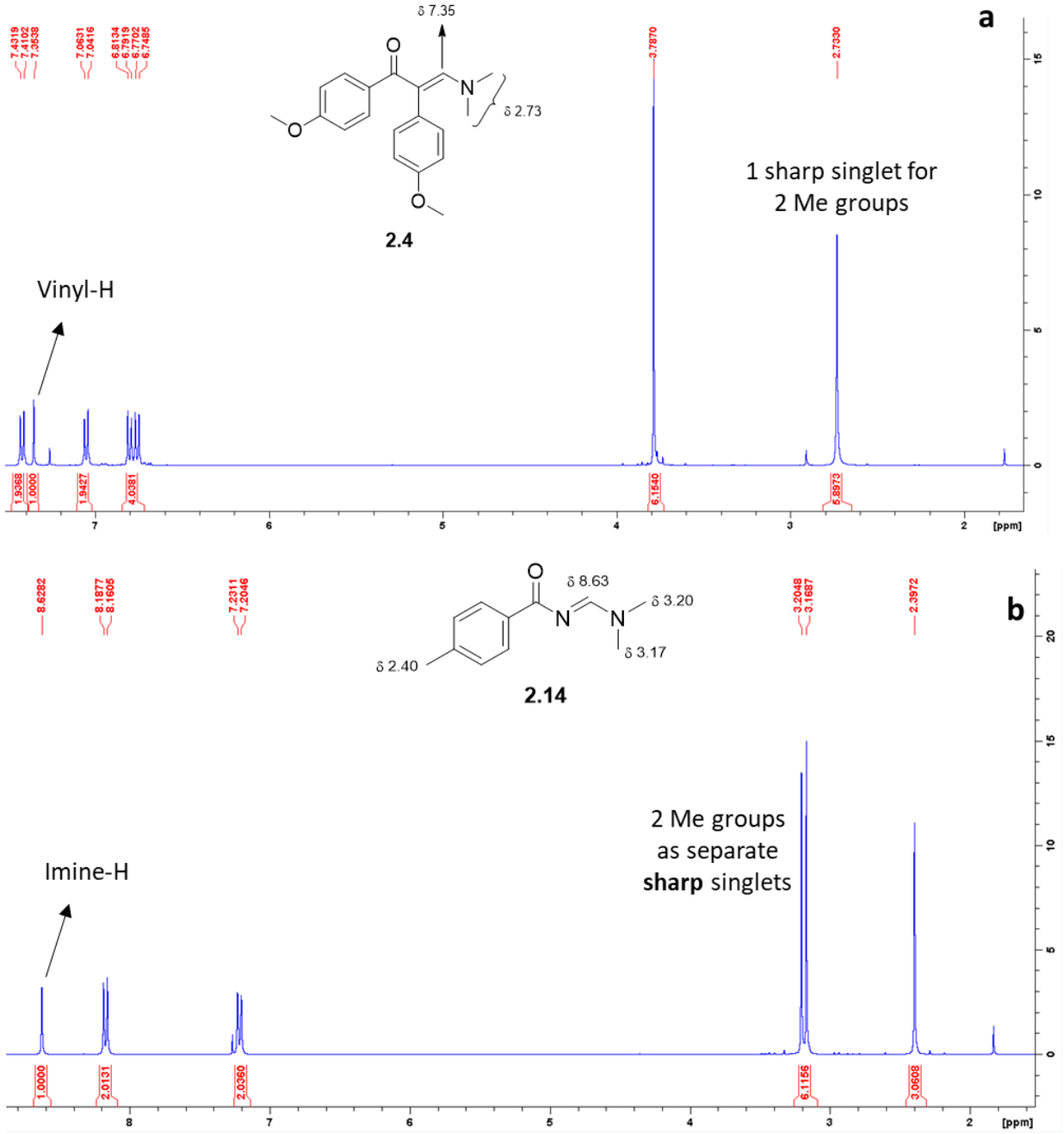

Figure 2.2: Selected ^{1}H-NMR spectra examples of enaminone products **2.4** (above) and **2.14** (below)

Substituting the C2-C3 double bond with the electron-withdrawing imine bond in analogue **2.14** results in a further downfield shift of 3-H to δ 7.93. An even more striking difference between the ^{1}H-NMR spectra of **2.4** and **2.14** is the appearance of the signal for the NMe_2 terminus. Unlike the ^{1}H-NMR spectrum of **2.1** the NMe groups for **2.4** are equivalent and resonate as a sharp singlet accounting for 6 H at δ 2.73 whereas, for **2.14** the NMe groups are markedly non-equivalent, presumably as a consequence of enhanced restricted rotation about the N-C3 bond during the NMR spectrum acquisition process, which stems from a more efficient delocalisation of the nitrogen atom lone pair resulting in an increase of the N-C bond order. These findings are in accordance with previous research work on analogous enaminone systems.[2]

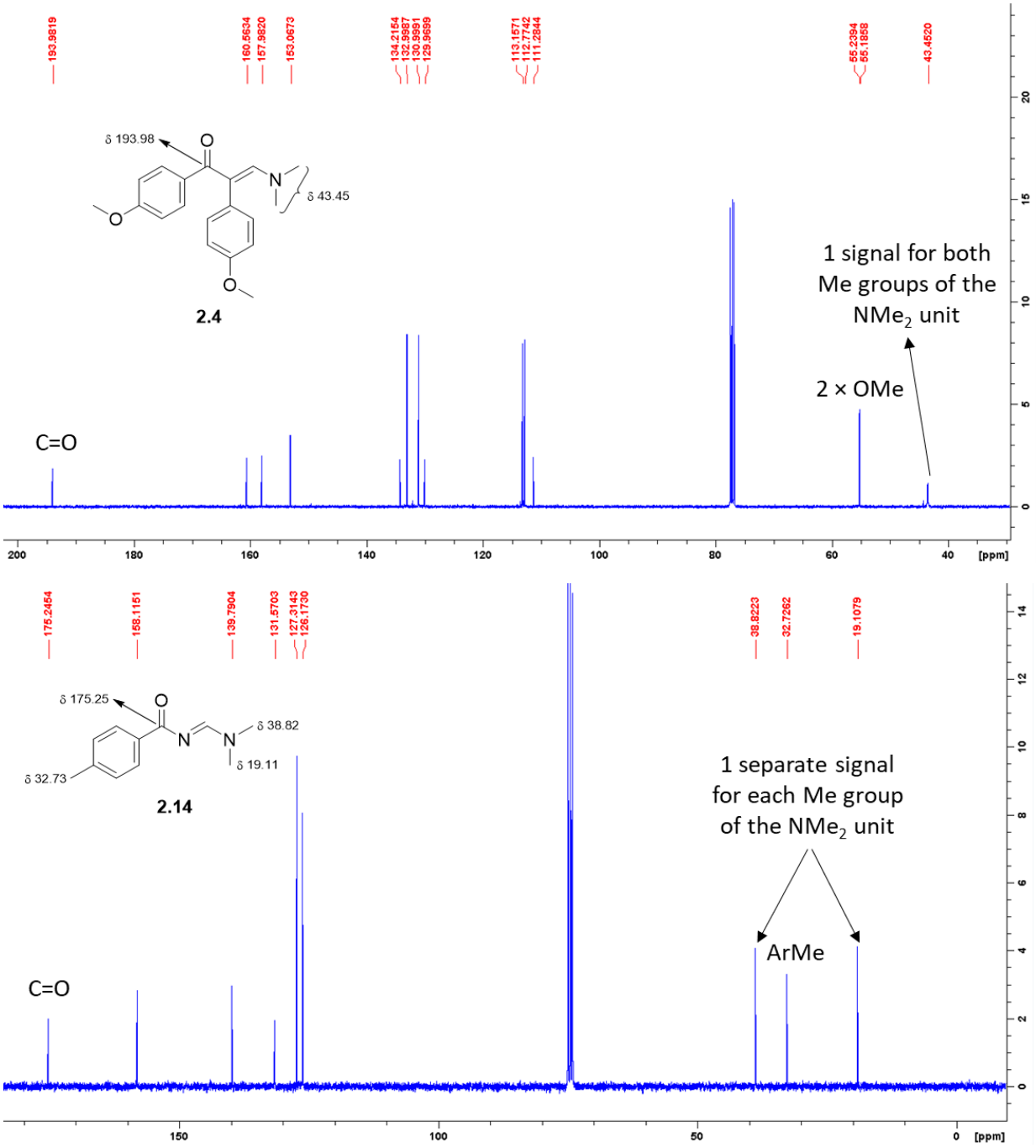

Figure 2.3: ^{13}C-NMR spectra of **2.4** and **2.14**

The behaviour leading to the appearance of the signals for the NMe groups noted in the ^{1}H-NMR spectra for **2.1**, **2.4** and **2.14** is also manifested in the respective ^{13}C NMR spectra with the one for **2.4** affording a weak singlet at δ 43.45, whereas the one for **2.14** affords distinct intense signals at δ 32.73 and δ 38.82. Further interest is presented by the *C* atom of the carbonyl unit of the enaminone, which appears to be typically highly deshielded (δ 193.98 for **2.4** and δ 175.25 for **2.14**) by virtue of the electron withdrawing adjacent double or imine bond (Figure 2.3).

Interestingly, in the ^{1}H-NMR spectrum of the thienyl analogue **2.8** the signal for the NMe_2 unit also appears as two slightly broadened singlets, similar to that of **2.1**, due to hindered (slow) N-C3 rotation during the acquisition of the NMR spectrum (Figure 2.4). Of further interest is the appearance of the signals for 2-H and for 3-H which resonate at δ 5.62 and δ 7.77 and appear as doublets with *J* = 12.3 Hz, which is typical for *trans*-alkene protons of enaminoketones.[2]

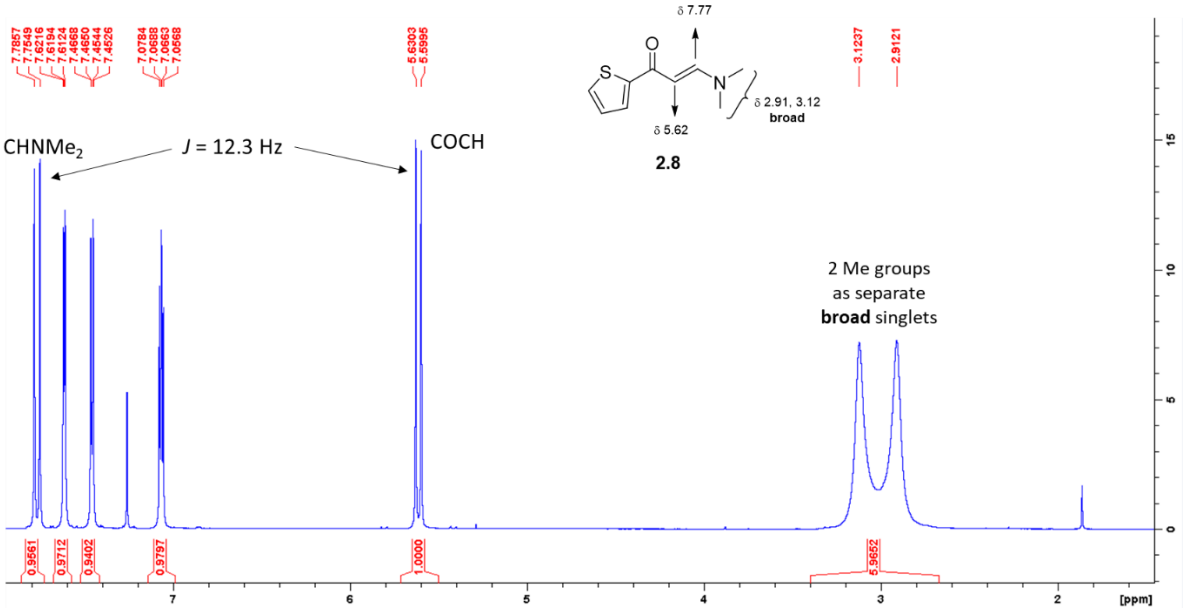

Figure 2.4: ^{1}H-NMR spectrum of **2.8**

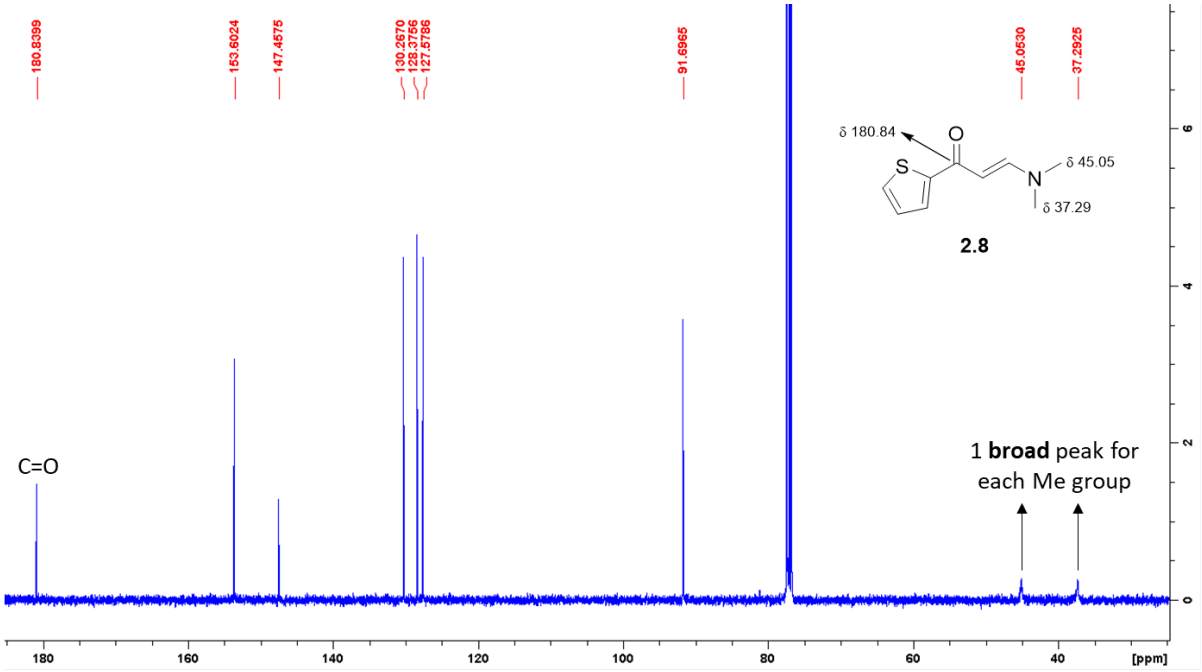

Figure 2.5: ^{13}C-NMR spectrum of **2.8**

The Me groups of the NMe_2 terminus reflect the broadened behaviour observed in the ^{1}H-NMR spectrum and in the ^{13}C-NMR spectrum of **2.8** they appear as two separate broad peaks, resonating at δ 37.29 and δ 45.05, thus providing further evidence of the restricted N-C3 bond rotation (Figure 2.5).
A comparison of the foregoing broad ^{13}C signals for the methyl groups on **2.8** with the two sharp peaks observed for the NMe units in the ^{13}C-NMR spectrum of the aza- derivative **2.14** (Figure 2.3) suggested that there is more extensive delocalisation leading to an essentially rigid system for **2.14**, which in turn is likely to have a much higher energy barrier for rotation.
The distinct differences for the NMe_2 signal between enaminones with different substituents on the 1- and 2-positions led to the postulate that the aforementioned restricted rotation suffered by the N-C3 bond was consistent amongst enaminone analogues and was directly affected by electronic effects imparted by the substituents. Further investigation of the behaviour of this bond rotation was thus deemed of interest, and Variable Temperature (VT)-NMR spectroscopy was employed in order to examine the respective rotation under a gradient of increasing temperature.[101] A sample of the furyl analogue **2.7** was used for this experiment with deuterated DMSO as the solvent, as the aforementioned derivative presented a ^{1}H-NMR spectrum that followed the signal pattern commonly seen for analogous compounds (*e.g.* phenyl (**2.1**) and thienyl (**2.8**) derivatives). Consecutive spectra acquisition after intervals of 10 °C temperature increase afforded a stacked plot of ^{1}H-NMR spectra between 25 °C and 70 °C (Figure 2.6). As is evident from the spectra, the initial two sharp singlets corresponding to the methyl groups of the NMe_2 unit broaden as the temperature increases, while they appear increasingly closer to each other, until they coalesce into a broad singlet from 55 ° to 65 °C, placing the coalescence temperature at approximately 60 °C. This is evidence of the two methyl groups gradually becoming equivalent at higher temperatures, which in turn indicates the anticipated acceleration of the N-C3 bond rotation speed upon the input of heat into the enaminone system. It can thus be suggested that the N-C3 bond rotates at a specific speed for each enaminone analogue and that this rotation speed can be tangibly influenced by electron donation or withdrawal effects from ambient substituents.

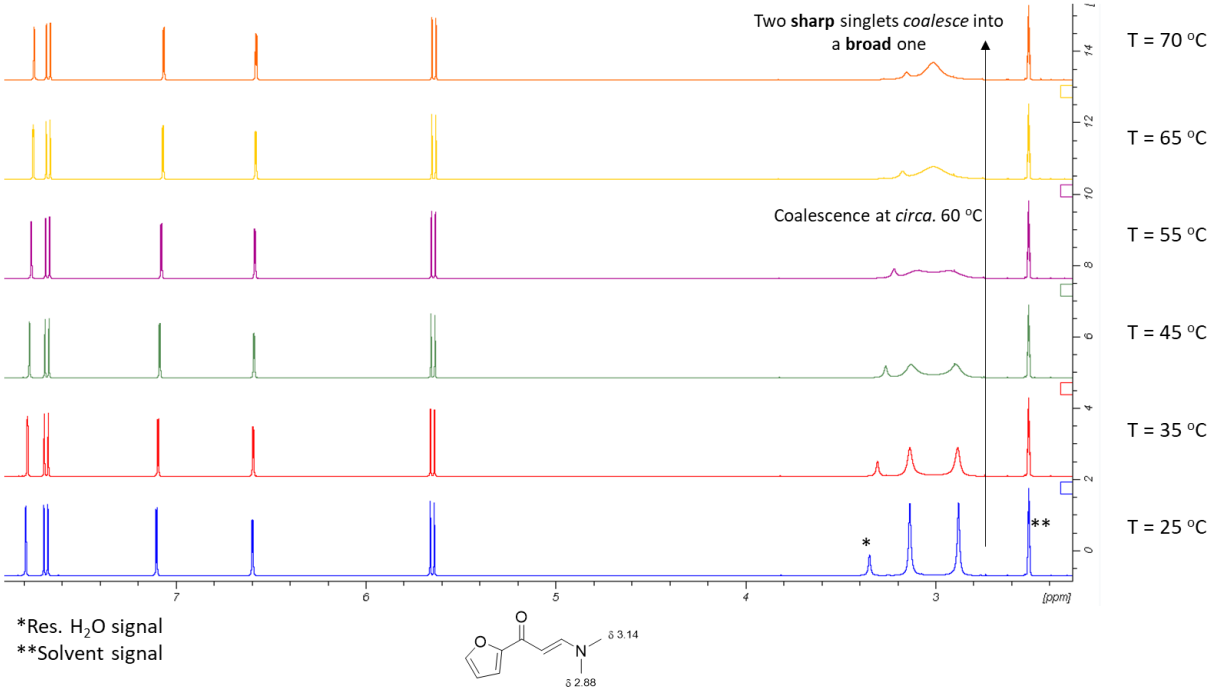

Figure 2.6: Overlaid spectra of VT-^{1}H-NMR run on analogue **2.8** from 25 ° to 70 °C at a 10 ° temperature increase pace (5 ° increase to reach 70 °C)

Apart from exploring the thermal features of enaminone systems, the coalescence temperature found by VT-NMR spectroscopy was further utilised in the calculation of the free enthalpy of rotation activation for the NMe_2 terminus, ΔG, during coalescence. If the coalescence of the two singlets into one broad singlet

is considered a chemical process with an exchange rate constant k_c occurring at 60 °C or 333 K, it is possible to use the Eyring equation for this calculation[102]:

$$k_c = \kappa \frac{k_b T_c}{h} e^{-\frac{\Delta G}{RT}}$$

where κ is the transmission coefficient, k_b is the Boltzmann constant and h is the Planck constant. With the transmission coefficient κ assumed to be equal to 1, solving the above equation for ΔG transforms it as follows (k_b =1.38 × 10^{-23} J/K, h = 6.63 × 10^{-34} Js):

$$k_c = \frac{k_b T_c}{h} e^{-\frac{\Delta G}{RT_c}} \rightarrow \frac{\Delta G}{RT_c} = \ln\frac{k_b T_c}{h} - \ln k_c \rightarrow \Delta G = RT_c\left(\ln\frac{k_b}{h} + \ln\frac{T_c}{k_c}\right) \rightarrow \Delta G = RT_c\left(23.759 + \ln\frac{T_c}{k_c}\right)$$

The constant k_c can be calculated at the coalescence temperature using the maximum peak separation in Hz at the lowest temperature (25 °C, spectrum acquired at 600 MHz):

$$k_c = \frac{\pi\Delta\nu}{\sqrt{2}} = \frac{\pi(3.13ppm - 2.88ppm)600MHz}{\sqrt{2}} = 333.1\ Hz$$

The previous equation can now produce the value for ΔG with R = 8.31 $Jmol^{-1}K$:

$$\Delta G = RT_c\left(23.759 + \ln\frac{T_c}{k_c}\right) = 8.31(Jmol^{-1}K^{-1})333(K)\left(23.759 + \ln\frac{333}{333.1}\right) = 65.745\ (KJmol^{-1})$$

This value is in good agreement with the free enthalpy of rotation activation for the phenyl analogue **2.1**, which has been studied in a similar fashion[103] and found to have a ΔG value of 63.7 $KJmol^{-1}$. It is clear that the foregoing calculations can be reproduced for any enaminone analogue with two distinct NMe_2 methyl group signals to ascertain the amount of energy that is required so that the respective N-C3 bond can rotate freely. This can be used to evaluate bond rotation speed between different derivatives, whereas it can further be used as an indication for the reactivity of a specific analogue.

The ^{1}H-NMR spectra of the styryl **2.9** and phenylethynyl **2.13** analogues merit some specific comments, as they are indicative of the differences between alkenyl and alkynyl- containing enaminone derivatives. In the case of the styryl- analogue **2.9,** the expected signals for the enamino unit (δ 5.28 for 2-H and δ 7.79 for 3-H, *J* = 12.4 Hz; δ 2.91 and δ 3.16 for the Me groups of the NMe_2 terminus) are joined by the alkene signals that appear as doublets at δ 6.85 and δ 7.58 with *J* = 15.7 Hz, a typical value of a *trans*-akene protons (Figure 2.7).[104] The absence of such protons on the triple bond of **2.13** attests that the two protons of the enaminone scaffold at δ 5.32 and δ 7.74 are the only olefinic protons in the compound, whilst the sharpness of the two singlets for the NMe_2 terminus at δ 2.91 and 3.16 can be directly correlated with the effect of the triple bond on the rotation of the N-C3 bond rotation; it appears that the presence of the triple bond has the apparent effect of decreasing this bond rotation to a greater extent than the double bond does, thus allowing for sharper singlets for these pivotal distinct Me moieties than the broadened signals seen on the styryl analogue **2.9**.

The triple bond adjacent to the carbonyl group in **2.13** was further found to have a profound effect on the sharpness of the N-Me signals in the ^{13}C-NMR spectrum (Figure 2.8). Examination of the relevant spectrum shows a broad peak at δ 174.78 that corresponds to the carbonyl carbon, as well as a signal at δ 102.17 and at δ 158.22 for the alkenyl carbons of the central double bond. The two alkynyl *C* atoms resonate closely at δ 86.53 and δ 87.79, with their peaks also being quite broadened, thus illustrating a spectroscopic behaviour that differs from the other previously observed enaminone examples. Conversely, the two methyl groups of the NMe_2 terminus appear as a sharp signal at δ 37.36 and at δ 45.36, which comes in tandem with previous spectroscopic observations on enaminones with electron-withdrawing substituents (*e.g.* **2.14**, Figure 2.3).

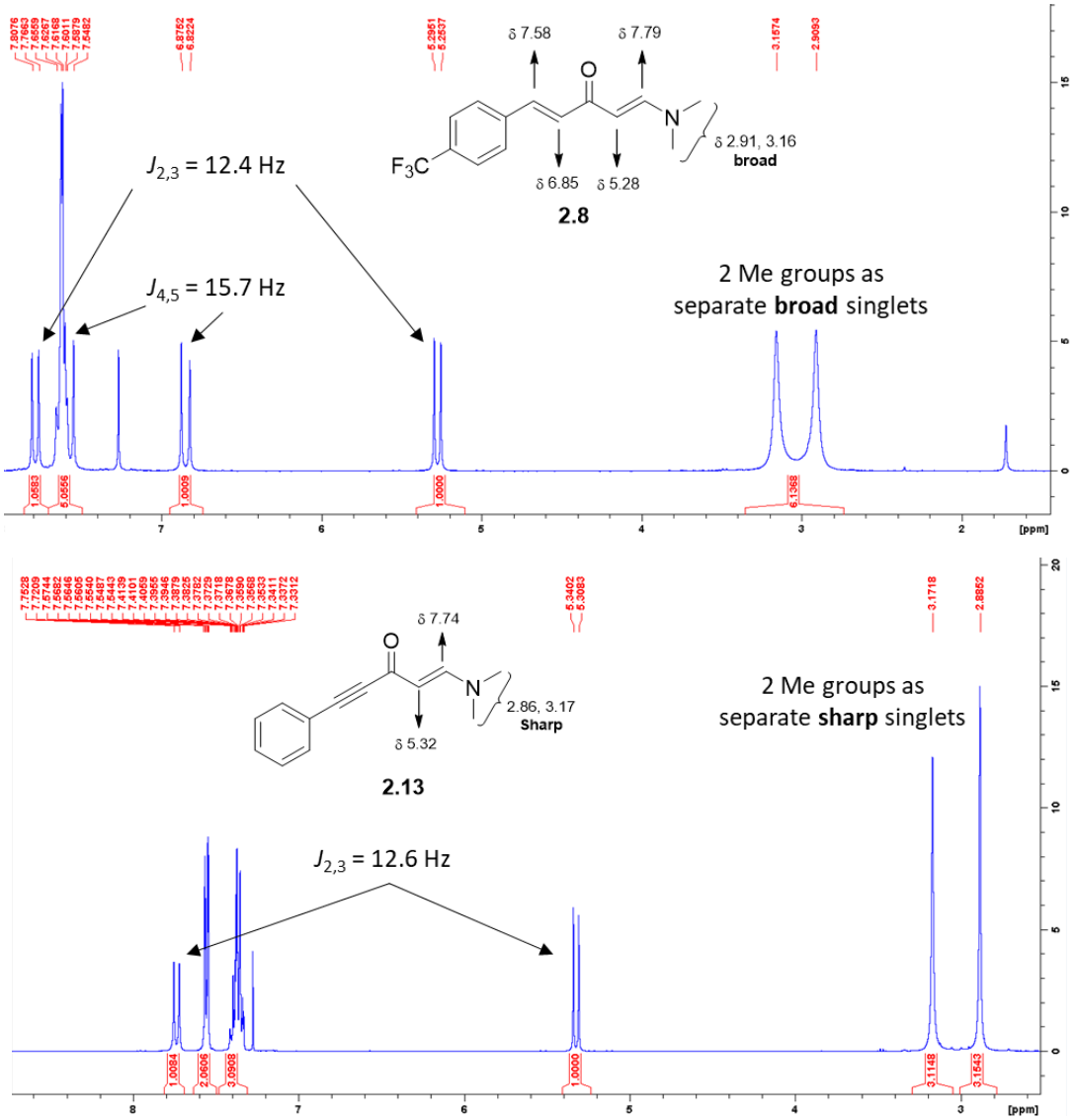

Figure 2.7: ^{1}H-NMR spectra of **2.8** and **2.13**

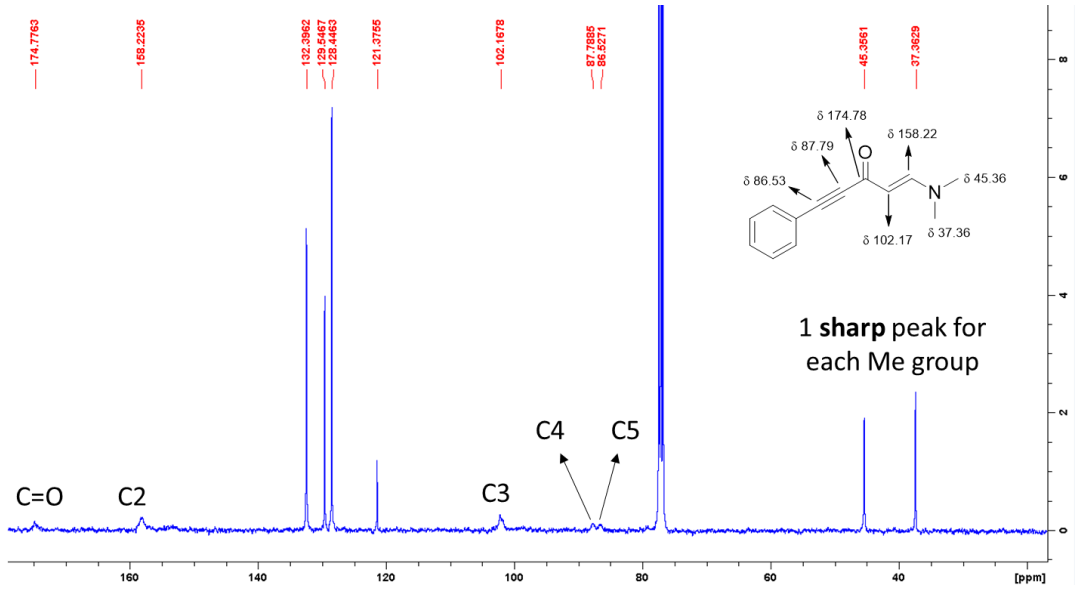

Figure 2.8: ^{13}C-NMR spectrum of **2.13**

The structure of prepared enaminones could be further verified by their IR spectroscopic profile; more specifically, the stretching band corresponding to the carbonyl unit was typically observed between 1550 and 1630 cm^{-1}. As previously commented, such C=O stretching band values deviate from the values that are common for unsaturated ketone systems (1685-1666 cm^{-1}). This decrease in frequency can be attributed to the extended conjugation caused by the neighbouring double bond in conjunction with the donation of electron density by the *N* atom of the amino terminus, with both of these effects allowing for C=O bond stretching at lower frequencies. This significant shift in the carbonyl stretching frequency unequivocally confirms the conversion of an α-methyleneketone precursor into its enaminone counterpart.

Whilst the geometry of the monosubstituted enaminoketones **2.1**, **2.6 - 2.13** could be readily established by examination of their 2-H – 3-H coupling constants, NOE NMR experiments were employed to determine the geometry of the 1,2-distubstituted compounds **2.2** - **2.4**. Specifically, the spatial proximity between the NMe_2 unit and the protons on the 2-substituent was examined to ascertain their position on the C2-C3 double bond. The NOE NMR spectrum of **2.2** is an indicative example, wherein two key spatial correlations can be seen, one between the vinyl proton and the Me groups of the NMe_2 unit and another between the foregoing aliphatic signals and a signal for the aromatic protons at *circa* δ 7.2 (Figure 2.9). Furthermore, the absence of a similar NOE contour between the vinyl proton and any of the aromatic signals provides supplementary evidence of a *Z*- configuration for the 2-phenyl group and the NMe_2 terminus, thus broadening the range of enaminones with *E*- geometry so as to include di-substituted enaminone systems as well as mono-substituted enaminone systems.

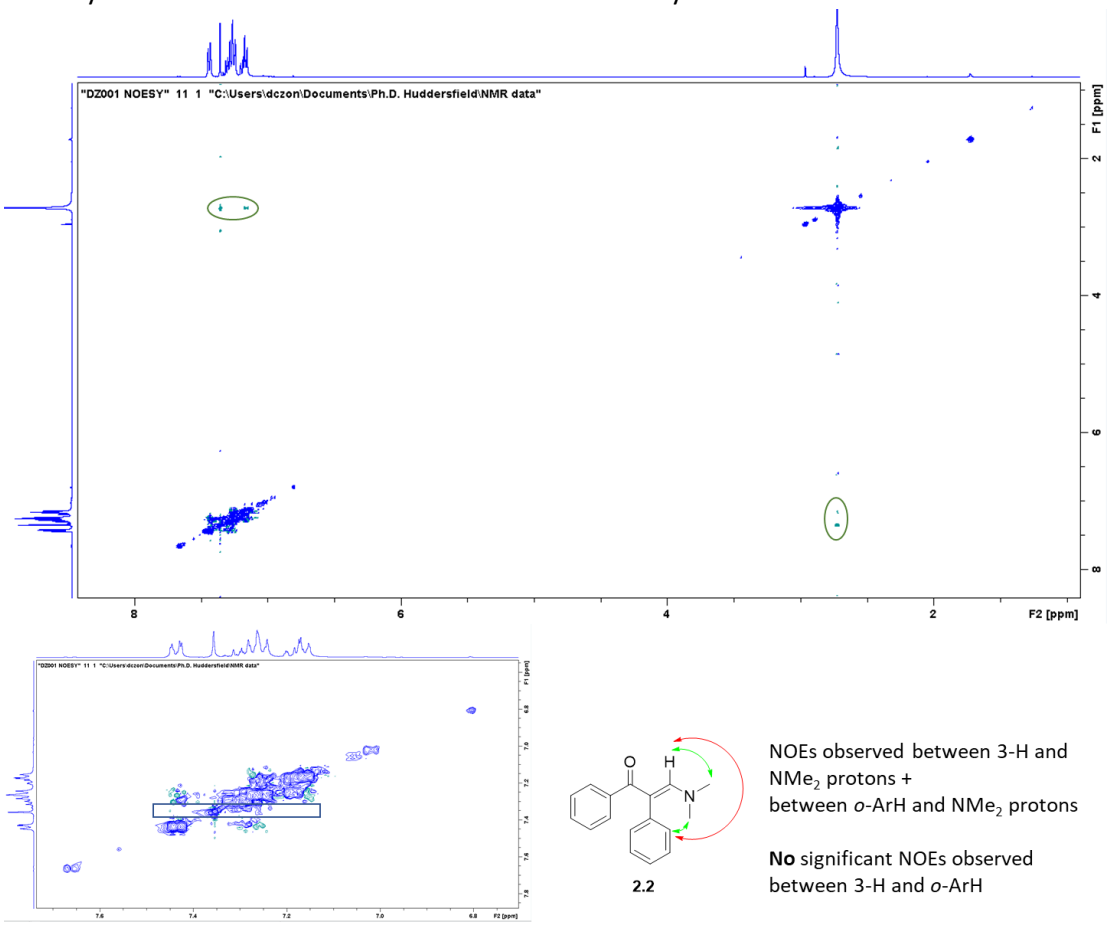

Figure 2.9: NOE NMR of **2.2** showing key correlations that denote a *cis* geometry

Given its effectiveness in ascertaining spatial relationships between proximal groups on the enaminones, NOE spectroscopy was limited by the requirement of protons being present on the 2-substituent. In analogues where the 2-substituent of the enaminoketone did not possess any H atoms, attempts to grow

crystals suitable for examination by X-ray crystallography were undertaken. This technique was specifically utilised for the cyano derivative **2.5**, prepared in 56.7 % yield by heating a solution of benzoylacetonitrile **2.15** in DMFDMA at reflux overnight (Scheme 2.2). The crystal structure of this analogue shows that the CN moiety is indeed *cis* to the amino terminus, thus confirming the preference for an *E*- geometry once more (Figure 2.10).

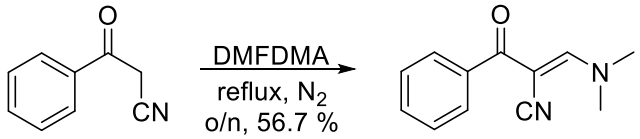

2.15 **2.5**

Scheme 2.2: Preparation of the cyano enaminone analogue **2.5**

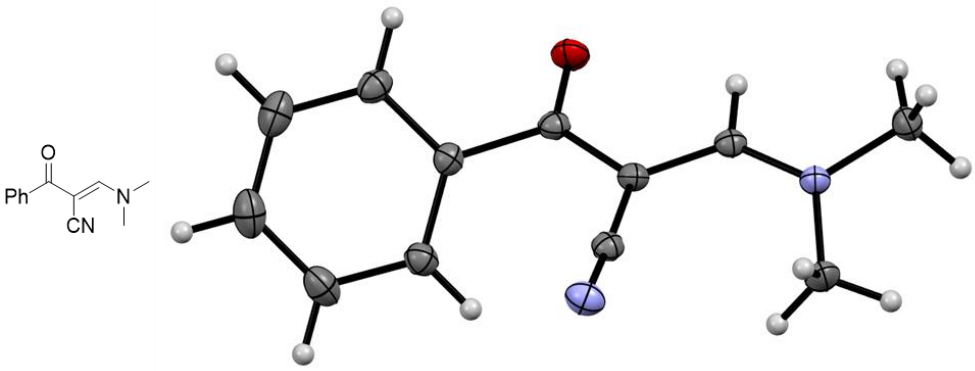

Figure 2.10: X-ray crystallography structure of analogue **2.5**, showing the adopted *E*- geometry (thermal ellipsoids shown at 50 % probability level)

The preparation of **2.5** was accompanied by an unexpected aspect: the formation of a stable ionic species arising from the union of two molecules of the starting material **2.15** (Scheme 2.3). During the foregoing DMFDMA addition to benzoylacetonitrile, a highly polar compound was isolated from the reaction mixture by column chromatography, which could not be unequivocally characterized after an extensive array of spectroscopic experiments; ^{1}H-NMR spectroscopy revealed the presence of 10 aromatic protons in the region of δ 7.39 – 7.52, along with a downfield singlet at δ 8.02 accounting for 1 proton and 1 singlet in the aliphatic region (δ 3.09) which integrated to 12 protons. The relevant ^{13}C-NMR spectrum hinted at the preservation of the carbonyl moiety due to a peak at δ 190.04, whereas the presence of three peaks at *circa* δ 54 could be interpreted as one carbon environment with splitting from a neighbouring ^{15}N nucleus[105,106]. Typical vibration frequencies at 2199 and 1612 cm^{-1} in the IR spectrum of this compound pinpointed the CN and CO groups respectively, but no further information could be inferred as to how these groups were connected. Fortunately, it was possible to grow crystals of suitable quality from EtOH/hexane for X-ray analysis, revealing that the side-product was a salt comprising of a carbanionic 'dimer' and a NMe_4^+ counterion (**2.5a**). Interestingly, a repeat of this preparation using PhMe as solvent at room temperature yielded the target compound **2.5** together with a different salt, the structure of which was also ascertained *via* X-ray crystallography and found to contain the aforementioned carbanionic unit bound with a different counterion ($Me_2NCH{=}N^+Me_2$, **2.5b**). A comparison of the yields recorded for the two routes towards the main product **2.5** also revealed that allowing more space to the reactants by using PhMe ameliorated the efficiency of the transformation (85.0 % for the solvent run at r.t. over 56.7 % for neat DMFDMA run at reflux), thus indicating that use of a solvent may be beneficial

for the formation of this derivative. The ^{1}H-NMR spectra obtained for these side-products are shown in Figure 2.11, whilst their 3D structures are presented in Figure 2.12.

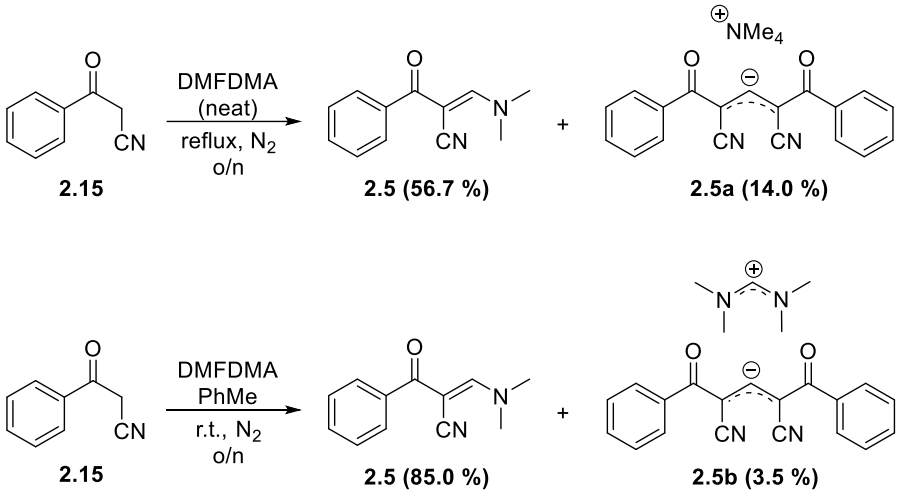

Scheme 2.3: Ionic species as side-products of enaminone formation

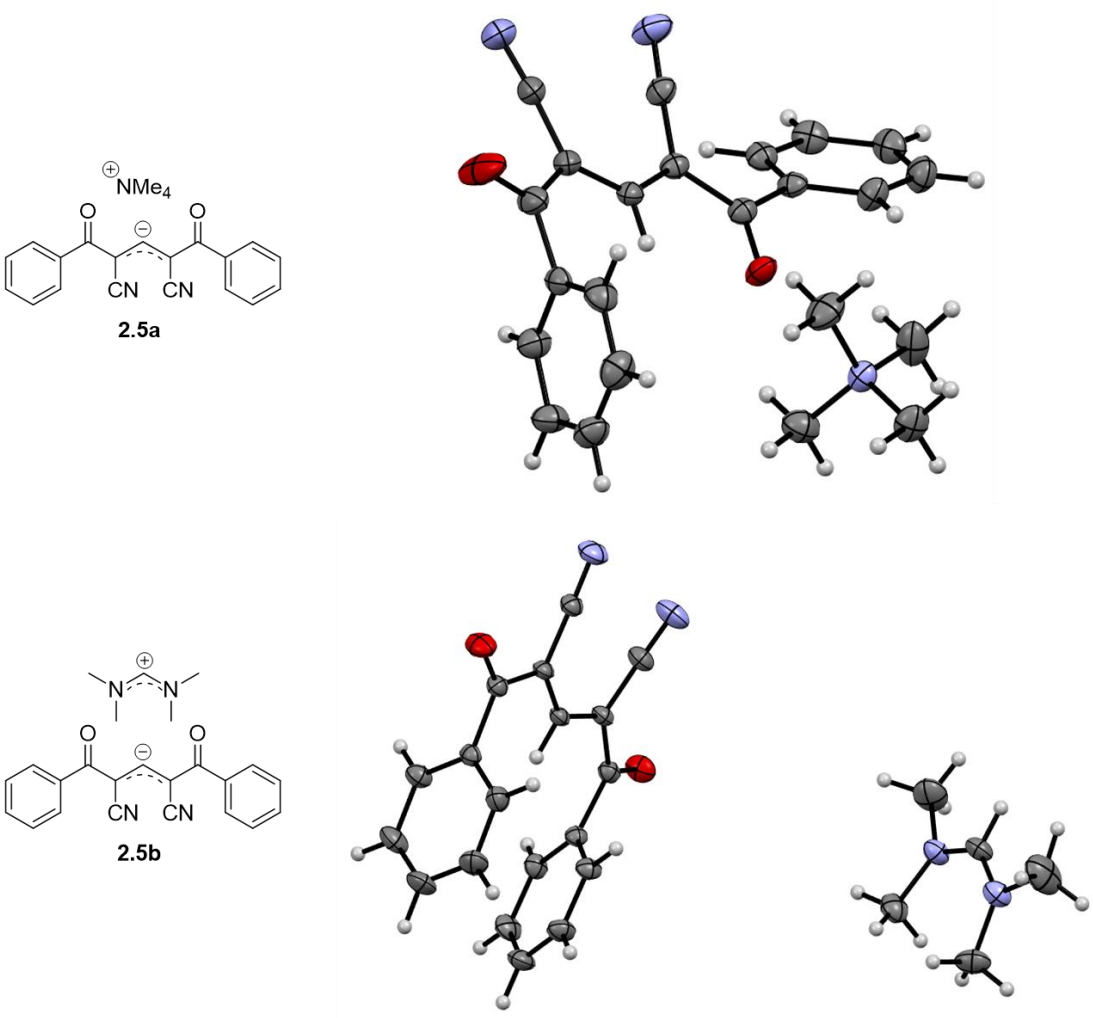

Figure 2.11: Crystal structure of ionic side-product obtained *via* the initial reaction protocol (**2.5a**) (above), Crystal structure of ionic species obtained by using PhMe as solvent (**2.5b**) (below)

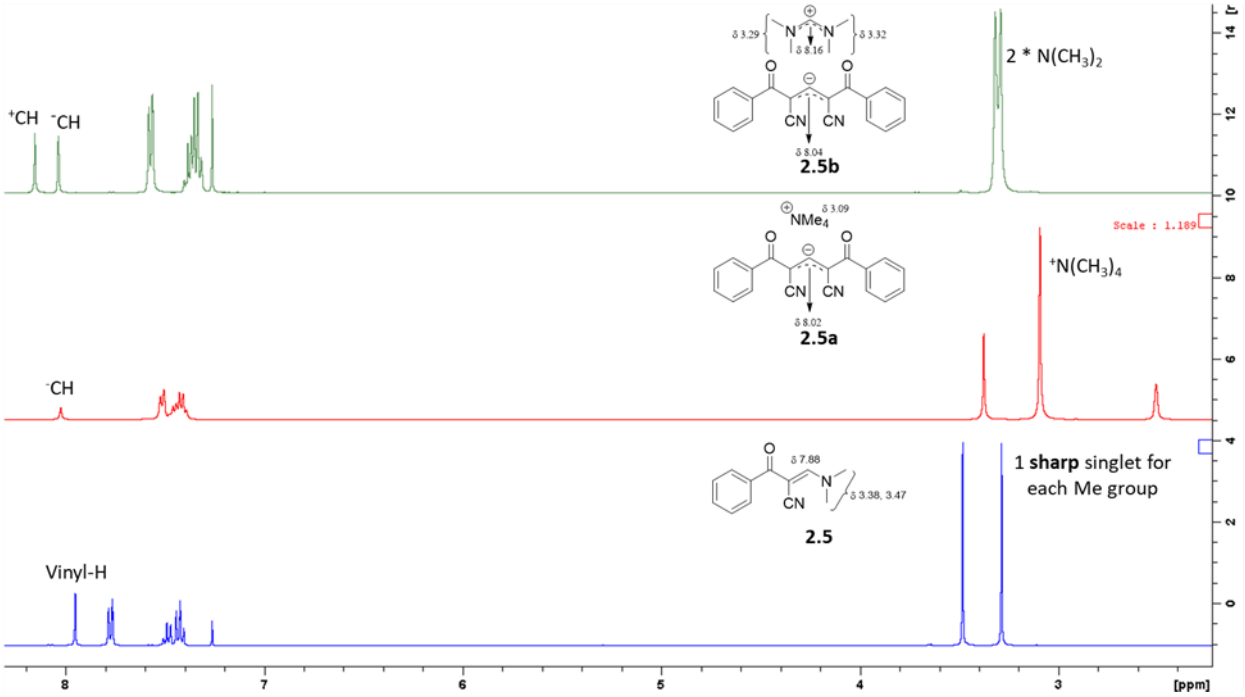

Figure 2.12: ^{1}H-NMR of the cyano analogue **2.5** and the two side-products **2.5a** and **2.5b**

In conjunction with the chemical behaviour of the reactants, the crystallographic data obtained for the structure of these side-products can be utilised to propose a mechanism for their formation (Scheme 2.4). It can be deduced that the presence of the strongly electron-withdrawing CN moiety in benzoylacetonitrile (**2.15**) is pivotal to the formation of the bis-benzoyl carbanion by stabilising the corresponding enolate, as no other starting ketone afforded similar dimer-like species upon treatment with DMFDMA, including the ester-containing analogue **2.3**. This feature can be viewed as a threshold of tendency towards "dimerization", which is subject to the electron-withdrawing character of the 2-substituent. In order to further explore this unusual behaviour, the isolated enaminone product (**2.5**) was re-dissolved in DMFDMA and heated to reflux over 22 h to test if the foregoing carbanion would be generated under these conditions, although unfortunately this only resulted in decomposition of the enaminone **2.5**; hence, it can be suggested that the formation of the side-products **2.5a** and **2.5b** involves both the starting material **2.15** and the enaminone product **2.5**, and a proposed route can be constructed (Scheme 2.4).
Such a route presumably includes the initial formation of the enolate ion **2.16**, which is followed by its transformation to the enaminone **2.5** through the established DMFDMA addition mechanism and its consequent addition to a second **2.16** ion to produce the dimer-like intermediate **2.17**. The dimethylamino unit on this species is able to be protonated and cleaved in the presence of MeOH, whereas the methoxy ion that forms as a result can cleave the acidic α-proton on the eliminated intermediate **2.18** towards the key carbanion **2.19**. Molecular clustering may favour this chain of transformations, as evident by the lower side-product yield (3.5 % for **2.5b** over 14.0 % for **2.5a**) when carrying out the conversion in a solvent. The presence of PhMe also appears to influence the mechanism that furnishes these ionic species, as the different counterions on the two ionic compounds have to arise from different rearrangements that take place during their formation. Solvent-free conditions were found to be suitable for an S_N2 attack on the electrophilic methyl group on the iminium fragment of DMFDMA (**2.20**, documented in section **1.1.2.2**[12,13]) by the aforementioned dimethylamine by-product towards the tetramethylammonium cation in **2.5a**[107], whereas the presence of PhMe led to the direct addition of Me_2NH to **2.20** and the formation of the bis-dimethylamino cation in **2.5b** instead.

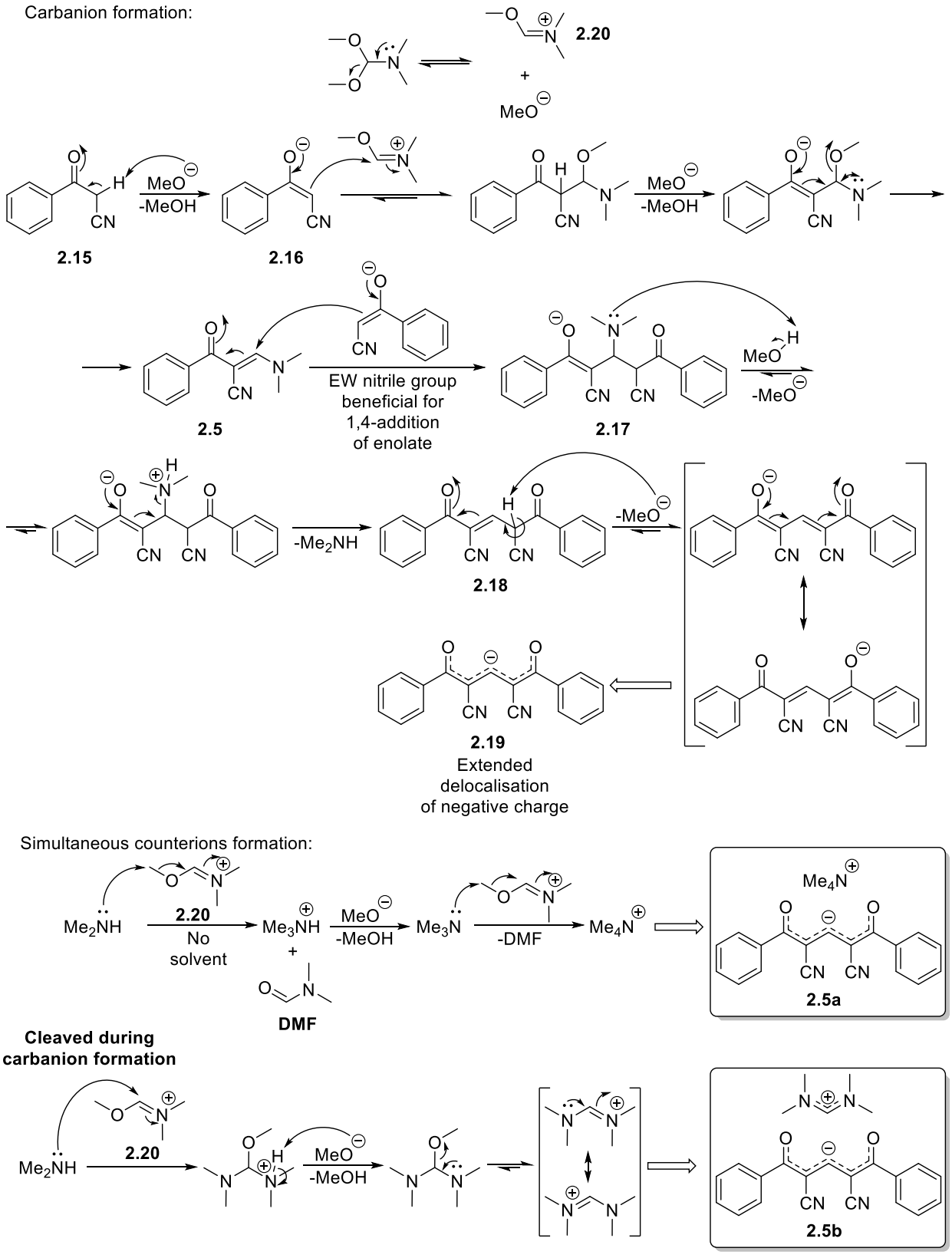

Scheme 2.4: Proposed mechanism for the formation of side-products **2.5a** and **2.5b**

Apart from **2.5**, the use of PhMe as solvent was further employed for the preparation of other enaminoketone analogues upon examination of the relevant literature. [22,25] For these derivatives, PhMe solutions of the starting ketones with DMFDMA were heated under reflux over varying time periods to produce the short series of enaminoketones shown in table 2.2.

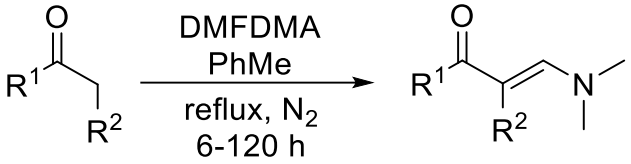

2.21 - 2.23

Entry	Compound No.	R^1	R^2	t (h)	Yield (%)
1	**2.21**	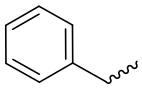	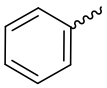	6	77.0
2	**2.22**	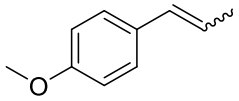	H	120	60.0
3	**2.23**	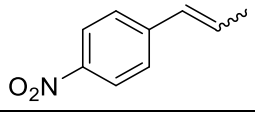	H	6	77.3

Table 2.2: Enaminones prepared using PhMe as solvent

The three derivatives (**2.21** – **2.23**) that were prepared *via* this iteration of the original protocol were afforded in good yields upon solvent removal and Et_2O trituration. Of note is the case of the methoxy analogue **2.22**, which required 6 days to reach reaction completion and was only isolated in a noticeably lower yield (60.0 %). Although this iteration provided satisfactory results, the initial method was efficient enough so that no further research regarding use of solvents was required.

The last alternative route evaluated for the reaction between α-methyleneketones and DMFDMA involved the use of L-proline as an organocatalyst, mirroring the research work discussed in section **1.1.2.2**.[20,21] The proposed mechanism, previewed for analogue **2.1** in Scheme 2.5, involves the formation of an imine intermediate (**2.24**) which can attack DMFDMA with consequent cleavage of MeOH, facilitated by the carboxylic end of the amino acid. Abstraction of the second acidic proton and loss of a second MeOH fragments affords an iminium intermediate (**2.25**), which is hydrolysed towards the enaminone target and the retrieved catalyst.

An assessment of the foregoing mechanism hints at a potential detrimental effect of a 2-substituent on the starting α-methyleneketone due to steric interference, which could also explain the screening of this catalytic process solely on mono-substituted starting materials.[20] To ascertain this hypothesis, specific derivatives (**2.1**, **2.5** and **2.6**), which had already been prepared, were synthesised again *via* this protocol, along with one new analogue (**2.26**), thus compiling a small compound library that is shown in table 2.3. In spite of the small number of prepared analogues, a few interesting insights can be obtained from the presented data. With regards to method reproducibility, juxtaposition of the obtained and the literature-reported yields illustrates that the catalytic conversion proceeds as anticipated, whilst any discrepancies in yields may derive from different purification procedures (recrystallisation instead of column chromatography).

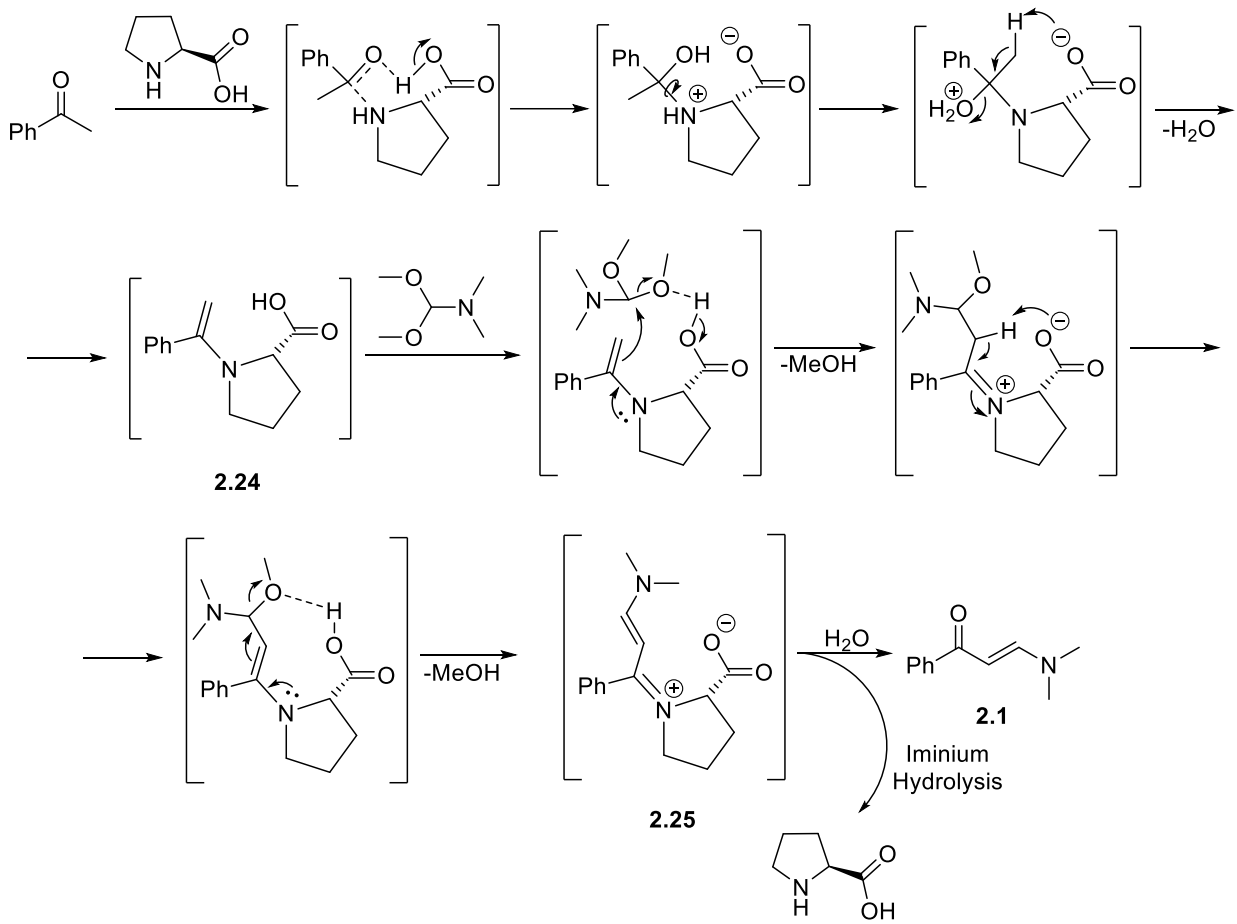

Scheme 2.5: Proposed mechanism of L-proline catalysis of dimethylaminomethylene addition

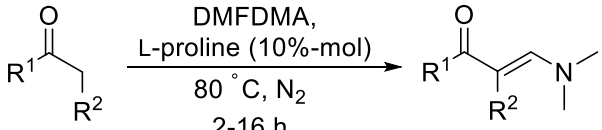

2.1, **2.5**, **2.6**, **2.26**

Entry	Compound No.	R^1	R^2	t (h)	Yield (%)	Reported t (h)[20,21]	Reported yield (%)[20,21]
1	**2.1**	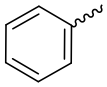	H	3.5	85.2	1	90.0
2	**2.5**	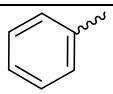	CN	3	62.0	-	-
3	**2.6**	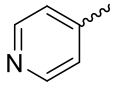	H	2	83.3	1	88.0
4	**2.22**	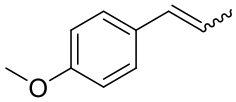	H	16	57.1	-	-
5	**2.26**	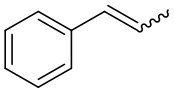	H	16	82.1	2	82.0

Table 2.3: Enaminone systems obtained *via* L-proline organocatalysis

Comparing the yields of the phenyl (**2.1**) and pyridyl (**2.6**) derivatives with the yields reported using the original, uncatalyzed method reveals that the expected increase in yield is not unilateral but dependent on the substituents on the substrate; although the phenyl analogue responds well (85.2 % after 3.5 h at 80 °C versus 69.0 % after reflux overnight), its pyridyl counterpart appears to be affected by the activation potency of the catalyst only in terms of shorter reaction time (2 h over 16 h), as evidenced by the practically identical yields between the two sets of conditions (83.3 % for the organocatalysis run at 80 °C and 84.9 % for the initial run). This "stagnancy" in yield is also evident in the case of the methoxystyryl analogue **2.22**, as the use of L-proline for the preparation of this enaminone (entry 4, Table 2.3) resulted in a 57.1 % yield after chromatographic purification, which is quite close to the yield recorded for the non-catalysed attempt of this reaction in PhMe (60.0 %, entry 2, Table 2.2) after trituration of the crude with Et_2O. Despite the inefficiency of this method in improving the synthesis of this analogue, the recorded yield was achieved after 16 h of reaction time, which is a significant improvement over the 120 h of reaction time required to reach a similar conversion extent during the solvent run. In the case of the 2-substituted cyano derivative **2.5**, use of the catalyst resulted in a marginally higher yield (62.0 % over 56.7 %), but this is noticeably lower than the yield reported when PhMe is used as solvent (85.0 %). These findings cement the claim of substitution on the 2-position hindering the ameliorating effect of L-proline, thus resulting in this method being avoided for further di-substituted analogues (Figure 2.13).

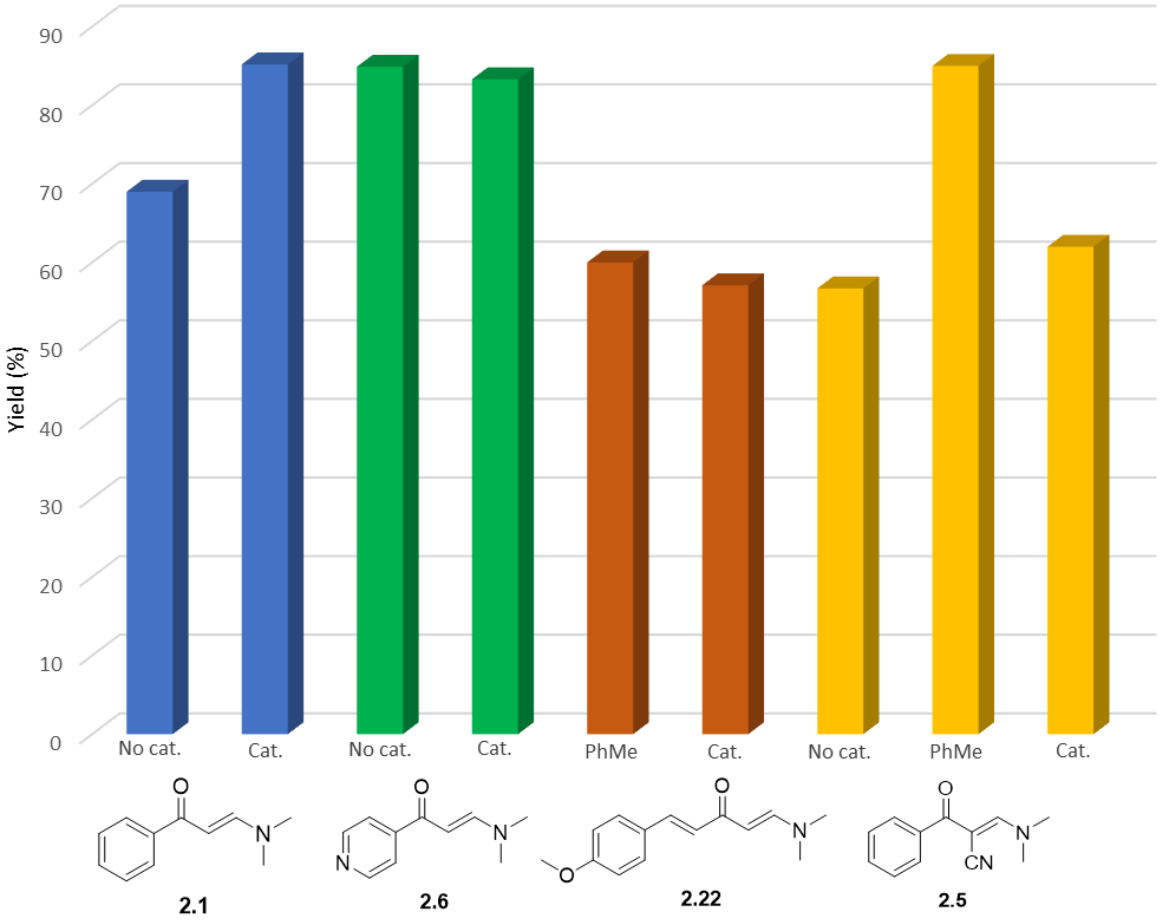

Figure 2.13: Effects of organocatalysis towards selected enaminones

2.1.2 Attempts at double substitution using DMFDMA

Another point of interest during the synthesis of the enaminone precursors revolved around the notion that a ketone with a methylene unit on either side of the carbonyl group would undergo two dimethylaminomethylene unit additions using at least two equivalents of DMFDMA, as established by the relevant literature.[22,23,24] Three target analogues (**2.30** - **2.32**) were selected to be prepared in order to test method efficiency along with substate tolerance, and the results of these attempts are shown in table 2.4.

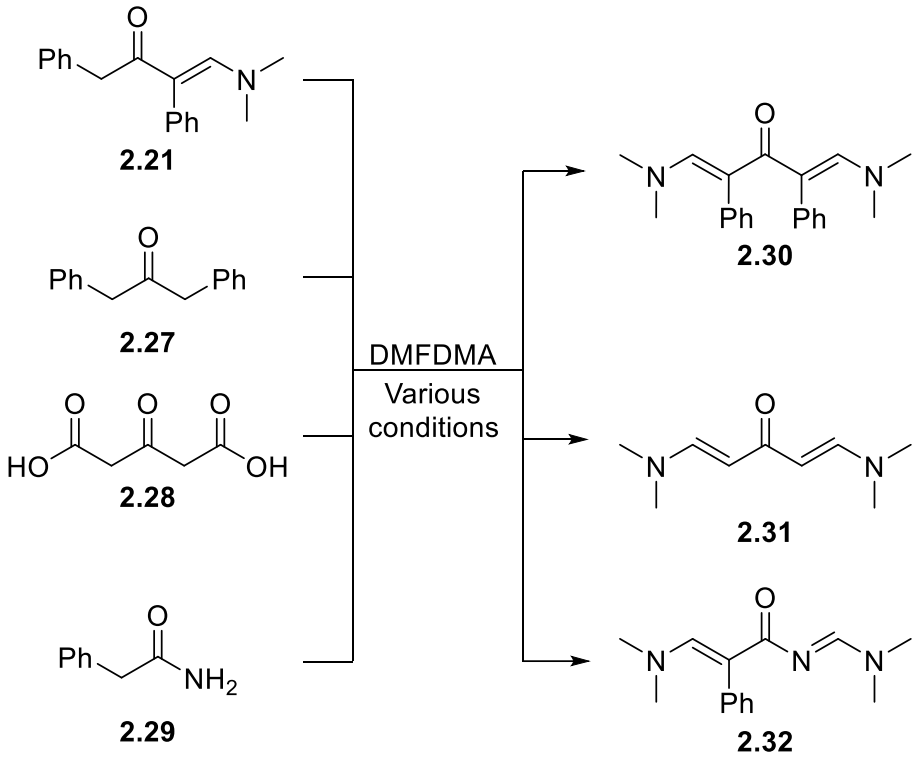

Entry	Substrate	Product	Solvent	Temperature (°C)	Catalyst	t (h)	Yield (%)
1	**2.27**	**2.30**	PhMe	110	-	24	n/a
2	**2.27**	**2.30**	-	103	-	16	n/a
3	**2.21**	**2.30**	-	80 to 103	L-proline	2	n/a
4	**2.28**	**2.31**	-	r.t. to 70	-	1	10.0
5	**2.28**	**2.31**	PhMe	0 to 35	-	3	59.1
6	**2.29**	**2.32**	-	103	-	6	70.1

Table 2.4: Attempts at double DMFDMA substitution

The findings from these reaction attempts indicate a discrepancy with the research work by Elnagdi *et al*., and by Taylor and Skotnicki, as the methods described in these publications[22,23] (Scheme 2.6) should have theoretically been replicated in terms of reagents and reaction conditions and resulted in the same results.

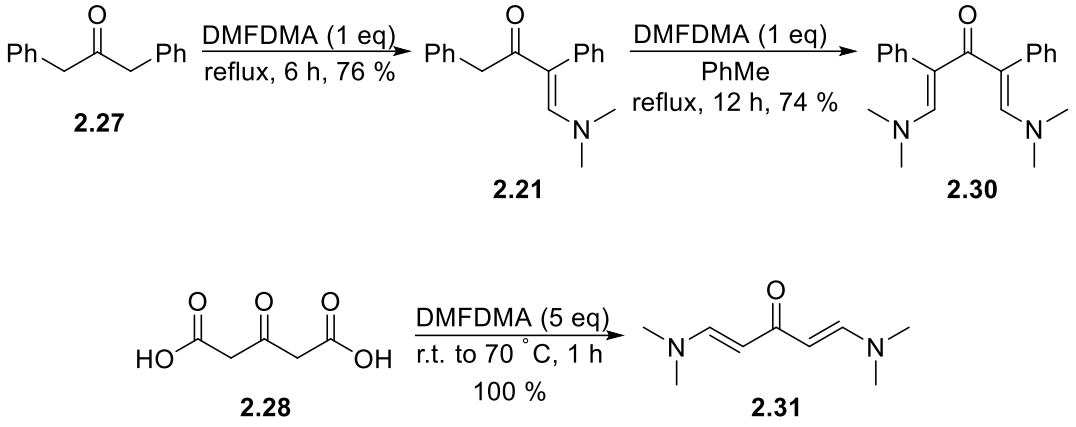

Scheme 2.6: Reported literature conditions for double DMFDMA substitution[22,23]

In the case of the diphenyl analogue **2.30**, heating a solution of the starting ketone **2.27** with DMFDMA in PhMe for 24 h (entry 1, Table 2.4) only afforded the monosubstituted species **2.21** (Figure 2.14a). Further attempts to obtain the bis-enaminone **2.30** from either **2.27** (entry 2, Table 2.4) or the mono-adduct **2.21** (entry 3, Table 2.4) using neat DMFDMA or L-proline organocatalysis did not fare any better, only affording a small amount of a side-product that was identified as the pyran-4-one derivative **2.33** (6.7 % yield) (Figure 2.14c,d); ^{1}H-NMR analysis of the crude reaction mixture before chromatographic purification showed no signals attributable to the 3,5-diphenylpyran-4-one **2.33** (Figure 2.14b), although two singlets at δ 7.49 and δ 2.58 were observed, presumably corresponding to the vinyl proton and the NMe_2 aliphatic protons.

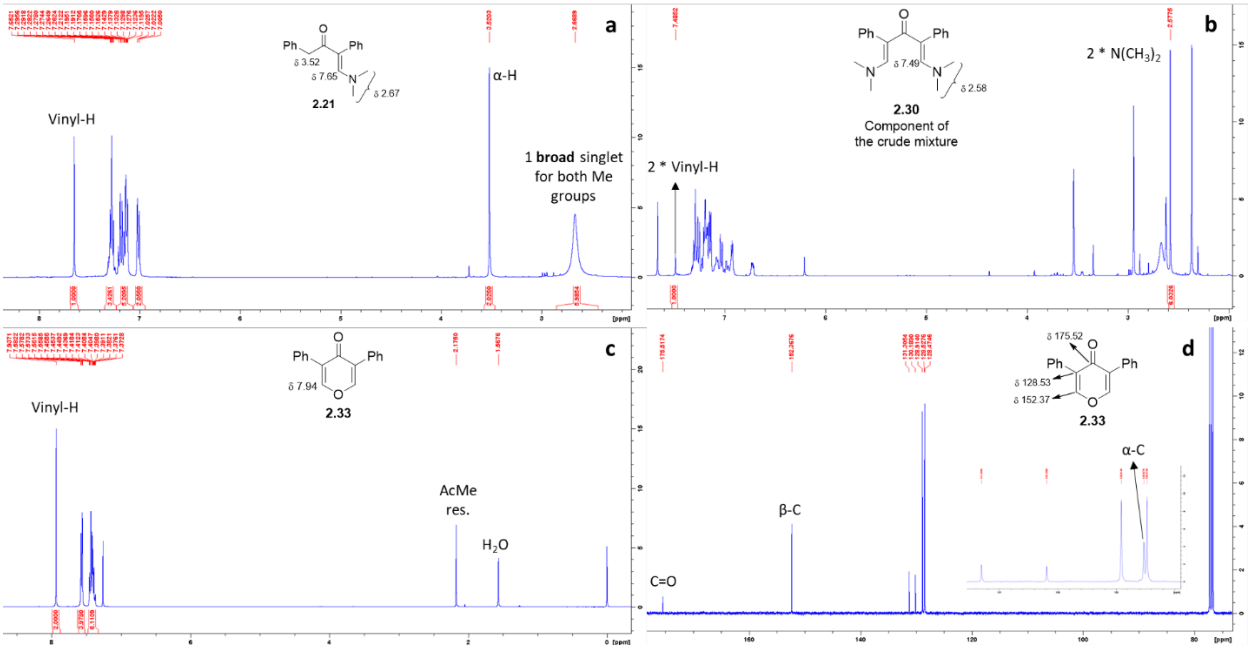

Figure 2.14: a) ^{1}H-NMR spectrum of the mono-substituted analogue **2.21**, b) ^{1}H-NMR of the final crude mixture towards **2.30**, showing potential signals for the bis-enaminone analogue, c) ^{1}H-NMR of pyran-4-one (**2.33**) side-product, d) ^{13}C-NMR spectrum of **2.33**

These findings denote that **2.30** does form to a small extent but, upon contact with atmospheric moisture or H_2O molecules trapped in the silica matrix, it can cyclise *in silica* towards the more stable conjugated system **2.33** (Scheme 2.7).

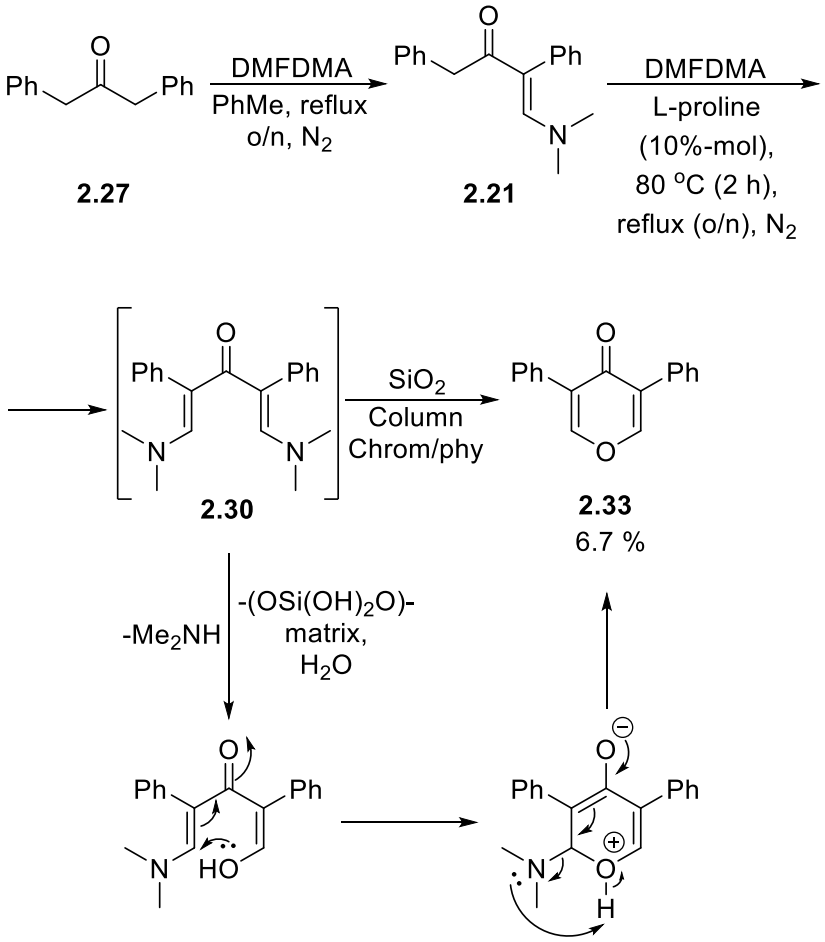

Scheme 2.7: Isolation of a pyranone heterocycle (**2.33**) upon a double DMFDMA substitution attempt

In search for a plausible explanation of the inactivation of **2.21** towards a second DMFDMA substitution, the signal corresponding to the dimethylamino group on **2.21** was examined. These two methyl groups afford a broadened singlet, which is indicative of relatively slow bond rotation and a high double-bond character for the C-N bond (examined in section **2.1.1**). It can thus be suggested that there is a significant resonance stabilisation effect, which is greater than that observed for typical enaminone systems exhibiting distinct sharp NMe_2 singlets in their ^{1}H-NMR spectra. Enolate formation actively negates this electron cloud delocalisation, hence α-deprotonation of **2.21** is tied to a high energy barrier that needs to be overcome before any further interaction of **2.21** with DMFDMA can occur (Scheme 2.8).

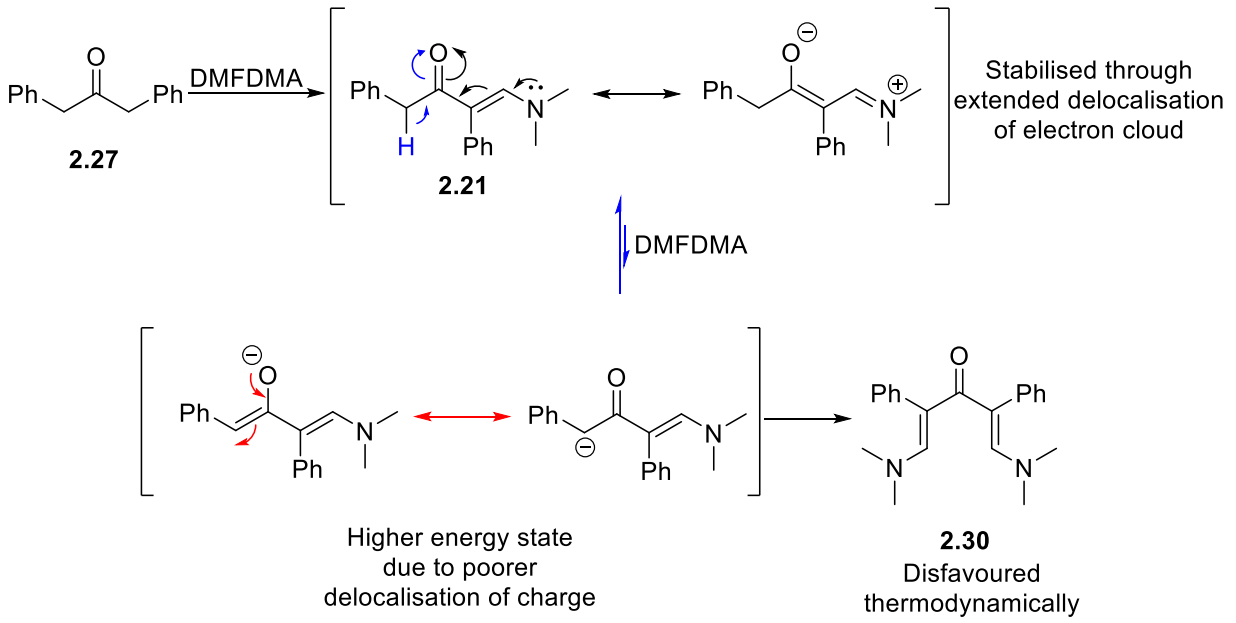

Scheme 2.8: Inactivation of **2.21** towards DMDMA substitution owing to stabilisation through resonance

Concerning the non-substituted analogue **2.31** (1,5-bis(dimethylamino)penta-1,4-dien-3-one), the intuitive strategy of using acetone as the starting ketone was abandoned due to concern that the foregoing behaviour of the diphenyl counterpart **2.27** would also manifest during the addition of DMFDMA to acetone. For this reason, synthesis of the bis-enaminone **2.31** required a different precursor, which was elected to be 3-oxopentanedioic acid (**2.28**), in accordance with the experimental protocol by Taylor and Skotnicki[23]. Unfortunately, repeating this experimental procedure led mostly to starting material decomposition, with the target compound being obtained at a low yield (10.0 %). Using a solvent (PhMe) and mixing the reagents at a lower temperature seems to have rectified this process, resulting a greatly ameliorated yield (59.1 %). The isolated compound could be readily identified *via* ^{1}H-NMR spectroscopy by the characteristic set of doublets at δ 4.97 and δ 7.52 (J = 12.8 Hz) for the two sets of *trans* protons, along with the anticipated singlet at δ 2.88 (Figure 2.15a). The ^{13}C-NMR validated this evidence on account of the carbonyl peak at δ 186.95, as well as the broadened signal at δ 41.09 corresponding to the 4 aliphatic *C* atoms of the 2 NMe_2 termini (Figure 2.15b).

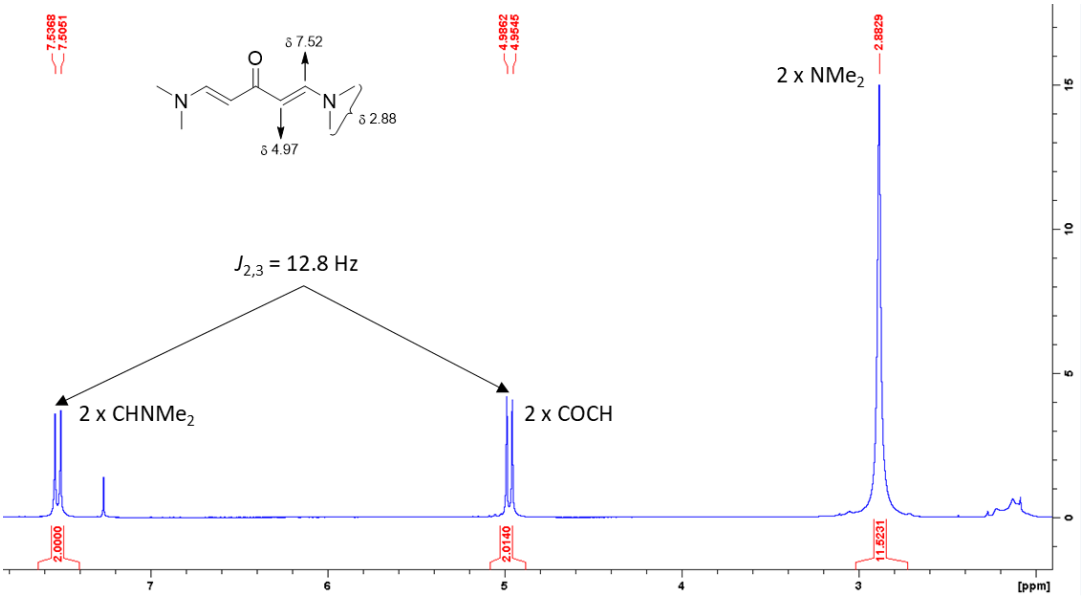

Figure 2.15a: ^{1}H-NMR spectrum of the bis-enaminone **2.31**

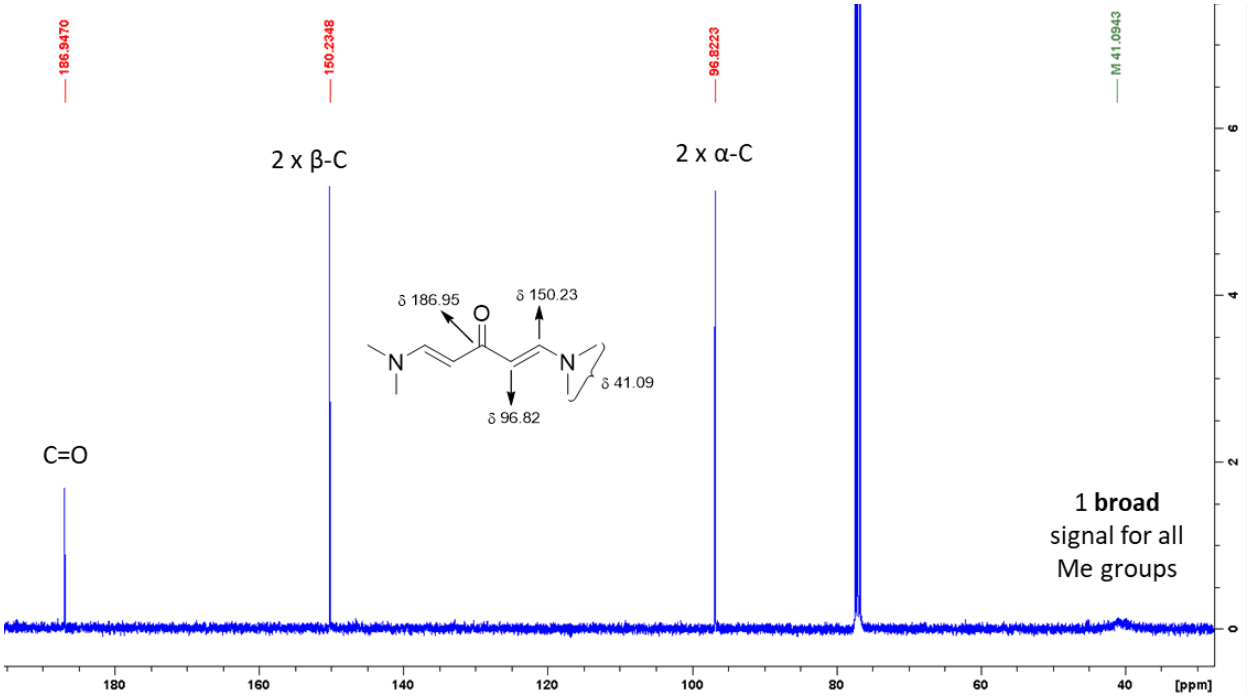

Figure 2.15b: ^{13}C-NMR spectrum of the bis-enaminone **2.31**

It can thus be inferred that higher temperatures are detrimental for the conversion, as the carboxyl moieties on the starting material can be deprotonated by the methoxy fragment of DMFDMA to produce an intermediate that is capable of undergoing rapid decarboxylation towards acetone. Such a process is thermodynamically favoured due to the release of CO_2, whereas the volatile acetone escapes the reaction mixture without interacting with DMFDMA (Scheme 2.9a). Conversely, a lower temperature allows for proton cleavage to occur at the α-positions towards an enolate ion that can attack the dimethylamino fragment of DMFDMA and afford the carboxyl intermediate **2.34**, which can be consequently converted into the desired enaminone **2.31** after an elimination process that includes decarboxylation and elimination of a methanol fragment.

Testing the same transformation to the analogous amide **2.29** was met with success without the use of a solvent or a catalyst, hinting at the pivotal role of the second *N* atom in containing the delocalisation of electron cloud on the enamine unit of the mono-substituted intermediate **2.35**. As a result, the carbonyl group has the capacity of being involved in the enolate formation that is necessary for the addition of the second dimethylaminomethylene moiety and the furnishing the target compound **2.32** (Scheme 2.9b). This analogue provides an interesting set of spectroscopic data, as the two dimethylamino termini appear to behave differently (Figure 2.16); the enone-adjacent group is observed as a singlet that denotes the equivalence of the two methyl groups, whereas the terminus in proximity to the imine moiety translates into two sharp singlets, which is evident of a high double bond character for the carbon-nitrogen bond. Moreover, the two olefinic signals are also influenced by the presence of the second *N* atom, as the proton of the imine group is further deshielded by virtue of a negative inductive effect. These assignments can also be aligned with previous enaminone examples (**2.2**, **2.14**) that include similar proton environments as those for **2.32**.

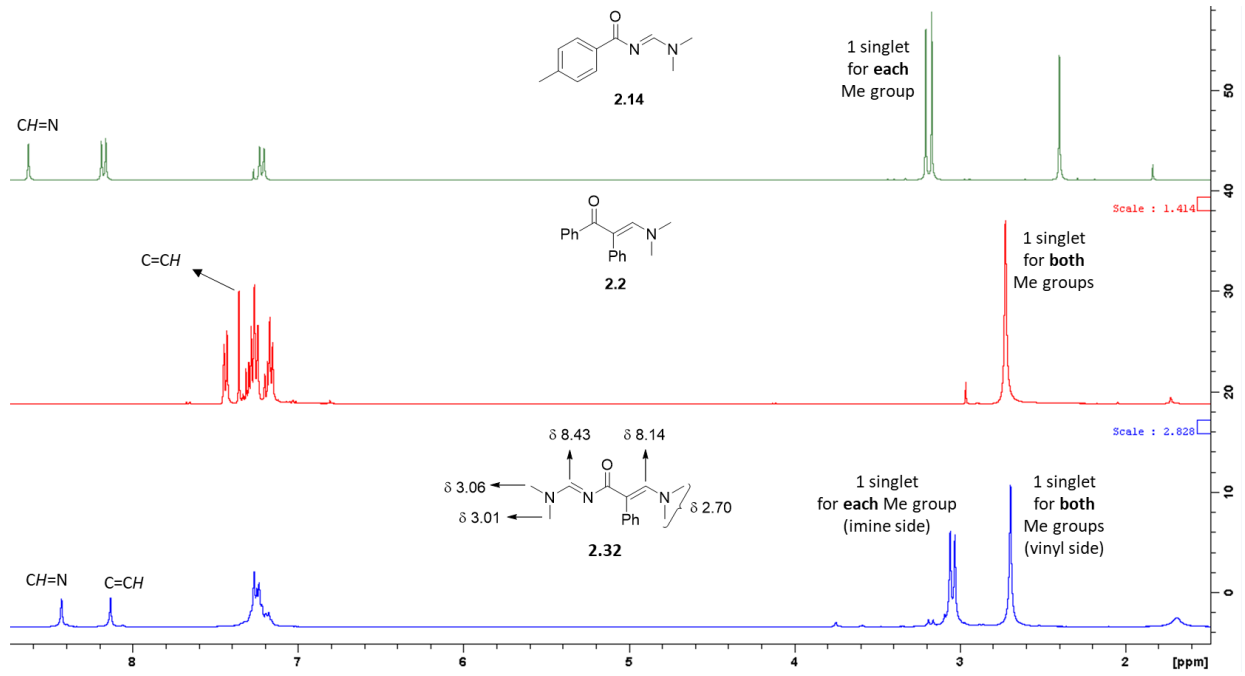

Figure 2.16: ^{1}H-NMR spectrum of the bis-enaminone **2.32** juxtaposed with the spectra of analogues **2.2** and **2.14**

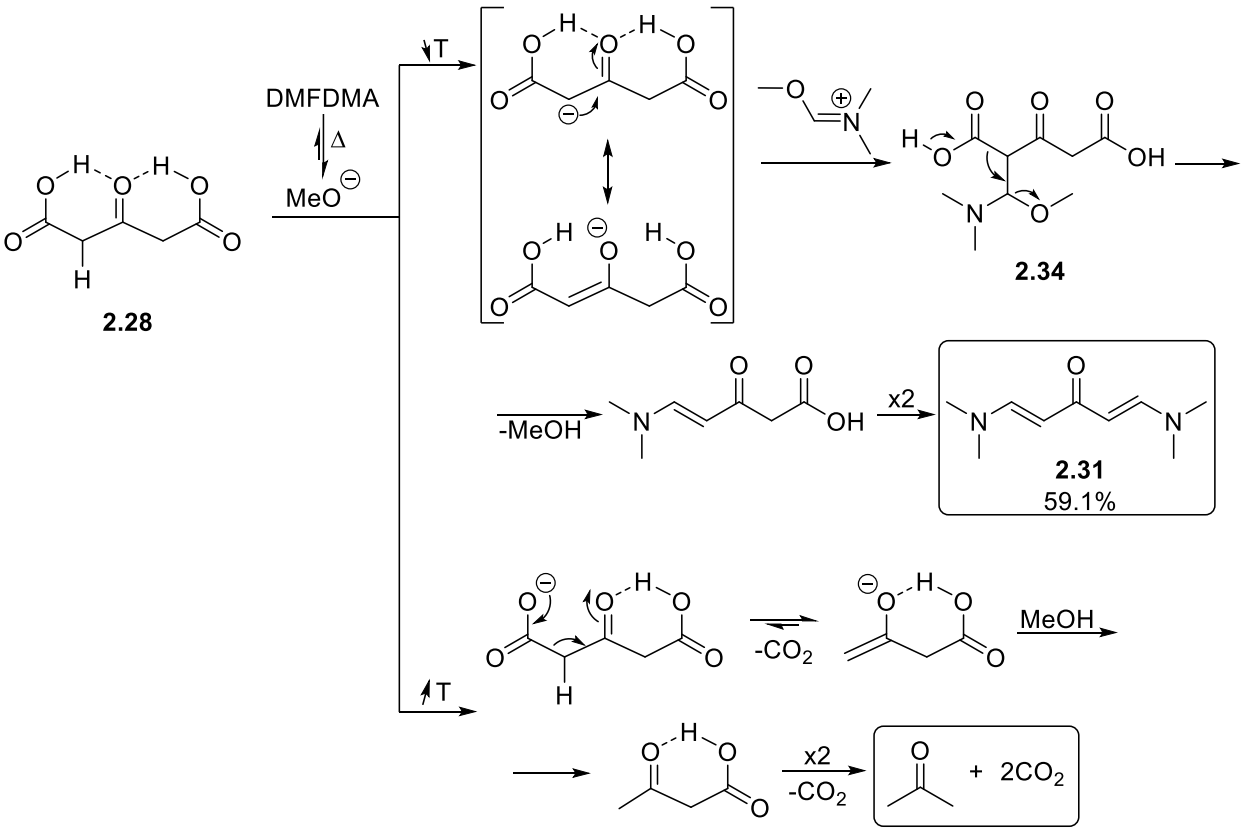

Scheme 2.9a: Observations on the formation of bis-enaminone **2.31**

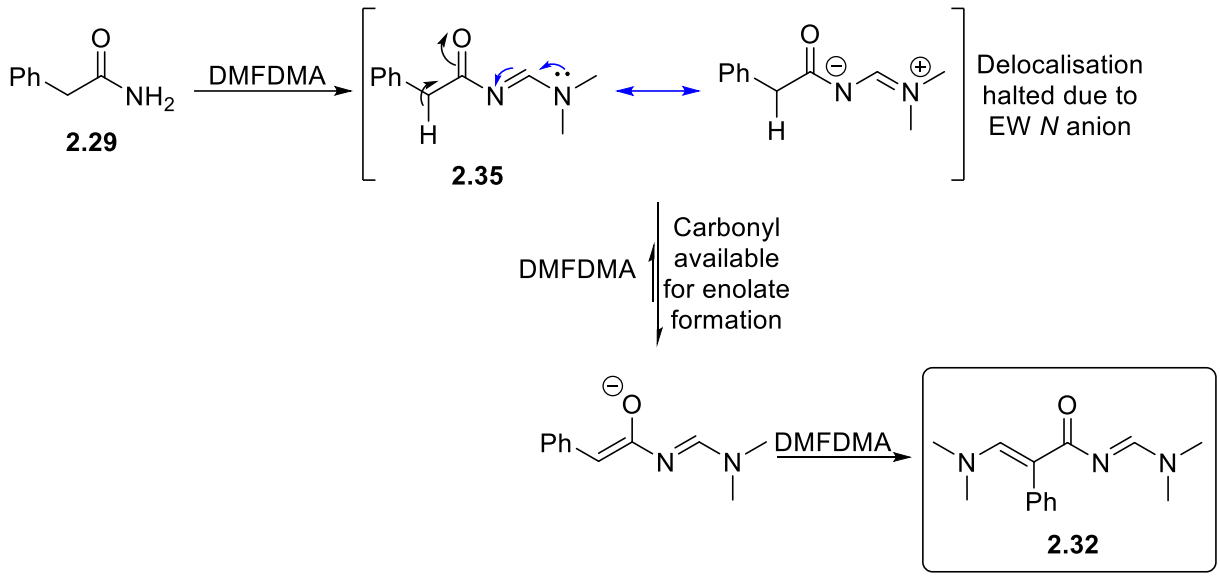

Scheme 2.9b: Observations on the formation of bis-enaminone **2.32**

2.2 Sulfene addition to enaminones towards 3,4-dihydro 1,2-oxathiine 2,2-dioxides

2.2.1 Analogue library and reaction overview

With the enaminone precursor library at hand, their cycloaddition with sulfenes was subsequently explored. In accordance with the research undertaken by Schenone *et al*. (discussed in sections **1.1.2.3** and **1.2.2.2**), the sulfenes used were prepared *in situ* from their corresponding sulfonyl chlorides upon treatment with Et_3N in the presence of the enaminone substrates. An aqueous work-up, followed by either crystallisation or column chromatography was used to isolate the pure product. The library of 3,4-dihydro-1,2-oxathiine 2,2-dioxide adducts produced by this conversion is detailed in table 2.5. Examination of the analogue structures juxtaposed with their respective yields presents valuable insights into the governing precepts of sulfene addition. There appears to be an increase in the yield when moving from lower to higher phenyl substitution patterns, as seen in the examples of the 6-phenyl (**2.52**, 37.4 %, entry 16), 3,6-diphenyl (**2.43**, 44.0 %, entry 8), 5,6-diphenyl (**2.41**, 78.1 %, entry 6) and 3,5,6-triphenyl (**2.36**, 77.0 %, entry 1) derivatives, which constitutes evidence of electron donating effects influencing the reaction. In contrast to this trend, EW groups on the 6- position of the heterocycle product appear to moderate the yield of the reaction (*e.g.* pyridyl analogue **2.44**, 9.7 %, entry 9, phenylethynyl analogue **2.51**, 34.8 %, entry 16), whereas withdrawal of electron density on the 2-position of the respective reacting enaminones seems to deactivate them completely (attempts towards **2.38**, **2.39** and **2.53**). This loss of reactivity can be correlated with the ^{1}H-NMR findings on such enaminone analogues (*e.g.* **2.11** and **2.14**), presented in section **2.1.1**. The resonance of the NMe_2 unit aliphatic signals as two distinct, sharp singlets (*e.g.* δ 3.29 and δ 3.48 for **2.5**, δ 3.17 and δ 3.21 for **2.14**) indicates that electron withdrawing groups permit electron density to be donated by the terminal *N* atom of the NMe_2 unit leading to a C3-N bond with a high double bond character. This discrepancy in the electron density on these analogues may in fact be the cause of their inability to interact with the sulfene species, given that all other analogues were found to undergo this transformation. This insight is particularly important, as it shows that, despite the presence of a nucleophilic centre on the sulfene (electron rich *C* atom) and an electrophilic unit on the enaminone (imino *C* atom), no bond formation occurs, inferring that the enone moiety is pivotal to the success of this addition which is indicative of a potential hetero Diels-Alder mechanistic route for the

formation of these heterocyclic adducts (Figure 2.17). The foregoing observations could pave the way for further experiments using a more extended series of structurally diverse enaminoketones in order to build up a series of empirical rules for substituent reactivity during sulfene additions to enaminoketones.

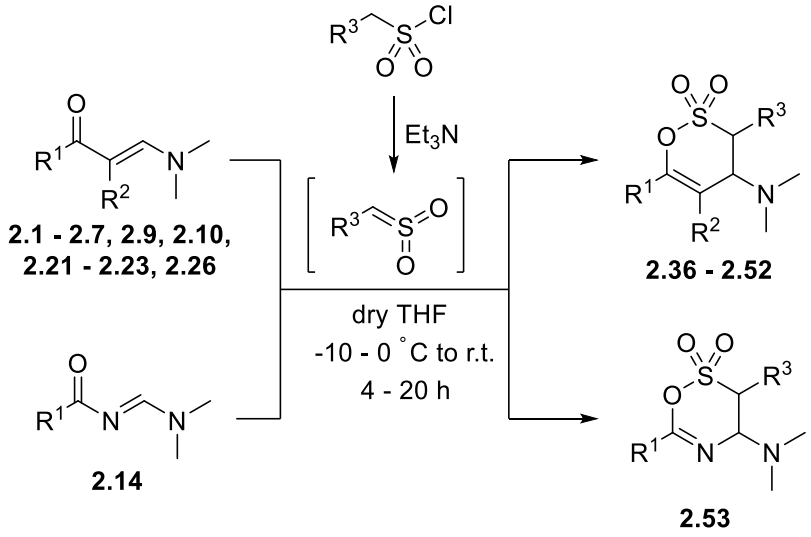

Entry	S. M. No.	Prod. No.	R^1	R^2	R^3	t (h)	Yield (%)
1	**2.2**	**2.36**	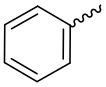	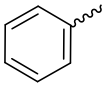	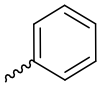	16	77.0
2	**2.2**	**2.37**	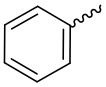	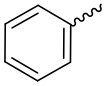	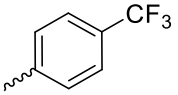	16	60.0
3	**2.5**	**2.38**	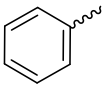	CN	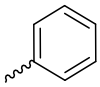	16	0.0
4	**2.3**	**2.39**	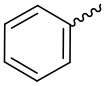	CO_2Et	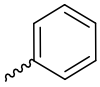	16	0.0
5	**2.21**	**2.40**	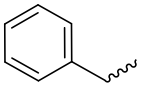	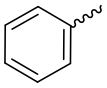	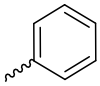	20	48.0
6	**2.2**	**2.41**	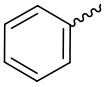	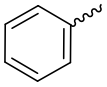	H	16	78.1
7	**2.4**	**2.42**	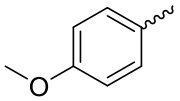	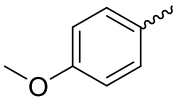	H	16	78.8
8	**2.1**	**2.43**	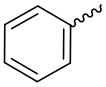	H	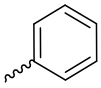	16	44.0
9	**2.6**	**2.44**	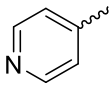	H	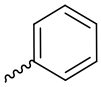	16	9.7
10	**2.26**	**2.45**	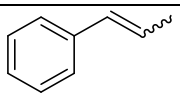	H	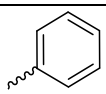	16	65.2

Table 2.5a: Library of 3,4-dihydro 1,2-oxathiine 2,2-dioxides with varying 3-, 5- and 6- substituents

Entry	S. M. No.	Prod. No.	R^1	R^2	R^3	t (h)	Yield (%)
11	**2.22**	**2.46**	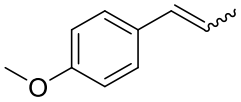	H	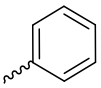	18	76.7
12	**2.23**	**2.47**	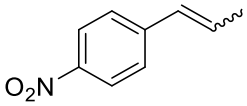	H	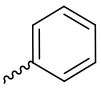	4	54.1
13	**2.9**	**2.48**	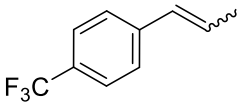	H	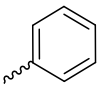	19	72.3
14	**2.10**	**2.49**	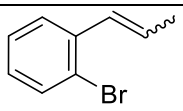	H	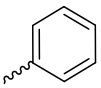	19	60.5
15	**2.7**	**2.50**	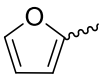	H	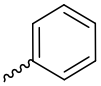	17	66.9
16	**2.13**	**2.51**	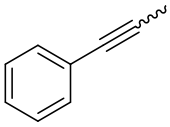	H	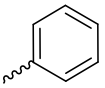	16	34.8
17	**2.1**	**2.52**	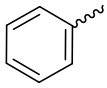	H	H	16	37.4
18	**2.14**	**2.53**	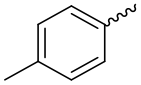	-*	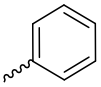	16	0.0
*N atom on the 2-position instead of a *C* atom							

Table 2.5b: Library of 3,4-dihydro 1,2-oxathiine 2,2-dioxides with varying 3-, 5- and 6- substituents

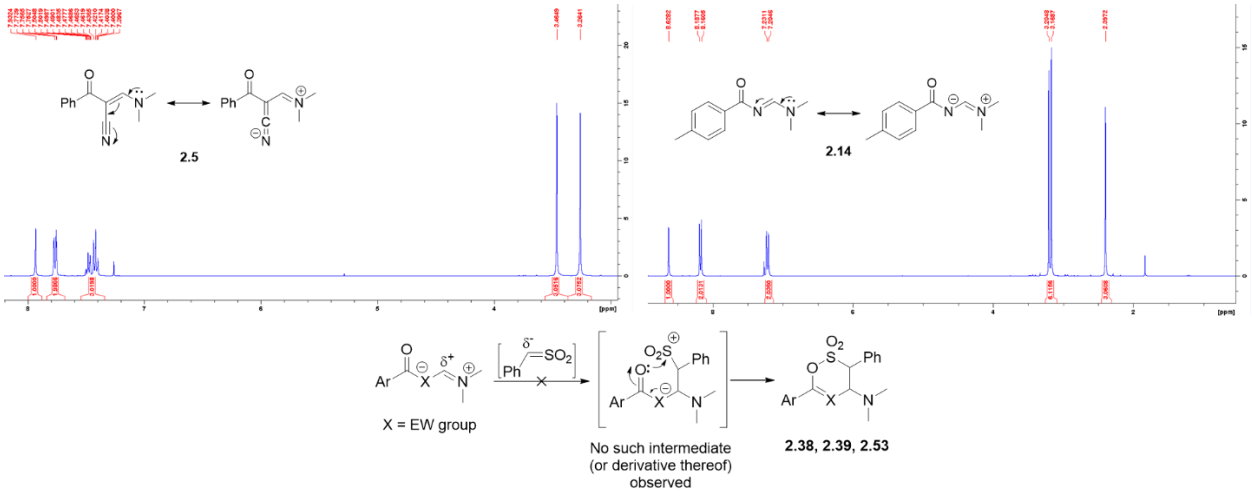

Figure 2.17: Failure of sulfene addition on enaminones with imine-like moieties hinting at a concerted mechanistic process with the enone as a diene requisite

Surprisingly, substitution on the 3-position of the 1,2-oxathiine 2,2-dioxide product seems to be inconsequential for the formation of the heterocycle products; when comparing the pair of phenyl substituted examples **2.36** and **2.41**, the presence of the 3-phenyl group seems to have practically no effect on the yields of the 1,2-oxathiine 2,2-dioxides (77.0 % for **2.36**, 78.1 % for **2.41**). Only the presence

of the EW trifluoromethyl (CF_3) moiety on the *para* position of the 3-phenyl ring (example **2.37**) seems to affect the yield, albeit to a small extent (60.0 % for **2.37**, 78.1 % for **2.41**). This "stagnant" response to the presence of an activating but bulky group, such as a phenyl ring, on the sulfene constitutes an indication that steric hindrance may prevail over electronic effect in the mechanism of this reaction.

The prepared heterocyclic systems share specific spectroscopic features that are characteristic for the 3,4-dihydro-1,2-oxathiine-2,2-dioxide group and thus indicative of the success of a sulfene addition. An examination of the ^{1}H-NMR spectra of selected analogues (Figure 2.18) reveals than the key signals correspond to the aliphatic protons of the 1,2-oxathiine backbone, observed between δ 3.0 and δ 5.0, along with the six NMe_2 protons that appear as a sharp singlet at *circa* δ 2.3 and the olefinic 5-H (whenever present) which is commonly observed near δ 6.0. Comparing signals for various substitution patterns highlights the effect of the 3-phenyl group in shielding the adjacent proton, whereas the 4-amino group is found to have the converse effect on 4-H due to a negative inductive effect by the *N* atom. An exception to this trend is seen in the case of 3,6-substituted analogues (*e.g.* furyl analogue **2.50** (Figure 2.18b)), where the peak for 3-H was always shifted upfield and was observed between the signals for 4-H and 5-H. With regards to analogues with no substituents on the 3-position (Figure 2.18c and d), the two diastereotopic protons 3-H and 3'-H appear to resonate at different frequencies and present different coupling constants when coupled to the neighbouring 4-H, thus affording a larger $J_{3,4}$ for the pair in an *anti*- arrangement and a smaller $J_{3',4}$ for the protons that are *syn* to each other. It should be noted that the aforementioned signals relate to only one of the two possible 3,4-dihydro-1,2-oxathiine 2,2-dioxide isomers that can be obtained from a sulfene addition to an enaminoketone, constituting a facet of these heterocycles formation that will be elaborated upon during later sections of this discussion.

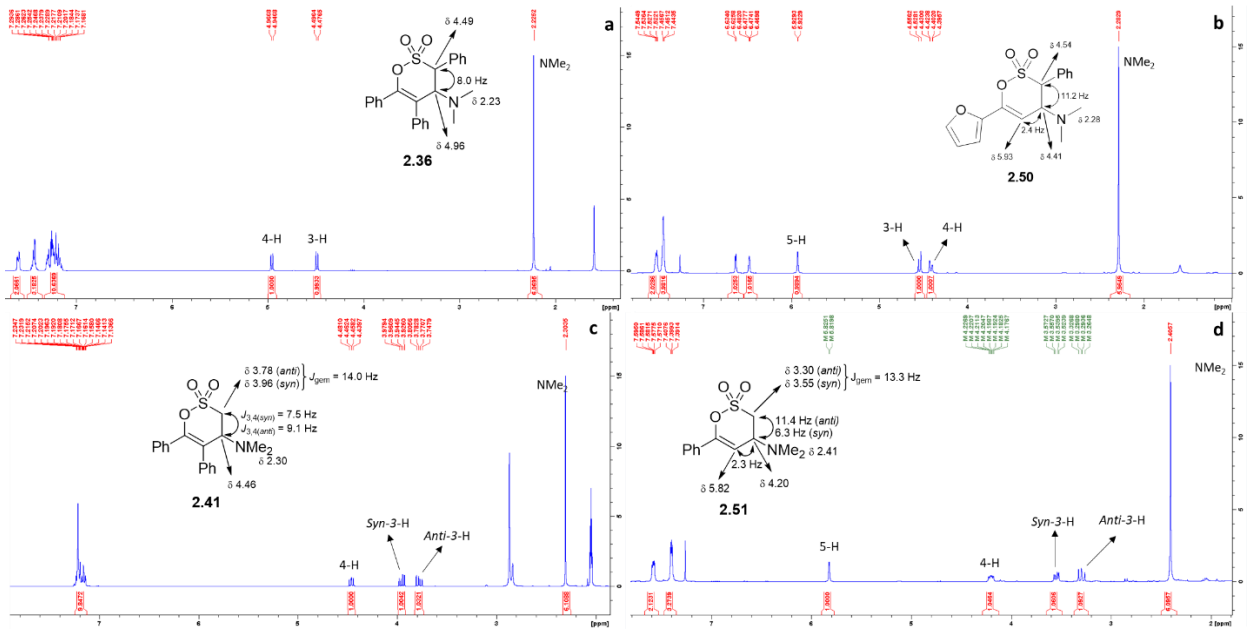

Figure 2.18: Representative examples of 3,4-dihydro-1,2-oxathiine-2,2-dioxide ^{1}H-NMR spectra (spectrum for **2.41** (c) was obtained from a d^6-AcMe sample)

As it can be deduced from the examples in Figure 2.18, examination of the *vicinal* coupling constants for the 3-H and 4-H doublets observed for the synthesised 1,2-oxathiine 2,2-dioxides can provide evidence of potential structural differences between analogues with different substitution patterns. The range of values for the four sets of isolated derivatives (3,5,6-substituted, 3,6-substituted, 5,6-substituted and 6-substituted) are detailed below (Table 2.6).

Substitution pattern	$^3J_{HH}$ (Hz)
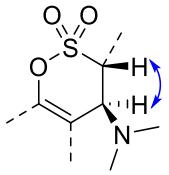	7.9 – 9.5
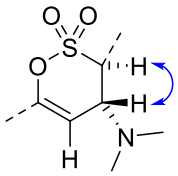	11.1 – 11.4
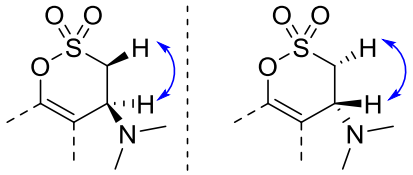	8.3 – 9.1
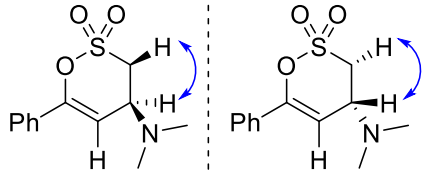	11.4

Table 2.6: Vicinal coupling constants of various 3,4-dihydro 1,2-oxathiine 2,2-dioxides

In the case of derivatives with substituted 6- and 5,6- positions, the three aliphatic protons are arranged in an AA'B spin pattern with two coupling constants where $J_{3,4(anti)} > J_{3,4(syn)}$, thus the larger *anti* coupling constant was utilised for comparable results. Evaluation of the contents of table 2.6 reveals that the absence of a substituent on the 5- position of the 1,2-oxathiine ring induces an increase on the *vicinal J* values from *circa* 8.4 Hz to *circa* 11.2 Hz, which is equivalent to a proportional increase on the *trans*-axial dihedral angles between the 3- and 4- protons[108,109]. This can be attributed to the empty space previously occupied by the 5- substituents, which allows for a different arrangement of the surrounding groups on the 3- (when present), 4- and 6- positions, leading to a potential distortion of the C3-C4-C5-C6-O plane towards a conformation of lower energy. The various substitution patterns of 3,4-dihydro 1,2-oxathiine systems can thus be divided into 2 groups, with the first one comprising of derivatives with a planar C3-C4-C5-C6-O backbone (3,5,6-substituted and 5,6-substituted analogues, also seen in section **1.2.2.1**[86]) and the second populated by derivatives with a "distorted" C3-C4-C5-C6-O unit (3,6-substituted and 6-substituted analogues). These results also indicate that the structure of a 3,4-dihydro 1,2-oxathiine 2,2-dioxide can be influenced by both the inherent torsion between the atoms of the 1,2-oxathiine ring and the substitution level of the molecule.

The effect of this structural alteration for 5-H analogues may be correlated with the unusual behaviour observed for derivative **2.43**; ^{1}H-NMR analysis of a 5-day-old $CDCl_3$ sample of this analogue afforded the product peaks along with an additional set of signals, which were identified as the signals of the starting enaminone **2.1** (Figure 2.19).

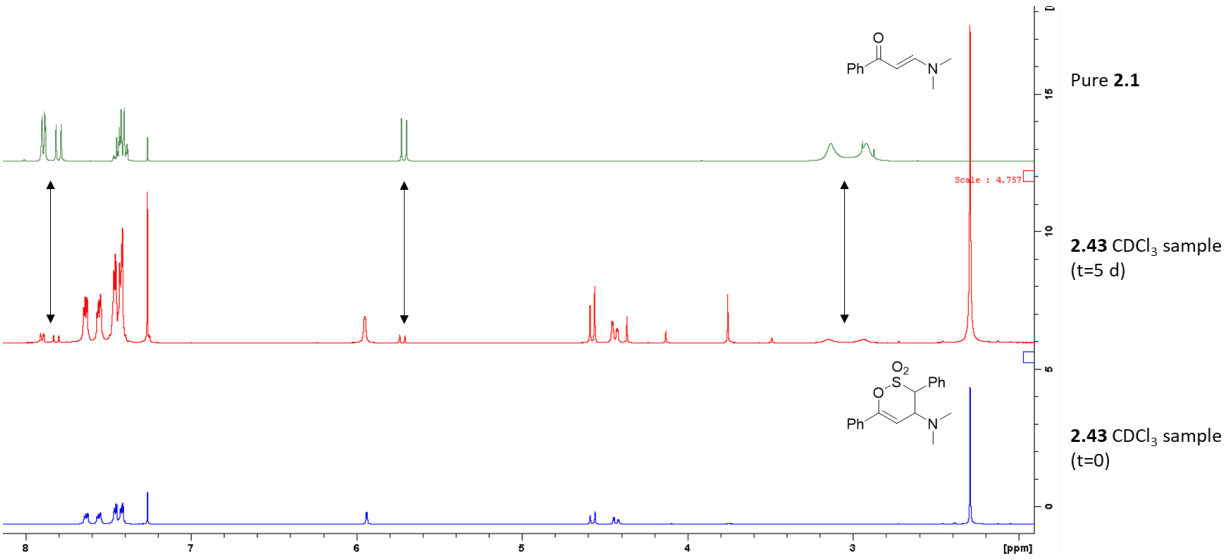

Figure 2.19: Appearance of starting material signals of a $CDCl_3$ sample of **2.43** after 5 days in solution

The foregoing data infers that the 3,4-dihydro 1,2-oxathiine product reverts back to its enaminoketone precursor **2.1**, whereas the phenylsulfene fragment potentially decomposes and the resulting phenyl ring signals and are not resolved from the aromatic signals in the spectrum. The extent of this reversion reaction was examined over time *via* consecutive ^{1}H-NMR measurements of $CDCl_3$ samples of **2.43** (deuterated solvent was used as supplied), along with the analogous **2.36** and **2.41**, between daily (or longer) intervals (Table 2.7).

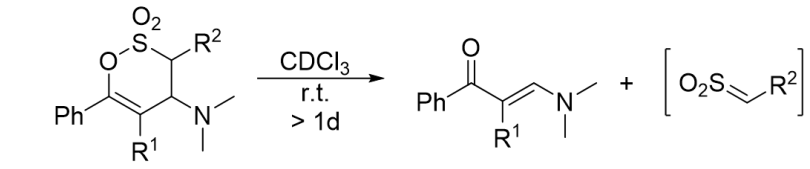

2.36 (R^1= R^2 = Ph)
2.41 (R^1 = Ph, R^2 = H)
2.43 (R^1 = H, R^2 = Ph)

2.1 (R^1 = H)
2.2 (R^1 = Ph)

t (d)	Reversion yield* (%)		
	2.36	2.41	2.43
0	0.0	0.0	0.0
1	0.0	0.0	4.6
4	0.0	0.0	8.9
5	0.0	0.0	9.8
6	0.0	0.0	11.3
25	0.0	0.0	16.0
26	0.0	0.0	16.8

*Calculated as % (S.M.) = $\frac{X_{S.M.}}{X_{S.M.}+X_{Prod.}}$
$X_{S.M.}$: Integral of enaminone precursor
$X_{Prod.}$: Integral of 1,2-oxathiine 2,2-dioxide

Table 2.7: Table of reversion yields between 3 analogous 3,4-dihydro 1,2-oxathiine 2,2-dioxides

As it can be seen in table 2.7, only the 3,6-substituted derivative **2.43** underwent reversion to the enaminone precursor, with the other two analogues (**2.36** and **2.41**) preserving their structural integrity after almost 1 month in solution to $CDCl_3$. Taking into consideration the results regarding the correlation between the coupling constants of various 3,4-dihydro-1,2-oxathiine systems and their respective structures (Table 2.6), it may be theorised that the "distorted" C3-C4-C5-C6-O backbone on **2.43** induces an increase in the total energy of this heterocyclic system, thus making it less stable and susceptible to cyclo-reversion when left in $CDCl_3$ solution for more than a few hours. It should be added that, regardless of the structure of the 1,2-oxathiine 2,2-dioxide heterocycle, the electron-donating effects of the phenyl group may also be a determining factor for this type of retro-transformation.
The behaviour 3,6-diphenyl derivative **2.43** was further investigated with regards to the effect of H_2O on its isolation from the reaction mixture. The general work-up procedure for the sulfene additions included

a H_2O wash of the reaction mixture upon complete conversion to remove triethylammonium chloride ($Et_3N^+HCl^-$, Scheme 2.10); however, such ionic species were found to be readily adsorbed onto the stationary phase during chromatographic purification of the products, thus an aqueous wash was deemed gratuitous as it lengthened the work-up process without meriting a full removal of ionic impurities. Moreover, washing the reaction mixture with water was also found to have an effect on the reaction yield. The first attempt at synthesising the 3,6-diphenyl analogue **2.43** was met with limited success (10.0 % yield) after a work-up process that included an aqueous wash (thorough contact with significant amount of H_2O), but a second run of the same reaction during which the crude product was only triturated with water without aqueous washing (brief contact with a small amount of H_2O) allowed for substantially better results (44.0 % yield). Aqueous washing was thus omitted from the general sulfene addition work-up process upon these findings.

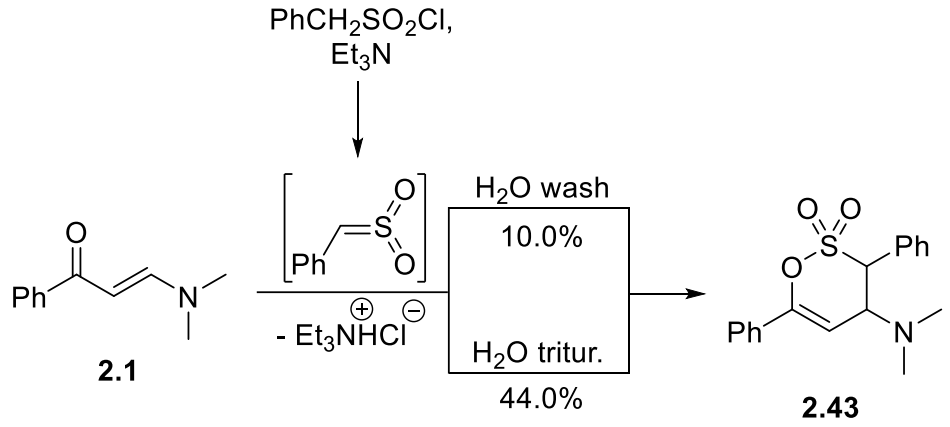

Scheme 2.10: Correlation between contact with H_2O and yield of 1,2-oxathiine 2,2-dioxide product

Parallel to the information accrued from the analysis of the ^{1}H-NMR spectra of the 3,4-dihydro-1,2-oxathine 2,2-dioxides, characteristic peaks were sought out from the ^{13}C-NMR spectra of the 3,4-dihydro-1,2-oxathiine 2,2-dioxide products, with key signals denoting the presence of the 1,2-oxathiine ring system. Using the 5,6-diphenyl analogue **2.41** as an example (Figure 2.20), the equivalent methyl groups of the amino terminus appear as a singlet at *circa* δ 40, while the two aliphatic carbons of the heterocycle are distanced significantly with C4 found at δ 43 and C3 at δ 64, on account of the electron-withdrawing SO_2 group deshielding C3. The olefinic pair of C5 and C6 are affected by the *O* atom in a similar fashion, with the former being observed at δ 122 (typical for alkenyl *C* environments) and the latter being deshielded to such an extent that its corresponding peak appears downfield at δ 149.

An additional piece of characterisation data that substantiates the conversion of enaminones to 1,2-oxathiine adducts regards the appearance of IR peaks which result from vibrations of the OSO_2 moiety and the loss of the C=O key signal at *circa* 1600 cm^{-1}. Indeed, the IR spectra of the isolated 3,4-dihydro-1,2-oxathiine 2,2-dioxides exhibited key bands at *circa* 1365 cm^{-1} and *circa* 1170 cm^{-1} which are in accordance with previous research work on the synthesis of such heterocyclic systems[41,42,43,44] (Figure 2.21).

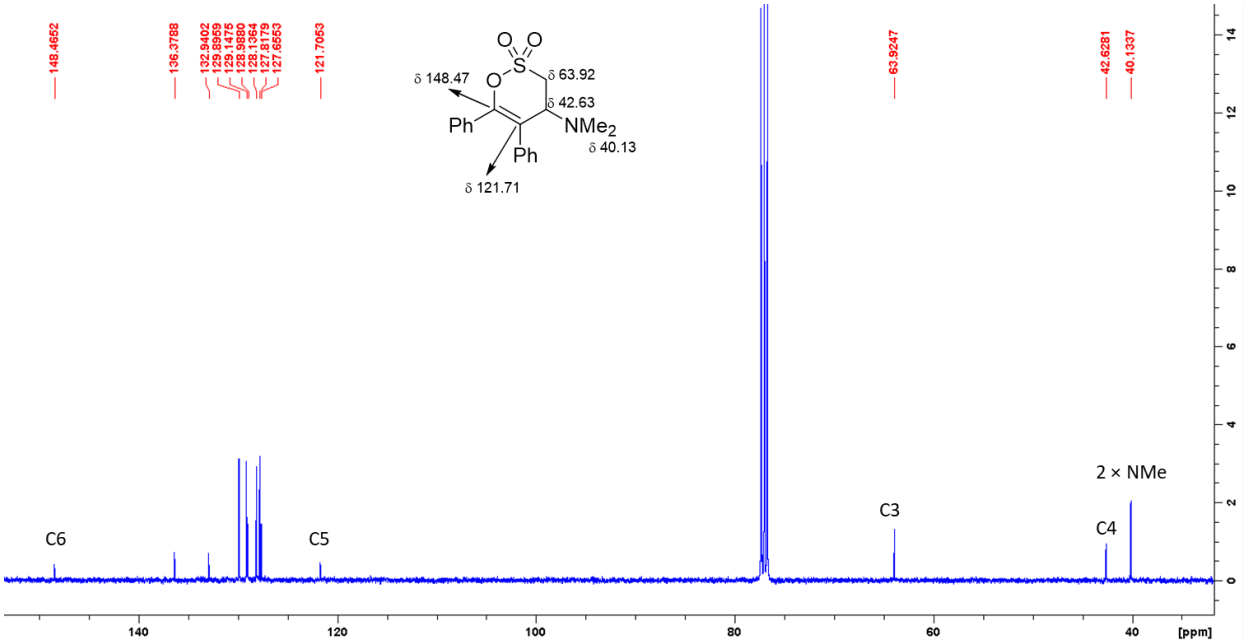

Figure 2.20: Typical ^{13}C-NMR spectrum of a 3,4-dihydro-1,2-oxathiine 2,2-dioxide system (**2.41**)

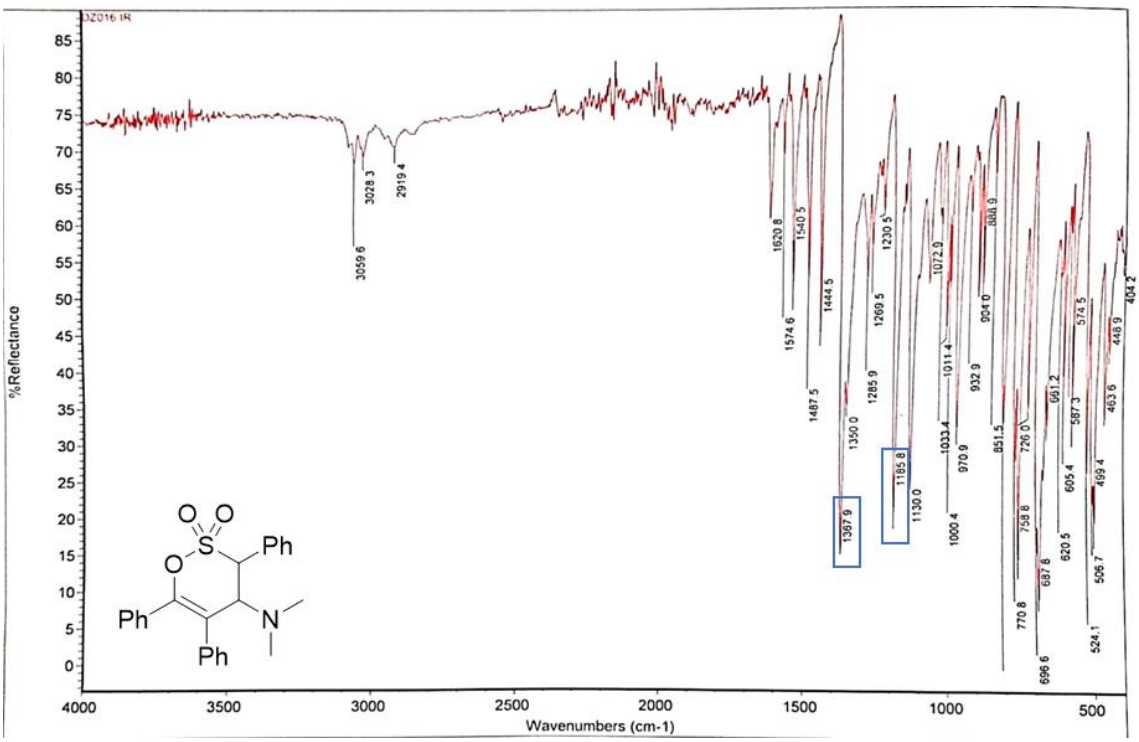

Figure 2.21: IR spectrum of **2.41**

The final piece of characterisation data involves the mass spectra of these heterocycles, through which their molecular weight could be ascertained. The mass spectrum of the triphenyl derivative **2.36** (Figure 2.22) presents a molecular ion at *m/z* 406.1471 $[M+H]^+$ which is in perfect agreement with the expected *m/z* of 406.1471 for $C_{24}H_{23}NO_3S$. A second peak is also present at *m/z* 297.1278, which interestingly closely aligns with that for 2,3,5-triphenylfuran (**2.54**) (expected *m/z* of 297.1235 $[M+H]^+$); this species may arise during the mass spectral analysis by loss of Me_2NH and SO_2 with concomitant ring contraction (Scheme 2.11).

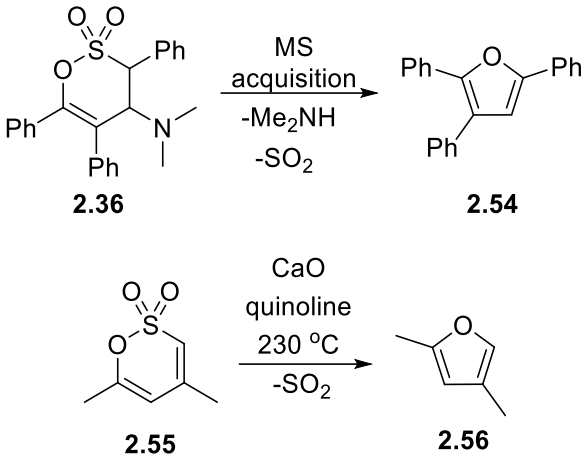

Scheme 2.11: (Above) Elimination and ring-contraction of **2.36** towards the furan derivative **2.54** during mass spectrum acquisition, (below) preceding research by Morel and Verkade[110] on the formation of the analogous furan system **2.56**

Such a process has been previously explored in the literature during documentation of the thermolysis of 4,6-dimethyl-1,2-oxathiine 2,2-dioxide (**2.55**) performed by Morel and Verkade[110] and their presented findings provided a synthetically useful route to 2,4-dimethylfuran (**2.56**, Scheme 2.11), which serves as a diene in cycloaddition chemistry and natural product synthesis.[111,112]

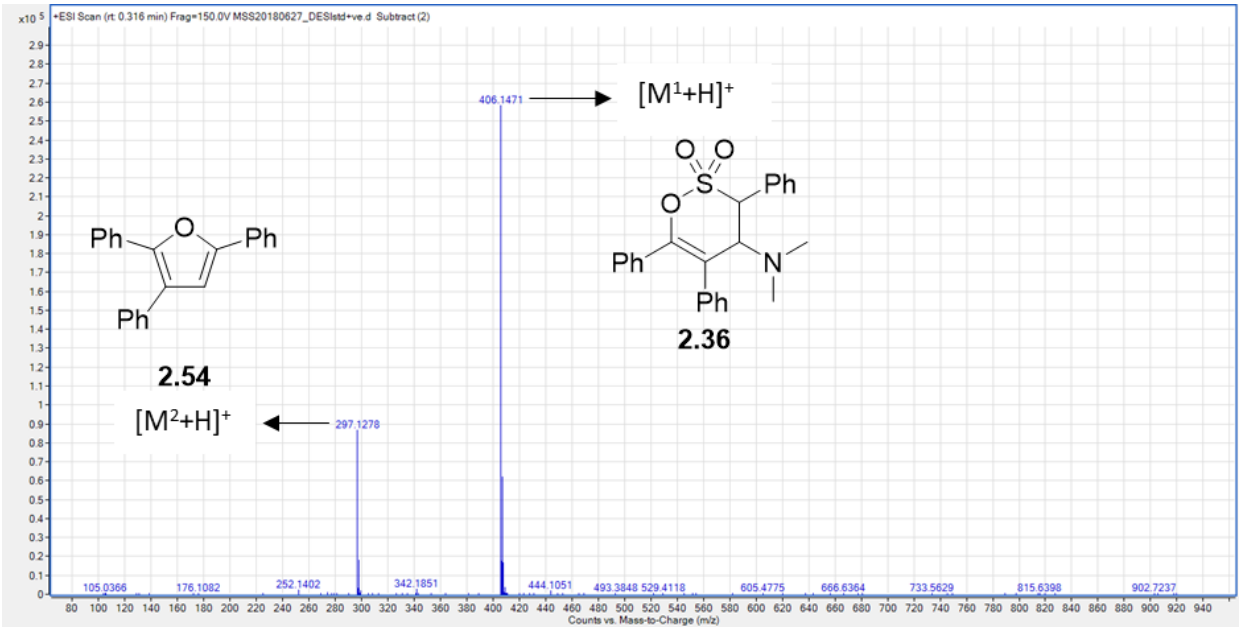

Figure 2.22: Mass spectra of **2.36** showing a molecular ion for **2.54**

As previously mentioned, the reported yields in table 2.5 and the previous characterisation discussion both relate to one isolated compound, even though two distinct 3,4-dihydro-1,2-oxathiine 2,2-dioxide isomers may arise from a sulfene addition, *i.e.* an *anti*- (Ph and NMe_2 on opposite sides) and a *syn*- (Ph and NMe_2 on the same side) diastereomer (Scheme 2.12). The *anti*- diastereomer was typically afforded as the major or sole isomer and for this reason all yields regarding 3,4-dihydro-1,2-oxathiine 2,2-dioxide systems refer to this isomer, unless otherwise stated. The minor *syn*- counterpart was not without interest, as its presence in the crude mixtures of these conversions seems to be dependent on the product substitution pattern; in fact, only tri-substituted 3,4-dihydro 1,2-oxathiine analogues afforded reaction mixtures that contained both isomers. Derivatives with 3,6-disubstitution patterns exhibited no minor isomer formation, albeit the presence of two chiral centres, whereas the absence of a 3-substituent on

the structure of 5,6-di-substituted systems connotes that no pairs of diastereomers may form for such analogues. Even when the *syn*- diastereomer was indeed observed, the almost identical polarity it shares with the major *anti*- isomer made its full isolation unattainable in almost all occasions. The ^{1}H-NMR spectrum of the crude mixture for analogue **2.36** presents a representative example, where except for the signals of the major product, an additional set of signals can be found with a $J_{3,4}$ = 5.9 Hz, indicating a *syn*- arrangement for 3-H and 4-H; comparison of this value with the one observed for the main set of doublets, $J_{3,4}$ = 8.0 Hz, conveys the fact that there is indeed a major *anti*- and a minor *syn*- isomer that have resulted from this addition at a 10 : 1 ratio (Figure 2.23). The chemical behaviour of these conformational isomers will be revisited in the following sections, as the proportion in which they form reveals a stereoselectivity effect, which may be tethered to the mechanism of the sulfene addition.

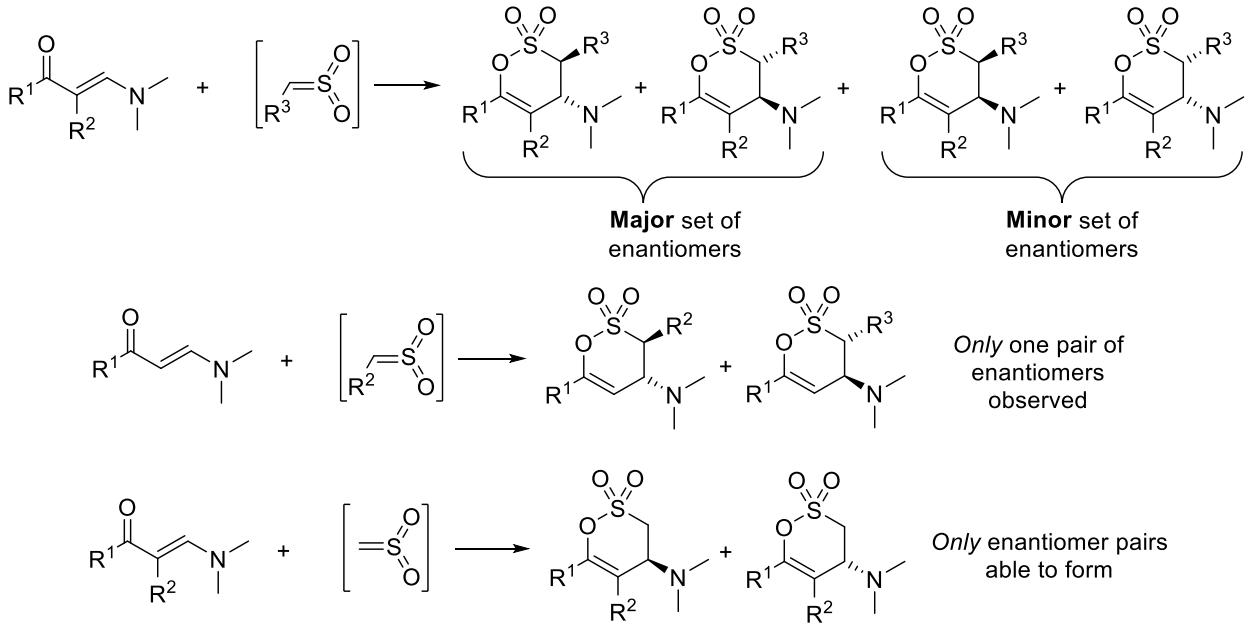

Scheme 2.12: Isomer products of specific sulfene additions

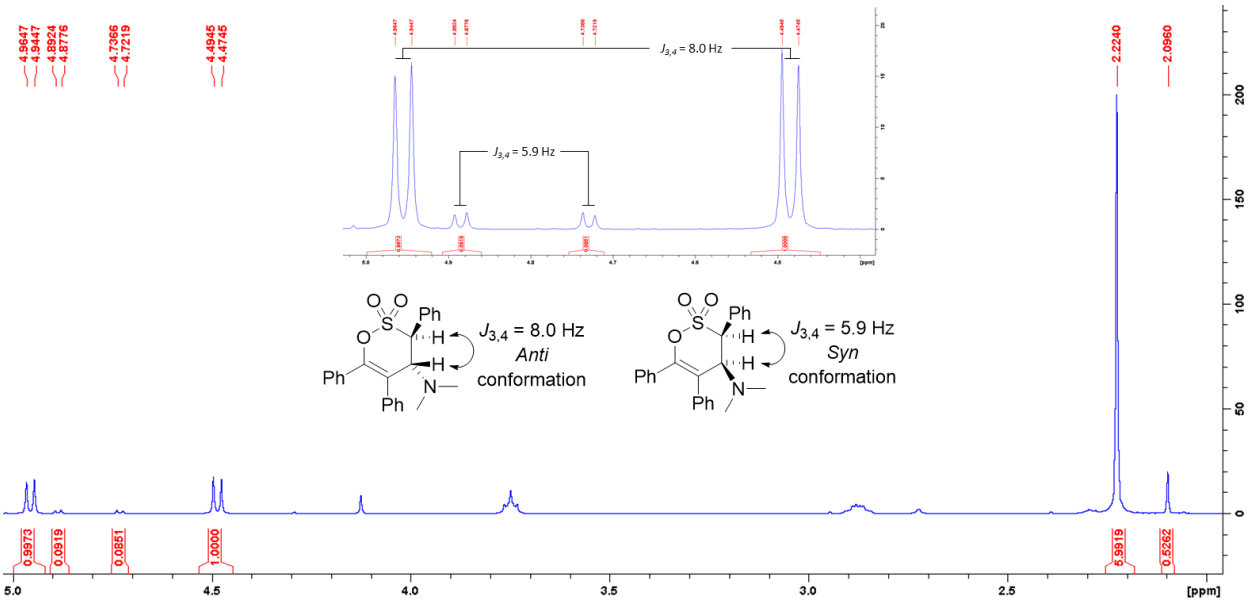

Figure 2.23: ^{1}H-NMR of isomer mixture for the triphenyl derivative **2.36**

Further insights to this reaction were gleaned from attempts to convert the bis-enaminone systems to their corresponding 3,4-dihydro-1,2-oxathiine 2,2-dioxides (Scheme 2.13). The addition of phenyl sulfene

to the bis-enaminone analogue **2.31** did not yield the desired heterocycle **2.57**, possibly due to extensive stabilisation of the enaminone through resonance. The imino counterpart **2.32** behaved more predictably under the same conditions and formed the expected heterocycle with sulfene, but its potential low stability led to the elimination of a $HNMe_2$ fragment, giving rise to the unsaturated analogue **2.58** in 8.8 % yield as the only isolated compound from this run. Examination of the ^{1}H-NMR spectrum of this compound conveys structural information that mirror those of its enaminone precursor (**2.32**, section **2.1.2**), as the terminal amino group appears as two singlets (one for each Me group) which points out the inability of the Me_2N-C bond to rotate due to its high double bond character (Figure 2.24). These data are evident of a 3,4-dihydro adduct forming at first but eliminating *in situ* towards a system with a higher level of conjugation. In turn, such an observation highlights the ability of the of the enaminone substituents to direct side-reactions on the desired 3,4-dihydro-1,2-oxathiine 2,2-dioxide adducts.

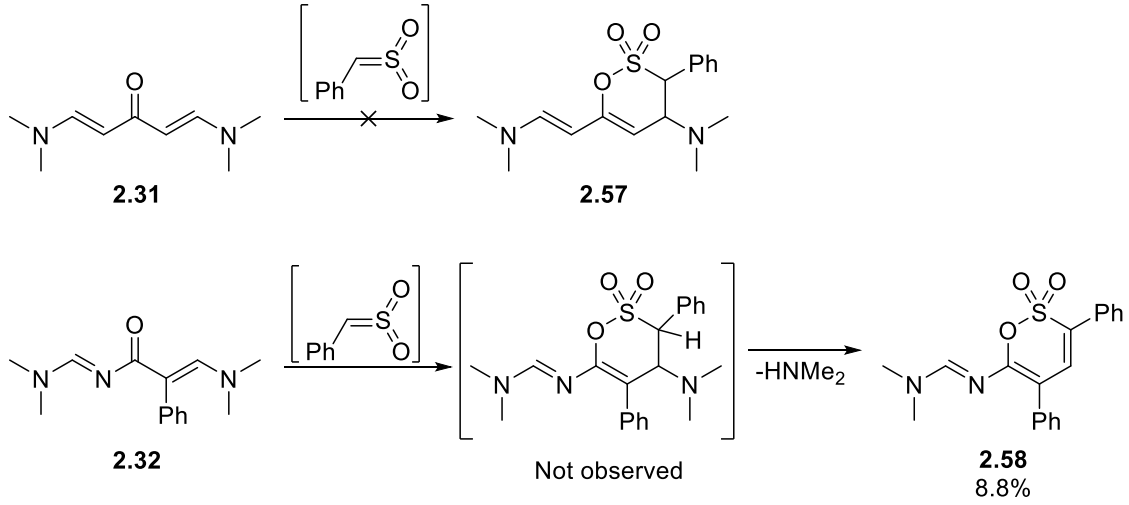

Scheme 2.13: Sulfene addition attempts using bis-enaminone systems

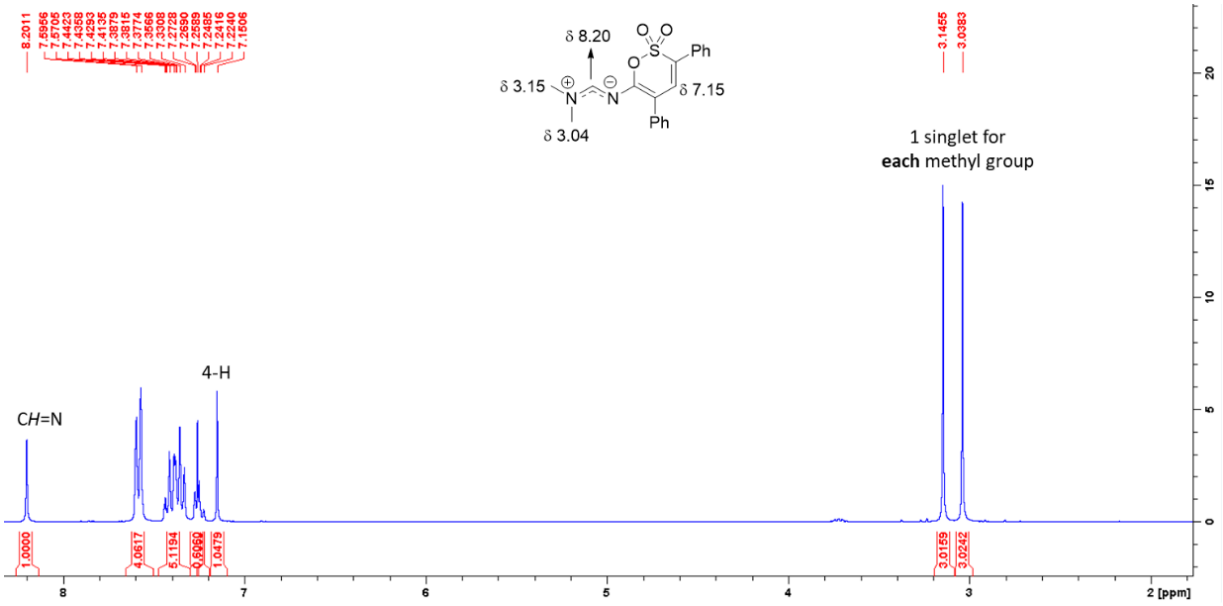

Figure 2.24: ^{1}H-NMR spectrum of the unsaturated derivative **2.58**

The use of excess amounts of sulfonyl chloride and Et_3N in order to ensure reaction completion presents another point of discussion, along with the side-products that arise as a result. A common trend that was always observed for additions of a substituted sulfene was the formation of dimerisation side-products

originating from the portion of the sulfene that did not react with the enaminone substrate. Although, the mechanism of their formation has already been documented (Section **1.1.3.2**[46,49]), isolating and characterising these compounds would confirm such literature data. The addition of Et_3N into a THF solution of phenylsulfonyl chloride **2.59** was carried out to that end. Analysis of the crude reaction mixture by ^{1}H-NMR spectroscopy revealed a significant aromatic load besides trace solvent and salt impurities, along with two singlets appearing at δ 6.62 and δ 7.14 with a 1 : 0.4 integral ratio, both of which signals had been observed in the reaction mixtures of various additions of phenylsulfene to enaminones (Figure 2.25). Moreover, the triplet and apparent sextet signals at *circa* δ 1.3 and δ 3.0, respectively in figure 2.25 can be assigned to the triethylamine hydrochloride by-product. Of note is the peak at *circa* δ 3.0, which appears to be more complex than a quartet on account of ^{15}N-H coupling manifested by the methylene protons on the ethyl groups.[113]

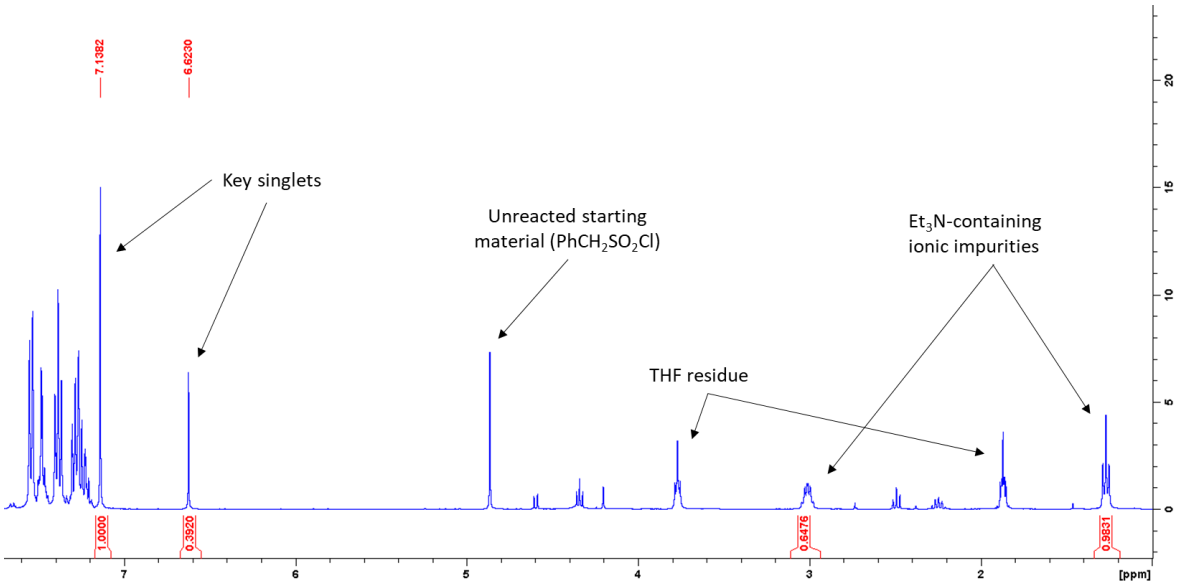

Figure 2.25: ^{1}H-NMR spectrum of the sulfene dimerization reaction mixture

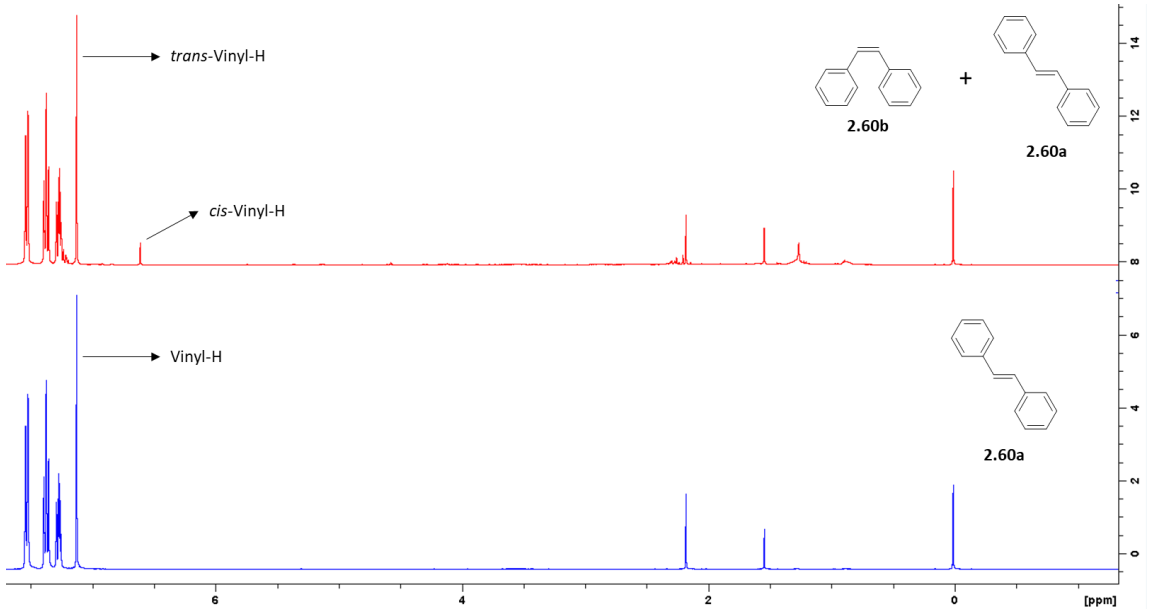

Figure 2.26: *Trans*/*Cis* isomers of stilbene (**2.60a/b**) isolated from the dimerization of phenylsulfene

Upon purification by recrystallisation, a mixture of the two compounds which exhibited a singlet at δ 6.62 and at δ 7.14 was subjected to chromatographic separation which afforded a co-eluted fraction containing

both components, followed by a second fraction containing a single component. Comparison of the ^{1}H-NMR signals of the isolated compound with literature sources[114] led to the conclusion that it was *trans*-stilbene **2.60a**, whereas the same research work validated the structure of *cis*-stilbene **2.60b** for the other compound (Figure 2.26).

As there is no singlet corresponding to the benzyl protons of a potential ionic dimer-like compound, it can be suggested that this by-product is triethylammonium chloride ($Et_3N^+HCl^-$), which consequently leads to the conclusion that any dimerisation of the *in situ* formed sulfene with itself or the starting sulfonyl chloride has exclusively one outcome, *i.e.* ring-closing to 4-membered dimeric intermediates (1,3-dithietane 1,1,3,3-tetraoxides) that are eventually converted into the stilbene isomers **2.60a** and **2.60b** *via* two consecutive SO_2 extrusions (Scheme 2.14), in accordance with the established literature[45,49].

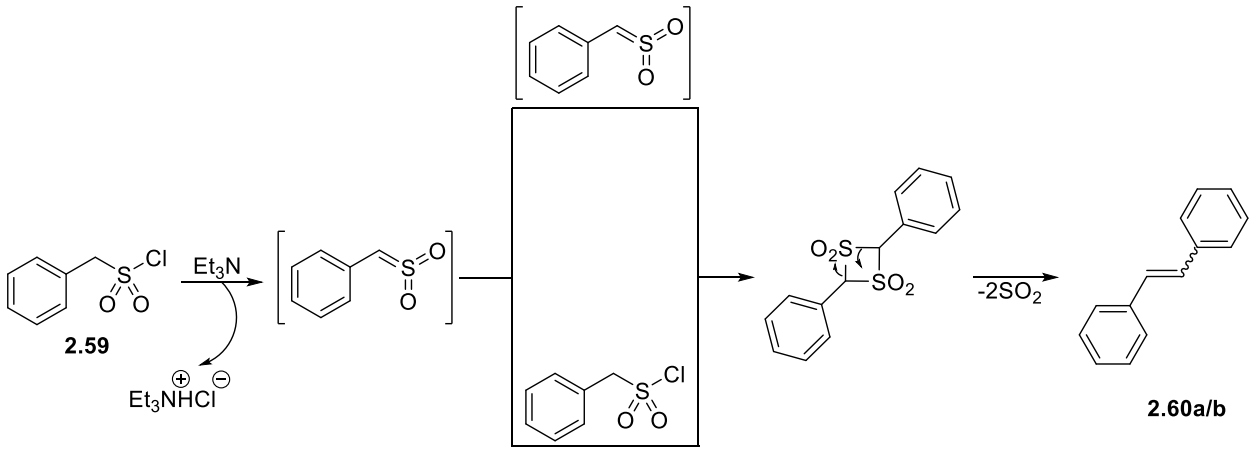

Scheme 2.14: Overview of sulfene dimerization/SO_2 extrusion to arrive at a pair of stilbene isomers **2.60a/b**

2.2.2 Exploration of the sulfene addition mechanism

The discovery of *anti*/*syn* diastereomer selectivity as a recurring trend during the synthesis of tri-substituted 3,4-dihydro-1,2-oxathiine systems (*e.g.* **2.36**, **2.40**), along with the effects of substituents in the reaction yield, incentivised the examination of the obtained information towards determining the mechanism for this specific transformation. Schenone *et al*.[44] isolated the ring-opened intermediate (**2.61**) of an analogous dichloroketene addition (Scheme 2.15, noted in section **1.1.2.3**), but no similar species were obtained by this or any other research group for the case of sulfene additions.

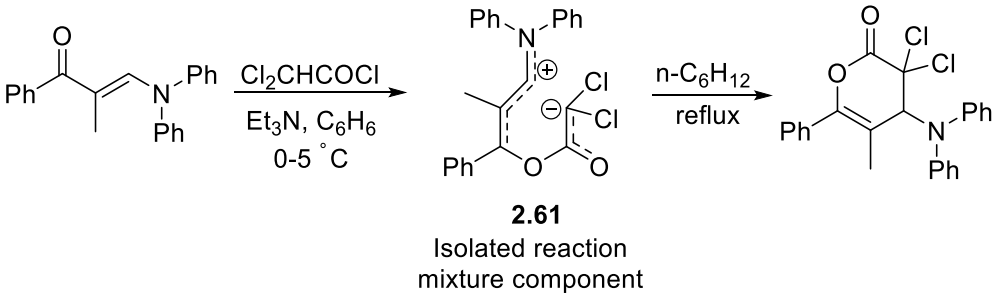

Scheme 2.15: Ring-open intermediate (**2.61**) isolated from a dichloroketene addition reaction mixture

The absence of any intermediate of this kind in the ^{1}H-NMR spectra of reaction mixture aliquots at various time points was the first observation suggestive of a concerted, hetero Diels-Alder process. In order to gain a more thorough understanding of how such a mechanism would operate, additional research on the

two obtained 3,4-dihydro-1,2-oxathiine 2,2-dioxide isomers was essential, although the *syn*- isomer was unattainable for examination using the initial work-up and purification processes due to its co-elution with the major *anti*- isomer during chromatographic separation, as seen for the benzyl example **2.40** (Figure 2.27).

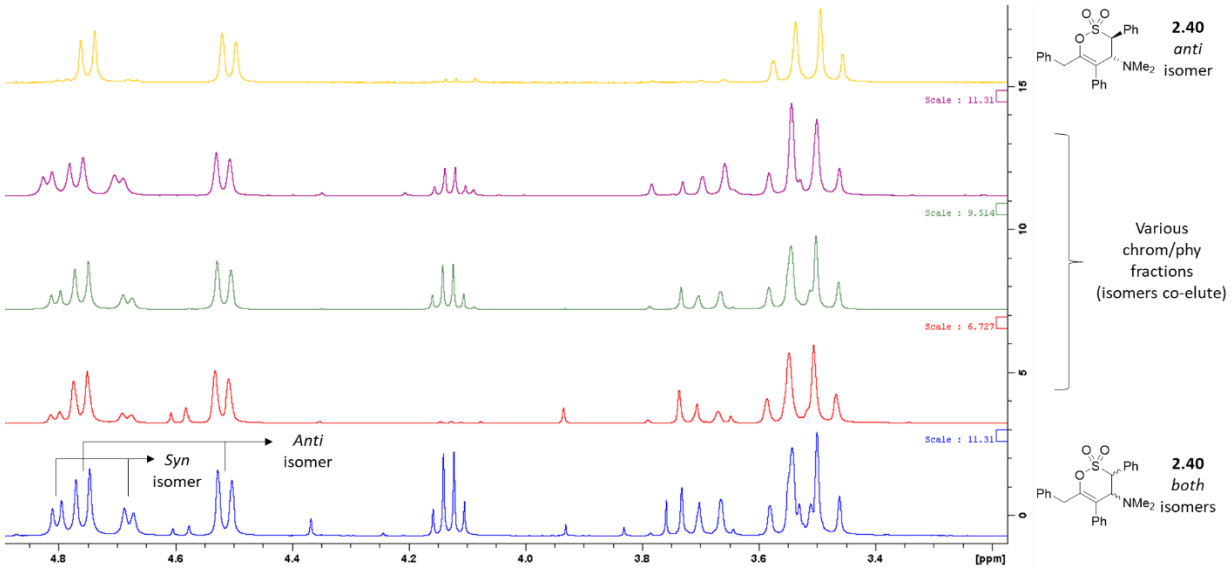

Figure 2.27: Co-elution of the *anti*/*syn* isomers of analogue **2.40**

Pleasingly, switching the silica for alumina for the chromatographic separation allowed for the successful isolation of the *syn*- isomer of **2.40**, **2.40b**, in 24.6 % yield (Scheme 2.16), as evident by the coupling constant between 3-H and 4-H being relatively smaller than that for the major *anti*- product **2.40a** ($J_{3,4(syn)}$ = 6.3 Hz as compared to $J_{3,4(anti)}$ = 9.5 Hz, Figure 2.28). An estimation of the proportion of these two isomers could only be obtained from the ^{1}H-NMR spectrum of the crude mixture for this repeat run, wherein they were observed in a 1 : 1.27 ratio (*anti*/*syn*) by comparing the integrals of the signal for 3-H for each isomer. Contrary to the first run of this sulfene addition (Figure 2.27), here the *syn*- diastereomer was the prevalent product instead of the *anti*- diastereomer, which had been hitherto unseen throughout the syntheses of 3,4-dihydro-1,2-oxathiine systems.

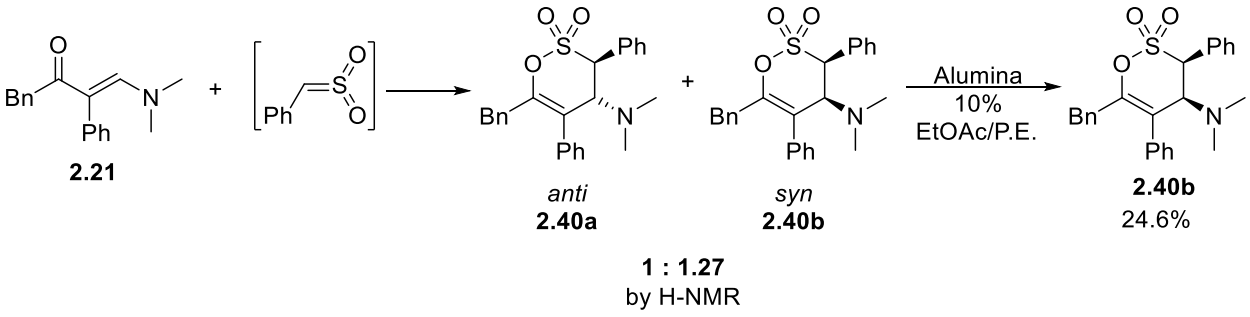

Scheme 2.16: Isolation of the *syn*- isomer from a sulfene addition reaction mixture

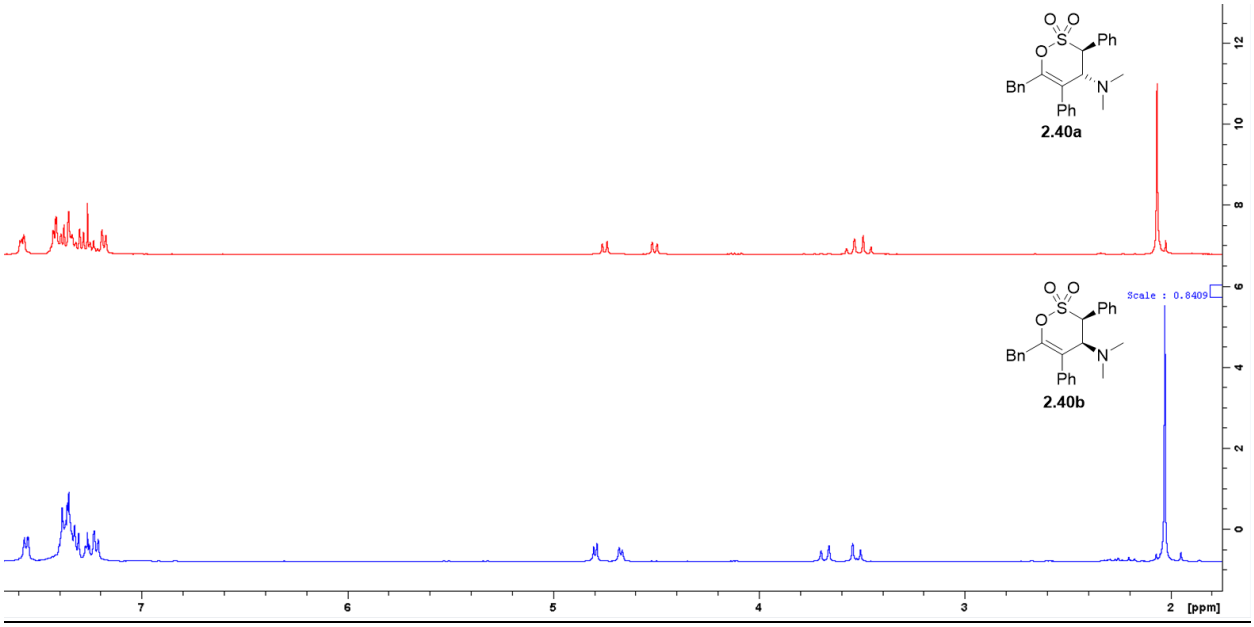

Figure 2.28: ^{1}H-NMR spectra of the *anti*- (**2.40a**, above) and *syn*- (**2.40b**, below) isomers of derivative **2.40**

Upon the isolation of this isomer, it was discovered that its $CDCl_3$ sample solution showed an additional set of signals after standing at room temperature for a few hours; this extra set of signals was attributed to the major *anti*- isomer **2.40a**. This interesting behaviour led to the conclusion that, when in solution with $CDCl_3$ (solvent used as purchased), this diastereomer was able to epimerise at C4 towards its more stable counterpart. A plot illustrating the gradual conversion of isomer **2.40b** to the *anti*- isomer **2.40a** over time is shown in Figure 2.29.

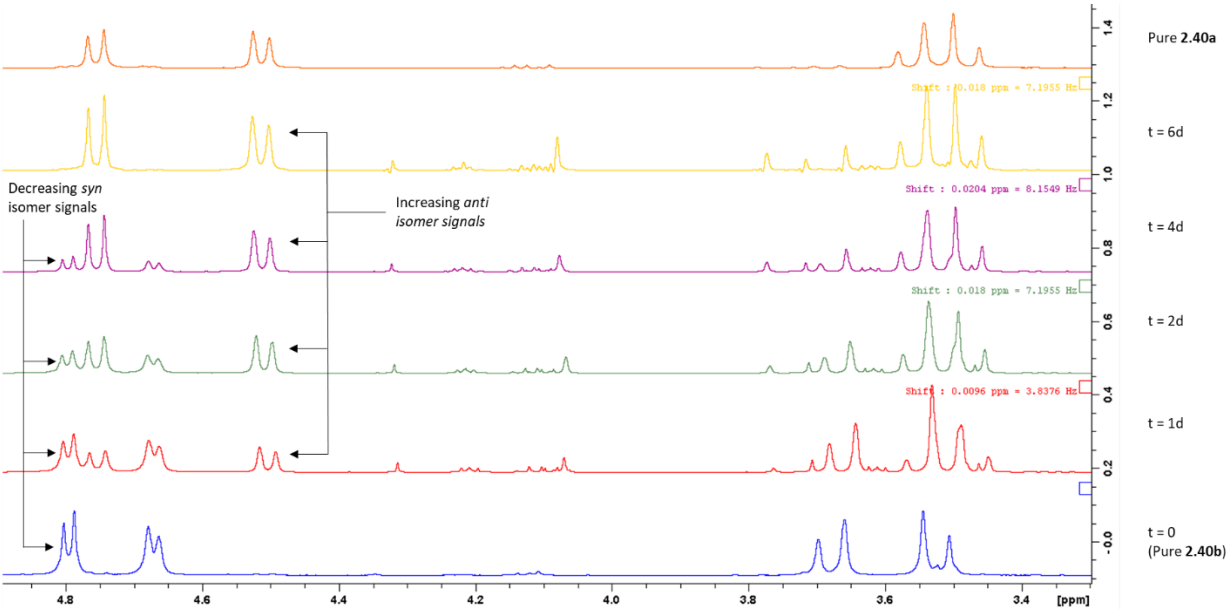

Figure 2.29: Developing signals of the major isomer in a $CDCl_3$ solution of the *syn*- isomer **2.40b** over 6 days

In order to further explore the epimerisation of **2.40b** to its *anti*- counterpart **2.40a**, a *circa* 1-year old sample of **2.40b** was subjected to ^{1}H-NMR analysis using d^{6}-AcMe as a solvent (Figure 2.30). A comparison of the obtained ^{1}H-NMR spectrum with an ^{1}H-NMR spectrum of **2.40a** in d^{6}-AcMe showed the full epimerisation of the *syn*- isomer, which clearly indicates that the NMR solvent has no pivotal effect on the epimerisation process, whereas the complete absence of a second set of key 3,4-dihydro-1,2-

oxathiine signals also hints at a potential *syn*/*anti* isomerisation of **2.40b** in solid state, which cements the postulation that there is a significant tendency of **2.40b** to convert into **2.40a** over time.

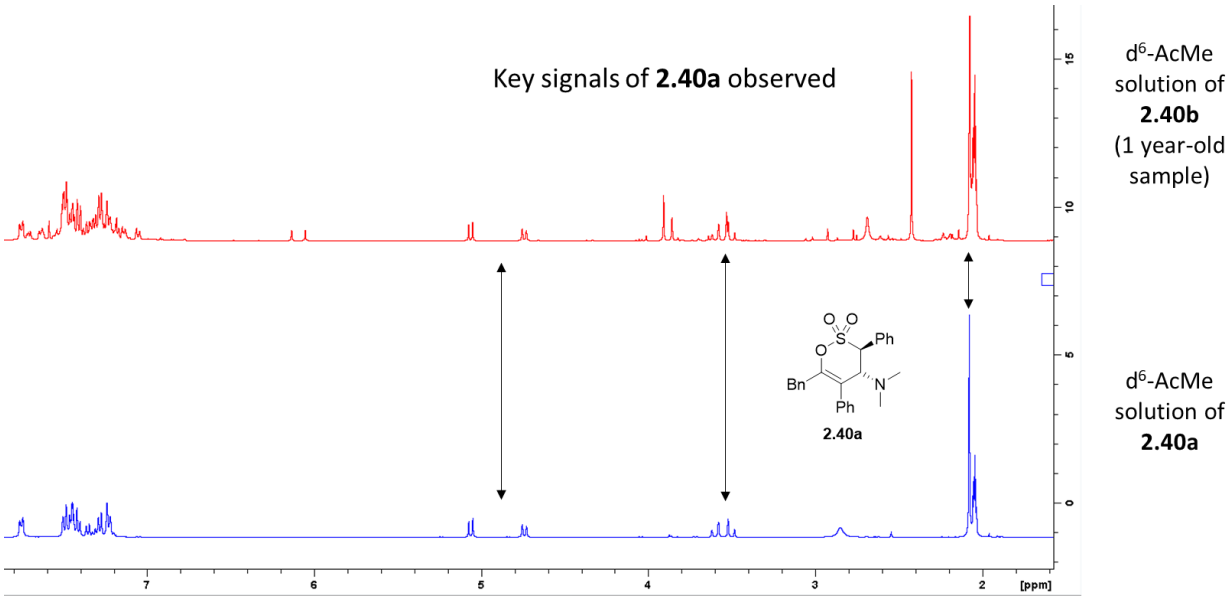

Figure 2.30: Full epimerisation of **2.40b** to **2.40a** in the solid state (1 year old stored sample)

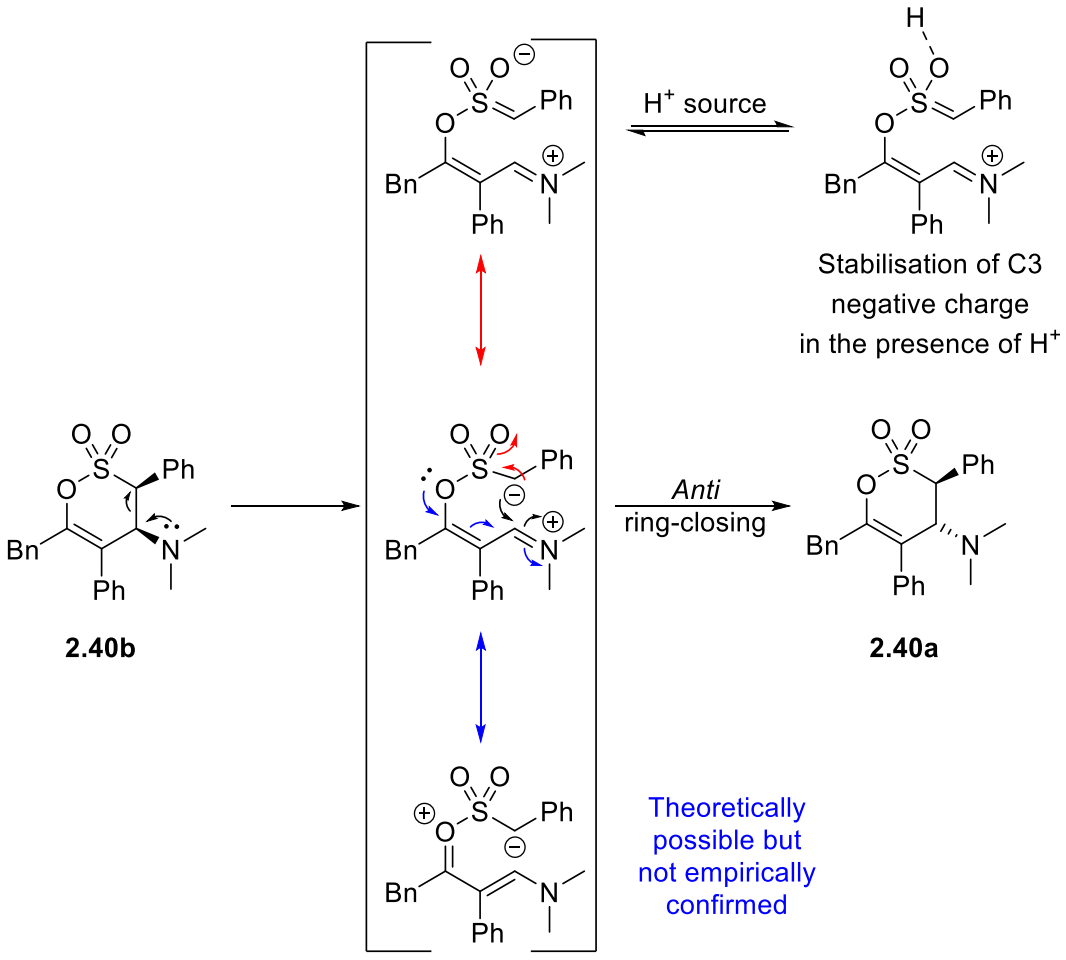

Scheme 2.17: Suggested epimerisation process of **2.40b** to **2.40a**

This gradual epimerisation may be possible due to the unstable *syn*- conformation of the NMe_2 and Ph groups, as well as a contribution from the NMe_2 moiety (Scheme 2.17). The C-C bond between the C3 and C4 substituents can shift towards the electron deficient C3 atom with concomitant donation of the lone pair of the amine, affording a ring-opened intermediate, in which the SO_2 unit can assist in the stabilisation of the negative charge centred on C3 (even further *via* protonation of one of the two *O* atoms when a proton source is present), and which is able to ring close with the two substituents *anti* to each other (Scheme 2.17). The proximal enol moiety may also facilitate such a process by stabilising the aforementioned intermediate, but at this stage its potency to behave as such had not been supported by any other experimental data.

This evident bias towards the *anti*- diastereomer was a valuable result, as it could be utilised to explain the trend of the *syn*- isomer being the minor isomer in almost all cases, as well as its challenging isolation. Furthermore, it proved that there is indeed a thermodynamic difference between the two possible 3,4-dihydro 1,2-oxathiine isomers that can be obtained from a sulfene addition.

Upon these observations, it was postulated that such differences in the thermal stability of the heterocyclic adducts could be utilised in order to acquire a foothold on the mechanistic aspects of the addition of sulfenes to enaminones. Since the benzyl analogue **2.40** was the 3,4-dihydro 1,2-oxathiine system with the most reaction runs and the highest minor isomer level, examination of the differences on the reaction conditions between the runs could be promisingly correlated with the ratio of the two diastereomers. The reaction was indeed repeated twice throughout these explorations. During the first run, 1,2 eq of Et_3N and phenylmethanesulfonyl chloride were used and the *in* situ formation of the sulfene was carried out at T = 0-5 ^oC, followed by a 4 h stirring at room temperature for reaction completion, although an additional 0.4 eq of the starting sulfonyl chloride and Et_3N were required for full consumption of the starting enaminone (again added at T = 0 - 5 ^oC) with subsequent stirring at room temperature overnight. Of note is that, as this run was performed prior to the optimisation of the reaction procedures, the reaction mixture received an aqueous wash during work-up. This protocol yielded an *anti*/*syn* ratio of 1 : 0.7. Repeating the reaction with 1,3 eq of the aforementioned reagents, sulfene formation at the same temperature and an overnight stirring at room temperature successfully converted the entirety of the starting material with a 1 : 1 ratio of diastereomers. Finally, when the same stoichiometric amounts were used at a lower temperature, *i.e.* -10 to -5 ^oC during sulfene formation, an *anti*/*syn* ratio of 1 : 1.27 revealed that the *syn*- isomer was the major component after an overnight stirring at room temperature. These findings are detailed in table 2.8.

Reaction run	**Eq of formed sulfene**	**T of sulfene formation (^oC)**	**T (h)**	**Aqueous wash**	**Isomer ratio (*anti* : *syn*)**
1	1.2 (+0.4)	0 - 5	20	☒	1 : 0.70
2	1.3	0 - 5	16	☐	1 : 1
3	1.3	(-10) - (-5)	16	☐	1 : 1.27

Table 2.8: Varying reaction conditions with the respective ratios of observed isomers (**2.40a** : **2.40b**)

As it can be seen in table 2.8, the use of additional amount of sulfene starting reagents may potentially influence the final isomer ratio, whereas the same can be implied about aqueous washing of the reaction mixture. More importantly, the temperature gradient over runs 2 and 3 resulted in the increase of the *syn*- isomer. This particular piece of data hints at a correlation between the temperature of the reaction and the preference of a specific isomer, thus prompting the conclusion that the *syn*- diastereomer is, in fact, the kinetic product of the reaction, favoured at lower temperatures, and that the *anti*- isomer is respectively the thermodynamic diastereomer, the stability of which allows for it to be favoured under higher reaction temperature (Scheme 2.18).

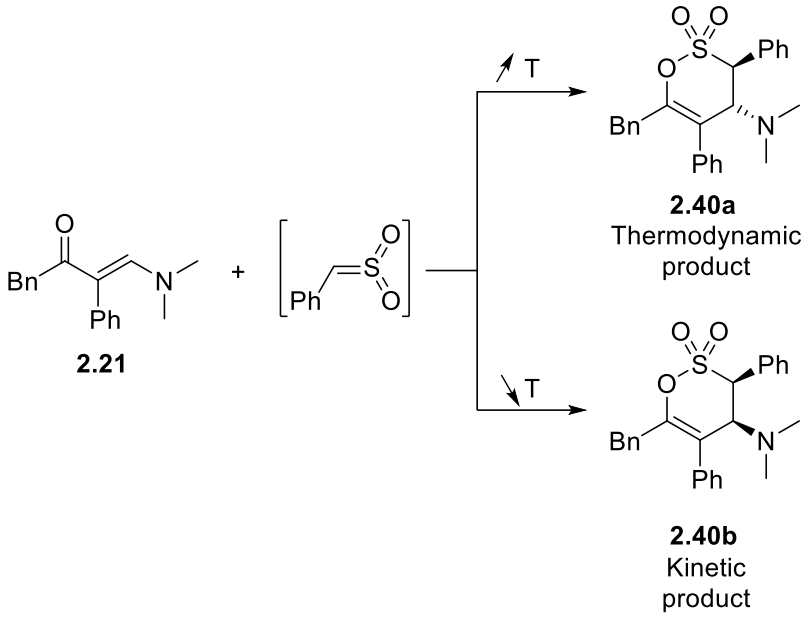

Scheme 2.18: Effect of temperature on the isomer preference during a sulfene addition

At this point, the potential acid-catalysed elimination of the *syn*- isomer **2.40b** towards the unsaturated derivative **2.62**, by virtue of the *anti*- arrangement of 3-H and the NMe_2 unit, was sought out in order to provide additional information about the behaviour of this diastereomer. Heating a PhMe solution of **2.40b** along with a catalytic amount of *p*-toluenesulfonic acid (*p*-TsOH) to reflux for 1.5 h resulted in its epimerisation into the *anti*- isomer, whereas a small amount of the unsaturated analogue **2.62** was also observed *via* ^{1}H-NMR examination, which may have originated from the elimination of either of the two isomers, hinting that the rate of epimerisation of **2.40b** is higher than the rate of its potential elimination (Figure 2.31a). Reflux overnight allowed for the elimination to proceed further, although a residual amount of the *anti*- isomer persisted (Figure 2.31b). Chromatographic separation of the obtained crude afforded a mixture where the eliminated product **2.62** was the prevailing component, affording an estimated yield of *circa* 15% (Figure 2.31c). The poor conversion may be a result of potential degradation, but this whole set of data indicates that epimerisation of the *syn*- isomer is favoured over its direct elimination, since the *anti*- diastereomer forms at a much higher amount as compared to the eliminated derivative **2.62** (Scheme 2.18).

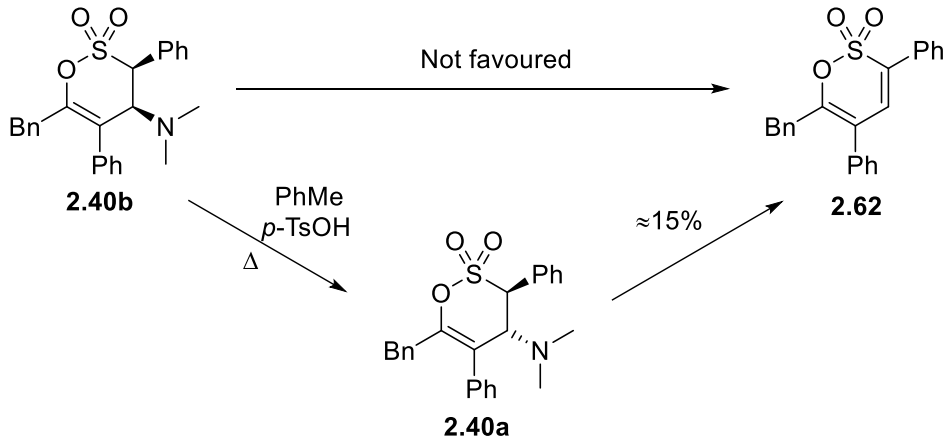

Scheme 2.19: *Syn*/*anti* epimerisation of **2.40** favoured over direct elimination to **2.62**

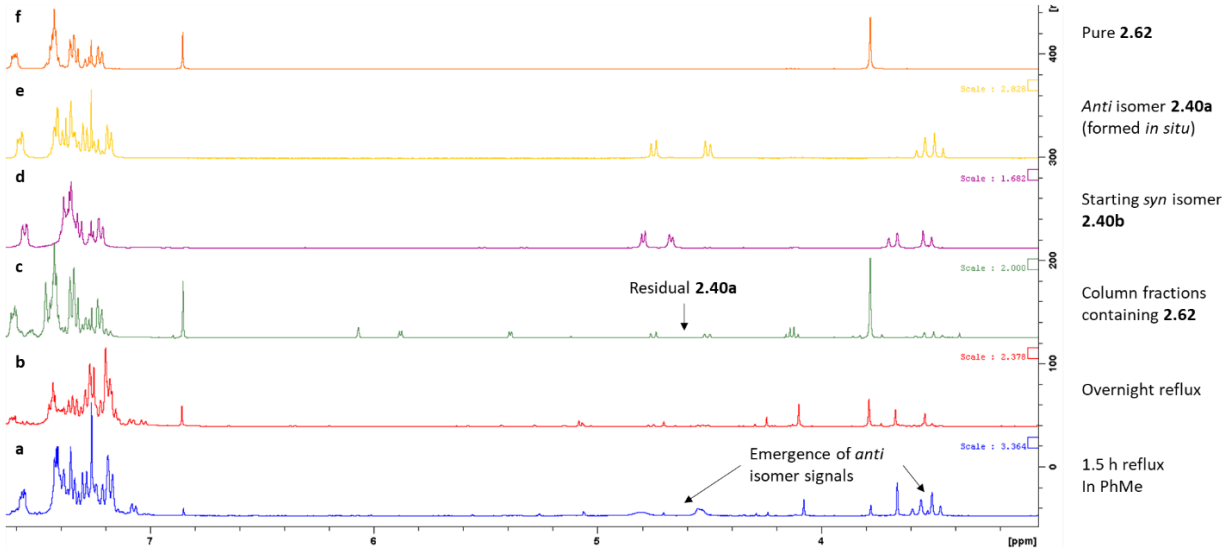

Figure 2.31: Acid-catalysed elimination attempts of the *syn*- isomer **2.40b**

The experimental findings described throughout this section, as well as the reactivity assessment in section **2.2.1**, contain several indications regarding the mechanism of sulfene addition. These can be summarised in the following points:

- Enaminones with an EW 2-substituent favouring delocalisation of the C2-C3 double bond are completely inactive towards sulfene addition
- Increasing the electron density on the reacting sulfene with a bulky ED group does not produce the expected increase in reactivity, as seen in analogues **2.36** and **2.41**
- For 3,5,6-substituted systems, the addition usually affords a major (*anti*) and a minor (*syn*) diastereomer, with the major *anti*- isomer being thermally favoured and the minor *syn*- isomer being kinetically favoured
- The *syn*- isomer is the less stable of the two, to the point of being able to readily epimerise towards the *anti*- isomer even at room temperature.

These main results converge to the general conclusion that the addition of sulfenes to enaminones proceeds through a concerted, hetero Diels-Alder mechanistic route, where the sulfene dienophile can approach the diene in either an *exo* or an *endo* manner to afford two sets of enantiomers that share a diastereomer relationship (Scheme 2.20). Taking into consideration the identical nature of enantiomeric compounds under NMR examination, these sets of products match the characterisation data of the prepared 3,4-dihydro 1,2-oxathiine targets.
This rationale was further explored in tandem with the Woodward-Hoffmann rules for cycloaddition reactions[115] and it was found to be in accordance with them. It is dictated by these rules that systems of [4+2] π-electrons can undergo thermal cycloadditions with disrotatory movement of the frontier lobes on the Highest Occupied Molecular Orbital (HOMO) of the diene, so that they can interact and form σ-bonds with the Lowest Occupied Molecular Orbital (LUMO) of the dienophile (Scheme 2.21).

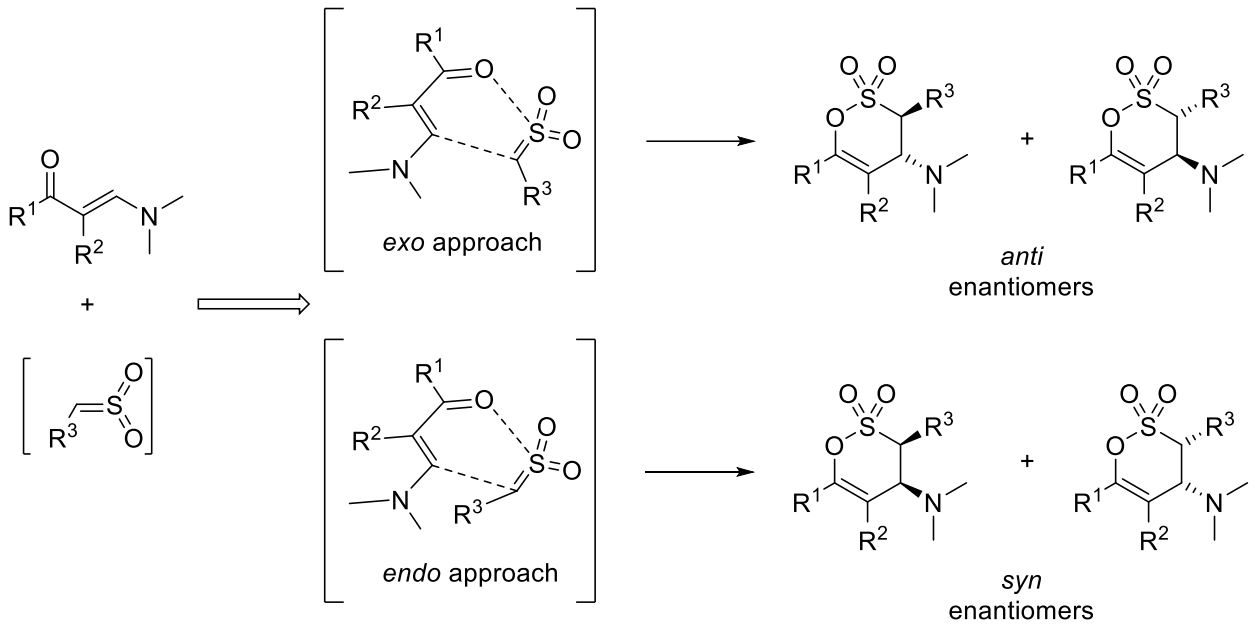

Scheme 2.20: *Exo*/*endo* approaches leading to an *anti*- and a *syn*- pair of enantiomers

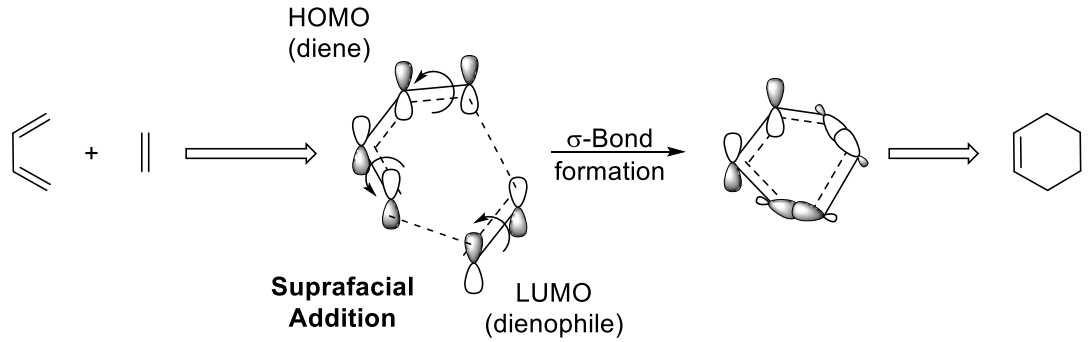

Scheme 2.21: Disrotatory movement of frontier orbitals allowing for the formation of σ-bonds

The dienophile can also approach from either one of the two sides of the plane defined by the diene towards enantiomer pairs. Although the regioselectivity of such cycloadditions is subject to the ambient substituents on both reactants under general Woodward-Hoffmann rules, the presence of clear electron-rich (enaminone O atom, sulfene sp^2 carbon) and electron poor (enaminone C4 atom, sulfene S atom) sites on both starting materials (as described in sections **1.1.2.1** and **1.1.3.1**) suffices for absolute regiospecificity during sulfene additions (Scheme 2.22).

When considering the *exo* and *endo* approaches of the dienophile, the Woodward-Hoffmann rules can be utilised to predict which of the two is the most favourable. During an *exo* addition, any side-groups on the dienophile are facing away from the diene system, as opposed to an *endo* addition, where these groups are proximal to the diene. Intuitively, the steric crowding that occurs during the latter case renders such an approach disfavoured by increasing the energy of its transition state, thus the major product of such a reaction is the *exo* adduct. This trend does not come without exceptions; specifically, the p orbitals of the diene HOMO have the potential of interacting with conjugated moieties appended on the dienophile *via* Secondary Orbital Interactions (SOIs). These interactions are able to stabilise the transition state of the *endo* approach to such an extent that the *endo* adduct is obtained as the major product of the cycloaddition (Scheme 2.23).

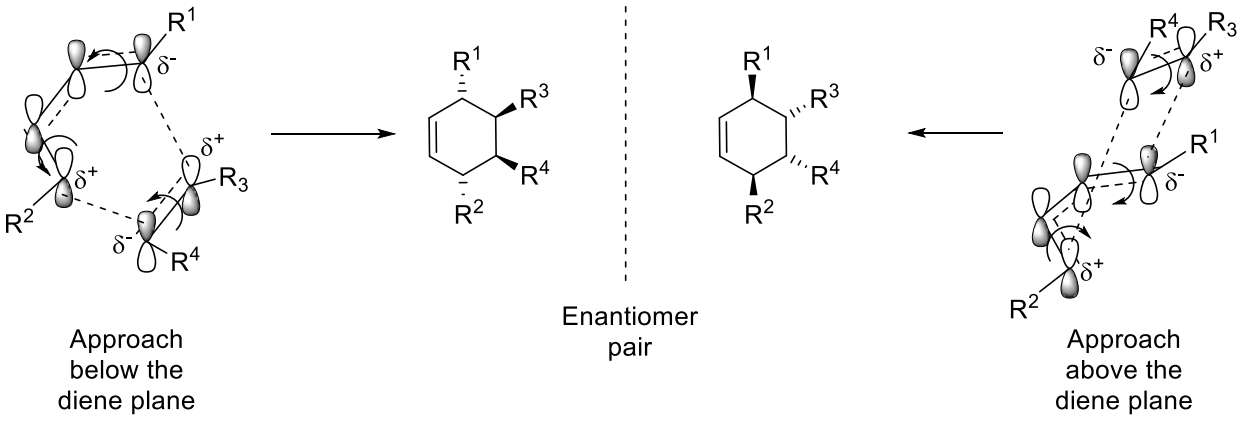

Scheme 2.22: Approaches from both sides of the diene plane afford pairs of enantiomers with substituent-dependent regioselectivity

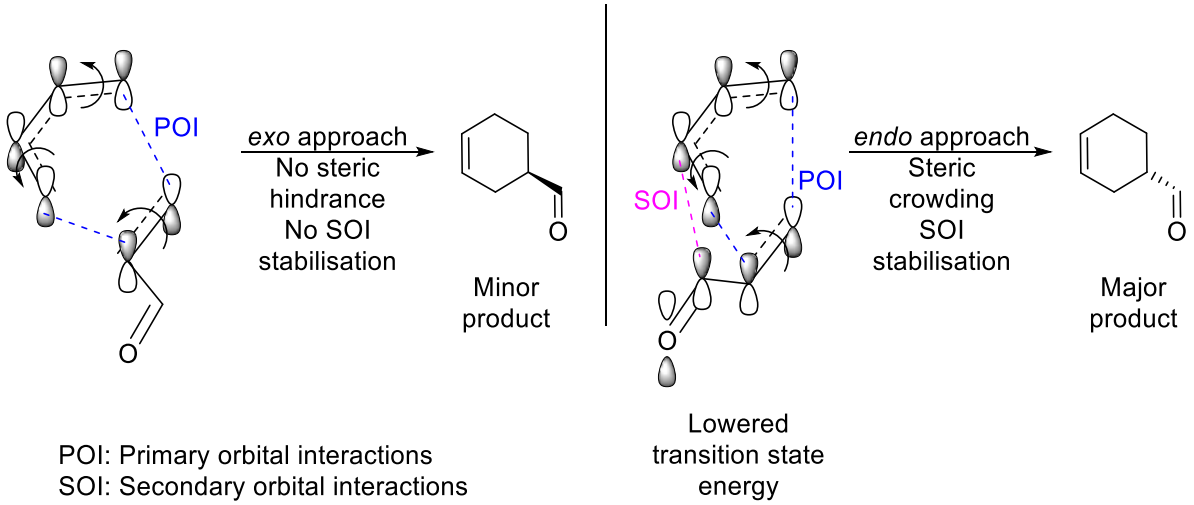

Scheme 2.23: Secondary orbital interactions as the driving force of the otherwise disfavoured *endo* approach

These tenets regarding Diels-Alder cycloadditions can be directly applied in sulfene additions, with the sulfene as the dienophile and the enaminone as the diene. The HOMO of the latter is sufficiently polarised by the carbonyl O atom and the terminal amino group to interact with the LUMO of the sulfene through disrotatory movement towards the 3,4-dihydro 1,2-oxathiine addition product. Following the general trend, the approach of the sulfene may occur in an *exo* or an *endo* fashion, but the presence of the aryl ring group on both the sp^2 sulfene carbon and the enaminone C2 creates a fertile ground for SOIs, potentially in the form of π-stacking between the aryl rings. This means that, in low temperatures, the transition state of the *endo* approach is stabilised enough to overcome the existing steric hindrance between the sulfene aryl group and the ambient moieties of the enaminone and make this approach more favourable over the *exo* one. At this point, a comprehensive description of the mechanistic process can be attempted; upon the *in situ* formation of the sulfene at a lowered temperature, the *endo* approach occurs to a greater extent, allowing the *syn*- diastereomer to be the prevalent isomer while the reaction is under kinetic control. Heating the reaction mixture to room temperature creates conditions of thermodynamic control, thus the sulfene molecules that form at this stage are mainly subject to steric interactions and the *exo* dienophile attack is favoured. Consequently, the *anti*- isomer is the preferred product, whereas concomitant epimerisation of the less thermally stable *syn*- isomer tips the balance further in favour of the former. By the time of full consumption of the starting enaminone, the *anti*-diastereomer is the major component inside the reaction mixture, which is confirmed by ^{1}H-NMR analysis of reaction mixture aliquots (Scheme 2.24). The amount of the minor isomer that has persisted is

dependent on the efficiency of the SOIs taking place during the initial stage of the reaction, as well as the inherent thermal stability of the diastereomer upon its formation.

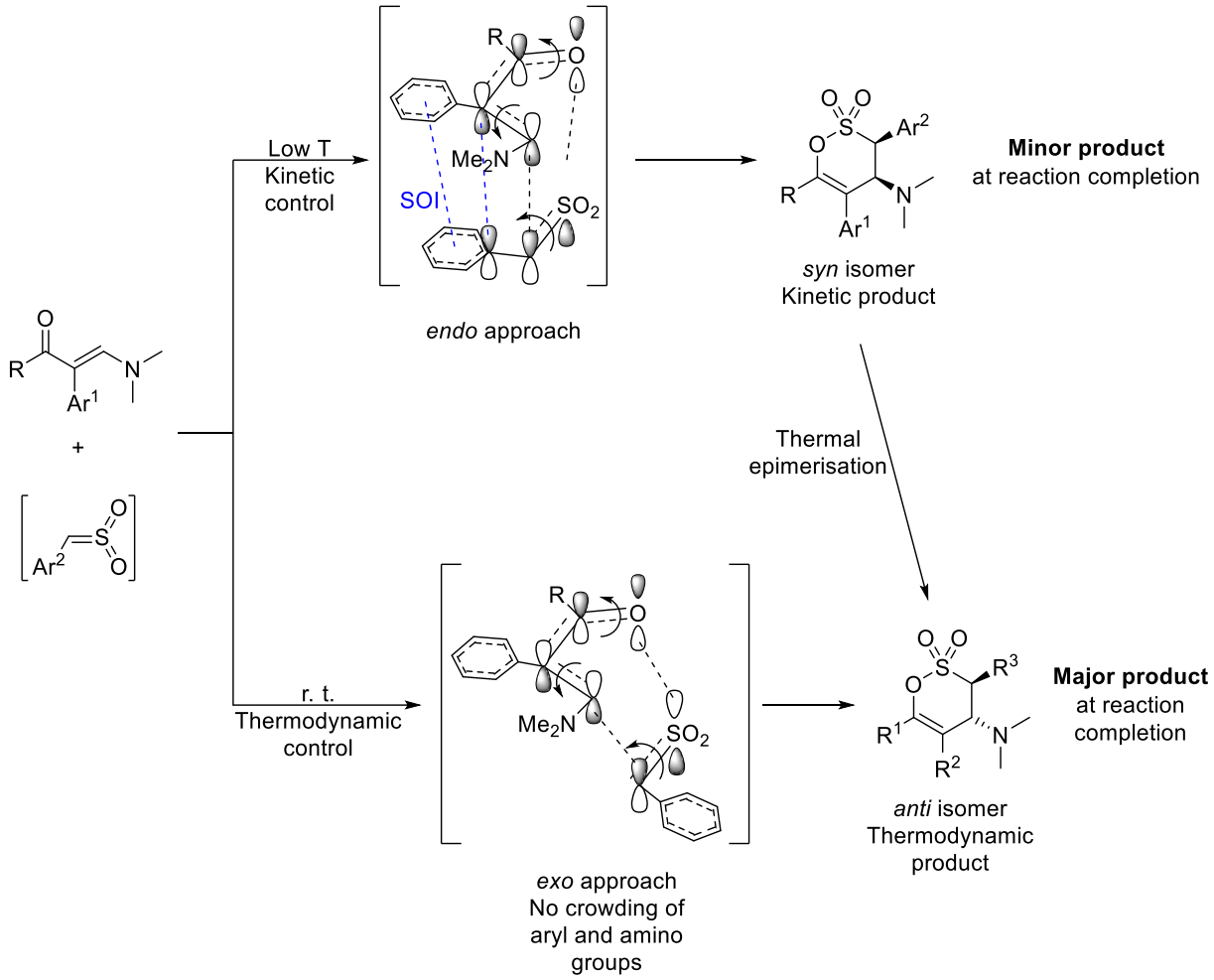

Scheme 2.24: Overview of the proposed mechanistic procedures of a sulfene addition

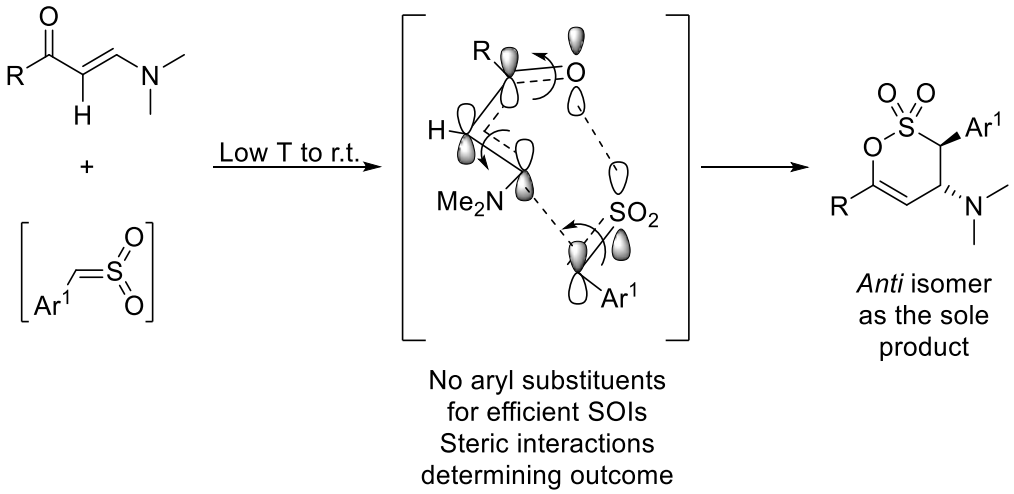

Scheme 2.25a: Mechanistic elements of sulfene additions towards 3,6-disubstituted systems

More conclusions can be drawn when examining sulfene additions with differing substitution patterns. Absence of an aryl substituent on the 2- position of the enaminone negates any prospect of SOIs with the sulfene aryl moiety, thus the addition is exclusively influenced by steric hindrance effects, resulting in the

formation of the *anti*- diastereomer with absolute selectivity. In the case of 5,6-di-substituted 3,4-dihydro 1,2-oxathiine derivatives, no substituents on the sulfene are consequent to the formation of one enantiomer pair since there is only one chiral centre on the heterocyclic products (Scheme 2.25a/b).

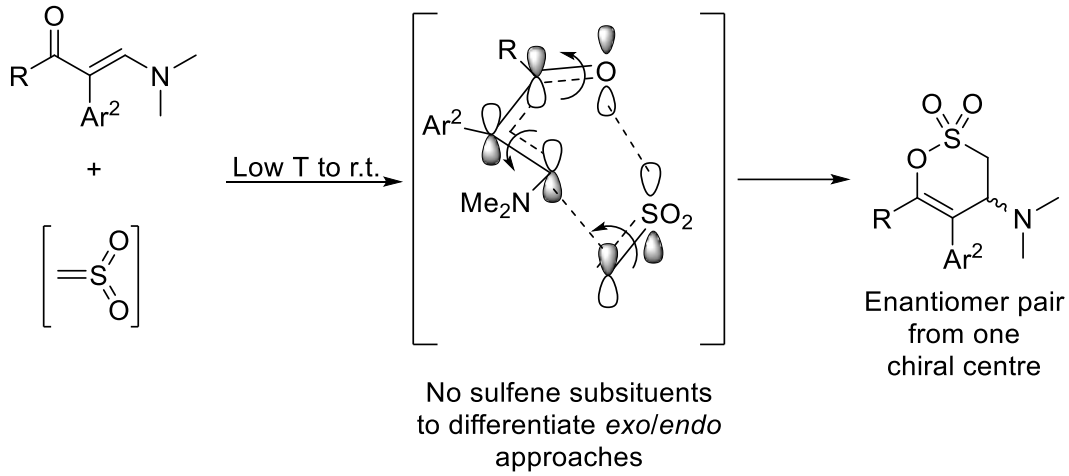

Scheme 2.25b: Mechanistic elements of sulfene additions towards 5,6-disubstituted systems

In order to finalise the framework for the proposed sulfene addition mechanism, the failed attempts towards analogues **2.38**, **2.39** and **2.53** have to be incorporated into it. It appears that, apart from steric interactions or SOIs between the enaminones and sulfenes, electronic effects also have a pivotal role in the fate of these conversions, enough so to overshadow the other factors (Scheme 2.26).

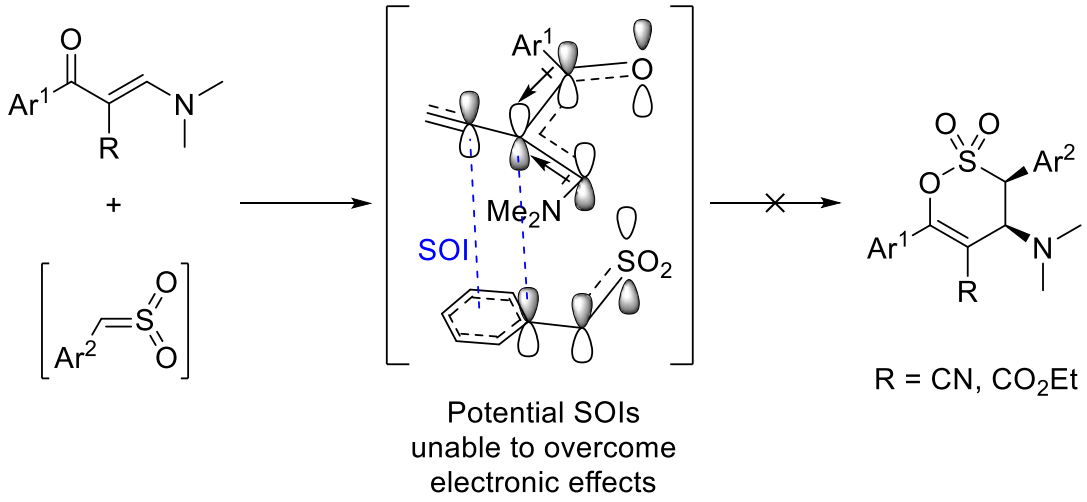

Scheme 2.26: Electron-withdrawing effects of nitrile and ester moieties as the determining factor of 1,2-oxathiine formation

In the cases of **2.38** and **2.39**, the presence of a p orbital-containing C atom on the 2- position of the enaminone and the potential SOIs it can form with the sulfene phenyl group do not suffice for the addition to occur, as the electron-withdrawing nitrile and ester groups restrain the "flow" of electrons and prevent the cycloaddition process. By extension, synthesising **2.53** fails for similar reasons, as any stabilising effects from interaction with the p orbital of the sp^2-hybridised N atom are completely countered by its electronegative character.

At this juncture, it is prudent to present a general scheme which indicates the likely possible products that arise from sulfene addition to an enaminone starting material *via* the *in situ* generation of the sulfene species from the sulfonyl chloride precursor (Scheme 2.27).

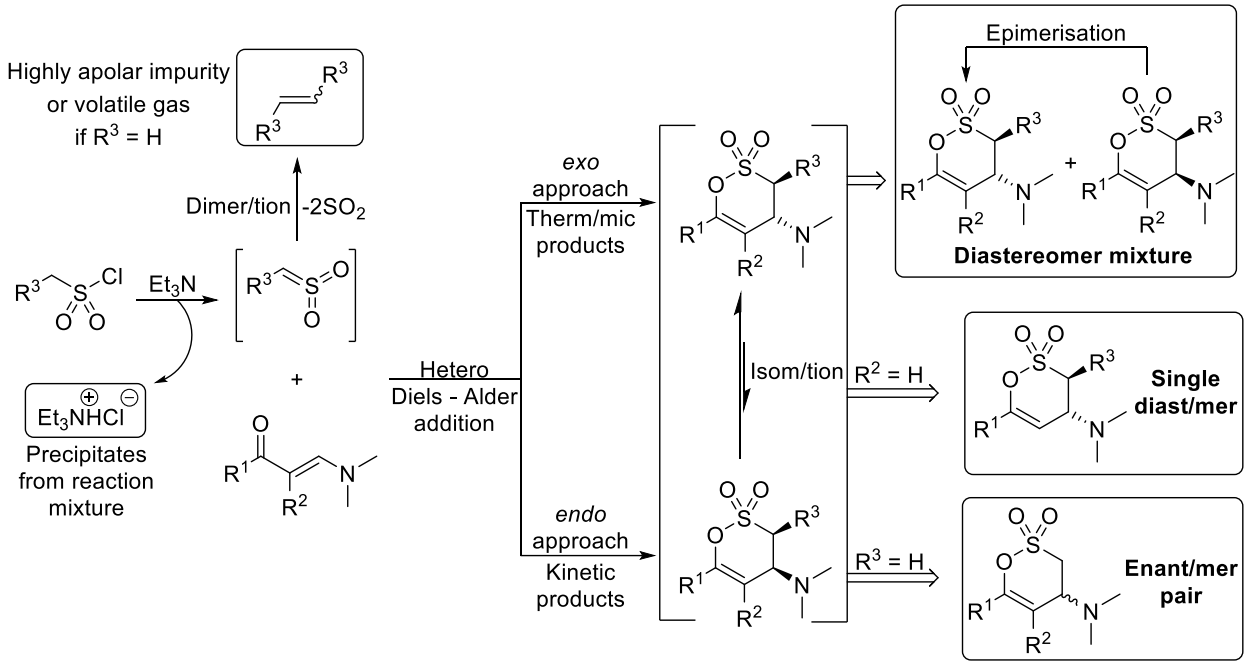

Scheme 2.27: General scheme of the range of products from the addition of a sulfene fragment to an enaminone species

At the beginning of this study it was anticipated that the addition of sulfenes to enaminoketones would provide a rapid access to the 3,4-dihydro-1,2-oxathiine 2,2-dioxide ring system for further exploration, based upon prior research on sulfene addition by Schenone *et al*., (Sections **1.1.2.3** and **1.2.2.2**). Whilst this approach was indeed efficient, it is apparent from the foregoing discussion that the sulfene addition process is complex and would merit much additional exploration. However, with a library of 3,4-dihydro-1,2-oxathiine 2,2-dioxides to hand, it was timely to explore their transformation into the unsaturated derivatives (1,2-oxathiine 2,2-dioxides) and study their subsequent reactivity.

2.3 Elimination towards 1,2-oxathiine 2,2-dioxides

2.3.1 Acid-catalysed elimination attempts

After a selection of saturated 3,4-dihydro-1,2-oxathiine 2,2-dioxides had been prepared, a suitable transformation was required for their conversion into their unsaturated 1,2-oxathiine 2,2-dioxide counterparts. Prior to obtaining the 6-imino (**2.58**) and 6-benzyl (**2.62**) analogues (Sections **2.2.1** and **2.2.2**), it had already been theorised that the saturated 1,2-oxathiine 2,2-dioxide systems had the potential to undergo elimination of the $HNMe_2$ unit irrespective of *anti*/*syn* isomerism, due to the acidity of 3-H and the leaving group potency of the amino moiety upon protonation (Scheme 2.28).
In order to ascertain the efficiency of such a conversion, two of the saturated analogues (**2.36** and **2.41**) were elected as preliminary examples. The first attempts were carried out using a gradient of increasing equivalents of *p*-TsOH in DCM under reflux overnight and afforded none of the desired unsaturated derivatives (**2.63** and **2.64**), as evidenced by TLC and ^{1}H-NMR analysis. Switching the solvent to PhMe, along with a catalytic amount of *p*-TsOH, allowed for the conversion to occur albeit incompletely, while

the obtained crude mixtures had multiple components (indicative of degradation under refluxing PhMe) and required chromatographic purification (Scheme 2.29).

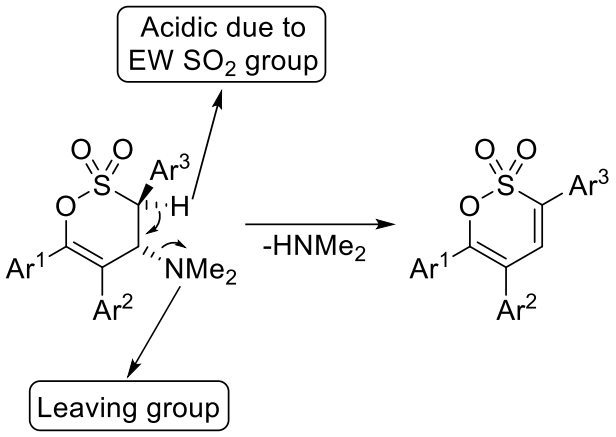

Scheme 2.28: Features of 3,4-dihydro-1,2-oxathiine 2,2-dioxides relating to elimination

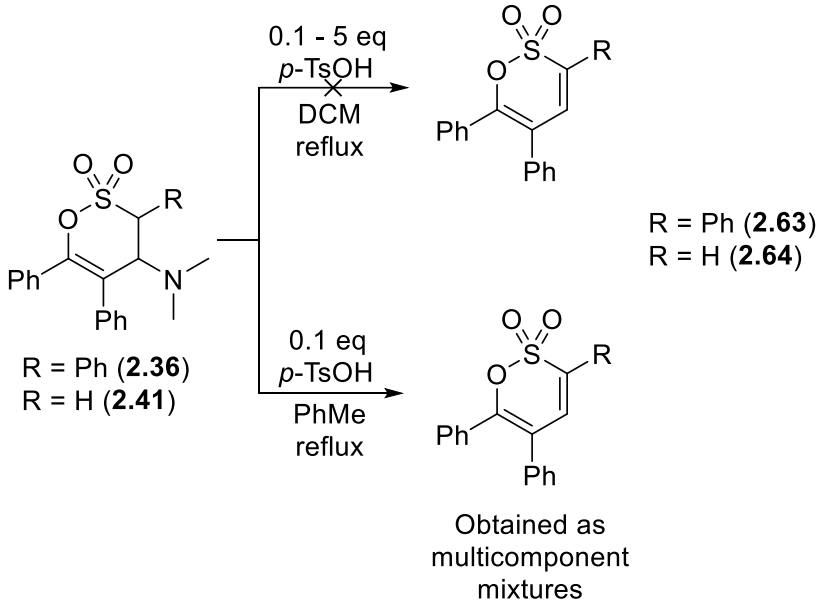

Scheme 2.29: Acid-catalysed elimination attempts on **2.36** and **2.41**

Full purification of the eliminated analogues **2.63** and **2.64** necessitated time-consuming chromatographic purifications of multicomponent mixtures of the unsaturated products and the saturated starting materials, along with decomposition side-products. For this reason, the isolation of **2.63** and **2.64** from the crude mixtures of the foregoing attempts was suspended so that a more robust elimination route could be developed for the efficient compiling of a library of unsaturated 1,2-oxathiine 2,2-dioxides.

2.3.2 Cope elimination: Reaction overview and substituent study

With the basic properties of the NMe_2 group unable to be exploited to a satisfactory extent, the *syn*-relationship between the amino moiety and the 3-H atom on the *anti*- isomer ring skeleton inferred that a *syn*- elimination strategy would be a viable alternative. One such strategy is the Cope elimination

protocol, which was first reported by Arthur C. Cope in 1949, regarding the thermal elimination of *N*,*N*-dialkylhydroxylamine from an trialkylamine-*N*-oxide containing a β-proton (generated by the *N*-oxidation of the respective amine) towards the formation of an alkene system (Scheme 2.30).[116,117] The protocol has a wide range of applications in organic synthesis and has been thoroughly reviewed over the years.[118,119,120]

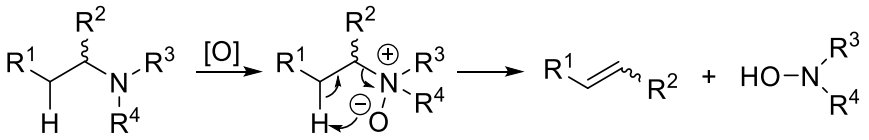

Scheme 2.30: General process of a Cope elimination

In the present work it was envisaged that oxidation of the nitrogen centre upon reaction with *m*-CPBA could bring forth an *N*-oxide capable of cleaving the proximal 3-H in a parallel fashion as shown in Scheme 2.30. Consequent formation of a C3-C4 double bond and cleavage of a $HONMe_2$ fragment would furnish the unsaturated target systems as seen in Scheme 2.31.

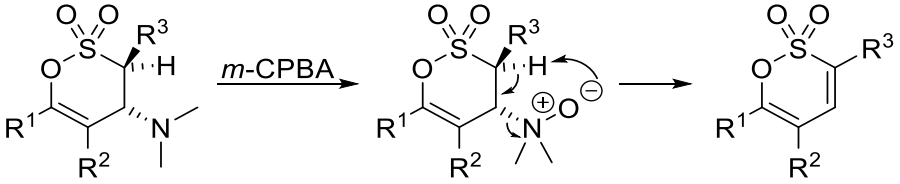

Scheme 2.31: Mechanistic overview of the Cope elimination conversion

Indeed, initial attempts of this reaction were successful and time-efficient; stirring a DCM mixture of the reacting 3,4-dihydro 1,2-oxathiine system and *m*-CPBA at room temperature overnight was sufficient for complete conversion, affording reaction mixtures which could be relieved of the residual oxidant during a work-up process of aqueous washes with reducing agents (Na_2SO_3) and strong bases (NaOH). The reaction allowed for consistent substituent tolerance, as illustrated by the library of analogues that is detailed in table 2.9.

The structure of unsaturated 1,2-oxathiine 2,2-dioxide products could be readily ascertained by ^{1}H-NMR spectroscopy, as previewed in figure 2.32. Tri-substituted analogues can be easily recognised by a singlet near δ 7.0, while 3,6-substituted systems presented pairs of doublets with $J_{4,5} \approx 7.0$ Hz, which is compatible with a single bond between two sp^2-hybridised *C* atoms. Substitution on the 5- and 6- positions leads the 3-H and 4-H to be parts of a *cis*-alkene system with an expected $J_{3,4}$ of *circa* 10 Hz, whereas the presence of one substituent results in the splitting of the signal for 4-H into a double doublet with the aforementioned typical values for $J_{3,4}$ and $J_{4,5}$. Of note is the observation that 4-H is always the more deshielded of the two (or three) protons of the 1,2-oxathiine centre due to a negative inductive effect by the SO_2 group which is amplified by conjugation with the C3-C4 double bond.

Additionally, a main indicator of a successful Cope elimination is the absence of the 1,2-oxathiine backbone aliphatic signals, as well as the 6H singlet for the NMe_2. This is evident by assessing the *C* environments on the ^{13}C-NMR spectra of the eliminated analogues, where the exclusive presence olefinic signals denotes the backbone sp^2 carbon chain of the 1,2-oxathiine ring (Figure 2.33). Further examination of the ^{13}C-NMR of examples **2.63**, **2.64**, **2.67** and **2.76** reveals that substitution of C3 or C5 with a phenyl group has a deshielding effect on these *C* atoms by virtue of the ring current caused by this substituent. Interestingly, C4 shifts upfield upon phenylation of the 3- position, presumably due to electron donation countering the SO_2-mediated electron density withdrawal, although it appears to be deshielded when the same substituent occupies the 5-position through a negative inductive effect.

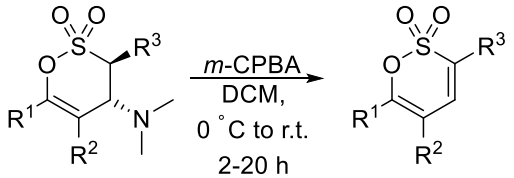

2.36, 2.37, 2.40 - 2.52 → **2.62 - 2.76**

Entry	Compound No.	R_1	R_2	R_3	t (h)	Yield (%)
1	**2.62**	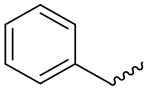	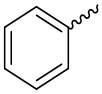	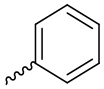	4.5	67.6
2	**2.63**	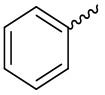	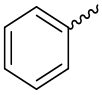	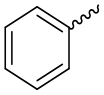	4	62.0
3	**2.64**	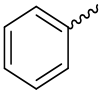	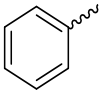	H	3	98.2
4	**2.65**	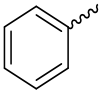	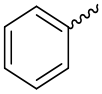	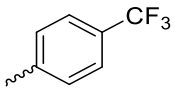	4	77.0
5	**2.66**	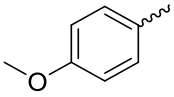	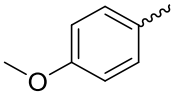	H	2	83.8
6	**2.67**	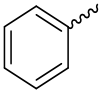	H	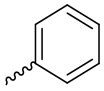	17	79.0
7	**2.68**	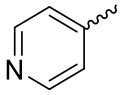	H	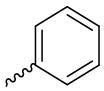	20	72.0
8	**2.69**	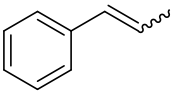	H	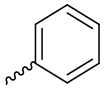	2	88.5
9	**2.70**	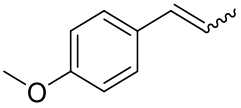	H	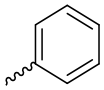	16	89.7
10	**2.71**	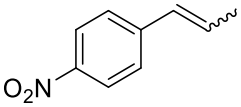	H	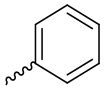	16	92.5
11	**2.72**	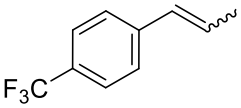	H	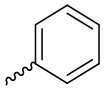	2	92.1
12	**2.73**	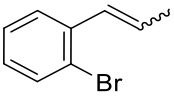	H	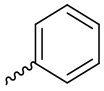	2	87.0
13	**2.74**	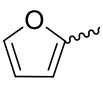	H	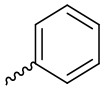	2.5	91.1

Table 2.9a: Library of unsaturated 1,2-oxathiine 2,2-dioxide products of a Cope elimination

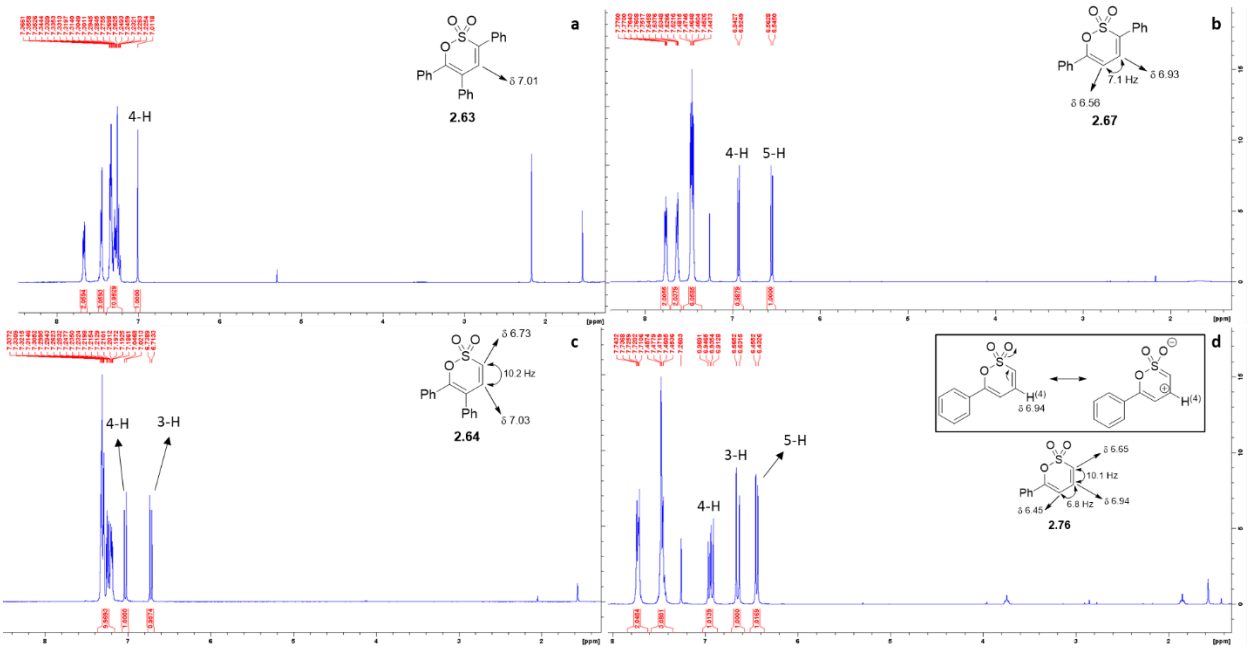

Figure 2.32: Representative examples of ^{1}H-NMR spectra for 1,2-oxathiine 2,2-dioxides (Insert in (d) shows the flow of electron density towards the EW SO_2 group causing deshielding of 4-H)

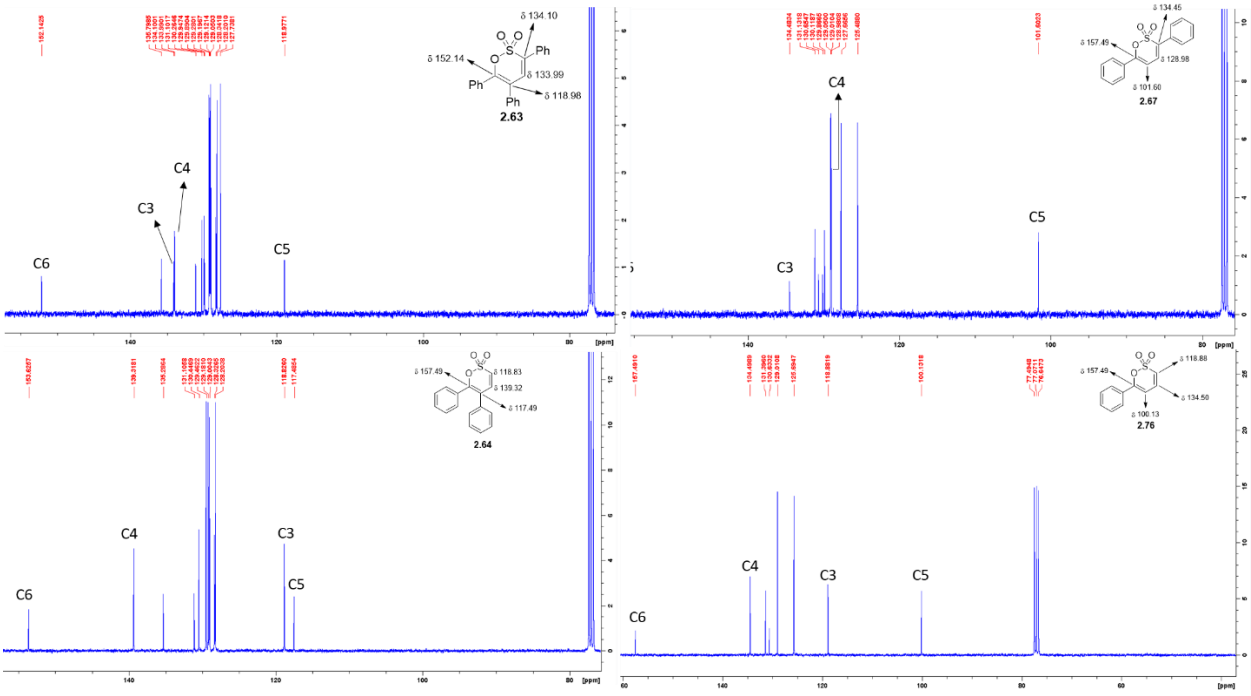

Figure 2.33: ^{13}C-NMR spectra of indicative 1,2-oxathiine 2,2-dioxide examples

Whilst the formation of the diene backbone was confirmed from the ^{1}H- and ^{13}C-NMR spectra of the unsaturated analogues, the preservation of the OSO_2 moiety throughout the elimination could be evaluated *via* IR spectroscopy. Two key bands at *circa* 1370 cm^{-1} and 1175 cm^{-1}, similar to those noted for the saturated analogues, could also be observed in the IR spectra of these compounds, thus proving unequivocally that the obtained products were the eliminated counterparts of the 3,4-dihydro species. With regards to mass spectrometry, the eliminated 1,2-oxathiine 2,2-dioxides were found to behave differently to their saturated precursors and fragment extensively during spectrum acquisition. Despite

the complexity of the resulting mass spectra, the *m/z* peak of the anticipated molecular weight was always prevalent, thus definitively verifying the success of the conversion (Figure 2.34a).

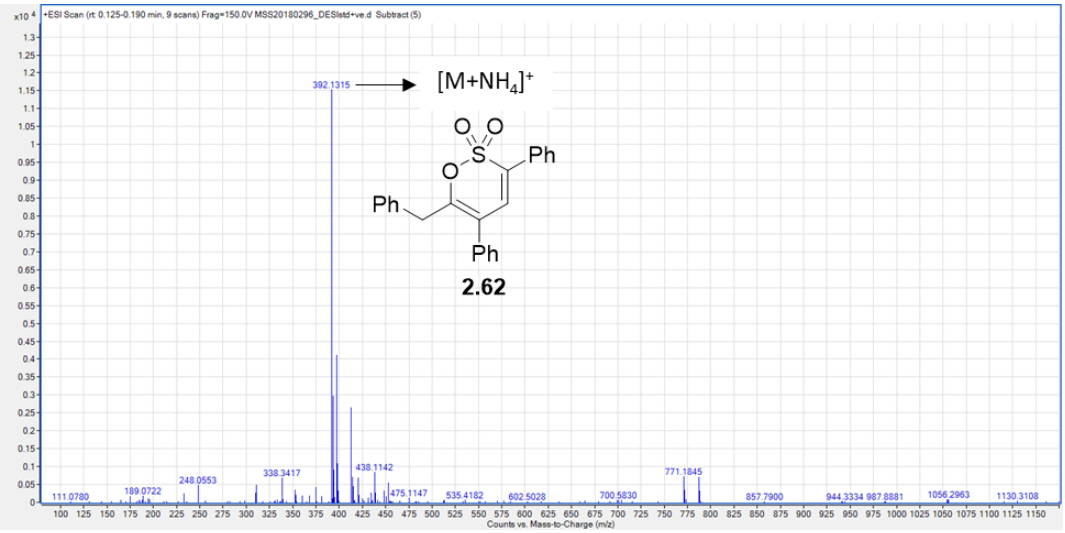

Figure 2.34: MS spectrum of the benzyl analogue **2.62**

Indicative of its good reproducibility, the Cope elimination produced good to excellent yields throughout the analogue library in table 2.9 and for this reason it was the most efficient step of the synthesis route to 1,2-oxathiine 2,2-dioxides from α-methylene containing ketones. It should be noted that broadening the range of 1,2-oxathiine heterocycles through this elimination protocol had been hitherto unexplored in the literature and its consistent efficiency clearly highlights its suitability for this type of amine-containing substrate. Hence, comparison of the obtained yields for the synthesised derivatives offers limited insights, as these attained yields do not fluctuate drastically. The styryl analogues (**2.69** – **2.73**) are of particular interest, as they all appear to be afforded in consistently very good yields, together with the 5,6-phenyl (**2.64**) and furyl (**2.74**) analogues. This consistent trend of effective conversions can be associated with the extended π systems on the 6-substituents. Since the formation of a C3-C4 double bond expands these conjugated systems, the elimination is favoured further in the case of these analogues as compared with the other entries in table 2.9. It can thus be postulated that this transformation is driven by factors relating to the emerging double bond on the eliminated product.

The exact structure of these unsaturated derivatives had already been explored *via* X-ray crystallography, as discussed in section **1.2.1.1**. However, the substitution pattern of these literature examples is different to that of the analogues that were prepared *via* the above Cope elimination protocol. In order to confirm the established structure, a crystal of the triphenyl derivative **2.63** was successfully grown by final year student Kelechi Anozie (University of Huddersfield) and subjected to X-ray analysis.[86] The 3D data obtained point out to the literature-anticipated "envelope" conformation, with the SO_2 group escaping the C3-C4-C5-C6-O plane and the S-C3-C4 angle measured at 114.7°, thus leading to the suggestion that this conformation of 1,2-oxathiine 2,2-dioxide ring systems seems to be prevalent regardless of their substitution patterns (Figure 2.35).

A final point of interest for this reaction is its convenient regioselectivity; a potential setback that escorted the synthesis of the pyridyl- analogue **2.68** was the undesired oxidation of the *N* atom to its respective *N*-oxide. This side-reaction could potentially cause problems with arriving at the desired product, although upon reaction completion and an aqueous washing work-up, the obtained product was pleasingly found to contain no extra O atoms, as evidenced by their mass spectra ($C_{15}H_{11}NO_3S$ requires an *m/z* of 286.0536 for $[M+H]^+$, Figure 2.36), which pointed out that the elimination had occurred regioselectively (Scheme 2.32). Nonetheless, it should be noted that no conclusive empirical data regarding the nature of this

regioselectivity was obtained; examination of the literature[121] suggests that pyridyl-*N*-oxides are able to preserve their integrity during washes with aqueous Na_2SO_3, thus it can be assumed that the oxidant (*m*-CPBA) forms an *N*-oxide exclusively with the NMe_2 moiety without interacting with the pyridine ring on **2.68**.

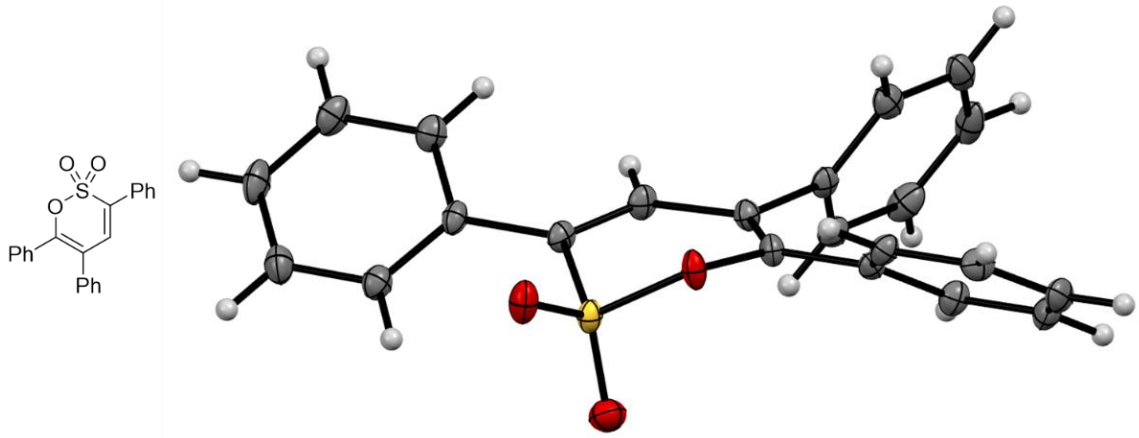

Figure 2.35: Crystal structure of analogue **2.63** (thermal ellipsoids shown at 50 % probability level)

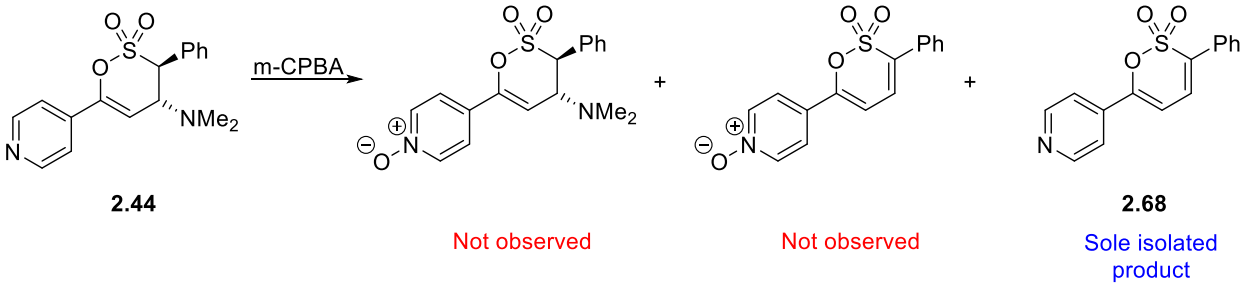

Scheme 2.32: Eliminated example **2.68** as an indicative example of the selective *m*-CPBA oxidation of the NMe_2 terminus

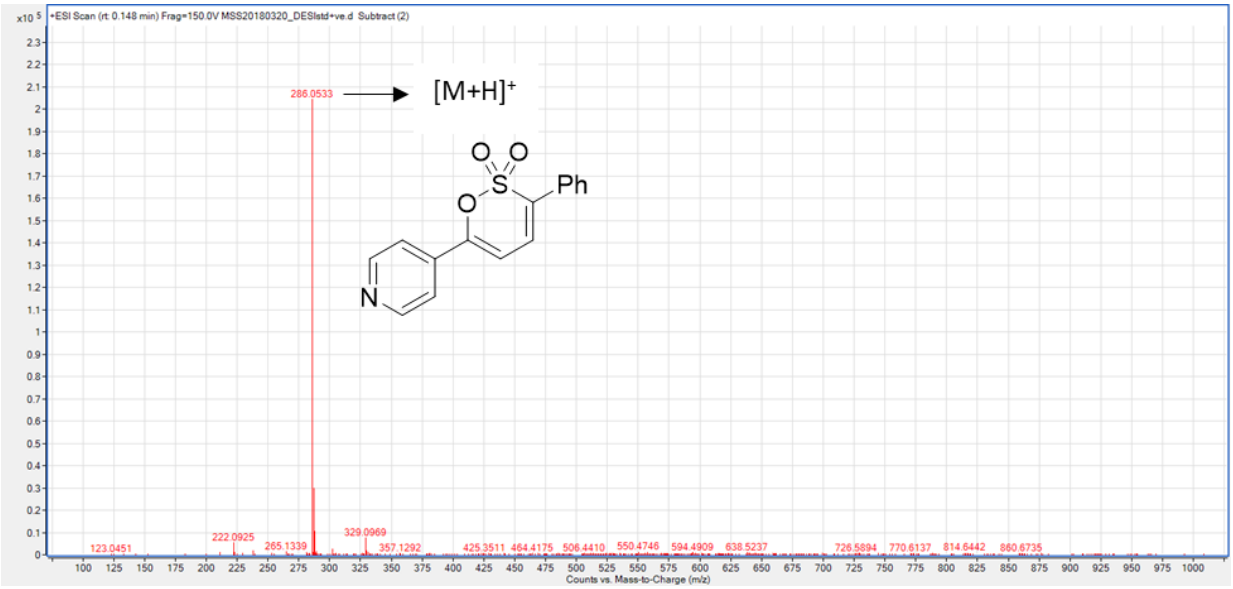

Figure 2.36: MS spectra of **2.68**, wherein no *m/z* peaks of a potential N-oxide can be observed

2.3.3 One-pot synthesis of 6-substituted 1,2-oxathiine 2,2-dioxides

Once the two key reactions (sulfene addition and Cope elimination) to arrive at the desired 1,2-oxathiine 2,2-dioxide species had been examined to a satisfactory effect, the iteration of their consecutive use on a starting enaminone to arrive directly at the unsaturated 1,2-oxathiine target system became a viable alternative to improve the time-efficiency of this synthetic route. As early as the synthesis of the first 3,4-dihydro 6-phenyl analogue **2.52**, the possibility of proceeding with the Cope elimination without purification of the saturated 3,4-dihydro system had been considered, due to the low yield of the latter. When the same sulfene addition was attempted on the pyridyl- enaminone substrate **2.6**, the 3,4-dihydro-1,2-oxathiine product **2.77** was unattainable through standard purification procedures, albeit being observed in the ^{1}H-NMR spectrum of the reaction mixture. In order to tackle this drawback, a repeat run of this sulfene addition was carried out where DCM was opted for the solvent for the sulfene generation and addition instead of THF (Scheme 2.33).

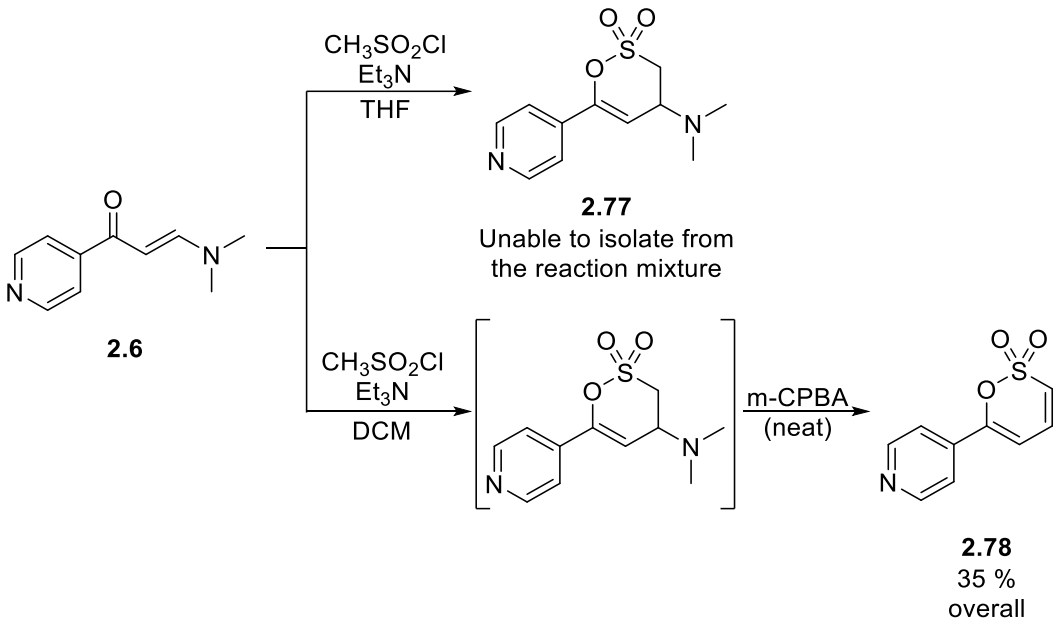

Scheme 2.33: "One-pot two steps" alternative towards 6-pyridyl-1,2-oxathiine 2,2-dioxide (**2.78**)

After the complete consumption of the starting enaminone, *m*-CPBA was immediately added to the reaction mixture, and the standard Cope elimination protocol was followed from this point onwards. Chromatographic purification of the resulting crude mixture afforded the unsaturated target analogue (**2.78**) in a 35% yield over the two steps, as indicated by the characteristic set of ^{1}H-NMR signals at δ 6.61, 6.77 and 6.97, denoting the presence of the C3-C6 chain, along with two signals at δ 7.56 and 8.75 corresponding to the pyridine ring (Figure 2.37).

This synthetic alteration not only served as a solution to arrive at a previously unobtainable derivative, but also paved the way for the utilisation of this one-pot synthesis alternative towards analogous mono-substituted 1,2-oxathiine 2,2-dioxide target compounds. The general procedure included the set-up of a sulfene addition on the starting enaminone as previously established, meticulous drying of the crude saturated intermediate upon filtration of the salt precipitate, re-dissolution in DCM and addition of the oxidising agent according to the general Cope elimination protocol. The obtained reaction mixtures were subjected to the standard work-up process of aqueous washes and the resulting crude products could be readily purified *via* sinter column chromatography. A library of the heterocyclic systems obtained using this method is shown in table 2.10.

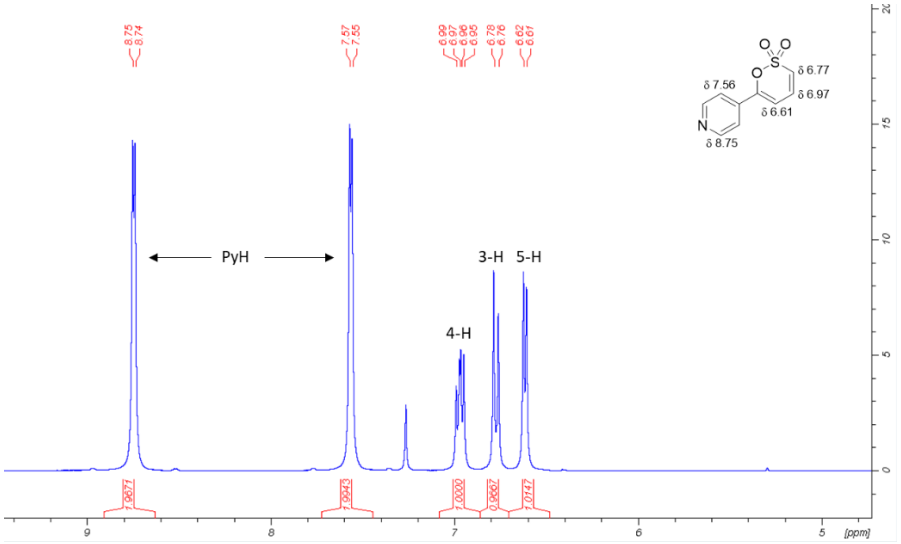

Figure 2.37: ^{1}H-NMR spectrum of **2.78**

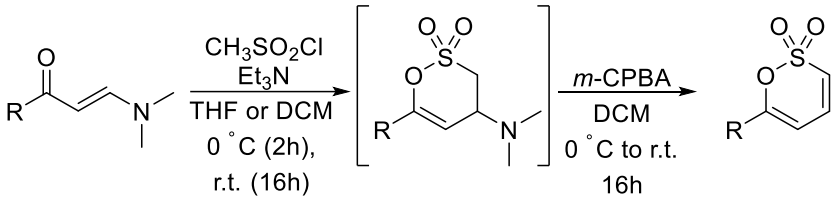

Entry	Compound No.	R	Sulfene Addition Solvent	Overall yield (%)
1	**2.76**	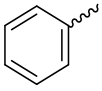	THF	63.7
2	**2.78**	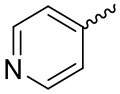	DCM	34.9
3	**2.79**	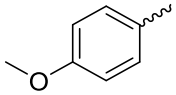	THF	78.7
4	**2.80**	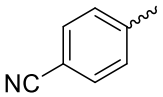	THF	55.9
5	**2.81**	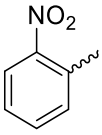	DCM	3.7
6	**2.82**	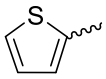	THF	34.0
7	**2.83**	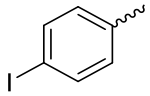	THF	44.8
8	**2.84**	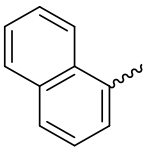	THF	15.8

Table 2.10: Analogue library of mono-substituted 1,2-oxathiine 2,2-dioxides prepared *via* the one-pot, two-step synthetic route

The findings in table 2.10 suggest that the one-pot method offers comparable results with the initial protocol of distinct sulfene addition / Cope elimination steps. Donation or withdrawal of electron density appear to have beneficial (anisyl analogue **2.79**, 78.7 % yield, entry 2) or detrimental (nitrophenyl analogue **2.81**, 3.7 % yield, entry 4) effects on the overall yield respectively; this is to be expected as the substituents on the 6- position of the 1,2-oxathiine heterocycle have been found to clearly influence the reactivity of enaminones during sulfene addition (Table 2.5), as well as the potency of the 3,4-dihydro-1,2-oxathiine analogue towards the Cope elimination process (Table 2.9). Moreover, heteroaromatic substituents seem to mitigate the extent of the conversion, as indicated by the overall yields for the pyridyl- (**2.78**, 34.9 %) and thienyl- (**2.82**, 34.0 %) analogues, whilst the presence of a strong electron withdrawing moiety on the *o*- position of the ambient phenyl group may hinder the 1,2-oxathiine formation even further, as evidenced by the particularly low yield for the *o*-nitrophenyl derivative (**2.81**), potentially due to steric interference during the addition of the sulfene fragment which does not occur when a similar substituent is appended on the *para* position (*e.g.* cyanophenyl analogue **2.80** obtained at 55.9 % overall yield).

To summarise, the addition of DMFDMA was found to convert α-methyleneketones to their enaminone derivatives bearing aryl, heteroaryl, alkenyl, alkynyl, ester and nitrile substituents in fair to excellent yields. Various protocols were evaluated for efficiency and suitability, and the only limitation appears to lie in the potency of the starting ketone to enolise. The library of enaminones was processed through a sulfene addition protocol towards 4-dimethylamino-3,4-dihydro-1,2-oxathiine 2,2-dioxides in moderate to fair yields with various aryl, heteroaryl, alkenyl and alkynyl substituents on the 3-, 5- and 6- positions, whereas enaminones with electron withdrawing substituents such as CN and CO_2R, were found to be inactive. Important aspects of the sulfene addition reaction were highlighted, and the obtained saturated derivatives were subjected to a very mild Cope elimination of the 4-dimethylamine moiety in order to produce their unsaturated 1,2-oxathiine 2,2-dioxide counterparts in good to excellent yields. The two foregoing transformations could also be conducted in a one-pot process to arrive at 1,2-oxathiine 2,2-dioxide species directly from their enaminone precursors.

CHAPTER 3: APPLICATION OF 1,2-OXATHIINE 2,2-DIOXIDE SYSTEMS AS PHOTOCHROMIC MATERIALS[c]

3.1 Preface

With an efficient route developed for the synthesis of 3,4-dihydro- and unsaturated 1,2-oxathiine 2,2-dioxides (Chapter 2) it was envisaged that the 1,2-oxathiine 2,2-dioxide moiety could be incorporated as the central core in a photochromic dithienylethene type system when appropriately substituted with (hetero)aryl groups. In particular, compound **2.64** and its dihydro precursor **2.36** could be considered as a variant of *cis*-stilbene **2.61b**, which is well known to undergo reversible photocyclization to afford a dihydrophenanthrene intermediate, which after irreversible aerial oxidation affords phenanthrene **3.1** (Figure 3.1).[122,123,124]

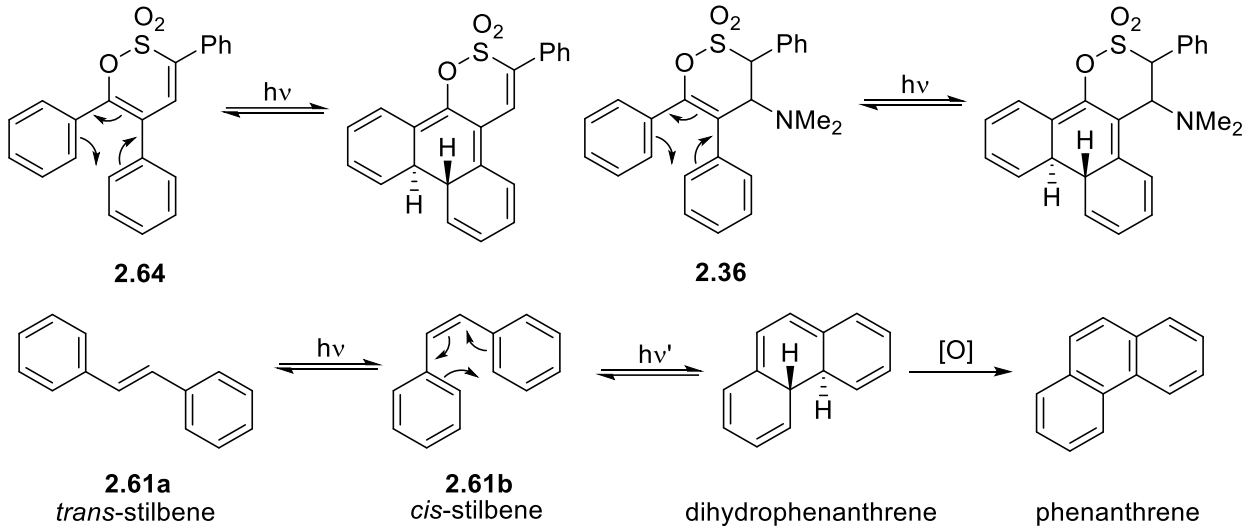

Figure 3.1: Stilbene photocyclization its parallel in triphenyl substituted 1,2-oxathiine 2,2-dioxide systems

Towards an understanding of such a conversion, the phenomenon of photochromism and in particular the niche of dithienylethene photochromic systems requires some introductory explanation.

3.2 Literature precedent

3.2.1 Photochromism and photochromic compounds

Glenn H. Brown, in his book 'Photochromism' (constituting volume III of the series Techniques of Chemistry[125]), defined photochromism as "a reversible change of a single chemical species between two states having distinguishably different absorption spectra, such change being induced in at least one direction by the action of electromagnetic radiation". A more general definition regards photochromism as a physicochemical phenomenon during which a molecule undergoes a reversible structural rearrangement upon absorbing electromagnetic (EM) radiation, commonly in the UV range, with the rearranged structure typically absorbing at longer wavelengths that fall within the visible region of the electromagnetic spectrum (Figure 3.2)[126,127,128,129,130]. When the photogenerated isomer is thermally stable

[c] Work contained within this chapter has contributed to the following publication (Appendix 2, p. 327): *Org. Biomol. Chem.*, **2019**, *17*, 9578-9584; DOI: https://doi.org/10.1039/C9OB02128K

but photochemically reversible the term “P-type photochromism” is applied (*e.g*. dithienylethene **3.2a**, Scheme 3.1a), whereas those photoisomers that thermally revert to their original colourless structure upon cessation of irradiation are called “T-type photochromes” (*e.g*. spiropyran **3.2b**, Scheme 3.1b). An important aspect of P-type photochromic molecules is that even though their photoisomers are thermally stable, they can be driven back to their initial form *via* a photochemical reversion transformation upon irradiation with a different wavelength of EM radiation.

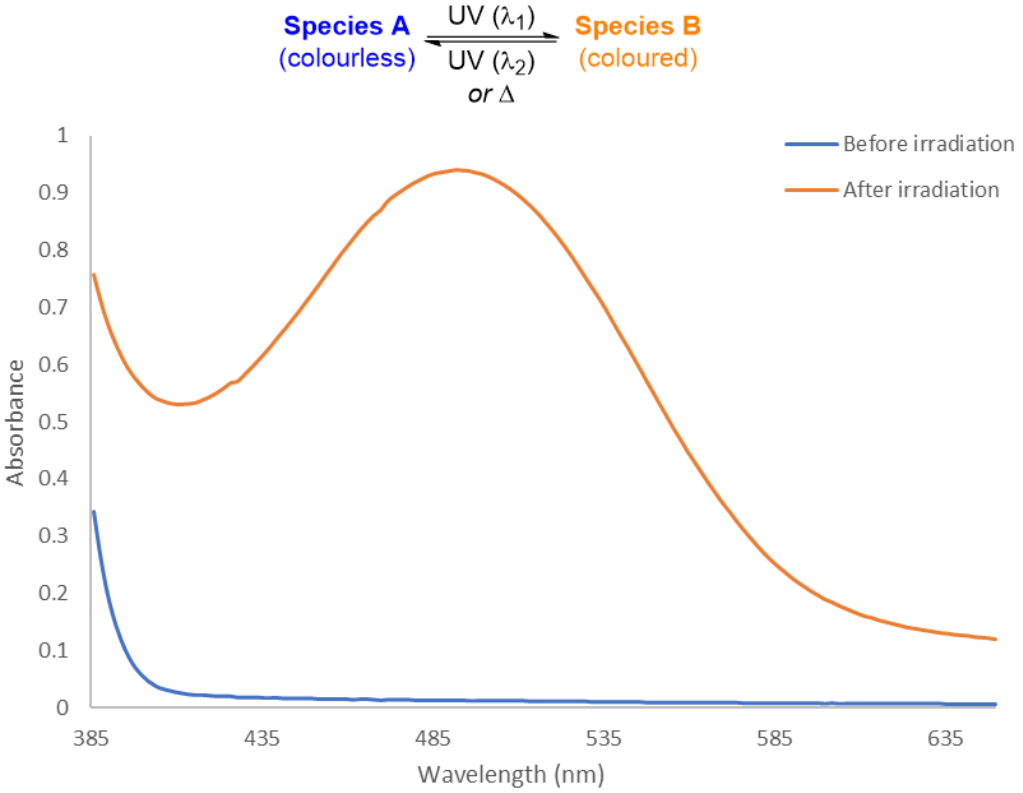

Figure 3.2: UV-Vis spectrum of a photochromic compound before (pale yellow) and after irradiation (red)

a

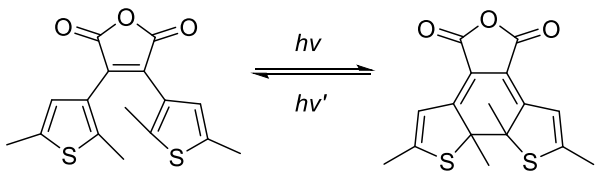

3.2a

P-type dithienyl ethene

b

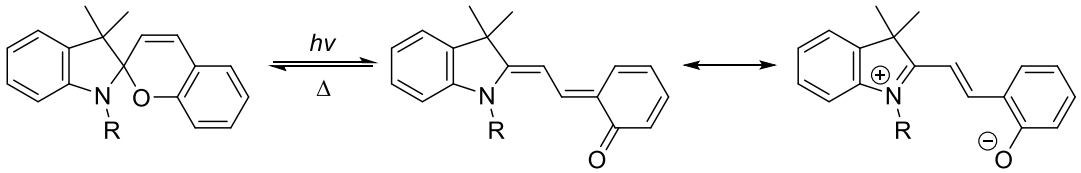

3.2b

T-type spiropyran

Scheme 3.1: (a) P-type and (b) T-type photochromic compounds

In the established literature, photochromic materials have been developed as classes of compounds, with each class having a specific photoresponsive moiety and a mechanism of conversion. The most widely explored classes are presented in Table 3.1.[131,132]

Spiropyrans[133,134] (X = CH), Spirooxazines[135] (X = N) **T-type** (UV induced ring-opening)	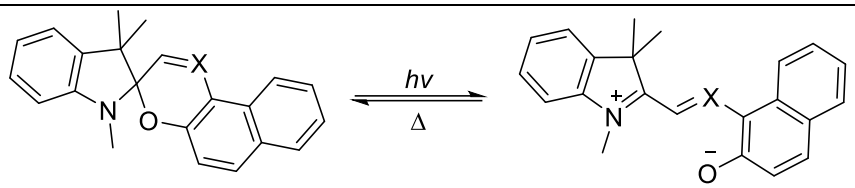 **3.3**
Naphthopyrans[136] **T-type** (UV induced electrocyclic ring-opening)	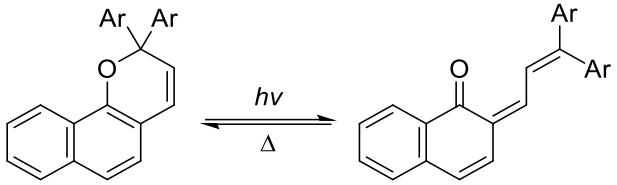 **3.4**
Substituted quinones[137] **P-type** (UV induced *para* – *ana* isomer inter-conversion)	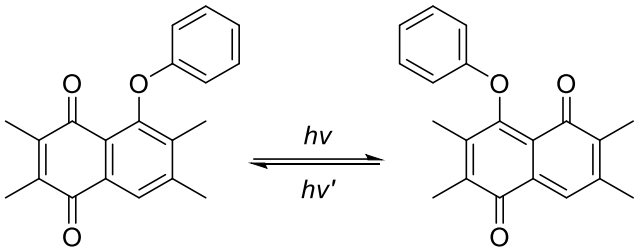 **3.5**
Azobenzenes[138] **P-type** *or* **T-type** (UV induced *trans-cis* isomerisation)	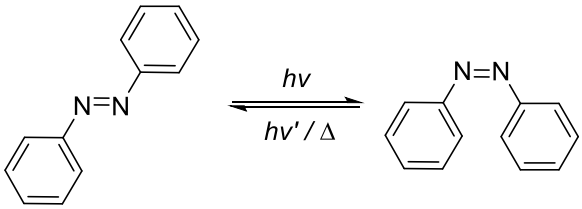 **3.6**
Diarylethenes[139] **P-type** (UV induced electrocyclic ring-closing)	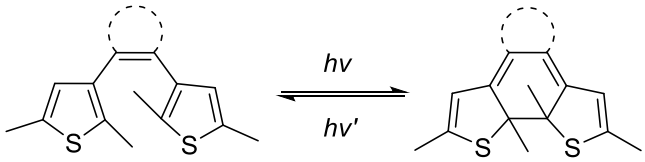 **3.7**
Fulgides[129,140] **P-type** (UV induced electrocyclic ring closing)	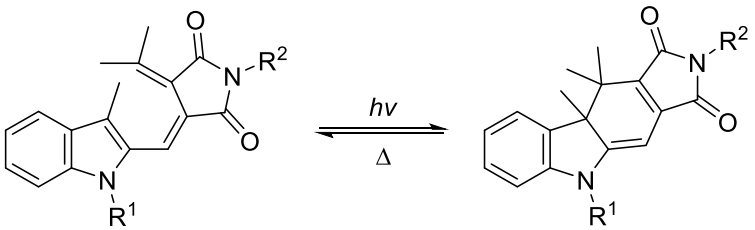 **3.8**

Table 3.1: Main classes of photochromic compounds

The compound classes in Table 3.1 highlight the variety of different conversions that bring about the photochromic activity of the foregoing molecules. Severe structural alterations, such as ring-opening (*e.g.*

spiropyrans/spirooxazines **3.3**, naphthopyrans **3.4**), ring-closing (diarylethenes **3.7**, fulgides **3.8**) and group migration reactions (*e.g.* quinone derivatives **3.5**) have been utilised for these purposes, along with less drastic transformations, *i.e. trans-cis* isomerisation processes (azobenzenes **3.6**).

Photochromism constitutes a research field that is met with significant commercial interest, as T-type photochromes such as spirooxazines **3.3**[141,142] and naphthopyrans **3.4**[143] are widely utilised in the optical lens industry in the production of high value ophthalmic photochromic sunglasses, *i.e.* sunglasses where the lens is capable of reversibly changing from colourless to either grey or brown upon exposure to sunlight. This is made possible by imbibing or coating the lens with photochromes which undergo T-type photochemical transformations as a result of their interaction with solar UV radiation. Further applications include optical memory storage units (P-type photochromes), where the changes in the absorption and transmittance of light is used to store and reproduce information[144,145], as well as molecular switches, in which case the changes in their properties and structure caused by photochromism allow for signal processing in optoelectronic systems[146,147,148]. As presented in the introductory preamble to this chapter, the synthetic route towards 1,2-oxathiine 2,2-dioxides allows for neighbouring substituents on positions 5- and 6- of the 1,2-oxathiine core that are separated by a double bond (as established in Chapter 2), thus resembling the general structure of diarylethene photochromic materials.

3.2.2 Diarylethene photochromic systems

Elaborating on the work reported by Mallory *et al.*[123], concerning the photocyclization of stilbenes, Kellogg *et al*. prepared heterocyclic derivatives of stilbenes (**3.9** - **3.13**) in which the terminal phenyl rings were replaced with heterocyclic units (thiophene and furan) and examined their thermally reversible photocyclization reactions in the presence of iodine as an oxidant (Scheme 3.2).[149]

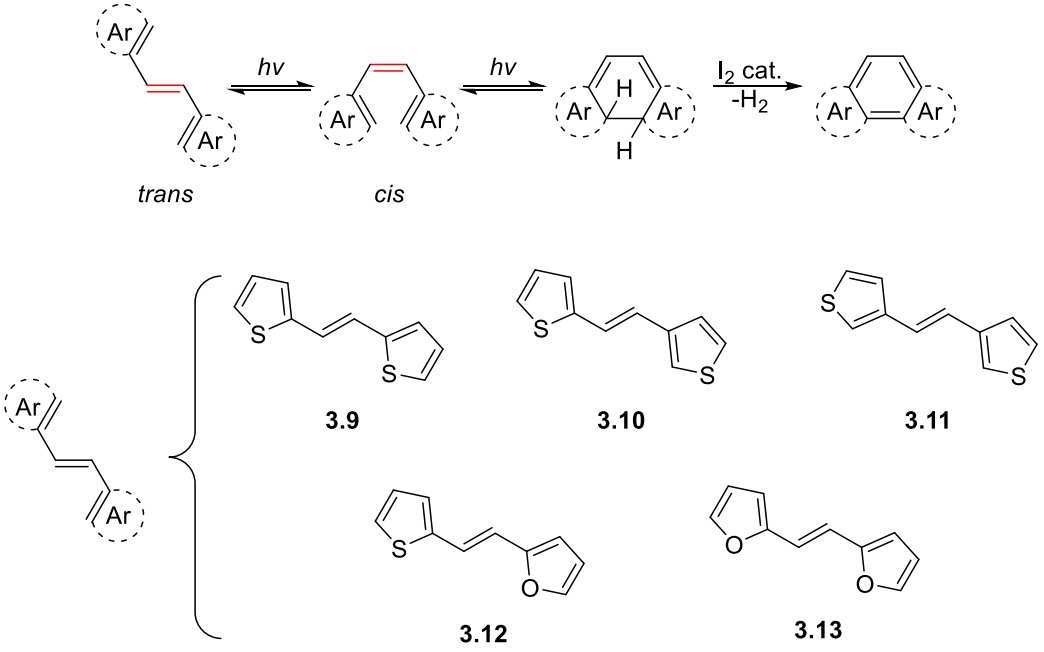

Scheme 3.2: Selected heterocyclic stilbene analogues investigated by Kellogg *et al.*[149]

Irie and Mohri capitalised upon the initial work of Kellogg and established the reversibility of (*E*)-1,2-di(thiophen-3-yl)ethene systems (**3.14**), termed "dithienylethenes", when the thiophene rings were appropriately substituted to produce the active hexatriene unit (Scheme 3.3).[150]

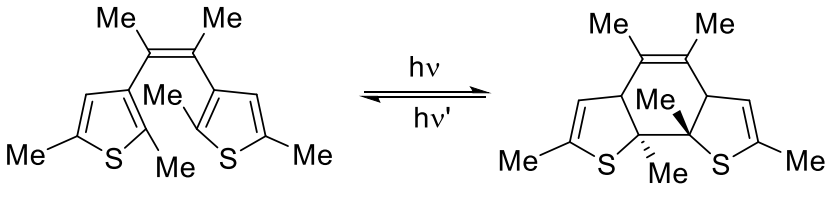

3.14

Scheme 3.3: Photochromic dithienylethene reported by Irie and Mohri

The structural array of this class of photochromes constitutes the basis of their photochromic activity, as it places three double bonds in the appropriate conformation for a UV-induced 6π-electrocyclisation reaction to occur. The result is a new ring system which possesses extended conjugation and thus absorbs in the visible spectrum (general structure **3.15**, Scheme 3.4).

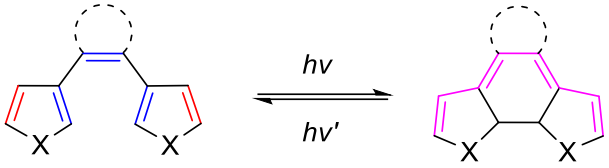

3.15

X = CHCH, O, NH, S

Scheme 3.4: Photochemical cyclisation of a dithienylethene photochromic moiety (**3.15**) leading to extension of the π-conjugated system

a

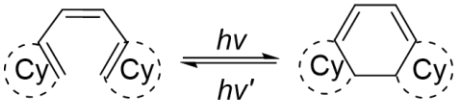

Cy	$\Delta E_{r\text{-}o \text{ to } r\text{-}c}$ (kcal/mol)	Cy	Half-life (T (°C))
Ph	27.3		1.5 min (20 °C)
	15.5		32 min (20 °C)
	9.2		12 h (80 °C)
	-3.3		12 h (80 °C)

b

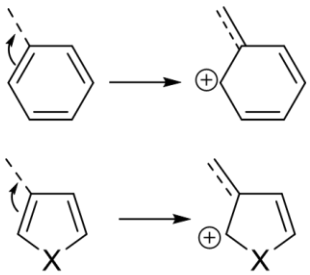

Group	Aromatic Stabilization Energy (kcal/mol)
Ph	27.7
X = NH	13.8
X = O	9.1
X = S	4.7

Table 3.2: High longevity and favourable thermal properties as driving factors of thiophene photochrome efficiency

Although heteroaromatic rings have been studied alongside phenyl groups in diarylethene units,[122,123,139,149] thiophene groups have prevailed as the commonly used building blocks; the efficiency of this heteroaromatic ring is illustrated in Table 3.2, which previews the longevity and thermal stability of a bis-thienyl photochrome unit compared to the other aromatic counterparts. In conjunction with these data, a comparison of the aromatic stabilisation energy of benzene, pyrrole, furan and thiophene indicated that the energy barrier required to be overcome for the ring-closing to occur is lowest in the

case of thiophene, thus confirming their advantage as diarylethene building blocks over other ring systems (Table 3.2).[151]

Moreover, the thermal stability of the ring-closed form can be enhanced by the presence of (usually) alkyl or aryl groups on the periphery of the three double bond system on the ring-open form. Further studies of di(hetero)aryl ethenes have also shown that, upon ring-closing, the *H* atoms of the newly formed single bond can be eliminated via contact with atmospheric O_2 (general structure **3.16**, Scheme 3.5), which can be countered if these positions are substituted (general structure **3.17**).[122]

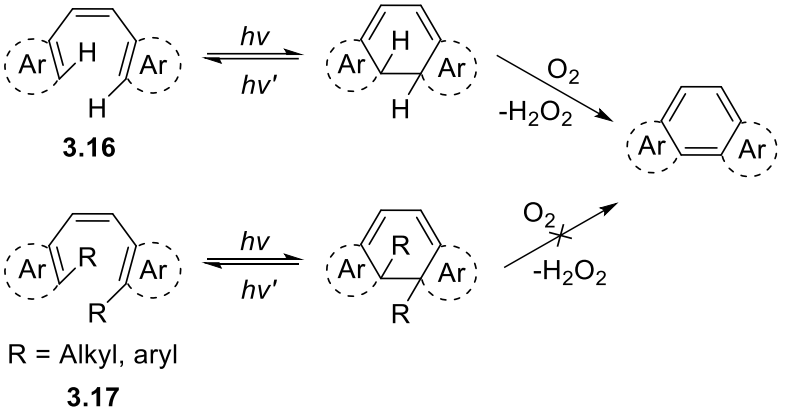

Scheme 3.5: Substitution on key positions of the photochrome unit suppresses undesired H_2 elimination

These structural requirements make for a large variety of di(hetero)aryl ethene analogues (**3.18** – **3.23**), where the two (hetero)aryl groups are either identical or different and the ethene backbone moiety is either an open or a closed ring system[152,153,154,155,156] (Figure 3.3). Another structural feature that is common amongst these species is the presence of a perfluorocyclopentene ring as the backbone of the photochrome unit, which was found to be beneficial for their photochromic activity by virtue of the stable F-C bonds allowing for fatigue resistance.[152]

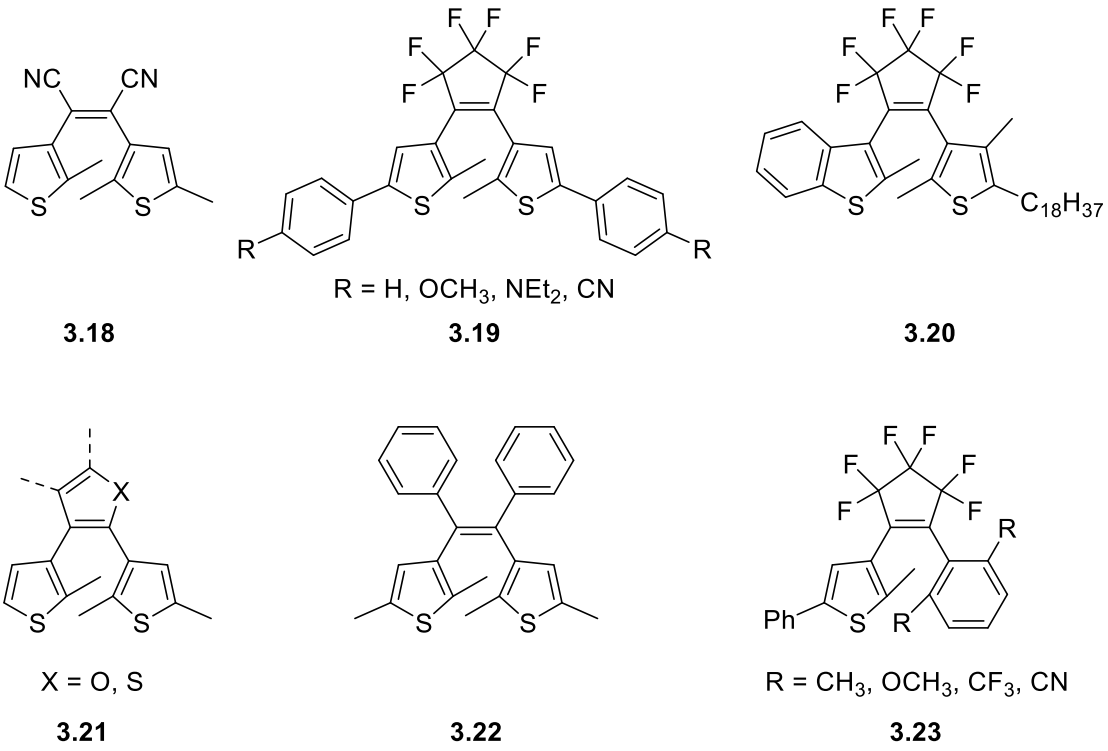

Figure 3.3: Typical examples of different types of di(hetero)aryl ethene photochromes

The conversion of diarylethenes to their ring-closed forms occurs via an electrocyclisation process, which needs to be in accordance with the Woodward-Hoffmann rules[115]: under photochemical conditions, the cyclisation proceeds through a conrotatory motion of the opposing bonds during the stage of the formation of the new bond (1,3,5-hexatriene example, Scheme 3.7a). As a result, an antiparallel conformation of the two aryl groups (**3.24**) is required for the photocyclisation to occur; the parallel conformation **3.25** is able to afford a ring-closed form only through disrotatory movement of the participating bonds, which is sterically hindered due to the presence of the two methyl groups, thus denying the possibility of a thermal cyclisation for these systems (Scheme 3.7b). This indicates that in a population of photochromic molecules, only the percentage that has the necessary conformation will undergo the cyclisation reaction, which constitutes the quantum yield of photochromic conversion in a solution of the compound.

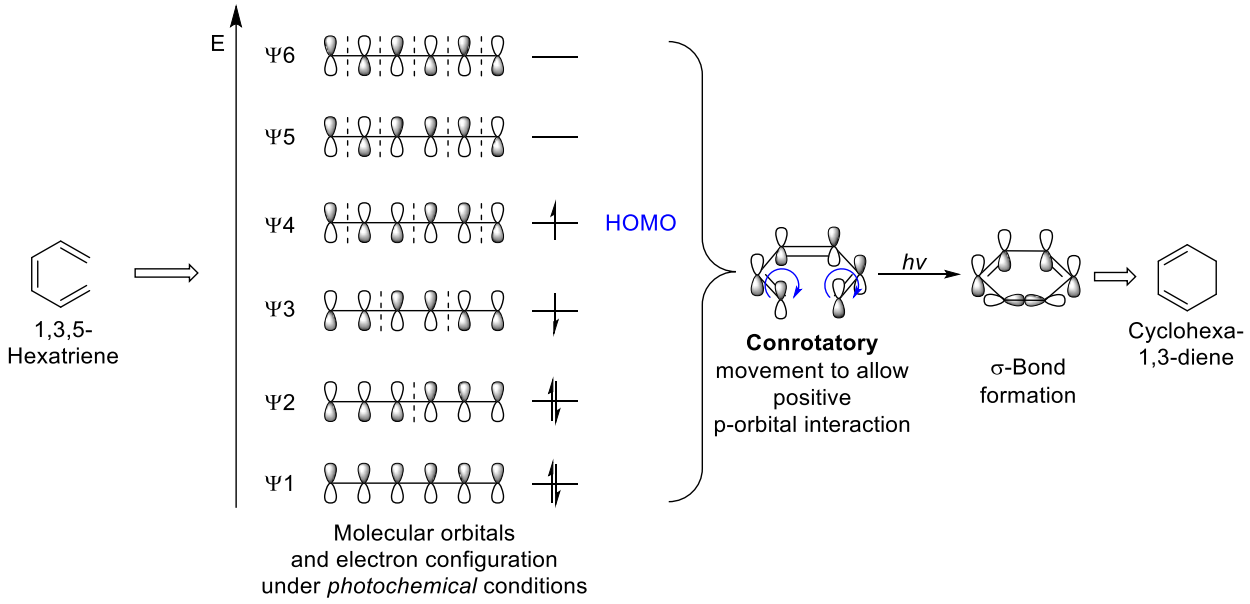

Scheme 3.6: Diagram of molecular orbitals for 1,3,5-hexatriene, highlighting the necessity of conrotatory orbital movement

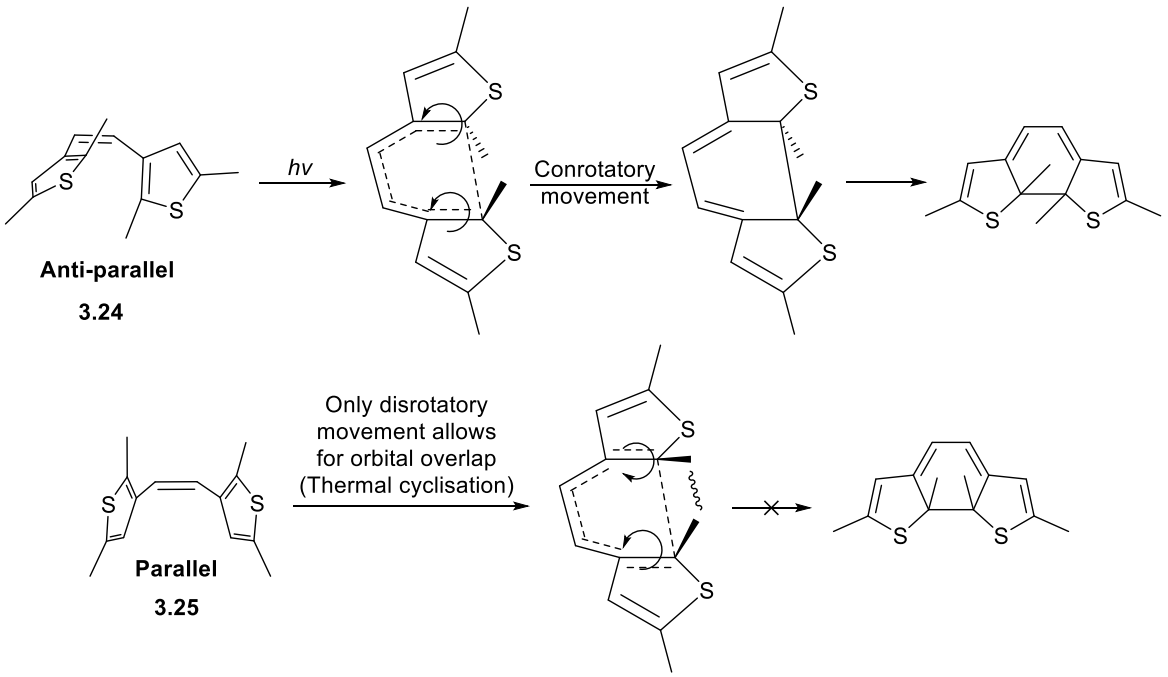

Scheme 3.7: Antiparallel conformation of bis-(2,5-dimethylthienyl)ethene as an inducing factor of photochromic activity

A valuable aspect of the photochromism of these systems is their ability to undergo multiple cycles of photocyclisation under UV irradiation followed by reversion to the initial ring-open form under visible light (colloquially known as bleaching)[157] (Figure 3.4). This endurance against fatigue caused by photochemical degradation makes di(hetero)aryl ethenes potent candidates as key components in molecular switches and optical memory units. [129,139]

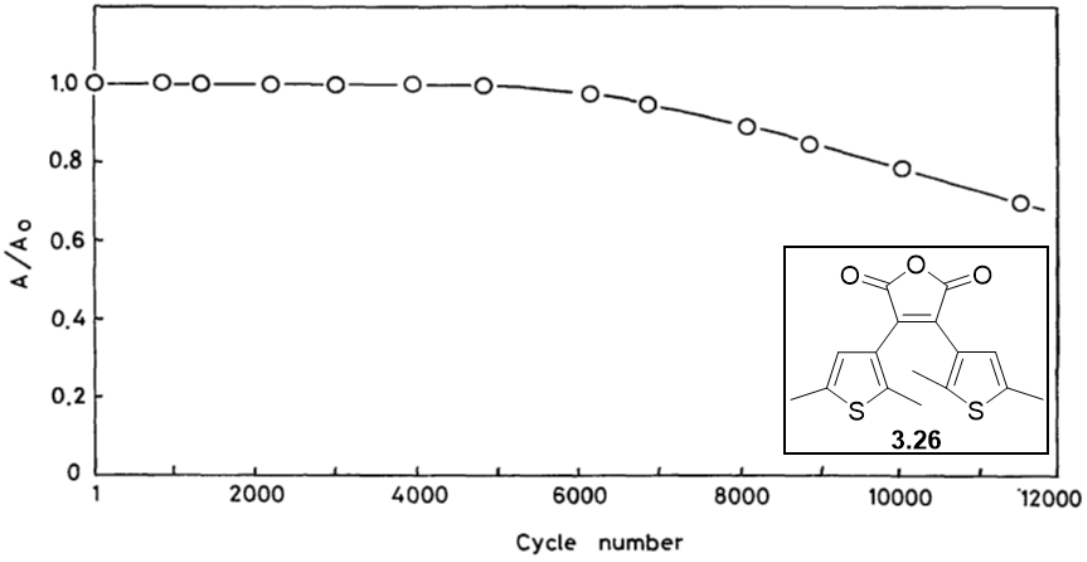

Figure 3.4: Performance of 2,3-bis-(2,4,5-trimethylthien-3-yl)maleic anhydride (**3.26**) during a high number of irradiation/photoreversion cycles, where fatigue occurs only after *circa* 5000 repeats (original picture taken from M. Irie, M. Mohri, *J. Org. Chem*., 1988, **53**, 803-808 and modified)[150]

Apart from the active diarylethene unit, the backbone moiety attached to the ethenic bond has also been explored in recent years. Concerning examples with internal alkene backbone scaffolds and two adjacent 2,5-dimethyl-3-thienyl groups, a search of the relevant literature revealed several ring systems connecting the two carbons of the central double bond on the photochrome. Cyclopropene and cyclobutene ring systems have been scarcely developed, presumably due to the difficulty of synthesising compounds with high internal angle strain (Scheme 3.8).[158,159]

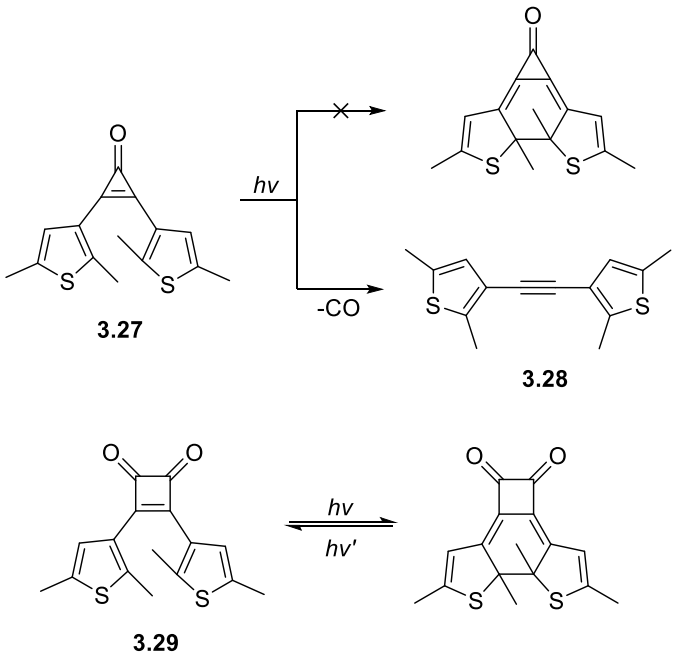

Scheme 3.8: Strained 3- and 4-membered ring systems as backbone groups on dithienylethene

Of note is the cyclopropenone **3.27** which undergoes a UV-mediated CO elimination towards the respective alkyne **3.28**, whereas introducing a second carbonyl, as seen for the cyclobutenyl analogue **3.29**, allows for the anticipated photocyclisation of the hexatriene fragment. Moving towards more thermally stable ring systems, *N*-containing 5-membered heterocycles (**3.30**, Scheme 3.9) have been utilised to host the two thienyl groups with the correct conformation to photocyclise under UV radiation and revert back to the ring-open forms with the use of visible light. Imidazole[160,161] and maleimide[162] systems have been developed to that end, while ionic species with imidazolium backbone moieties[163] have also been explored.

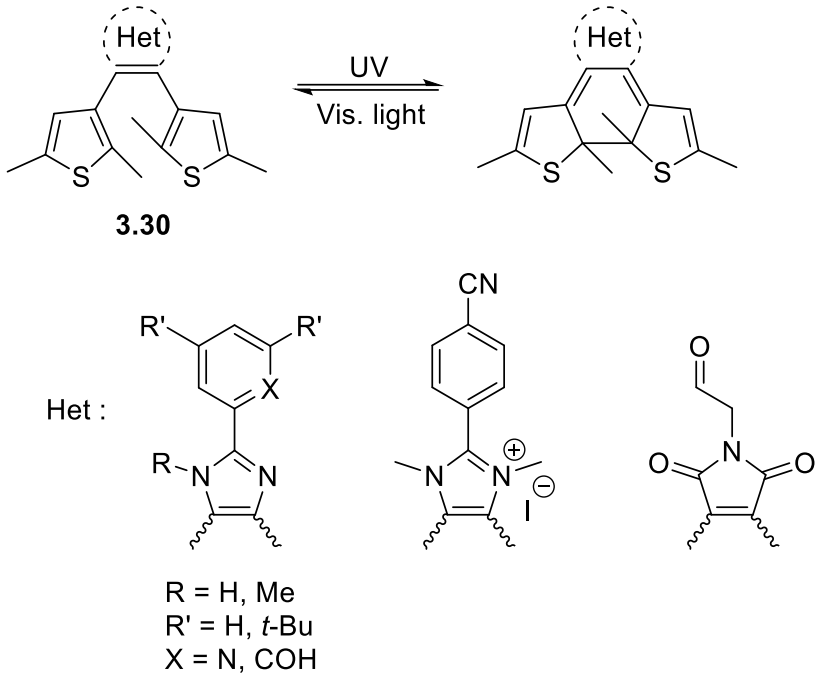

Scheme 3.9: Nitrogen-based heterocyclic dithienylethene photochromes

In a similar fashion, 5-membered heterocyclic arrays that contain one or more *S* atoms (**3.31**) have been examined for their effect on the photochromic activity of the dithienylethene active site. Thiophene[164,165], dithiole[166] and thiazole[167] systems were found to manifest the anticipated activity, although the thione-containing analogue **3.32** was interestingly found to undergo the 6π-electrocyclisation without producing a coloured ring-closed form[166] (Scheme 3.10). Fused thiophene systems with appended phosphole units are of particular note, as they demonstrate further remote functionalisation of the ambient structure of the photochrome[154].

The fused thiophene analogues in Scheme 3.10 were also furnished with a furan ring as the backbone for the dithienylethene unit, leading to furyl-dithienylethene systems[154] (**3.33**) with comparable results. Further research on furan-based photochromes (examples **3.34**) offered less promising results[168], as the ring-closed forms were thermally unstable and susceptible to fatigue upon consecutive cycles of UV irradiation/ visible light photoreversion (Scheme 3.11).

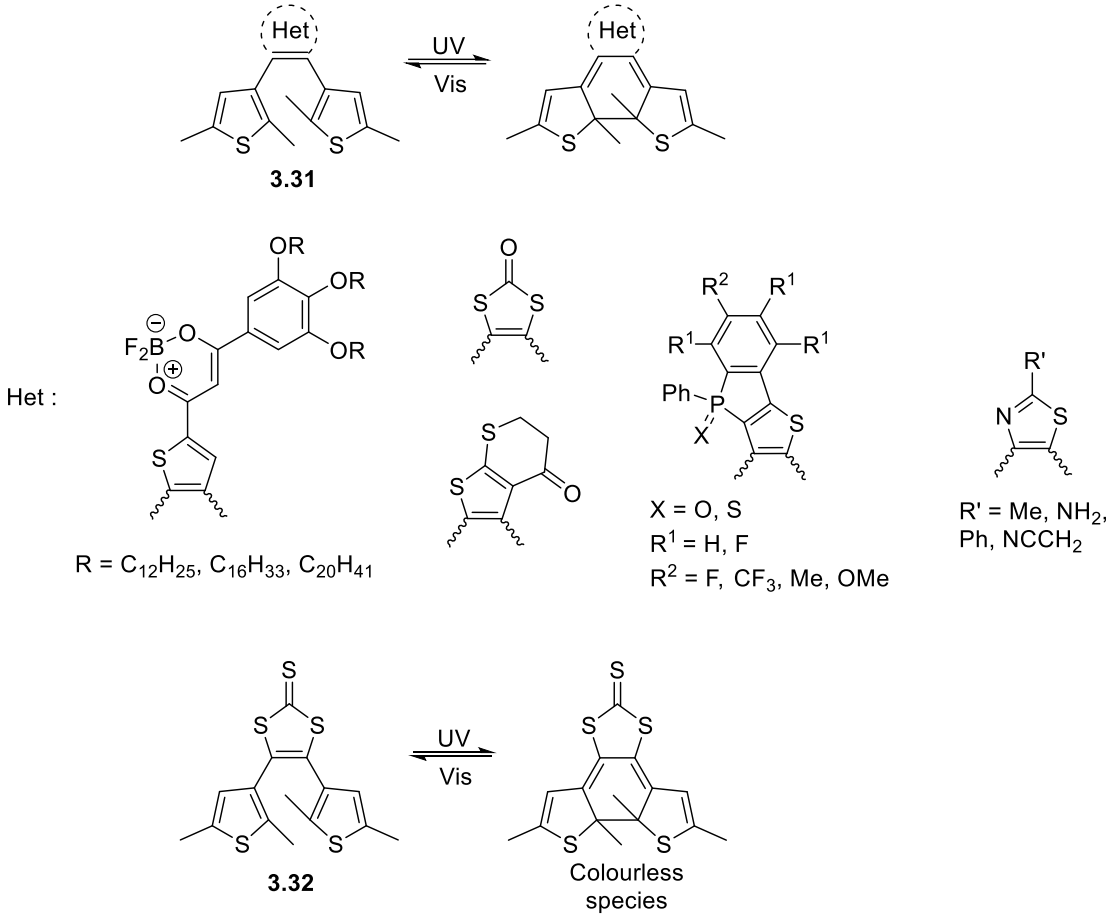

Scheme 3.10: Sulfur-based heterocyclic scaffolds on dithienylethene systems

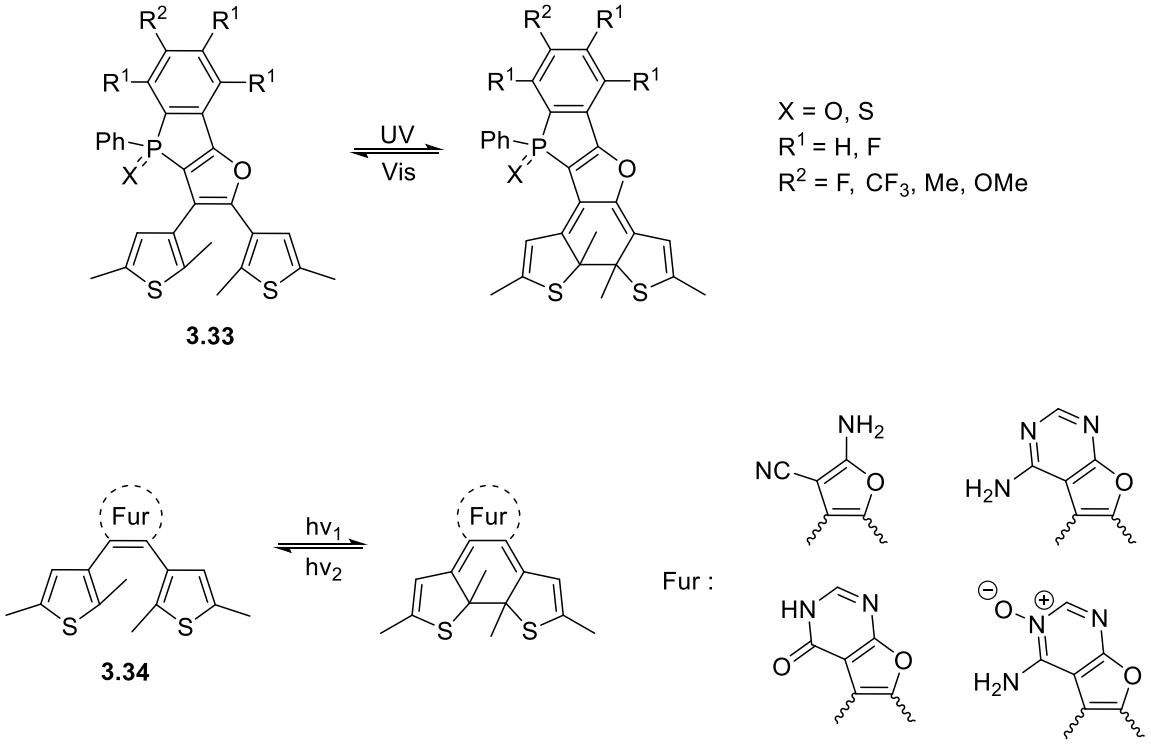

Scheme 3.11: Photochromic candidates with a central furan ring system

In addition to the more common *N*-, *O*- and *S*- heterocycles, silole and phosphole rings (**3.35**, **3.36**) that contain the key double bond of the hexatriene unit have also been explored, although they reportedly failed to produce photochromes that photocyclise reversibly[169]. However, further developments in this area brought forth phosphole systems that are fused with polycyclic scaffolds[170] (**3.37**) and manifest satisfying photochromic properties (Scheme 3.12).

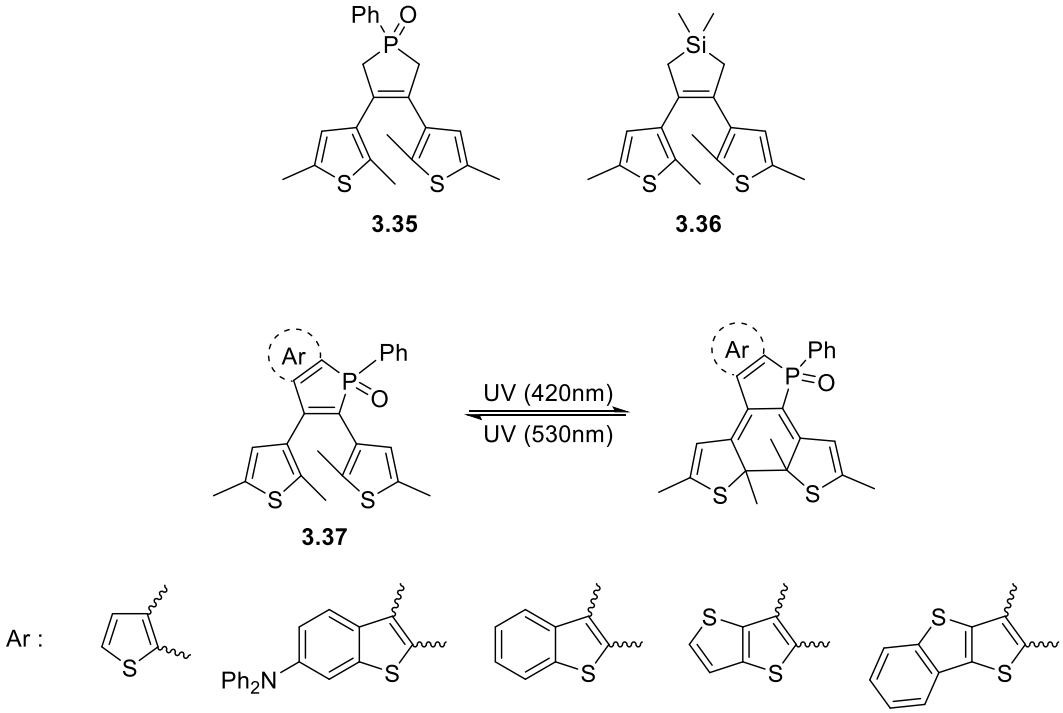

Scheme 3.12: Silicon and phosphorus as heteroatoms on cyclic backbone moieties of photochromic candidates

With regards to 6-membered cyclic backbone systems, the examples described in the literature comprise a broad range of nitrogen-, oxygen- and sulfur-based heterocycles that are able to host the two key thiophene groups and allow for reversible photocyclisation (Scheme 3.13a,b).[171,172,173]

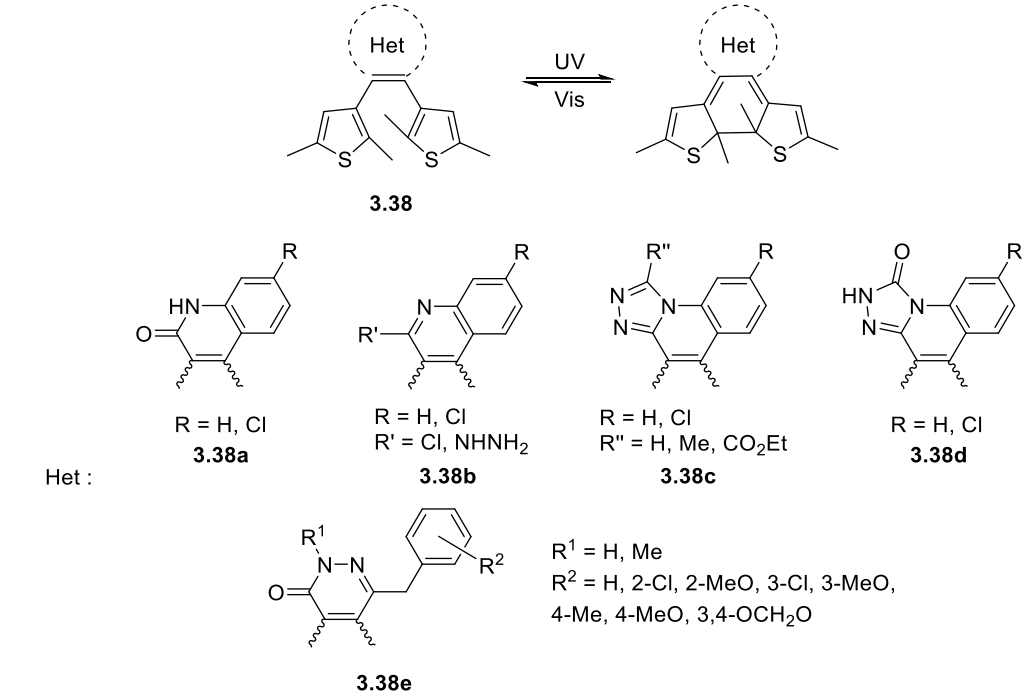

Scheme 3.13a: Classes of bis-2,5-dithienyl ethene photochromes with heterocyclic backbones

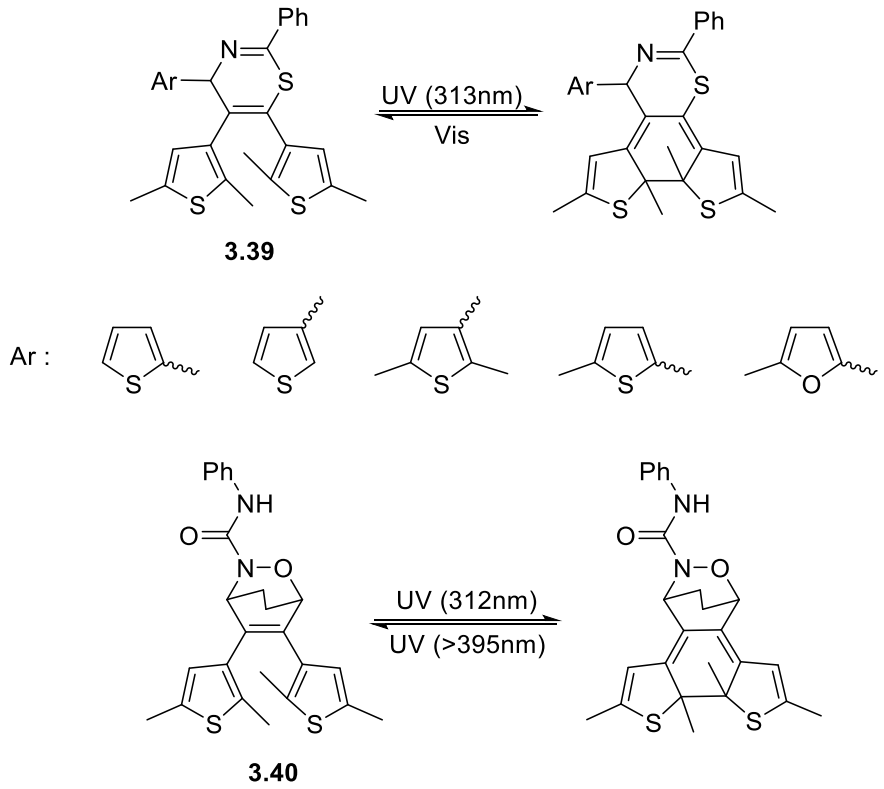

Scheme 3.13b: Classes of bis-2,5-dithienyl ethene photochromes with heterocyclic backbones

Various research groups have developed quinolones (**3.38a**), quinolines (**3.38b**), fused triazoloquinolines (**3.38c** and **3.38d**), pyridazinones (**3.38e**) and thiazines (**3.39**) as capable backbone scaffolds. The bridged oxazine system **3.40** is of further interest, as it requires light on the cusp of the visible – UV boundary at 395 nm for the photoreversion reaction, which falls outside the typical range of visible light irradiation wavelength (*circa* 570 nm).

Finally, 7-membered systems have also been utilised but to a much more limited extent.[174] Interestingly, the photochromic system **3.41** is also a dimeric species with two independent dithienylethene units appended to it, leading to an intermediate where only one of the dithienylethene units has generated the ring-closed form and the final isomer wherein both dithienylethene units have undergone photocyclisation (Scheme 3.14).

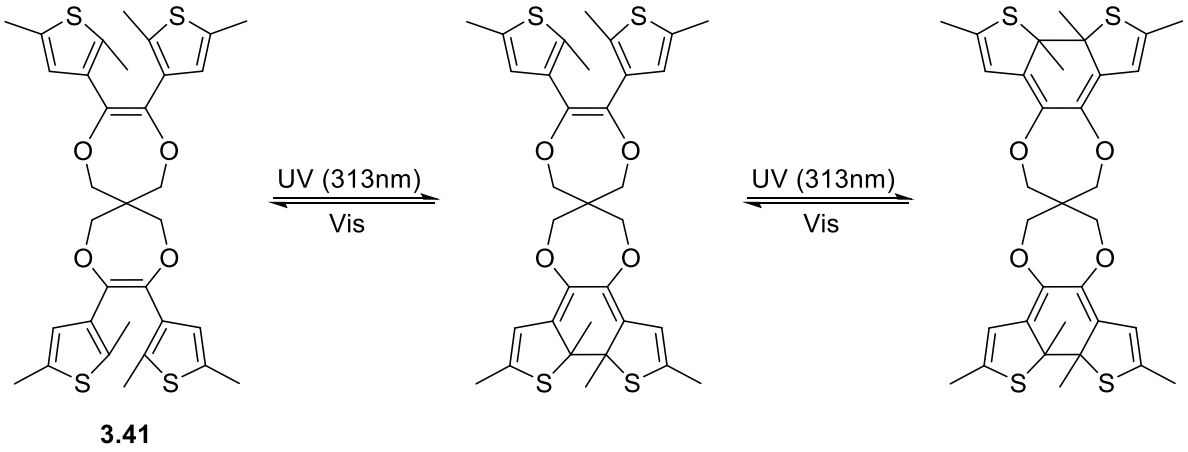

Scheme 3.14: Dimeric species **3.41** as an example of a 7-membered heterocyclic backbone core

As it can be deduced from the aforementioned literature findings, the synthesis of novel dithienylethenes with derivatised heterocyclic backbone units remains an active area of research, as the central ring has an

active role on the features of the photochromic activity. Given this potential influence, novel diarylethene candidates with 3,4-dihydro-1,2-oxathiine 2,2-dioxide and 1,2-oxathiine 2,2-dioxide backbones will be synthesised using the methodology discussed in Chapter 2 and then examined for photochromic properties.

Note: Compounds already synthesised in chapter 2 with the general structure numbering **2.*XX*** have been renumbered in this chapter with the general numbering **3.*XX*** for ease of reading and continuity.

3.3 Explorations on photochromic activity of 1,2-oxathiine 2,2-dioxide systems

3.3.1 Synthesis of diarylethene photochrome candidates based upon a 1,2-oxathiine 2,2-dioxide core

Key to the synthesis of the target photochromic systems **3.43** - **3.46** and **3.48** - **3.51** which are presented in Figure 3.5 are the three thiophene containing methylene ketones **3.52**, **3.53** and **3.54** (Figure 3.6), whereas the synthesis of **3.42** and **3.47** commencing from commercially available deoxybenzoin has been described in chapter 2.

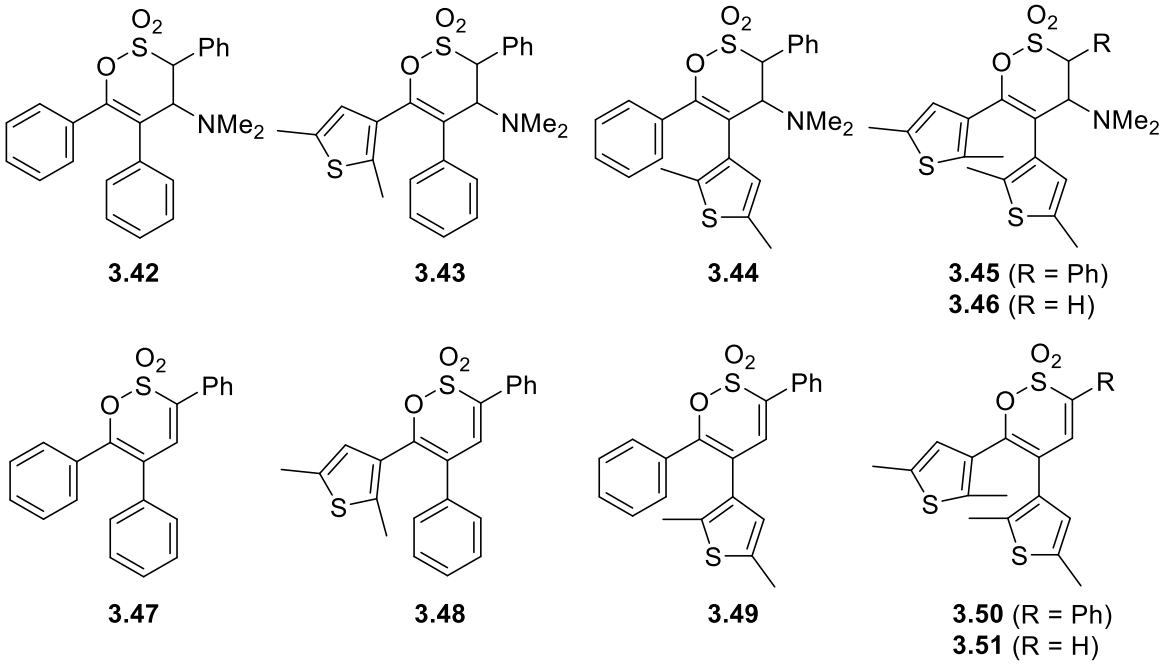

3.42 **3.43** **3.44** **3.45** (R = Ph) **3.46** (R = H)

3.47 **3.48** **3.49** **3.50** (R = Ph) **3.51** (R = H)

Figure 3.5: Target structures of the 1,2-oxathiine 2,2-dioxide photochrome candidates

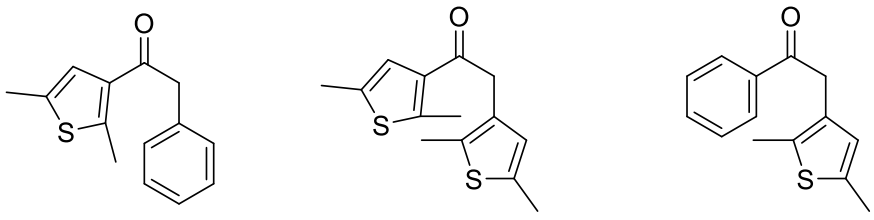

3.52 **3.53** **3.54**

Figure 3.6: Target thiophene containing α-methylene ketones

The most readily accessible methylene ketone was **3.52** which could conveniently be prepared from commercially available starting materials, 2,5-dimethylthiophene and phenylacetyl chloride, by a Friedel-

Crafts acylation reaction. Examination of the literature revealed two additional routes to **3.52**, an early report which employed a Friedel-Crafts acylation using CS_2 as the solvent and $AlCl_3$ as the Lewis acid catalyst[175] and a more recent Pd-catalyzed carbonylative Suzuki cross-coupling protocol between benzyl halides with potassium aryltrifluoroborates[176] (Scheme 3.15).

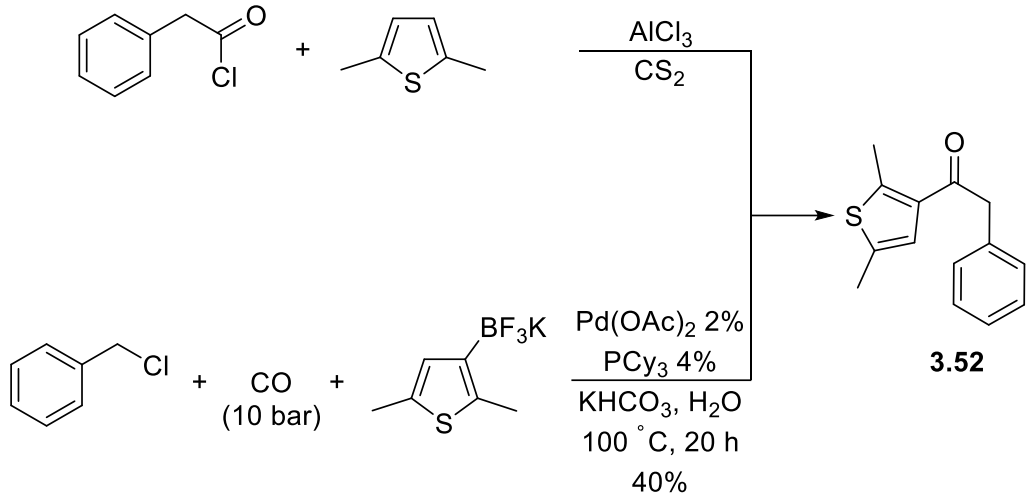

Scheme 3.15: Previous research work on furnishing methyleneketone **3.52**

Upon opting for an $AlCl_3$-catalysed Friedel-Crafts acylation method, it was deemed necessary to use a solvent able to efficiently dissolve the inorganic Lewis acid and keep it in solution with the starting chloride **2.55** and 2,5-dimethylthiophene **2.56**. A mixture of $MeNO_2$ and DCM was utilised to that end and after a short reaction time the target ketone was obtained in 77.1 % yield after distillation (Scheme 3.16).

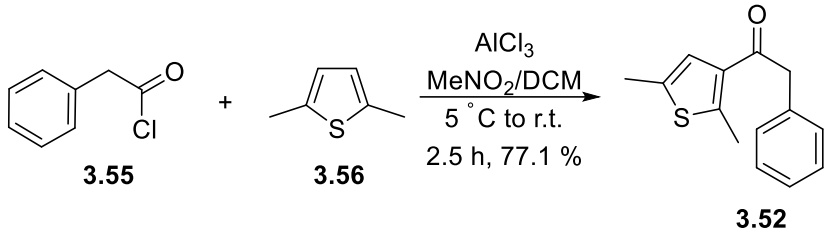

Scheme 3.16: Friedel-Crafts acylation of 2,5-dimethylthiophene towards ketone **3.52**

Confirmation of this product was made possible by NMR analysis, wherein the characteristic singlets for the protons of the thiophene ring and substituents at δ 2.42 (Me), 2.68 (Me) and 7.09 (4-H), as well as the α-methylene protons at δ 4.11, were identified in the ^{1}H-NMR spectrum (Figure 3.7). Of note is the observation that the proton on the thiophene ring is split by the protons of the proximal methyl group with $^4J \approx 1.0$ Hz, giving rise to apparent singlets which resolve into multiplets upon a Gaussian multiplication of the ^{1}H-NMR spectrum (Figure 3.8). Locating the 3 aliphatic carbon environments at δ 15.07, 16.19 and 48.40, along with the carbonyl *C* atom at δ 193.57, on the ^{13}C-NMR spectrum also highlights the structural features of this compound (Figure 3.7), while the anticipated C=O stretching of the carbonyl moiety is observed at 1663 cm^{-1} on the respective IR spectrum.

This acylation follows the established mechanistic route of Friedel-Crafts conversions (Scheme 3.17); cleavage of the chloride leaving group by $AlCl_3$ affords the acylium intermediate, which is attacked by the 3- position of the disubstituted thiophene ring. Loss of a proton completes the electrophilic aromatic substitution process with the thiophene ring regaining its aromaticity.

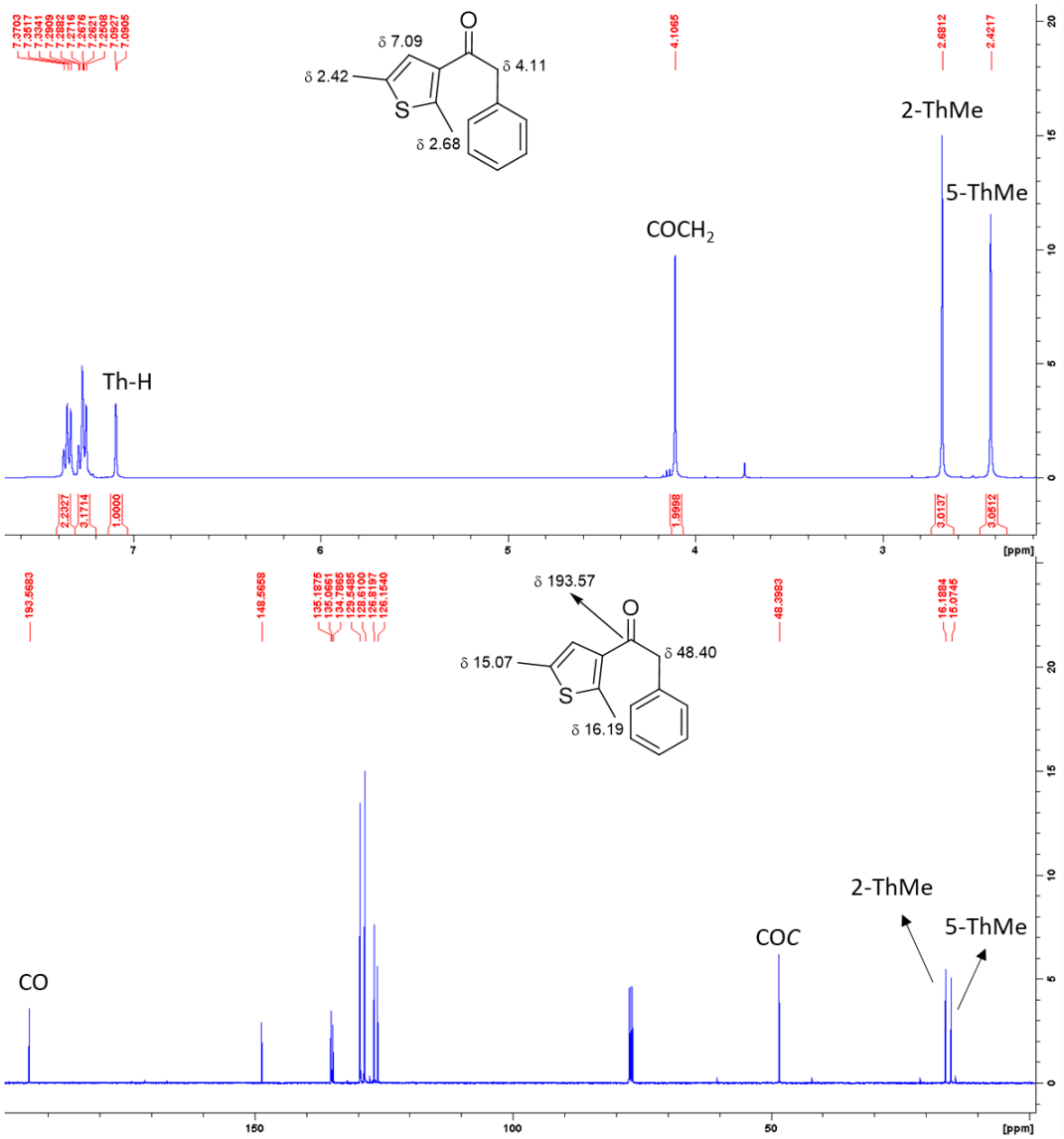

Figure 3.7: ^{1}H-NMR (above) and ^{13}C-NMR spectra (below) of methyleneketone **3.52**

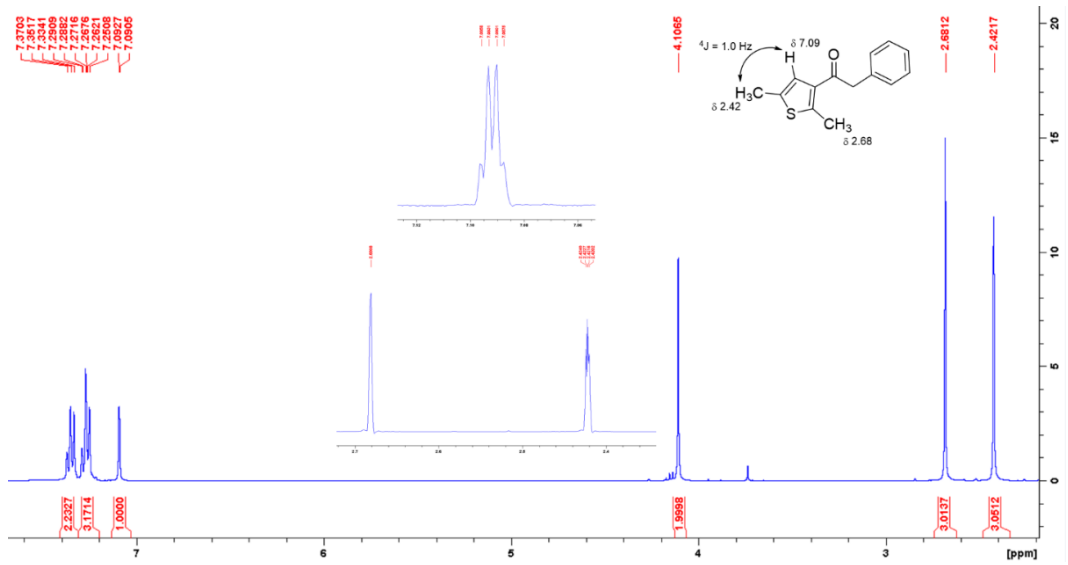

Figure 3.8: Long-range (^{4}J) coupling between thienyl proton and proximal methyl group protons on **3.52**

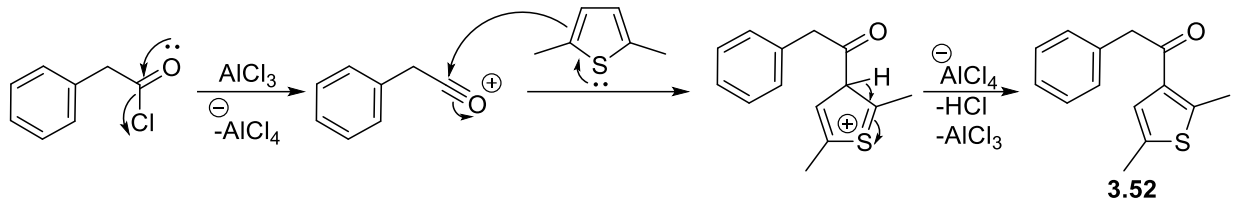

Scheme 3.17: Mechanism of the Friedel-Crafts acylation towards methyleneketone **3.52**

After the initial success of the Friedel-Crafts acylation protocol in furnishing the foregoing ketone **3.52**, the same strategy was sought out to produce the analogous bis-thienyl ketone **3.53**. The literature-established routes for this compound comprised of the conversion of a hydroxy-ketone precursor **3.57** to the corresponding thiol and its subsequent cleavage under basic conditions[177], as well as a Friedel-Crafts acylation of 2,5-dimethylthiophene by the acid chloride **3.58** mediated by $SnCl_4$ instead of the more common $AlCl_3$[178] (Scheme 3.18).

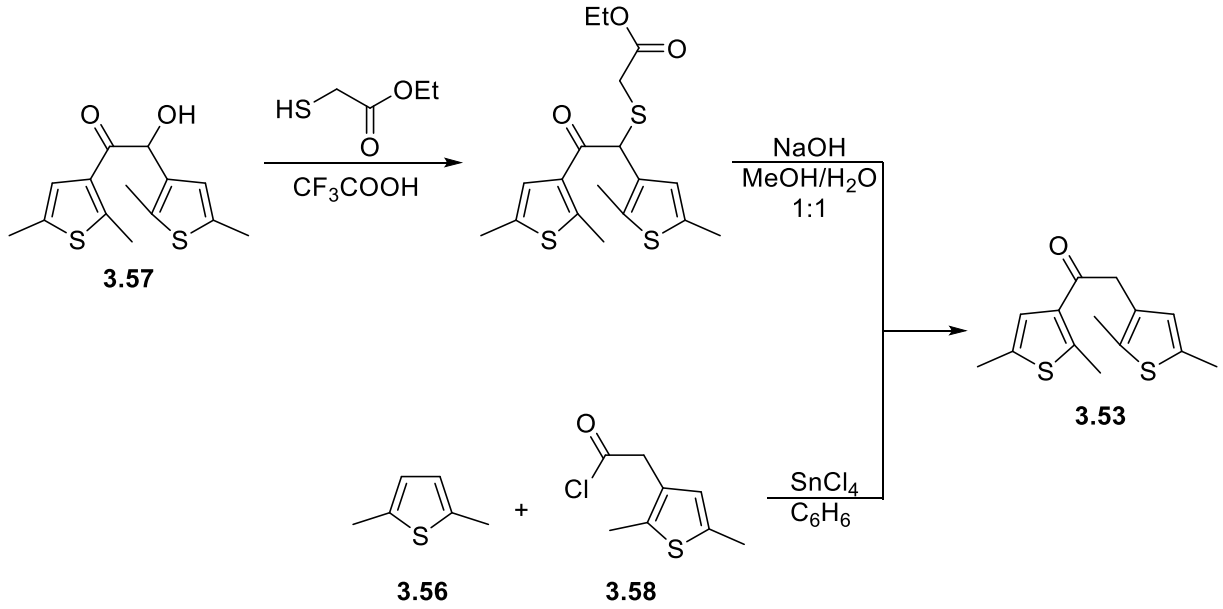

Scheme 3.18: Literature-based synthetic routes towards the bisthienyl ketone **3.53**

Given the relatively simple structure, the acid chloride **3.58** was deemed a more suitable precursor, thus a Friedel-Crafts acylation approach was opted for to arrive at **3.53** (Scheme 3.19). The lack of commercial availability necessitated the synthesis of **3.58** from suitable precursors, and examination of the relevant literature[179,180] cemented a preparative route comprising of three steps, in which 2,5-dimethylthiophene **3.56** would be acylated with ethyl chloroglyoxylate (ethyl chlorooxoacetate) **3.59** and the resulting ketoester **3.60** would hydrolyse with concomitant reduction of the α-keto group employing H_2NNH_2 in a Wolff-Kishner Huang Minlon modification reduction process. The resulting carboxylic acid **3.61** would subsequently be treated with $SOCl_2$ to afford the required chloride **3.58**, which in turn can be used in the Friedel-Crafts protocol that was previously selected for the phenyl ketone counterpart **3.52**.

The initial acylation with ethyl chloroglyoxylate to arrive at the ester **3.60** proceeded efficiently in $MeNO_2$ with a 70.0 % yield. The structure of the product was confirmed by ^{1}H-NMR spectroscopy, as the presence of a triplet and a quartet at δ 1.40 and 4.39 respectively, in conjunction with the characteristic thiophene singlet at δ 7.09 (4-H), denote a thienyl-containing ester. Moreover, the two key signals of the carbonyl units at δ 164.04 and 180.59 on the ^{13}C-NMR spectrum of **3.60** clearly highlight the α-keto ester moiety, as the former signal appears quite upfield on account of the electron-donating adjacent *O* atom (Figure 3.9a/b). These groups provide additional characteristic evidence *via* IR spectroscopy, by means of their vibration resonating at 1668 cm^{-1} (α-keto group) and 1732 cm^{-1} (ester C=O bond).

The transformation follows the aforementioned mechanistic aspects of a Friedel-Crafts acylation, *i.e.* formation of an acylium ion, attack by the thiophene starting material and loss of a proton to restore the aromaticity of the thiophene group, as discussed earlier for ketone **3.52** (Scheme 3.17).

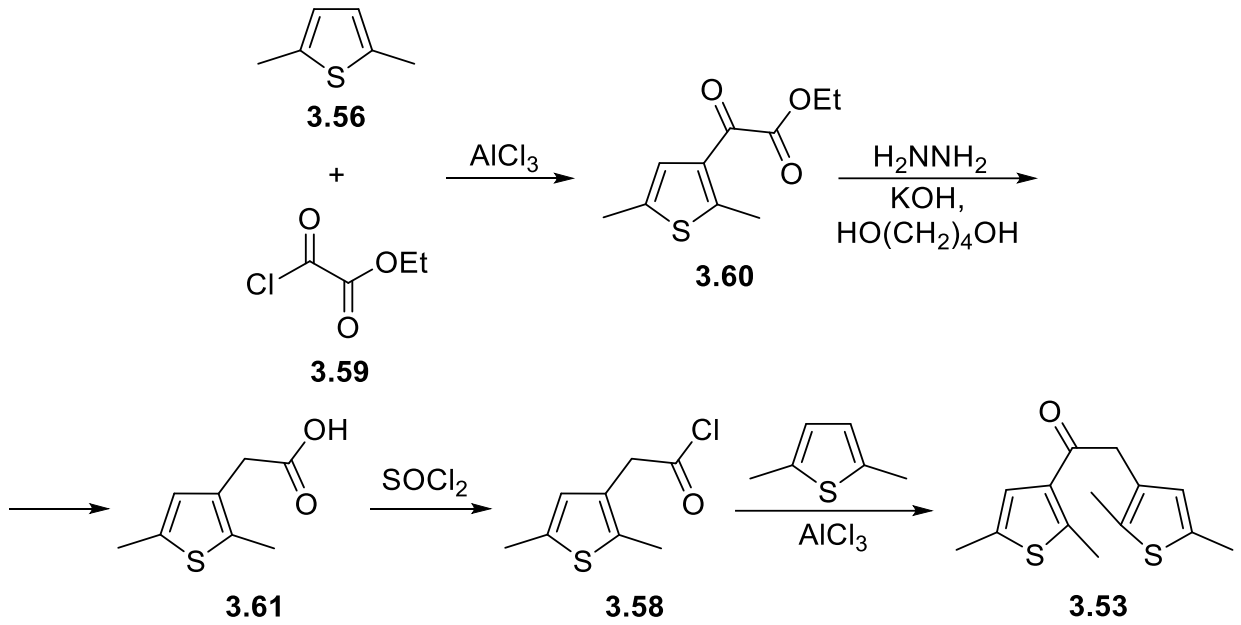

Scheme 3.19: Synthetic route for the preparation of ketone **3.53**

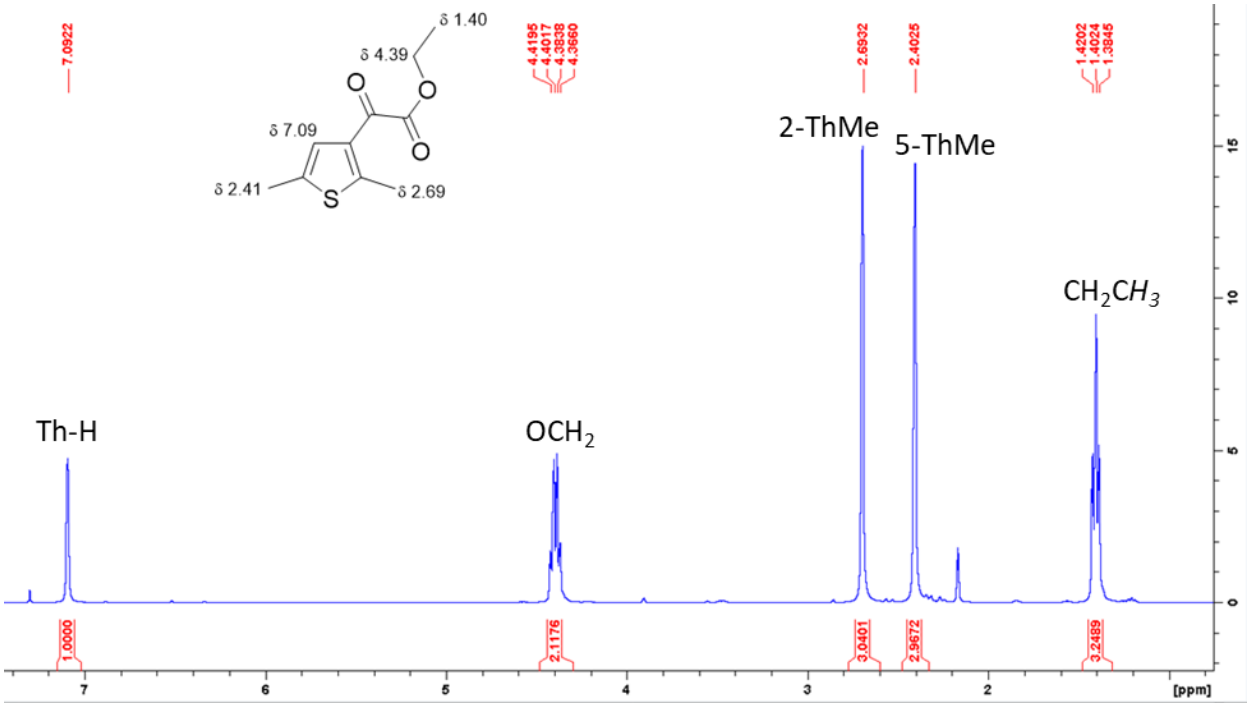

Figure 3.9a: ^{1}H-NMR spectrum of glyoxylate ester **3.60**

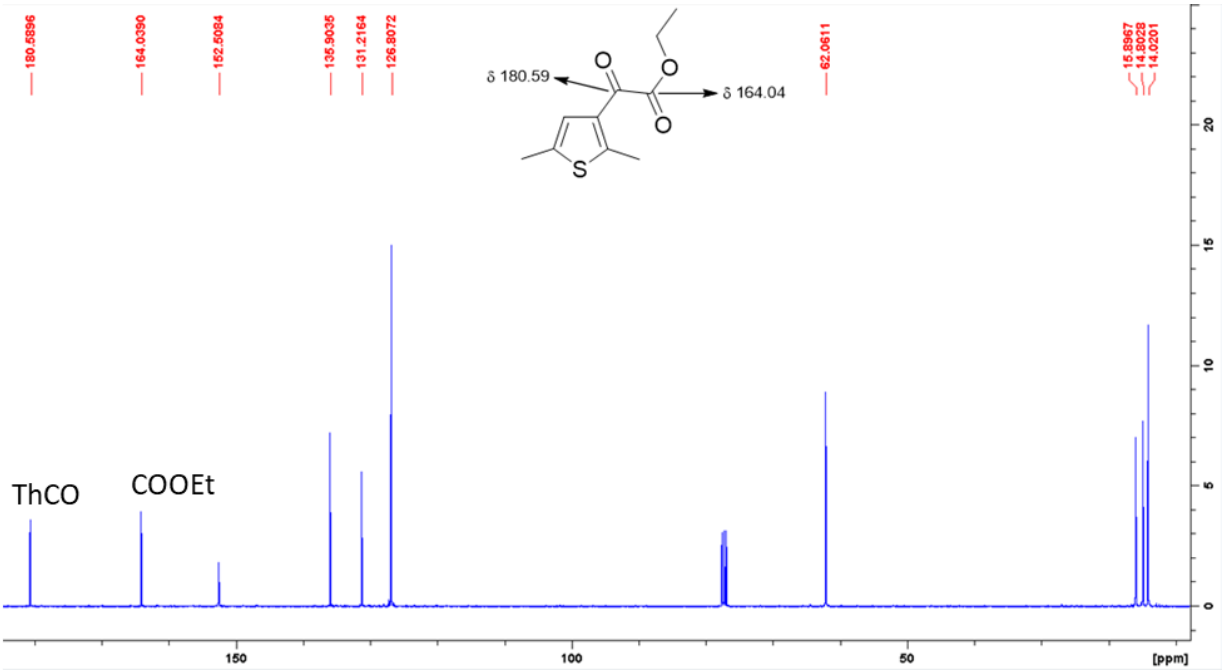

Figure 3.9b: ^{13}C-NMR spectrum of glyoxylate ester **3.60**

Reducing the bridging carbonyl group to a methylene unit and hydrolysing the ester moiety was carried out in ethylene glycol using H_2NNH_2 to form the hydrazone intermediate and a subsequent excess of KOH to both complete the Wolff-Kishner Huang Minlon reduction process and hydrolyse the ester bond (Scheme 3.20). The final carboxylic acid product **3.61**, isolated in 92.0 % yield, could be readily recognised by the established spectroscopic techniques; apart from the expected set of singlets (δ 2.33 (Me), 2.39 (Me) and 6.55 (4-H)), the methylene moiety resonates as a singlet at δ 3.50 and the carboxylic proton can be observed as a broad singlet at δ 10.94. The reduction conversion can be further ascertained by the presence of an aliphatic signal at δ 33.79, while in a similar fashion, the carboxylic *C* atom resonates at δ 177.86 (Figure 3.10). Definitive characterisation data is also offered by IR spectroscopy, as the carboxyl group produces a strong sharp CO peak at 1690 cm^{-1}, due to the effect of the electronegative *O* atom in reducing the CO bond length and increasing the vibration frequency, as well as a broad strong peak at 2917 cm^{-1} on account of the OH stretch.

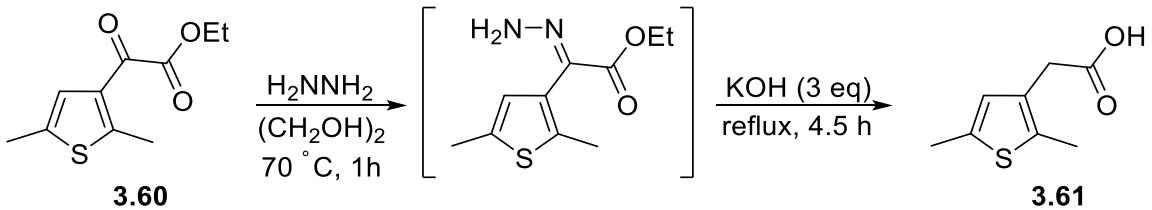

Scheme 3.20: Wolff-Kishner Huang Minlon reduction and ester hydrolysis towards **3.61** *via* use of H_2NNH_2 and KOH

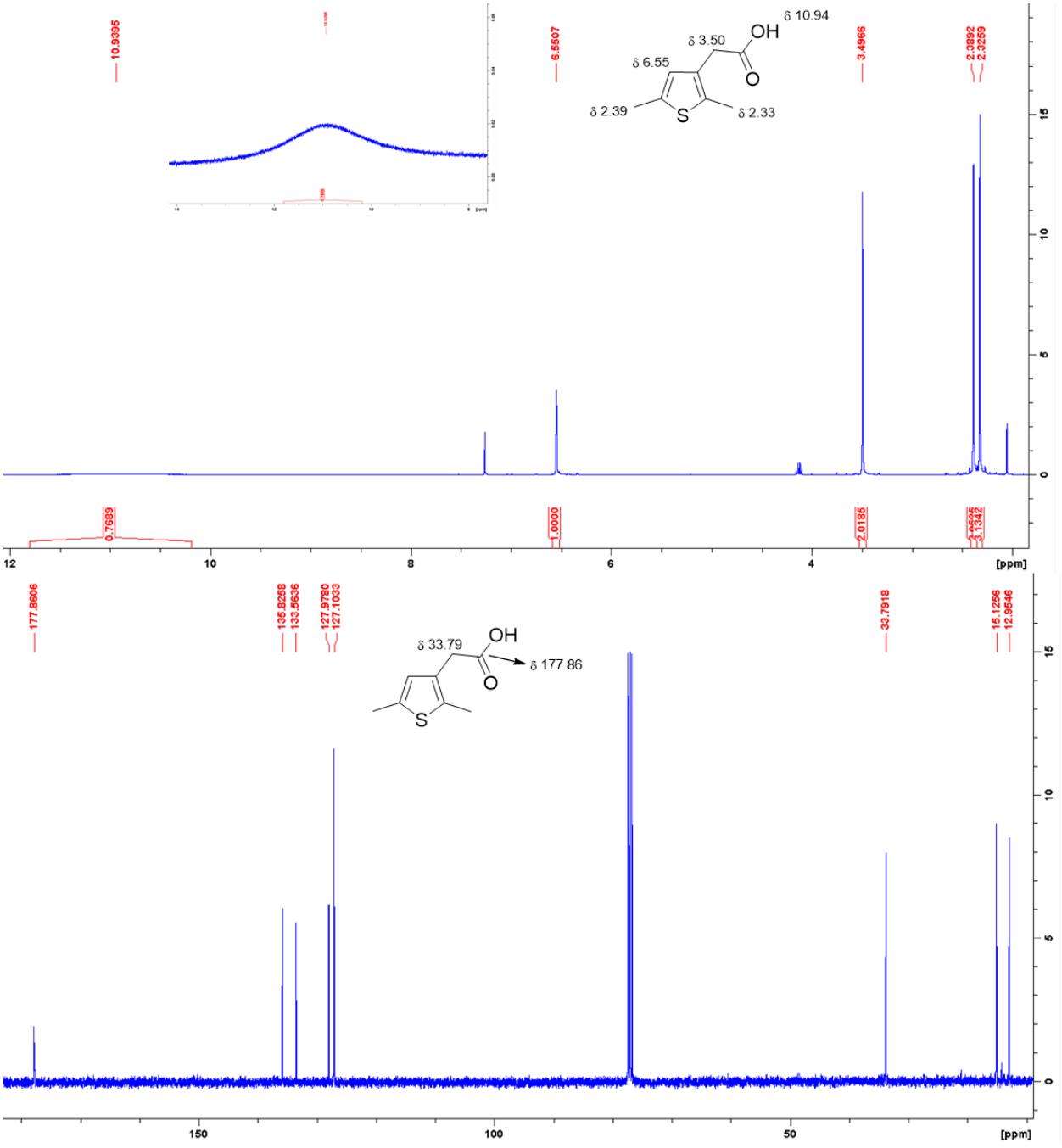

Figure 3.10: ^{1}H-NMR (above) and ^{13}C-NMR (below) spectra of carboxylic acid **3.61**

The Wolff-Kishner Huang Minlon transformation begins with an attack of the α-keto group by hydrazine and formation of a hydrazone by an addition – elimination process. Addition of the KOH prompts the deprotonation of the terminal NH_2 group, with the electron density flowing towards the α-carbon, which is protonated by the resulting H_2O. Further deprotonation results in the cleavage of a N_2 fragment and the recurrence of the enolate ion that receives a proton from the ambient H_2O, whereas the large excess of KOH allows for a concomitant attack on the ester carbonyl bond with consequent cleavage of the ethoxy moiety group and the furnishing of the desired acid **3.61** (Scheme 3.21).

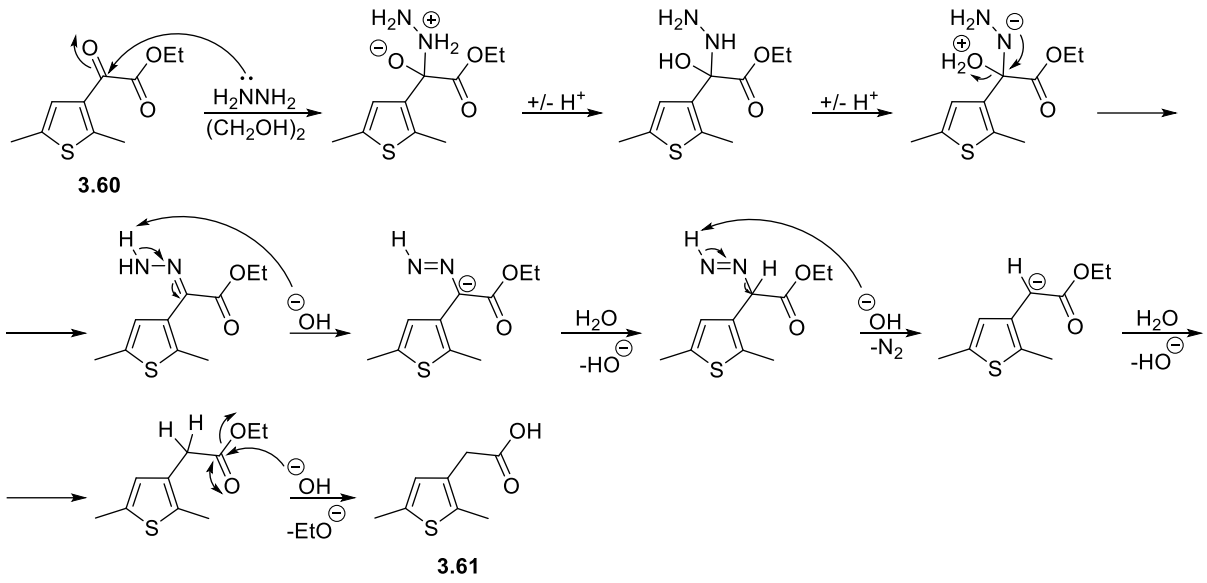

Scheme 3.21: Mechanism of the Wolff-Kishner Huang Minlon reduction/ester hydrolysis to afford the acid **3.61**

Upon arriving at the carboxylic acid **3.61**, its conversion to the corresponding chloride **3.58** was carried out efficiently through use of $SOCl_2$ as the source of the chloride group and DMF as the catalyst. The acid chloride was used for the next step without further purification to preserve the integrity of the compound. Use of the foregoing Friedel-Crafts protocol with 2,5-dimethylthiophene as the nucleophile successfully yielded the target ketone **3.53** in 46.7 % overall yield from **3.61** (Scheme 3.22).

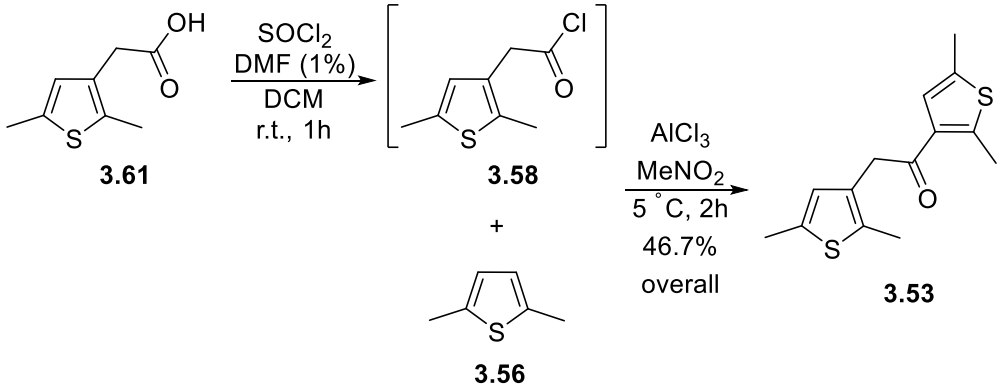

Scheme 3.22: Final steps towards the bis-thienyl ketone **3.53**

Juxtaposition of the ^{1}H-NMR spectrum of the obtained product with literature data[177,178] provides clear evidence of the success of the reaction, as the 4 key singlets of the Me groups are observed between 2.30 and δ 2.70 and the 2 signals for the thiophene ring protons appear at δ 6.48 and 7.05. The pivotal α-methylene protons also have a distinctive resonance at δ 3.92, thus revealing the presence of the ketone moiety. The 5 foregoing aliphatic proton environments are also reflected on the ^{13}C-NMR spectrum of **3.53**, wherein their respective *C* atoms are observed between δ 13.44 and 16.13 (4 methyl groups) and δ 41.14 (methylene carbon), while the carbonyl *C* atom is apparent at δ 193.24 as anticipated (Figure 3.11). The characteristic vibration frequency of 1666 cm^{-1} is furthermore observed on the IR spectrum as clear evidence of a carbonyl functional group being present in the compound.

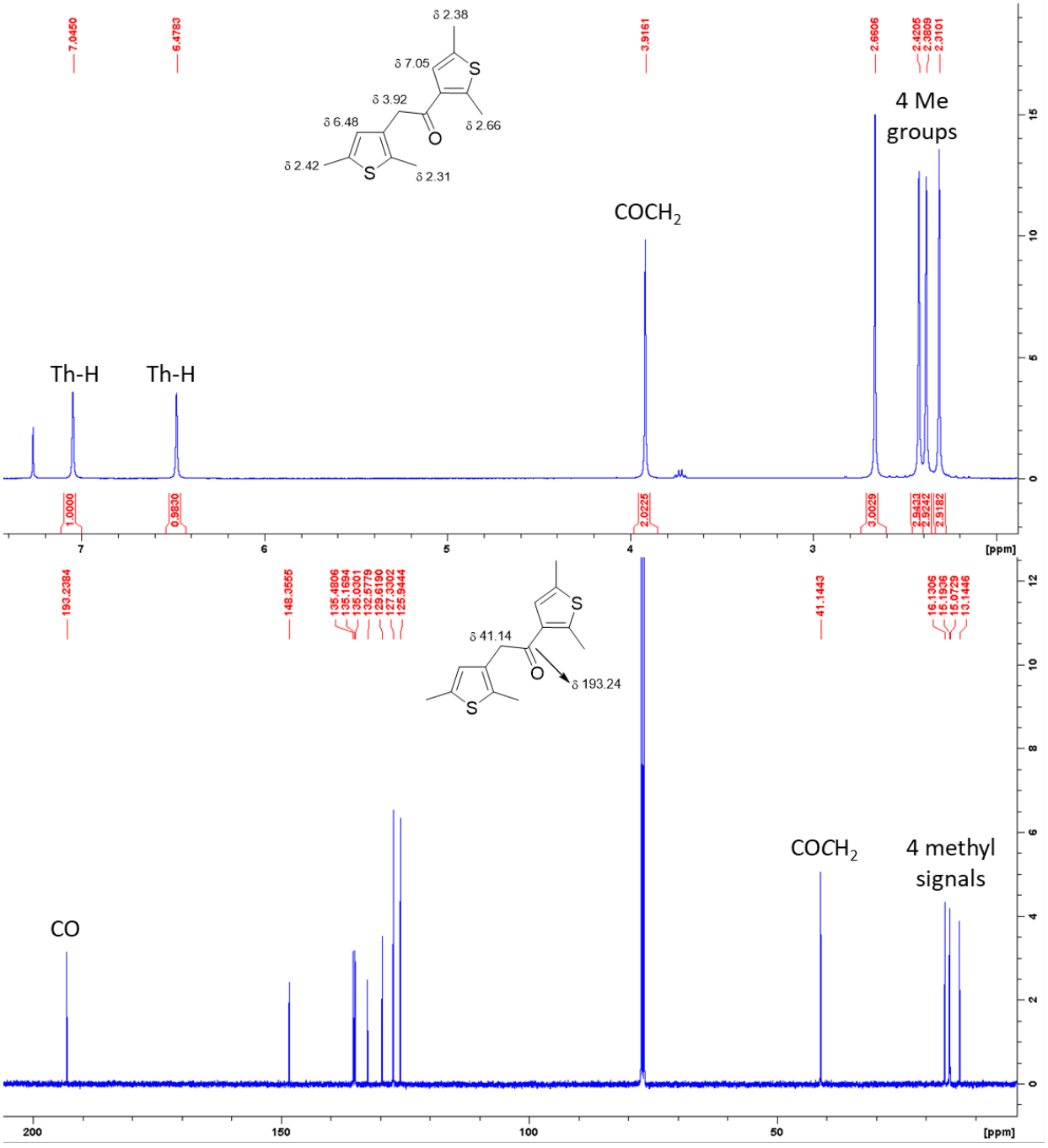

Figure 3.11: ^{1}H-NMR (above) and ^{13}C-NMR (below) spectra of ketone **3.53**

The mechanism of the chlorination of **3.61** is brought about by $SOCl_2$ in the presence of a catalytic amount of DMF (Scheme 3.23). The latter is able to activate the chlorinating agent by forming a chloroiminium ion (Vilsmeier reagent) which interacts with the carboxylic acid towards an intermediate that allows for the migration of the chloride, followed by the regeneration of the catalyst and the formation of the desired chloride derivative **3.58**. This reactive species can readily undergo a nucleophilic substitution by the electron rich 2,5-dimethylthiophene system *via* the mechanism established earlier.

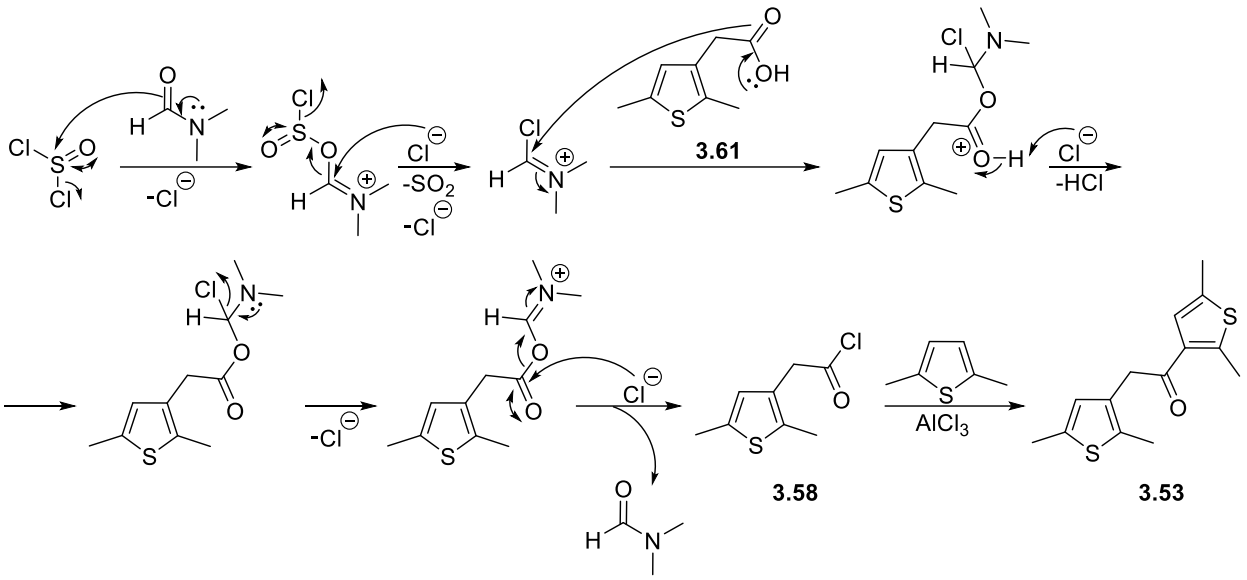

Scheme 3.23: Chlorination mechanism of **3.61** with consequent Friedel-Crafts acylation with 2,5-dimethylthiophene towards **3.53**

After the successful formation of the bis-thienyl ketone **3.53**, it was postulated that the aforementioned Friedel-Crafts protocol would be effective in yielding the 1-phenyl isostere **3.54**, upon combining the acid chloride **3.58** with benzene in the presence of $AlCl_3$. Interestingly, applying this strategy failed to afford **3.54**, since an examination of the ^{1}H-NMR and ^{13}C-NMR spectral data obtained for the only isolated compound showed none of the signals reported for the target compound as described in the literature[177] (Figure 3.12a).

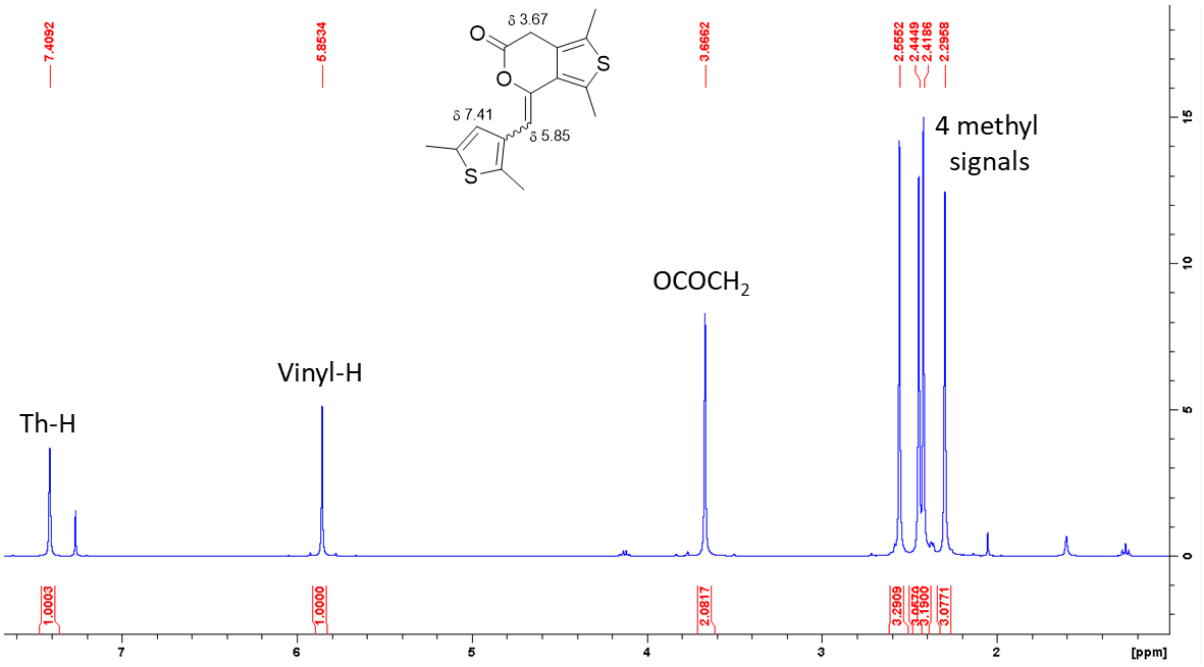

Figure 3.12a: ^{1}H-NMR spectrum of the thienopyranone **3.62**

Moreover, absence of any aromatic signals denoted that no incorporation of the benzene moiety had occurred in any fashion. The presence of a singlet at δ 5.85 and at δ 7.41, along with 4 aliphatic singlets between δ 2.30 and 2.56, hinted at the presence of two thiophene ring moieties which existed in

conjunction with two α-methylene protons, as suggested by the singlet at δ 3.67. These findings indicated the formation of a ketone-containing dimer-like species, although an explanation was required for the sole observed deshielded aliphatic proton environment. To that end, the observation of an upfield carbonyl carbon environment on the ^{13}C-NMR spectrum pointed out to an ester bond (Figure 3.12b), which was confirmed by the relevant IR peak at 1756 cm^{-1}. This ester group could be the product of an aldol condensation between the two carbonyl groups of this "dimeric" compound, which would fit in with the ^{1}H-NMR data if the singlet at δ 5.85 was attributed to a vinyl proton. Indeed, the appearance of two alkene carbon environments at δ 104.37 and 126.74 revealed the presence of an enol ether fragment and prompted the assignment of the thieno[3,4-*c*]pyranone structure to the obtained side-product **3.62** (Scheme 3.24), which was proven to be correct after the respective *m/z* was observed on the MS spectrum (305.0660 for [M+H]$^{+}$, $C_{16}H_{16}O_2S_2$ requires an *m/z* of 305.0664 for [M+H]$^{+}$).

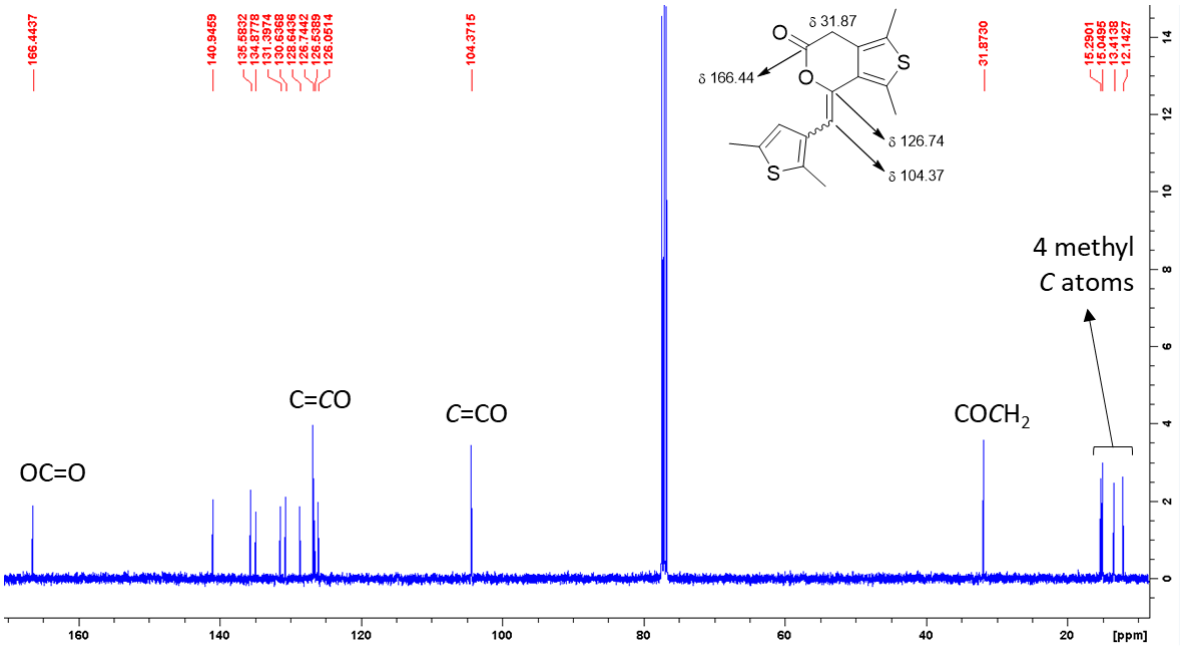

Figure 3.12b: ^{13}C-NMR spectrum of the thienopyranone **3.62**

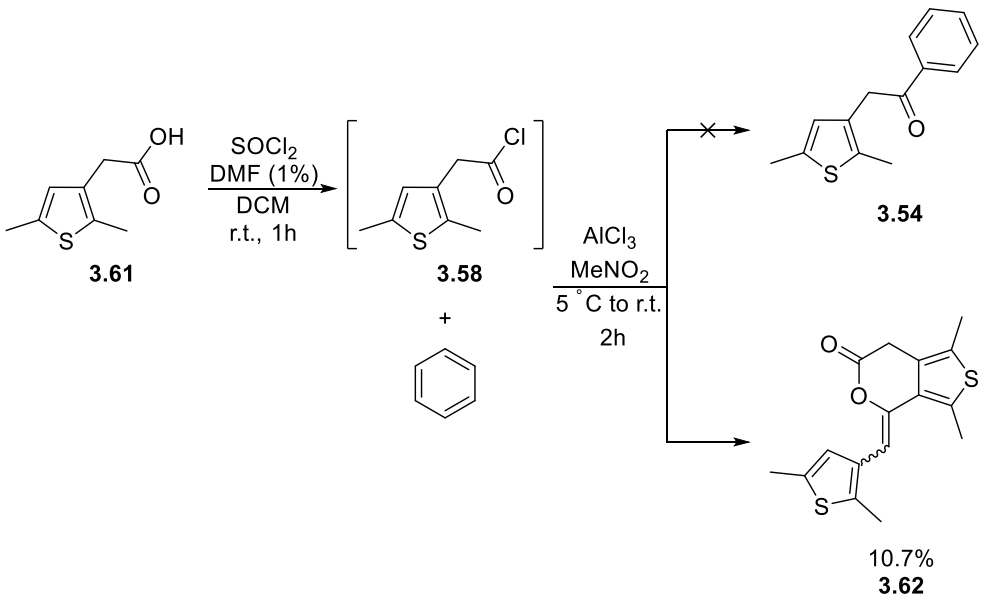

Scheme 3.24: Failed attempt at synthesising 1-phenyl analogue **3.54** with the serendipitous formation of the fused pyranone **3.62**

Based on the characterisation data of this side-product, it can be theorised that the chloride **3.58** undergoes a 'homo Friedel-Crafts' reaction in the presence of $AlCl_3$ rather than interacting with benzene, leading to a keto-chloride dimer-like intermediate that is able to tautomerise to the enol form under acidic conditions. This brings forth a nucleophilic *O* atom on one monomer which is capable of a nucleophilic attack on the acid chloride moiety of the other monomer towards an ester bond with concomitant cleavage of the chloride leaving group. Deprotonation of the foregoing oxygen atom eventually affords the thieno[3,4-*c*]pyranone derivative **3.62** (Scheme 3.25).

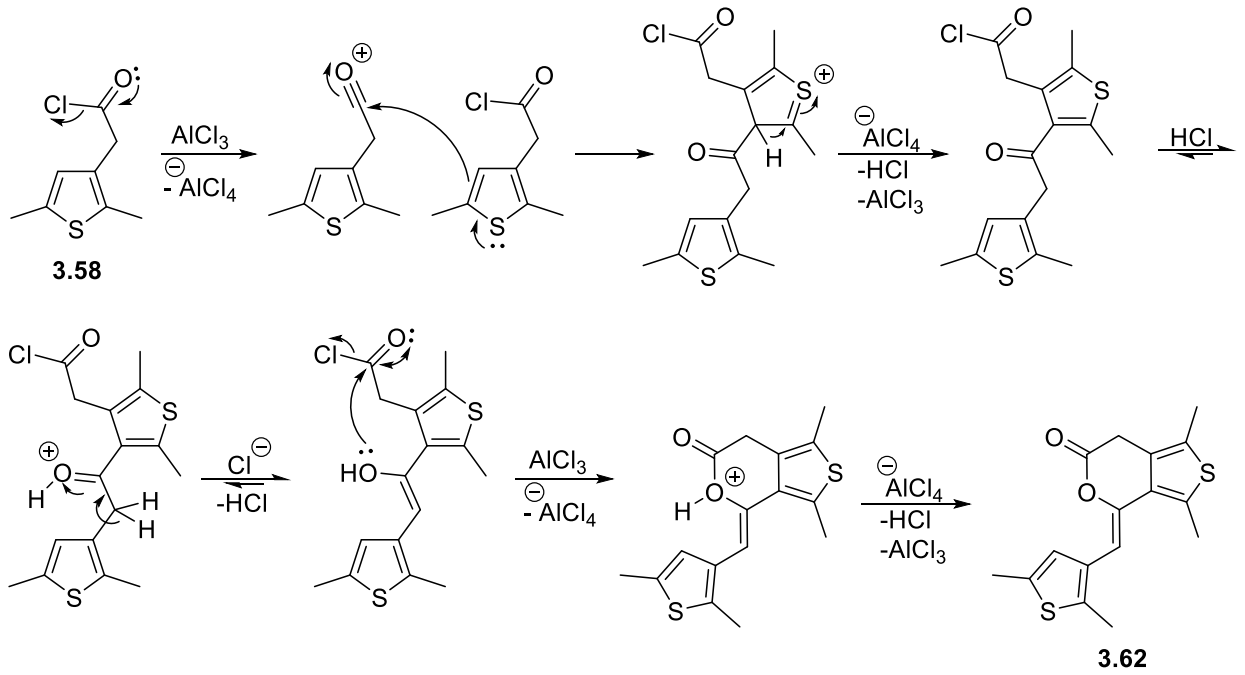

Scheme 3.25: Proposed mechanism for the formation of the fused pyranone derivative **3.62**

The formation of this novel compound can be attributed to the fact that the thiophene moiety on the starting acid chloride is more electron rich than benzene and is thus a more favoured substrate for the pivotal acylation step, whereas the ring-closing step is also beneficial by virtue of the suitable proximity of the enol *O* atom and the chloride carbonyl group towards the formation of a thermodynamically stable 6-membered pyranone ring. A final point of interest for this interesting side-product regards the *E*/*Z* geometry of the central double bond. Ascertaining this structural feature was made possible by examination of the NOESY spectrum of **3.62**, which revealed two key correlations that pinpoint the vinyl proton between 2 thienyl methyl groups, in addition to only one correlation for the thienyl proton, thus pointing out to the *Z*-isomer (Figure 3.13).

Due to the aforementioned setback during the preparation of ketone **3.54**, an alternative strategy was required. The previously noted method of producing the ketone from a thiol precursor had been successfully attempted towards this analogue[177], although a synthetic route for the initial hydroxy-ketone (**3.63**) was deemed quite time-consuming a prerequisite. A further search of the literature provided an additional route towards this compound by utilising an enol-ether precursor (**3.64**) but this strategy also required several complex reagents in order to be carried out[181] (Scheme 3.26).

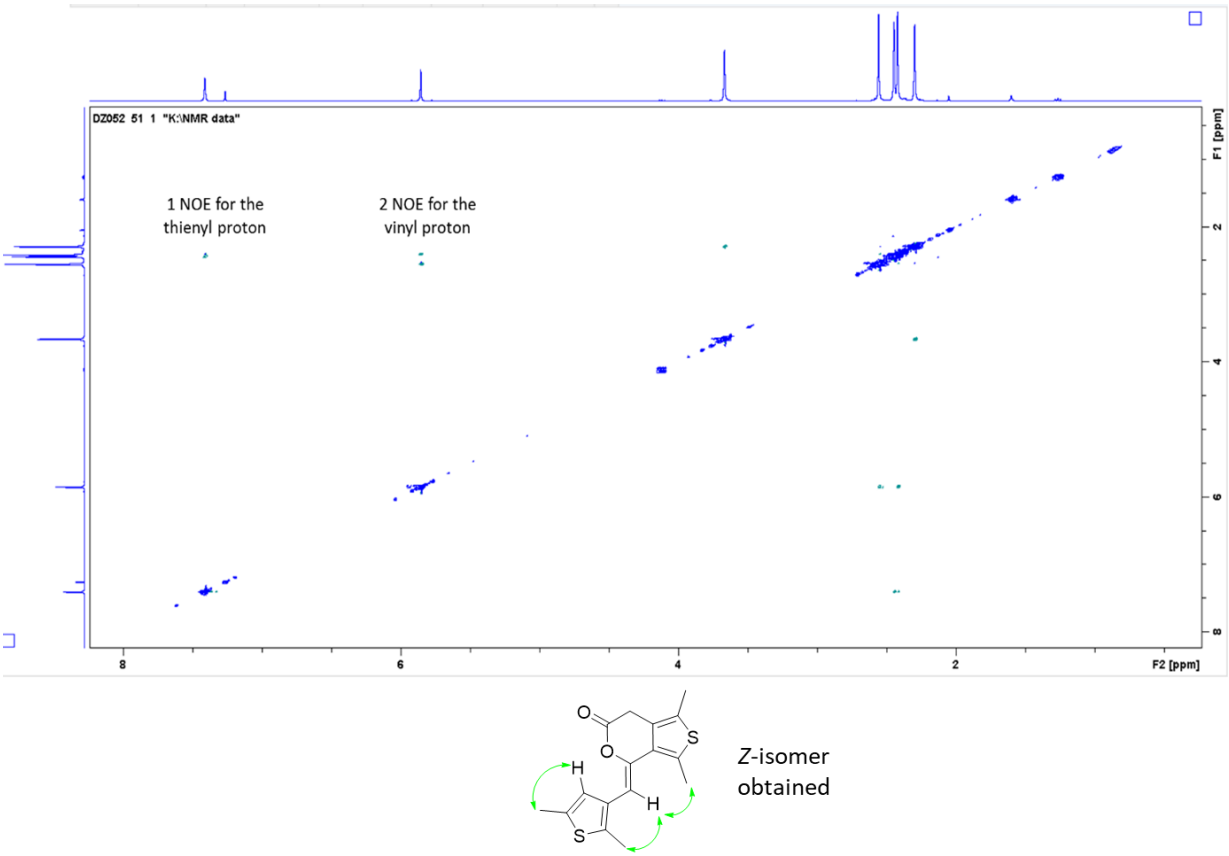

Figure 3.13: NOESY spectrum of **3.62**

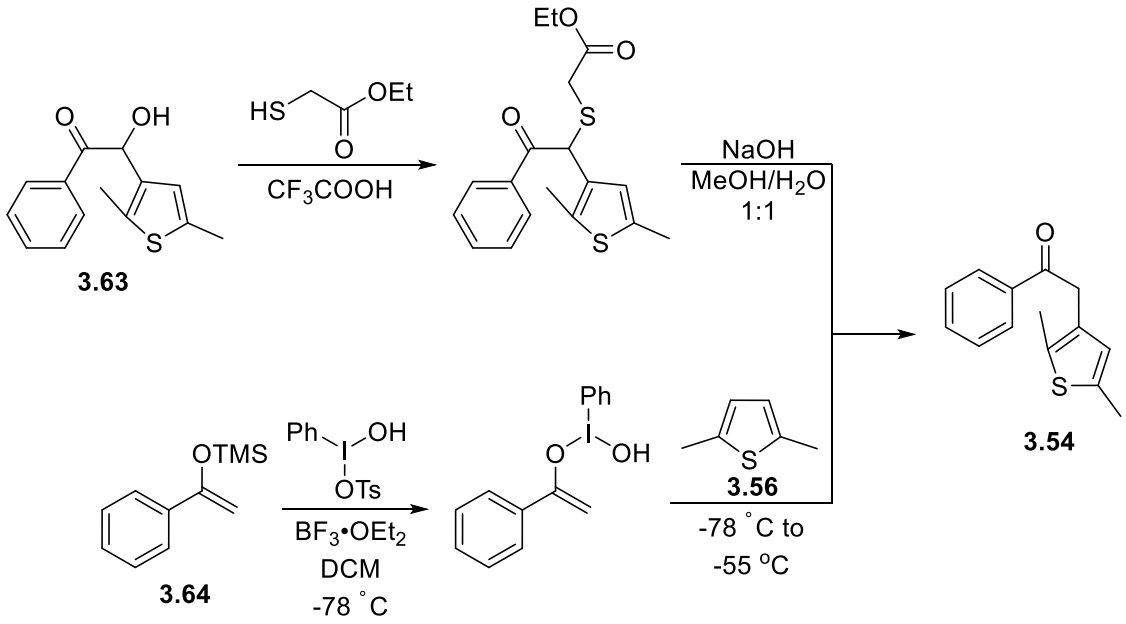

Scheme 3.26: Literature-established alternatives towards the 1-phenyl ketone **3.54**

Before any of these routes were examined in further detail, the possibility of attaining **3.54** *via* the formation of a Weinreb amide intermediate was examined. This class of reactive amides have been thoroughly explored in literature[182,183,184] and an important aspect of their reactivity regards their affinity towards nucleophilic species in carbonyl substitution reactions. It was thus envisaged that converting the carboxylic acid **3.61** to the corresponding chloride **3.58** and reacting this with *N*,*O*-dimethylhydroxylamine

would furnish the amide analogue **3.65**, which would interact with a phenyl nucleophile, *e.g.* phenyllithium, to afford the target ketone (Scheme 3.27).

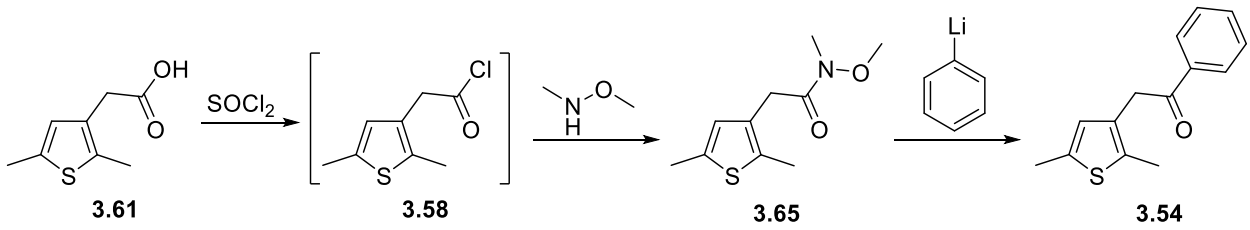

Scheme 3.27: Suggested synthetic route of **3.54** *via* a Weinreb amide intermediate (**3.65**)

Fortunately, treating a solution of the crude acid chloride **3.58** with *N,O*-dimethylhydroxylamine hydrochloride and pyridine in DCM in accordance with literature protocols[185,186] produced the anticipated Weinreb amide **3.65**, as confirmed upon characterisation of the isolated product (Figure 3.14).

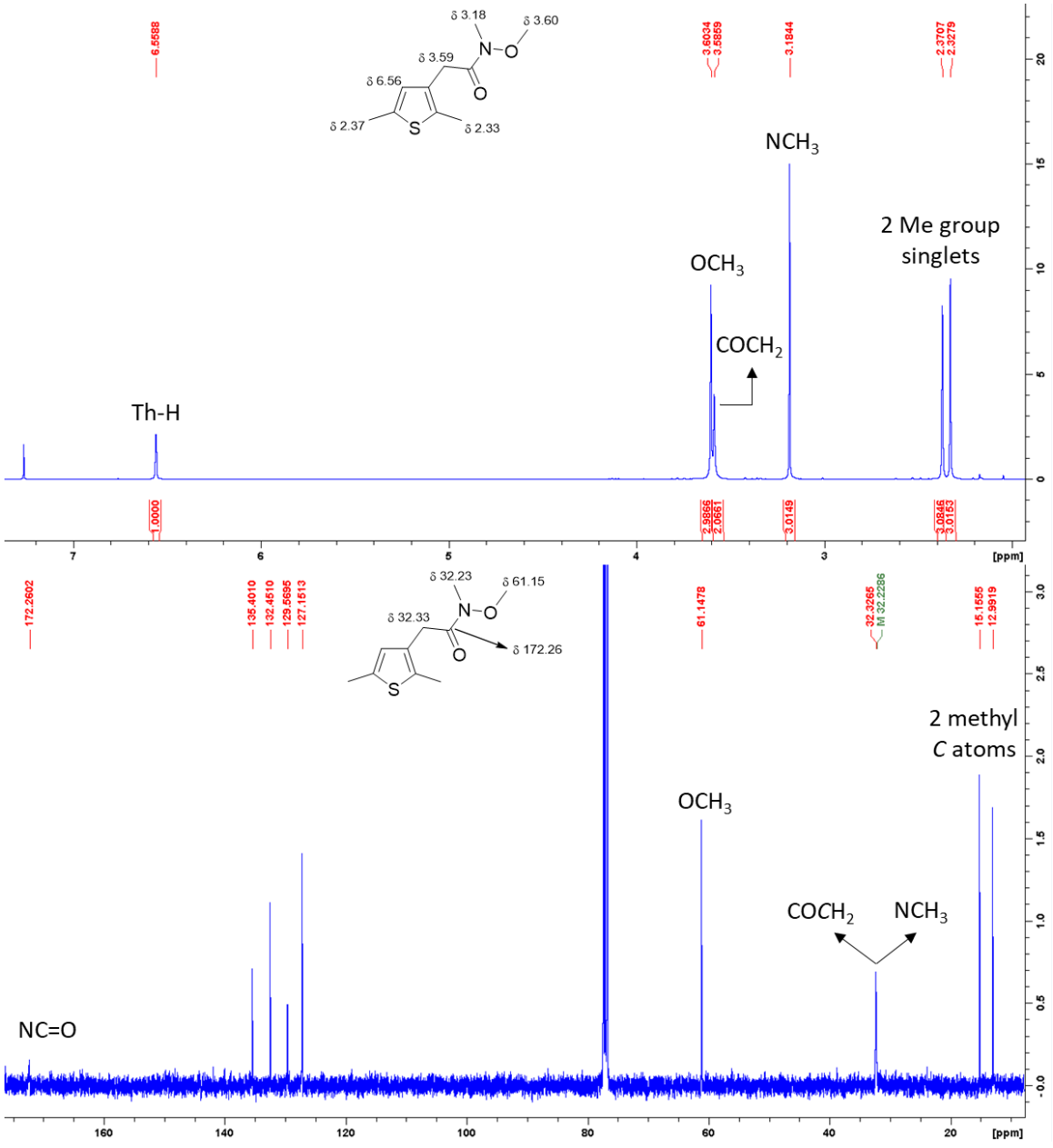

Figure 3.14: ^{1}H-NMR (above) and ^{13}C-NMR (below) spectra of the Weinreb amide species **3.65**

The acquired ^{1}H-NMR spectrum shows the common 3 signals for the substituted thiophene moiety (2 singlets at δ 2.33 (Me) and 2.37 (Me), 1 singlet at δ 6.56 (4-H)), in addition to 3 singlets at δ 3.18, 3.59 and 3.60, which correspond to the two methyl groups of the amide terminus and the α-methylene unit, respectively. Locating these aliphatic signals between 12.99 and 61.15 (two peaks at *circa* δ 32) along with the shielded amide CO peak at δ 172.26 provides additional evidence of the success of the transformation, as does the respective IR stretching band at 1665 cm^{-1}, which is in accord with the typical range of amide carbonyl vibration frequencies.

Upon its successful isolation in 62.0 % yield, the amide **3.65** was treated with PhLi in anhydrous THF at -70 °C and was pleasingly converted to the phenylketone **3.54** in 50.6 % yield after aqueous NH_4Cl solution quenching. A repeat of these two steps in order to reach a larger amount of obtained ketone (64.8 % for Weinreb amide formation and 65.8 % for phenyllithium addition) managed to both ascertain the reproducibility and scalability of this method as well as establish this strategy as a novel and efficient synthetic route towards **3.54** (Scheme 3.28). Characterisation of ketone **3.54** validated this method by direct comparison with literature data (Figure 3.15a,b).[177,181]

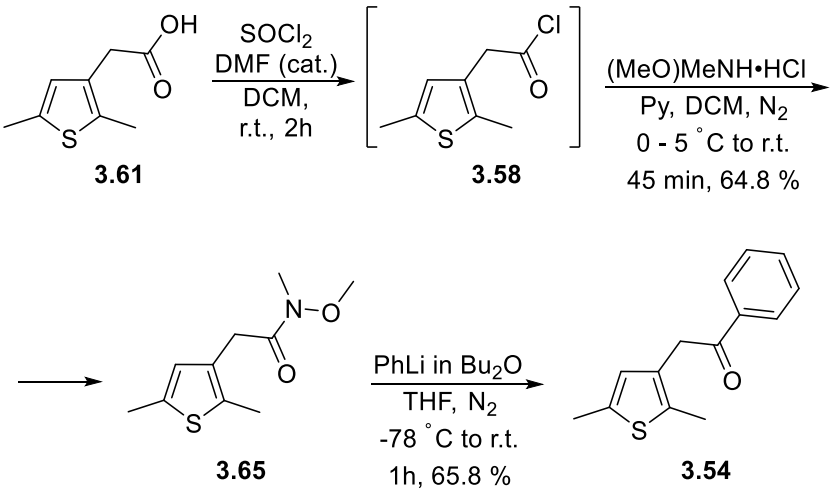

Scheme 3.28: Synopsis of the Weinreb amide alternative route to furnish **3.54**

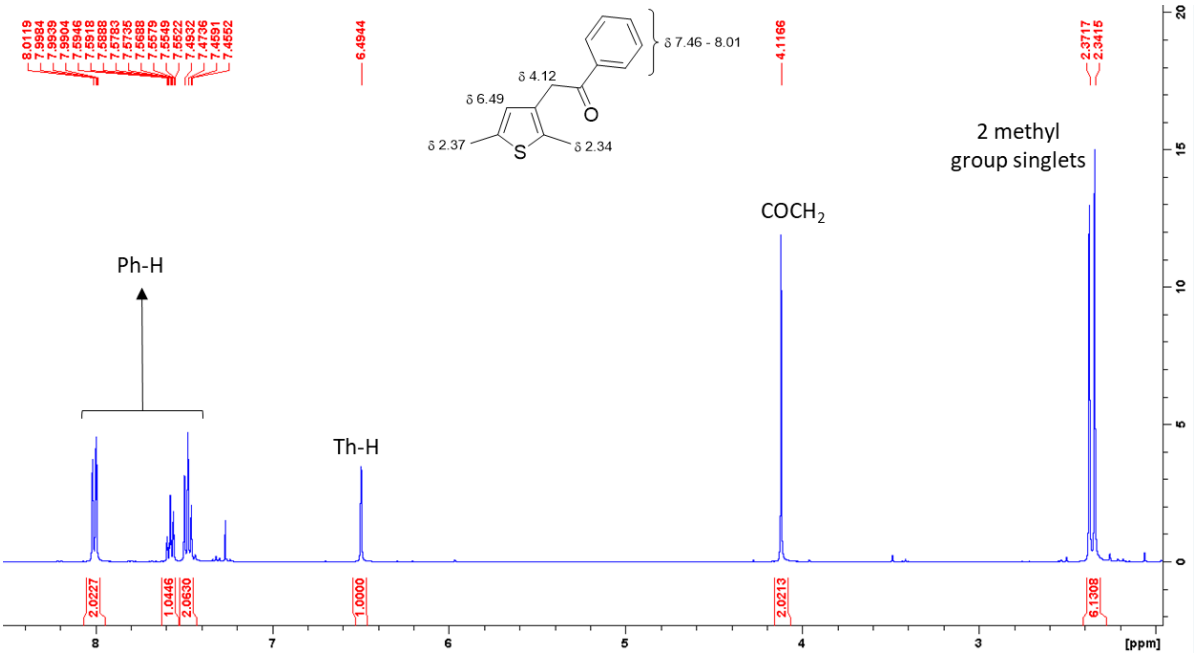

Figure 3.15a: ^{1}H-NMR spectrum of ketone **3.54**

The phenyl ring signals that were absent in the previous attempt to prepare **3.54** (Scheme 3.23) could be observed between δ 7.46 and 8.01 in the ^{1}H-NMR spectrum, and the presence of the 4 key singlets for the thiophene ring, the methyl groups and the methylene unit illustrate the remainder of the ketone structure. Further evidence for successful acylation can be found from the ^{13}C-NMR spectrum, wherein the carbonyl *C* atom resonates at δ 197.31 and the adjacent α-methylene carbon appears at δ 38.42. The carbonyl key stretching frequency of 1683 cm^{-1} was observed on the IR spectrum for **3.54**.

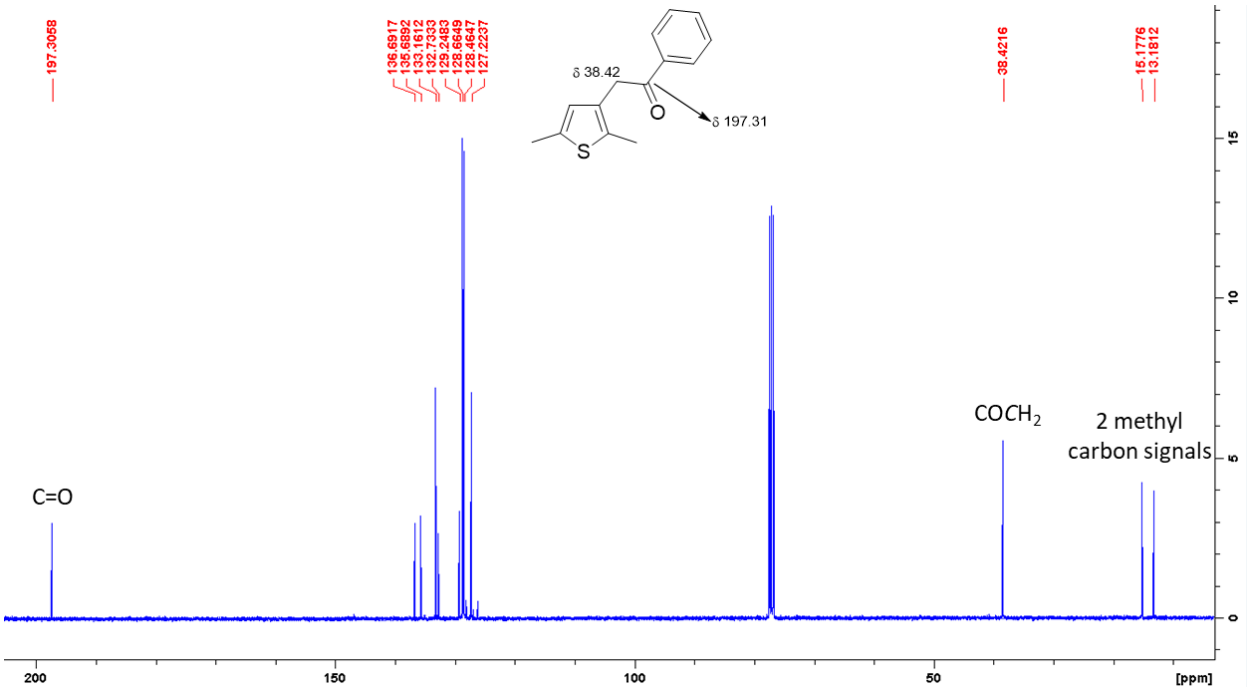

Figure 3.15b: ^{13}C-NMR spectrum of ketone **3.54**

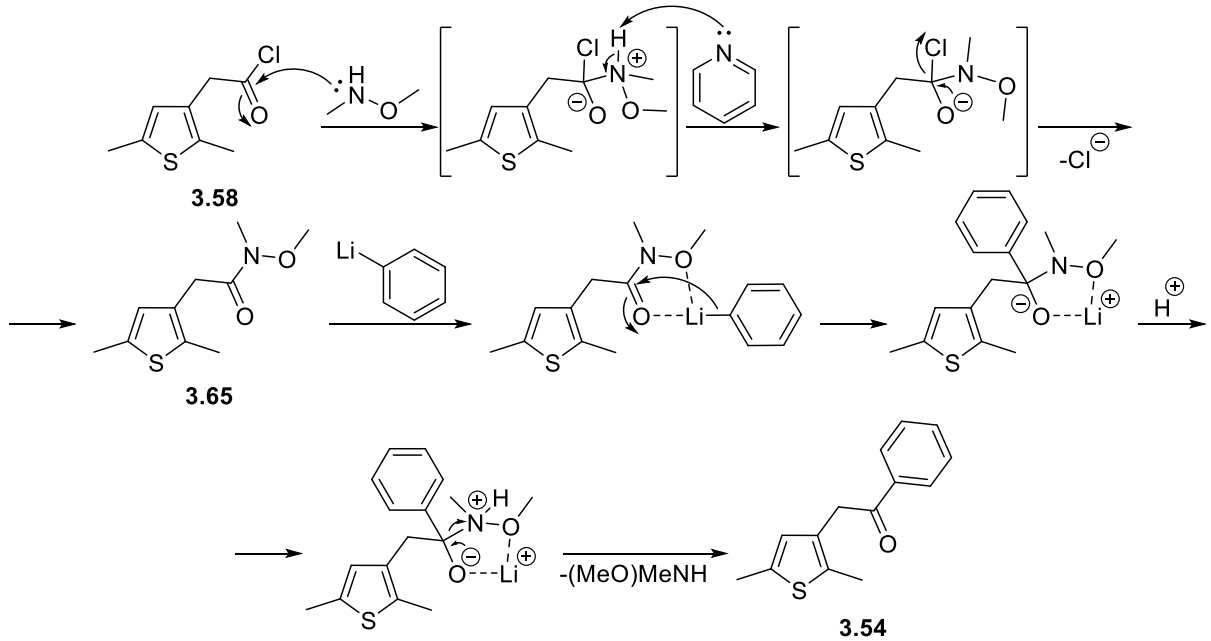

Scheme 3.29: Mechanism of the formation of Weinreb amide **3.65** and its subsequent phenylation towards **3.54**

The mechanistic route to arrive at **3.54** presumably includes two consecutive nucleophilic substitutions on the pivotal carbonyl group of the acid chloride **3.58** (Scheme 3.29). Attack by the electron rich *N* atom of the reacting amine bring forth a quaternary intermediate that is converted to the amide product **3.65**

through cleavage of the chloride leaning group and deprotonation of the amino moiety. Subsequent attack of this amide by the extremely reactive phenyl anion is carried out efficiently as the Weinreb amide species has the ability to coordinate with the lithium cation and stabilise the intermediate of this transformation due to the oxygen atom on the methoxy group. Finally, cleavage of the amide bond upon quenching the reaction mixture with a weak acid (NH_4Cl aq.) restores the carbonyl unit and yields the desired ketone. The foregoing synthetic routes that led to the compilation of the three methylene ketones, **3.52** – **3.54**, are summarised in Scheme 3.30.

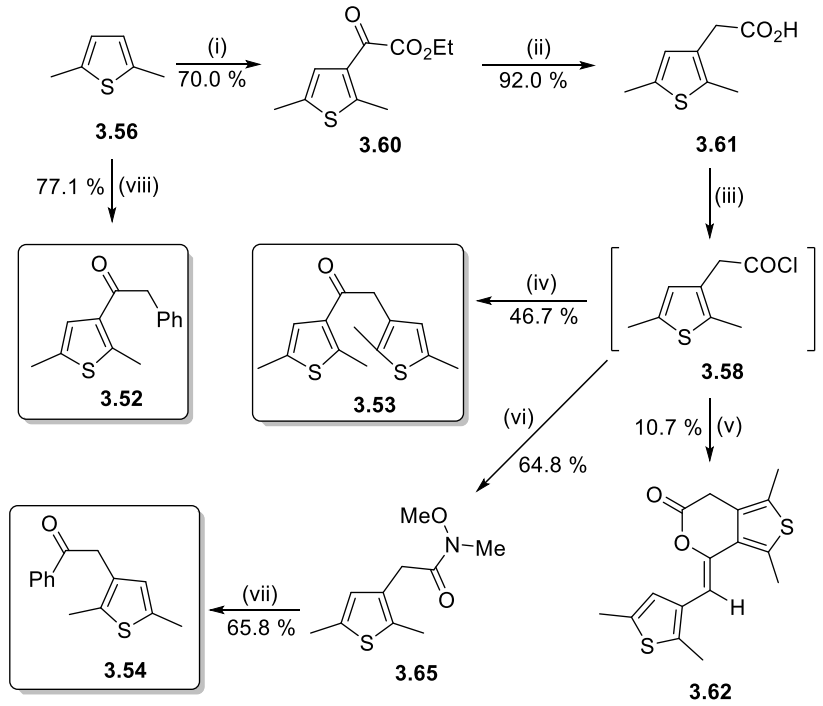

Reagents and conditions: (i) ethyl oxalyl chloride, $AlCl_3$ anyhd., $MeNO_2$, 5 °C – r.t.; (ii) $NH_2NH_2{\cdot}H_2O$, $HOCH_2CH_2OH$, then KOH, 70 °C – reflux; (iii) $SOCl_2$, cat. DMF, CH_2Cl_2; (iv) 2,5-dimethylthiophene, $AlCl_3$ anyhd., $MeNO_2$, 5 °C – r.t.; (v) PhH, $AlCl_3$ anyhd., $MeNO_2$, 5 °C – r.t.; (vi) MeNHOMe·HCl, pyridine, CH_2Cl_2, N_2, 0 - 5 °C – r.t.; (vii) PhLi in Bu_2O, THF anhyd., N_2, -78 °C – r.t., (viii) $PhCH_2COCl$, $AlCl_3$ anyhd., CH_2Cl_2 , $MeNO_2$, 5 °C – r.t.;
Scheme 3.30: Summary of routes to the thienylketones **3.52**, **3.53** and **3.54**

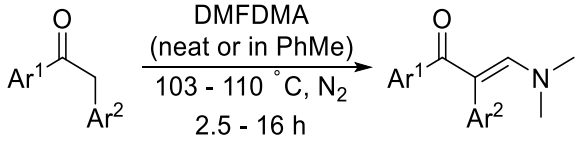

3.52 - 3.54 **3.66 - 3.68**

Entry	Ar^1	Ar^2	Enaminone No.	Solvent	Temperature (°C)	Time (h)	Yield (%)
1	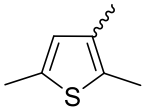	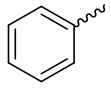	**3.66**	-	103	16	82.1
2	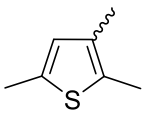	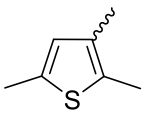	**3.67**	-	103	16	60.0
3	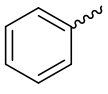	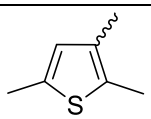	**3.68**	PhMe	110	2.5	85.5

Table 3.3: DMFDMA addition on the 3 α-methylene ketones **3.52 – 3.54**

The methylene ketones **3.52 – 3.54** were transformed into their respective enaminones **3.66 – 3.68** in fairly good yields upon reaction with DMFDMA employing the protocols established in chapter 2 (Table 3.3). In a similar fashion to the other enaminone systems visited in chapter 2, these thienyl-containing analogues present key signals on their NMR spectra, as seen for the bis-thienyl example **3.67** (Figure 3.16). In addition to the previously noted singlets of the thiophene methyl groups between δ 2.12 and 2.42 and the thiophene ring protons found between δ 6.43 and 6.45, the vinyl proton resonates at δ 7.30 and the NMe_2 unit is observed as a broadened signal at δ 2.77.

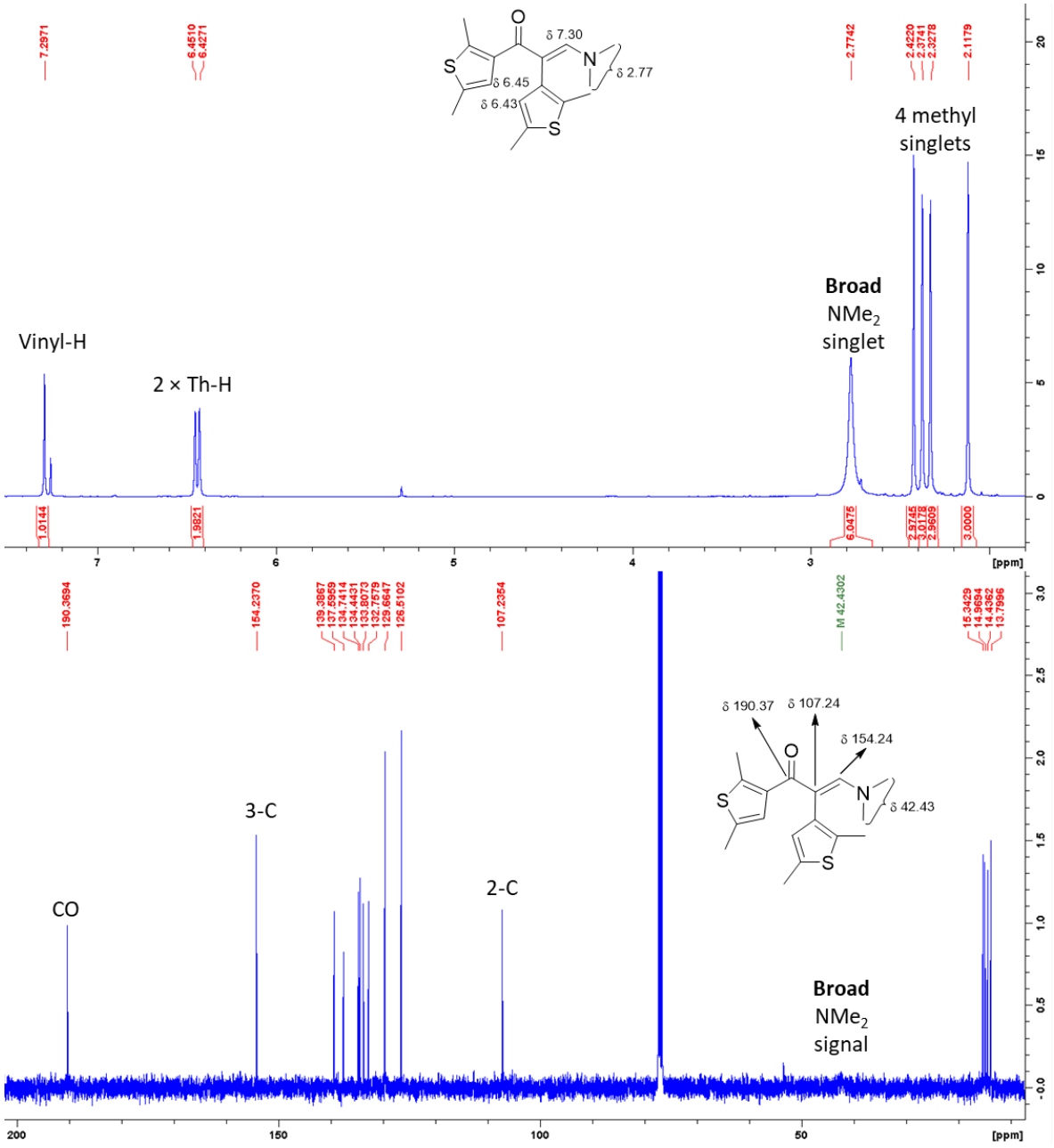

Figure 3.16: ^{1}H-NMR and ^{13}C-NMR spectra of enaminone system **3.67**

The ^{13}C-NMR spectrum proves further structural evidence, with the key CO signal observed at δ 190.37 and the two carbon atoms of the double bond affording two olefin signals at δ 107.24 and 154.24 (Figure 3.16). The remaining characteristic signal for the two methyl groups of the NMe_2 unit appeared obscured initially, but analysis by HSQC-NMR showed a contour that connects the NMe_2 ^{1}H-NMR singlet at δ 2.77 with a broadened ^{13}C-NMR signal at δ 42.43 (Figure 3.17).

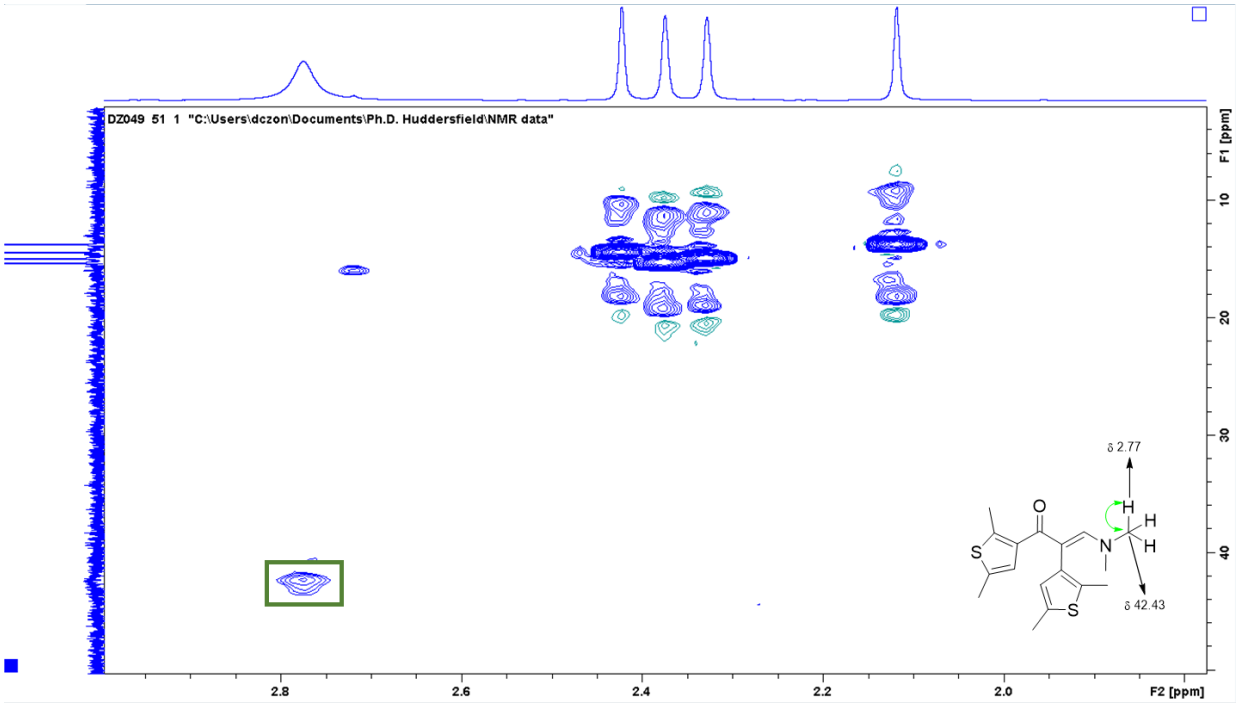

Figure 3.17: Key ^{1}H-^{13}C correlation between the protons and carbons of the NMe_2 terminus on **3.67**

Upon the preparation of **3.67**, it was postulated that the presence of two proton-containing thiophene rings could be utilised to provide evidence of an *E*-geometry for this enaminone by means of NOE spectroscopy, as shown in Figure 3.18.

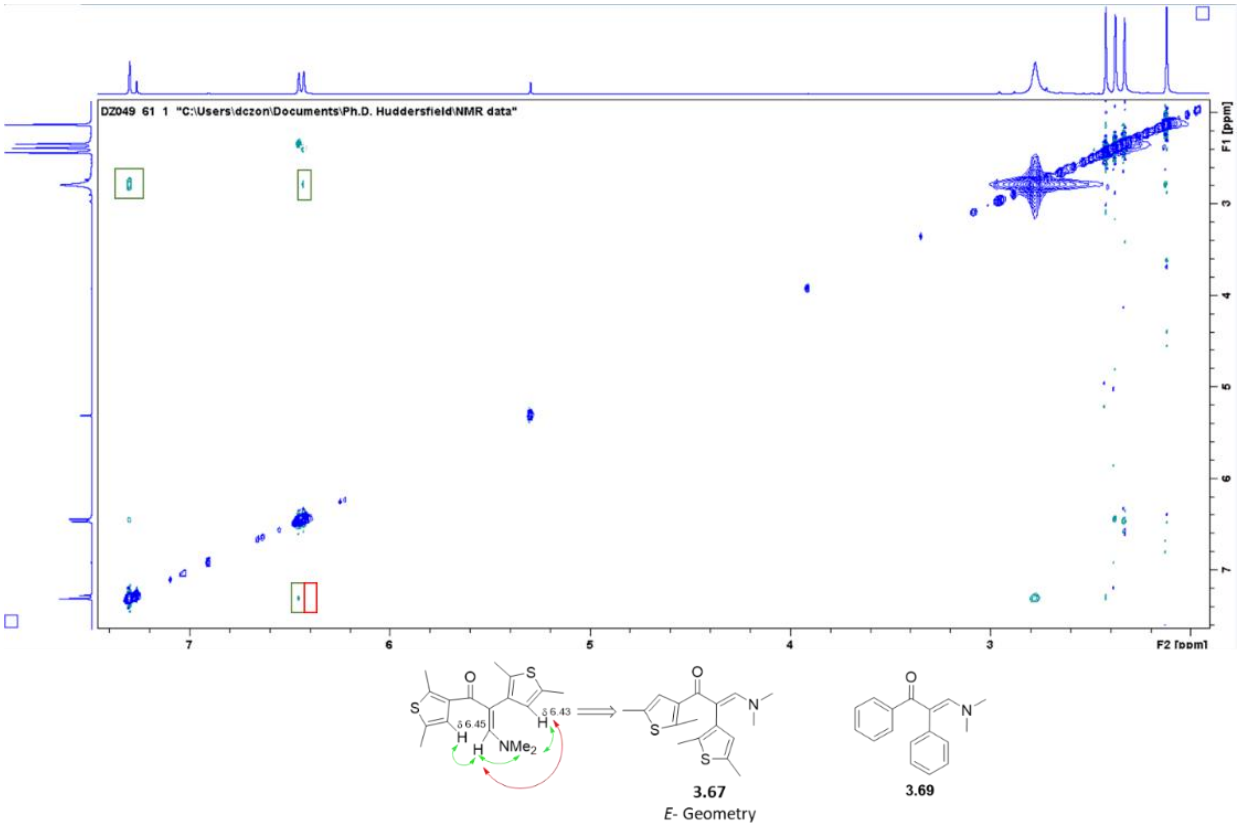

Figure 3.18: NOE NMR deployed to ascertain the *E* geometry of analogue **3.67** parallel to its bis-phenyl counterpart **3.69**

In a similar fashion to the bis-phenyl analogue **3.69**, the 6 NMe_2 protons present the predicted correlations with the vinyl proton at δ 7.30, as well as the backbone proton of the adjacent thienyl group on C2 at δ

6.43. This particular proton shows no correlation with its vinyl counterpart, thus illustrating that the thienyl moiety at C2 and the NMe_2 terminus share a *cis* configuration, whereas the vinyl proton at δ 7.30 also shows the anticipated correlation with the backbone proton of the thienyl group on C1 (δ 6.45), evident of an s-*trans* conformation for the single bond of the enone unit and, consequently, an *E* geometry for the bis-thienyl analogue **3.67**.

A final point of interest for the enaminones **3.66** – **3.69** was encountered during comparison of their ^{1}H-NMR spectra, wherein the NMe_2 unit on each derivative produced a singlet of different width. This variation in the sharpness of these signals could be directly correlated to the rate of the C3-N bond rotation in each enaminone analogue (Figure 3.19). As it can be seen on the overlaid spectra, the broadest singlets belong to **3.67** and **3.68**, indicating that the presence of a 2,5-dimethylthienyl group on the α-position of the enaminone structure restricts the rotation of the aforementioned bond and lowers its rate of rotation, potentially by virtue of unfavourable steric interactions between the 2 pairs of methyl groups on the thienyl moiety and the amino terminus. Absence of such moieties in analogues **3.66** and **3.69** allows the unfettered bond rotation, leading to a greater rate of rotation and, as a result, sharper ^{1}H-NMR signals for the *N*-methyl groups. In order to confirm this steric effect on the rotation speed, a VT-NMR experiment was carried out using a deuterated DMSO sample of the 2-dimethylthienyl derivative **3.68**, with an increasing temperature gradient from 25 ° to 70 °C. The broad NMe_2 singlet at δ 2.74 was indeed found to sharpen consistently as the temperature increased, which was evident of the C-N bond rotating at a higher rate, as the aforementioned steric clashes are mitigated by the introduction of thermal energy to the enaminone system, mirroring the VT-NMR finding presented in Chapter 2 (Figure 3.20). This influence of the substituent of the 2-position on the rotation of the NMe_2 unit places the two substituents in close proximity and, as a result, constitutes indirect evidence of the *E*-geometry being a general structural feature for enaminone systems with the foregoing substitution patterns.

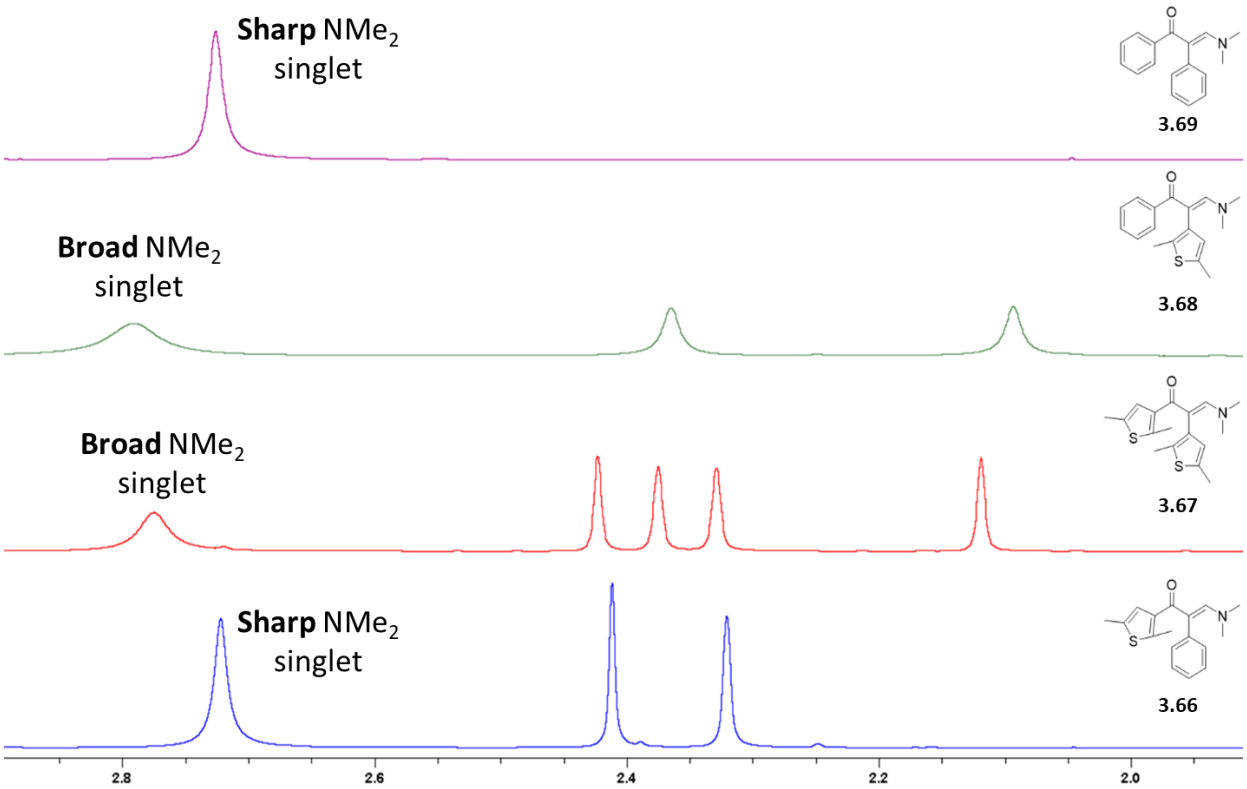

Figure 3.19: Overlaid ^{1}H-NMR spectra for **3.66** (blue), **3.67** (red), **3.68** (green) and **3.69** (purple), presenting the key singlets at δ 2.6 – 2.8 for the NMe_2 protons

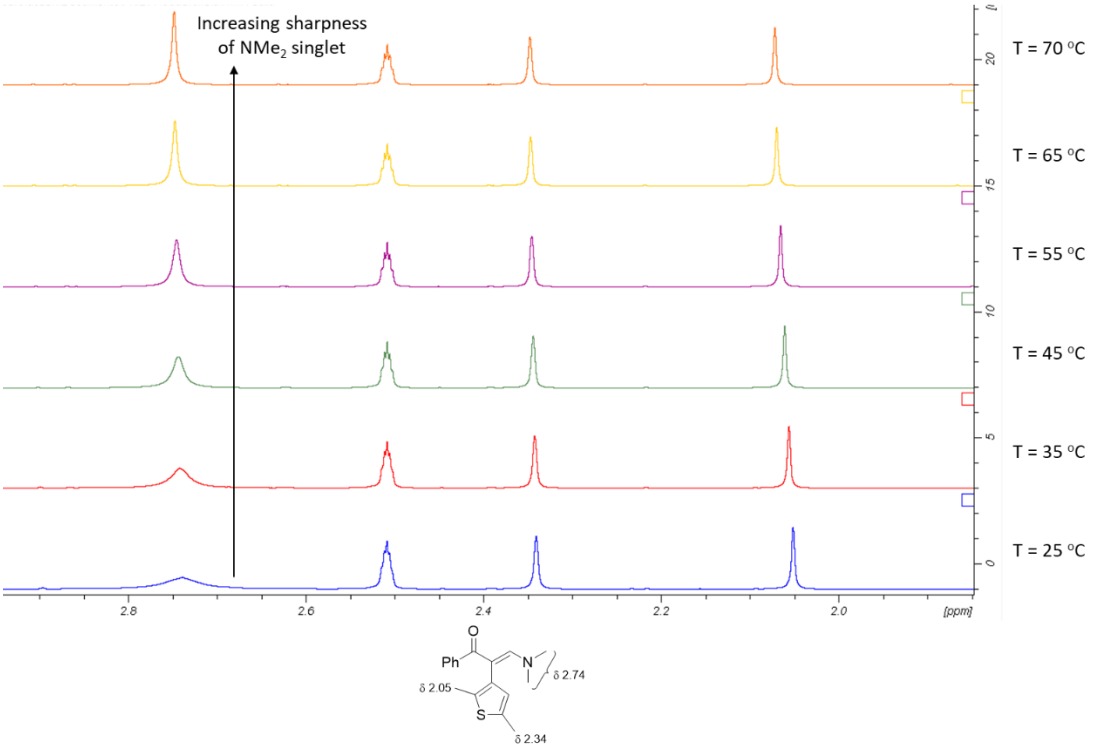

Figure 3.20: Overlaid VT-NMR spectra of **3.68** between 25 °and 70 °C, illustrating the increasing C-N bond rotation rate

Upon arriving at this enaminone series **3.66** – **3.68**, the corresponding 3,4-dihydro-4-dimethylamino-1,2-oxathiine 2,2-dioxide photochromic candidates **3.43 – 3.46** were constructed in good yields *via* the sulfene addition reaction detailed in section **2.2**. The results of this conversion are summarised in Table 3.4. As expected, the common spectroscopic features of 3,4-dihydro-1,2-oxathiine 2,2-dioxides that were mapped out in Chapter 2 were observed during the characterisation of the thienyl-containing analogues **3.43** – **3.46**.

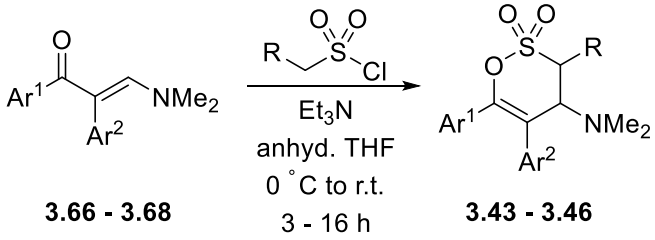

3.66 - 3.68 **3.43 - 3.46**

Entry	Ar^1	Ar^2	R	Product No.	Time (h)	Yield (%)
1	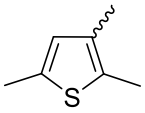	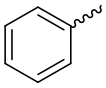	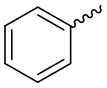	**3.43**	16	71.0
2	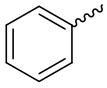	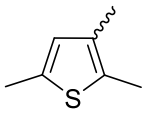	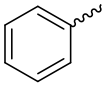	**3.44**	3	52.6
3	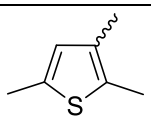	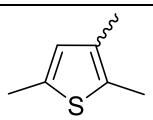	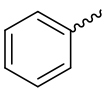	**3.45**	4	52.7
4	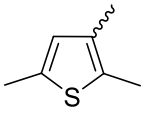	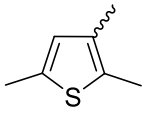	H	**3.46**	3	55.0

Table 3.4: Sulfene addition towards the 3,4-dihydro-1,2-oxathiine 2,2-dioxides **3.43 – 3.46**

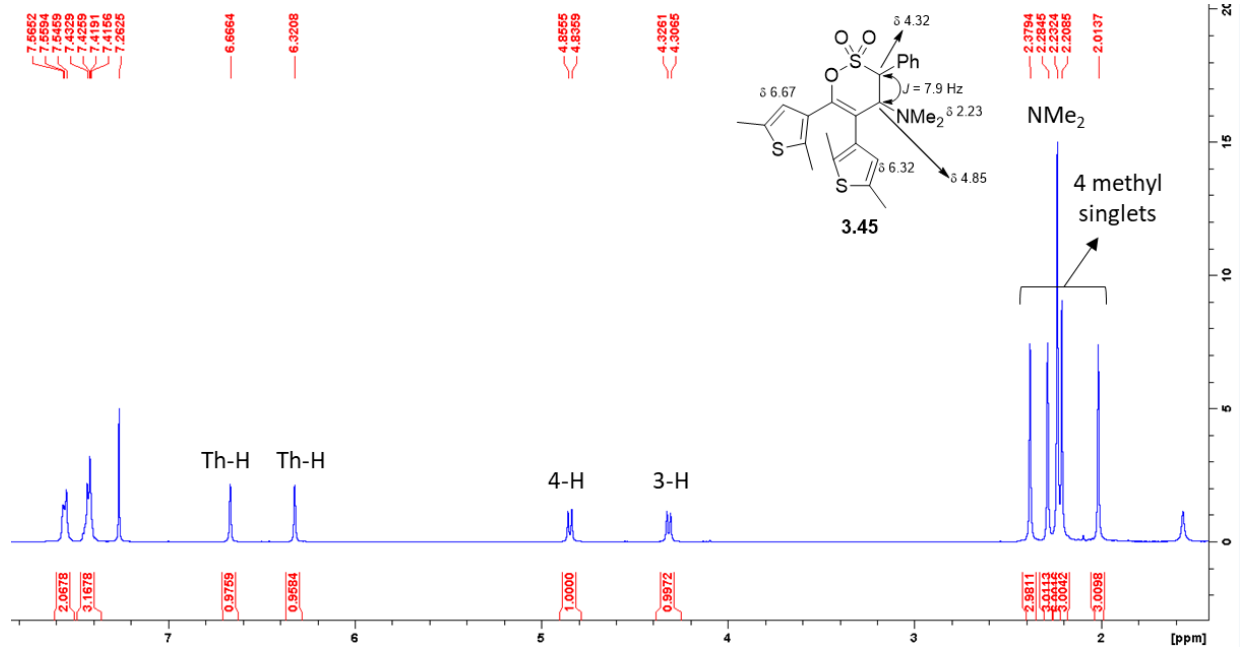

Figure 3.21: 1H-NMR spectra of the bis-thienyl analogue **3.45**

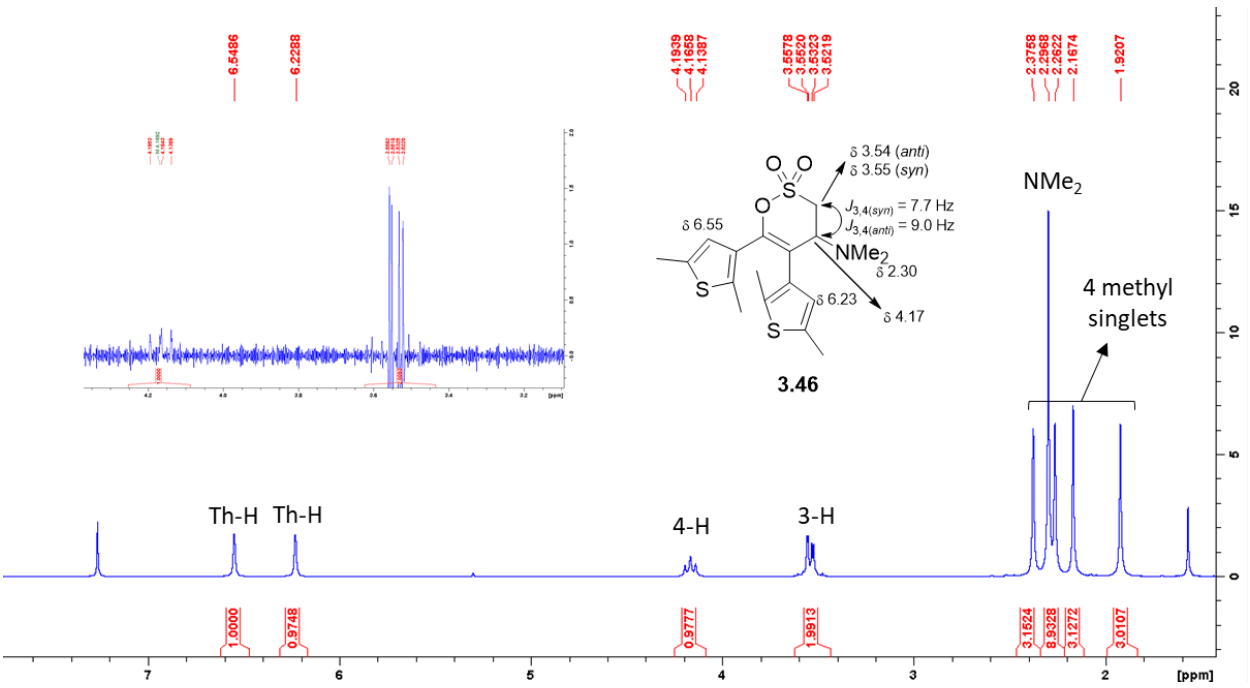

Figure 3.22: ^{1}H-NMR spectra of **3.46** (insert shows the deconvolution of peaks *via* a Gaussian multiplication of the ^{1}H-NMR spectrum)

As seen on the ^{1}H-NMR spectra of examples **3.45** and **3.46** (Figure 3.22), the key signals for the 3-H and 4-H appear between δ 3.5 - 5.0, with a coupling constant of 7.9 Hz in case of the phenyl analogue **3.45** and an AA'B pattern with $J_{3,4(syn)}$ = 7.7 Hz and $J_{3,4(anti)}$ = 9.0 Hz for analogue **3.46**. Moreover, the NMe_2 units in both compounds resonate in the range between δ 2.23 – 2.30, while the substituted thienyl groups on the 5- and 6- positions produce the commonly noted four aliphatic (δ 1.92 – 2.38) and two near-aromatic (δ 6.23 – 6.67) signals.

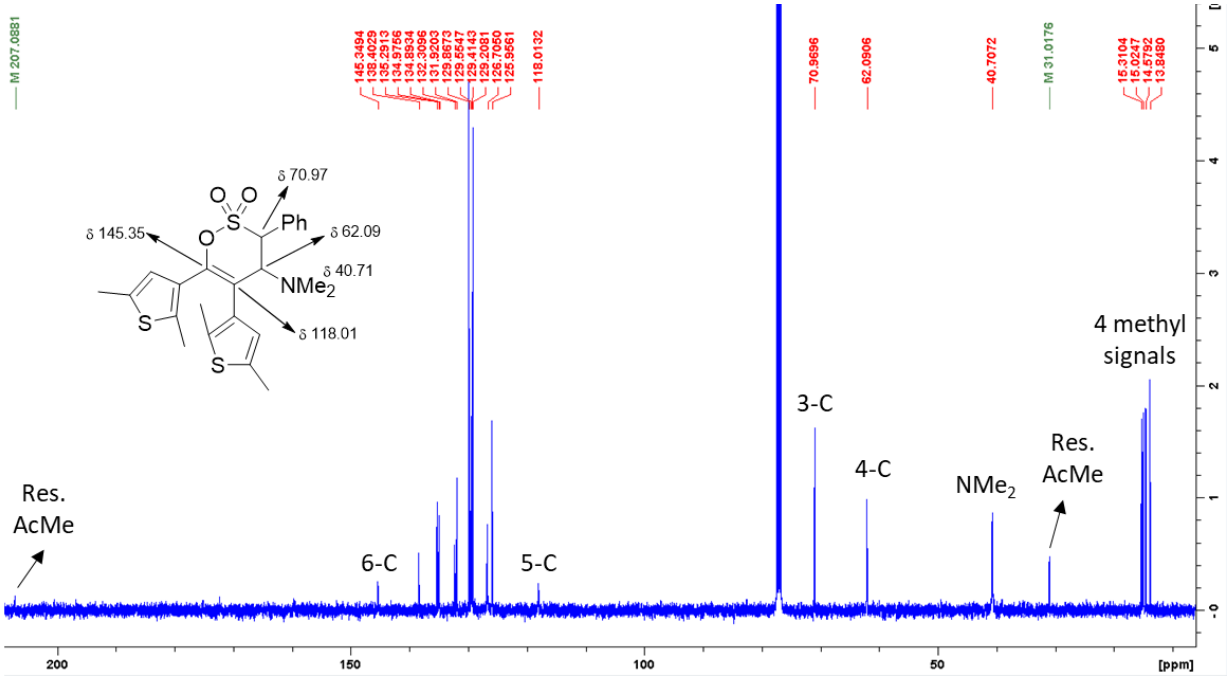

Figure 3.23: ^{13}C-NMR spectrum of the bis-thienyl analogue **3.45**

The heterocyclic scaffolds of **3.43** – **3.46** were also confirmed by ^{13}C-NMR spectroscopy (Figure 3.23), as their key spectroscopic elements were successfully located. The two aliphatic carbons C3 and C4 on the bis-thienyl analogue **3.45** produce two signals at δ 70.97 and 62.09 respectively, while the olefinic C5 resonates at δ 118.01 and the deshielded C6 at δ 145.35. The pivotal NMe_2 signal is also found at δ 40.71 and the remaining characteristic peaks of the thiophene methyl groups are observed between δ 13.85 and δ 15.31. The key vibration frequencies of the SO_3 fragment could also be successfully located on the IR spectrum of **3.45** as sharp peaks at 1385 and 1153 cm^{-1}.

Finally, unequivocal evidence of the sulfene addition success was obtained *via* mass spectrometry (Figure 3.24), in accordance with the findings for the 3,4-dihydro-1,2-oxathiine 2,2-dioxide analogues of Chapter 2. The HRMS spectrum of **3.45** shows a peak at *m/z* 474.1236 for a $[M_1+H]^+$ fragment which matches the theoretical value of 474.1226 for the *m/z* of a $[M_1+H]^+$ fragment for the formula $C_{24}H_{23}NO_3S$. As was previously noted in section **2.2.1**, the base peak at *m/z* 365.1040 correlates to the furan system **3.70**, which is formed during MS analysis through pyrolysis of the 1,2-oxathiine 2,2-dioxide centre unit and has the formula $C_{22}H_{20}OS_2$ with an anticipated *m/z* value of 365.1032 (Scheme 3.31).

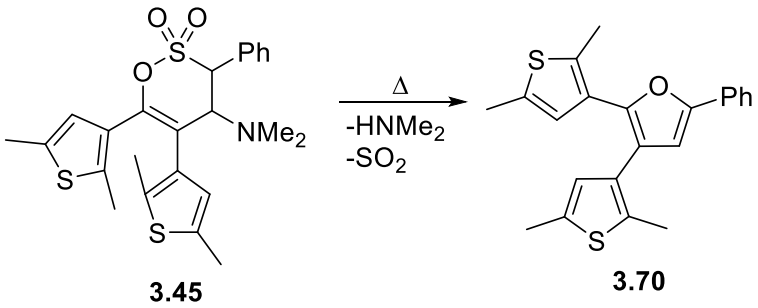

Scheme 3.31: Pyrolysis of **3.45**

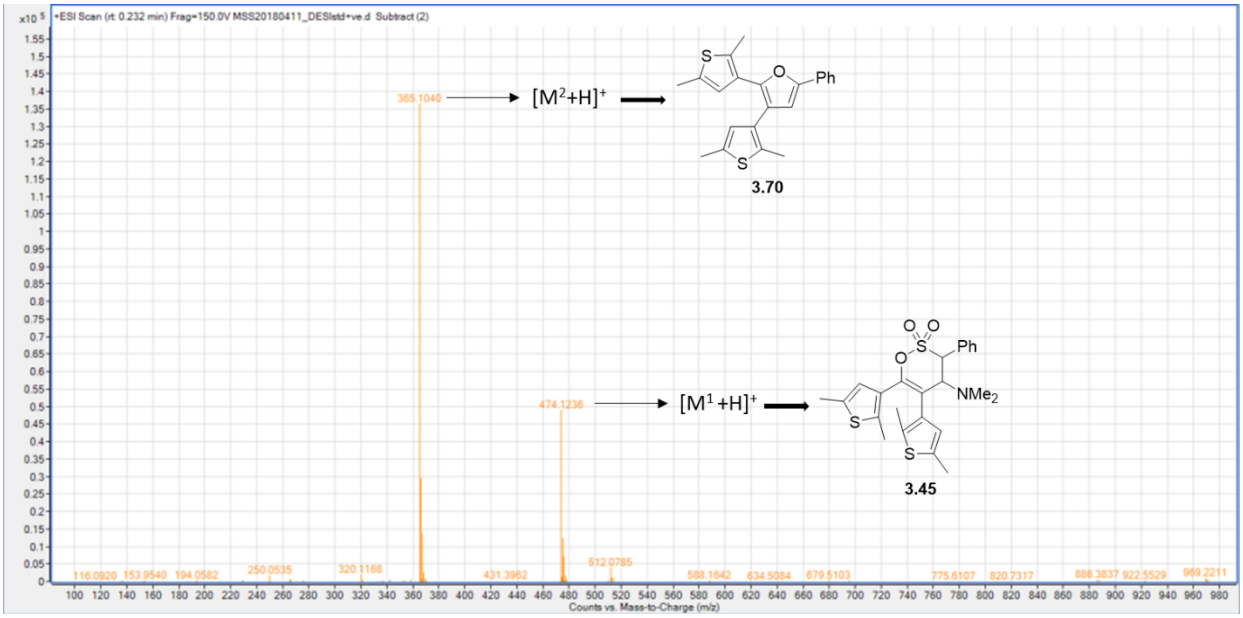

Figure 3.24: MS spectrum of **3.45**, illustrating the presence of the *in situ* formed furan derivative **3.70**

In tandem with acquiring spectroscopic data for the compiled analogue library, crystals of adequate quality for single crystal X-ray crystallographic analysis were obtained for the bis-thienyl analogue **3.45** from Et_2O and hexane (stored at -20 °C for 24 h) in order to illustrate its exact 3D configuration (Figure 3.25). The crystal structure proves that the 3-H and 4-H atoms are in a *trans*-axial arrangement with a torsion angle of *circa* 155° for H-C3-C4-H, which is in accordance with the coupling constant of 7.9 Hz recorded for their corresponding doublets. The rest of the 1,2-oxathiine backbone in this structure illustrates that the "envelope" conformation mentioned in section **1.2.2.1**[86] is not only adopted for the tri-phenyl analogue but seems to be a structural trend for such heterocyclic systems with the SO_2 group escaping the C3-C4-C5-C6-O plane in a similar fashion, with the S-C3-C4 angles measured at 110.3°.
An important issue that arose during the synthesis of these photochromic candidates was whether the two neighbouring thiophene units would adopt the antiparallel conformation which is requisite for a reversible photochemical cyclisation.[187] Further examination of the crystal structure seen of **3.45** highlights that the heteroaromatic rings are indeed positioned in this array, which is a promising indication of photochromic activity. It should be noted that these findings do not point out to any other analogues adopting the desired antiparallel conformation.

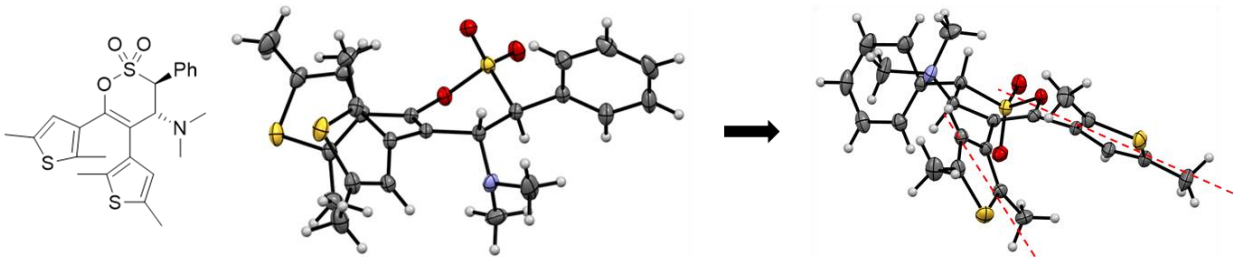

Figure 3.25: Crystal structure of **3.45** (various viewpoints, thermal ellipsoids shown at 50 % probability level)

The final step for the preparation of the photochromic candidate library of **3.42** – **3.51** involved the employment of the Cope elimination protocol described in section **2.3.2** to furnish the eliminated derivatives **3.48** – **3.51** from their saturated precursors **3.43** – **3.46** in very good yields (Table 3.5).

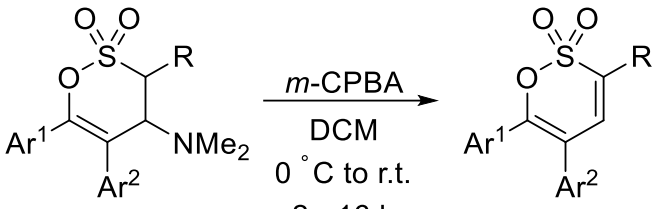

3.43 - 3.46 **3.48 - 3.51**

Entry	Ar^1	Ar^2	R	Product No.	Time (h)	Yield (%)
1	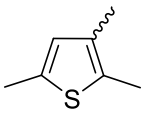	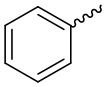	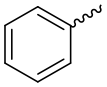	**3.48**	16	71.1
2	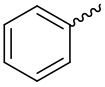	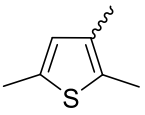	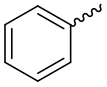	**3.49**	2	78.0
3	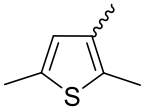	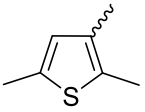	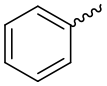	**3.50**	2	83.5
4	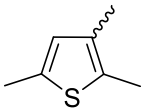	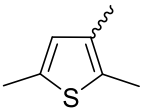	H	**3.51**	3	77.7

Table 3.5: Cope elimination runs towards analogues **3.48** – **3.51**

As was the case for the analogues presented in chapter 2, the 1,2-oxathiine 2,2-dioxides **3.48** – **3.51** were examined by NMR spectroscopy to ensure the success of the elimination step (Figure 3.26). In the ^{1}H-NMR spectrum of analogue **3.48**, the vinyl proton appears to resonate at δ 7.04 and the thienyl proton at δ 6.38, while the methyl group signals appear at δ 2.15 and 2.29. Further structural evidence can be obtained by the ^{13}C-NMR spectrum of **3.48**, wherein the C3-C6 backbone chain is identified by signals at δ 119.48, 133.90, 135.68 and 149.48. Moreover, the key IR peaks at 1359 cm^{-1} and 1178 cm^{-1} complete the identification of the 1,2-oxathiine centre by illustrating the presence of the SO_3 moiety of the heterocycle. The non-substituted analogue **3.51** presents an additional spectroscopic feature, as in this instance there are protons on the 3- and 4-positions which produce a set of doublets at δ 6.61 and 6.90 with $J_{3,4}$ = 10.2 Hz (Figure 3.27).

It was anticipated that, upon exposure of either of the candidates **3.42** – **3.51** to UV radiation, a reversible electrocyclic reaction would occur towards a coloured ring-closed species with extended conjugation (red-coloured conjugated system in **3.42-closed** – **3.51-closed**, Scheme 3.32). It was postulated that the coloured species would be thermally stable so that they could remain intact until the reverse reaction would be initiated by irradiation with visible light. Furthermore, the extension of lateral conjugation accomplished by the 3,4-double bond on the unsaturated analogues, in addition to the presence of a 3-phenyl ring, would be studied to ascertain their effect on the photochromic response.

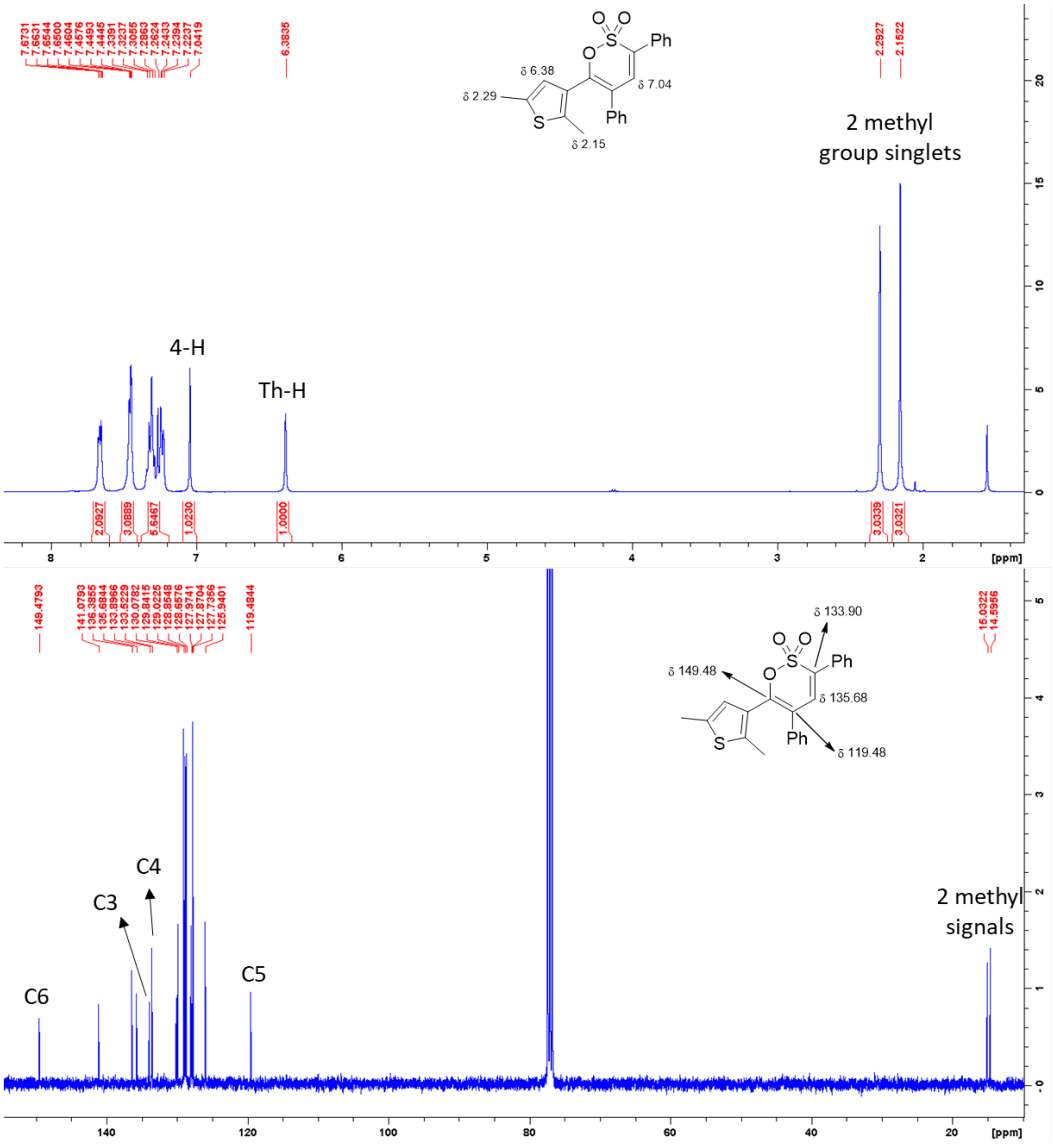

Figure 3.26: ^{1}H-NMR (above) and ^{13}C-NMR (below) spectra of the unsaturated analogue **3.48**

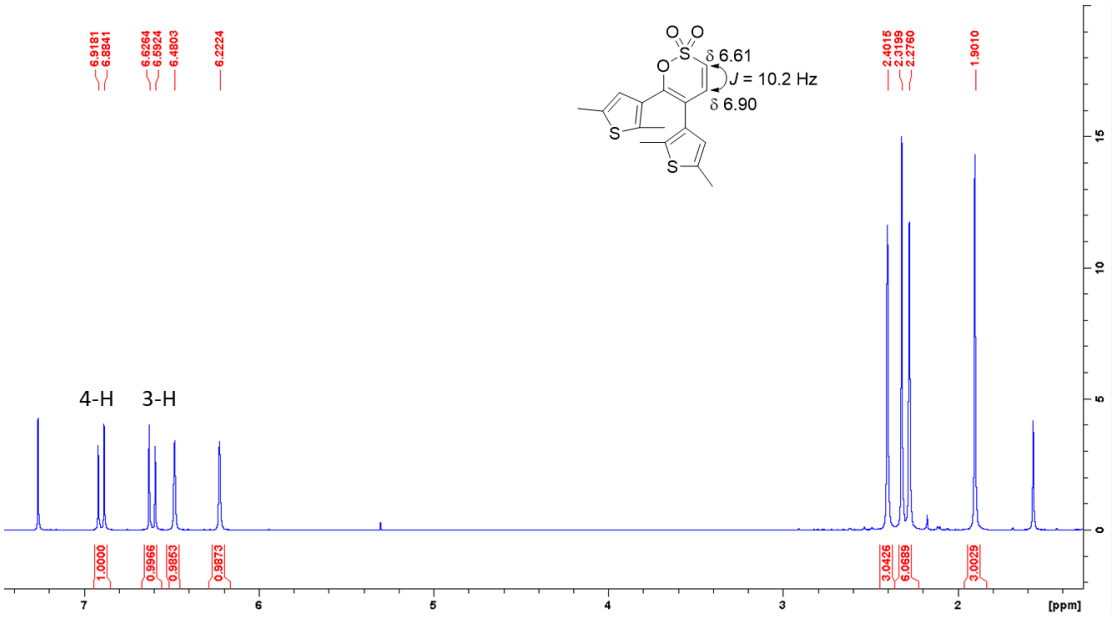

Figure 3.27: ^{1}H-NMR spectrum of **3.51** showing the characteristic doublets for 3-H and 4-H

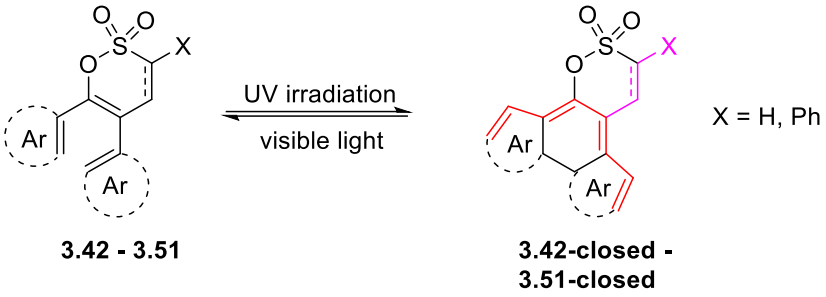

3.42 - 3.51 **3.42-closed - 3.51-closed**

Scheme 3.32: Photoconversion to the ring-closed forms and reversion with visible light

3.3.2 UV-Vis spectrophotometric studies

With the series of 1,2-oxathiine 2,2-dioxides **3.42 - 3.51** fully prepared, their photochromic response in dilute hexane solutions was examined using the bespoke UV-Vis-NIR Shimadzu spectrophotometer equipped with an 'in cell' UV-Vis irradiation system (Figure 3.28**Error! Reference source not found.**).

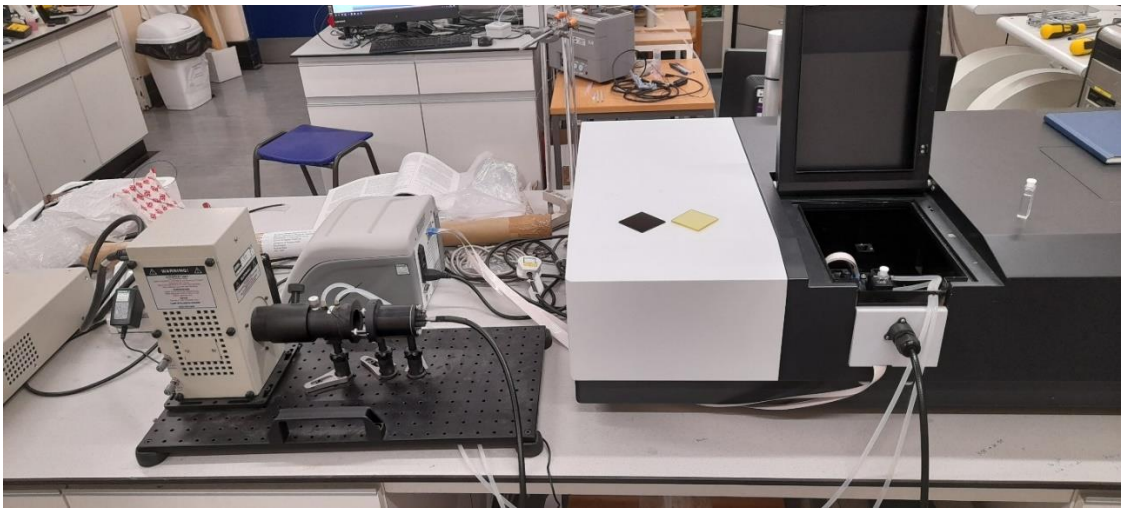

Figure 3.28: Irradiation equipment used for the UV-Vis spectrophotometric studies

Exposing hexane solutions of the 3,4-dihydro analogues **3.43** - **3.46** to UV radiation (λ_{irr} = 260 – 380 nm, 150 W) induced a yellow/orange colour development with λ_{max} in the range 413 to 441 nm. Prolonged irradiation times of up to 155 min led to a photostationary state (PSS) for each analogue, *i.e.* a point where no further increase in absorption would be observed on the UV-Vis spectrum (Figure 3.29). The absorption and λ_{max} values for each analogue, along with the irradiation times, molar absorption coefficients and percentages of ring-closed forms, are summarised in Table 3.6. The 5,6-diphenyl analogue **3.42** showed no observable photochromic response and is thus omitted from Table 3.6, whereas the remaining four analogues showed various levels of activity, with the 3-phenyl bis-thienyl example **3.45** affording the highest absorption value at a PSS, followed by its non-substituted counterpart **3.46** with a notably lower A_{max}, evident of a potential benefit to the activity by the 3-phenyl group. The "mixed aryl" derivatives **3.43** and **3.44** were less active, but the significant difference between the absorption values on their PSS is met with interest, as it suggests that the phenyl and thienyl groups require specific positions for an optimal photochemical interaction. Although the findings in Figure 3.29 constitute evidence of a photochemical response to UV irradiation which reflects the anticipated cyclisation, any attempts at converting the ring-closed forms (**3.43-closed** – **3.46-closed**) into their ring-open counterparts (**3.43** – **3.46**) *via* irradiation with visible light failed to proceed completely, indicating that the observed photochromic activity is not fully reversible.

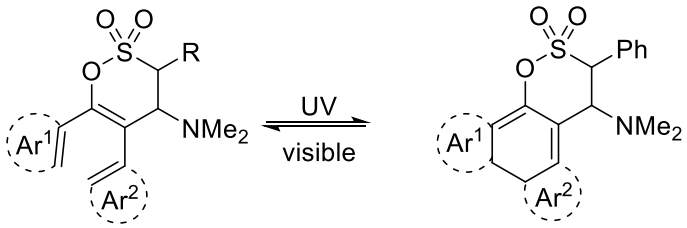

3.43/3.43-closed: Ar^1 = 2,5-dimethyl-3-thienyl, Ar^2 = Ph, R = Ph
3.44/3.44-closed: Ar^1 = Ph, Ar^2 = 2,5-dimethyl-3-thienyl, R = Ph
3.45/3.45-closed: Ar^1 = Ar^2 = 2,5-dimethyl-3-thienyl, R = Ph
3.46/3.46-closed: Ar^1 = Ar^2 = 2,5-dimethyl-3-thienyl, R = H

Compounds No.	λ_{max} (nm)	Absorbance at λ_{max}		ε_m at PSS (mol^{-1} dm^3 cm^{-1})	Time to PSS (s)	% Closed form*
		A_0	A_{PSS}			
3.43/3.43-closed	474	0	0.03	61	20 min	2
3.44/3.44-closed	413	0.01	0.23	489	30 min	5
3.45/3.45-closed	414	0.01	0.55	1300	2 h 35 min	2
3.46/3.46-closed	441	0.01	0.38	1524	2 h 15 min	8
* Calculated by the ring-closed/ring-open integral ratios of the respective thiophene ring protons on the ^{1}H-NMR spectra of post-irradiation samples						

Table 3.6: Key UV-Vis values of the saturated 1,2-oxathiine 2,2-dioxide analogues (**3.43** – **3.46**)

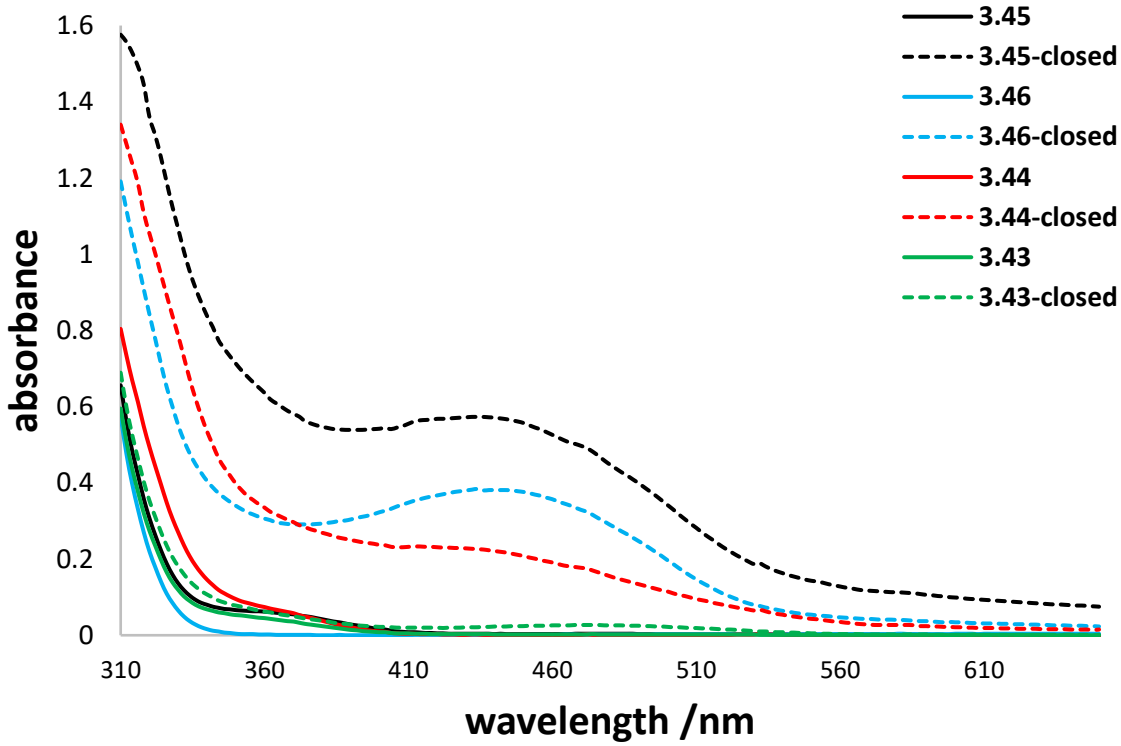

Figure 3.29: Absorption spectra (in hexane) of 3,4-dihydro-1,2-oxathiine 2,2-dioxides **3.43** – **3.46** before irradiation and at the photostationary state (PSS)

The photochromic potency of the unsaturated species **3.48** – **3.51** in hexane solutions was next examined by UV irradiation (λ_{irr} = 260 – 380 nm, 120 W) (Figure 3.30) and the findings are previewed in Table 3.7. In a similar manner to **3.42**, the solution of **3.47** failed to exhibit any photochromism, hence it is not included in the table below. Overviewing the behaviour of the active candidates shows that, in the case of the unsaturated 1,2-oxathiine 2,2-dioxide systems, absence of the phenyl group on the 3-position results in an increase in the absorption maxima (A_{max} = 0.82 for **3.50**/ A_{max} = 0.94 for **3.51**), which is a contrasting trend to that observed for their 3,4-dihydro counterparts (A_{max} = 0.55 for **3.45**/ A_{max} = 0.38 for **3.46**, Table 3.6). Further evaluation of these UV-Vis findings reveals that the introduction of the C3-C4 double bond augments the activity for the bis-thienyl derivatives **3.50** and **3.51** in terms of maximum absorption but mitigates it for the thienyl/phenyl analogues **3.48b** and **3.49**, as evidenced by the exceptionally weak red hue that was observed upon irradiation to the PSS.

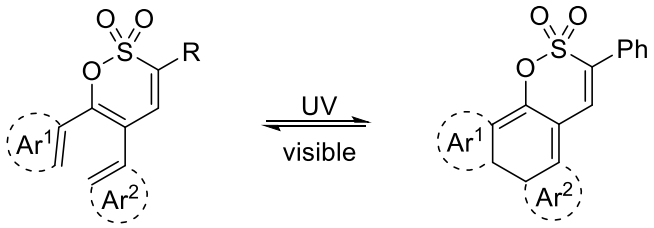

3.48/3.48-closed: Ar^1 = 2,5-dimethyl-3-thienyl, Ar^2 = Ph, R = Ph
3.49/3.49-closed: Ar^1 = Ph, Ar^2 = 2,5-dimethyl-3-thienyl, R = Ph
3.50/3.50-closed: Ar^1 = Ar^2 = 2,5-dimethyl-3-thienyl, R = Ph
3.51/3.51-closed: Ar^1 = Ar^2 = 2,5-dimethyl-3-thienyl, R = H

Compounds No.	λ_{max} (nm)	Absorbance at λ_{max}		ε_m at PSS (mol^{-1} dm^3 cm^{-1})	Time to PSS (s)	% Closed form*
3.48/3.48-closed	513	0	0.01	25	15 min	2
3.49/3.49-closed	481	0.01	0.07	125	20 min	0.5
3.50/3.50-closed	503	0.03	0.82	1708	45 min	38
3.51/3.51-closed	494	0.01	0.94	1541	50 min	9
* Calculated by the ring-closed/ring-open integral ratios of the respective 4-H protons on the ^{1}H-NMR spectra of post-irradiation samples						

Table 3.7: Key UV-Vis values of the unsaturated 1,2-oxathiine 2,2-dioxide analogues (**3.48** – **3.51**)

Juxtaposition of the findings in Table 3.6 and Table 3.7 presents an additional insight on the photochromic behaviour of these compounds (Scheme 3.33); comparing of the absorption and λ_{max} values for the 3,4-dihydro candidates **3.43** – **3.46** with those of the unsaturated **3.48** – **3.51** suggests that the presence of a double bond between C-3 and C-4 not only induces a consistent decrease in the time required to establish a PSS, but also results in a bathochromic shift in the wavelength of maximum absorption, with the specific examples of the λ_{max} for **3.50-closed** (503 nm) and **3.51-closed** (494 nm) being considerably higher than those for their 3,4-dihydro precursors **3.45-closed** (414 nm) and **3.46-closed** (441 nm). Presumably, this can be directly connected to the increase in the level of conjugation that transpires when moving from the saturated **3.43** – **3.46** to the eliminated systems **3.48** – **3.51**. Supporting this conclusion, an additional bathochromic shift can be observed when the conjugation level is further extended with the C3 phenyl group, as seen by examining the λ_{max} of **3.50 and 3.51** (503 nm and 494 nm respectively).

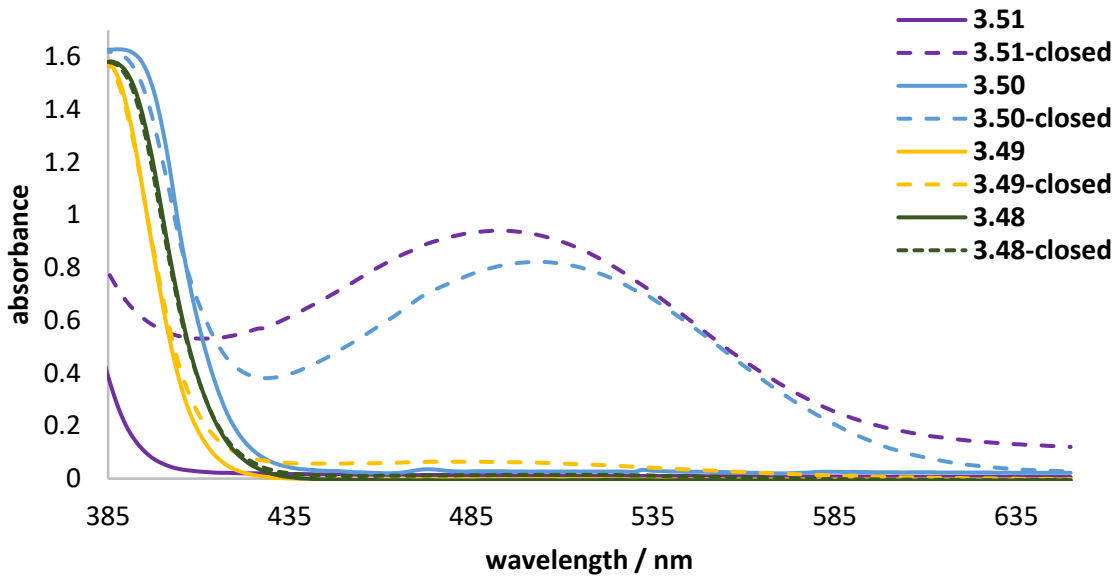

Figure 3.30: Absorption spectra (in hexane) of the unsaturated 1,2-oxathiine 2,2-dioxides **3.48** – **3.51** before irradiation and at photostationary state

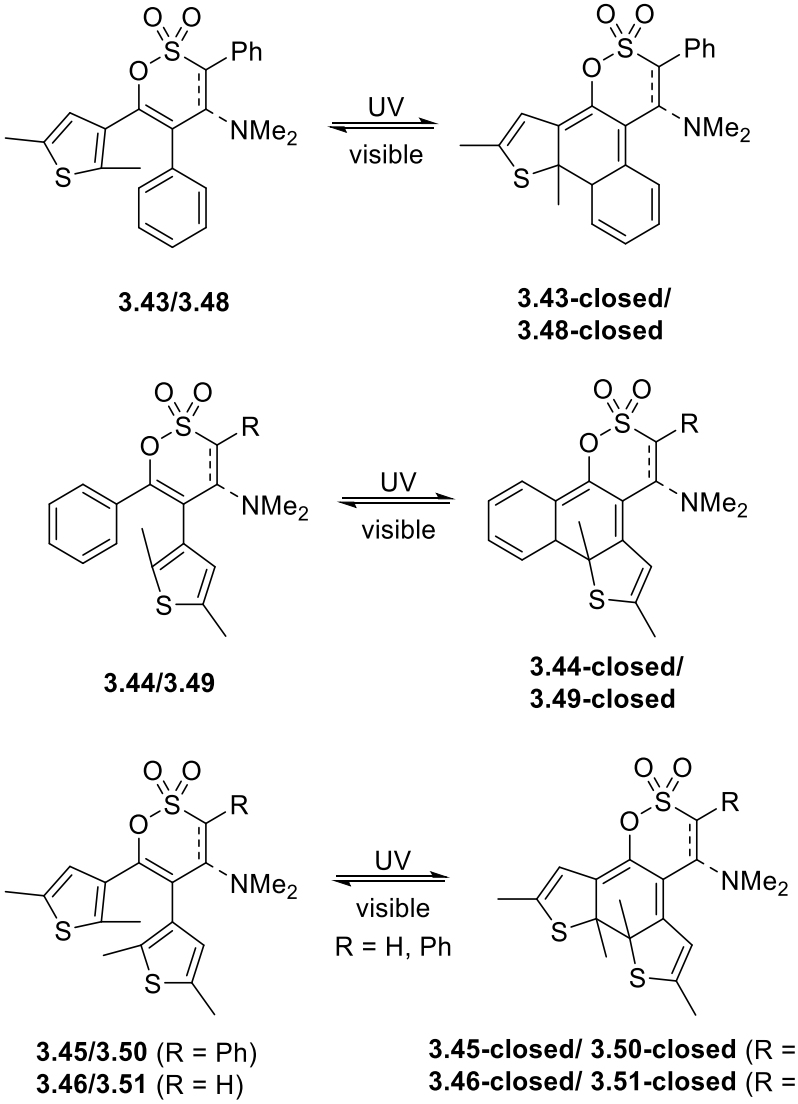

Scheme 3.33: Structures of the active candidates **3.23** and **3.24** *before* and *after* irradiation

More clearly defined absorption peaks for the unsaturated analogues **3.50** and **3.51** as compared with their saturated precursors **3.45** and **3.46** led to additional explorations on reversion of the photocyclisation by visible light. A hexane solution of **3.50** was UV irradiated for 45 min until it reached its PSS, with the generation of an intense red hue (λ_{max} = 503 nm) (Figure 3.31 and attached inserts) confirming the presence of the ring-closed isomer **3.50-closed** (Scheme 3.33). Subsequently, visible light bleaching (λ_{irr} = 455 – 650 nm) of the foregoing red solution was efficiently accomplished after 25 min. The colouration and bleaching cycle of **3.50** in a PhMe solution was repeated 10 times to illustrate the reversibility of this process (insert (a), Figure 3.31), with substantial resistance to fatigue due to decomposition.

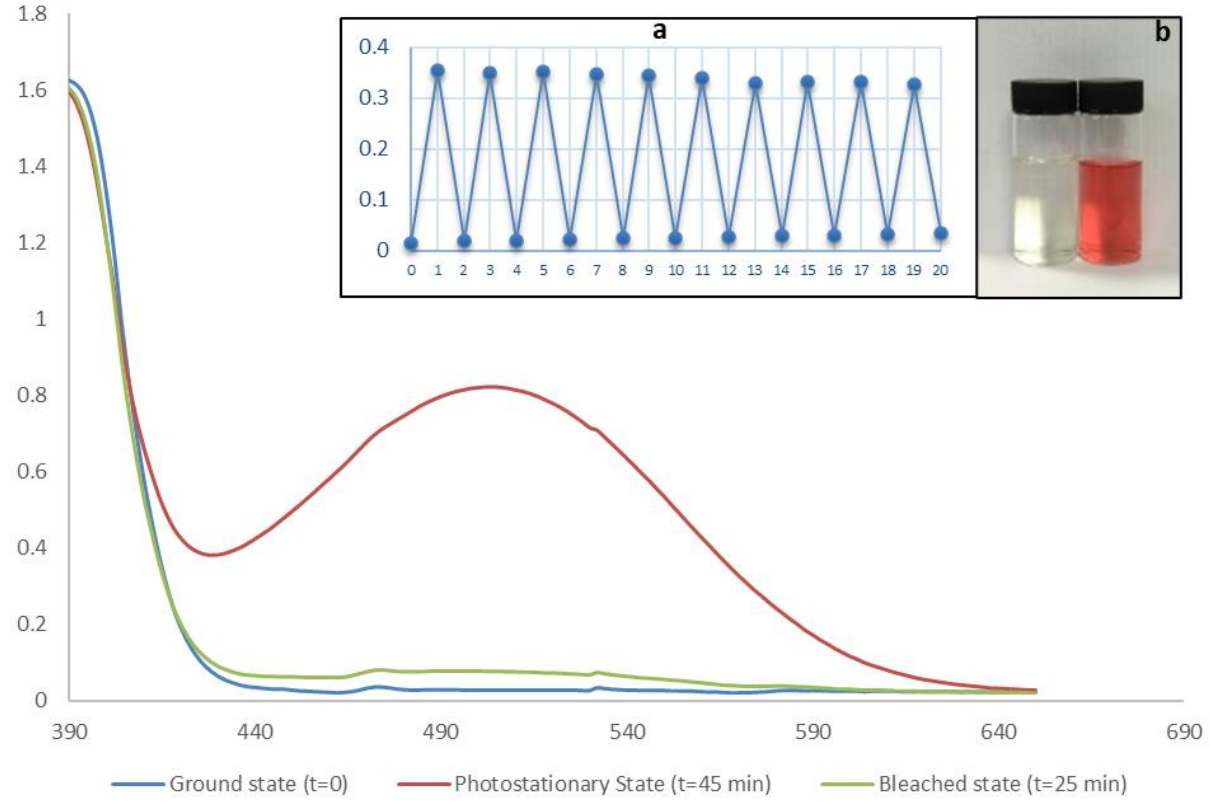

Figure 3.31: Absorption spectra of **3.50** (initial, after UV activation and after visible light bleaching), insert (a): recyclability after 10 UV activation and visible light bleaching cycles, insert (b): **3.50** hexane solution before (right) and after (left) UV irradiation

In tandem with these spectrophotometric evaluations, the photochemical cyclisation could be further explored *via* ^{1}H-NMR spectroscopy. Repeating the UV irradiation experiment of **3.50** in $CDCl_3$ and recording consecutive ^{1}H-NMR spectra over time revealed the presence of new signals attributed to **3.50-closed** at δ 2.05, 2.11, 2.12, and 2.22 for the thiophene methyl groups, at 5.96 and 6.07 for the thienyl protons and at δ 6.83 for 4-H (Figure 3.32).

Comparison of the integrals for 4-H in **3.50** (δ 6.89) and **3.50-closed** (δ 6.83) of the $CDCl_3$ solution revealed a ratio of 5 : 3 (**3.50**/**3.50-closed**) at the photostationary state. The presence of two possible conformations, parallel and antiparallel, may substantiate this finding, since only the latter conformers may yield a photochromic response.

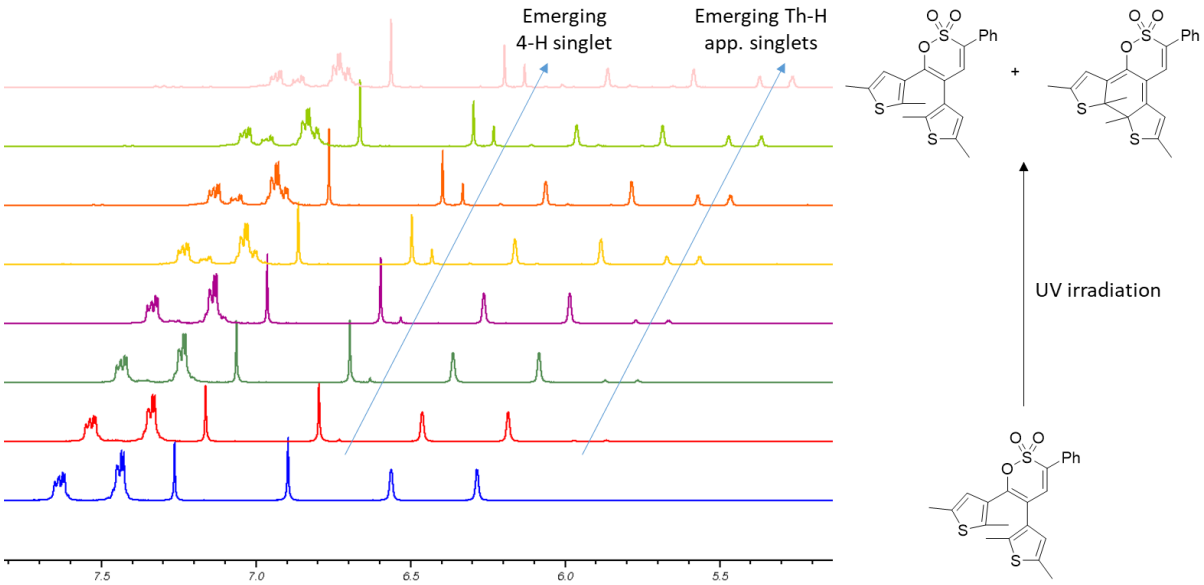

Figure 3.32: Stacked ^{1}H-NMR spectra (δ 5.5 – 7.7, $CDCl_3$) after increasing UV irradiation intervals (10 min to 2.5 h) showing the gradual emergence of signals for **3.50-closed** upon irradiation of a solution of **3.50**

Repeating these experiments for the analogous **3.51** afforded comparable results; upon 50 min of irradiation, the previously seen strong red hue was observed again at λ_{max} = 494 nm, revealing a bathochromic shift accompanying the presence of a phenyl group on the 3-position of the oxathiine ring. A $CDCl_3$ solution of this derivative displayed similar signals to those for its 3-phenyl counterpart (**3.50**) when irradiated for 30 min, which were attributed to **3.51-closed**: the methyl groups were observed at δ 2.01, 2.08, 2.11 and 2.22, the thiophene ring protons at *circa* δ 5.92 and 5.99 and the two 1,2-oxathiine 2,2-dioxide protons 3-H and 4-H at δ 6.38 and 6.82 (Figure 3.33).

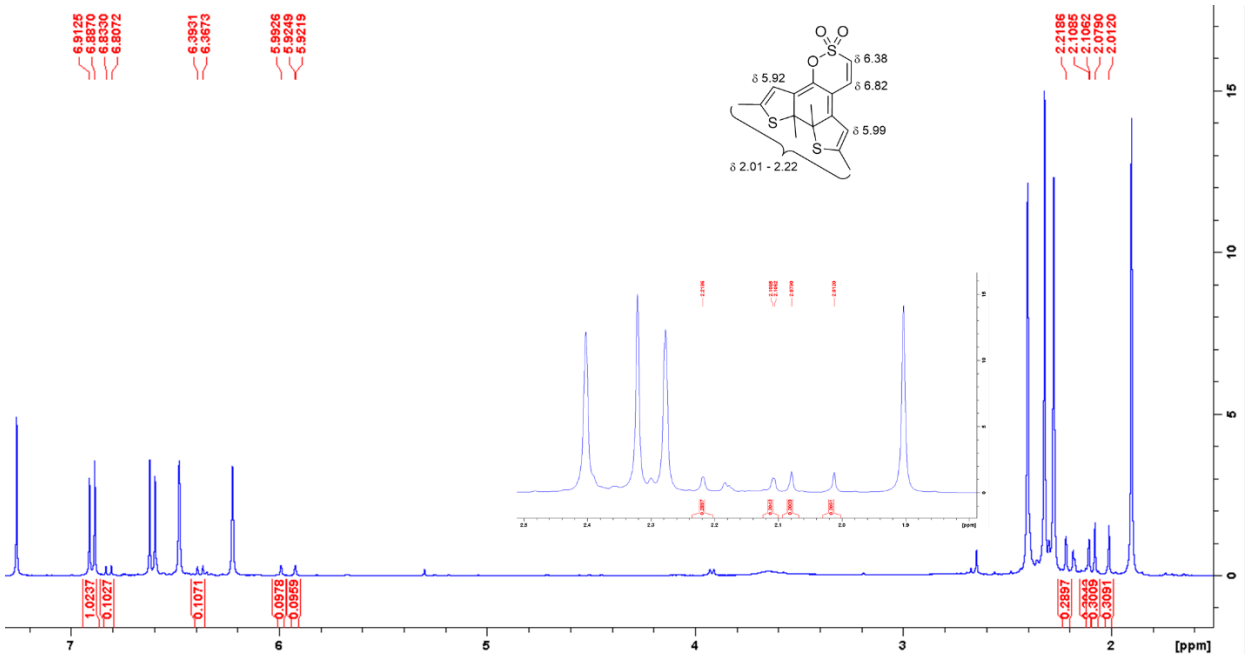

Figure 3.33: ^{1}H-NMR of analogue **3.51** after 30 min of UV irradiation, illustrating the protons of the ring-closed form

The multiplicity observed for the upfield thienyl proton at δ 5.92 and the methyl group at δ 2.11 is an indication of long-range coupling between these two nuclei, with a ^{4}J = 1.0 Hz, previously touched upon in section **3.3.1**. Moreover, irradiation for more than 30 min afforded additional decomposition signals, which prevented the calculation of a **3.51**/**3.51-closed** ratio at the PSS. At t = 30 min, the ratio of integrals

for the 4-H protons of the two isomers (δ 6.90 for **3.51**, δ 6.82 for **3.51-closed**) was found to be 10 : 1 as seen in Figure 3.33.

A final point of interest concerned the potential of these photochromic 1,2-oxathiine systems to exhibit solid-state photochromism. This aspect of photochromic compounds has been studied by various research groups and allows for a broader range of potential applications for such systems.[188,189,190] To ascertain the potential of solid-state photochromism, a preliminary investigation was carried out, wherein a finely powdered sample of the unsaturated bis-thienyl phenyl analogue **3.50** was irradiated with a hand-held TLC inspection lamp (Spectroline, 8 W, 365 nm) for 30 s, causing a drastic change in the colour of the powder from pale yellow to red-brown. Upon its irradiation, the sample remained stable for several hours, before being partially bleached by irradiation with a white light source for 20 min (flashlight tool, Samsung Galaxy A2117F/DSN® mobile phone), leading to a colour change from red-brown to orange (Figure 3.34**Error! Reference source not found.**). The fast response of this derivative clearly highlights its proclivity towards the ring-closing conversions examined earlier (Scheme 3.33), while also paving the way for future optimisation of its photochromic properties.

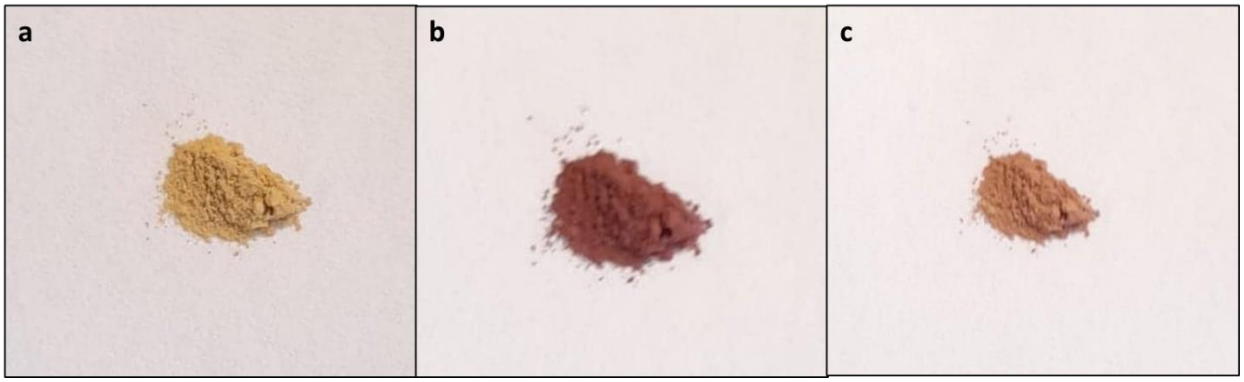

Figure 3.34: (a) Pre-irradiated **3.50** solid sample, (b) Post-irradiation photograph of **3.50** solid sample (30 s), (c) Bleaching of 3.50 solid sample after 20 min of visible light irradiation

In summary, the sulfene addition strategy previously described in chapter 2 has been applied to three new 2,5-dimethylthiophene containing enaminoketones, which were obtained from three α-methylene ketone precursors furnished *via* various synthetic routes. The resulting 3,4-dihydro-1,2-oxathiine 2,2-dioxides **3.43** – **3.46** underwent a smooth Cope elimination of the dimethylamino function to afford the 1,2-oxathiine 2,2-dioxides **3.48** – **3.51**. Both the saturated and unsaturated series of analogues were subjected to spectrophotometric studies, wherein their P-type photochromic activity was mapped out and correlated with their structural features.

CHAPTER 4: REACTIVITY OF 1,2-OXATHIINE 2,2-DIOXIDES

4.1 Preface

Given the immense interest in the properties of small heterocyclic entities by both the pharmaceutical and materials sectors and the present paucity of examples of diversely substituted 1,2-oxathiine 2,2-dioxides in the literature.[64,67,191] It was envisaged that the ready access to 1,2-oxathiine 2,2-dioxides described in chapter 2 could be capitalised upon by exploration of their reactivity leading to further functionalised examples thus providing a more extensive library of 1,2-oxathiine 2,2-dioxides.
On account of the advances reported in modern day transition metal-mediated chemistry, an obvious reaction to examine was that of bromination which would subsequently enable Pd-mediated coupling reactions, such as the Suzuki coupling[192,193,194] and the Miyaura borylation[195] reaction, to be examined. Furthermore, the non-brominated 1,2-oxathiine 2,2-dioxide substrates could be examined in a complementary C-H activated coupling study (Scheme 4.1).[196]

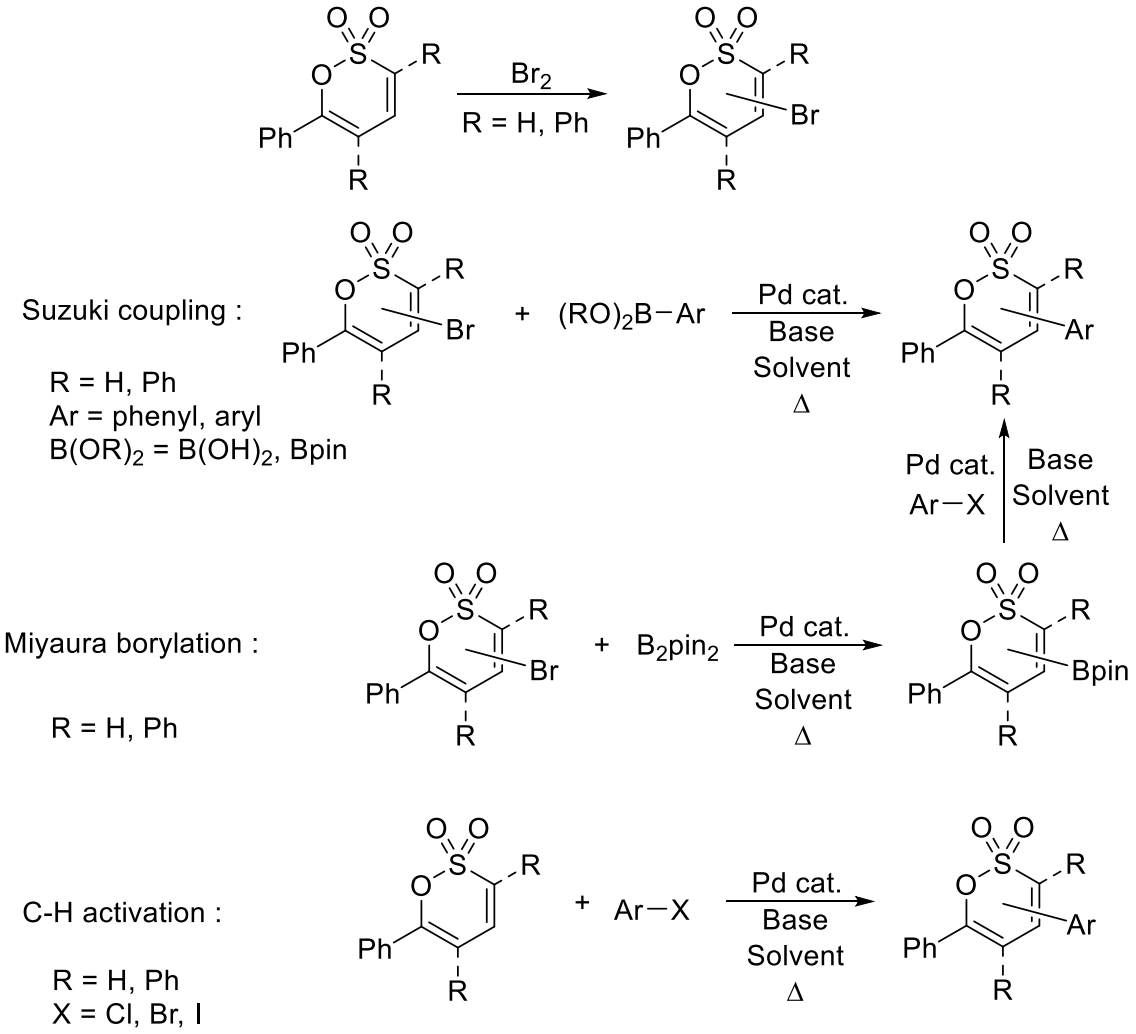

Scheme 4.1: Bromination and palladium-catalysed cross-coupling reactions on 1,2-oxathiine 2,2-dioixide systems

Cycloadditions, such as the Diels-Alder and hetero Diels-Alder reaction, provide an efficient approach to complex carbocyclic and heterocyclic systems.[197,198,199] As a consequence of having to hand a short series of 6-substituted 1,2-oxathiine 2,2-dioxides, in which the 6-substituent contains an unsaturated group and thus affords an extended conjugated moiety comprising of the C5-C6 unit and the unsaturated 6-

substituent, (hetero) Diels-Alder transformations leading to a series of novel fused 1,2-oxathiine 2,2-dioxides will be explored (Scheme 4.2).

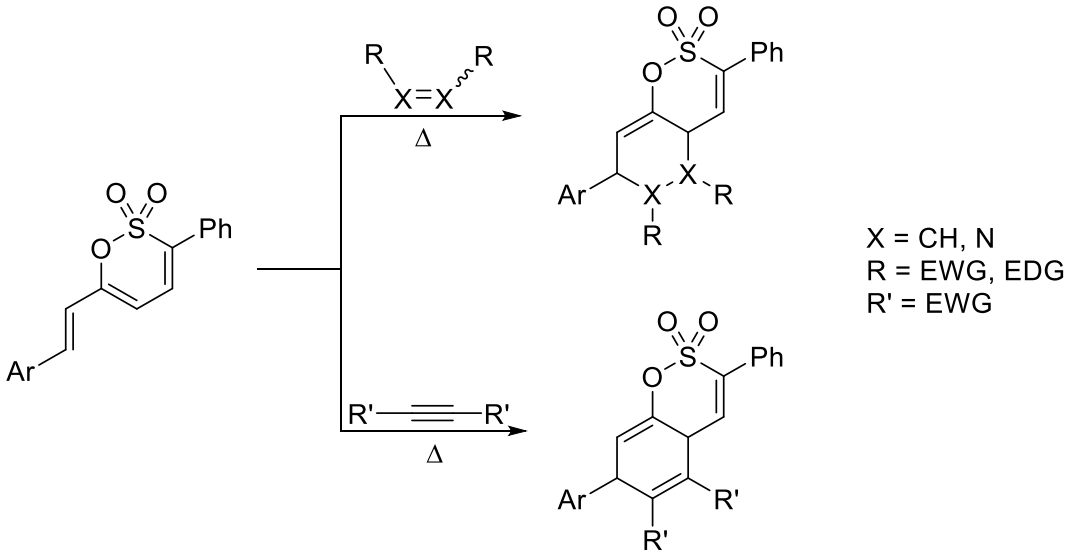

Scheme 4.2: (Hetero) Diels-Alder reactions on 6-alkenyl-1,2-oxathiine 2,2-dioxide analogues

The application of benzyne chemistry has also featured prominently in recent years providing a facile approach to arylation *via* bond insertion reactions and also to the formation of benzo-fused analogues though cycloadditions.[200,201,202,203,204,205] Thus, it is anticipated that exploration of the behaviour of 1,2-oxathiine 2,2-dioxides towards benzyne (Scheme 4.3) would provide a complementary link between the proposed Pd-mediated chemistry and investigations of cycloadditions.

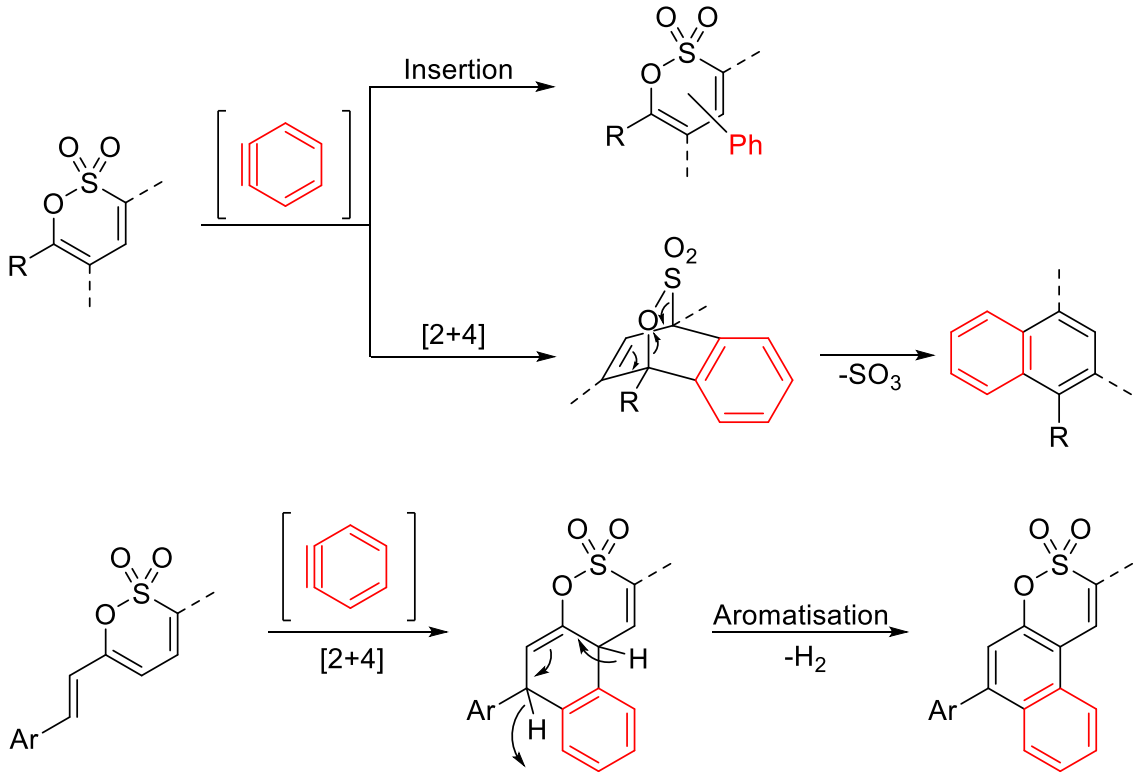

Scheme 4.3: Benzyne transformations of substituted 1,2-oxathiine 2,2-dioxides

Note: Compounds already synthesised in chapter 2 with the general structure numbering **2.*XX*** have been renumbered in this chapter with the general numbering **4.*XX*** for ease of reading and continuity.

4.2 Bromination of mono-, di- and tri- phenyl-substituted 1,2-oxathiine 2,2-dioxides

After the compilation of a small library of 1,2-oxathiine 2,2-dioxides with mono-, di- and tri- aryl substitution (Chapter 2), the reactivity of these variously substituted systems towards molecular bromine was examined. The proposed mechanistic processes for the formation of brominated products follows the literature findings detailed in the introduction chapter (Chapter 1),[67,69,81] with an additional focus on the potential bromine substitution at the 4- or the 5- positions in analogues where the 3-position is already substituted and thus unavailable (Scheme 4.4).

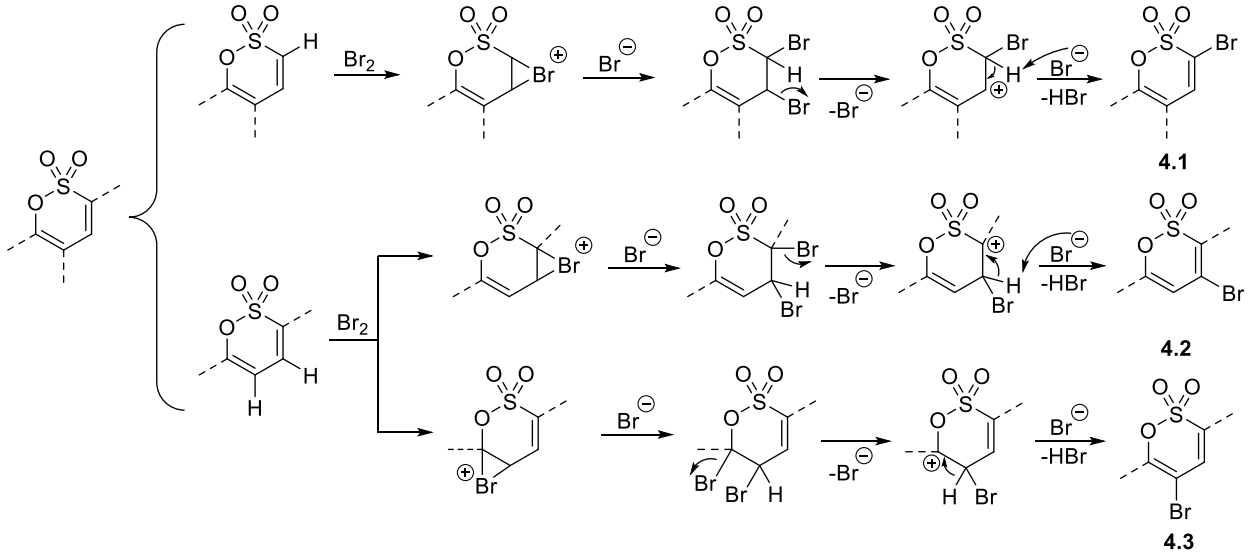

Scheme 4.4: General mechanism of 1,2-oxathiine 2,2-dioxide bromination, previewing the possible sites of Br_2 attack

The addition of Br_2 involves the established bromonium mechanism *via* interaction of Br_2 with the less sterically hindered and most reactive of the two double bonds. The electron-withdrawing SO_2 moiety is able to deactivate the C3-C4 bond as well as allow for negative charge stabilisation on C3; therefore, in systems where the C3-C4 bond is less hindered than the C5-C6 bond, the former may be favoured for bromonium ion formation. The subsequent elimination of HBr towards the 3-bromo product **4.1** may occur via an E1 mechanism, as the proton on the 3-position and the bromine cannot adopt the antiperiplanar arrangement required for an E2 elimination route on a closed ring conformation. It was also postulated that absence of a proton on the 3-position would result in the cleavage of 4-H as the only available proton, thus furnishing a 4-bromo oxathiine system (**4.2**); alternatively, formation of a bromonium ion about the C3-C4 double bond would be disfavoured on 3-substituted 1,2-oxathiine 2,2-dioxides and instead the oxathiine ring could undergo bromination at C-5 (**4.3**, Scheme 4.4). Apart from assessing the reactivity of 1,2-oxathiine 2,2-dioxide systems, testing these hypotheses would afford a library of brominated 1,2-oxathiine 2,2-dioxides to be further converted into highly substituted systems. The findings from these bromination attempts are summarised in table 4.1.

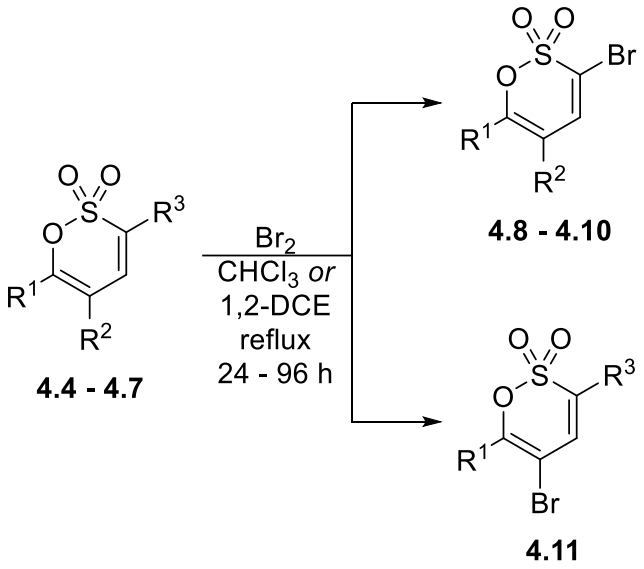

Entry	Starting material No.	R^1	R^2	R^3	Product No.	Solvent	Time (h)	Eq of Br_2	Yield (%)
1	**4.4**	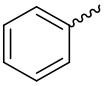	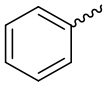	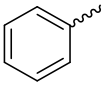	**4.8**	$CHCl_3$	24	1.5	0.0
2	**4.5**	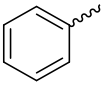	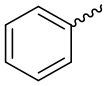	H	**4.9**	$CHCl_3$	72	1.0	73.2
3	**4.6**	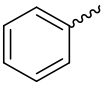	H	H	**4.10**	$CHCl_3$	24	1.1*	86.6
4	**4.7**	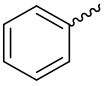	H	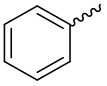	**4.11**	1,2-DCE	96	2.7	45.9
*0.25 eq of pyridine was added to achieve reaction completion after a further 15 min reflux time									

Table 4.1: Bromination attempts on different phenyl-substituted 1,2-oxathiine 2,2-dioxides

Overnight reflux of the 3,5,6-triphenyl derivative **4.4** in $CHCl_3$ with Br_2 was unsuccessful, thus pointing out that the absence of the aforementioned reactive protons on the 3- and 5-positions, along with the steric hindrance caused by the three phenyl groups, prevented any Br_2 addition. Moreover, as it can been seen in table 4.1, bromination on the 4-position of the 1,2-oxathiine centre was not observed despite the consistent availability of this position amongst analogues **4.4** – **4.7**.

In order to examine the bromination at lower substitution levels, the 5,6-diphenyl analogue **4.5** was studied next. In this instance the bromination was complete after 72 h of reflux in $CHCl_3$. The dibromo intermediate **4.9a** (Scheme 4.5) was observed as indicated by the presence of two sets of upfield doublets (δ 5.38 and δ 5.58) with $J_{3,4}$ = 5.2 Hz in a sample withdrawn from the reaction mixture during the first hour of the 72 h reflux period. Due to the vinyl proton signal of **4.9** resonating in the aromatic region at δ 7.62, an additional NMR measurement in d_6-AcMe was required to unequivocally pinpoint the 4-H singlet (Figure 4.1).

Confirming the theorised mechanistic route in scheme 4.4, an overview of this conversion is shown in scheme 4.5. It should be noted the observed regioselectivity of this transformation derives from the increased acidity for 3-H, which in turn is a result from the withdrawal of electron density towards the SO_2 group on the 1,2-oxathiine ring.

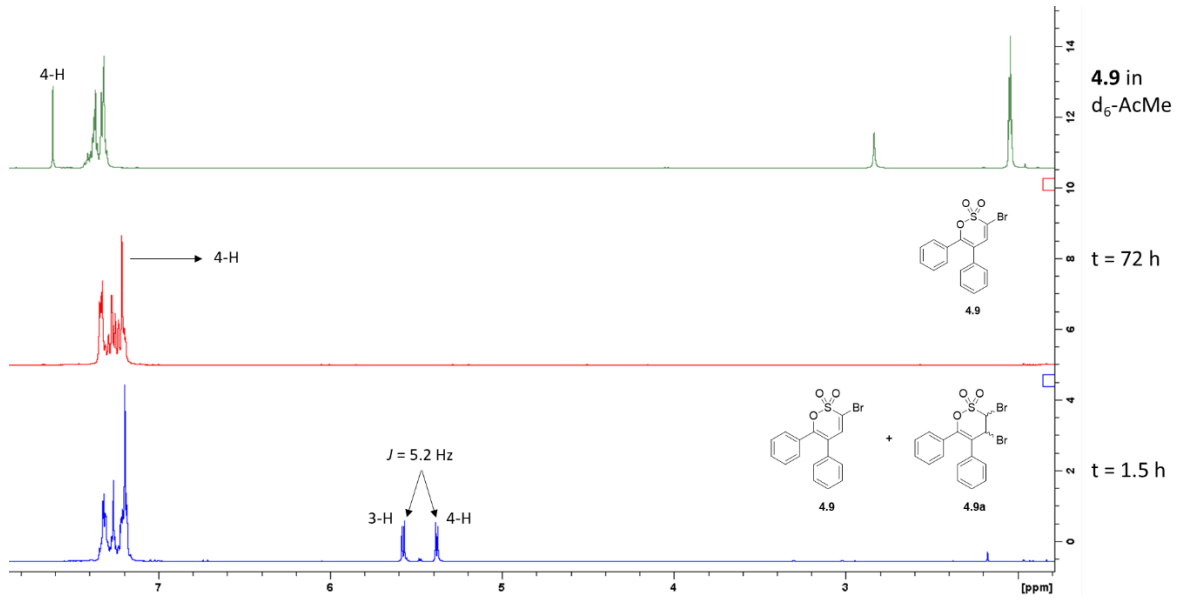

Figure 4.1: Stacked ^{1}H-NMR spectra after 1.5 h and 72h of reaction time, illustrating the doublet signals of the 3-H and 4-H on the 3,4-dibromo intermediate **4.9a** and pinpointing the vinyl proton of **4.9** in a d_6-AcMe solution

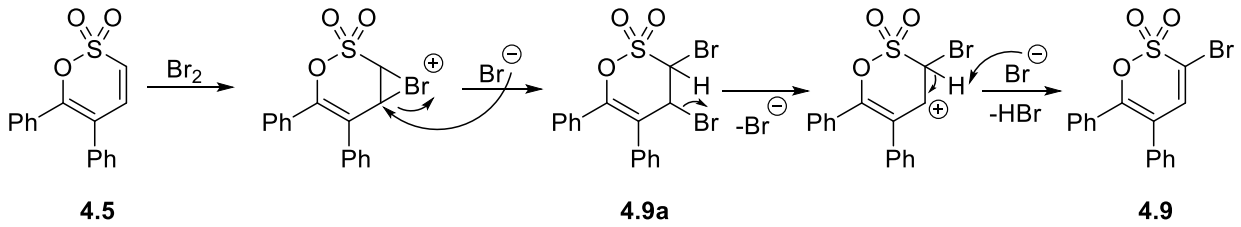

Scheme 4.5: Mechanism for the bromination of analogue **4.5**

Parallel to the assessment of the ^{1}H-NMR spectrum of **4.9**, additional data was required to clearly indicate the presence of bromine on the obtained product. Utilising the typical behaviour of bromo compounds in mass spectrometry, the relevant mass spectrum of **4.9** offered unequivocal evidence of a bromine atom by virtue of the two *m/z* peaks at 384.9500 and 386.9481 which are attributed to the two isotopes of bromine ($[M+Na]^+$ and $[M+Na+2]^+$ for ^{79}Br and ^{81}Br respectively). In nature these isotopes share a 1:1 ratio[206], which is directly translated to the 1:1 ratio of the foregoing *m/z* peaks, as seen in figure 4.2.

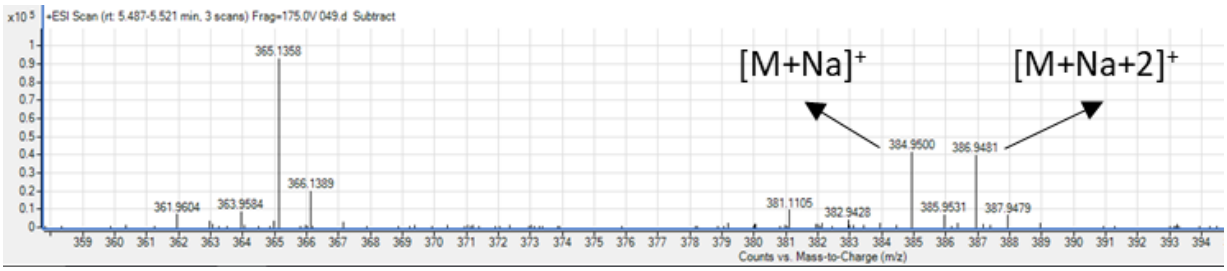

Figure 4.2: Mass spectrum of **4.9**, showing the key pair of *m/z* peaks hinting at the two bromine isotopes

The reactivity for the two double bonds in the 1,2-oxathiine 2,2-dioxide ring was more thoroughly examined in the case of 6-phenyl-1,2-oxathiine 2,2-dioxide **4.6** (Scheme 4.6). The formation of **4.10** was confirmed by ^{1}H-NMR spectroscopy which revealed a doublet at δ 6.32 and at δ 7.10 with $J_{4,5}$ = 7.3 Hz (Figure 4.3). No products other than **4.10** were obtained or observed during this attempt which confirms that the conversion proceeds regioselectively towards this 3-bromo product under these conditions.

Moreover, the use of a small amount of pyridine (0.25 eq) as a base in order to ensure the complete deprotonation of the dibromo intermediate towards the mono-brominated **4.10** suggests that the absence of the stabilising phenyl group on the 5-position is detrimental to the elimination of HBr.

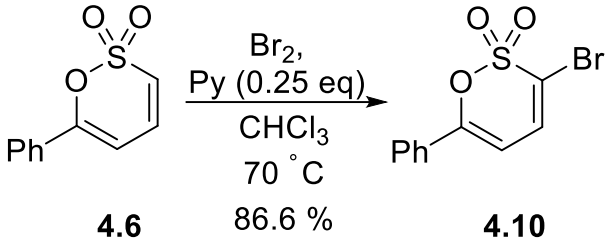

Scheme 4.6: Bromination of the 6-phenyl analogue **4.6**

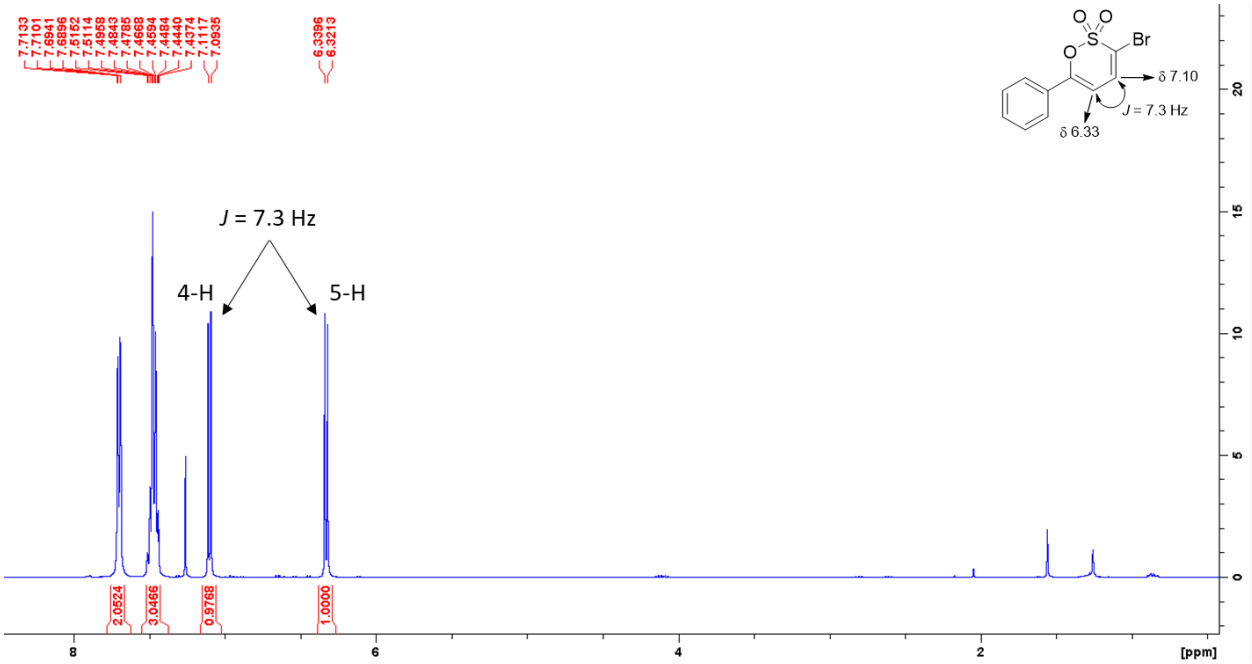

Figure 4.3: ^{1}H-NMR spectrum of **4.10** with the characteristic ~7 Hz coupling between 4-H and 5-H

Finally, the 3,6-diphenyl analogue **4.7** was examined in order to complete the assessment of the reactivity of the 1,2-oxathiine ring double bonds. Initial attempts using $CHCl_3$ as a solvent, along with pyridine as a base, resulted in partial starting material consumption and consequently low yields (13 – 22 %) of brominated product **4.11**. The only efficient alternative was to switch the solvent to 1,2-dichloroethane (1,2-DCE), so as to utilise its higher boiling point (83 °C over 61 °C) and achieve a higher conversion. Even under these conditions, only a moderate yield of **4.11** (45.9 %) was achieved after 96 h of reflux, illustrating a significant difference in reactivity between the C3 – C4 and the C5 – C6 double bonds.

Bromination at the 5- position of **4.11** was initially ascertained by comparison of the ^{13}C-NMR spectrum of **4.11** with that of **4.7** (Figure 4.4). The C5 atom was found to be shielded to a small extent (upfield shift from δ 102 to 100) due to the bromine atom, while the neighbouring C4 is conversely deshielded (δ 129 to 134).

The small shielding effect noted for C5 upon its bromination is observed in contrast to the increased electronegativity of bromine over carbon (Pauling electronegativity value of 2.96 and 2.55 respectively[207]); such a contradictory finding can be attributed to the considerable atomic size difference between the two elements, which factors for poor orbital overlap and a consequent poor electron-withdrawing effect by bromine, resulting in C5 resonating at similar frequencies on the ^{13}C-NMR spectra of **4.11** and **4.7**.

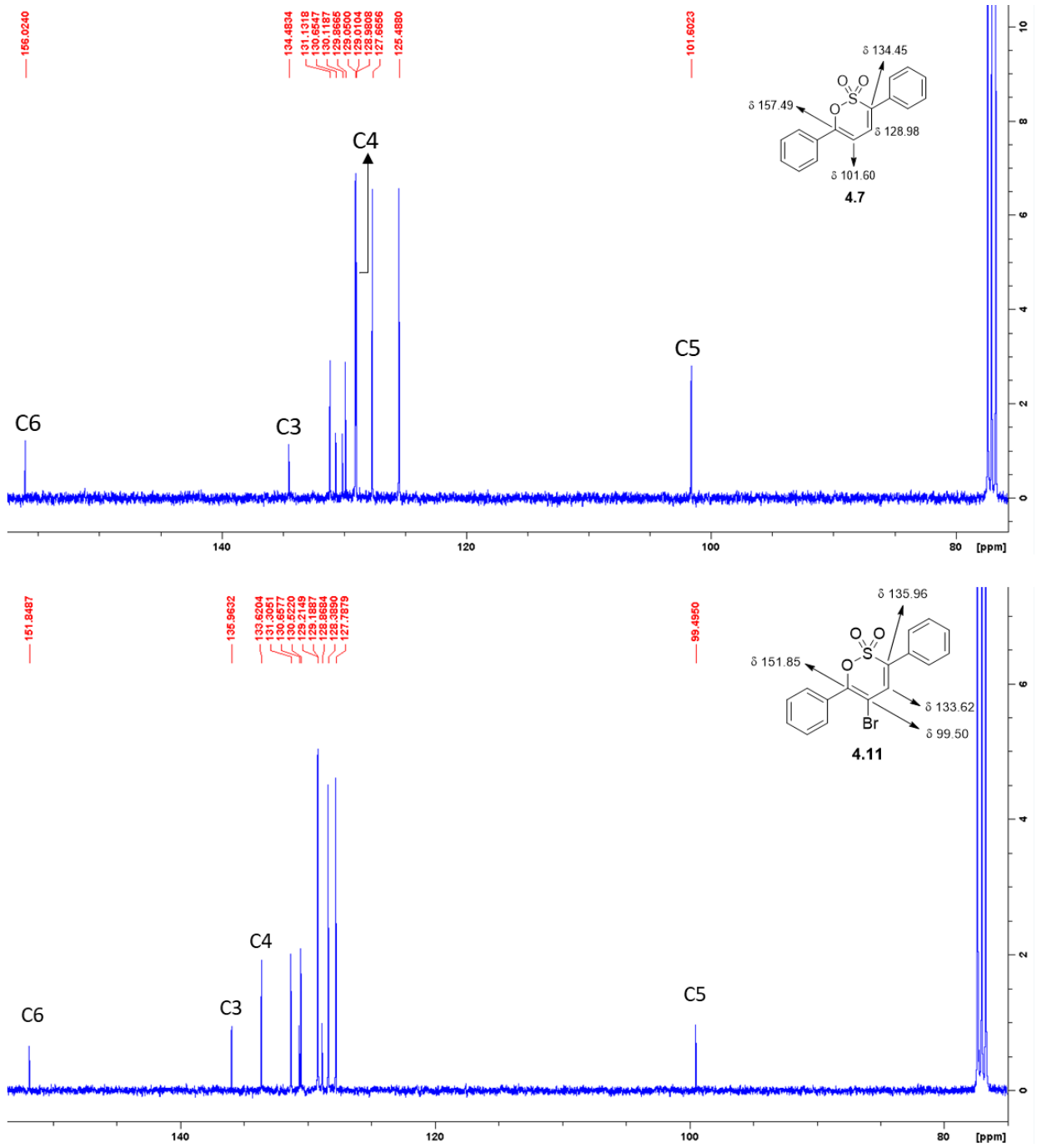

Figure 4.4: Overlaid ^{13}C-NMR spectrum of **4.11** (bottom) and **4.7** (top), illustrating the upfield shift of C5 and downfield shift of C4 due to bromine substitution

Although the observed chemical shifts are in accordance with the theoretical precepts of this transformation (Scheme 4.4), definitive data was required to confirm the anticipated 5-bromo structure. To that end, HMBC and NOESY experiments were carried out, so that the proton of the 1,2-oxathiine ring could be pinpointed on the 4- position. As seen in the HMBC spectrum of **4.11** (Figure 4.5a), the pivotal *C* atom at δ 151.85 has a long range correlation with the signal at δ 7.87 accounting for two aromatic protons. This illustrates that these protons belong to the 6-phenyl group so it can be inferred that the multiplet at δ 7.64 corresponds to the *ortho* protons of the 3-phenyl group by process of elimination. The key correlation between these two aromatic protons and their vinyl counterpart at δ 7.02 (observed on

the NOESY spectrum, Figure 4.5b) places the latter on the 4- position and unequivocally attests the assigned 5-bromo structure of **4.11** (Scheme 4.7).

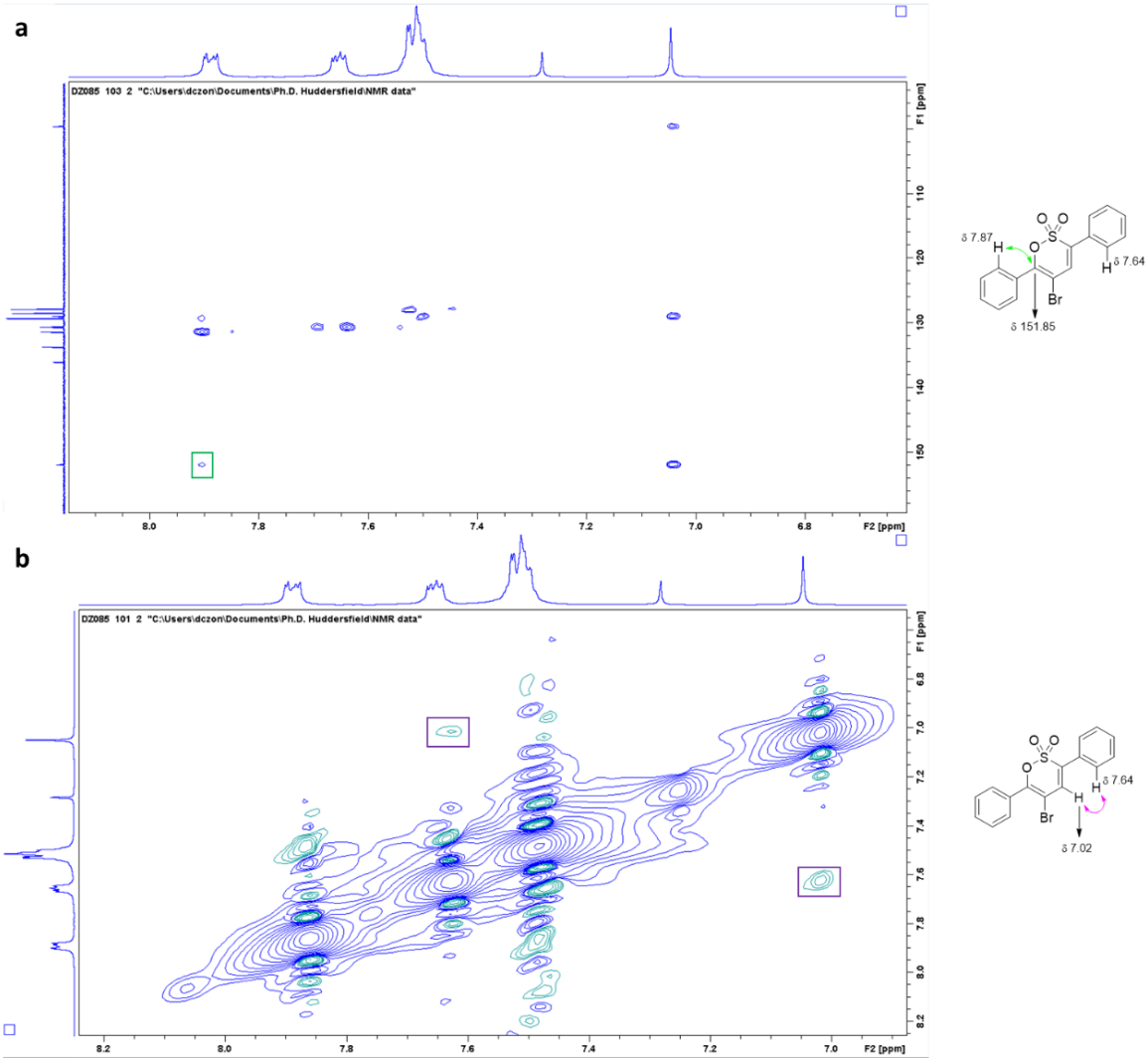

Figure 4.5: a) HMBC spectrum of **4.11**, showing the long-range correlation between C6 and the *ortho* protons on the 6-phenyl group, b) NOESY spectrum of **4.11**, bearing the key correlation between the aromatic protons at δ 7.64 and 4-H at δ 7.02

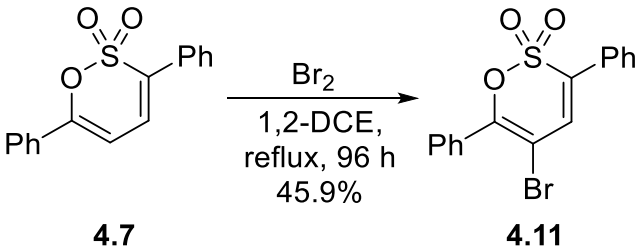

4.7 **4.11**

Scheme 4.7: Bromination of 3,6-diphenyl analogue **4.7**

This difficulty in attaining reaction completion for analogue **4.11** points to the unreactivity of the C5-C6 double bond, which may be associated with the SO_3 fragment of the 1,2-oxathiine ring. Even though the *O*-1 atom is capable of lone pair donation as a means of increasing the reactivity of the proximal double bond, such a process is countered by the electron-withdrawing SO_2 fragment opposing the presence of any adjacent positive charge. Moreover, the absence of any 4-substituted bromo products arising from the conversions presented in table 4.1 suggests that the 4-position is the least reactive site on the 1,2-

oxathiine scaffold, thus highlighting an order of decreasing reactivity between the three substitution sites on these heterocyclic systems (Figure 4.6).

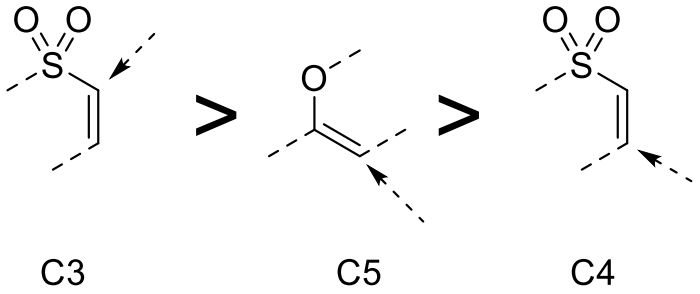

Figure 4.6: Order of decreasing reactivity between different sites of a 1,2-oxathiine 2,2-dioxide system

The last bromination test regarded the attempted substitution on the 4-position *via* use of a different protocol. It was thought that N-bromosuccinimide (NBS) in aq. DMSO would pose as an alternative source of bromine and interact with the 5,6-diphenyl analogue **4.5** towards the bromonium intermediate shown in scheme 4.1, which may permit a nucleophilic attack of H_2O on C3 to bring forth a bromohydrin product (**4.12**). Unfortunately, no addition was detected, even at increased NBS/H_2O equivalence and temperature (Scheme 4.8).

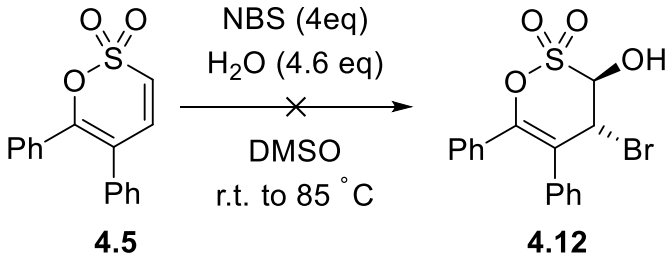

Scheme 4.8: Attempt at furnishing the bromohydrin **4.12**

4.3 Reactions with brominated 1,2-oxathiine 2,2-dioxides

4.3.1 Bromine-lithium exchange attempts

Upon their syntheses, the brominated 1,2-oxathiine 2,2-dioxide derivatives **4.9** – **4.11** were examined with regards to their performance as substrates for various transformations. The first of these involved a lithium/bromine exchange[208,209] to arrive at lithiated intermediates (*e.g.* **4.13**, Scheme 4.9) capable of attacking electrophilic reagents and functionalising the starting 1,2-oxathiine 2,2-dioxides. Applying established literature protocols[210,211,212] on analogues **4.9** and **4.11** with anhydrous DMF as the electrophile resulted in apparent degradation of the starting materials even at -78 °C, with no isolation of the desired products **4.14** and **4.15**.

The apparent sensitivity of bromo- 1,2-oxathiine 2,2-dioxides in the presence of organolithium reagents directed the scope of research towards alternate approaches to functionalisation employing the bromo-oxathiine 2,2-dioxide substrates.

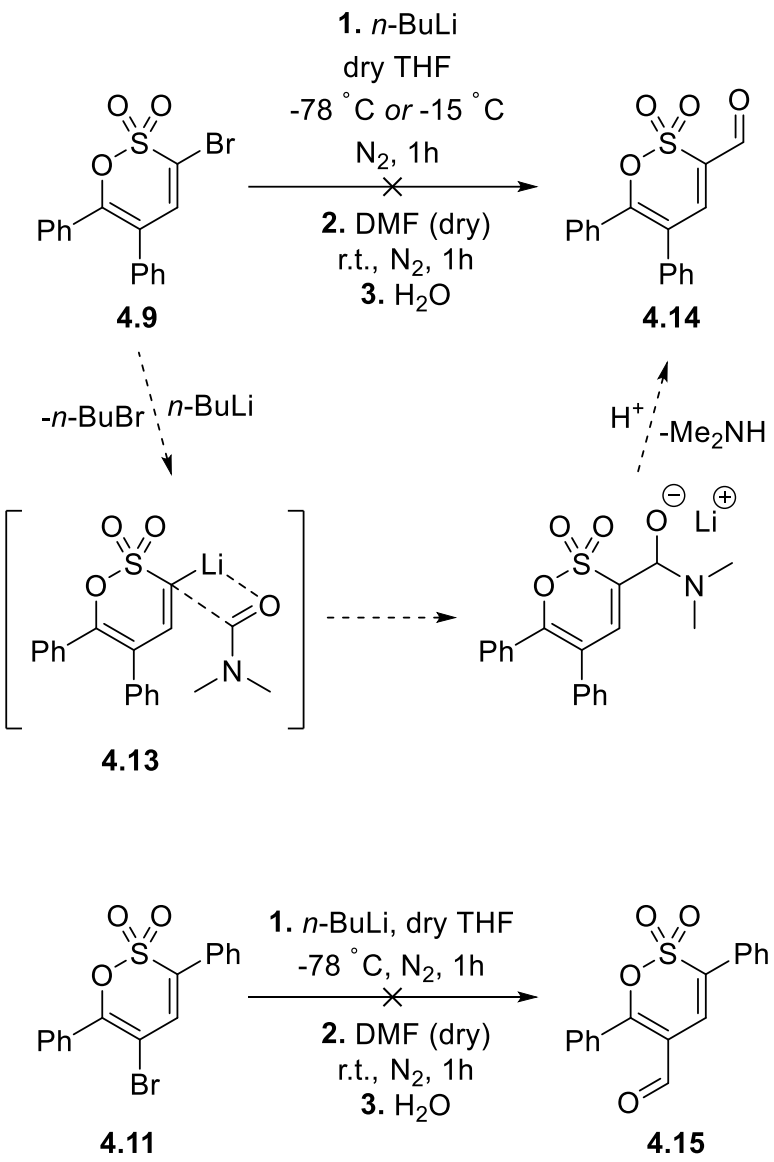

Scheme 4.9: Attempts to functionalise **4.9** and **4.11** through lithium-bromine exchange and consecutive formylation using DMF

4.3.2 Suzuki coupling reactions

After the foregoing explorations of organolithium-based reactions, the next aspect of organometallic chemistry regarded the use of the brominated 1,2-oxathiine 2,2-dioxides as substrates in Suzuki cross-coupling reactions. This transformation was first explored by Suzuki *et al*. in 1979[213], wherein the coupling of alkenyl or alkynyl halides (**4.17**, **4.19**) to alkenyl boronic esters (**4.16**) towards dienes (**4.18**) or enynes (**4.20**) was accomplished *via* the use of a palladium(0) catalyst and a suitable base (Scheme 4.10).

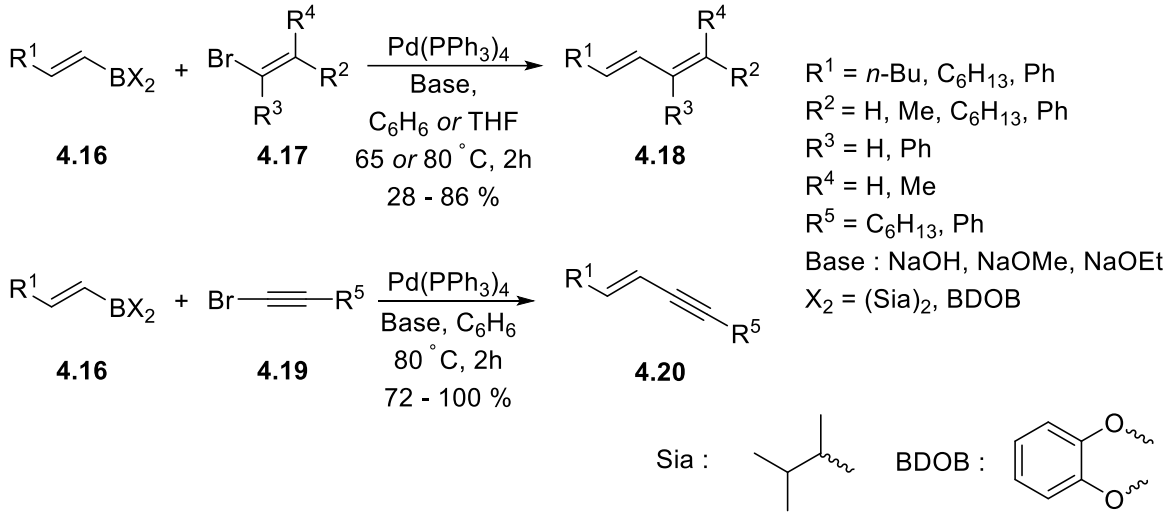

Scheme 4.10: First Pd-mediated cross-coupling attempts by Suzuki *et al*.[213]

In the years after the discovery of this transformation, its scope was broadly expanded to allow for the formation of C-C bonds between various halides (**4.21**) and boron containing species (**4.22**) by utilising palladium-based catalytic arrays (Scheme 4.11a).[214,215] Given the commercial availability of a wide range of such boronic acids and esters, this cross-coupling protocol was attempted with the bromo-1,2-oxathiine 2,2-dioxides using the set of conditions developed by Wu *et al*. in their attempt to furnish arylated 2-pyrones (**4.25**) from their bromo/ pseudo-halo precursors (**4.23**) and various boronic acids (**4.24**), on account of the structural similarity between 2-pyrone and 1,2-oxathiine 2,2-dioxide heterocycles (Scheme 4.11b).[216]

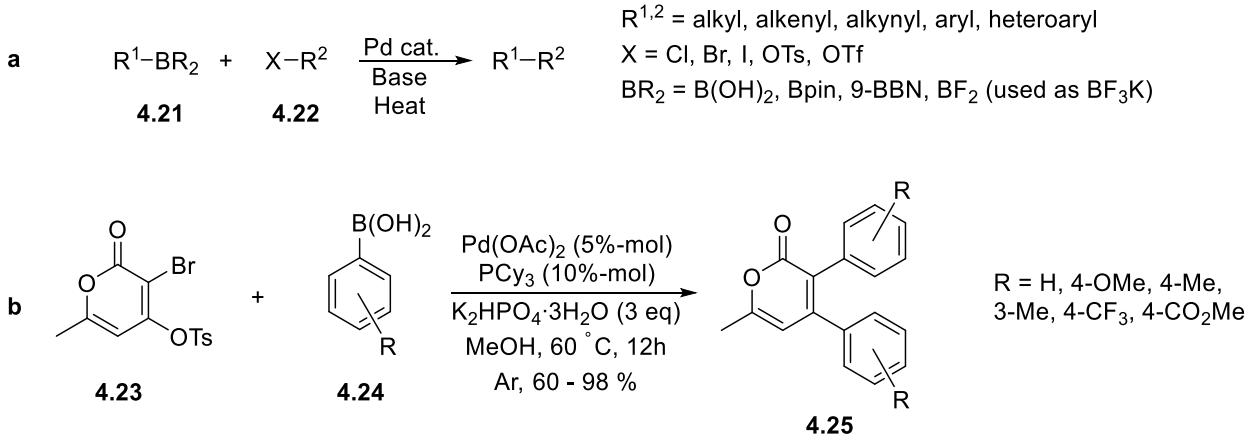

Scheme 4.11: (a) General scope of Suzuki cross-coupling transformations, (b) experimental conditions selected for attempting the transformation on bromo-1,2-oxathiine 2,2-dioxide analogues

In accordance with the adopted literature protocol, different aryl boronic acids / esters were used as coupling partners to the brominated 1,2-oxathiine 2,2-dioxides, while $Pd(OAc)_2$ was selected as the catalyst, PCy_3 was utilised as a ligand and $K_2HPO_4{\cdot}3H_2O$ as the base. In the case of the solvent, the reacting bromo-1,2-oxathiine 2,2-dioxides were found to be only partially soluble in MeOH, prompting the use of dimethylacetamide (DMA) as solvent. The results from the attempted couplings are summarised in table 4.2.

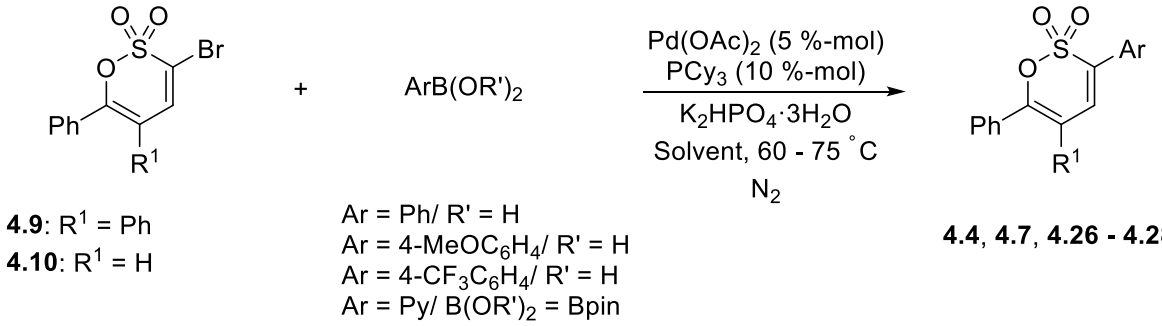

4.9: R^1 = Ph
4.10: R^1 = H

Ar = Ph/ R' = H
Ar = 4-$MeOC_6H_4$/ R' = H
Ar = 4-$CF_3C_6H_4$/ R' = H
Ar = Py/ $B(OR')_2$ = Bpin

4.4, **4.7**, **4.26 - 4.28**

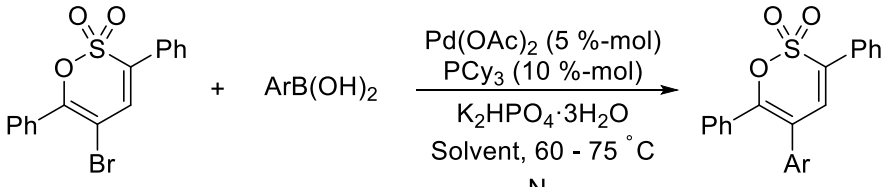

4.11 **4.4**

A/a	S.m. No.	R^1	Ar	Product No.	Solvent	Temp/re (°C)	Time (d)	Yield (%)
1	**4.9**	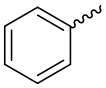	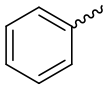	**4.4**	DMA	60	2	40.0
2	**4.10**	H	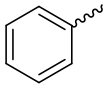	**4. 7**	DMA	70	1	27.5*
3	**4.11**	-	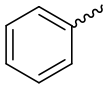	**4.4**	DMA	70	2	0.0
4	**4.9**	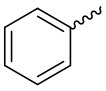	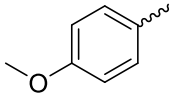	**4.26**	DMA	75	4	16.3
5	**4.9**	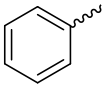	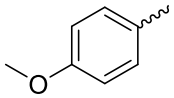	**4.26**	DMA/ MeOH 1:1	60	1	58.1
6	**4.9**	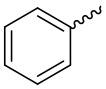	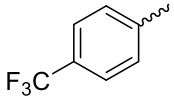	**4.27**	DMA/ MeOH 1:1	60	1	36.2
7	**4.10**	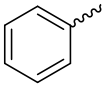	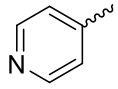	**4.28**	DMA/ MeOH 1:1	65	1	0.0
* Dimer-like species **4.29** also obtained in 10.0 % yield (Scheme 4.12a)								

Table 4.2: Suzuki coupling attempts towards various 1,2-oxathiine 2,2-dioxides

Despite the initial success in appending a phenyl group at C3 **4.9** and **4.10**, the same conversion was found to fail completely in the case of the 5-bromo derivative **4.11**, which is indicative of either a strong steric hindrance caused by the neighbouring 6-phenyl substituent and/or the unreactivity of the 5-bromo position as discussed previously (Section **4.2**). The formation of the homo-coupling derivative (6,6'-diphenyl-[3,3'-bi(1,2-oxathiine)] 2,2,2',2'-tetraoxide **4.29**) in 10.0 % yield during the attempt of phenyl coupling to **4.10** presented an additional point of interest, as it hinted at the tendency of this heterocyclic substrate to favour C-C bond formation between proximal 1,2-oxathiino ligands (Scheme 4.12a). The catalytic route of this side-reaction probably involves a transfer of a 1,2-oxathiino ligand *via*

transmetalation to a Pd complex that already contains this ligand, followed by the final isomerisation and reductive elimination steps to furnish **4.29** (Scheme 4.12b).

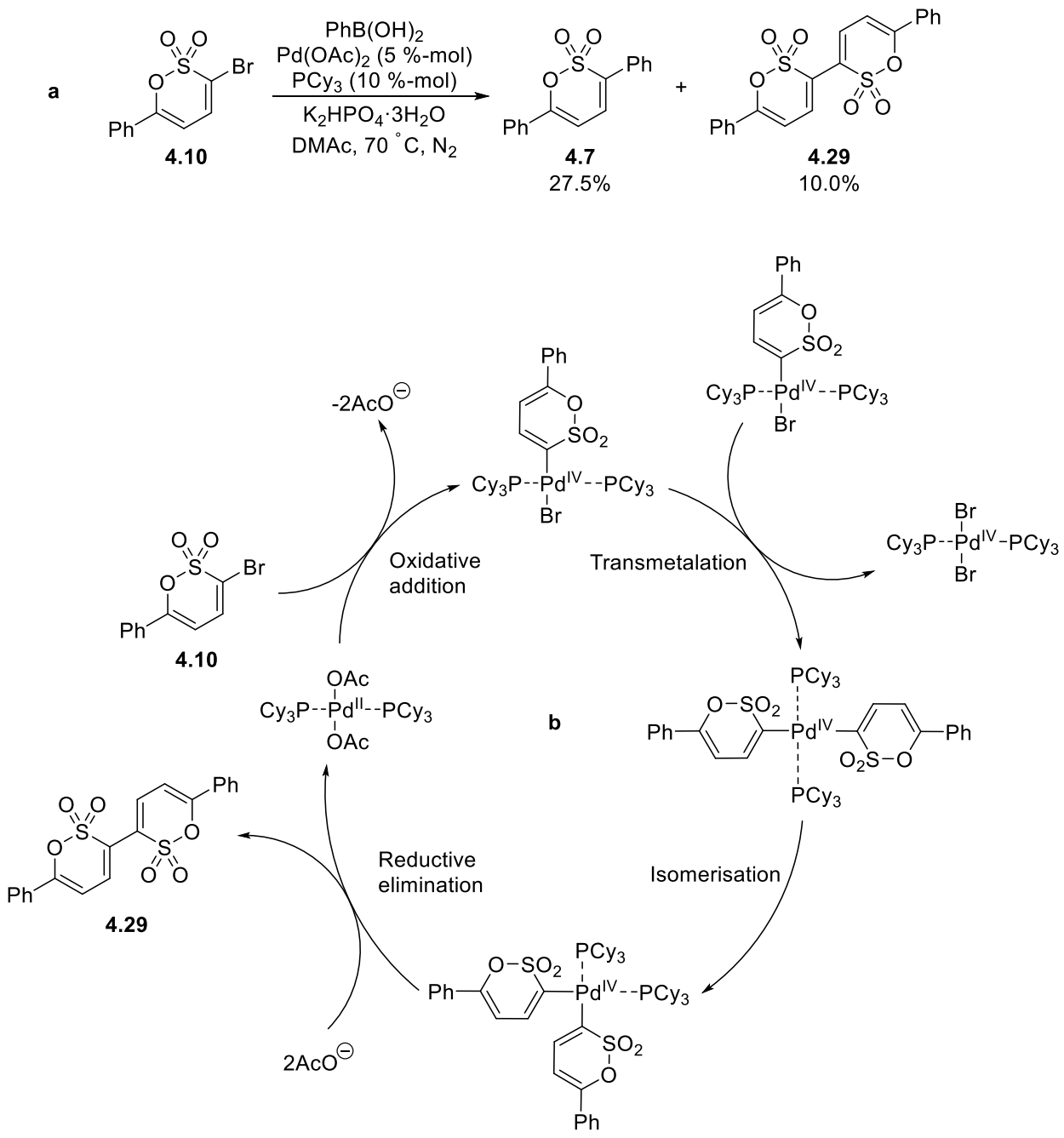

Scheme 4.12: a) Obtained products **(4.7** and **4.29**) from the Suzuki coupling on **4.10**, b) Proposed catalytic cycle towards the formation of the dimer-like compound **4.29**

The corresponding ^{1}H-NMR spectrum of 4.32 showed two characteristic doublets at δ 6.63 and δ 7.48 with $J_{4,5}$ = 7.4 Hz for both pairs of 4-H and 5-H (Figure 4.7). The dimeric structure of **4.29** was further corroborated by mass spectrometry which gave a molecular ion $[M+Na]^+$ of 437.0126 which is in good agreement with that calculated for the $[M+Na]^+$ ion of **4.29** at *m*/*z* 437.0132. The formation of this side-product indicated that a Pd-catalysed homo-coupling conversion would be favoured in brominated 1,2-oxathiine 2,2-dioxides systems, although such dimer-like species were not obtained during the formation of the other coupling products.

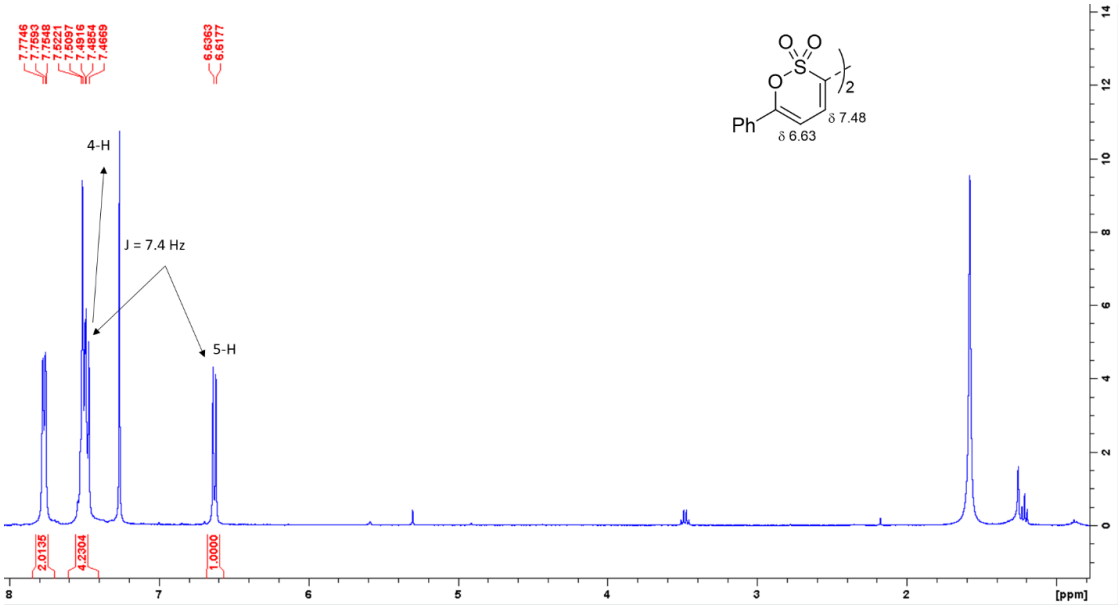

Figure 4.7: ^{1}H-NMR spectrum of **4.29**

Apart from the 1,2-oxathiine 2,2-dioxide substrates being consumed in homo-coupling processes, poor solubility of the base in DMA was also suspected of mitigating the efficiency of the conversion. Employing the initial protocol to produce the 3-anisyl analogue **4.26** afforded the product in an unexpectedly low yield (16.3 %, entry 4, Table 4.2), illustrating that this method offered poor reproducibility, and the large amount of solid residue observed in the reaction mixture during the reaction directly supported the claim that DMA was unable to contain all reagents in solution to allow for an efficient conversion. This necessitated a modification in the reaction set-up and a mixture of DMA/MeOH 1:1 was consequently selected as a more suitable solvent system. The drastic increase in yield (58.1 %, entry 5, Table 4.2) confirmed that tackling the solubility issue proved indeed to be beneficial to the fate of the transformation. Adopting this optimised set of conditions, the trifluoromethylphenyl analogue **4.27** was readily obtained albeit in low yield (36.2 %), presumably due to the electron-withdrawing effect of the CF_3 group. An attempt to effect the coupling of **4.10** with pyridyl pinacol ester afforded no oxathiine 2,2-dioxide coupling products but instead 4,4'-bipyridine (**4.30**) was observed by ^{1}H-NMR analysis of an aliquot of the reaction mixture as a homo-coupling side-product[217], along with the unreacted starting material (Scheme 4.13). The most plausible explanation for this loss of reactivity involves the complete deactivation of the reacting boronic ester caused by the pyridyl ring, which places a significant energy barrier on any interaction with substrate **4.9**.

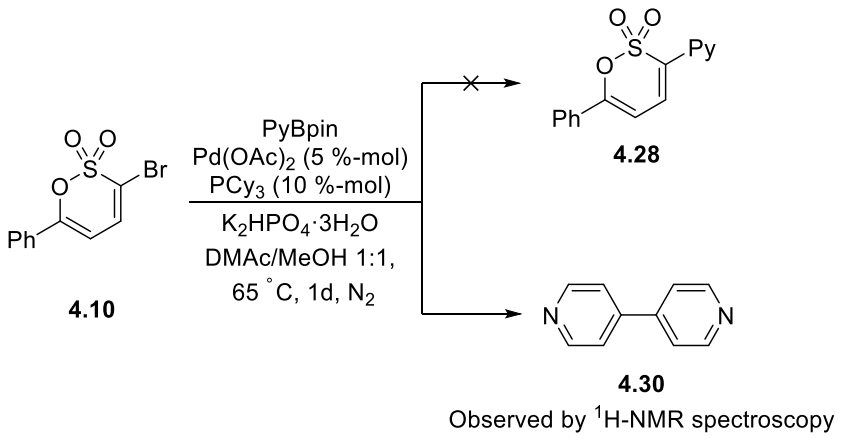

Scheme 4.13: Homo-coupling of the pyridyl boronic ester as the preferred route over the formation of **4.28**

4.3.3 Suzuki-Miyaura borylation

In a complementary manner to the foregoing Suzuki cross-coupling reactions, the Suzuki-Miyaura Pd-catalysed borylation of the 5,6-diphenyl analogue **4.9** was attempted in order to provide a borylated 1,2-oxathiine 2,2-dioxide derivative (**4.31**) that could be subsequently coupled to an aryl halide under Suzuki cross-coupling conditions.[218,219] Although the initial attempt using $Pd(OAc)_2$ was unsuccessful, further attempts with $Pd(dppf)Cl_2$ and varying equivalents of the borylating agent (B_2pin_2) and the base (KOAc) revealed an inclination of the starting brominated heterocycle to react with itself leading to the 5,5',6,6'-tetraphenyl-[3,3'-bi(1,2-oxathiine)] 2,2,2',2'-tetraoxide **4.32** (analogous to the 6-phenyl dimeric species **4.29** observed earlier), rather than afford the anticipated boronic ester **4.31** from the addition of a Bpin fragment (Scheme 4.14).

The formation of this product was first postulated due to the absence of any Bpin aliphatic signals on the ^{1}H-NMR spectrum of **4.32** (Figure 4.8a) and this claim was confirmed by mass spectrometry (Figure 4.8b), in conjunction with a literature precedent that presented analogous cases of borylation/dimerization processes.[220,221] Obtaining this dimer-like derivative highlighted the dimerisation potency of brominated 1,2-oxathiine 2,2-dioxides that was first encountered during the Suzuki cross-coupling attempt, although the stark difference in reaction conditions between the Suzuki and Suzuki-Miyaura protocols merited an explanation of the behaviour of **4.9** during borylation. To that end, different conditions were used to explore this side reaction and the findings are presented in table 4.3.

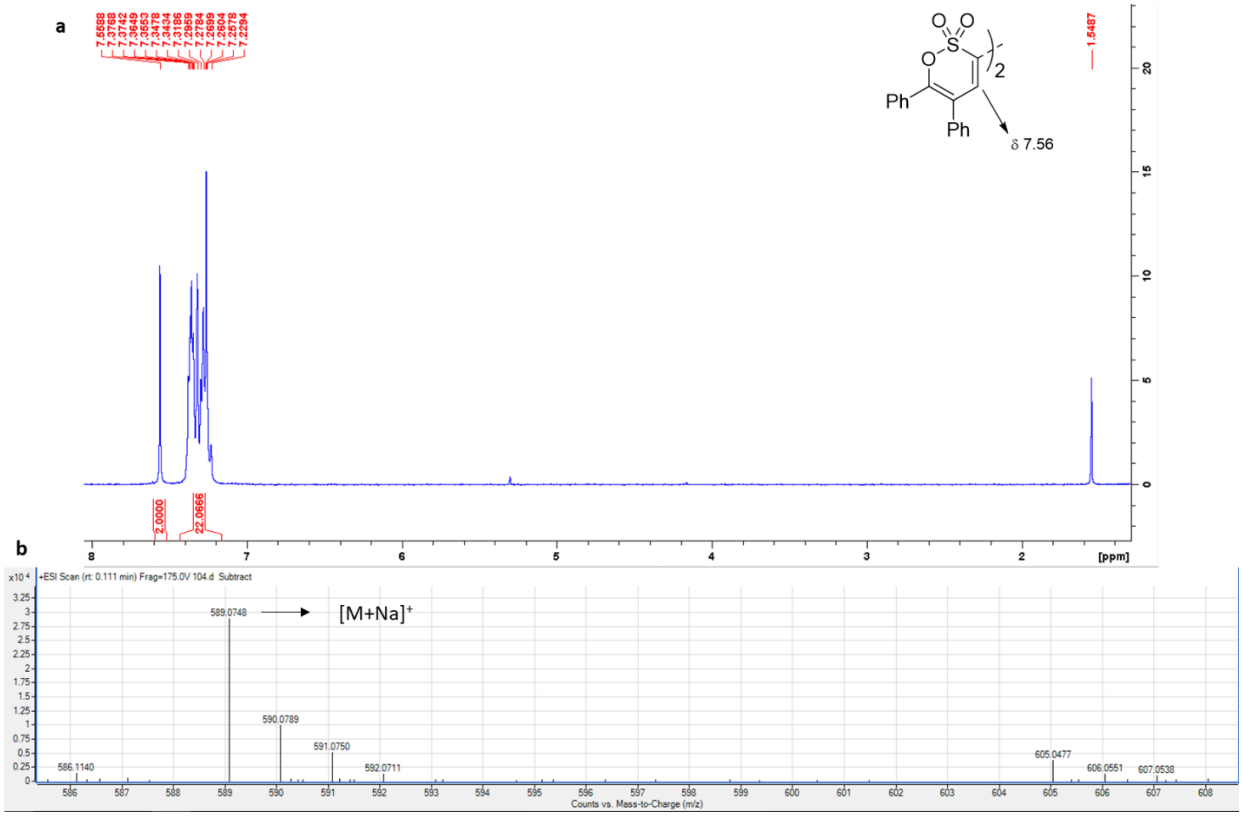

Figure 4.8: a) ^{1}H-NMR spectrum of **4.32**, b) Mass spectrum of **4.32**

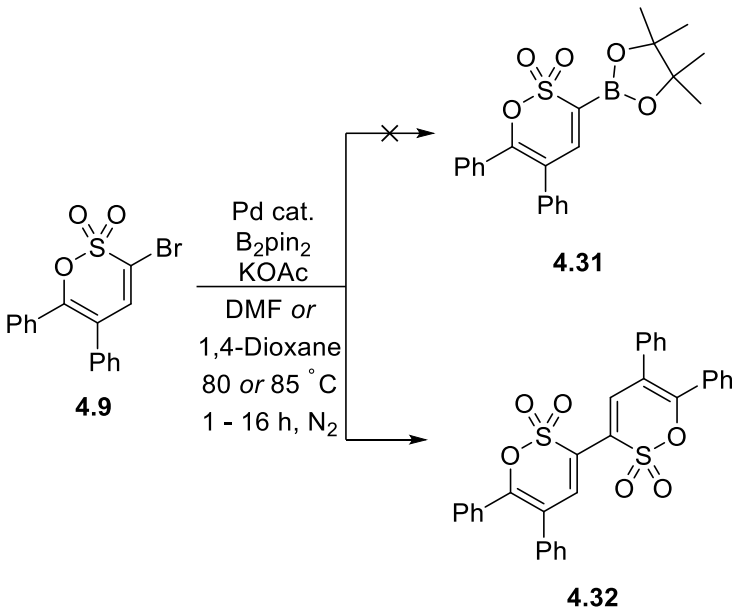

Scheme 4.14: Suzuki-Miyaura borylation attempt on **4.9**

A/a	Pd cat. (%-mol)	eq B_2pin_2	eq KOAc	Solvent	Temperature (°C)	Time (h)	Yield of 4.32 (%)
1	$Pd(OAc)_2$ (3 %-mol)	1.1	3.0	DMF	85	5	0.0
2	$Pd(dppf)Cl_2$·DCM (10 %-mol)	2.0	3.0	1,4-Dioxane	80	16	13.3
3	$Pd(dppf)Cl_2$·DCM (10 %-mol)	0.5	3.0	1,4-Dioxane	80	16	25.6
4	$Pd(dppf)Cl_2$·DCM (10 %-mol)	0.5	2.5	1,4-Dioxane	80	1.5*	**51.3**
5	$Pd(dppf)Cl_2$·DCM (10 %-mol)	2.0	1.0	1,4-Dioxane	80	1	37.4
*16 h stir at room temperature, followed by 1.5 h heating at 80 °C							

Table 4.3: Variation of reaction conditions for a Suzuki-Miyaura catalysed homo-coupling of **4.9**

As is evident from the table above, the greatest yield of **4.32** resulted when 0.5 eq of B_2pin_2 and 2.5 eq of KOAc are used, which was indicative of the boron ester **4.31** being formed *in* situ but immediately coupled to the bromo precursor **4.9** towards **4.32**. This increased "dimerisation" tendency can be attributed to the polarisation of the carbon-boron bond on the reactive ester **4.31** caused by the electron-withdrawing nature of the adjacent SO_2 moiety, which suggests that brominated 1,2-oxathiine 2,2-dioxides are more efficient substrates in Suzuki cross-coupling protocols. Interestingly, no boronic ester was obtained even at 1 eq of base and 2 eq of B_2pin_2 (entry 5, Table 4.3); instead, the homo-coupling product, along with the 3,4-dihydro precursor **4.5**, were observed in a 2:1 ratio by ^{1}H-NMR analysis of the crude mixture. The foregoing finding relays the fact that, at *x* eq of **4.9** at the start of a high B_2pin_2 excess reaction run, *x*/*3* eq of **4.9** reacts with *x*/*3* eq of KOAc in a Suzuki-Miyaura borylation cycle towards the boronic ester **4.31**, which is subsequently coupled to another *x*/*3* eq of **4.9** in a Suzuki coupling cycle mediated by the remaining 2 *x*/*3* eq of KOAc to furnish **4.32**. The final *x*/*3* eq of 4.9 is concomitantly consumed by the excess B_2pin_2 and is converted to **4.5** during the aqueous wash, thus producing the observed 2:1 ratio of **4.32**/ **4.5** (Scheme 4.15).

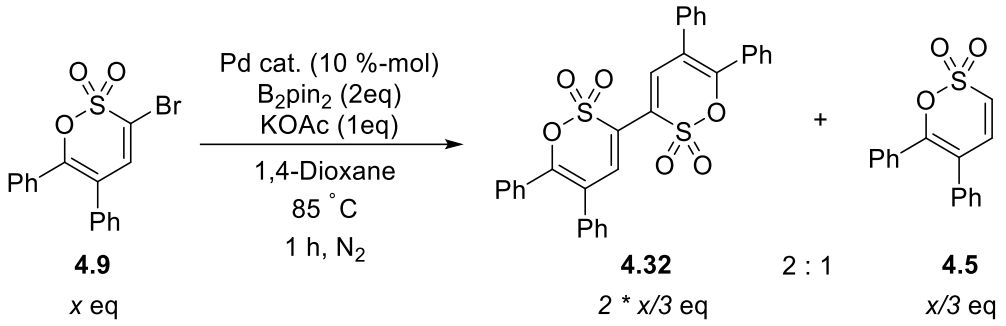

Scheme 4.15: Obtained products from a Suzuki-Miyaura borylation attempt with 2 eq of B_2pin_2 and 1 eq KOAc

The foregoing observations can be combined to cement a proposed mechanistic cycle that gives rise to the homo-coupling species **4.32**. Upon the initial oxidative addition of **4.9** to the Pd complex and the Br^-/OAc^- ligand exchange, the Bpin fragment is introduced to the intermediate complex **4.31A** via transmetalation, followed by an isomerisation process to arrive at a cis arrangement of the 1,2-oxathiine 2,2-dioxide and Bpin ligands. The C-B bond formation can thus occur during the final reductive elimination step to afford the reactive boronic ester **4.31** (Scheme 4.16).

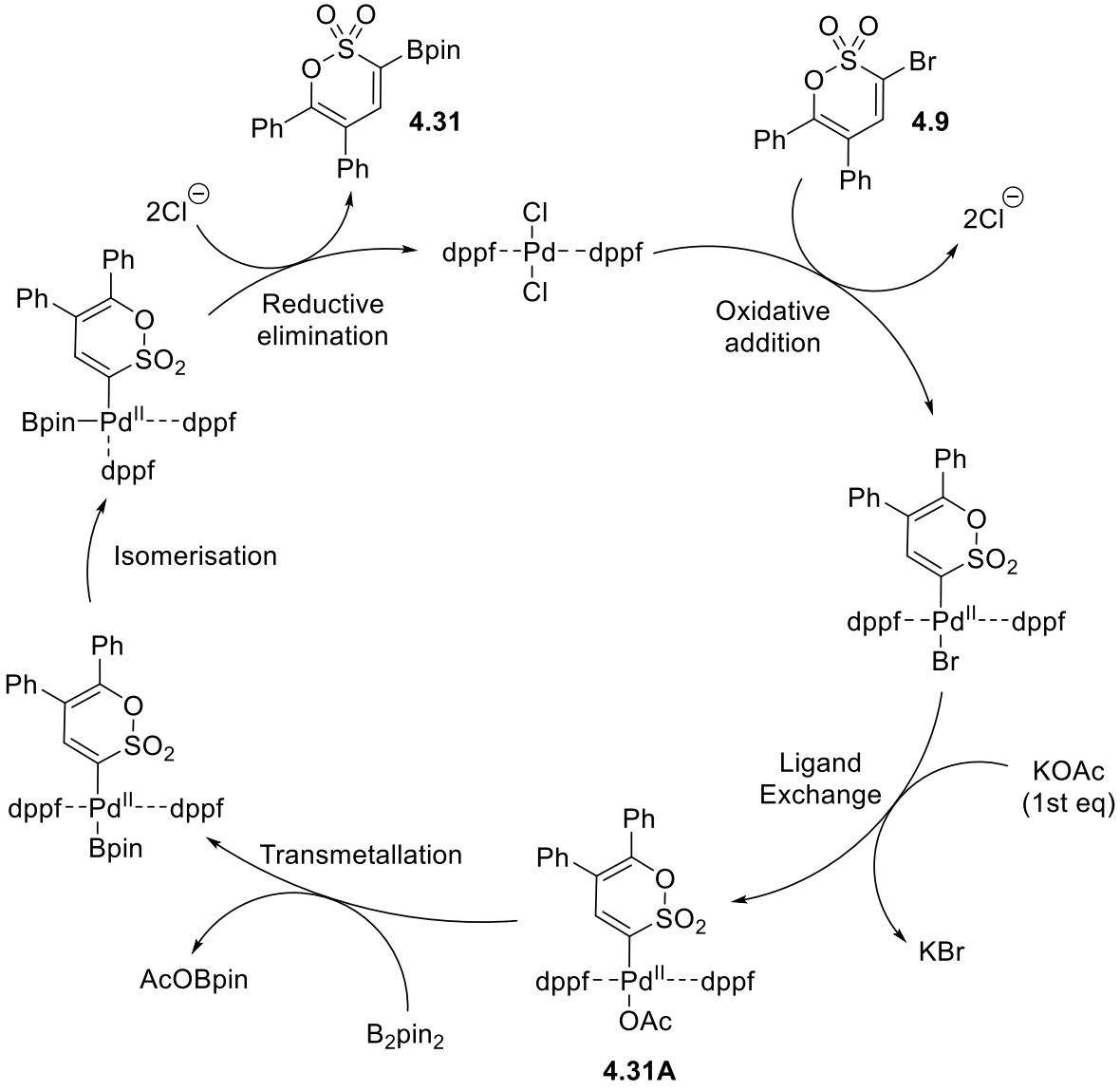

Scheme 4.16: First catalytic cycle towards the boronic ester **4.31**

In a second catalytic cycle, the intermediate **4.31A** forms again but interacts with the boronate species **4.33** that derives from the addition of an AcO^- ion to the nascent boronic ester **4.31**. Isomerisation of the resulting complex **4.31B** leads to the two 1,2-oxathiine 2,2-dioxide fragments adopting a *cis* disposition and couple into **4.32** *via* reductive elimination (Scheme 4.17).

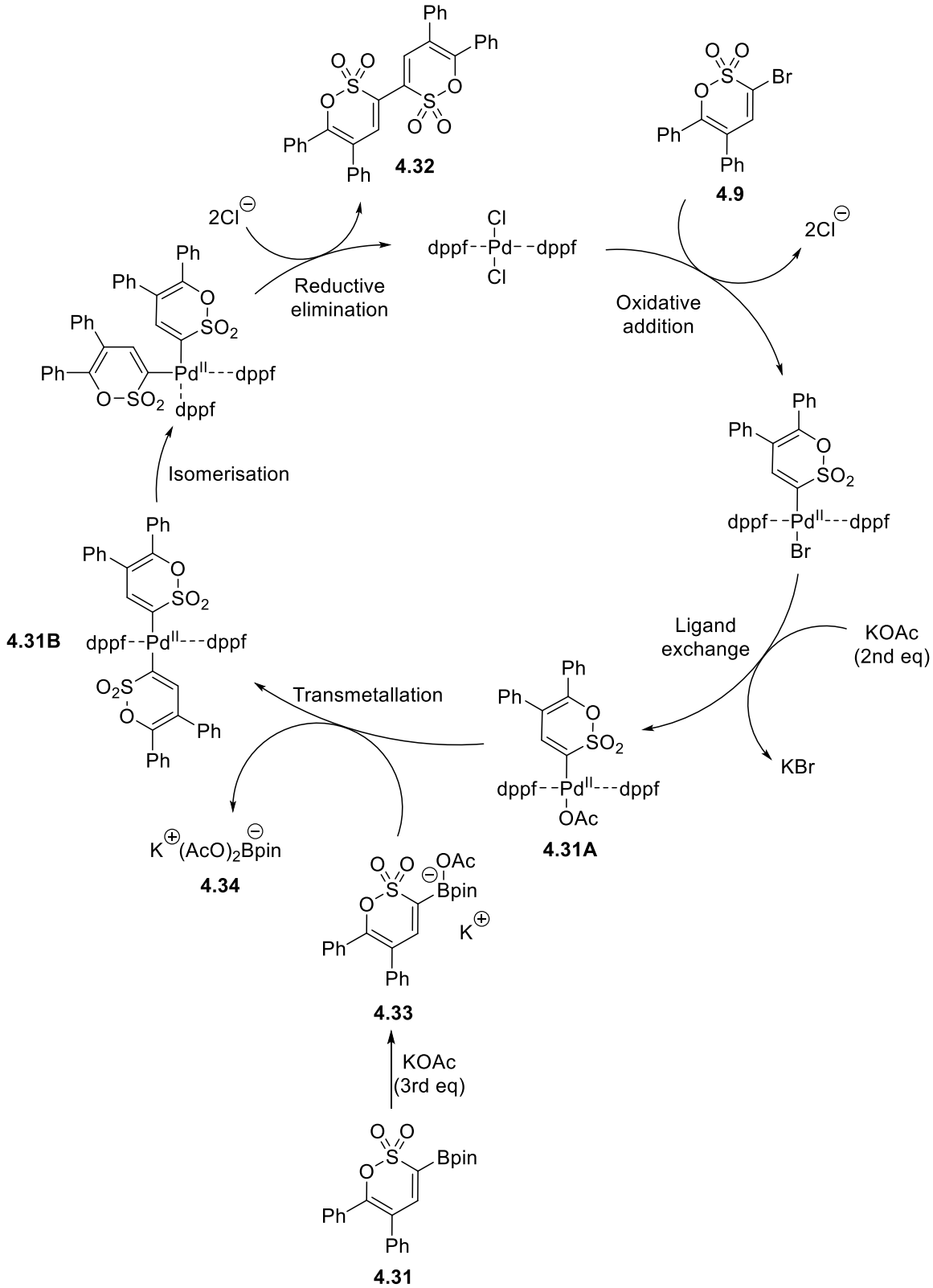

Scheme 4.17: Second catalytic cycle towards 5,5',6,6'-tetraphenyl-[3,3'-bi(1,2-oxathiine)] 2,2,2',2'-tetraoxide **4.32**

With regards to the precursor oxathiine 2,2-dioxide **4.5**, a similar cycle to that on scheme 4.16 includes the Br^-/OAc^- ligand exchange step towards **4.31A** with use of a different AcO^- source, *i.e.* the boronate by-product **4.34** (Scheme 4.17), while the excess B_2pin_2 allows for the consecutive transmetallation step. The boronic ester **4.31** that is eventually furnished can potentially undergo a Pd-catalysed hydrolysis[222] upon aqueous quenching during the reaction work-up, thus affording **4.5** as the minor product of this conversion (Scheme 4.18).

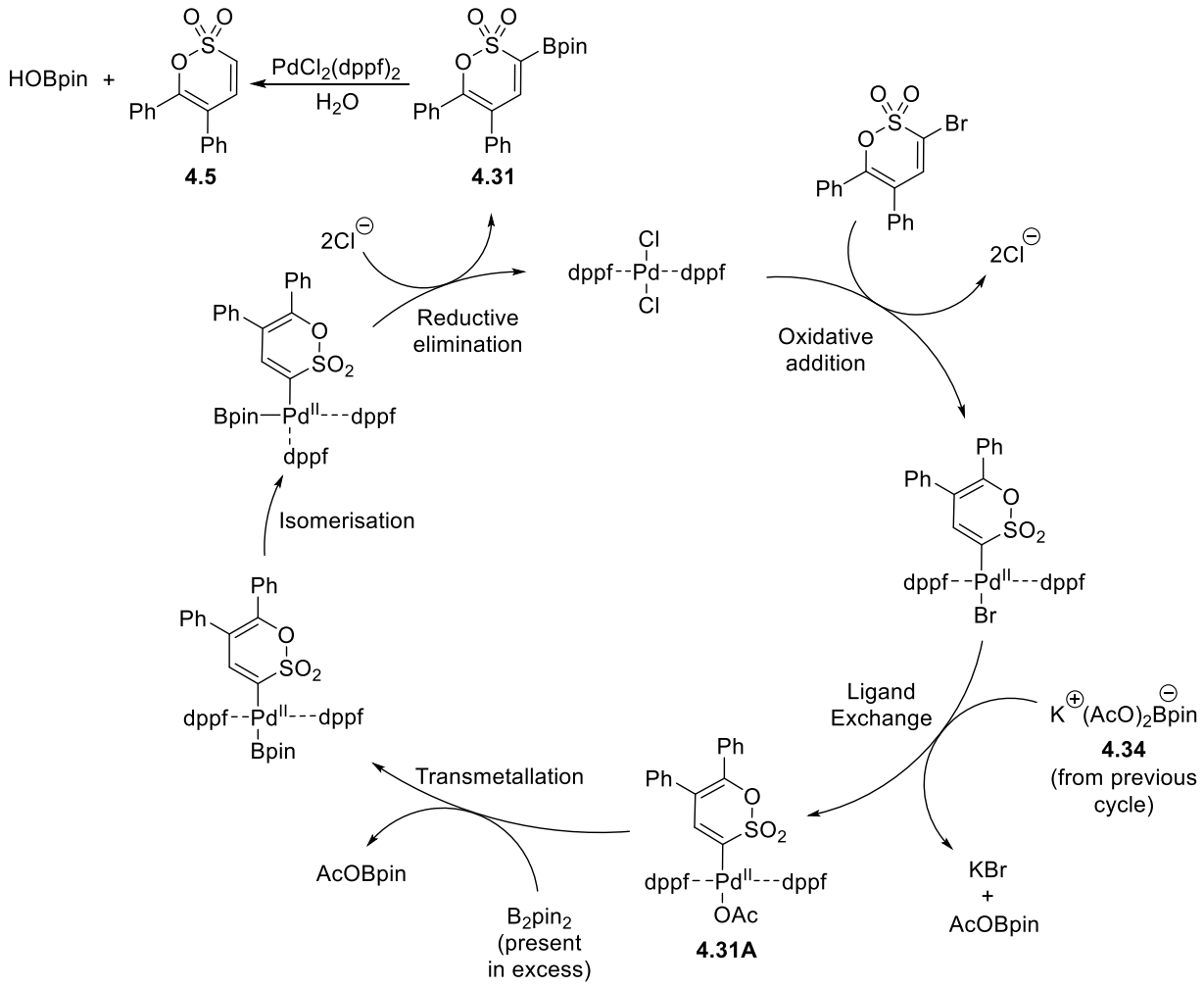

Scheme 4.18: Catalytic cycle furnishing the dihydro precursor **4.5**

Absence of a B_2pin_2, as was the case for the highest yield attempt (entry 4, Table 4.3), presumably allows for a higher amount of the dimer-like system **4.32** through the first two catalytic cycles of boronic ester (**4.31**) furnishing and C-C bond formation (Scheme 4.16, Scheme 4.17), since there is not enough B_2pin_2 to divert the intermediate **4.31A** from being transmetallated into **4.31B** and, eventually, converted into **4.32**. Moreover, comparison of entries 3 and 4 in table 4.3 shows that long reaction times (>1.5 h) can be detrimental for this transformation, as evident by the drop in yield when the reaction remains at 80 °C overnight.

This preliminary survey of the reactivity of brominated 1,2-oxathiine 2,2-dioxides in traditional Pd-mediated coupling reactions illustrated that these heterocycles are more suitable for coupling with aryl boronic acids under Suzuki coupling conditions, rather than being converted into boronic esters *via* the Suzuki-Miyaura borylation and subsequently coupled to aryl halides through the aforementioned Suzuki

protocols. This conclusion connotates a general feature of these analogues as “electron-poor” bromides and for this reason, alternative methods of C-C bond formation were sought out.

4.4 Reactions with unsaturated 1,2-oxathiine 2,2-dioxides

4.4.1 C-H activation coupling reactions

Following on from the exploration of the reactivity of the brominated 1,2-oxathiine 2,2-dioxides towards Pd-catalysed coupling reactions, it was rationalised that the next area of research should regard the possibility of functionalising the unsaturated systems **4.5** – **4.7** through C-H activation cross-coupling protocols[223,224] that utilised aryl halides as coupling partners. Indeed, ascertaining the success of such a conversion would be quite useful in further exploring the reactivity of 1,2-oxathiine 2,2-dioxides, as well as in establishing an interesting and more efficient alternative to furnishing poly-substituted derivatives through traditional bromination and Suzuki coupling reactions. The work of Pereira *et al.* was elected as a suitable literature template[225], since the coumarin systems **4.35** that were used as substrates to afford selectively substituted counterparts (**4.36**) contained an α,β-unsaturated lactone unit that was considered to be analogous to the α,β-unsaturated sultone unit of the 1,2-oxathiine 2,2-dioxide starting materials (Scheme 4.19).

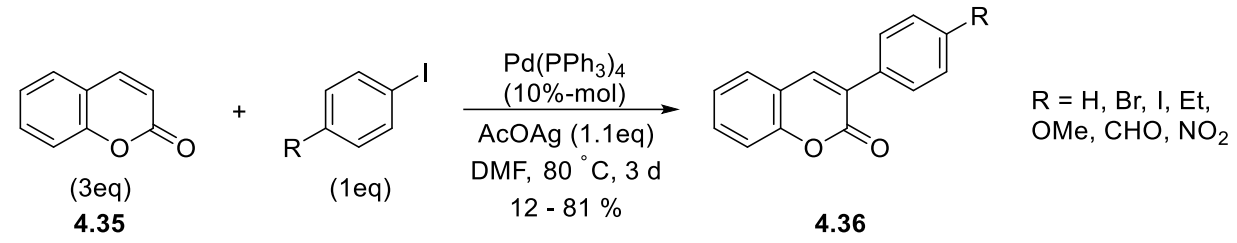

Scheme 4.19: Literature-established attempt towards 3-substituted coumarin systems through a C-H activation cross-coupling protocol

Initial application of this protocol to the 1,2-oxathiine 2,2-dioxide **4.5** was met with poor reproducibility, as the excess of the starting material (3 eq for 1 eq of PhI, Scheme 4.20) allowed for its Pd-catalysed dimerization in a parallel manner to that observed for the brominated derivatives in sections **4.3.2** and **4.3.3**. Specifically, overnight heating at 80 °C of the coupling partners, $Pd(PPh_3)_4$ and AcOAg in DMF afforded a mixture of unreacted starting material **4.5**, coupling product **4.4** and the [3,3'-bi(1,2-oxathiine)] 2,2,2',2'-tetraoxide **4.32** at a 1 : 0.56 : 0.35 ratio, as calculated by the integrals of the respective singlets on the ^{1}H-NMR spectrum of the crude mixture (Figure 4.9).

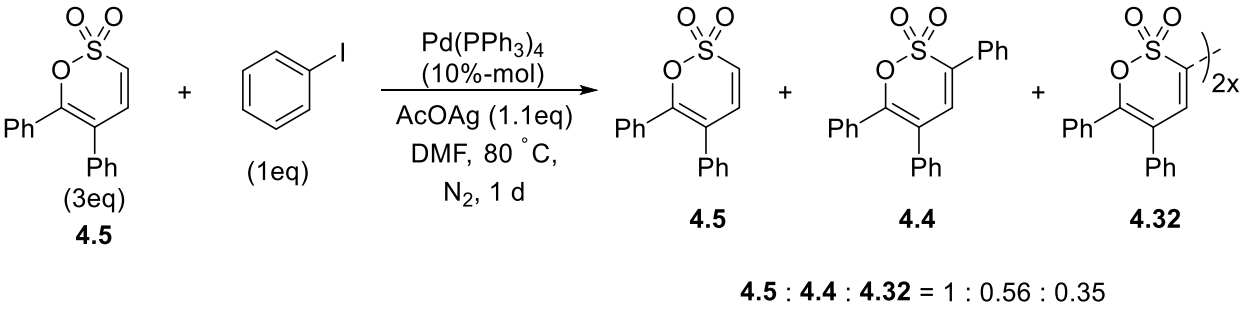

4.5 : **4.4** : **4.32** = 1 : 0.56 : 0.35

Scheme 4.20: Initial C-H activated coupling attempt of the 5,6-diphenyl analogue **4.5** with PhI towards **4.4**

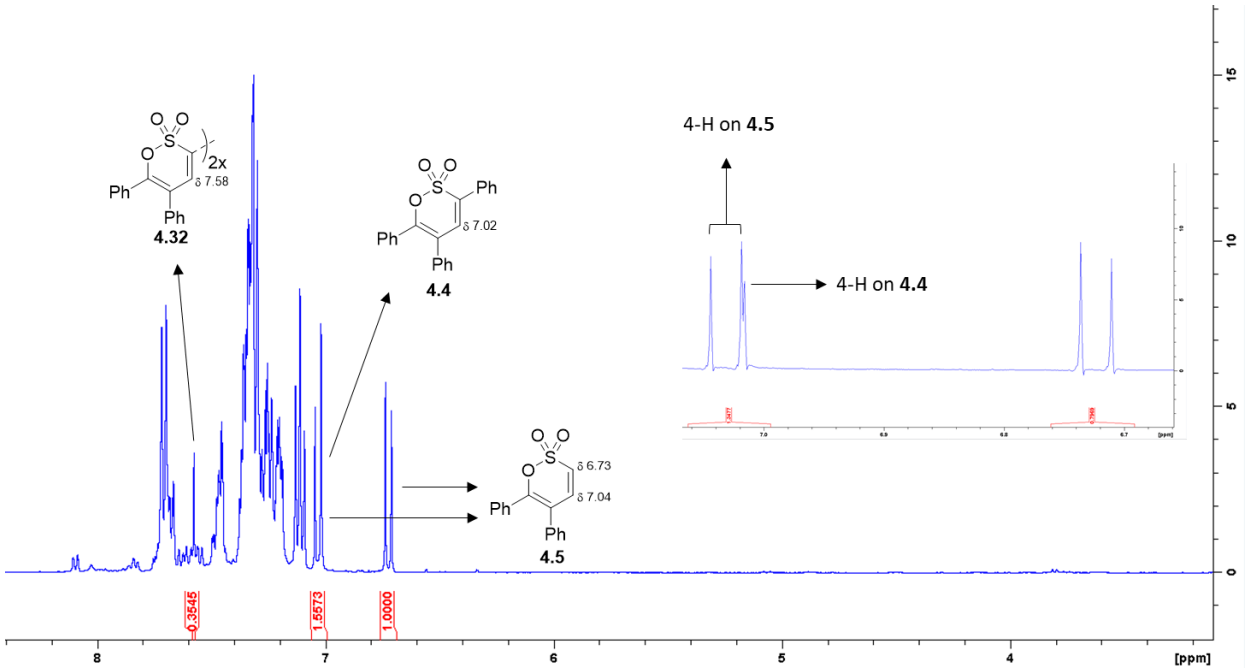

Figure 4.9: ^{1}H-NMR spectrum of the crude mixture from the C-H activated coupling attempt on **4.5**

This finding further cemented the previously observed tendency of 1,2-oxathiine 2,2-dioxide systems to undergo homo-coupling processes in the presence of Pd-catalysts. Unfortunately, the aforementioned three components were found to have very similar R_f values, thus rendering their routine chromatographic separation ineffective. The coupling reaction was consequently repeated using 1 eq of the starting 1,2-oxathiine 2,2-dioxide and 3 eq of the iodide. Pleasingly, this iteration yielded the triphenyl product **4.4** in 39.2 % yield with absence of the dimeric side-product **4.32**, prompting further attempts of this transformation with varying aryl iodide reagents (Table 4.4). Evaluation of the foregoing findings shows several interesting insights on the behaviour of 1,2-oxathiine 2,2-dioxides under C-H activation coupling conditions. Comparison of the yields between the attempts using the 5,6-diphenyl (**4.5**) and the 6-phenyl analogue (**4.6**) indicates that the presence of a phenyl group on the 5-position is moderately beneficial for this conversion (39.2 % for **4.5** over 32.1 % for **4.6**), mirroring the reactivity of their respective 3-bromo analogues during the Suzuki coupling explorations (Section **4.3.2**). Following on similar behaviour, the 3,6-diphenyl derivative **4.7** was found to be completely inactive in terms of coupling on the 5-position, in a similar fashion to the brominated counterpart **4.11**. As the best results from these attempts were obtained using the 5,6-diphenyl analogue **4.5**, it was used as the starting material for further attempts using varying aryl iodides. A very interesting trend was revealed after the isolation of the methoxyphenyl (**4.26**) and trifluorophenyl (**4.27**) analogues at 25.9 % and 56.7 % yield respectively; there appears to be a gradient of increasing yield when moving from aryl iodides with an ED substituent to aryl iodides with an EW group (25.9 % for **4.26**, 39.2 % for **4.5** and 56.7 % for **4.27**). The opposite trend can be inferred from the findings of the Suzuki attempts toward the same analogues regarding the reactivity of boronic acids, with an EW substituent on the aryl group mitigating the extent of the conversion and an ED one increasing it (58.1 % for **4.26**, 40.0 % for **4.5** and 36.2 % for **4.27**, Figure 4.10).

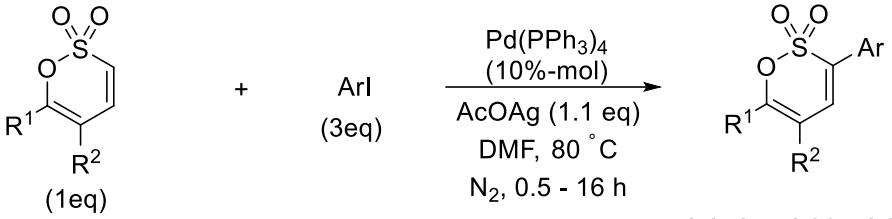

4.5: $R^1 = R^2 = Ph$
4.6: $R^1 = Ph$, $R^2 = H$
4.37: $R^1 = An$, $R^2 = An$
4.39: $R^1 = PhCH{=}Ch$, $R^2 = H$

4.4, **4.7**, **4.26 - 4.28**, **4.38, 4.40**

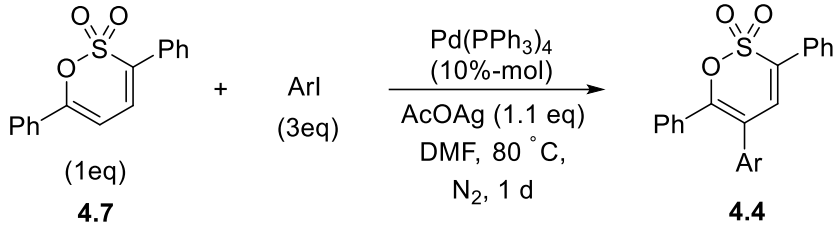

4.7 **4.4**

Entry	Substrate No.	R^1	R^2	Ar	Product No.	Time (h)	Yield (%))
1	**4.5**	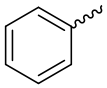	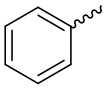	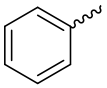	**4.4**	16	39.2
2	**4.6**	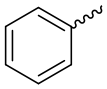	H	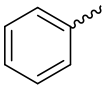	**4.7**	16	32.1
3	**4.7**	-	-	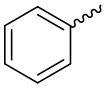	**4.4**	16	0.0
4	**4.5**	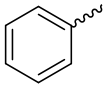	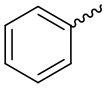	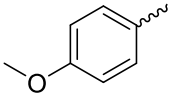	**4.26**	16	25.9
5	**4.5**	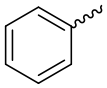	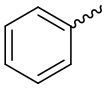	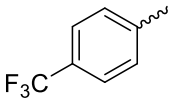	**4.27**	2	56.7
6	**4.5**	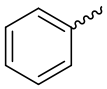	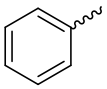	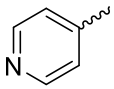	**4.28**	1	68.0
7	**4.5**	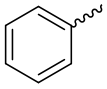	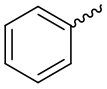	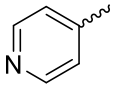	**4.28**	16	0.0*
8	**4.37**	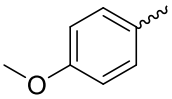	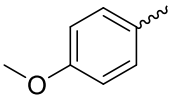	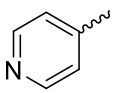	**4.38**	0.5	32.8
9	**4.39**	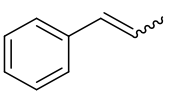	H	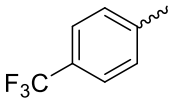	**4.40**	2	82.3

*Dimer-like species **4.32** observed by ^{1}H-NMR spectroscopy on the reaction mixture

Table 4.4: C-H activated coupling of 1,2-oxathiine 2,2-dioxides with varying aryl iodides

This is a clear indication that the Suzuki coupling protocol shows a reactivity profile which is complementary to that of the C-H activation coupling reaction, prompting an even more general conclusion with respect to the use of these transformations towards the functionalisation of 1,2-oxathiine

2,2-dioxides: employing a Suzuki coupling reaction is evidently a more reliable strategy towards appending electron-rich groups on the 3-position of the 1,2-oxathiine scaffold, whereas the coupling of electron-poor groups on the same position can be carried out more efficiently by opting for C-H activation as the coupling protocol. Moreover, the complete unreactivity of the 5-position of the 1,2-oxathiine 2,2-dioxide during both coupling protocols highlights that any substituent on this position has to be introduced during the preparation of the 1,2-oxathiine core unit, *i.e.* its presence is necessary on the enaminone precursor discussed in Chapter 2.

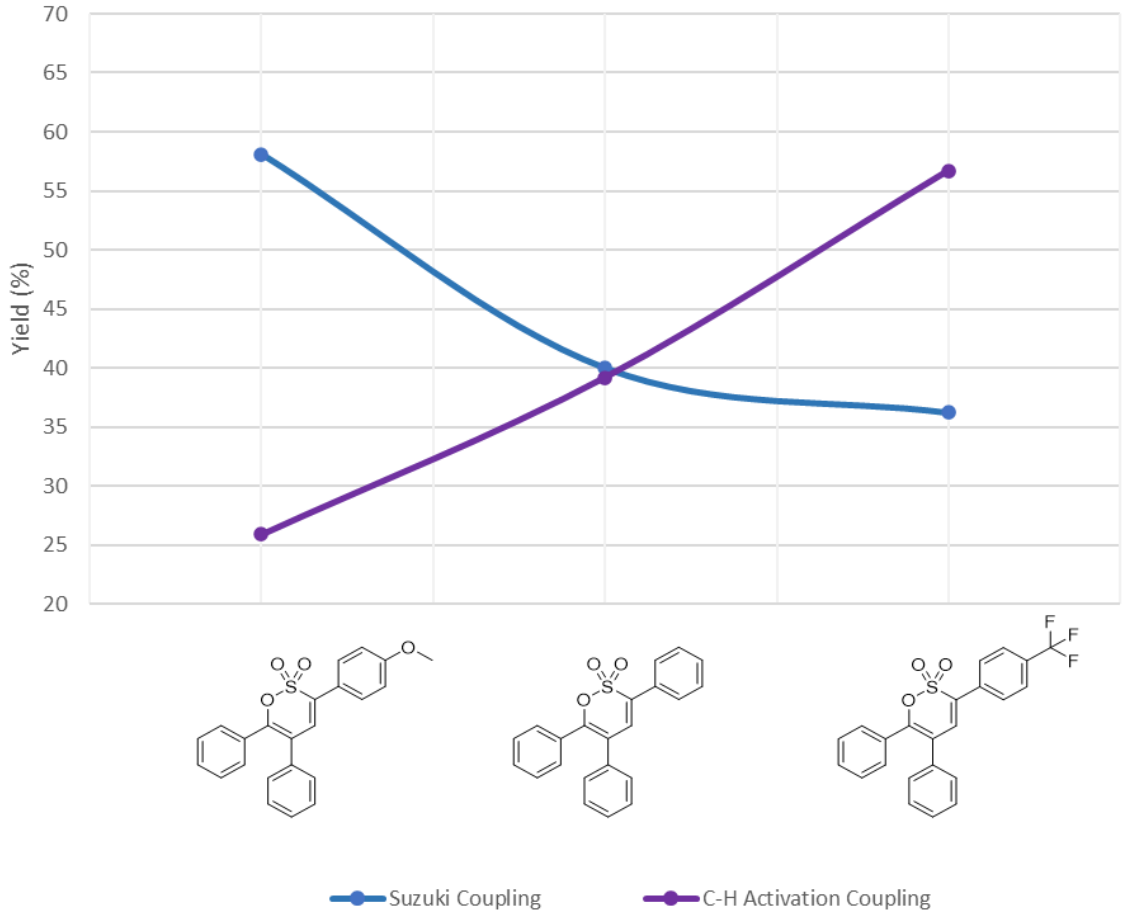

Figure 4.10: Correlation between yields and 3-aryl substituents across Suzuki and C-H activation coupling protocols

Apart from the electronic effects on the yields observed for this coupling protocol, the reaction time was also found to have a profound influence on its success. Careful TLC monitoring of the reaction progress for the trifluorophenyl analogue **4.27** ascertained that the starting material **4.5** was fully consumed after 2 hours of heating at 80 °C, rendering the overnight heating period redundant. The time expediency of this reaction was even more pronounced in the case of the pyridyl group coupling, which required only 1 hour to completion and afforded the 3-pyridyl 1,2-oxathiine 2,2-dioixide analogue **4.28** in 68.0 % yield. A repeat of this reaction, wherein the reaction mixture was given the initial overnight heating period, failed to afford the target compound **4.28** and the only product observed in the ^{1}H-NMR spectrum of the reaction mixture was the dimeric side-product **4.32** (Scheme 4.21). This finding emphasises the importance of a reduced reaction time towards reaction success, as long reaction times are not only time-consuming, but they allow for the dimerisation of the starting materials, which is presumably a slower process than the desired coupling process. The dimeric side-product formation can be further examined using these data; the isolation of the 3-pyridyl coupling product **4.28** after a short reaction time (1 h),

along with the fact that the same attempt affords the dimerization product **4.32** as the sole product after a full overnight period of heating at 80 °C, may indicate that the coupling product **4.28** forms initially but, due to the significant EW character of the pyridine substituent, interacts with the palladium catalyst at longer heating periods towards complexes that lead to the homo-coupling of the 1,2-oxathiine starting material through transmetallation processes that are favoured by virtue of the aforementioned thermal stability of the dimer-like species **4.32** (Scheme 4.21).

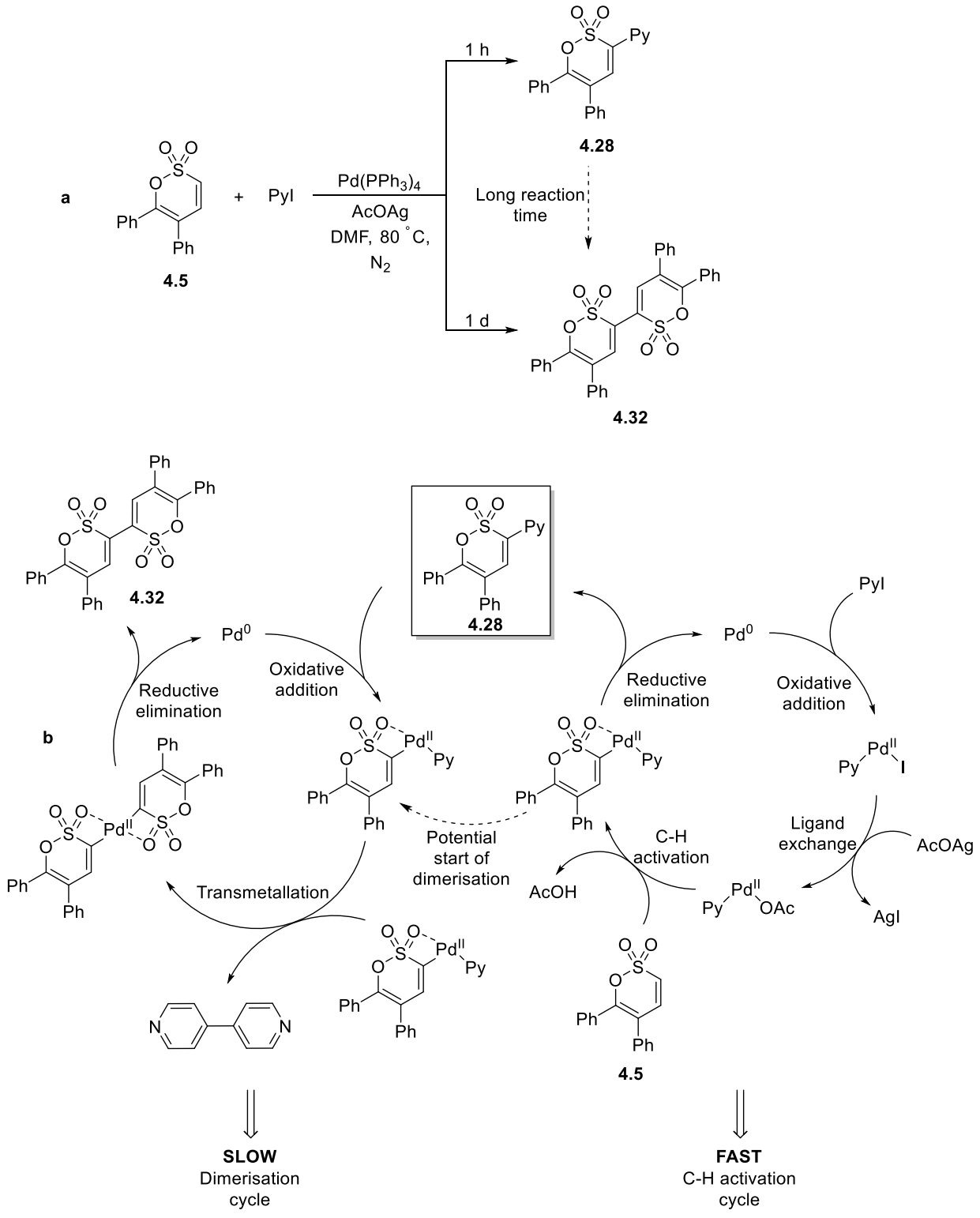

Scheme 4.21: Effect of reaction time on the formation of different products **4.28** and **4.32**

However, given the presence of trace amounts of **4.32** in the reaction mixture of **4.28** after 1 h of reaction time (as observed by TLC), this proposed route does not preclude the possibility of the dimerization occurring before the formation of the coupling product (through interaction between identical Pd-complexes as seen under Suzuki coupling conditions (Scheme 4.12), yet it still presents an additional pathway of product loss which further cements the importance of short reaction times and meticulous monitoring of the reaction.

After this modification on the reaction time, the versatility of this conversion was tested by varying the 5- and 6-substituents of the 1,2-oxathiine substrate. The 5,6-dianisyl derivative **4.38** was obtained in a lower yield to its 5,6-diphenyl counterpart **4.28** (32.8 % over 68.0 %, Figure 4.11), while 6-styryl 1,2-oxathiine 2,2-dioxide **4.39** offered the best results amongst these coupling attempts, as it was efficiently coupled to iodobenzotrifluoride towards the 3,6-disubstituted analogue **4.40** in 82.3 % yield.

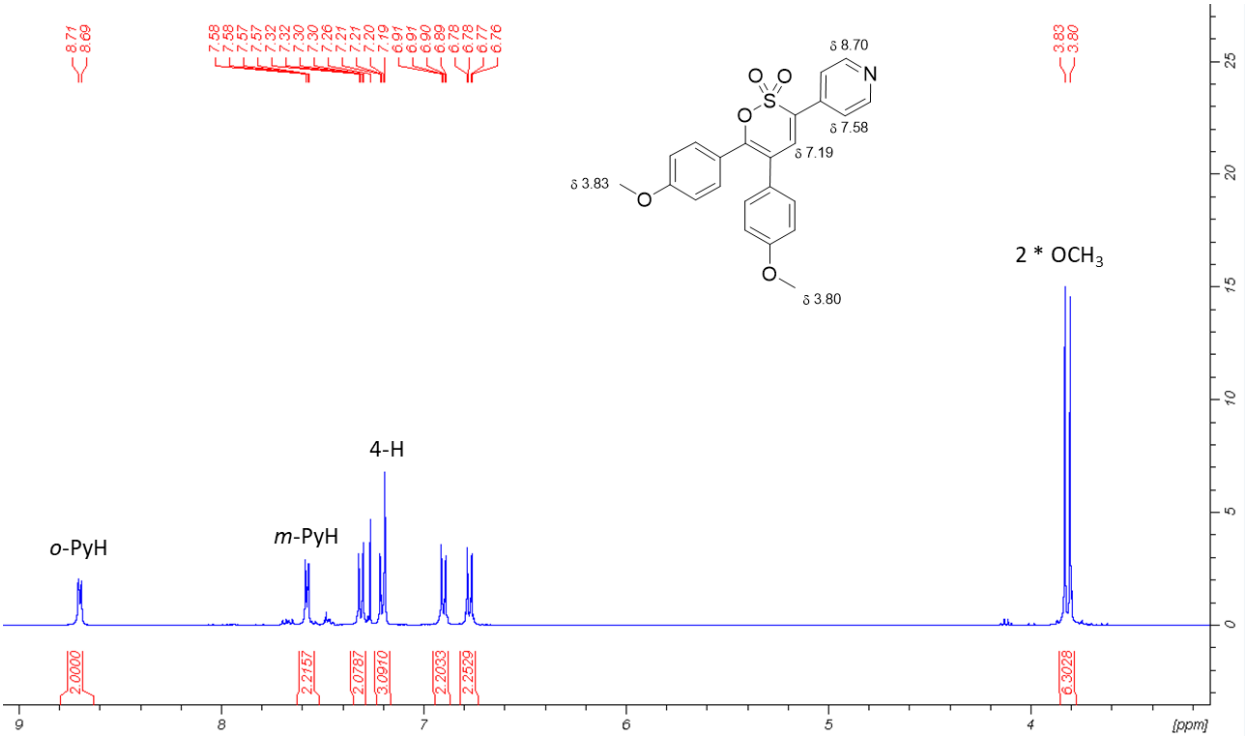

Figure 4.11: ^{1}H-NMR spectrum of the 3-pyridyl-5,6-dianisyl 1,2-oxathiine analogue **4.38**

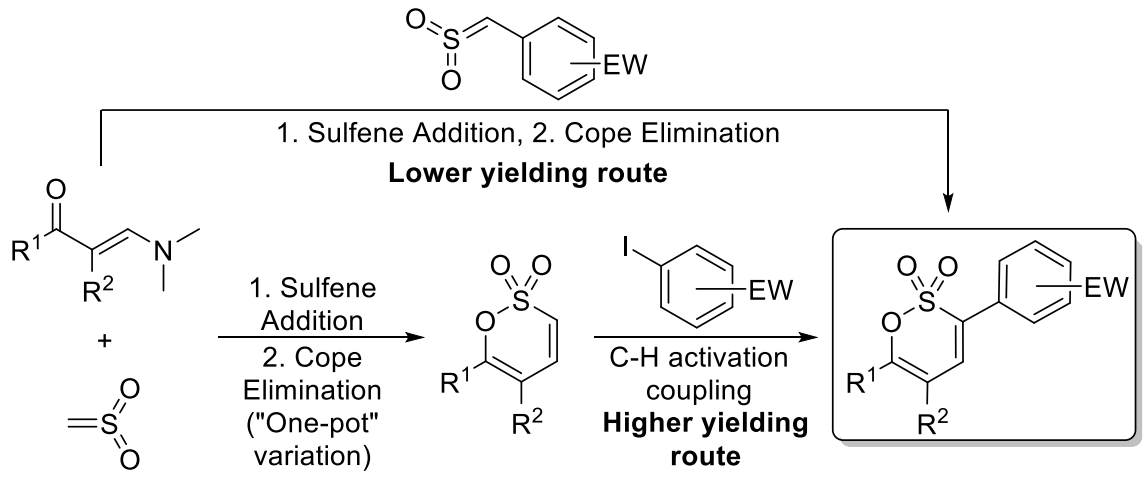

Scheme 4.22: Synthetic strategy towards 1,2-oxathiine 2,2-dioxide analogues with electron-poor aryl 3-substituents

In summary, C-H activation coupling was thoroughly explored as a viable method of appending an aryl group on the 3-position of the 1,2-oxathiine 2,2-dioxide scaffold, with particular efficiency in electron-

poor aryl groups. Furthermore, the general synthetic route of preparing a 1,2-oxathiine 2,2-dioxide as discussed in Chapter 2, with the desired 5- and 6- substituents already present as moieties on the enaminone precursor, and subsequently functionalising the 3-position *via* C-H activation coupling constitutes a valuable strategy that allows access to 3-substituted 1,2-oxathiine systems that would presumably be more challenging to prepare through addition of electron-poor sulfenes to enaminone substrates.

4.4.2 Exploration of cycloaddition reactions

After the activity of unsaturated 1,2-oxathiine 2,2-dioxide systems in Pd-catalysed cross-coupling conditions was explored, a different facet of their reactivity was sought to be mapped out through cycloaddition / (hetero) Diels-Alder transformations. During the initial exploration of the reactivity of these compounds, examination of the relevant literature[66,82] had highlighted their diene-like properties by virtue of their conversion into poly-substituted benzenes (**4.43**) or fused cyclic anhydrides **4.44**, even though these reactions were found to only occur under forcing conditions, *e.g.* pressures of up to 1300 MPa and temperatures of up to 150 °C (Scheme 4.23, also seen in section **1.2.1.3**. A common element of these surveys was the use of 2,4-disbustituted 1,2-oxathiines 2,2-dioxides (**4.41**) and triple bond-containing dienophiles (*e.g.* DMAD, **4.42**) in Diels-Alder/ retro Diels-Alder routes, which prompts the need for further examinations using different dienophiles.

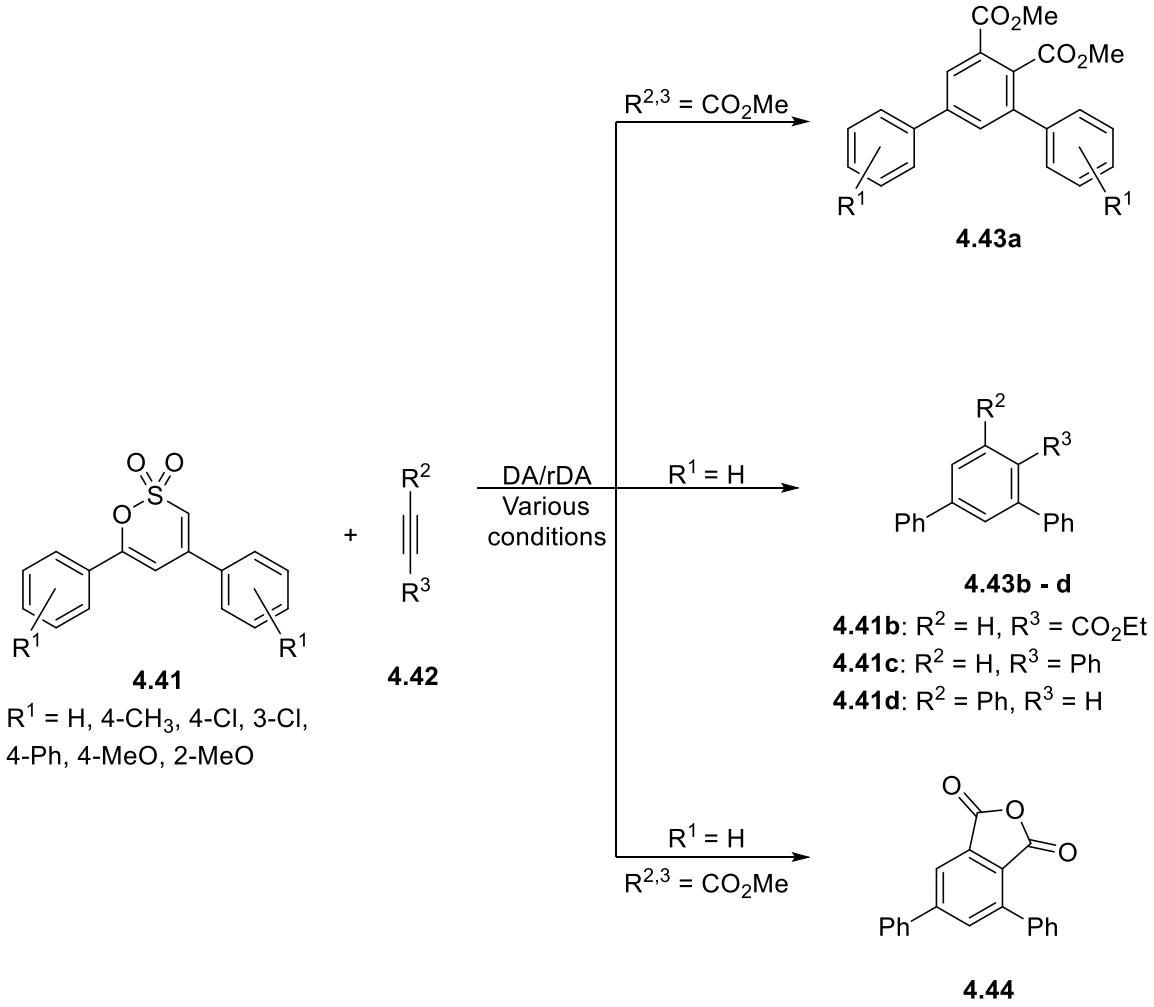

Scheme 4.23: Literature findings on Diels-Alder/retro Diels-Alder conversions of 1,2-oxathiine 2,2-dioxides

Moreover, the use of high temperature and elevated pressure is indicative of a relative "reluctancy" of these heterocycles to undergo cycloadditions; hence, it was proposed that vinyl or ethynyl groups on the periphery of the 1,2-oxathiine ring would constitute alternative diene moieties along with one of the two internal double bonds of the 1,2-oxathiine ring (bonds in red, **4.45** – **4.50**, Figure 4.12). The use of different dienophiles would also be of interest in ascertaining the behaviour of such compounds and expanding the range of different cycloadducts.

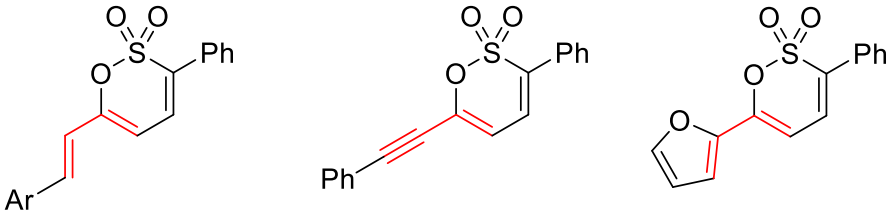

4.45: Ar = Ph
4.46: Ar = 4-$MeOC_6H_4$
4.47: Ar = 4-$CF_3C_6H_4$
4.48: Ar = 4-$NO_2C_6H_4$

4.49 **4.50**

Figure 4.12: Library of starting materials for cycloaddition reactions

The first heterodienophile that was used for these explorations was 4-phenyl-1,2,4-triazoline-3,5-dione **4.51** (PTAD).[226] The synthesis of this triazoline heterocycle is commonly brought about *via* the oxidation of 4-phenyl urazole **4.52** using various oxidising agents, with the presence of **4.51** being readily monitored by its characteristic wine red colour owing to the N=N bond (Scheme 4. 24).[227] One particularly effective oxidising agent is iodobenzene diacetate which when mixed with finely ground **4.52** in DCM results in the formation of **4.51** in *circa* 30 min.[228]

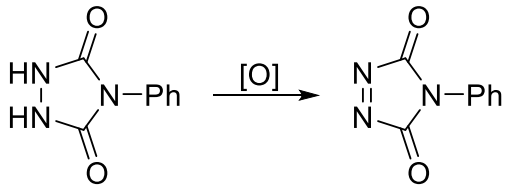

4.52 **4.51**

Scheme 4. 24: Preparation of PTAD (**4.51**) through the oxidation of 4-phenylurazole **4.52**

The heterocyclic scaffold in PTAD contains a urea-like fragment that draws electron density away from the N=N bond, thus making it quite reactive as a dienophile by virtue of its low energy LUMO.[229] For this reason, PTAD is a commonly used reagent in various cycloaddition transformations that have been documented in the literature. As can be expected, hetero Diels-Alder conversions where PTAD participates towards the formation of pyridazine-based heterocycles have been found to occur using a broad range of diene substrates, which is not limited to common butadiene derivatives[226,230] but also includes polyaromatic, bicyclic and 7-membered functionalised ring systems (Scheme 4.25).[231,232,233] The increased reactivity of PTAD has been interestingly utilised in its use as a protecting group of ring-closed diene systems (**4.53**), as it can be added to them towards bridged bicyclic adducts (**4.54**) and subsequently be cleaved through treatment with a base (Scheme 4.26).[234]

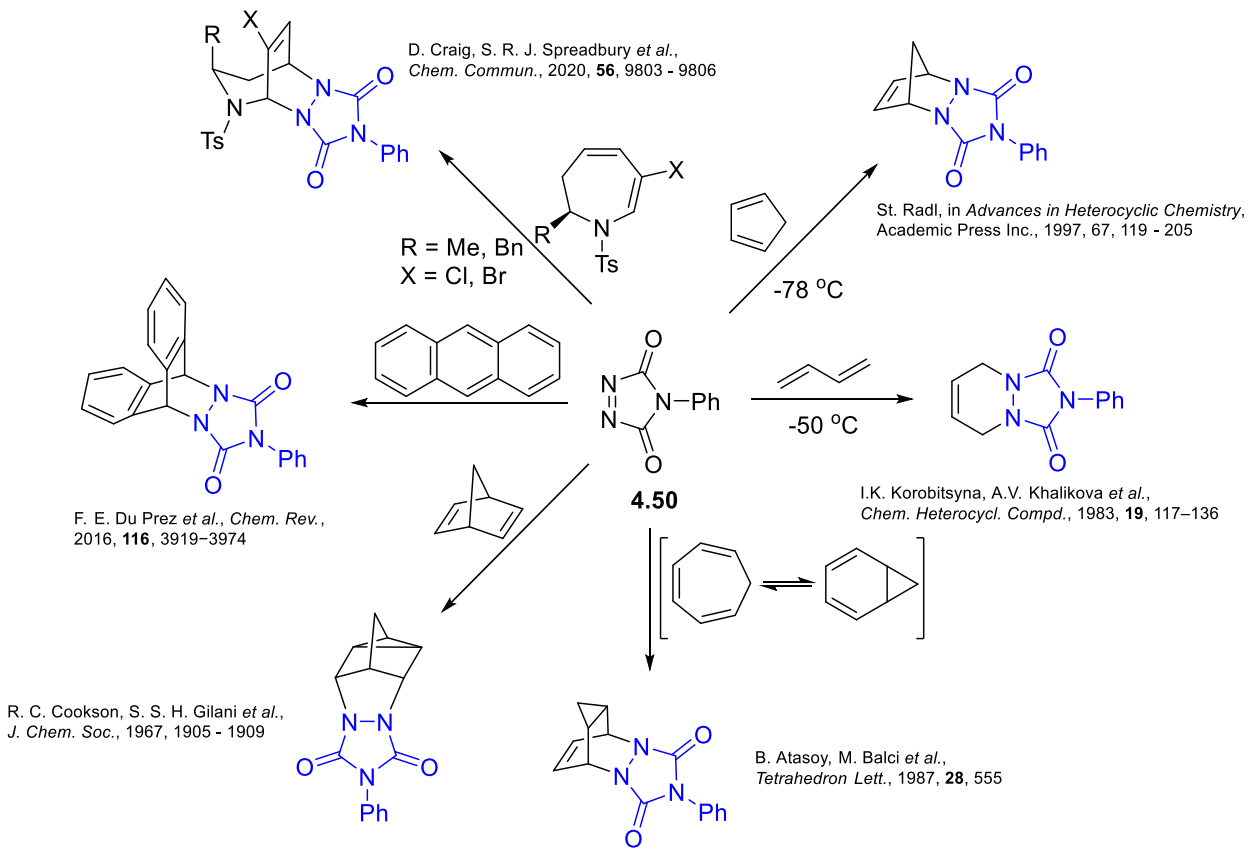

Scheme 4.25: Range of Diels-Alder cycloadditions of PTAD to various diene systems[226,230,231,232,233]

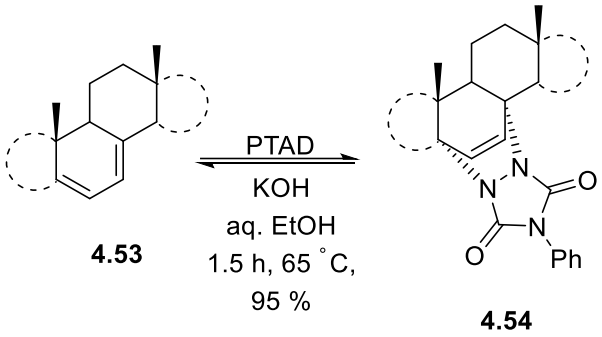

Scheme 4.26: Protection of a diene moiety *via* conversion to a PTAD cycloadduct **4.54** and deprotection under basic conditions

The ability of PTAD to interact with olefins can be further demonstrated with alkenyl compounds in [2+2] cycloadditions. Although theoretically such conversions do not occur thermally and require electromagnetic irradiation to proceed according to the Woodward/Hoffmann rules[115], the key N=N double bond on PTAD permits the formation of dipolar intermediates (**4.55**) that afford the 4-membered cycloaddition products through a stepwise mechanism (Scheme 4.27).[229,235] Starting from vinyl ethers, polycyclic systems and adamantene derivatives, various 4-membered *N*-heterocycles have been furnished through this transformation, thus expanding the spectrum of synthetic applications for PTAD.[236,237,238] The N=N double bond is alternatively able to interact with olefins bearing protons on the allylic position and form diradical intermediate species (**4.56**). This results in the cleavage of these neighbouring protons *via* an "ene" mechanistic route towards ring-open adducts where only one of the key *N* atoms is tethered to the starting material.[239] Simple alkene systems, as well as cyclic, polycyclic and silyl species, have been used as substrates, highlighting the potency of PTAD for "ene" transformations (Scheme 4.27).[226,229,230,240,241]

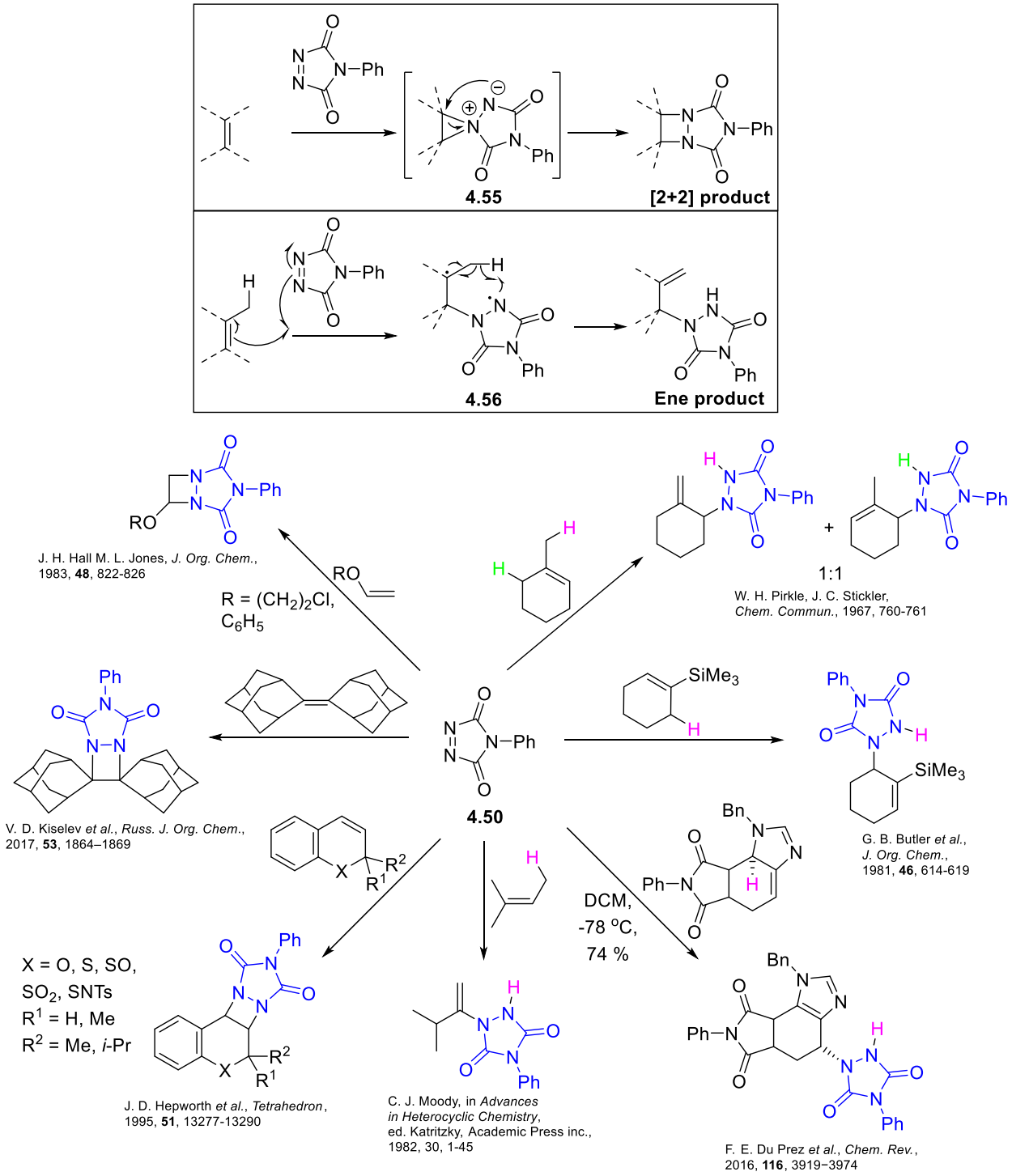

Scheme 4.27: Scope of [2+2] 'cycloadditions' and "ene" reactions of PTAD[226,229,230,236,237,238,240,241]

As can be deduced, this profound versatility of PTAD can be the underlying cause of regioselectivity issues during its interaction with multifunctional substrates; however, examination of the relevant literature sources indicates that these foregoing conversions manifest a gradient of thermodynamic preference; the [2+2] cycloaddition has been found to yield the strained but kinetically favoured diazetidine adducts at low temperatures, whereas the more thermally stable ring-open "ene" products are obtained at higher temperatures.[228] Similarly, additional research on the addition of PTAD to styrene (**4.57**) revealed that the addition of PTAD yields a reactive intermediate that can undergo an "ene" reaction at low temperatures to afford the ring-open aromatic analogue **4.58**, as opposed to the bridged bicyclic Diels-Alder adduct

4.59, which is obtained at room temperature (Scheme 4.28a).[229] These observations have significant importance in employing suitable conditions to guide the behaviour of PTAD according to the desired synthetic target, as it is shown in the example of (*E*)-5-methylhexa-1,3-diene (**4.60**, Scheme 4.28b).

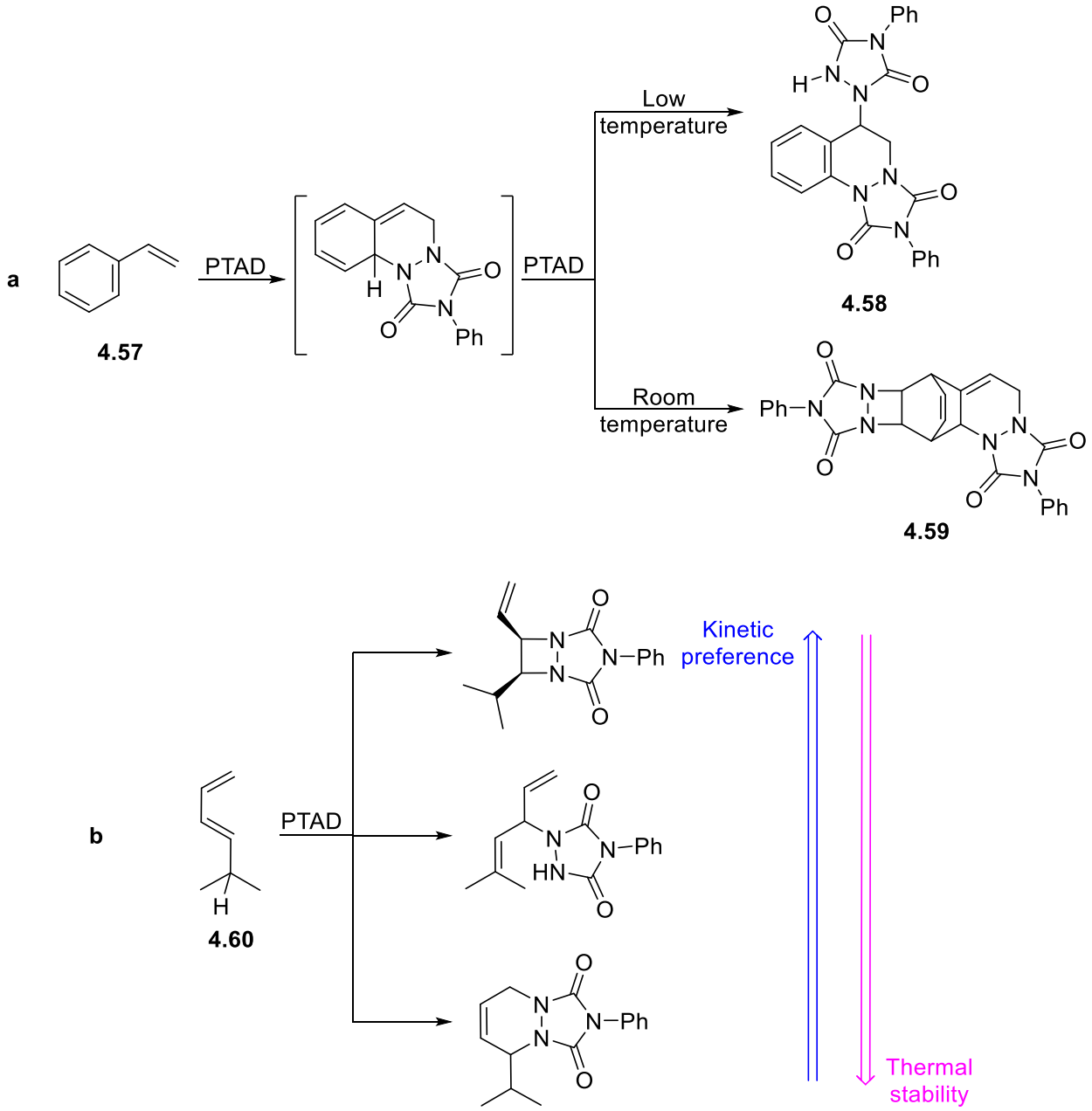

Scheme 4.28: Thermodynamic precepts of PTAD additions, illustrated in the examples of styrene (**4.57**) and the diene **4.60**

For the present project, PTAD was synthesised from finely ground commercially available phenylurazole (**4.52**) upon treatment with iodobenzene diacetate in DCM. The oxidation process was apparent by virtue of the gradual colour change of the reaction mixture from opaque white (the phenylurazole is highly insoluble in DCM) to wine red, whereas trituration of the crude product obtained upon filtration of unreacted starting material provided the target reagent in 58.2 % yield (Scheme 4.29).

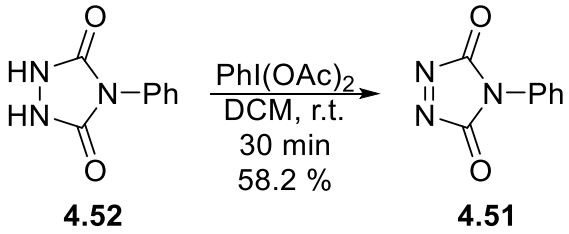

4.52 **4.51**

Scheme 4.29: Preparation of PTAD using iodobenzene diacetate as the oxidising agent

Prior to any attempts at a hetero Diels-Alder reaction between PTAD and the styryl analogues 4.43 – 4.46, it was deemed essential to screen one of the phenyl-substituted 1,2-oxathiine 2,2-dioxides against this hetero-dienophile, in order to ascertain the potential formation of either a [2+2] or hetero Diels-Alder adduct. In the case of such adducts being observed or isolated, this would pose a regioselectivity problem during the addition to the styryl derivatives, taking into consideration the foregoing literature observations on PTAD regioselectivity. Interestingly, stirring a solution of the 5,6-diphenyl analogue **4.5** at either room temperature or at reflux did not yield any of the potential cycloaddition products **4.61** or **4.62** and the starting material was retrieved intact (Scheme 4.30). Based on this finding, the addition of PTAD could be attempted without any regioselectivity concerns.

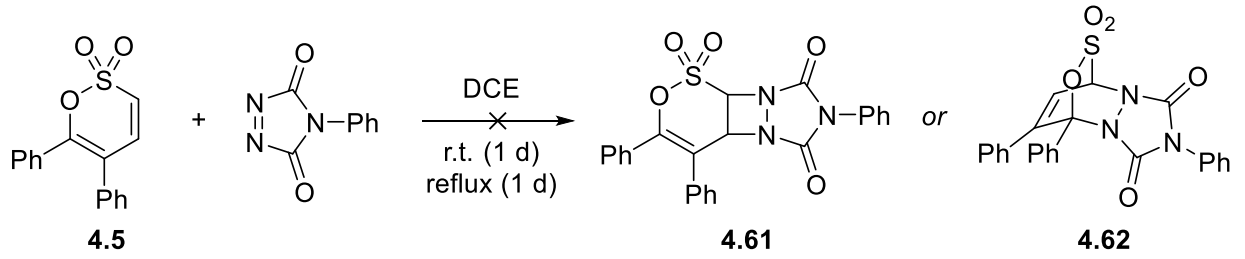

4.5 **4.61** **4.62**

Scheme 4.30: Attempt at the [2+2] or Diels-Alder cycloaddition of PTAD to the C3-C6 diene moiety of a 1,2-oxathiine 2,2-dioxide system (**4.5**)

Overnight stirring of a solution of the styryl 1,2-oxathiine 2,2-dioxide **4.45** and PTAD in 1,2-DCE resulted in the loss of the characteristic wine red colour of the heterodienophile, which was indicative of a potential addition to the starting material. Examination of the crude mixture *via* NMR spectroscopy confirmed the presence of an adduct (**4.63a**), as evidenced by three complex signals at δ 5.37, δ 5.82 and δ 6.32 attributed to protons 10a-H, 5-H and 6-H respectively, as well as the absence of any peaks of the starting material (Figure 4.13). Although not observed initially, it was theorised that the additional required signal for 10-H resonated in the same region as the aromatic protons of the three phenyl groups. Interestingly, purification of this product through a column of chromatography silica with DCM as the eluent afforded a white solid with a significantly different ^{1}H-NMR spectrum to that shown in figure 4.13. Here the purported fourth key proton had shifted upfield and was visible as a doublet of doublets at δ 7.12, whilst the other three complex peaks seen on the ^{1}H-NMR of the crude product also appeared at different chemical shifts (δ 5.48, δ 5.96 and δ 6.15) as doublets (Figure 4.14). These findings indicate that, upon chromatographic separation, a new product (**4.63b**) is obtained to that originally obtained from the reaction mixture, pointing out to a potential rearrangement / isomerisation of the initial adduct during contact with silica.

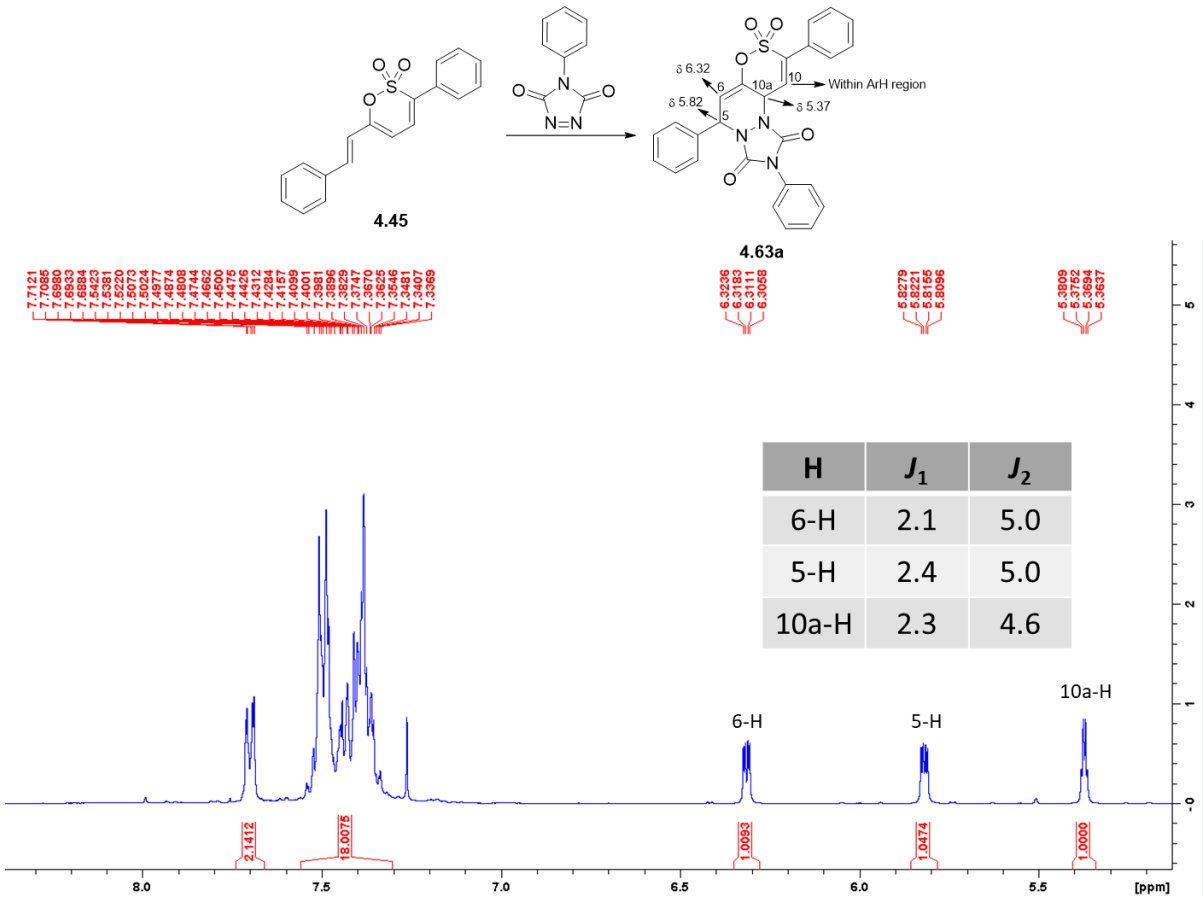

Figure 4.13: ^{1}H-NMR of the crude mixture from the addition of PTAD to the styryl analogue **4.45**

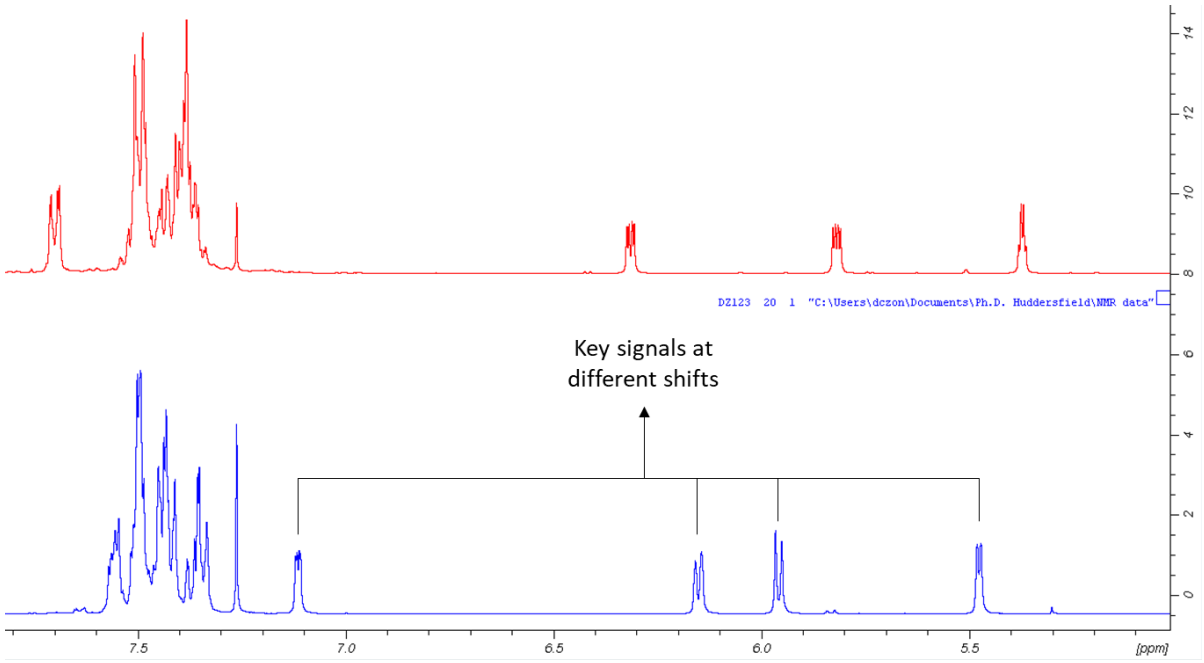

Figure 4.14: ^{1}H-NMR spectrum of the compound of **4.63b**, as obtained from chromatographic treatment (blue), compared with the foregoing spectrum of the respective crude mixture (red)

Performing a Gaussian multiplication on this ^{1}H-NMR spectrum of **4.63b** decreased the line broadening and improved the resolution of the spectrum to reveal that the doublet at δ 6.14 and the doublet of doublets at δ 7.11 to each be doublets of doublets of doublets (ddd), whereas the initial doublets at δ 5.48 and δ 5.96 were found to be doublets of doublets (dd), (Figure 4.15). The coupling constants of these signals are shown in the table of figure 4.15, illustrating specific spatial relationships between the protons which correspond to these signals; The most deshielded of the four (δ 7.11) is adjacent to the most shielded proton at δ 5.48 (*J* = 3.6 Hz), while also being proximal to the proton resonating at δ 6.14 (*J* = 1.7 Hz), as well as to the proton at 5.96 ppm (*J* = 0.5 Hz). Similarly, the proton at δ 6.15 appears to neighbour the proton at δ 5.96 with *J* = 6.1 Hz and be coupled to the protons at δ 7.11 (*J* = 1.7 Hz) and δ 5.48 (*J* = 1.0 Hz). The presence of long-range coupling between the protons at δ 6.15 and δ 7.11, in conjunction with the absence of such coupling for the protons at δ 5.48 and δ 5.96, points to an ABCD pattern for the 4 protons, wherein the two deshielded protons B and C at δ 6.14 and δ 7.11 are placed in close proximity and the two shielded protons (A, D) are placed in the periphery, far enough from each other so that no long-range coupling can occur. This pattern leads to the suggested structure **4.63b** shown below, where the C9-C10 double bond has "migrated" between C10 and C10a (presumably upon contact with silica), so that a central butadiene fragment can connect the olefinic protons, with the aliphatic protons appended on each end of this unit.

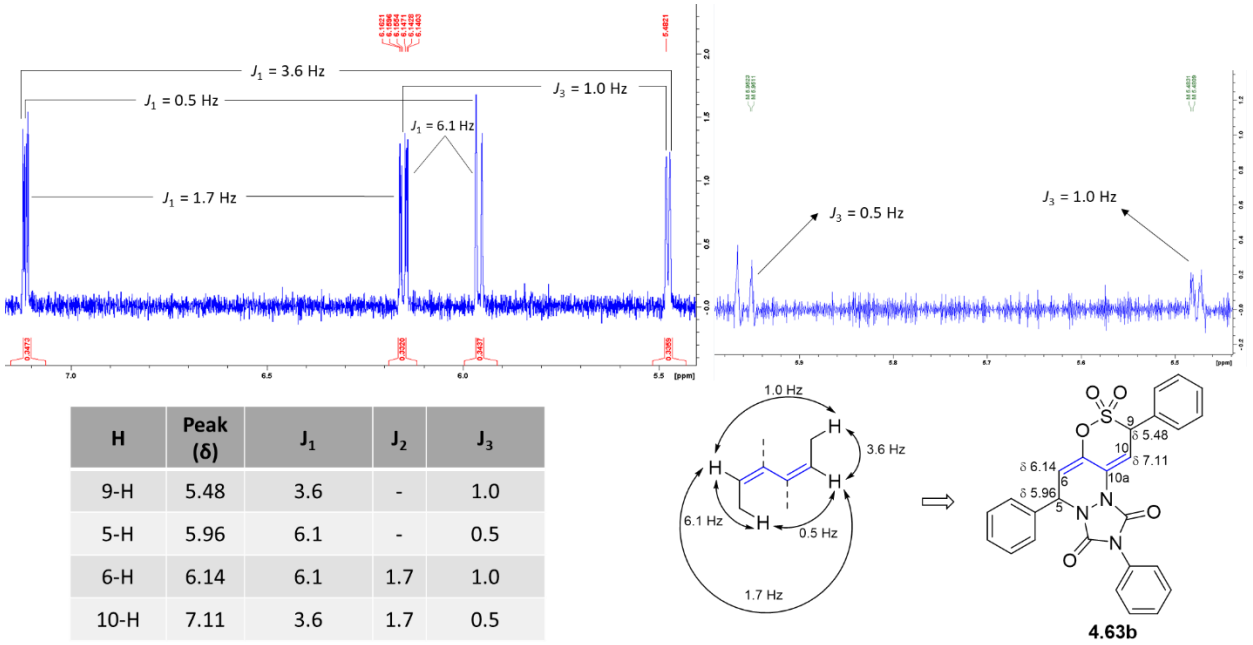

H	Peak (δ)	J_1	J_2	J_3
9-H	5.48	3.6	-	1.0
5-H	5.96	6.1	-	0.5
6-H	6.14	6.1	1.7	1.0
10-H	7.11	3.6	1.7	0.5

Figure 4.15: Spectroscopic features of post-purification product **4.63b**

Additional evidence for the proposed structure **4.63b** was obtained *via* 2D-NMR experiments that provided more information regarding the position of 9-H at δ 5.48 (Figure 4.16). In particular, the HSQC spectrum of **4.63b** suggested that the foregoing proton is situated on a *C* atom that resonates at δ 63.07. Utilising this information, the HMBC spectrum of the compound presented a long-range correlation of this carbon with the adjacent proton at δ 7.11, as well as one with the aromatic protons at *circa* δ 7.56; as theorised, no such correlation was observed with either of the other protons of the tricyclic core (δ 5.96 and δ 6.14), thus this aliphatic carbon had to be pinpointed as the "isolated" 9-position, which is in direct agreement with the butadienyl structure shown above (Figure 4.15).

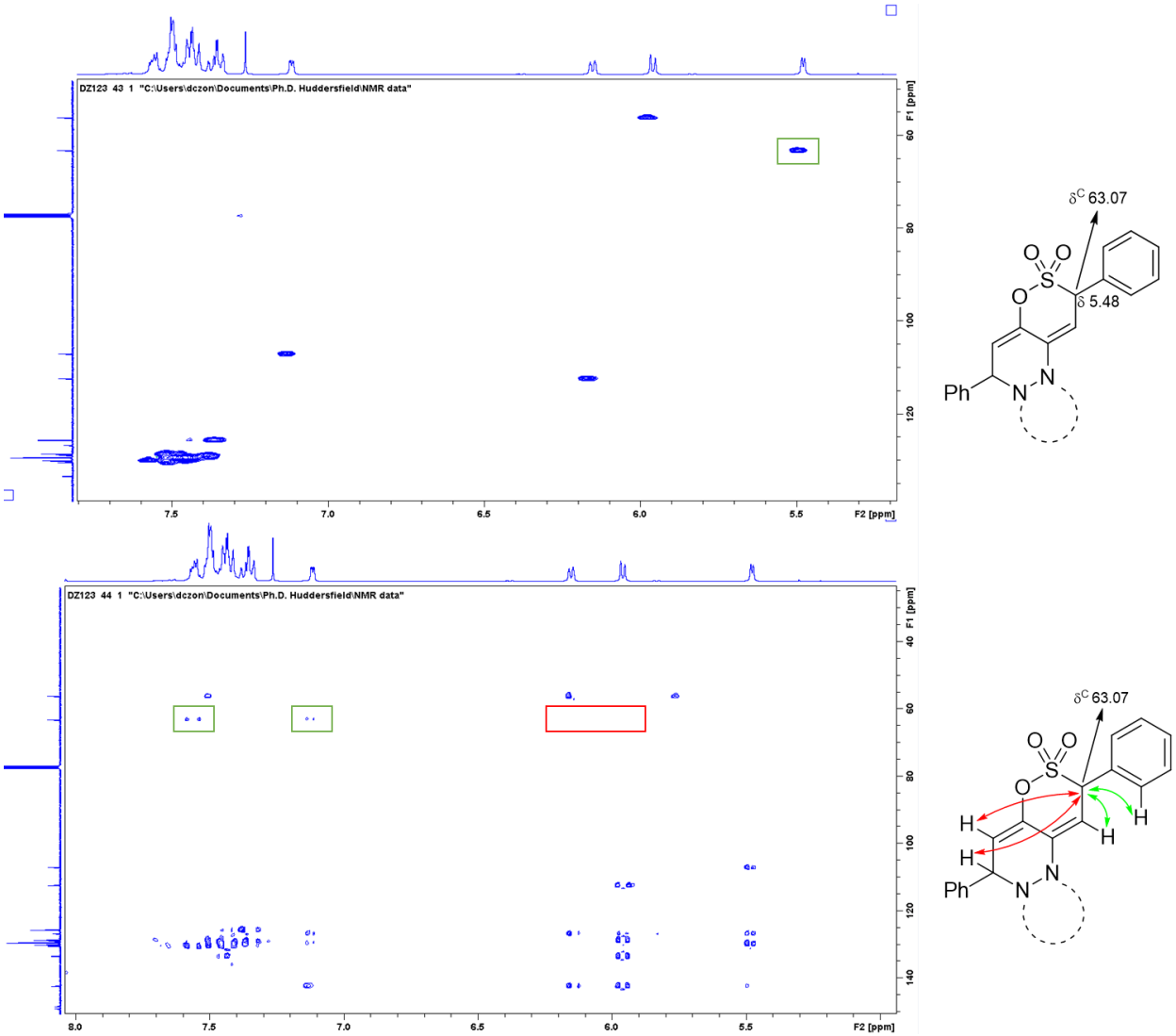

Figure 4.16: Locating the *C* atom of the pivotal proton at 5.48 ppm by HSQC-NMR (above) and placing it on the 9- position by observing two long-range correlations on the HMBC-NMR (below) of **4.63b**, as well as noticing the absence of such correlations (red box) with the other two distanced protons (5-H and 6-H)

At this point, the need to provide definitive evidence of the triazolinedione ring fragment having maintained structural integrity throughout the observed rearrangement became a pressing matter, as it required suitable characterisation data that highlighted the presence of the key functional groups of this heterocycle. Fortunately, the presence of two amide bonds in **4.63b** could be readily utilised in searching for the corresponding vibration frequency of the amide carbonyl group, which was indeed found at 1712 cm^{-1} on the IR spectrum of **4.63b**; the standard vibration frequencies of the SO_3 moiety were also observed at 1384 and 1165 cm^{-1}, thus illustrating the suggested tricyclic scaffold of an 1,2-oxathiine 2,2-dioxide and a triazolinedione ring system.

After the acquisition of these findings, it was postulated that the initial product of the hetero Diels-Alder reaction **4.63a** was susceptible to a migration of the C9-C10 double bond, on account of the acidity of the 10a-H and the consequent activation of the aforementioned vinyl moiety. When in contact with the silica gel, this double bond could cleave the acidic protons of the silanol matrix with concomitant elimination of 10a-H towards the more acid-stable **4.63b** isomer (Scheme 4.31).

It is of special note that this hetero Diels-Alder cycloaddition protocol of PTAD to the 6-styryl 1,2-oxathiine 2,2-dioxide analogue **4.45** affords a 1*H*-[1,2]oxathiino[5,6-*c*][1,2,4]triazolo[1,2-*a*]pyridazine-1,3(2*H*)-dione 8,8-dioxide system which is a novel condensed heterocyclic ring system.

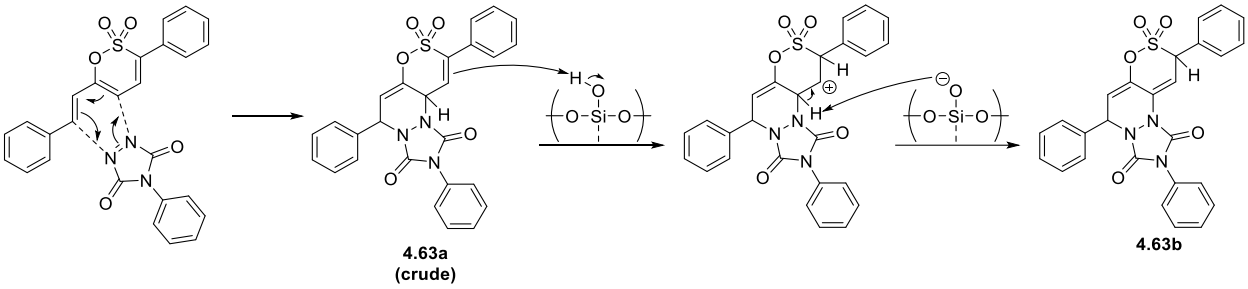

Scheme 4.31: Formation of the tricyclic adduct **4.63a**, followed by silica-mediated isomerisation to **4.63b**

In order to ascertain the reproducibility of this cycloaddition – rearrangement transformation and further establish whether this behaviour is common between this type of polycyclic system, the other styryl analogues **4.46** – **4.48** were also reacted with PTAD under the foregoing conditions and the results of these attempts are summarised below (Table 4.5). Parallel with these attempts, the phenylalkynyl analogue **4.49** was also treated with PTAD under the similar set of reaction conditions, with the starting material **4.49** being retrieved unaltered even upon heating the reaction mixture to reflux, whereas a similar attempt using the furyl analogue **4.50** was also met without success and unfortunately led to the degradation of the compound with no cycloadduct identified.

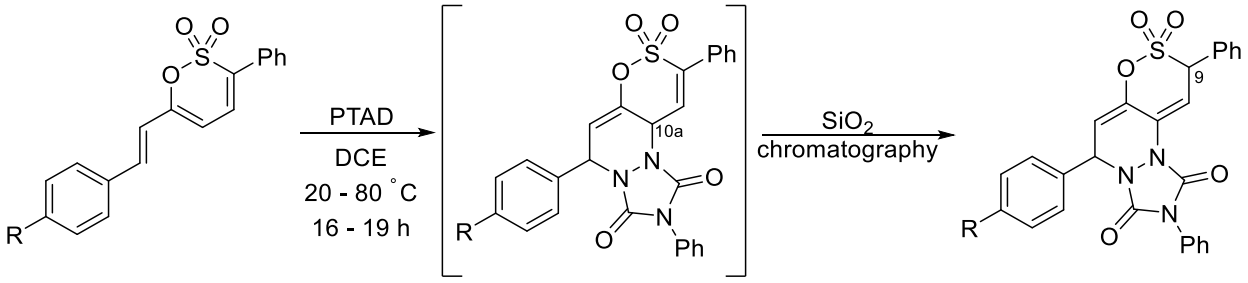

4.45 - 4.48 **4.63a - 4.66a** **4.63b - 4.66b**

Entry	S. M. No.	R	Temperature (°C)	Time (h)	Intermediate No.	10a-H (δ)	Product No.	9-H (δ)	Yield (%)
1	**4.45**	H	20	16	**4.63a**	5.37	**4.63b**	5.48	60.3
2	**4.46**	MeO	20	16	**4.64a**	5.36	**4.64b**	5.48	66.7
3	**4.47**	CF_3	50	19	**4.65a**	5.40	**4.65b**	5.49	38.6
4	**4.48**	NO_2	20 (16 h)/ 80 (22 h)	38	**4.66a**	5.41	**4.66b**	-	n/a*
*Product observed in the ^{1}H-NMR spectrum of the crude mixture but decomposed during purification									

Table 4.5: Attempts towards the formation of variously substituted tricyclic 1,2-oxathiine 2,2-dioxides

The findings in table 4.5 follow the anticipated behaviour of these analogues during a thermal cycloaddition reaction; analogue **4.46** is activated by the electron donating MeO- group and was converted in a higher yield than its non-substituted counterpart (66.7 % over 60.3 %). Similarly, electron withdrawal caused by the CF_3 group prevented the full conversion of the starting material **4.47** and led to a lower yield for the respective tricyclic adduct **4.65b** (38.6 %). Even greater deactivation of the diene

moiety by the *p*-NO_2 group in **4.48** reduced the reactivity even further, with the adduct **4.66a** only being observed in the ^{1}H-NMR spectrum of a reaction mixture aliquot (Figure 4.17).

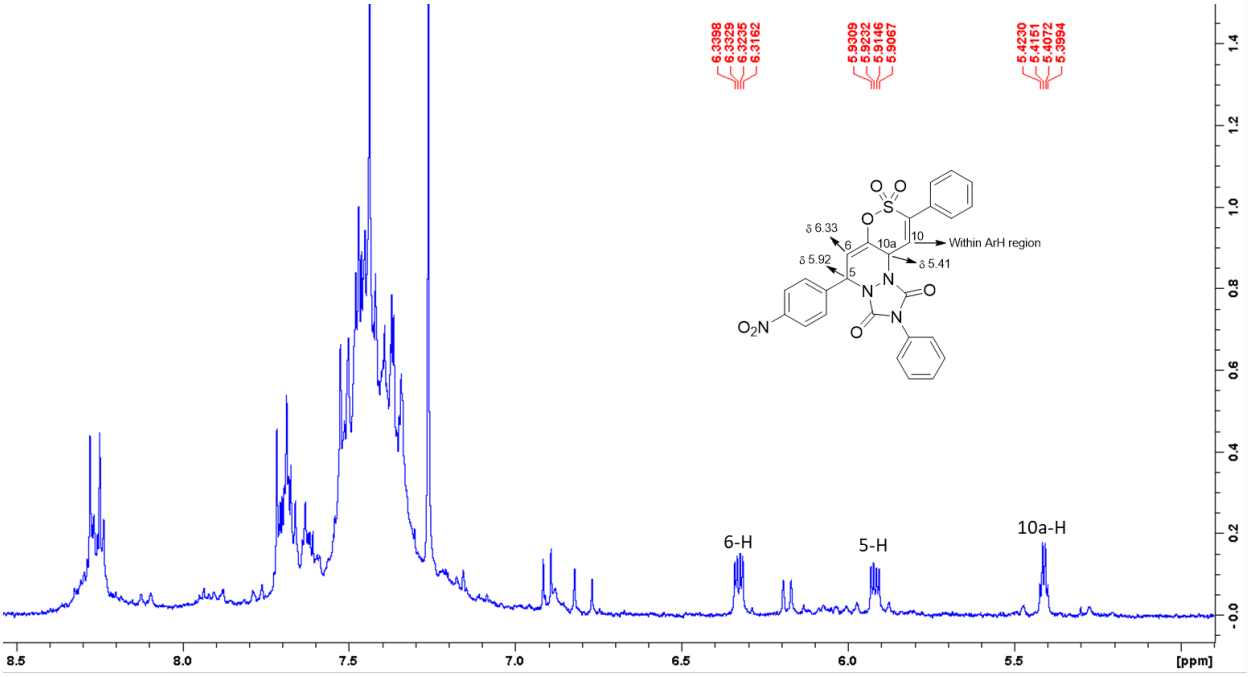

Figure 4.17: ^{1}H-NMR of the crude mixture from the addition of PTAD to the nitrophenyl analogue **4.46**

The isolation of PTAD adducts **4.63b** – **4.65b** prompted the additional challenge of acquiring a pure sample of the initial adduct 4.64a solely for the purposes of the elaboration of the structural relationships that were initially observed on the phenyl analogue **4.63a**. Repeating the PTAD addition on **4.46** and **4.47** afforded the crude adducts **4.64a** and **4.65a**, respectively; all attempts at crystallisation failed to afford pure material, however triturating the crude adduct mixtures with AcMe afforded sufficiently pure, small quantities of each adduct **4.64a** and **4.65a**, without any reorganisation of their structure. Unfortunately, this trituration process was accompanied by very significant loss of mass and would thus be unsuitable as a general purification protocol. The methoxy analogue **4.64a** merited a useful example of identifying the location of the key protons through 2D NMR spectroscopic techniques, as well as confirming the foregoing structural rearrangement by comparison with data from the silica-treated **4.63b**.

Starting with the COSY spectra of **4.64a**, the correlations found between the aliphatic proton at δ 5.37 and the protons at δ 5.79 and δ 6.39 points out the proximity of 5-H and 6-H to the central 10a-H, which can be achieved in a 1,4-dihydropyridazine scaffold (Figure 4.18). These correlations disappear in the COSY spectrum of **4.64b**, constituting evidence of a migration of the aliphatic proton of the 10a- position away from 5-H and 6-H. Moreover, the absence of any correlations between the olefinic protons at δ 6.13 and δ 7.09 on the COSY spectrum of **4.64b** confirms the earlier postulation that the two aliphatic/olefinic proton pairs are distanced with each other in this analogue.

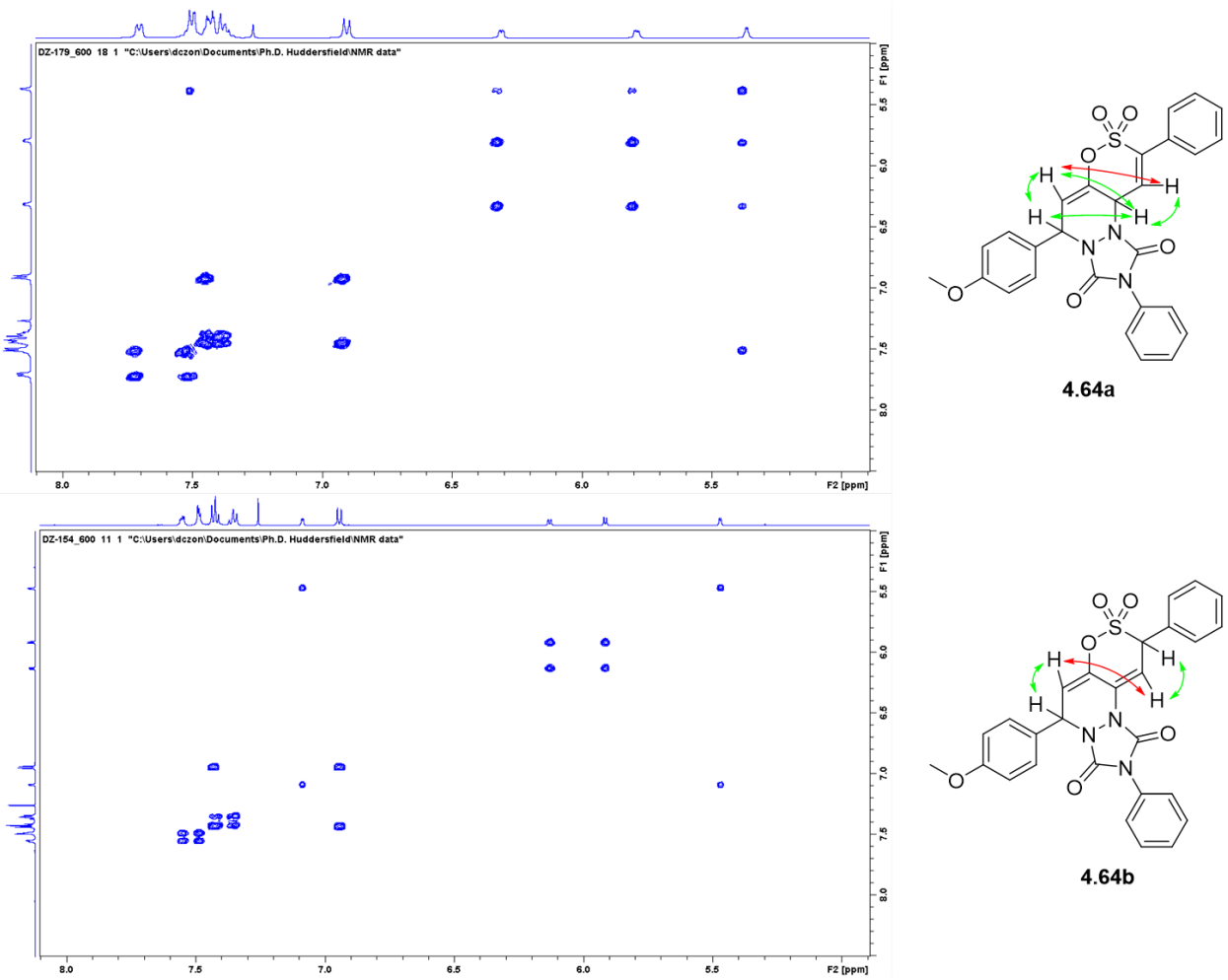

Figure 4.18: Differences in the COSY correlations between **4.64a** and **4.64b** highlighting the silica-enabled migration of the aliphatic 10a-H

Placing the migrating proton on the carbon adjacent to the SO_2 group (C9) on **4.64b** can be cross-checked by examining its proximity to the phenyl group that is appended on this carbon. Performing NOESY experiments for **4.64a** and **4.64b** cements this hypothesis (Figure 4.19); the absence of a correlation between the *ortho* aromatic protons at δ 7.70 and the aliphatic proton at δ 5.36 on **4.64a** requires the interjection of the vinyl 10-H (δ 7.49) between these two proton environments to prevent any spatial proximity, whereas further absence of correlations with any of the aromatic protons on the compound necessitates that the proton at δ 5.36 occupies the central 10a- position.

Conversely, such contours can be observed on the NOESY spectrum of **4.64b**, wherein the respective aliphatic proton at δ 5.48 is in clear proximity with the distinct *ortho* aromatic protons of the 9-phenyl group (δ 7.55). A similar contour is seen for the vinyl 10-H (δ 7.09) and these two aromatic protons, albeit having a lower magnitude than the aforementioned contour of the aliphatic proton 9-H; this drop in contour "intensity" indicates that this aliphatic proton occupies a position closer to the 9-phenyl group than the vinyl proton, thus placing it on the 9- position. The aliphatic/olefinic pair of 5-H and 6-H shows analogous correlations with the proximal aromatic protons of the anisyl group on both isomers, thus illustrating that this side of the tricyclic system is not affected throughout treatment with silica. The foregoing findings for both pairs of isomers **4.63a/b** and **4.64a/b** establish repeating structural patterns for their tricyclic backbone units, thus unequivocally assigning the 10a-hydro structure for the pre-silica derivatives **4.63a** – **4.66a** and the 9-hydro structure for the rearranged derivatives **4.63b** – **4.66b**.

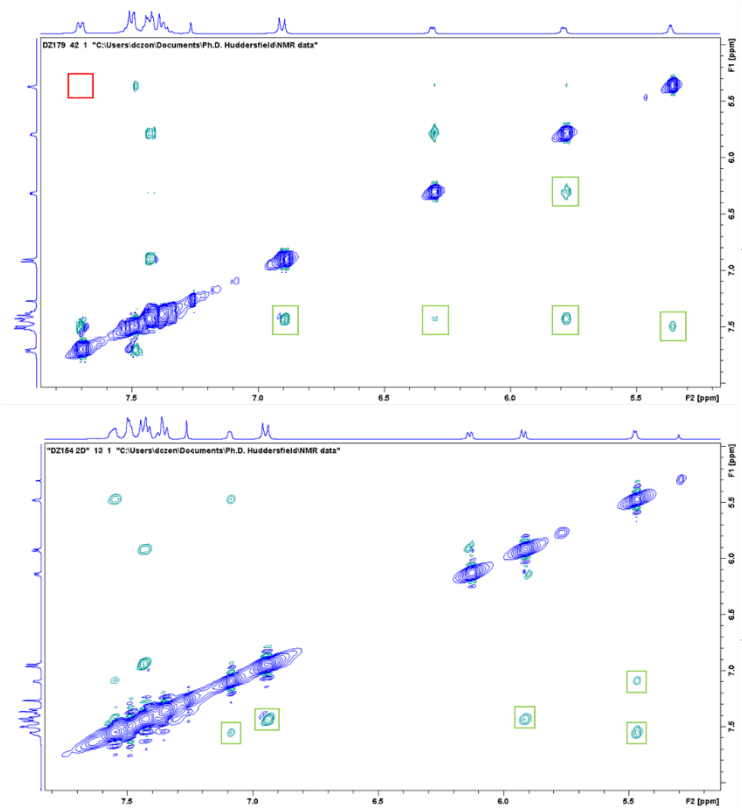

4.64a

H	Peak (δ)
10a-	5.36
5-	5.78
6-	6.31
10-	7.49

4.64b

H	Peak (δ)
9-	5.48
5-	5.92
6-	6.13
10-	7.09

Figure 4.19: Spatial proximity of pivotal protons on **4.64a** and **4.64b** supporting their suggested structures

In conjunction with the foregoing spectroscopic data, mass spectrometry was employed to verify the occurrence of an isomerisation process and not any other, "molecular weight-altering" reaction. Examination of the mass spectrum of the pre-silica adduct **4.65a** shows that the compound is observed as the $[M-H]^-$ molecular ion with an *m/z* value of 552.0846, which is in quite good agreement with the calculated *m/z* value of 552.0843 for $C_{27}H_{18}F_3N_3O_5S$. A different molecular ion, $[M+H]^+$, is observed on the respective mass spectrum of **4.65b**, with the *m/z* value of 576.0815 matching the calculated value of 576.0819 for the aforementioned $C_{27}H_{18}F_3N_3O_5S$ formula. Evident of the identical chemical formulas of the two adducts **4.65a** and **4.65b**, this data indicates that the molecular weight of **4.65a** is preserved during contact with silica, thus clearly pointing out to a isomerisation process towards **4.65b**.

Although the foregoing spectroscopic data provided multifaceted evidence of the suggested structures and *in silica* transformations, the complexity of these cycloadducts suggested the need for X-ray crystallography in order to confirm their structural features by examining their crystal structures. Unfortunately, all attempts to grow crystals of suitable quality for X-ray crystallographic analysis were unsuccessful, as these compounds appear inclined to form amorphous material (*i.e.* fine powders), rather than crystals with established matrices.

The foregoing explorations of PTAD cycloadditions highlighted that the hetero-dienophile interacted with the styryl-substituted 1,2-oxathiine 2,2-dioxides **4.45** – **4.48** in a regioselective [4+2] process, despite the presence of a double bond between C3 and C4 on the 1,2-oxathiine ring core. The phenyl substituent on the 3- position was thought to deter contact with PTAD in a potential [2+2] addition, but in the absence of such a group, as in the 6-styryl analogue **4.67**, it was postulated that PTAD could initially interact with the diene moiety of **4.67** towards the established mono-adduct **4.68** with concomitant disruption of the three-double bond conjugated system, leading to the reactive C3-C4 double bond being available for cycloaddition towards the bis-adduct **4.69** (Scheme 4.32).

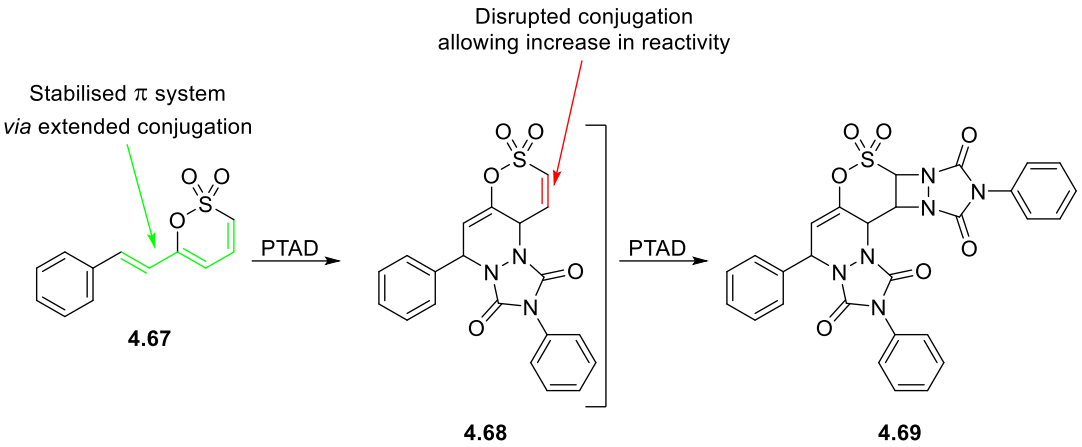

Scheme 4.32: Suggested route of "double" PTAD addition towards polycyclic adduct **4.69**

In order to examine this potential transformation, a solution of **4.67** and 1 eq of PTAD in 1,2-DCE was stirred at room temperature overnight, with gradual loss of the characteristic wine red colour. TLC monitoring showed that the reaction was incomplete, hinting at the formation of 0.5 eq of the theorised adduct **4.69** and 0.5 eq the starting material remaining unreacted. Interestingly, addition of a second equivalent of PTAD and stirring the reaction mixture for further 3 h did not complete the conversion, whereas the ^{1}H-NMR spectrum of a reaction mixture aliquot showed three complex signals that mirrored the ones observed for the 3-phenyl analogue **4.63a** (Figure 4.13). Heating the solution at 50 °C appeared to drive the reaction further towards completion (indicative of a thermodynamic conversion) and the resulting crude mixture was purified in a silica column as established earlier. Examination of the ^{1}H-NMR spectrum of the obtained solid provided particularly insightful data about this conversion (Figure 4.20).

H (δ)	$J_{H/H'}$	$^{3}J_{anti/syn}$	^{3}J	$^{5}J_{l\text{-}r}$	$^{6}J_{l\text{-}r}$
4.26	17.6	5.5/4.9	-	-	0.7
5.93	-	-	6.0	-	-
6.11	-	-	6.0	1.7	0.7
6.98	-	5.5/4.9	-	1.7	0.7

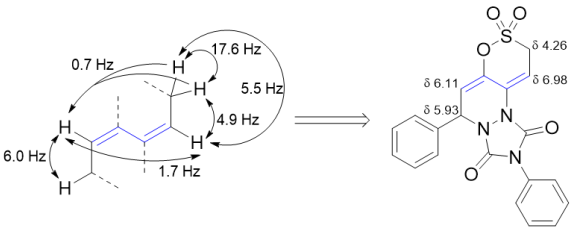

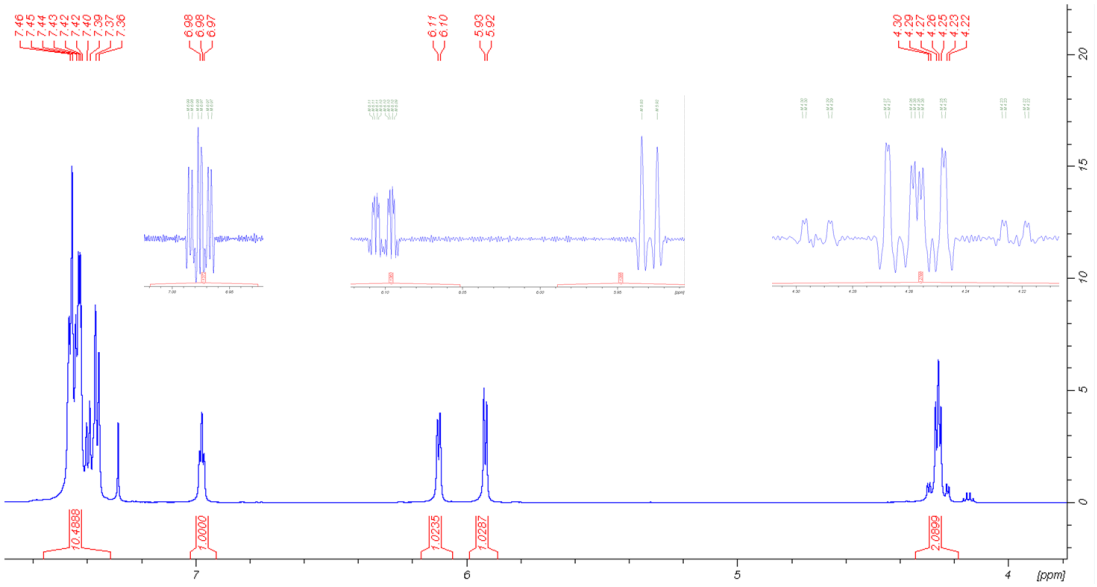

Figure 4.20: ^{1}H-NMR spectrum of **4.70** depicting the spin pattern seen for previous PTAD adducts (inserts show regions of the same spectrum after Gaussian multiplication)

The four signals commonly found amongst the isomerised adducts **4.63b** – **4.66b** were also observed in this case, although the most upfield one was found to correspond to two diastereotopic protons as a doublet of doublets of doublets (ddd). The same multiplicity was seen for the signals at δ 6.11 and δ 6.98, whilst the proton at δ 5.93 was found to be split only by the proton at δ 6.11. The presence of two diastereotopic protons as part of a methylene unit could be confirmed by use of DEPT ^{13}C-NMR spectroscopy (Figure 4.21). Two aliphatic signals resonating at δ 46.92 and δ 56.05 are seen on the ^{13}C-NMR of **4.70**, with the one δ 46.92 appearing negatively phased on the DEPT90 ^{13}C-NMR spectrum, which points out to the anticipated CH_2 carbon environment. This finding, in conjunction with the overwhelming resemblance of the ^{1}H-NMR spin pattern of **4.70** with the spectra recorded for the phenyl analogues **4.63b** – **4.66b**, provides unequivocal evidence that the mono-adduct **4.68** is the sole product of this attempt, with the assorted, silica-mediated rearrangement occurring as usual to produce the regioisomer **4.70** in 69.8 % yield.

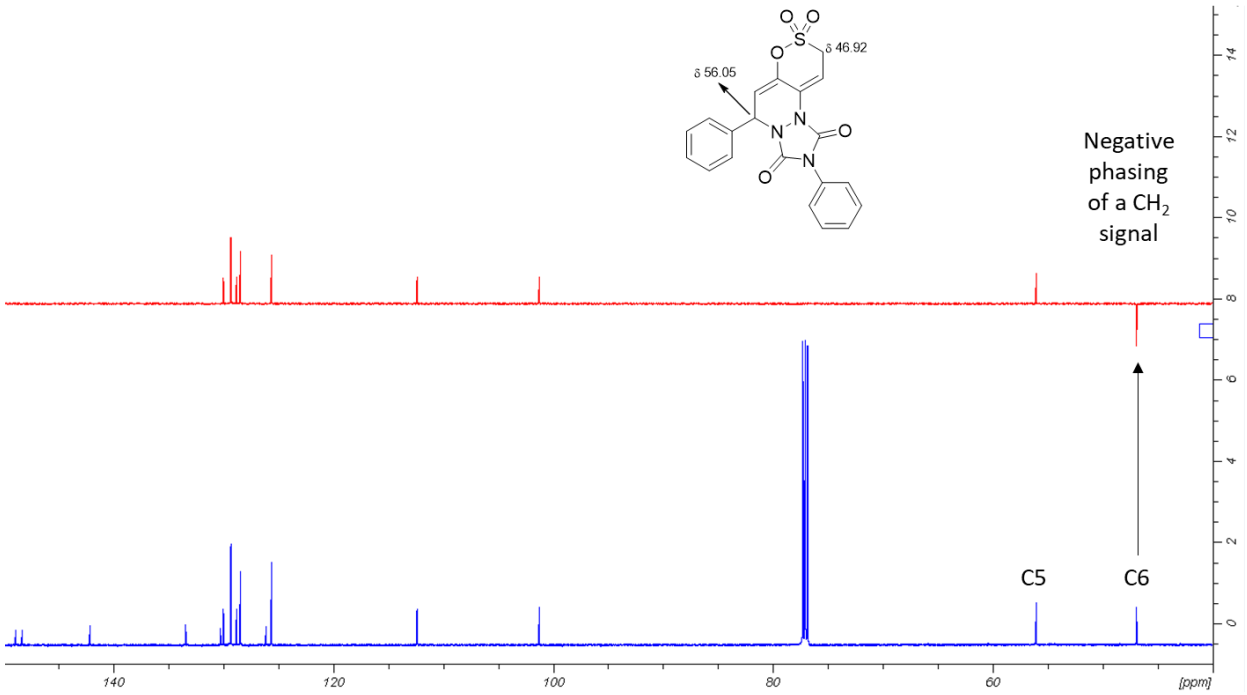

Figure 4.21: (Below) ^{13}C-NMR spectrum of **4.70**, (above) DEPT90 ^{13}C-NMR spectrum of **4.70**, showing the negatively phased CH_2 signal

Upon the confirmation of its structure, the formation route for **4.70** can substantiate further insights on the compatibility of 1,2-oxathiine 2,2-dioxides with PTAD. The conclusion that no [2+2] cycloaddition occurs even at 2 eq of PTAD is a clear indication that the C3-C4 double bond of the 1,2-oxathiine ring system can be kept inactive towards PTAD at room temperature, potentially due to low reactivity by virtue of the adjacent, electron-withdrawing SO_2 function (Scheme 4.27). With the cycloaddition occurring regioselectively towards **4.68**, the aforementioned C3-C4 double bond is unencumbered and is readily protonated by the acidic silanol matrix towards **4.70** (Scheme 4.33).

After the PTAD addition to a styryl analogue with no substituent on the 3-position, the same conversion was attempted on a styryl derivative bearing an electron-withdrawing 3-aryl substituent, in order to further assess the influence of this position on the behaviour of these 1,2-oxathiine 2,2-dioxide analogues in the presence of this hetero-dienophile. To that end, the 3-(4-trifluoromethylphenyl)-6-styryl 1,2-oxathiiine derivative **4.40** was treated with PTAD following the foregoing method and performing a chromatographic purification of the crude product. Unfortunately, even after a prolonged heating period at 50 °C, the cycloaddition product **4.71** was only obtained at 17.6 % yield, as evidenced by the key four

signals on the ^{1}H-NMR spectrum of the isolate product (Scheme 4.34), indicating a significant deactivating effect credited to the 3-trifluoromethylphenyl group of the 1,2-oxathiine core unit.

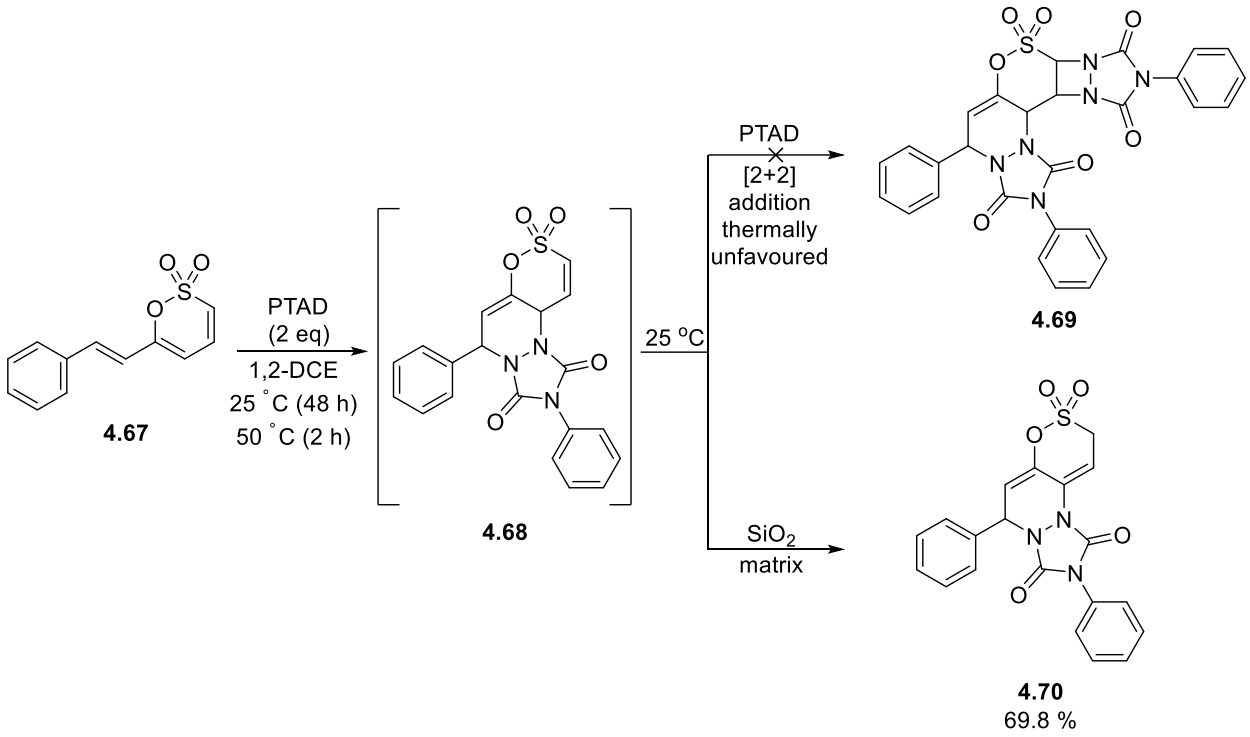

Scheme 4.33: Regioselective [4+2] addition of PTAD to **4.67** with subsequent rearrangement towards **4.70**

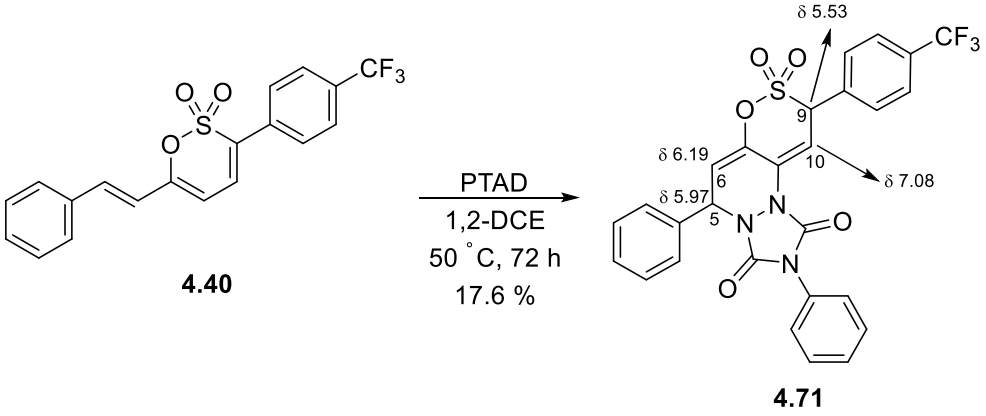

Scheme 4.34: Attempt at the addition of PTAD to the 3-trifuoromethylphenyl analogue **4.40**

Following the thorough exploration of PTAD addition to the series of styryl substituted 1,2-oxathiine 2,2-dioxides, a series of different dienophiles were examined in their ability to undergo similar transformations with the styryl analogues **4.46** and **4.47**. These attempts at Diels-Alder conversions are shown in table 4.6.

Unfortunately, the methoxy-containing 6-styryl 1,2-oxathiine system **4.46** was found to be completely inactive when heated to various temperatures in the presence of different dienophiles, *i.e.* dimethyl fumarate, maleic anhydride and dimethyl acetylenedicarboxylate (DMAD). In all cases, the starting material either decomposed due to prolonged heating times or it was retrieved unchanged. A variation of such a transformation was attempted with **4.47** and 3,4-dihydro-2*H*-pyran in an inverse demand Diels-Alder addition attempt, but even after 6 days of heating the two compounds in *o*-xylene, no adducts were observed by either TLC or ^{1}H-NMR spectroscopy.

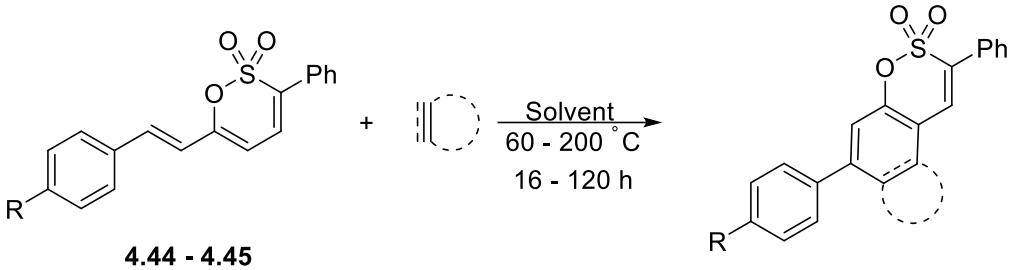

4.44 - 4.45

4.65 - 4.69

Entry	S. M. No.	R	Dienophile	Product No.	Solvent	Temperature (°C)	Time (h)	Yield (%)
1	**4.46**	MeO	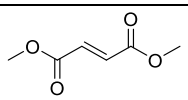	**4.72**	PhMe	110	120	0.0
2	**4.46**	MeO	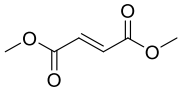	**4.72**	Ph_2O	200	16	0.0
3	**4.46**	MeO	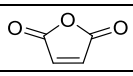	**4.73**	PhMe	80	16	0.0
4	**4.46**	MeO	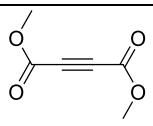	**4.74**	-	195	16	10.0*
5	**4.47**	CF_3		**4.75**	*o*-xylene	80	120	0.0
*Aromatised derivative obtained instead (**4.76**).								

Table 4.6: Diels-Alder attempts using the styryl analogues **4.46** and **4.47**

Of note is the attempt at the cycloaddition of DMAD to **4.46** (Entry 4, Table 4.6) in the absence of solvent. In this instance, the aromatised adduct (dimethyl 7-(4-methoxyphenyl)-3-phenylbenzo[*e*][1,2]oxathiine-5,6-dicarboxylate 2,2-dioxide) **4.76** was isolated in 10.0 % yield, presumably upon dehydrogenation of the nascent Diels-Alder product **4.74** (Scheme 4.35). This derivative was serendipitously isolated during chromatographic separation of the crude mixture components and an examination of the ^{1}H-NMR spectrum showed singlets at δ 7.41 and δ 7.63, along with 3 aliphatic singlets at δ 3.65, δ 3.86 and δ 3.93, suggestive of a structure with 2 protons on the central polycyclic unit (Figure 4.22). This requisite is met for the fused structure **4.76**, whereas the presence of two ^{13}C-NMR signals at δ 165.94 and δ 167.71 also indicates the presence of the two ester moieties which are appended on the central phenyl unit. Furthermore, the vibrations of these groups are observed in the IR spectrum appear as stretches at 1719 and 1728 cm^{-1}, falling within the range where ester C=O vibrations are commonly observed. Locating the established SO_3 vibration frequencies at 1180 and 1373 cm^{-1} reassures that the 1,2-oxathiine ring has been preserved, thus definitively proving that this side-product has the proposed 1,2-benzooxathiine structure. It should finally be noted that this observed DMAD addition/ aromatisation sequence constitutes a novel route towards benzo-fused 1,2-oxathiine 2,2-dioxide ring systems, which may form an attractive strategy to construct diversely substituted analogues upon future optimisation to ameliorate yields.

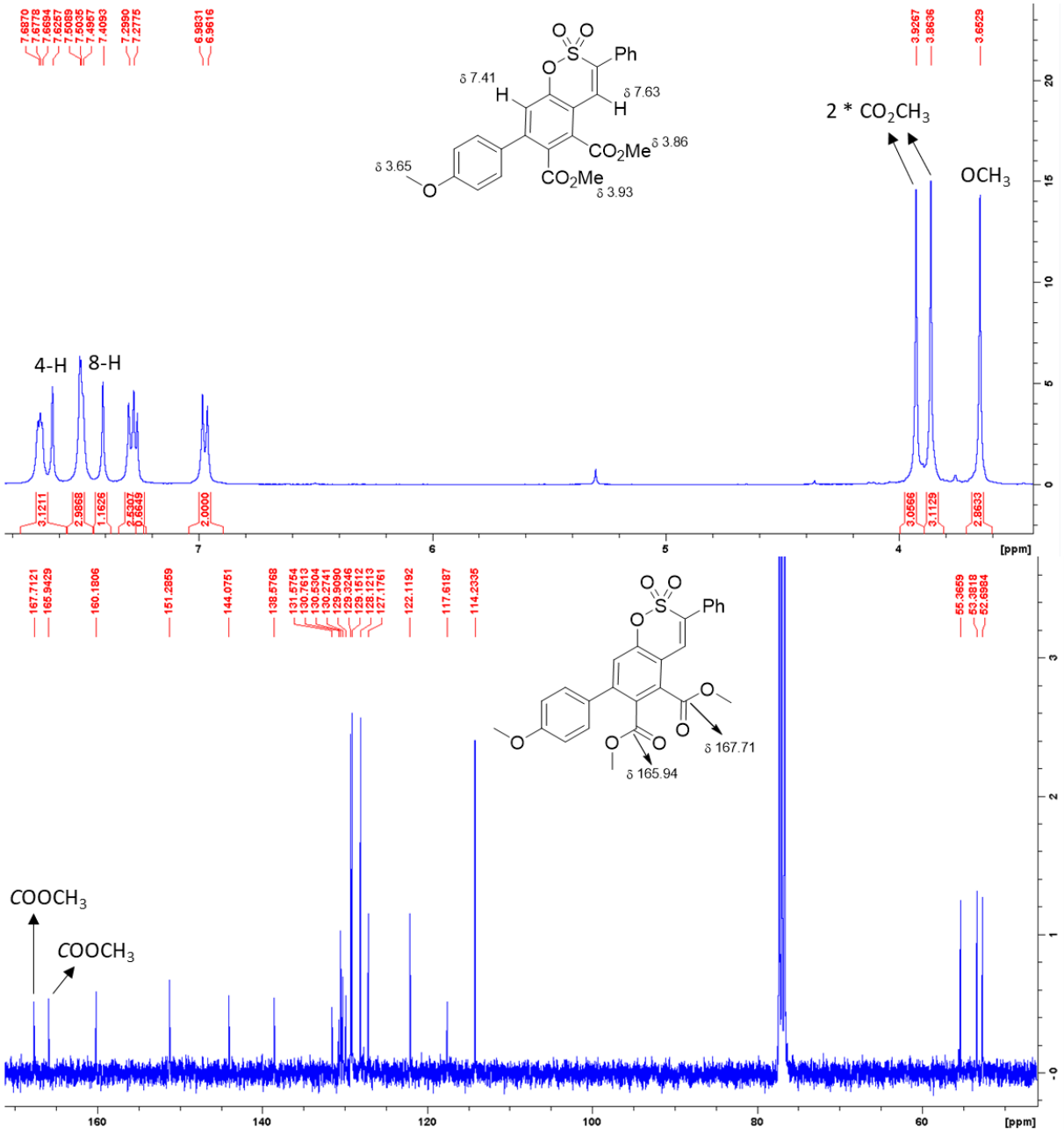

Figure 4.22: ^{1}H-NMR (above) and ^{13}C-NMR (below) spectra of side-product **4.76**

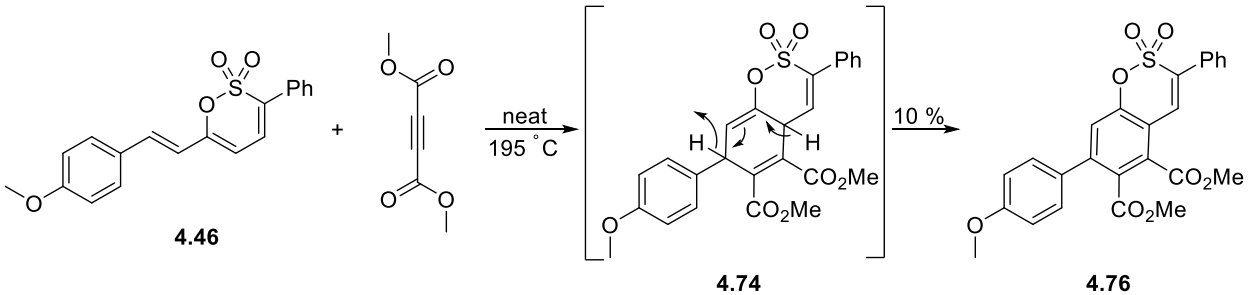

Scheme 4.35: Formation of the Diels-Alder adduct **4.74**, followed by its dehydrogenation towards the aromaticity-stabilised benzo derivative **4.76**

4.4.3 Attempted benzyne addition to 1,2-oxathiine 2,2-dioxides

The last reaction which was used to probe the reactivity of 1,2-oxathiine 2,2-dioxide systems was the addition of benzyne, in an attempt to explore the diene-like properties of the C3-C6 diene moiety in less forcing conditions than those seen in the preceding literature.[41,42] The reactive benzyne species has been met with great interest in recent literature and the most convenient method of preparation involves the use of a disubstituted benzene precursor, *i.e.* 2-(trimethylsilyl)phenyl trifluoromethanesulfonate **4.77** (Scheme 4.36). The silicon centre on this compound has high affinity to fluorine, so interaction with a fluoride source, *e.g.* CsF, would allow for the cleavage of the trimethylsilyl group and the sulfonate ion to furnish the beznyne intermediate *in situ*.[204,242] In accordance with this preparation protocol, adding a MeCN solution of 2-(trimethylsilyl)phenyl trifluoromethanesulfonate **4.77** in a solution of the 6-anisyl analogue **4.78** with suspended CsF and stirring the resulting mixture overnight at room temperature yielded a non-polar product (**4.80**) in a meagre 8.2 % yield which was identified as 1-(4-methoxyphenyl)naphthalene by comparing the ^{1}H-NMR signals with literature-sourced data (Figure 4.23). The isolation of this compound indicated that, upon their interaction, the 6-anisyl 1,2-oxathiine substrate and the *in situ* formed benzyne species must undergo a cycloaddition reaction towards a bridged bicyclic adduct (**4.79**), which presumably collapses into the 1-substituted naphthalene system **4.80** through loss of an SO_3 fragment *via* a retro Diels-Alder process (Scheme 4.36).

Despite the low yield, this transformation showed that the 1,2-oxathiine 2,2-dioxide ring system had potency for interacting with benzyne in cycloaddition processes, thus pointing out to further explorations of this reaction by varying the substitution pattern of the reacting heterocycle. To that end, four phenyl-substituted 1,2-oxathiine analogues **4.4** – **4.7**, along with the 6-(4-cyanophenyl) derivative **4.81**, were reacted in a similar manner with benzyne with a view to their conversion into substituted naphthalenes; the results of these attempts are presented in table 4.7.

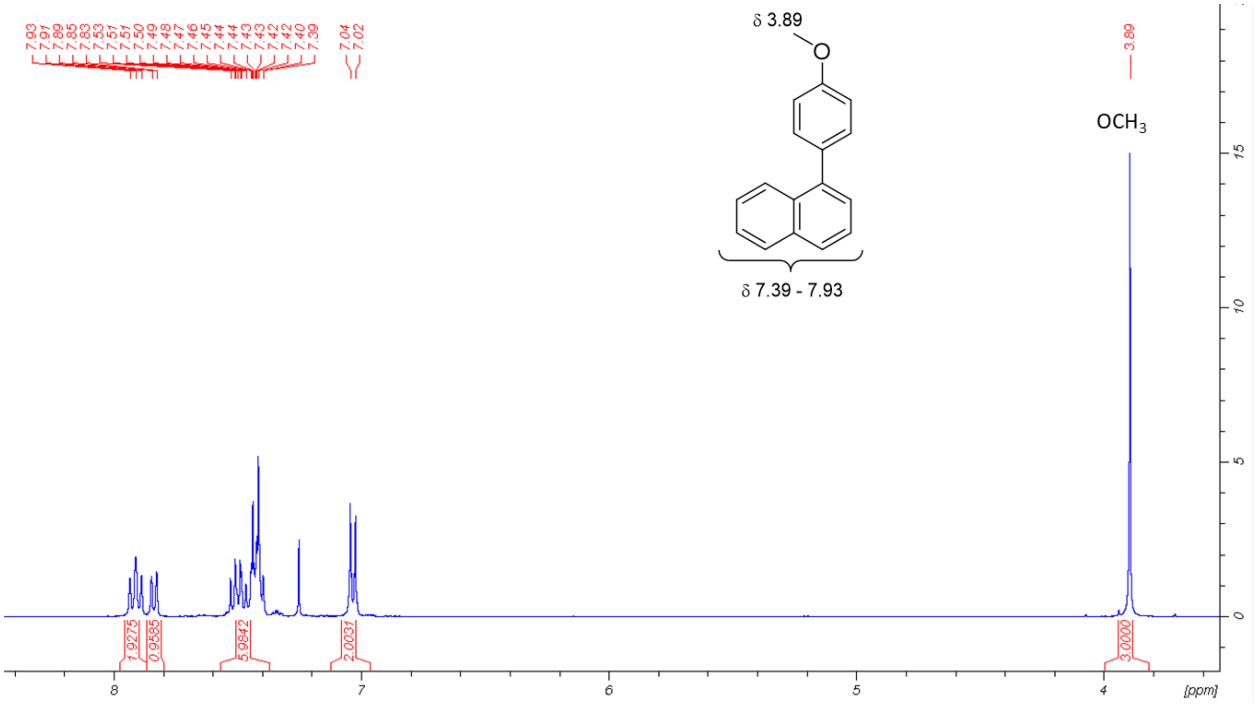

Figure 4.23: ^{1}H-NMR spectrum of **4.80**

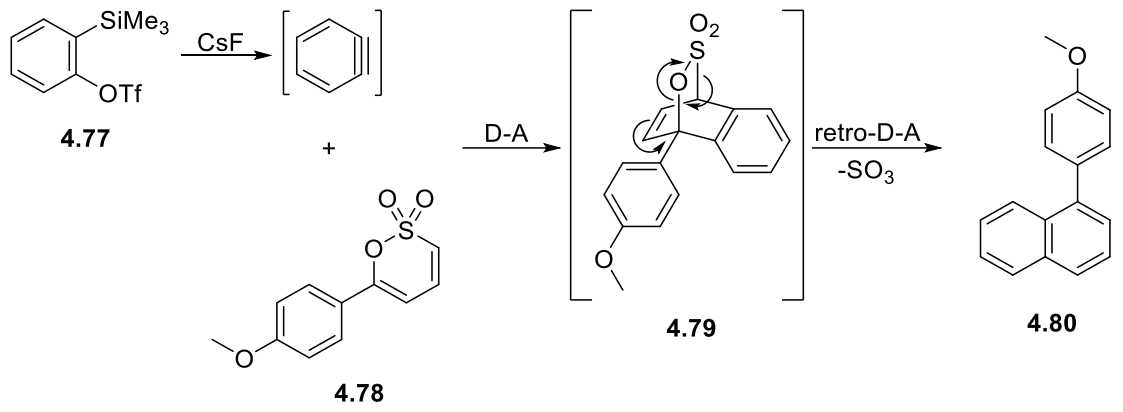

Scheme 4.36: Generation of benzyne species and subsequent addition to a 1,2-oxathiine 2,2-dioxide analogue (**4.78**)

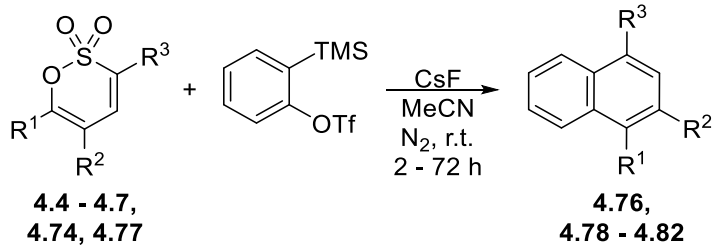

Entry	S.M. No.	R^1	R^2	R^3	Product No.	Time (h)	Yield (%)
1	**4.74**	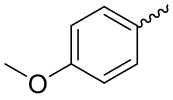	H	H	**4.80**	16	8.2
2	**4.6**	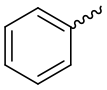	H	H	**4.82**	2	0.0
3	**4.81**	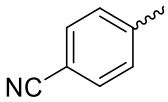	H	H	**4.83**	2	0.0
4	**4.5**	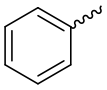	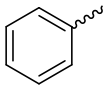	H	**4.84**	2.5	0.0
5	**4.4**	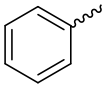	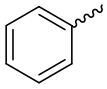	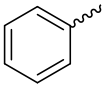	**4.85**	3.5	32.0
6	**4.7**	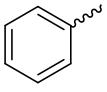	H	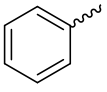	**4.86**	16	22.0

Table 4.7: Attempted cycloaddition of benzyne to 1,2-oxathiine 2,2-dioxide analogues

The findings in table 4.7 portray an interesting reactivity profile for the interaction of 1,2-oxathiine 2,2-dioxides with benzyne. Comparing the results for the naphthalene derivatives **4.80**, **4.82** and **4.83** clearly indicates that starting analogues with only one aryl group on the 6-position appear to be completely inactive and require an ED substituent as part of the aryl group to manifest diene-like behaviour. Introducing a second phenyl group, as is the case with starting analogue **4.5**, does not appear to improve the reactivity, as no naphthalene product was obtained from this attempt. However, the presence of three phenyl groups on the 3-, 5- and 6- positions of the 1,2-oxathiine 2,2-dioxide scaffold appears to offer much

better results, with the 1,2,4-triphenylnaphthalene adduct **4.85** being isolated in 32.0 % yield. With the 3- and 6- substituents in place, the absence of the 5-phenyl group appears to be mildly detrimental to the conversion, as the 1,4-diphenylnaphthalene product **4.86** could be isolated in a lower yield than its triphenyl counterpart (22.0 % over 32.0 %). Of note is the fact that the initial reaction time of 16 h (overnight, *e.g.* anisyl analogue **4.80**) had to be reduced to 2 - 3.5 h for subsequent analogues, on account of additional side-products being observed by TLC as weak spots over longer time periods. An exception to this modification was seen in the case of the 1,4-diphenyl analogue **4.86**, wherein the presence of phenyl groups on the two ends of the diene moiety is presumably able to direct the benzyne species towards the desired [4+2] cycloaddition.
This substituent-mediated increase in diene-like activity provides additional information about the chemical reactivity of 1,2-oxathiine 2,2-dioxides, albeit offering moderate to low conversion yields which require future optimisation. Evidently, phenyl groups on the 3- and 6- position of the 1,2-oxathiine unit are pivotal for the conversion to occur in a tangible yield, whereas 5-phenyl substitution is capable of a beneficial effect only in cases when the aforementioned heterocyclic core is already activated on the "termini" of the diene moiety (Figure 4.24).

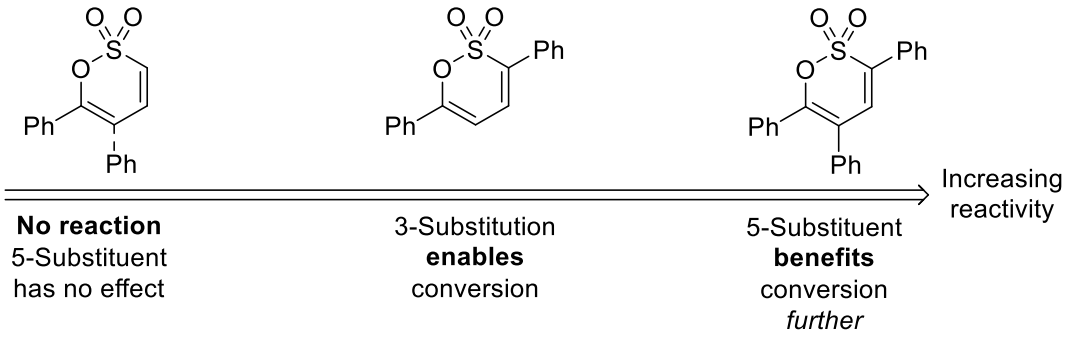

Figure 4.24: Effect of different substitution patterns in the success of benzyne addition

It should finally be noted that the foregoing transformations constitute the first examples of a Diels-Alder/retro Diels-Alder process involving 1,2-oxathiine 2,2-dioxide heterocycles without the use of forcing conditions (such as high temperatures and pressures), while they also highlight the general effect that the ambient substituents have on directing the reactivity of the 1,2-oxathiine centre unit towards further functionalisation.

To summarise, the reactivity of 1,2-oxathiine 2,2-dioxides was probed by use of four prominent, phenyl-substituted analogues. After the examination of how these compounds behaved in the presence of molecular bromine, the successfully synthesised brominated derivatives were tested in bromine-lithium exchange processes and Pd-catalysed cross-coupling reactions. The former did not provide any tangible results, while the latter allowed for the functionalisation of the brominated positions, despite persisting limitations. Employing a C-H activation cross-coupling method as an alternative was found to solve the setbacks encumbering previous functionalisation protocols, whereas the dimerisation side-reaction of the 1,2-oxathiine 2,2-dioxide starting materials that was prevalent throughout the palladium chemistry explorations was thoroughly examined. The styryl, ethynyl and furyl analogues were also utilised in the attempt to expand the 1,2-oxathiine 2,2-dioxide scaffold into more complex polycyclic structures *via* cycloaddition reactions, wherein the most prominent was the addition of PTAD to styryl-containing derivatives. The structure of these hetero Diels-Alder products was elucidated by various 2D-NMR spectroscopic techniques and their behaviour on exposure to silica was tentatively examined. PTAD was also attempted to interact with the diene moiety of the 1,2-oxathiine 2,2-dioxide unit without any success, prompting the use of benzyne as a prospective dienophile. Albeit at a limited extent, the [4+2] addition

of benzyne to the 1,2-oxathiine starting materials was ascertained but found to occur only in analogues where the two ends of the diene moiety were phenyl-substituted.

CHAPTER 5: CONCLUSIONS

5.1 General comments

The results and discussion presented in the previous three chapters of this thesis provide a multitude of information with respect to the enaminoketone precursors, the 3,4-dihydro-1,2-oxathiine 2,2-dioxide sulfene adducts and the unsaturated 1,2-oxathiine 2,2-dioxide systems. The conclusions that derived from evaluating this information are summarised in the following sections.

5.2 Conclusions Pertaining to Chapter 2

The enaminone derivatives, which were used as the fundamental precursor units for the development of 1,2-oxathiine 2,2-dioxide systems, were synthesised in 51 – 99 % yields from the reaction of α-methylene-containing ketones and DMFDMA. After using different reaction conditions (*i.e.* reflux of neat compounds, use of solvent, organocatalysis) and tailoring the synthetic protocol to the requirements of each starting material, a library of enaminone analogues was successfully compiled. The characterisation of these species by NMR spectroscopy presented consistent features, with the key alkenyl protons resonating as either a pair of doublets in the range δ 5 – 8 with *J* of the order of 12.5 Hz (mono-substituted analogues) or a singlet in the range δ 7 – 8 (di-substituted analogues). The aliphatic protons on the NMe_2 moiety of these compounds were of particular interest, as their ^{1}H-NMR signals could be used as a direct indicator for the electron density throughout the enaminone structural scaffold. Electron-withdrawing substituents, as well as the absence of a 2-substituent, appear to allow for the delocalisation of electrons between the *O* and *N* termini, resulting in a higher order C-N bond with relatively reduced rotation about the bond and subsequent non-equivalence of the methyl groups of the NMe_2 unit.

Furnishing enaminone analogues with two enamine functions on their structure proved to be more challenging than it was described in the relevant literature. It appears that the addition of the first dimethylaminomethylene unit to a ketone precursor with two α-methylene groups drastically reduces the reactivity of the second set of α-protons, leading to a thermodynamic barrier for the formation of a "double enaminone" system. This conclusion contradicts preceding research work claiming that such derivatives were readily isolated, while it further presents the need for synthetic alternatives in order to achieve the synthesis of such analogues, *e.g.* use of dioic acids instead of acetone derivatives.

The preparation of the known enaminone derived from benzoylacetonitrile was met with a remarkable observation that, in addition to the isolated (*E*)-2-benzoyl-3-(dimethylamino)acrylonitrile (57 - 85 %), a unique extensively delocalised room temperature stable carbanion, (*E*)-2,4-dicyano-1,5-dioxo-1,5-diphenylpent-3-en-2-ide, was obtained accompanied by a cation counterion that varied depending upon the severity of the reaction conditions. X-ray crystallography was employed to elucidate the structure of the anion and each counterion, whereas the formation of these ionic side-products deviates from the literature precedent and illustrates further aspects of enaminone synthesis.

The addition of an *in situ* prepared sulfene derivative, derived from the action of Et_3N on the respective sulfonyl chloride, to an enaminone substrate towards a 3,4-dihydro-1,2-oxathiine 2,2-dioxide ring proved to have more facets than those presented previously in the literature. Enaminone analogues with electron-withdrawing substituents or extensively delocalised electron density (*i.e.* "double enaminone" analogues) were found to be completely inactive towards the sulfene addition, whereas the rest of the analogues afforded the heterocyclic adduct in various yields (10 - 79 %). The obtained 3,4-dihydro-1,2-oxathiine 2,2-dioxide adducts could be readily recognised by ^{1}H-NMR spectroscopy by virtue of the key signals for the aliphatic (δ 3.5 - 4.5 for 3-H, δ 4.2 - 5.0 for 4-H) and (wherever present) the olefinic protons (5-H resonating at δ 5.8 - 6.0) of the 1,2-oxathiine 2,2-dioxide core, as well as the characteristic singlet

corresponding to the NMe_2 group at δ 2.1 – 2.4. Further characterisation was made possible by ^{13}C-NMR spectroscopy, as the aliphatic carbon environments could be readily observed between δ 60 – 35, along with the deshielded signal for C6 being (commonly) the most downfield peak of the spectrum at *circa* δ 150. The IR stretching frequencies of the SO_3 fragment at *circa* 1065 and 1170 cm^{-1} served as confirming evidence of the O-S bond formation, with the values of these frequencies fluctuating to a limited extent between different analogues. The mass spectral fragmentation pattern of the 3,4-dihydro-1,2-oxathiine 2,2-dioxides was of interest exhibiting the expected molecular ion and a base peak, which corresponded to elimination of the NMe_2 and SO_2 functions to afford a polysubstituted furan system.

The coupling constants of the protons on the 3- and 4- positions of the 3,4-dihydro-1,2-oxathiine 2,2-dioxide ring system were more thoroughly examined by being screened against the substitution patterns of the respective derivatives. The comparison of how these constants varied in response to changes in substitution pattern highlighted the fact that the ambient substituents of the 1,2-oxathiine ring unit had a distinct effect on the geometry of the heterocyclic ring. In particular, the absence of a substituent on the 5- position in 3,6-disubstituted derivatives was correlated to a different conformation of the C3-C6 carbon chain, which caused an increase in the dihedral angle between 3-H and 4-H that was indicated by an increase of the $J_{3,4}$ value (11.1 – 11.4 Hz, as compared with the 7.9 – 9.5 Hz range for 3,5,6- and 5,6-substituted analogues). This difference in conformation has been tentatively associated with a tendency of the 3,6-disubstituted analogues to revert back to their enaminone precursors over time through a retro Diels-Alder process, which was interestingly not observed for 3,5,6- and 5,6-substituted derivatives.

The regioselectivity of the sulfene addition was efficiently probed using styryl-containing, as well as imine-containing enaminone precursors; the exclusive formation of the desired 1,2-oxathiine 2,2-dioxide adducts in both cases pointed out to the enamine fragment of the starting material having a clear directing effect on the adding sulfene.

An aspect of the sulfene addition to enaminones barely having been explored by previously published research was the mechanism of the addition. The observation that there were two sets of signals present in the ^{1}H-NMR spectra of the crude mixtures for 3,5,6-trisubstituted analogues of 3,4-dihydro-1,2-oxathiine 2,2-dioxides hinted at the formation of an *anti*- and a *syn*- diastereomer of the heterocyclic product. Repetition of the sulfene addition under different sets of conditions on a specific enaminone analogue, revealed evidence of a thermodynamic (*anti*) and a kinetic (*syn*) product. It was thus concluded that the addition of sulfene followed the concerted mechanism of a hetero Diels-Alder reaction; an *exo* approach, influenced by steric interactions between the enaminone and the sulfene, produces the thermally stable *anti*- isomer, whereas secondary orbital interactions are able to favour the kinetic product (*syn*- isomer). Absence of a pro-chiral centre on the reacting sulfene leads to no diastereomers of the 5,6-substituted analogues, whereas mono-substituted enaminones offer no substituents for secondary orbital interactions and thus only the *anti*- isomers of the 3,6-substituted analogues are afforded from the addition. These claims highlight the effect of the reaction conditions on the stereoselectivity of the addition, thus paving the ground for future attempts that may potentially allow for the asymmetric synthesis of either one of the two observed diastereomers for the3,5,6-trisubstituted analogues.

After initial attempts at the acid-catalysed elimination of 3,4-dihydro-1,2-oxathine 2,2-dioxides (*p*-TsOH in refluxing PhMe) was found to be troublesome due to long reaction times, incomplete conversions and difficulty of product purification, the Cope elimination reaction was employed instead to furnish 1,2-oxathine 2,2-dioxide derivatives. This protocol offered high reproducibility and good to excellent yields under exceptionally mild conditions (DCM, 0 – 10 ^{o}C). Indeed, utilising an oxidant to produce the *N*-oxide of the NMe_2 group allowed for its elimination with concomitant formation of a C3-C4 double bond. It was further observed that the conversion occurred with complete regioselectivity, as no epoxides deriving from oxidation of the C5-C6 double bond were observed. In the case of the styryl-containing analogues, not only was epoxide formation not observed, but the increase in the extent of delocalisation on the

product appears to favour the elimination, resulting in consistently high yields for these derivatives. Chemoselectivity was an additional beneficial aspect of this protocol, as it was shown that ambient oxidisable groups on specific 1,2-oxathiine substrates remained chemically unaltered throughout the oxidation/ elimination process. The elimination products could be readily identified by ^{1}H-NMR spectroscopy, where the key protons of the diene C3-C6 chain were observed as sets of doublets (or one singlet for trisubstituted analogues) at δ 6.5 - 7.1 with coupling constants that were typical of *cis* alkene protons or vinyl protons connected *via* a single bond. The observation that no aliphatic ^{13}C-NMR signals corresponding to the sp^3-hybridised *C* atoms of the 1,2-oxathiine ring unit or the adjacent NMe_2 moiety served as additional evidence that the elimination had succeeded, whereas the preservation of the SO_3 connecting function was ascertained by IR spectroscopy, wherein the aforementioned key stretching frequencies were again observed. Unequivocal evidence of their structure was finally obtained by X-ray crystallography, which illustrated the desired heterocyclic structure having an "envelope" conformation, with the C3-C4-C5-C6-O chain being relatively planar and the SO_2 group escaping this plane.

After the foregoing sulfene addition and Cope elimination transformations were explored to a satisfactory extent, the two-step synthetic route that they constituted was further developed into a "one-pot" process that included the sulfene addition to an enaminone precursor, removal of the solvent (if THF was used), and immediate oxidant addition on the crude 3,4-dihydro intermediate. The standard work-up procedure of the Cope elimination, followed by chromatographic purification of the final mixture, afforded various 6-substituted 1,2-oxathiine 2,2-dioxide analogues. Even though the recorded yields for this "one-pot" protocol were found to fluctuate vastly depending on the electronic and steric features of the 6-substituent, comparing the yields of the original two step transformation and the "one-pot" method for the same analogue pointed out a significant yield increase when the latter was employed. This variation could thus be adopted in future attempts towards 1,2-oxathiine 2,2-dioxide systems; however, a more thorough examination of the crude saturated intermediate would be warranted in order to determine whether the Cope elimination can be carried out immediately or if the 3,4-dihydro analogue requires full purification before its elimination.

A broader understanding of enaminone synthesis using DMFDMA was achieved, highlighting the potential effects of solvent use, reaction conditions and catalysis. The addition of sulfenes on enaminones was investigated in order to assess the structural features of the 3,4-dihydro 1,2-oxathiine products, as well as arrive at a plausible mechanism suggestion, whereas Cope elimination was found to be particularly efficient in producing fully unsaturated 1,2-oxathiine analogues. Future research work may use the above route to furnish 1,2-oxathiine 2,2-dioxides with various ambient substituents, able to be functionalised or interact with each other towards analogue libraries of increasing complexity.

5.3 Conclusions Pertaining to Chapter 3

Upon the development of 1,2-oxathiine 2,2-dioxide analogues using the foregoing route, it became apparent that the 5- and 6- positions of the heterocyclic core could be occupied by dimethylthienyl substituents leading to a 1,2-oxathiine 2,2-dioxide moiety that could exhibit potential photochemically reversible photochromic activity. To that end, three non-commercially available α-methylene ketones were obtained through a branching synthetic route starting from 2,5-dimethylthiophene.

The first of these ketones was afforded *via* use of a Friedel-crafts acylation of 2,5-dimethylthiophene with oxalyl chloride towards an α-keto ester, a Wolff-Kishner Huang Minlon reduction/ ester hydrolysis to furnish a carboxylic acid, derivatisation into the acid chloride, and a second Friedel-Crafts acylation using 2,5-dimethylthiophene to afford the desired ketone, 1,2-bis(2,5-dimethylthiophen-3-yl)ethan-1-one. Appending a phenyl group adjacent to the carbonyl unit by using benzene in the foregoing acylation protocol proved to be more challenging, by virtue of the decreased reactivity of benzene compared to the dimethylthiophene moiety, resulting in the starting acid chloride undergoing a self-acylation to yield a

novel, fused pyranone derivative, (*Z*)-4-((2,5-dimethylthiophen-3-yl)methylene)-1,3-dimethyl-4*H*-thieno[3,4-*c*]pyran-6(7*H*)-one. Overcoming this setback required the conversion of the aforementioned chloride into a Weinreb amide and the subsequent addition of phenyllithium to arrive at the target isostere ketone, 1-phenyl-2-(2,5-dimethylthiophen-3-yl)-ethanone. The third ketone (1-(2,5-dimethylthiophen-3-yl)-2-phenylethanone) presented a more straightforward synthesis, involving a Friedel-Crafts acylation of 2,5-dimethylthiophene with phenyl acetyl chloride.

Reaction of the obtained 2,5-dimethylthienyl substituted methyleneketones with DMFDMA proceeded smoothly to afford the anticipated enaminoketones. The addition of sulfenes to which, afforded the 4-dimethylamino-3,4-dihydro-1,2-oxathiine 2,2-dioxide adducts in good yield, and a subsequent Cope elimination gave the unsaturated 2,5-dimethylthiophene substituted 1,2-oxathiine 2,2-dioxides. The 2,5-dimethylthiophene rings of 5,6-bis(2,5-dimethylthiophen-3-yl)-3-phenyl-1,2-oxathiine 2,2-dioxide were shown, by X-ray crystallography, to adopt an antiparallel conformation and thus facilitate photochromic behaviour upon UV-irradiation which promoted a reversible electrocyclic ring-closure to afford a coloured photoisomer.

The UV-Vis spectrophotometric studies were carried out on the 3,4-dihydro and unsaturated 2,5-dimethylthienyl substituted 1,2-oxathiine 2,2-dioxides and provided several insights into their photochromic behaviour; both series of 1,2-oxathiine analogues exhibited a photochromic response with that exhibited by the unsaturated derivatives being more pronounced than that of the 3,4-dihydro analogues. The presence of a C3-C4 double bond was shown to cause a bathochromic shift of the λ_{max} of the ring-closed, coloured photoisomer, measured at the photostationary state. The influence of the C3 phenyl group on the photochromic properties was also determined and induced an additional bathochromic shift in both the 3,4-dihydro and unsaturated series of molecules. Further confirmation of the photochromic activity was achieved by ^{1}H-NMR spectroscopy, as the UV-mediated formation of the ring-closed form of the photochromic unit could be readily monitored by consecutive cycles of UV irradiation/ ^{1}H-NMR measurement on an unsaturated candidate (5,6-bis-(2,5-dimethylthiophen-3-yl)-3-phenyl-1,2-oxathiine 2,2-dioxide) and observation of the emerging signals of the ring-closed coloured form. Finally, solid state photochromism was also explored, with a powdered sample of 5,6-bis-(2,5-dimethylthiophen-3-yl)-3-phenyl-1,2-oxathiine 2,2-dioxide undergoing a dramatic colour change after a short period of UV irradiation. It should be noted that the photochromic properties of 1,2-oxathiine 2,2-dioxide have potential for future exploration; different thiophene-based substituents can be incorporated on the 1,2-oxathiine core unit to screen their photochromic response, whereas the 3-substituent of the 6-membered heterocycle could be further functionalised to bear electron-donating and electron withdrawing groups in order to examine their potential effect on the photochromic properties of the photochrome candidate.

Literature protocols were successfully adopted or modified as required to arrive at methylene ketones containing mixed aryl groups. The established sulfene addition/ Cope elimination route was used to arrive at a small library of 1,2-oxathiine photochrome candidates, which were examined in spectrophotometric studies to assess their photochromic properties, along with how these are affected by the backbone 1,2-oxathiine scaffold. Functionalisation of the 3-position can be utilised to further investigate the photochromic response of these species in future research.

5.4 Conclusions Pertaining to Chapter 4

This chapter was concerned with increasing the structural diversity of the synthesised 1,2-oxathiiine 2,2-dioxides by application of selected chemical transformations and also with examining the 1,2-oxathiine 2,2-dioxide ring as a heterocyclic building block. The first reaction that was attempted was the bromination of selected unsaturated 1,2-oxathiine 2,2-dioxides with varying phenyl substitution patterns. Bromination revealed that, between the 3-, 4- and 5- positions of the 1,2-oxathiine ring, the 3-position is the most reactive, followed by the 5-position, which required a greater heat input and longer reaction

time to be substituted by bromine, and lastly the 4-position, which was completely inactive towards substitution, presumably due to its significant deficiency in electron density.

Functionalisation of the brominated 1,2-oxathiine analogues was initially attempted by bromine-lithium exchange and subsequent quenching of the anion with an electrophilic, although this method was found to be ineffective, as it led to the degradation of the brominated starting at -70 ^{o}C reaction temperature. Opting for less forceful conditions, a Suzuki cross-coupling protocol using aryl boronic acids and esters bearing electron-donating and electron-withdrawing groups was examined next. Upon optimising the reaction solvent to ensure sufficient dissolution of all reagents, the recorded yields, whilst moderate, pointed out a beneficial effect of electron-rich boronic acids and a complementary mitigating effect of electron-poor coupling agents on the extent of the transformation. An additional facet of this reaction regarded the isolation of a homo-coupled bis-1,2-oxathiine derivative, (6,6'-diphenyl-[3,3'-bi(1,2-oxathiine)] 2,2,2',2'-tetraoxide, which was isolated along with the target coupling product. The formation of this bis-1,2-oxathiine was rationalised by the transmetallation of the 1,2-oxathiino ligands between identical Pd-complexes, whereas extended conjugation and consequent thermal stability favoured it over the desired coupling products. The scope of this coupling protocol was thus limited to use of electron-rich boronic reagents, meriting future optimisation towards developing a catalytic system which allows the hetero-coupling mechanism to proceed seamlessly with various boronic reagents.

Further inability of the Suzuki coupling reaction to allow the incorporation of electron-withdrawing aryl groups (*e.g.* pyridyl group) on the 1,2-oxathiine 2,2-dioxide system required an alternative method to be adopted. The Miyaura borylation was examined for this purpose, however consecutive attempts of this protocol consistently resulted in the exclusive formation of a homo-coupled species similar to that isolated during the Suzuki cross-coupling attempts. Further attempts at Miyaura borylation were abandoned in favour of a more efficient coupling method; different bromo-1,2-oxathiine 2,2-dioxide substrates could be screened in future attempts in order to ascertain the consistency of the foregoing homo-coupling trend. The catalytic system used could also be adjusted to reduce its reactivity, in the hopes that it can selectively catalyse the borylation process without interacting with the formed boronic ester any further.

The attempted Pd-catalysed cross-coupling reactions on the brominated 1,2-oxathiine 2,2-dioxides illustrated that the electron-poor nature of these substrates (owing to the electron-withdrawing SO_2 group) renders their functionalisation fairly troublesome and in need of substantial optimisation. The last coupling protocol alternative that was explored involved the use of the parent unsaturated counterparts, 1,2-oxathiine 2,2-dioxides, along with aryl iodides in a C-H activation cross-coupling protocol. The results of this transformation were much more promising than the previous coupling methods, with a small library of coupling products being compiled in 32 – 82 % yield, including analogues with either a 6-styryl substituent or a 3-(4-pyridyl) group that had been completely unattainable *via* previous protocols. The diverse range of coupling products allowed for a comparison of the reactivity between the aryl iodides, with electron-poor analogues offering better results than electron-rich ones. The advantage of this method, as compared to previous protocols, is further pronounced by the shorter synthetic route it offers, since the bromination step can be omitted, resulting in higher yields of functionalised products. It should be noted that the successful incorporation of a pyridyl function on the 1,2-oxathiine 2,2-dioxide structure could aid in the future synthesis of a 3,6-bi(4-pyridyl) derivative that could be further developed into a novel electrochromic 'viologen-like' species by quaternising the terminal *N* atoms. The last valuable insight obtained from the C-H activation coupling regarded the profound effect of the reaction time on the obtained products, as long heating periods seem to favour the formation of the homo-coupled products, even after the desired coupling product has successfully formed.

Cycloaddition reactions on 1,2-oxathiine 2,2-dioxides bearing alkenyl or alkynyl groups were examined using various dienophiles and most prominently 4-phenyl-1,2,4-triazole-3,5-dione (PTAD). A small series of 3-phenyl-6-styryl analogues was found to afford novel tricyclic adducts in 39 – 67 % yield upon

interaction with PTAD in 1,2-DCE at either room temperature or reflux, with electron-donating effects ameliorating the yield of this conversion. These novel 1*H*-[1,2]oxathiino[5,6-*c*][1,2,4]triazolo[1,2-*a*]pyridazine derivatives presented an unexpected point of interest, as the aforementioned yields do not regard the anticipated Diels-Alder adducts but their rearranged, diene-containing counterparts instead, which form during the chromatographic purification process, presumably upon contact with the silanol matrix on the silica gel. Avoiding chromatography by means of AcMe trituration afforded pure samples of the initial Diels-Alder adducts with their structure intact and their characterisation was combined with extensive 2D spectroscopy analysis in order to validate the proposed rearrangement. The phenylethynyl and furyl substituted 1,2-oxathiine derivatives remained inactive towards PTAD addition or fully degraded under the foregoing conditions.

PTAD was also added to (*E*)-6-styryl-1,2-oxathiine 2,2-dioxide, which is devoid of a 3-substituent, in order to examine whether the unhindered C3-C4 double bond was reactive. Interestingly, no C3-C4 double bond addition was observed even with excess amounts of PTAD, and the formed mono-adduct behaved in the aforementioned fashion of being rearranged during purification. In an attempt to explore the electronics of the addition further, a styryl analogue with an electron-withdrawing 4-$CF_3C_6H_4$- group on the 3-position was combined with PTAD, with the low yield of the resulting adduct offering clear evidence of the influence that the surrounding substituents may have on the diene reactivity of any styryl-containing analogue. In contrast to the interesting findings of the PTAD addition, attempting similar Diels-Alder reactions using other dienophiles (dimethyl fumarate, maleic anhydride), failed to afford any cycloadducts, with the exception of a fused product, dimethyl 7-(4-methoxyphenyl)-3-phenylbenzo[*e*][1,2]oxathiine-5,6-dicarboxylate 2,2-dioxide, that was obtained in low yield (*circa* 10 %) after a DMAD Diels-Alder addition/ aromatisation process.

These cycloaddition reactions present ample room for future work; as the addition of PTAD to 6-styryl derivative was covered to a satisfactory level, further interest would be drawn in the reaction being attempted on a 3-styryl analogue to afford a novel, alternate condensed heterocyclic ring system. Finally, the obtained tricyclic adducts (rearranged or not) could be screened for their reactivity in specific reactions, such as oxidation using DDQ towards a highly conjugated tricyclic system and basic cleavage of the PTAD fragment towards a fused pyridazine system.

The last reaction that was utilised to probe the reactivity of 1,2-oxathiine 2,2-dioxides was the addition of benzyne that was generated *in situ* from the effect of fluoride ion on 2-(trimethylsilyl)phenyl trifluoromethanesulfonate (Kobayashi's reagent). The initial attempt of this addition led to the isolation of a naphthalene analogue (1-(4-methoxyphenyl)naphthalene) in 8 % yield, deriving from the addition of benzyne to the 1,2-oxathiine core and consequent retro Diels-Alder cleavage of SO_3. Further attempts at benzyne addition showed its extent to be quite limited, with most 6-substituted and 5,6-substituted starting materials being retrieved unaltered. However, the presence of a substituent on the 3-position of the 1,2-oxathiine ring appeared to contradict the foregoing trend of low reactivity, with examples of 3,6- and 3,5,6-substituted naphthalenes being isolated in moderate yields (22 – 32 %). These findings highlight the importance of substitution on the 3- and 6- positions of the C3-C6 chain of the reacting 1,2-oxathiine 2,2-dioxides, so that they can exhibit measurable diene-like properties. Future developments of this reaction would encompass the extensive optimisation of yields for the naphthalene adducts, along with use of benzyne variants (pyridyne, indolyne) to assess their compatibility with 1,2-oxathiine 2,2-dioxides.

Bromination of selected 1,2-oxathiine 2,2-dioxide analogues provided valuable insights about the reactivity of these heterocycles. Adopting different coupling protocols allowed for functionalisation of the 3-position of the 1,2-oxathiine ring, while cycloaddition reactions afforded novel fused derivatives and naphthalene products. Increasing the range of different 1,2-oxathiine analogues by use of these reactions, exploring the reactivity of the fused adducts and using 1,2-oxathiine 2,2-dioxides in more reactions to further screen their chemical behaviour are all promising niches of future research regarding these heterocyclic systems.

CHAPTER 6: EXPERIMENTAL SECTION

6.1 Equipment and Reagents

Reagents were purchased from Alfa Aesar, Acros, Apollo Scientific, Fluorochem, Manchester Organics, Sigma Aldrich and VWR and were used as supplied unless indicated otherwise.

Reactions were stirred / heated using stirrer hotplates supplied by either Heidolph MR3001K or Asynt ADS HP-NT, employing Asynt 'DrySyn' aluminium heating blocks.

Thin Layer Chromatography separations were performed on either Merck TLC Aluminium sheets (silica gel 60 Å F254), or on Alugram pre-coated TLC sheets (silica gel 60 Å F254) or on Fluorochem aluminium backed TLC sheets (silica gel 60 Å F254), employing a variety of eluent systems of differing polarity. Flash and short column (sinter) chromatographic separations were performed on either Aldrich chromatography silica (60 Å, 230-400 mesh, 40-63 µm) or (60 Å, 70-230 mesh, 63-200 µm), or on Fluorochem chromatography silica (60 Å, 40-63 µm), or on Acros Organics neutral Al_2O_3 (50-200 µm 60 Å). Al_2O_3 was activated by mixing Al_2O_3 (300 g) with H_2O (9 mL) prior to flash column chromatography separations.

NMR spectra were recorded on a Bruker Avance 400 instrument (^{1}H 400 MHz, ^{13}C 100 MHz, ^{19}F 376 MHz) in commercial deuterated solvents which typically contained tetramethylsilane (TMS) as a chemical shift reference (Fluorochem). FT-IR spectra were recorded on neat samples using a Nicolet 380 FT-IR equipped with a diamond probe ATR attachment. Accurate mass measurements were obtained from the Innovative Physical Organic Solutions (IPOS) centre at the University of Huddersfield. Melting points were determined in capillary tubes, using a Stuart SMP10 melting point apparatus, and are uncorrected.

UV-visible spectra were recorded for spectroscopic grade hexane solutions of the samples (10 mm path length quartz cuvette, PTFE capped, concentration in the range 10^{-2} - 10^{-6} moldm^{-3}). A bespoke Shimadzu UV-3600 Plus UV-Vis-NIR spectrophotometer was used and equipped with a single cell Peltier temperature controlled (23 °C) stirred fluorescence cell holder attachment. The spectrophotometer sample chamber door was modified to accept activating irradiation delivered from the light source by liquid light guides (Newport 77557, Newport 77569). Irradiation was provided by a xenon ozone free arc lamp (Newport 6255) powered by an Oriel 300-Watt xenon arc lamp source (Newport 66906) with power manually limited to either 120 or 150 Watts. An in-line destilled water liquid filter (Newport 6177), multiple filter holder (Newport 62020), UG11 filter (Newport FSO-UG11), fibre optic coupler (Newport 77799) completed the irradiation equipment. Spectra (350 - 750 nm) were recorded prior to (ground state) and immediately after cessation of activating irradiation to a photostationary state (PSS) or steady state (sample dependent irradiation time). Activation of the colourless ring-opened forms of the photochromic dithienylethenes to a PSS was achieved by using UV irradiation using different Newport filters 255 - 390 nm (GG420, UG11, KG3, GG455, BG3, BG40, GG400). Bleaching of the coloured (ring-closed forms) was induced by irradiation with visible light > 455 nm (filters Newport FSQ-GG455). For the fatigue cycles, the colourless ring-opened forms of the photochromic dithienylethenes were activated to a photostationary state using a Spectroline hand-held UV TLC inspection Lamp ENF-280C/FE (8 watts).

The following 4-arylbut-3-en-2-one precursors for Chapter 2 were obtained by a standard base-catalysed aldol procedure, see for example Zhu *et al.*,[25] and possessed spectroscopic and physical data in agreement with literature data: (*E*)-4-(4-methoxyphenyl)but-3-en-2-one[243], (*E*)-4-(4-nitrophenyl)but-3-en-2-one[244], (*E*)-4-(4-(trifluoromethyl)phenyl)but-3-en-2-one[25], (*E*)-4-(2-bromophenyl)but-3-en-2-one[245].

5,6-Bis(4-methoxyphenyl)-1,2-oxathiine 2,2-dioxide and (*E*)-6-styryl-1,2-oxathiine 2,2-dioxide were prepared using the optimised sulfene addition/ Cope elimination synthetic methods devised in Chapter 2

of this thesis by final year student Ochola W. Ogwang (University of Huddersfield) as part of their final year research project module.

6.2 Chapter 2 Compounds

6.2.1 Preparation of enaminoketones

6.2.1.1 Preparation of 3-(dimethylamino)-1-(aryl)prop-2-en-1-ones

(*E*)-3-(Dimethylamino)-1-phenylprop-2-en-1-one 2.1

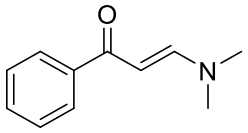

Acetophenone (8.75 mL, 75.0 mmol) was dissolved in DMFDMA (40.00 mL, 301.1 mmol, 2.5 eq) under a N_2 atmosphere and the solution was stirred at reflux overnight. Upon cooling, evaporation of the volatiles *under reduced pressure* afforded an orange solid, which was purified by recrystallisation from EtOAc/ Hexane to afford the product (9.03 g, 69%) as yellow/orange filamentous crystals; R_f= 0.7 (10% EtOAc/ Hexane); m.p. = 91 - 93 (from EtOAc/ Hexane, lit. m.p. = 89 - 92 °C)[246]; ν_{max} (neat): 2981, 2904, 2806, 1639 (C=O), 1595, 1581, 1537, 1482, 1428, 1409, 1362, 1310, 1272, 1231, 1205, 1121, 1051, 1024, 1014 cm^{-1}; ^{1}H-NMR (400 MHz, $CDCl_3$): δ 2.92 (s, 3H, NMe), 3.13 (s, 3H, NMe), 5.71 (d, *J* = 12.4 Hz, 1H, α-vinyl-H), 7.39-7.45 (m, 3H, ArH), 7.80 (d, *J* = 12.4 Hz, 1H, β-vinyl-H), 7.88-7.90 (m, 2H, ArH); ^{13}C-NMR (100 MHz, $CDCl_3$): δ 37.24, 45.02, 92.23, 127.50, 128.13, 130.88, 140.55, 154.25, 188.71.

(*E*)-3-(Dimethylamino)-1-(4-pyridyl)-2-propen-1-one 2.6

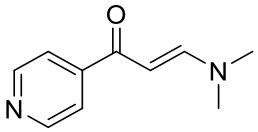

4-Acetylpyridine (10.00 g, 82.5 mmol) was mixed with DMFDMA (12.82 mL, 99.0 mmol, 1.2 eq) under a N_2 atmosphere and the resulting mixture was heated to 80° C. L-proline (0.95 g, 10 %-mol) was subsequently added and the reaction mixture was stirred at the same temperature for 2h and 15 min. After the removal of the volatile components under reduced pressure, the crude solid so obtained was recrystallised twice from EtOAc/ Hexane to yield the product (12.11 g, 83.3 %) as a pale brown solid. R_f = 0.2 (50% EtOAc/ Hexane); m.p. = 109 -111 °C (from EtOAc/ Hexane, lit. m.p. = 115-117 °C)[247]; ν_{max} (neat): 3031, 2912, 2821, 1635 (C=O), 1593, 1559, 1520, 1484, 1430, 1409, 1365, 1319, 1271, 1235, 1129, 1057, 1012 cm^{-1}; ^{1}H-NMR (400 MHz, $CDCl_3$): δ 2.96 (s, 3H, NMe), 3.19 (s, 3H, NMe), 5.65 (d, *J* = 12.2 Hz, 1H, α-vinyl-H), 7.68 (m, 2H, Py-H), 7.84 (d, *J* = 12.2 Hz, 1H, β-vinyl-H), 8.70 (m, 2H, Py-H); ^{13}C-NMR (100 MHz, $CDCl_3$): δ 37.45, 45.34, 91.72, 121.22, 147.22, 150.21, 155.24, 186.64.

(*E*)-3-(Dimethylamino)-1-(furan-2-yl)prop-2-en-1-one 2.7

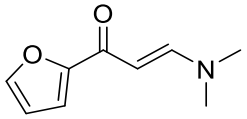

2-Acetylfuran (5.00 g, 45.4 mmol) was dissolved in DMFDMA (15.07 mL, 113.5 mmol, 2.5 eq) under a N_2 atmosphere and the mixture was heated to reflux overnight. Upon reaction completion, all volatile components were removed under reduced pressure. The obtained crude was crushed into a thin powder and triturated with Et_2O to afford the title compound (6.33 g, 84.4 %) as a brown solid; R_f = 0.4 (4 % MeOH/ $CHCl_3$); m.p. = 83 - 85 °C (from DMFDMA, lit. m.p. = 83 - 84 °C)[248]; v_{max} (neat): 3111, 2914, 2808, 1635 (C=O), 1573, 1537, 1491, 1461, 1385, 1350, 1285, 1256, 1160, 1123, 1061, 1020 cm^{-1}; ^{1}H-NMR (400 MHz, $CDCl_3$): δ 2.90 (s, 3H, NMe), 3.11 (s, 3H, NMe), 5.66 (d, *J* = 12.5 Hz, 1H, α-vinyl-H), 6.45 - 6.46 (m, 1H, furyl-H), 7.03 - 7.04 (m, 1H, furyl-H), 7.46 - 7.47 (m, 1H, furyl-H), 7.78 (d, *J* = 12.5 Hz, 1H, β-vinyl-H); ^{13}C-NMR (100 MHz, $CDCl_3$): δ 37.27, 45.00, 91.47, 111.77, 113.27, 144.11, 153.48, 154.83, 177.45.

(*E*)-3-(Dimethylamino)-1-(thiophen-2-yl)prop-2-en-1-one 2.8

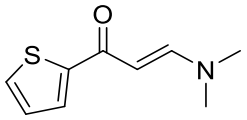

2-Acetylthiophene (2.57 mL, 23.8 mmol) was dissolved in DMFDMA (7.90 mL, 59.4 mmol, 2.5 eq) under a N_2 atmosphere and the solution was stirred at reflux overnight. Upon full consumption of the starting material as monitored by TLC, the volatile components were removed under reduced pressure. The resulting crude solid was triturated with Et_2O to afford the title compound (4.25 g, 98.6 %) as an orange solid; R_f = 0.2 (50% EtOAc/ Hexane); m.p. = 112 - 115 °C (from DMFDMA, lit. m.p. = 122 - 124 °C (from xylene))[249]; v_{max} (neat): 1632 (C=O), 1542, 1514, 1483, 1432, 1408, 1352, 1284, 1247, 1202, 1112, 1085, 1065, 1012 cm^{-1}; ^{1}H-NMR (400 MHz, $CDCl_3$): δ 2.91 (s, 3H, NMe), 3.12 (s, 3H, NMe), 5.62 (d, *J* = 12.3 Hz, 1H, α-vinyl-H), 7.06 - 7.08 (m, 1H, thienyl-H), 7.45 - 7.47 (m, 1H, thienyl-H), 7.61 - 7.62 (m, 1H, thienyl-H), 7.77 (d, *J* = 12.3 Hz, 1H, β-vinyl-H); ^{13}C-NMR (100 MHz, $CDCl_3$): δ 37.29, 45.05, 91.70, 127.58, 128.38, 130.27, 147.46, 153.60, 180.84.

(*E*)-3-(Dimethylamino)-1-(4-iodophenyl)prop-2-en-1-one 2.11

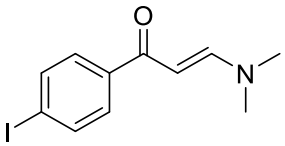

4'-Iodoacetophenone (3.00 g, 12.2 mmol) was dissolved in DMFDMA (4.05 mL, 30.5 mmol, 2.5 eq) under a N_2 atmosphere and the solution was heated at reflux overnight. Upon removal of volatile components under reduced pressure, the obtained crude mixture was triturated with Et_2O to afford the target compound (3.15 g, 85.8 %) as an orange solid; R_f = 0.3 (50 % EtOAc/ Hexane); m.p. = 116 - 118 °C (from DMFDMA); v_{max} (neat): 2360, 2342, 1634 (C=O), 1562, 1515, 1472, 1409, 1350, 1301, 1268, 1233, 1177, 1104, 1062, 1049, 1005 cm^{-1}; ^{1}H-NMR (400 MHz, $CDCl_3$): δ 2.92 (br. s, 3H, NMe), 3.15 (br. s, 3H, NMe), 5.65 (d, *J* = 12.6 Hz, 1H, α-vinyl-H), 7.61 - 7.63 (m, 2H, ArH), 7.74 - 7.76 (m, 2H, ArH), 7.80 (d, *J* = 12.6 Hz, 1H, β-vinyl-H); ^{13}C-NMR (100 MHz, $CDCl_3$): δ 37.36, 45.16, 91.62, 97.91, 129.19, 137.31, 139.86, 154.55, 187.44; HRMS: Found $[M+H]^+$ = 302.0036, $C_{11}H_{12}INO$ requires $[M+H]^+$ = 302.0040.

(*E*)-3-(Dimethylamino)-1-(naphthalen-2-yl)prop-2-en-1-one 2.12

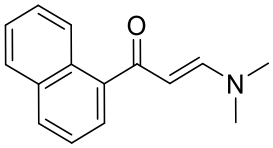

1-Acetylnaphthalene (1.79 mL, 11.8 mmol) was dissolved in DMFDMA (3.90 mL, 29.4 mmol, 2.5 eq) under a N_2 atmosphere and the resulting reaction mixture was heated at reflux overnight. Upon removal of the volatile components under reduced pressure, the crude oil eluted through a sinter column (silica, wet loading, 0 % to 20 % EtOAc in DCM) to yield the target compound (2.09 g, 78.6 %) as an orange oil; R_f = 0.1 (50 % EtOAc/ Hexane); v_{max} (neat): 2910, 1639 (C=O), 1544, 1502, 1460, 1417, 1392, 1347, 1308, 1267, 1234, 1208, 1174, 1140, 1089, 1058, 1022 cm^{-1}; ^{1}H-NMR (400 MHz, $CDCl_3$): δ 2.88 (s, 1H, NMe), 3.06 (s, 1H, NMe), 5.53 (d, *J* = 12.6 Hz, 1H, α-vinyl-H), 7.44 - 7.57 (m, 5H, ArH), 7.85 - 7.86 (m, 1H, ArH), 7.85 (d, *J* = 12.6 Hz, 1H, β-vinyl-H), 8.26 (app. s, 1H, ArH); ^{13}C-NMR (100 MHz, $CDCl_3$): δ 37.22, 45.03, 98.61, 124.77, 124.97, 125.98, 126.12, 126.49, 128.12, 129.32, 130.47, 133.74, 140.31, 155.11, 193.70.

6.2.1.2 Preparation of 1-(dimethylamino)-5-(aryl)penta-1,4-dien-3-ones and 1-(dimethylamino)-5-phenylpent-1-en-4-yn-3-one

(1*E*, 4*E*)-1-(Dimethylamino)-5-phenylpenta-1,4-dien-3-one 2.26

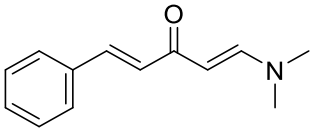

Under a N_2 atmosphere, 4-phenyl-3-buten-2-one (5.00 g, 34.2 mmol) was dissolved in DMFDMA (11.4 mL, 85.5 mmol, 2.5 eq) and heated to 80 °C, before the addition of L-proline (0.39 g, 3.4 mmol, 10 %-mol). The reaction mixture remained stirring at 80 °C overnight. Upon reaction completion, the volatile components were removed by rotary evaporation and the crude solid so obtained was triturated with Et_2O to afford the title compound as a yellow-brown solid (5.65 g, 82.1 %); R_f = 0.3 (4% MeOH/ $CHCl_3$); m.p. = 90 - 95 °C (from DMFDMA, lit. m.p. = 94 - 96 °C (from EtOAc/ Hexane))[25]; v_{max} (neat): 3020, 2916, 1639, 1616 (C=O), 1577, 1549, 1496, 1484, 1432, 1365, 1345, 1275, 1219, 1200, 1158, 1116, 1030 cm^{-1}; ^{1}H-NMR (400 MHz, $CDCl_3$): δ 2.88 (s, 3H, NMe_2), 3.12 (s, 3H, NMe_2), 5.27 (d, *J* = 12.5 Hz, 1H, 2-H), 6.79 (d, *J* = 15.8 Hz, 1H, 4-H), 7.29 - 7.37 (m, 3H, ArH), 7.53 - 7.55 (m, 2H, ArH), 7.55 (d, *J* = 15.7 Hz, 1H, 5-H), 7.75 (d, *J* = 12.5 Hz, 1H, 1-H); ^{13}C-NMR (100 MHz, $CDCl_3$): δ 37.27, 44.99, 96.39, 127.88, 128.31, 128.71, 129.23, 135.82, 138.49, 153.46, 186.32.

(1*E*,4*E*)-1-(Dimethylamino)-5-(4-methoxyphenyl)penta-1,4-dien-3-one 2.22 Method 1

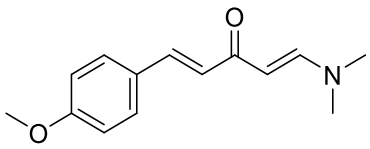

(*E*)-4-(4-Methoxyphenyl)but-3-en-2-one (6.93 g, 39.3 mmol) was dissolved in PhMe (50 mL) and mixed with DMFDMA (15.6 mL, 118.0 mmol, 3 eq) under a N_2 atmosphere. The mixture was refluxed for 5 d. Upon reaction completion (monitored by ^{1}H-NMR) the volatile components of the mixture were removed under reduced pressure. The resulting solid was triturated with Et_2O to afford the product (5.46 g, 60.0

%) as a yellow solid; R_f = 0.2 (4 % MeOH/ DCM); m.p. = 100 - 102 °C (from DMFDMA); ν_{max} (neat): 2996, 2909, 2837, 1653, 1610, 1597 (C=O), 1573, 1531, 1509, 1434, 1417, 1405, 1355, 1300, 1269, 1247, 1170, 1144, 1084, 1026 cm^{-1}; ^{1}H-NMR (400 MHz, $CDCl_3$): δ 2.89 (s, 3H, NMe), 3.08 (s, 3H, NMe), 3.82 (s, 3H, MeO), 5.25 (d, *J* = 12.5 Hz, 1H, 2-H), 6.67 (d, *J* = 15.9 Hz, 1H, 4-H), 6.87 - 6.89 (m, 2H, ArH), 7.48 - 7.50 (m, 2H, ArH), 7.53 (d, *J* = 15.9 Hz, 1H, 5-H), 7.73 (d, *J* = 12.5 Hz, 1H, 1-H); ^{13}C-NMR (100 MHz, $CDCl_3$): δ 37.43, 44.90, 55.33, 96.40, 114.17, 126.16, 128.55, 129.40, 138.26, 153.14, 160.61, 186.54; HRMS: Found $[M+H]^+$= 232.1334, $C_{14}H_{17}NO_2$ requires $[M+H]^+$= 232.1335.

(1*E*,4*E*)-1-(Dimethylamino)-5-(4-methoxyphenyl)penta-1,4-dien-3-one 2.22 Method 2

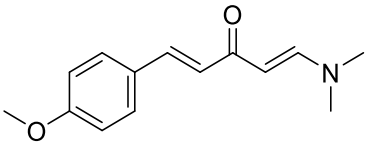

(*E*)-4-(4-Methoxyphenyl)but-3-en-2-one (0.05 g, 0.3 mmol) was dissolved in DMFDMA (2 mL) and heated to 80 °C. L-proline (3.5 mg, 0.03 mmol, 10 %-mol) was added and the reaction mixture remained at this temperature overnight. The volatile components were subsequently removed under reduced pressure and the crude product so obtained was purified by column chromatography (silica, wet loading, 0 % to 2 % MeOH/ DCM) to yield the title compound (0.04 g, 57.1 %) as a yellow solid; with identical ^{1}H-NMR signals to **2.22** prepared above;

(1*E*,4*E*)-1-(Dimethylamino)-5-(4-nitrophenyl)penta-1,4-dien-3-one 2.23

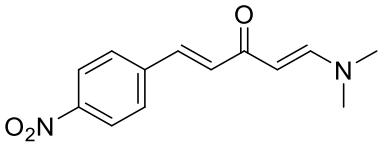

(*E*)-4-(4-Nitrophenyl)but-3-en-2-one (1.00 g, 5.2 mmol) was dissolved in PhMe (25 mL) and mixed with DMFDMA (1.73 mL, 13.0 mmol, 2.5 eq) under a N_2 atmosphere. The reaction mixture was refluxed for 6h and the volatile components were removed under reduced pressure. The crude product so obtained was filtered through a sinter column (silica, wet loading, 0% to 5% MeOH/ $CHCl_3$) and trituration of the obtained brown solid with Et_2O afforded the title compound (0.99 g, 77.3 %) as an orange solid; R_f = 0.3 (4 % MeOH/ $CHCl_3$); m.p. = 152 - 154 °C (from MeOH/ $CHCl_3$); ν_{max} (neat): 3035, 2912, 1650, 1614 (C=O), 1593, 1537, 1505, 1436, 1424, 1355, 1335, 1302, 1265, 1089 cm^{-1}; ^{1}H-NMR (400 MHz, $CDCl_3$): δ 2.91 (s, 3H, NMe), 3.17 (s, 3H, NMe), 5.28 (d, *J* = 12.2 Hz, 1H, 2-H), 6.89 (d, *J* = 15.9 Hz, 1H, 4-H), 7.58 (d, *J* = 15.9 Hz, 1H, 5-H), 7.65 - 7.68 (m, 2H, ArH), 7.80 (d, *J* = 12.2 Hz, 1H, 1-H), 8.20 - 8.22 (m, 2H, ArH); ^{13}C-NMR (100 MHz, $CDCl_3$): δ 37.35, 45.18, 96.54, 124.05, 128.31, 132.38, 135.54, 142.37, 147.79, 154.12, 184.94; HRMS: Found $[M+H]^+$= 247.1082, $C_{13}H_{14}N_2O_3$ requires $[M+H]^+$= 247.1080.

(1*E*,4*E*)-1-(dimethylamino)-5-(4-(trifluoromethyl)phenyl)penta-1,4-dien-3-one 2.9

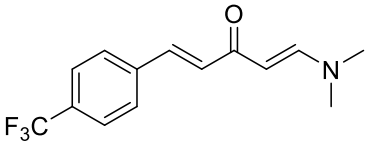

(*E*)-4-(4-(Trifluoromethyl)phenyl)but-3-en-2-one was dissolved in DMFDMA (7.75 mL, 58.3 mmol, 2.5 eq) under a N_2 atmosphere. The mixture was heated to reflux overnight. Upon reaction completion, all volatile components were removed under reduced pressure and the obtained crude was crushed into a powder

and triturated with 1:1 Et_2O/ P.E. to yield the product (3.17 g, 50.6 %) as a yellow solid; R_f = 0.3 (4 % MeOH/ $CHCl_3$); m.p. = 131 - 133 °C (from DMFDMA); ν_{max} (neat): 3062, 2916, 2803, 1653, 1613 (C=O), 1537, 1422, 1360, 1318, 1264, 1161, 1111, 1089, 1063, 1009 cm^{-1}; ^{1}H-NMR (300 MHz, $CDCl_3$): δ 2.91 (s, 3H, NMe), 3.16 (s, 3H, NMe), 5.28 (d, *J* = 12.4 Hz, 1H, 2-H), 6.85 (d, *J* = 15.7 Hz, 1H, 4-H), 7.58 (d, *J* = 15.7 Hz, 1H, 5-H), 7.59 - 7.66 (m, 4H, ArH), 7.79 (d, *J* = 12.4 Hz, 1H, 1-H); ^{13}C-NMR (100 MHz, $CDCl_3$): δ 37.29, 45.13, 96.42, 124.05 (q, *J* = 272 Hz, CF_3), 125.65 (q, *J* = 3.8 Hz, *o*-Ar*C*-CF_3), 127.93, 130.63, 130.65 (q, *J* = 32 Hz, *C*-CF_3), 136.61, 139.35, 153.86, 185.55; ^{19}F-NMR (376.5 MHz, $CDCl_3$) δ -62.66 (s, 3F); HRMS: Found $[M+H]^+$ = 270.1100, $C_{14}H_{14}F_3NO$ requires $[M+H]^+$ = 270.1103.

(1*E*,4*E*)-1-(2-Bromophenyl)-5-(dimethylamino)penta-1,4-dien-3-one 2.10

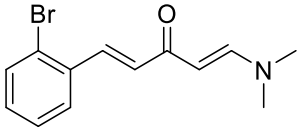

(*E*)-4-(2-Bromophenyl)but-3-en-2-one was dissolved in DMFDMA (7.40 mL, 55.5 mmol, 2.5 eq) under a N_2 atmosphere and the reaction mixture was heated to reflux overnight. Upon reaction completion (as monitored by TLC), the reaction mixture was condensed under reduced pressure to remove the volatile components. The product was thus obtained (5.77 g, 92.8 %) as a black-brown oil that was sufficiently pure for further use; R_f = 0.3 (4 % MeOH/ $CHCl_3$); ν_{max} (neat): 2908, 2803, 1654, 1610 (C=O), 1541, 1463, 1416, 1351, 1258, 1217, 1199, 1082, 1020 cm^{-1}; ^{1}H-NMR (300 MHz, $CDCl_3$): δ 2.90 (s, 3H, NMe), 3.14 (s, 3H, NMe), 5.31 (d, *J* = 12.5 Hz, 1H, 2-H), 6.71 (d, *J* = 15.8 Hz, 1H, 4-H), 7.14 - 7.19 (m, 1H, ArH), 7.27 - 7.30 (m, 1H, ArH), 7.57 - 7.63 (m, 2H, ArH), 7.75 (d, *J* = 12.5 Hz, 1H, 1-H), 7.86 (d, *J* = 15.8 Hz, 1H, 5-H); ^{13}C-NMR (100 MHz, $CDCl_3$): δ 37.27, 45.08, 95.90, 125.26, 127.51, 127.62, 130.16, 131.42, 133.27, 135.95, 136.83, 153.71, 186.03; HRMS: Found $[M+H]^+$ = 280.0328, $C_{13}H_{14}{}^{79}BrNO$ requires $[M+H]^+$ = 280.0331.

(*E*)-1-(Dimethylamino)-5-phenylpent-1-en-4-yn-3-one 2.13

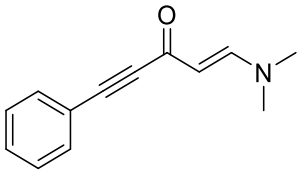

4-Phenylbut-3-yn-2-one (3.03 mL, 20.8 mmol) was dissolved and mixed with DMFDMA (6.92 mL, 52.0 mmol, 2.5 eq, an additional 5 mL were added to ensure smooth stirring of the mixture) under a N_2 atmosphere. The resulting reaction mixture was heated at reflux overnight. Upon reaction completion, the volatile components of the mixture were removed under reduced pressure and the obtained crude oil was mixed with Et_2O prompting the precipitation of the title compound, which was filtered and crushed into a pale brown powder (3.18 g, 76.8 %); R_f = 0.1 (20 % EtOAc/ Hexane); m.p. = 80 - 82 °C (from DMFDMA, lit. m.p. = 86 - 87 °C from EtOAc/Hexane)[26]; ν_{max} (neat): 1621 (C=O), 1558, 1488, 1441, 1405, 1343, 1308, 1267, 1207, 1193, 1178, 1115, 1025 cm^{-1}; ^{1}H-NMR (400 MHz, $CDCl_3$): δ 2.89 (s, 3H, NMe), 3.17 (s, 3H, NMe), 5.33 (d, *J* = 12.6 Hz, 1H, α-vinyl-H), 7.33 - 7.41 (m, 3H, ArH), 7.54 - 7.57 (m, 2H, ArH), 7.74 (d, *J* = 12.6 Hz, 1H, β-vinyl-H); ^{13}C-NMR (100 MHz, $CDCl_3$): δ 37.36, 45.36, 86.53, 87.79, 102.17, 121.38, 128.45, 129.55, 132.40, 158.22, 174.78; HRMS: Found $[M+H]^+$ = 200.1068, $C_{13}H_{13}NO$ requires $[M+H]^+$ = 200.1073.

6.2.1.3 Preparation of 1,2-disubstituted 3-(dimethylamino)prop-2-en-1-ones

(*E*)-3-(Dimethylamino)-1,2-diphenylprop-2-en-1-one 2.2

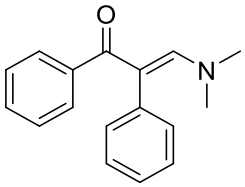

Deoxybenzoin (15.00 g, 76.4 mmol) was dissolved in DMFDMA (25.00 mL, 188.0 mmol, 2.5 eq) under a N_2 atmosphere and the mixture was stirred under reflux overnight. Upon cooling, evaporation of the volatiles under reduced pressure afforded a yellow - orange solid, which was purified by recrystallisation (EtOAc/ Hexane). The product (16.45 g, 87%) was isolated as pale yellow crystals; R_f = 0.3 (50 % EtOAc/ Hexane, alumina); m.p. = 130 - 131°C (from EtOAc/ Hexane), (lit. m.p. = 129 - 130.5 °C)[250]; ν_{max} (neat): 2915, 1616, 1578, 1542 (C=O), 1495, 1440, 1421, 1402, 1384, 1320, 1300, 1225, 1184, 1156, 1118, 1081, 1052, 1025 cm^{-1}; ^{1}H-NMR (400 MHz, $CDCl_3$): δ 2,73 (s, 6H, NMe_2), 7.15-7.20 (m, 3H, ArH), 7.24-7.31 (m, 5H, ArH), 7,36 (s, 1H, vinyl-H), 7.42-7.44 (m, 2H, ArH); ^{13}C-NMR (100 MHz, $CDCl_3$): δ 43.58, 111.98, 126.30, 127.60, 127.64, 128.75, 129.24, 132.13, 137.32, 141.81, 153.73, 194.84.

(*E*)-Ethyl 2-benzoyl-3-(dimethylamino)-acrylate 2.3

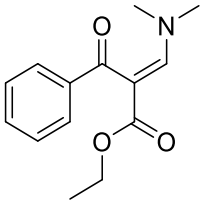

Under a N_2 atmosphere, ethyl benzoylacetate (10,0 g, 52,0 mmol) was dissolved in DMFDMA (17.3 mL, 130.1 mmol, 2.5 eq) and the solution was stirred at reflux overnight. The volatile components were removed under reduced pressure and the resulting orange-brown oil was mixed with brine (300 mL) and the product was extracted with EtOAc (5 x 75 mL). The extracts were washed with brine (3 x 30 mL) and H_2O (100 mL), dried with Na_2SO_4 and the solvent evaporated under reduced pressure. The orange oil so obtained was triturated with DCM, prompting the product to precipitate as yellow crystals that were filtered and recrystallised from EtOAc (7.26 g, 57.0 %); R_f = 0.5 (50 % EtOAc/ Hexane); m.p. = 63 - 65 °C (from EtOAc, lit. m.p. = 63 - 65 °C (from Et_2O/ Heptane))[251]; ν_{max} (neat): 2983, 2927, 2817, 2360, 2341, 1680 (C=O), 1615, 1583 (OC=O), 1484, 1430, 1366, 1309, 1269, 1214, 1161, 1139, 1083, 1028, 1002 cm^{-1}; ^{1}H-NMR (400 MHz, $CDCl_3$): δ 0.87 (t, *J* = 6.3 Hz, 3H, OCH_2CH_3), 2.96 (br s, 6H, NMe_2), 3.94 (d, *J* = 6.5 Hz, 2H, OCH_2CH_3), 7.36-7.46 (m, 3H, ArH), 7.72-7.79 (m, 3H, ArH/ vinyl-H); ^{13}C-NMR (100 MHz, $CDCl_3$): δ 13.89, 41.90, 46.86, 59.68, 99.72, 127.96, 128.87, 131.70, 141.04, 155.82, 168.76, 194.18.

(*E*)-3-(Dimethylamino)-1,2-bis(4-methoxyphenyl)prop-2-enone 2.4

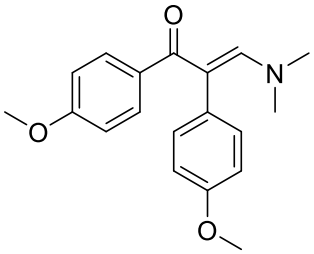

Deoxyanisoin (2.50 g, 9.8 mmol) was dissolved in DMFDMA (3.23 mL, 24.4 mmol, 2.5 eq) under a N_2 atmosphere and the mixture was heated at reflux overnight. After the reaction completion was confirmed by TLC, the volatile components of the mixture were removed through rotary evaporation, thus affording the title compound (2.95 g, 97.2 %) as an off white solid; R_f = 0.2 (20% EtOAc/ Hexane); m.p. = 119 - 121 °C (from DMFDMA, lit. m.p. = 119 - 120 °C)[252]; ν_{max} (neat): 2987, 2964, 2929, 2834, 1622, 1601, 1579, 1556 (C=O), 1504, 1456, 1439, 1410, 1382, 1293, 1234, 1168, 1119, 1103, 1081, 1054, 1021 cm^{-1}; ^{1}H-NMR (400 MHz, $CDCl_3$): δ 2.73 (s, 6H, NMe_2), 3.79 (s, 6H, 2 × OMe), 6.75 - 6.81 (m, 4H, ArH), 7.04 - 7.06 (m, 2H, ArH), 7.35 (s, 1H, vinyl-H), 7.41 - 7.43 (m, 2H, ArH); ^{13}C-NMR (100 MHz, $CDCl_3$): δ 43.45, 55.19, 55.24, 111.28, 112.77, 113.16, 129.97, 131.00, 133.00, 134.22, 153.07, 157.98, 160.56, 193.98.

(*E*)-2-Benzoyl-3-(dimethylamino)-acrylonitrile 2.5 Method 1

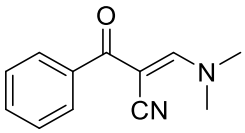

Benzoylacetonitrile (12.0 g, 82.7 mmol) was dissolved in DMFDMA (27.4 mL, 206.7 mmol, 2.5 eq) under a N_2 atmosphere and was heated under reflux overnight. Upon cooling, the volatile components of the reaction mixture were removed under reduced pressure and the resulting crude product was purified by column chromatography (silica, wet loading, 4% to 10% MeOH in DCM) to yield two fractions:
Fraction 1: (*E*)-2-Benzoyl-3-(dimethylamino)-acrylonitrile **2.5** (9.36 g, 56.7 %) as an off-white solid; R_f = 0.6 (10 % MeOH/ EtOAc); m.p. = 111°- 113° C (from MeOH/ DCM, lit. m.p. = 128-129 °C (from EtOH))[253]; ν_{max} (neat): 2924, 2191 (CN), 1640 (C=O), 1586, 1568, 1444, 1426, 1412, 1318, 1300, 1229, 1180, 1135, 1095, 1070, 1056, 1027; ^{1}H-NMR (400 MHz, ($CDCl_3$): δ 3.29 (s, 3H, NMe), 3.48 (s, 3H, NMe), 7.40-7.51 (m, 3H, ArH), 7.76-7.79 (m, 2H, ArH), 7.95 (s, 1H, vinyl-H); ^{13}C-NMR (100 MHz, $CDCl_3$): δ 39.0, 48.3, 79.7, 120.3, 128.1, 128.2, 131.5, 138.5, 159.4, 190.3.

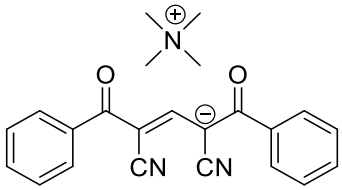

Fraction 2: Tetramethylammonium (*E*)-2,4-dicyano-1,5-dioxo-1,5-diphenylpent-3-en-2-ide **2.5a** as yellow crystals; R_f = 0.3 (10% MeOH/ DCM); m.p. : Decomposition after 150 °C (from MeOH/DCM); ν_{max} (neat): 3031, 2199 (CN), 2186 (CN), 1612 (C=O), 1596, 1574, 1483, 1448, 1316, 1295, 1241, 1176, 1109, 1074, 1026, 1002; ^{1}H-NMR (400 MHz, d^6-DMSO): δ 3.09 (s, 12H, $^+NMe_4$), 7.51-7.39 (m, 10H, ArH), 8.02 (s, 1H, vinyl-H); ^{13}C-NMR (100 MHz, $CDCl_3$): δ 54.38 (t, *J* = 4 Hz), 86.68, 118.62, 127.75, 127.96, 130.21, 139.76, 152.52, 190.04; HRMS: Found $[M\text{-}NMe_4]^-$= 299.0825, $C_{23}H_{23}N_3O_2$ requires $[M\text{-}NMe_4]^-$= 299.0821.

(*E*)-2-Benzoyl-3-(dimethylamino)-acrylonitrile 2.5 Method 2

A solution of 2-benzoylacetonitrile (2.00 g, 13.8 mmol) in PhMe (50 mL) containing DMFDMA (2.02 mL, 15.2 mmol, 1.1 eq) under a N_2 atmosphere was stirred overnight and the solvent was subsequently removed under reduced pressure. Recrystallisation of the obtained crude mixture from EtOH afforded a precipitate (solid 1), while the filtrate yielded a second precipitate (solid 2) upon cooling:
Solid 1: (*E*)-2-Benzoyl-3-(dimethylamino)-acrylonitrile **2.5** (2.34 g, 85.0 %) as yellow filamentous crystals; with identical ^{1}H-NMR signals to **2.5** prepared above.

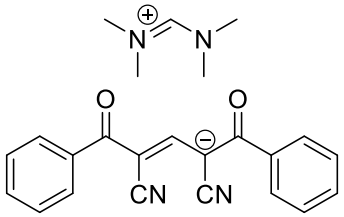

Solid 2: *N*-((Dimethylamino)methylene)-*N*-methylmethanaminium (*E*)-2,4-dicyano-1,5-dioxo-1,5-diphenyl pent-3-en-2-ide **2.5b** (90 mg, 3.5 %) as a sub-white solid; R_f = 0.1 (4% MeOH/DCM); m.p. = 146 - 147 °C (from EtOH); ν_{max} (neat): 3044, 2203 (CN), 2195 (CN), 1698 (C=O), 1605, 1574, 1495, 1442, 1423, 1413, 1369, 1337, 1250, 1168, 1114, 1066, 1025, 1001; ^{1}H-NMR (400 MHz, $CDCl_3$): δ 3.29 (s, 6H, NMe_2), 3.32 (s, 6H, $[=NMe_2]^+$), 7.26-7.40 (m, 6H, ArH), 7.56-7.58 (m, 4H, ArH), 8.04 (s, 1H, vinyl-H), 8.16 (s, 1H, Me_2NCH); ^{13}C-NMR (100 MHz, $CDCl_3$): δ 39.35, 46.51, 87.86, 120.09, 128.12, 128.32, 130.51, 139.77, 154.69, 157.49, 192.16; HRMS: Found $[M\text{-}Me_2N{=}CHNMe_2]^-$ = 299.0824, $C_{24}H_{24}N_4O_2$ requires $[M\text{-}Me_2N{=}CHNMe_2]^-$ = 299.0826.

(*E*)-2-Benzoyl-3-(dimethylamino)-acrylonitrile 2.5 Method 3

2-Benzoylacetonitrile (3.00 g, 20.6 mmol) was suspended in DMFDMA (3.29 mL, 24.8 mmol, 1.2 eq) under a N2 atmosphere and the mixture was heated to 80 °C with full dissolution. L-proline (0.24 g, 2.1 mol, 10 %-mol) was added and the resulting reaction mixture was stirred overnight at the same temperature. The volatile components were removed under reduced pressure and the crude mixture so obtained was purified by column chromatography (silica, wet loading, 0 % to 10 % MeOH/ DCM) to afford the product (2.56 g, 62.0 %) as an off-white solid with identical ^{1}H-NMR signals to **2.5** prepared above;

(*E*)-4-(Dimethylamino)-1,3-diphenylbut-3-en-2-one 2.21

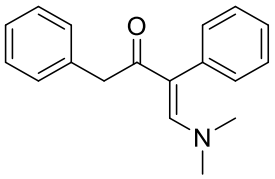

1,3-Diphenylacetone (10.00 g, 47.5 mmol) was dissolved in PhMe (75 mL) and DMFDMA (7.57 mL, 57.0 mmol, 1.2 eq) was added under a N_2 atmosphere. The resulting reaction mixture was stirred at reflux for 6h. The volatile components of the reaction mixture were removed under reduced pressure to afford a crude mixture that was purified by Kugelrohr distillation as an orange oil (9.74, 77%) that turned into a yellow solid over the course of *circa* 3 weeks; R_f= 0.2 (20% EtOAc/ Hexane); m.p.= 44 - 48 °C (from PhMe); ν_{max} (neat): 3056, 3025, 2919, 2806, 1626, 1598, 1562 (C=O), 1491, 1452, 1419, 1406, 1385, 1312, 1265, 1208, 1182, 1151, 1100, 1058, 1029; ^{1}H-NMR (400 MHz, $CDCl_3$): δ 2.67 (s, 6H, NMe_2), 3.52 (s, 2H, α-CH_2), 7.00 - 7.02 (m, 2H, ArH), 7.12 - 7.22 (m, 5H, ArH), 7.26 - 7.31 (m, 3H, ArH), 7.65 (s, 1H, vinyl-H); ^{13}C-NMR

(100 MHz, $CDCl_3$): δ 43.10 (br), 45.87, 110.48, 125.94, 126.83, 127.87, 128.07, 129.26, 132.70, 137.02, 137.86, 149.79, 196.04; HRMS: Found $[M+H]^+$= 266.1539, $C_{18}H_{19}NO$ requires $[M+H]^+$= 266.1539.

3,5-Diphenyl-4*H*-pyran-4-one 2.33 (Attempted preparation of (1*E*,4*E*)-1,5-bis(dimethylamino)-2,4-diphenylpenta-1,4-dien-3-one **2.30**)

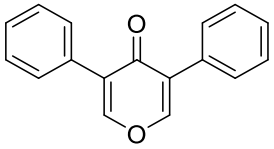

Diphenylacetone (10.0 g, 47.5 mmol) was dissolved in PhMe (50 mL) and mixed with DMFDMA (13.90 mL, 104.5 mmol, 2.2 eq) and refluxed overnight. The volatile components were removed under reduced pressure and a fresh amount of DMFDMA (7.57 mL, 57.0 mmol, 1.2 eq) was added. Upon heating to 80 °C, L-proline (0.55 g, 4.8 mmol, 10 %-mol) was added, and the reaction mixture was stirred for 2h, before being further heated to reflux overnight. Evaporation of the volatile components under reduced pressure produced a crude mixture which was chromatographed in a silica column (wet loading, 10% to 50% EtOAc/Hexane) to produce a solid that was recrystallised from EtOAc/ Hexane to afford the title compound (0.8 g, 6.8 %) as an off white solid; R_f = 0.2 (10 % EtOAc/ Hexane); m.p. = 185 - 186 °C (from EtOAc/ Hexane, lit. m.p. = 185 - 186 °C)[254]; ν_{max} (neat): 3024, 2846, 2355, 1683 (C=O), 1636, 1614, 1596, 1576, 1556, 1515, 1491, 1445, 1397, 1354, 1337, 1298, 1277, 1242, 1154, 1109, 1085, 1072, 1027, 1001 cm^{-1}; ^{1}H-NMR (400 MHz, $CDCl_3$): δ 7.93 (s, 2H, 2 × vinyl-H), 7.58 - 7.55 (m, 4H, ArH), 7.45 - 7.37 (m, 6H, ArH); ^{13}C-NMR (100 MHz, $CDCl_3$): δ 175,5 (1C, CO), 152,4 (4C, 2C=C), 131.3, 130.2, 128.9, 128.5, 128.4.

6.2.1.4 Preparation of enaminones from amides and carboxylic acids

(*E*)-*N*-((Dimethylamino)methylene)-4-methylbenzamide 2.14

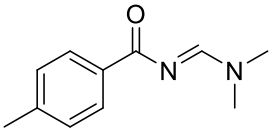

p-Toluamide (2.00 g, 14.8 mmol) was dissolved in DMFDMA (4.92 mL, 37.0 mmol, 2.5 eq) under a N_2 atmosphere and the solution was heated at reflux overnight. Upon reaction completion as monitored by TLC, the volatile components of the reaction mixture were removed under reduced pressure and the obtained solid was triturated with Et_2O to afford the title compound as a white solid (2.23 g, 79.1 g); R_f = 0.7 (10 % MeOH/ DCM); m.p. = 109 - 112 °C (from DMFDMA); ν_{max} (neat): 3275, 2938, 1720, 1668 (C=O), 1610, 1573, 1516, 1444, 1382, 1364, 1316, 1252, 1208, 1184, 1125, 1067, 1037 cm^{-1}; ^{1}H-NMR (300 MHz, $CDCl_3$): δ 2.40 (s, 3H, *Me*C_6H_4), 3.17 (s, 3H, NMe), 3.21 (s, 3H, NMe), 7.21 - 7.23 (m, 2H, ArH), 8.16 - 8.19 (m, 2H, ArH), 8.63 (s, 1H, vinyl-H); ^{13}C-NMR (75 MHz, $CDCl_3$): δ 19.11, 32.73, 38.82, 126.17, 127.31, 131.57, 139.79, 158.12, 175.25; HRMS: Found $[M+H]^+$ = 191.1175, $C_{11}H_{14}N_2O$ requires $[M+H]^+$ = 191.1255.

(*E*,*E*)-1,5-(dimethylamino)-penta-1,4-dien-3-one 2.31

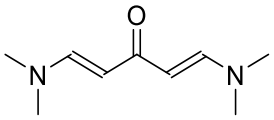

Under a N_2 atmosphere, 1,3-acetonedicarboxylic acid (2.00 g, 13.7 mmol) was suspended in PhMe (40 mL) and cooled to 0 °C in a flame-dried flask. DMFDMA (4.00 mL, 30.1 mmol, 2.2 eq) was subsequently added dropwise at the same temperature. Upon complete addition, the reaction mixture was heated to 35 °C prompting effervescence, before being allowed to reach room temperature over 3h. Upon reaction completion as monitored by ^{1}H-NMR, the reaction mixture was condensed under reduced pressure and the resulting crude mixture was triturated with Et_2O to yield the title compound (1.36 g, 59.1 %) as a brown solid; R_f = 0.7 (4% MeOH/ DCM); m.p. = 102 - 105 °C (decomposition after 58 °C, from PhMe, lit. m.p. = 108 - 110 °C (from cyclohexane))[23]; ν_{max} (neat): 3346, 2884, 2801, 2360, 2342, 1581 (C=O), 1494, 1415, 1349, 1266, 1225, 1155, 1053 cm^{-1}; ^{1}H-NMR (400 MHz, ($CDCl_3$): δ 2.88 (s, 12H, 2 × NMe_2), 4.97 (d, *J* = 12.7 Hz, 2H, 2 × β-vinyl-H), 7.52 (d, *J* = 12.7 Hz, 2H, 2 × α-vinyl-H); ^{13}C-NMR (100 MHz, $CDCl_3$): δ 41.09, 96.82, 150.23, 186.95.

(*E*)-3-(Dimethylamino)-N-((*E*)-dimethylamino)methylene)-2-phenylacrylamide 2.32

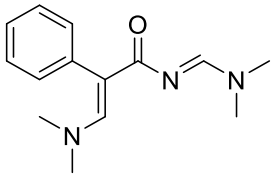

Under a N_2 atmosphere, phenylacetamide (5.00 g, 35.4 mmol) was dissolved in DMFDMA (26.4 mL, 198.7 mmol, 5.6 eq) and the solution was heated to 100 °C for 4h in a distillation array (MeOH distilled at 70°-95° C). Due to the formation of the stable monosubstituted product, an additional amount of DMFDMA (6mL) was added, followed by 2h of reflux heating, to ensure reaction completion. Upon removal of the volatile components by rotary evaporation, the crude mixture was triturated with EtOAc/ P.E. (1:1) to yield the product (6.15 g, 70.1 %) as a pale yellow solid; R_f = 0.5 (4% MeOH/DCM); m.p. = 107 - 111 °C (from DMFDMA); ν_{max} (neat): 3013, 2911, 2818, 1628, 1593 (C=O), 1552, 1495, 1435, 1421, 1384, 1328, 1283, 1266, 1204, 1173, 1086 cm^{-1}; ^{1}H-NMR (400 MHz, $CDCl_3$): δ 2.69 (s, 6H, NMe_2), 3.03 (s, 3H, NMe), 3.06 (s, 3H, NMe), 7.17-7.32 (m, 5H, ArH), 8.13 (s, 1H, C=C*H*), 8.43 (s, 1H, N=C*H*); ^{13}C-NMR (100 MHz, $CDCl_3$): δ 34.79, 40.93, 43.22, 107.56, 125.72, 127.15, 132.19, 138.28, 150.34, 158.41, 179.31; HRMS: Found $[M+H]^+$ = 246.1600, $C_{14}H_{19}N_3O$ requires $[M+H]^+$ = 246.1601.

6.2.2 Preparation of 3,4-Dihydro-1,2-oxathiine 2,2-dioxides

6.2.2.1 Sulfene additions to 1,2-disubstituted enaminone precursors

4-(Dimethylamino)-3,5,6-triphenyl-3,4-dihydro-1,2-oxathiine 2,2 dioxide 2.36

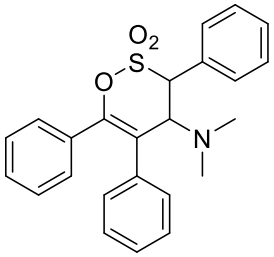

(*E*)-(Dimethylamino)-1,2-diphenylprop-2-en-1-one **2.2** (10.0 g, 39.7 mmol) was dissolved in THF (120 mL), warmed to facilitate dissolution and mixed with Et_3N (6.17 mL, 44.5 mmol, 1.1 eq). The mixture was subsequently cooled to 5 °C, before the dropwise addition of a solution of phenylmethanesulfonyl chloride (8.48 g, 44.5 mmol, 1.1 eq) in THF (80 mL) under an N_2 atmosphere at the same temperature. The reaction mixture was allowed to reach room temperature overnight. Filtration through alumina and solvent removal under reduced pressure afforded an orange oil which was dissolved in EtOAc (100 mL) and washed with water (50 mL). The organic layer was dried over Na_2SO_4, condensed under reduced pressure and the resulting solid yielded the title compound (12.52 g, 77.0 %) as a white solid after recrystallisation from EtOH/ Hexane; R_f = 0.9, (10 % EtOAc/ Hexane); m.p. = 139 - 142 °C (from EtOAc); ν_{max} (neat): 2972, 2938, 2899, 1644, 1494, 1455, 1446, 1365 (O-SO_2), 1332, 1266, 1227, 1182 (O-SO_2), 1169, 1154, 1102, 1093, 1071, 1036, 1025, 1001 cm^{-1}; ^{1}H-NMR (400 MHz, $CDCl_3$): δ 2.23 (s, 6H, NMe_2), 4.49 (d, *J* = 8.0 Hz, 1H, 4-H), 4.96 (d, *J* = 8.0 Hz, 1H, 3-H), 7.17 - 7.31 (m, 10H, ArH), 7.42 - 7.45 (m, 3H, ArH), 7.59 - 7.61 (m, 2H, ArH); ^{13}C-NMR (100 MHz, $CDCl_3$): δ 40.65, 62.28, 71.71, 122.80, 127.71, 127.85, 128.22, 129.02, 129.14, 129.25, 129.50, 129.88, 129.95, 131.73, 132.82, 137.27, 148.25; HRMS: Found $[M+H]^+$ = 406.1471, $C_{24}H_{23}NO_3S$ requires $[M+H]^+$ = 406.1471.

6-Benzyl-4-(dimethylamino)-3,5-diphenyl-3,4-dihydro-1,2-oxathiine 2,2-dioxide 2.40a

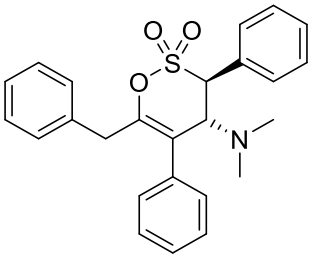

4-(Dimethylamino)-1,3-diphenylbut-3-en-2-one **2.21** (5.00 g, 18.8 mmol) was dissolved in THF (50 mL) and mixed with Et_3N (3.14 mL, 22.6 mmol, 1.2 eq). The mixture was cooled to *circa* 3 °C, before a solution of phenylmethanesulfonyl chloride (4.30 g, 22.6 mmol, 1.2 eq) in THF (40 mL) under a N_2 atmosphere was added dropwise over 15 min with the temperature maintained under 5 °C. Upon complete addition, the reaction mixture was allowed to reach room temperature overnight (additional amounts (0,4 eq) of reagents added until no starting material was observed by TLC). Filtration through a thin alumina afforded a filtrate which had the solvent removed by rotary evaporation. The resulting crude was dissolved in EtOAc (80 mL), washed with H_2O (2 × 80 mL), dried with Na_2SO_4 and condensed under reduced pressure. The crude mixture was purified by column chromatography (silica, dry loading, 10% to 30% EtOAc/ Hexane) and the obtained solid was recrystalised from EtOAc/ Hexane to yield the product (3.78 g, 48.0 %) as a white solid; R_f = 0.5 (20% EtOAc/ Hexane); m.p. = 133 - 136 °C (from EtOAc/ Hexane); ν_{max} (neat): 2935,

2834, 2788, 2010, 1667, 1600, 1495, 1454, 1442, 1428, 1361 (O-SO_2), 1313, 1223, 1182 (O-SO_2), 1119, 1091, 1067, 1031 cm^{-1}; ^{1}H-NMR (400 MHz, $CDCl_3$): δ 2.07 (s, 6H, NMe_2), 3.48 (d, *J* = 15.3 Hz, 1H, PhCH), 3.56 (d, *J* = 15.3 Hz, 1H, PhCH), 4.51 (1H, d, *J* = 9.5 Hz, 4-H), 4.76 (1H, d, *J* = 9.5 Hz, 3-H), 7.18- 7.45 (m, 13H, ArH), 7.57- 7.60 (m, 2H, ArH); ^{13}C-NMR (100 MHz, $CDCl_3$): δ 30.97, 37.89, 40.82, 62.59, 70.51, 122.86, 126.84, 127.88, 128.42, 128.57, 128.69, 129.06, 129.18, 129.53, 129.80, 131.03, 135.84, 137.10, 148.67; HRMS: Found $[M+H]^+$= 420.1627, $C_{25}H_{25}NO_3S$ requires $[M+H]^+$= 420.1628.

4-(Dimethylamino)-3,5,6-triphenyl-3,4-dihydro-1,2-oxathiine 2,2 dioxide 2.40b

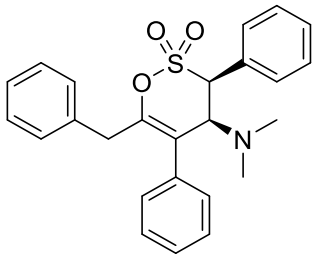

(*E*)-(Dimethylamino)-1,3-diphenylbut-3-en-2-one **2.21** (5.00 g, 18.8 mmol) was dissolved in THF (125 mL), mixed with Et_3N (3.42 mL, 24.5 mmol, 1.3 eq) and cooled down to -10 °C. To it, a solution of $PhCH_2SO_2Cl$ (4.67 g, 24.5 mmol, 1.3 eq) in THF (100 mL) was added dropwise under a N_2 atmosphere, with the temperature maintained under 0 °C. The resulting reaction mixture was allowed to reach room temperature overnight, before being filtered through alumina. Removal of the solvent under reduced pressure afforded a crude mixture which was purified by column chromatography (alumina, dry loading, 10 % EtOAc/ Hexane) to afford the desired isomer as a white solid (1.94 g, 24.6 %); R_f = 0.4 (20 % EtOAc/ Hexane); m.p. = 101 - 102 °C (from EtOAc/ Hexane); ν_{max} (neat): 2863, 2796, 1657, 1600, 1493, 1453, 1362 (O-SO_2), 1290, 1247, 1187, 1163 (O-SO_2), 1102, 1071, 1041 cm^{-1}; ^{1}H-NMR (400 MHz, $CDCl_3$): δ 2.06 (s, 6H, NMe_2), 3.52 (d, *J* = 15.3 Hz, 1H, PhC*H*), 3.68 (d, 15.3 Hz, 1H, PhC*H*), 4.67 (d, *J* = 6.3 Hz, 1H, 4-H), 4.79 (d, *J* = 6.3 Hz, 1H, 3-H), 7.21 - 7.41 (m, 13H, ArH), 7.55 - 7.57 (m, 2H, ArH); ^{13}C-NMR (100 MHz, $CDCl_3$): δ 37.80, 42.03, 64.76, 68.09, 120.74, 126.88, 127.89, 128.29, 128.61, 128.64, 128.78, 129.33, 129.44, 129.79, 130.58, 136.18, 136.90, 148.37; HRMS: Found $[M+H]^+$ = 420.1627, $C_{25}H_{25}NO_3S$ requires $[M+H]^+$ = 420.1631.

4-(Dimethylamino)-5,6-diphenyl-3-(4-(trifluoromethyl)phenyl)-3,4-dihydro-1,2-oxathiine 2,2 dioxide 2.37

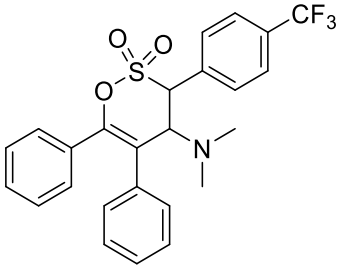

A solution of trifluoromethylphenylmethanesulfonyl chloride (4.50 g, 17.4 mmol, 1.1 eq) in dry THF (35 mL) was added dropwise over *circa* 20 min into a vigorously stirred solution of (*E*)-(dimethylamino)-1,2-diphenylprop-2-en-1-one **2.2** (3.9 g, 15.5 mmol) and Et_3N (2.42 mL, 17.4 mmol, 1.1 eq) in THF (50 mL) under a N_2 atmosphere, while the temperature remained under 5 °C. Once the addition was completed, the reaction mixture was allowed to reach room temperature overnight. Filtration through aluminna gel yielded a filtrate which was condensed under reduced pressure to afford an orange oil. Dissolution in EtOAc (60 mL) was followed by two washings with H_2O (50 mL), and the obtained organic layer was dried over Na_2SO_4 and had the solvent removed by rotary evaporation towards a crude mixture that afforded

the product (4.40 g, 60.0 %) as a white solid through recrystallisation from EtOAc/ Hexane; R_f = 0.9 (50 % EtOAc/ Hexane, alumina); m.p.= 124 - 128 °C (from EtOAc/ Hexane); ν_{max} (neat): 2833, 2794, 2248, 2222, 2179. 2159, 2041, 2028, 2005, 1978, 1955, 1662, 1620, 1491, 1446, 1421, 1371, 1364 (O-SO_2), 1323, 1223, 1186, 1162 (O-SO_2), 1114, 1098, 1069, 1049, 1035, 1018, 1000 cm^{-1}; ^{1}H-NMR (400 MHz, d^6-AcMe): δ 2.22 (s, 6H, NMe_2), 4.79 (1H, d, *J* = 8.7 Hz, 4-H), 5.42 (1H, d, *J* = 8.7 Hz, 3-H), 7.22 - 7.27 (8H, m, ArH), 7.35 - 7.38 (2H, m, ArH), 7.85 - 7.87 (m, 2H, ArH), 8.05 - 8.07 (m, 2H, Ar-H); ^{13}C-NMR (100 MHz, d^6-AcMe): δ 40.13, 61.90, 70.88, 124.2 (q, *J* = 270.0 Hz, *C*F_3), 123.58, 125.84 (q, *J* = 4.0 Hz, *o*-ArC-CF_3), 127.65, 127.97, 128.07, 129.06, 129.08, 130.06, 130.76 (q, *J* = 32 Hz, *C*-CF_3), 131.05, 133.29, 136.66, 137.03, 147.83; ^{19}F-NMR (376.5 MHz, d^6-AcMe) δ -63.20 (s, 3F); HRMS: Found $[M+H]^+$ = 474.1333, $C_{25}H_{22}F_3NO_3S$ requires $[M+H]^+$ = 474.1345.

4-(Dimethylamino)-5,6-diphenyl-3,4-dihydro-1,2-oxathiine 2,2-dioxide 2.41

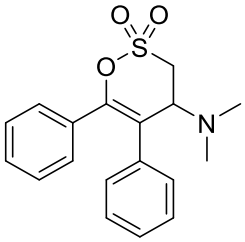

Under a N_2 atmosphere, (*E*)-(dimethylamino)-1,2-diphenylprop-2-en-1-one **2.2** (13.00 g, 52.0 mmol) was dissolved in anhydrous THF (60 mL), followed by the addition of Et_3N (8.20 mL, 58.5 mmol, 1.1 eq). The solution was cooled down to *circa* 0 °C and the mixture was stirred vigorously throughout the dropwise addition of a methanesulfonyl chloride (4.34 mL, 56.0 mmol, 1.05 eq) solution in THF (40 mL) over *circa* 20 min, while the temperature remained below 5 °C. Upon complete addition, the reaction mixture was allowed to reach room temperature overnight and was subsequently filtered through alumina. The filtrate was washed with H_2O (50 mL), dried over Na_2SO_4 and the solvent was removed under reduced pressure to afford a crude mixture that was purified by recrystallisation from EtOAc/ Hexane. The title compound (10.03 g, 53.0 %) was thus obtained as a white solid; R_f = 0.4 (50 % EtOAc/ Hexane); m.p. = 157 - 159 °C (from EtOAc/ Hexane); ν_{max} (neat): 3398, 2830, 2781, 1658, 1493, 1443, 1370 (O-SO_2), 1339, 1280, 1260, 1225, 1192, 1173 (O-SO_2), 1149, 1114, 1101, 1072, 1045, 1004 cm^{-1}; ^{1}H-NMR (400 MHz, d^6-AcMe): δ 2.30 (s, 6H, NMe_2), 3.78 (dd, *J* = 9.1, 14.0 Hz, 1H, *anti*-3-H), 3.95 (dd, *J* = 7.5, 14.0 Hz, 1H, *syn*-3-H), 4.46 (dd, J = 7.5, 9.1 Hz, 1H, 4-H), 7.14-7.23 (m, 10H, ArH); ^{13}C-NMR (100 MHz, d^6-AcMe): δ 39.32, 42.25, 63.76, 122.41, 127.26, 127.84, 127.86, 128.82, 129.09, 129.97, 133.74, 136.98, 148.00; HRMS: Found $[M+H]^+$= 330.1155, $C_{18}H_{19}NO_3S$ requires $[M+H]^+$= 330.1158.

4-(Dimethylamino)-5,6-bis(4-methoxyphenyl)-3,4-dihydro-1,2-oxathiine 2,2-dioxide 2.42

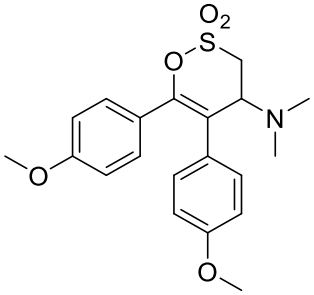

Under a N_2 atmosphere, (*E*)-3-(dimethylamino)-1,2-bis(4-methoxyphenyl)prop-2-enone **2.4** (2.00 g, 6.4 mmol) was dissolved in THF (40 mL), mixed with Et_3N (1.35 mL, 9.5 mmol, 1.5 eq) and then cooled down

to -5 °C. A solution of $MeSO_2Cl$ (0.75 mL, 9.5 mmol, 1.5 eq) in THF (10 mL) was subsequently added dropwise, while the temperature was maintained at *circa* 0 °C. Upon complete addition, the reaction mixture was allowed to reach room temperature overnight, before being filtered through alumina. The filtrate had the solvent removed under reduced pressure and the crude mixture so obtained was purified in a sinter column (alumina, wet loading, n. DCM) and obtained as a pale yellow colloid (1.97 g, 78.8 %); R_f = 0.3 (20% EtOAc/ Hexane); m.p. = 39 - 65 °C (from DCM, wide range/colloid); ν_{max} (neat): 2936, 2835, 2783, 1606, 1575, 1509, 1455, 1413, 1366 (O-SO_2), 1283, 1245, 1167 (O-SO_2), 1094, 1030, 1014 cm^{-1}; ^{1}H-NMR (400 MHz, $CDCl_3$): δ 2.29 (s, 6H, NMe_2), 3.61 (d, *J* = 8.3 Hz, 2H, 2 × 3-H), 3.74 (s, 3H, OMe), 3.77 (s, 3H, OMe), 4.27 (t, *J* = 8.3 Hz, 1H, 4-H), 6.66 - 6.68 (m, 2H, ArH), 6.75 - 6.78 (m, 2H, ArH), 7.07 - 7.11 (m, 4H, ArH); ^{13}C-NMR (100 MHz, $CDCl_3$): δ 40.12, 42.71, 55.13, 55.20, 63.92, 113.24, 113.64, 119.95, 125.48, 128.78, 130.57, 131.07, 148.14, 158.85, 159.75; HRMS: Found $[M+H]^+$= 390.1377, $C_{20}H_{23}NO_5S$ requires $[M+H]^+$= 390.1373.

6.2.2.2 Sulfene additions to 1-aryl enaminone precursors

4-(Dimethylamino)-3,6-diphenyl-1,2-oxathiine 2,2-dioxide 2.43

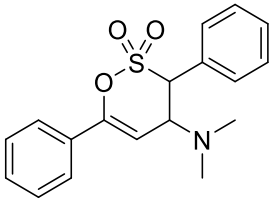

3-(Dimethylamino)-1-phenylprop-2-en-1-one **2.1** (12.00 g, 68.5 mmol) was dissolved in anhydrous THF (200 mL) and cooled to *circa* 5 °C. After the addition of Et_3N (15.20 mL, 109.6 mmol, 1.6 eq), a solution of phenylmethanesulfonyl chloride (20.90 g, 109.6 mmol, 1.6 eq) in anhydrous THF (120 mL) was added dropwise under a N_2 atmosphere, with the temperature maintained under 5 °C. The reaction mixture was subsequently allowed to reach room temperature overnight, before the formed solid was filtered and washed twice with H_2O to afford the title compound (15.96 g, 44.0 %) as a pale yellow solid; R_f = 0.4 (50 % EtOAc/ Hexane); m.p. = 142 – 145 °C (from THF); ν_{max} (neat): 3388, 2831, 2783, 1659, 1575, 1494, 1469, 1452, 1367 (O-SO_2), 1313, 1272, 1222, 1178 (O-SO_2), 1117, 1105, 1072, 1039 cm^{-1}; ^{1}H-NMR (400 MHz, d^6-AcMe): δ 2.34 (6H, s, NMe_2), 4.46 (1H, dd, *J* = 2.5, 11.6 Hz, 4-H), 4.96 (1H, d, *J* = 11.6 Hz, 3-H), 6.25 (1H, d, *J* = 2.5 Hz, 5-H), 7.46 - 7.49 (m, 6H, ArH), 7.65 - 7.68 (m, 2H, ArH), 7.70 - 7.74 (m, 2H, ArH); ^{13}C-NMR (100 MHz, d^6-AcMe): δ 41.27, 63.08, 64.60, 104.38, 125.02, 128.69, 129.24, 129.36, 129.76 (2C), 129.86, 131.81, 150.51; HRMS: Found $[M+H]^+$ = 330.1159, $C_{18}H_{19}NO_3S$ requires $[M+H]^+$ = 330.1158.

4-(Dimethylamino)-3-phenyl-6-(pyridin-4-yl)-3,4-dihydro-1,2-oxathiine 2,2-dioxide 2.44

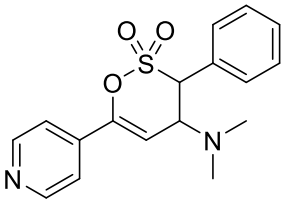

3-(Dimethylamino)-1-(4-pyridyl)-2-propen-1-one **2.6** (5.00 g, 28.4 mmol) was heated in THF (50 mL) to dissolution and mixed with Et_3N (10.3 mL, 73.8 mmol, 2.6 eq). The solution was cooled down to *circa* 5 °C, before the dropwise addition of a solution of phenylmethanesulfonyl chloride (14.08 g, 73.8 mmol, 2.6 eq) in THF (60 mL) over 20 min under a N_2 atmosphere, with the temperature remaining under 5 °C. The

reaction mixture was allowed to reach room temperature overnight, before being poured into H_2O and extracted with EtOAc (9 × 200 mL) and DCM (2 × 450 mL). The combined extracts were dried over Na_2SO_4, condensed under reduced pressure and the resulting crude was attempted to be purified by recrystallisation from EtOAc. During heating, the formation of a black precipitate prompted the decantation of the mother liquor, which was cooled to room temperature affording orange crystals that were filtered and recrystallized from EtOAc to afford the product (0.95 g, 9.7 %) as yellow-orange crystals; R_f = 0.3 (4% MeOH/ DCM); m.p. = 124 - 126 °C (from EtOAc); ν_{max} (neat): 3046, 2979, 2942, 2800, 2359, 1651, 1594, 1548, 1495, 1474, 1454, 1410, 1368 (O-SO_2), 1315, 1278, 1220, 1178 (O-SO_2), 1117,1099, 1072, 1056, 1040 cm^{-1}; ^{1}H-NMR (400 MHz, $CDCl_3$): δ 2.29 (s, 6H, NMe_2), 4.45 (dd, *J* = 2.6, 11.3 Hz, 1H, 4-H), 4.61 (d, *J* = 11.3 Hz, 1H, 3-H), 6.17 (d, *J* = 2.6 Hz, 1H, 5-H), 7.46-7.51 (m, 5H, ArH/PyH), 7.54-7.56 (m, 2H, ArH), 8.68-8.70 (m, 2H, PyH); ^{13}C-NMR (100 MHz, $CDCl_3$): δ 41.35, 63.20, 64.62, 108.46, 118.70, 128.82, 129.34, 129.71, 129.97, 138.99, 148.14, 150.49; HRMS: Found $[M+H]^+$ = 331.1117, $C_{17}H_{18}N_2O_3S$ requires $[M+H]^+$ = 331.1111.

4-(Dimethylamino)-6-(furan-2-yl)-3-phenyl-3,4-dihydro-1,2-oxathiine 2,2-dioxide 2.50

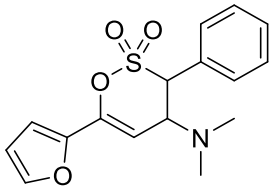

(*E*)-3-(dimethylamino)-1-(furan-2-yl)prop-2-en-1-one **2.7** (3.00 g, 18.2 mmol) was dissolved in THF (50 mL), mixed with Et_3N (3.80 mL, 27.2 mmol, 1.5 eq) and cooled down to -5 °C. A solution of $PhCH_2SO_2Cl$ (5.19 g, 27.2 mmol, 1.5 eq) in THF (60 mL) was then added dropwise under a N_2 atmosphere with the temperature maintained at below 0 °C. Upon complete addition, the reaction mixture was stirred at *circa* 0 °C for 1h, before being allowed to reach room temperature overnight. Reaction completion was ascertained by ^{1}H-NMR and the mixture was filtered through alumina. Evaporation of the solvent on the filtrate under reduced pressure afforded a crude mixture which was purified by column chromatography (alumina, dry loading, 20 % to 50 % EtOAc/ Hexane). The obtained yellow solid was triturated with Et_2O and crushed into an off-white powder (3.88 g, 66.9 %); R_f = 0.2 (20 % EtOAc/ Hexane); m.p. = 123 - 126 °C (from EtOAc/ Hexane); ν_{max} (neat): 3153, 2978, 2951, 2866, 2834, 2790, 1670, 1565, 1488, 1454, 1375 (O-SO_2), 1343, 1315, 1225, 1185 (O-SO_2), 1160, 1115, 1102, 1074, 1039, 1025 cm^{-1}; ^{1}H-NMR (400 MHz, $CDCl_3$): δ 2.28 (s, 6H, NMe_2), 4.41 (dd, *J* = 2.4, 11.2 Hz, 1H, 4-H), 4.54 (d, *J* = 11.2 Hz, 1H, 3-H), 5.93 (d, *J* = 2.4 Hz, 1H, 5-H), 6.47 - 6.48 (m, 1H, furyl-H), 6.62 - 6.63 (m, 1H, furyl-H), 7.44 - 7.46 (m, 4H, ArH, furyl-H), 7.52 - 7.54 (m, 2H, ArH); ^{13}C-NMR (100 MHz, $CDCl_3$): δ 41.19, 63.85, 64.47, 101.69, 109.13, 111.74, 129.07, 129.24, 129.82, 142.70, 143.85, 145.94; HRMS: Found $[M+H]^+$ = 320.0955, $C_{16}H_{17}NO_4S$ requires $[M+H]^+$ = 320.0954.

4-(Dimethylamino)-6-phenyl-3,4-dihydro-1,2-oxathiine 2,2-dioxide 2.52

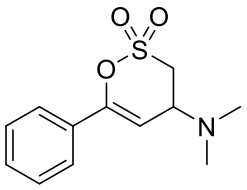

(*E*)-3-(dimethylamino)-1-phenylprop-2-en-1-one **2.1** (12.00 g, 68.5 mmol) was dissolved in THF (200 mL) and mixed with Et_3N (12.41 mL, 89.1 mmol, 1.3 eq). The resulting solution was cooled down to 0 - 5 °C, before a solution of $MeSO_2Cl$ (6.91 mL, 89.1 mmol, 1.3 eq) in THF (80 mL) was added dropwise under a N_2

atmosphere, with the reaction temperature monitored under 5 °C. After the addition, the reaction mixture was allowed to reach room temperature overnight (an additional 1.5 eq of the sulfonyl chloride and trimethylamine were required to achieve reaction completion). The mixture was subsequently filtered through alumina and the solvent was removed under reduced pressure. Consecutive triturations with EtOAc and EtOH afforded the title compound (6.49 g, 37.4 %) as a white solid; R_f = 0.7 (50% EtOAc/ Hexane); m.p. = 173 - 175 °C (from THF, lit. m.p. = 77 °C (from Et_2O))[41]; ν_{max} (neat): 2972, 2918, 2439, 1676, 1512, 1492, 1474, 1448, 1379 (O-SO_2), 1251, 1272, 1226, 1187, 1167, 1136 (O-SO_2), 1105, 1078, 1026 cm^{-1}; ^{1}H-NMR (400 MHz, D_2O): δ 3.01 (s, 6H, NMe_2), 4.20 (dd, J = 9.1, 14.0 Hz, 1H, *anti*-3-H), 4.30 (dd, 6.7, 14.0 Hz, 1H, *syn*-3-H), 4.88 (ddd, *J* = 3.3, 6.7, 9.1 Hz, 1H, 4-H), 6.08 (d, *J* = 3.1 Hz, 1H, 5-H), 7.46 - 7.54 (m, 3H, ArH), 7.66 - 7.68 (m, 2H, ArH); ^{13}C-NMR (100 MHz, D_2O): δ 38.35, 40.32, 42.34, 59.52, 95.92, 125.45, 128.91, 130.21, 131.27, 154.34; HRMS: Found $[M+H]^+$ = 254.0853, $C_{12}H_{15}NO_3S$ requires $[M+H]^+$ = 254.0845.

6.2.2.3 Sulfene additions to 1-styryl enaminone precursors

(*E*)-4-(Dimethylamino)-3-phenyl-6-styryl-3,4-dihydro-1,2-oxathiine 2,2-oxide 2.45

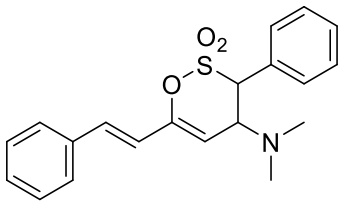

(1*E*, 4*E*)-1-(Dimethylamino)-5-phenylpenta-1,4-dien-3-one **2.26** (2.5 g, 12.4 mmol) was dissolved in THF (35 ml), mixed with Et_3N (6.05 mL, 43.4 mmol, 3.5 eq) and cooled to -10 °C. A solution of phenylmethanesulfonyl chloride (8.27 g, 43.4 mmol, 3.5 eq) in THF (35 mL) was then added dropwise under a N_2 atmosphere with the temperature maintained at *circa* 0 °C. The reaction mixture reached room temperature overnight, before being filtered through alumina, and the obtained filtrate had the solvent removed through rotary evaporation. The crude product so obtained was purified by column chromatography (alumina, dry loading, 20% to 30% EtOAc/ Hexane) to yield the product (2.87 g, 65.2 %), as a pale yellow solid; R_f = 0.5 (20% EtOAc/ Hexane); m.p. = 124 - 126 °C (from EtOAc/ Hexane); ν_{max} (neat): 2830, 2793, 1651, 1496, 1468, 1454, 1368 (O-SO_2), 1315, 1268, 1228, 1191, 1170 (O-SO_2), 1073, 1039 cm^{-1}; ^{1}H-NMR (400 MHz, $CDCl_3$): δ 2.25 (s, 6H, NMe_2), 4.38 (dd, *J* = 2.4, 11.2 Hz, 1H, 4-H), 4.53 (d, *J* = 11.2 Hz, 1H, 3-H), 5.50 (d, *J* = 2.6 Hz, 1H, 5-H), 6.55 (d, *J* = 15.9 Hz, 1H, PhC*H*=CH), 7.04 (d, *J* = 15.9 Hz, 1H, PhCH=C*H*), 7.32 - 7.39 (m, 3H, ArH), 7.44 - 7.46 (m, 5H, ArH), 7.52 - 7.55 (m, 2H, ArH); ^{13}C-NMR (100 MHz, $CDCl_3$): δ 41.24, 63.35, 64.58, 108.09, 119.62, 127.06, 128.77, 128.83, 129.23, 129.26, 129.75, 129.76, 131.72, 135.59, 149.60; HRMS: Found $[M+H]^+$ = 356.1323, $C_{20}H_{21}NO_3S$ requires $[M+H]^+$ = 356.1315.

(*E*)-4-(Dimethylamino)-6-(4-methoxystyryl)-3-phenyl-3,4-dihydro-1,2-oxathiine 2,2-dioxide 2.46

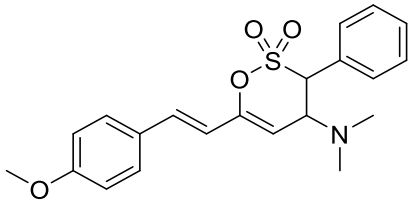

(1*E*,4*E*)-1-(Dimethylamino)-5-(4-methoxyphenyl)penta-1,4-dien-3-one **2.22** (5.00 g, 21.6 mmol) was dissolved in THF (60 mL) and DCM (15 mL), mixed with Et_3N (7.53 mL, 54.0 mmol, 2.5 eq) and the mixture was cooled to -5 °C. A solution of $PhCH_2SO_2Cl$ (10.30 g, 54.0 mmol, 2.5 eq) in THF (60 mL) and DCM (10

mL) was subsequently added dropwise under a N_2 atmosphere over 20 min at *circa* 0 °C. Upon complete addition, the reaction mixture was stirred for 2h at 0 °C, before being allowed to reach room temperature overnight. Reaction completion was verified via ^{1}H-NMR spectroscopy of an aliquot of reaction mixture, prompting the filtration of the reaction mixture through alumina and the evaporation of THF under reduced pressure. The crude product was purified by column chromatography (alumina, dry loading, 20 % to 50 % EtOAc/ Hexane). Collected fractions had the solvents removed under removed pressure and triturated with hexane to afford the title compound (6.39 g, 76.7 %) as a yellow solid; R_f = 0.25 (20 % EtOAc / Hexane); m.p. = 125 - 127 °C (from EtOAc/ Hexane); ν_{max} (neat): 2976, 2938, 2831, 2781, 1601, 1510, 1495, 1453, 1372 (O-SO_2), 1319, 1251, 1226, 1169 (O-SO_2), 1109, 1015 cm^{-1}; ^{1}H-NMR (400 MHz, $CDCl_3$): δ 2.25 (s, 6H, NMe_2), 3.83 (s, 3H, OMe), 4.39 (dd, *J* = 2.2, 11.1 Hz, 1H, 4-H), 4.52 (d, *J* = 11.1 Hz, 1H, 3-H), 5.43 (d, *J* = 2.5 Hz, 1H, 5-H), 6.43 (d, *J* = 15.9 Hz, 1H, ArC*H*=CH), 6.88 - 6.91 (m, 2H, ArH), 6.99 (d, *J* = 15.9 Hz, 1H, ArCH=C*H*), 7.38 - 7.41 (m, 2H, ArH), 7.44 - 7.45 (m, 3H, ArH), 7.53 - 7.55 (m, 2H, ArH); ^{13}C-NMR (100 MHz, $CDCl_3$): δ 41.18 (2C), 55.35, 63.32, 64.61, 106.79, 114.29, 117.42, 128.35, 128.44, 129.21, 129.36, 129.72, 129.74, 131.32, 149.89, 160.18; HRMS Found $[M+H]^+$ = 386.1417, $C_{21}H_{23}NO_4S$ requires $[M+H]^+$ = 386.1424;

(*E*)-4-(Dimethylamino)-6-(4-nitrostyryl)-3-phenyl-3,4-dihydro-1,2-oxathiine 2,2-dioxide 2.47

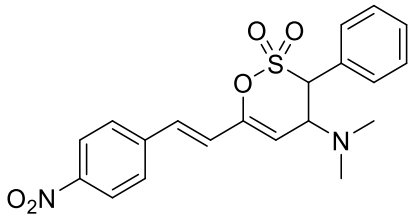

(1*E*,4*E*)-1-(dimethylamino)-5-(4-nitrophenyl)penta-1,4-dien-3-one **2.23** (0.92 g, 3.7 mmol) was dissolved in THF (15 mL) and DCM (20 mL) and then mixed with Et_3N (0.90 mL, 6.7 mmol, 1.8 eq). The mixture was cooled to -10 °C before the dropwise addition of a solution of $PhCH_2SO_2Cl$ (1.27 g, 6.7 mmol, 1.8 eq) in THF (15 mL) under a N_2 atmosphere at *circa* -7 °C. The resulting reaction mixture was stirred at -5 °C for 2h and was subsequently allowed to reach room temperature over 1h. Filtration of the salt precipitate through alumina and subsequent removal of solvents and other volatile components under reduced pressure afforded a crude mixture that was purified by column chromatography (alumina, dry loading, 20 % to 100% EtOAc/ Hexane), yielding a solid which was triturated with Et_2O and crushed into an off-yellow solid (0.80 g, 54.1 %); R_f = 0.1 (20 % EtOAc/ Hexane); m.p. = 156 - 158 °C (from EtOAc/ Hexane); ν_{max} (neat): 2787, 2359, 2341, 1619, 1590, 1506, 1498, 1456, 1377 (O-SO_2), 1335, 1267, 1226, 1189, 1139 (O-SO_2), 1107, 1072, 1053, 1038 cm^{-1}; ^{1}H-NMR (400 MHz, $CDCl_3$): δ 2.26 (s, 6H, NMe_2), 4.40 (dd, *J* = 2.5, 11.3 Hz, 1H, 4-H), 4.55 (d, *J* = 11.3 Hz, 1H, 3-H), 5.64 (d, *J* = 2.5 Hz, 1H, 5-H), 6.70 (d, *J* = 15.8 Hz, 1H, ArC*H*=CH), 7.07 (d, *J* = 15.8 Hz, 1H, ArCH=C*H*), 7.45 - 7.54 (m, 5H, ArH), 7.58 - 7.60 (m, 2H, ArH), 8.22 - 8.24 (m, 2H, ArH); ^{13}C-NMR (100 MHz, $CDCl_3$): δ 41.25, 63.30, 64.69, 123.78, 124.22, 124.30, 127.56, 128.90, 129.02, 129.24, 129.32, 129.70, 129.95, 141.92, 147.55; HRMS: Found $[M+H]^+$ = 401.1168, $C_{20}H_{20}N_2O_5S$ requires $[M+H]^+$ = 401.1169.

(*E*)-4-(Dimethylamino)-3-phenyl-6-(4-(trifluoromethyl)styryl)-3,4-dihydro-1,2-oxathiine 2,2-dioxide 2.48

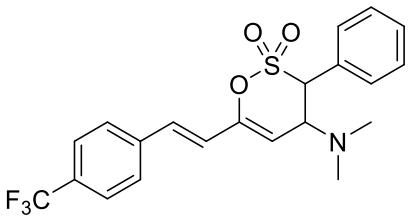

(1*E*,4*E*)-1-(dimethylamino)-5-(4-(trifluoromethyl)phenyl)penta-1,4-dien-3-one **2.9** (3.00 g, 11.1 mmol) was dissolved in THF (50 mL), mixed with Et_3N (2.77 mL, 20.0 mmol, 1.8 eq) and cooled to -5 °C. A solution of $PhCH_2SO_2Cl$ (3.80 g, 20.0 mmol, 1.8 eq) in THF (50 mL) was then added dropwise under a N_2 atmosphere at the same temperature. The resulting mixture was stirred for 2h at -10 °C and was subsequently allowed to reach room temperature overnight. The salt precipitate was filtered through alumina and the filtrate had the solvent removed under reduced pressure. The obtained crude mixture was purified by column chromatography (alumina, dry loading, 30 % to 50 % EtOAc/ Hexane) and the obtained solid was triturated with Et_2O and crushed into an off-white powder (3.40 g, 72.3 %); R_f = 0.1 (20 % EtOAc/ Hexane); m.p. = 128 - 129 °C (from EtOAc/ Hexane); ν_{max} (neat): 2980, 2948, 2359, 2341, 1652, 1613, 1496, 1455, 1414, 1376 (O-SO_2), 1321, 1267, 1221, 1188, 1163 (O-SO_2), 1105, 1063, 1044, 1013 cm^{-1}; ^{1}H-NMR (400 MHz, $CDCl_3$): δ 2.26 (s, 6H, NMe_2), 4.39 (dd, *J* = 2.7, 11.1 Hz, 1H, 4-H), 4.54 (d, *J* = 11.1 Hz, 1H, 3-H), 5.58 (d, *J* = 2.7 Hz, 1H, 5-H), 6.63 (d, *J* = 15.9 Hz, 1H, ArC*H*=CH), 7.05 (d, *J* = 15.8 Hz, 1H, ArCH=C*H*), 7.45 - 7.46 (m, 3H, ArH), 7.53 - 7.55 (m, 4H, ArH), 7.61 - 7.63 (m, 2H, ArH); ^{13}C-NMR (100 MHz, $CDCl_3$): δ 41.22, 63.35, 64.63, 109.77, 122.02, 124.04 (q, *J* = 270 Hz, CF_3), 125.79 (q, *J* = 3.7 Hz, *o*-Ar*C*-CF_3), 127.17, 129.07, 129.27, 129.73, 129.85, 130.13, 130.34 (q, *J* = 32 Hz, *C*-CF_3), 139.04, 149.16; ^{19}F-NMR (376.5 MHz, $CDCl_3$) δ -62.64 (s, 3F); HRMS: Found $[M+H]^+$ = 424.1191, $C_{21}H_{20}F_3NO_3S$ requires $[M+H]^+$ = 424.1192.

(*E*)-6-(2-Bromostyryl)-4-(dimethylamino)-3-phenyl-3,4-dihydro-1,2-oxathiine 2,2-dioxide 4.29

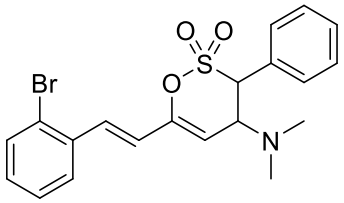

(1*E*,4*E*)-1-(2-bromophenyl)-5-(dimethylamino)penta-1,4-dien-3-one **2.10** (5.00 g, 17.8 mmol) was dissolved in THF (60 mL), mixed with Et_3N (5.46 mL, 39.2 mmol, 2.2 eq) and cooled to -5 °C. At this temperature, a solution of $PhCH_2SO_2Cl$ (7.45 g, 39.2 mmol, 2.2 eq) in THF (60 mL) was added dropwise under a N_2 atmosphere. The resulting reaction mixture was stirred for 2 h at -10 °C and then allowed to reach room temperature overnight. Filtration of the reaction mixture through alumina and removal of the solvent under reduced pressure afforded a crude mixture which was purified by column chromatography (alumina, dry loading, 30 % EtOAc/ Hexane). The solid so obtained was triturated with Et_2O and crushed into a pale yellow powder (4.68 g, 60.5 %); R_f = 0.1 (20 % EtOAc/ Hexane); m.p. = 128 - 130 °C (from EtOAc/ Hexane); ν_{max} (neat): 2978, 2936, 2863, 2837, 2794, 2359, 2343, 1657, 1496, 1458, 1437, 1364 (O-SO_2), 1337, 1310, 1280, 1259, 1207, 1186 (O-SO_2), 1171, 1149, 1092, 1076, 1046, 1022 cm^{-1}; ^{1}H-NMR (400 MHz, $CDCl_3$): δ 2.26 (s, 6H, NMe_2), 4.37 (dd, *J* = 2.4, 11.4 Hz, 1H, 4-H), 4.55 (d, *J* = 11.4 Hz, 1H, 3-H), 5.55 (d, *J* = 2.4 Hz, 1H, 5-H), 6.50 (d, *J* = 15.4 Hz, 1H, ArC*H*=CH), 7.14 - 7.18 (m, 1H, ArH), 7.28 - 7.32 (m, 1H, ArH), 7.34 (d, *J* = 15.4 Hz, 1H, ArCH=C*H*), 7.45 - 7.46 (m, 3H, ArH), 7.53 - 7.55 (m, 3H, ArH), 7.55 - 7.61 (m, 1H, ArH); ^{13}C-NMR (100 MHz, $CDCl_3$): δ 41.23, 63.33, 64.58, 109.35, 122.49, 124.63, 126.95, 127.55, 129.21, 129.24, 129.75, 129.78, 129.80, 130.35, 133.37, 135.68, 149.41; HRMS: Found $[M+H]^+$ = 434.0421, $C_{20}H_{20}{}^{79}BrNO_3S$ requires $[M+H]^+$ = 434.0423.

6.2.2.4 Preparation of 4-(Dimethylamino)-3-phenyl-6-(phenylethynyl)-3,4-dihydro-1,2-oxathiine 2,2-dioxide 2.51

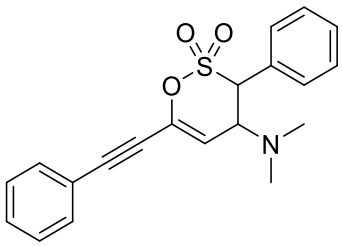

(*E*)-1-(Dimethylamino)-5-phenylpent-1-en-4-yn-3-one **2.13** (2.00 g, 10.0 mmol) was dissolved in THF (30 mL), mixed with Et_3N (4.20 mL, 30.0 mmol, 3.0 eq) and cooled down to -10 °C. To this, a solution of $PhCH_2SO_2Cl$ (5.73 g, 30.0 mmol, 3.0 eq) in THF (30 mL) was added dropwise under a N_2 atmosphere with the temperature maintained at *circa* -5 °C. Upon complete addition, the reaction mixture was stirred at -10 °C for 2 h and was then allowed to reach room temperature overnight. Filtration of the precipitated salts through alumina and removal of the solvent under reduced pressure afforded a crude mixture that was purified by column chromatography (alumina, dry loading (n. DCM), 10 % to 20 % EtOAc/ P.E.). The fractions containing the product were combined and condensed under reduced pressure to produce a yellow solid that was triturated with Et_2O to yield the target compound (1.23 g, 34.8 %) as an off-white solid; R_f = 0.3 (20 % EtOAc/ Hexane); m.p. = 128 - 130 °C (from EtOAc/ P.E.); ν_{max} (neat): 2779, 2214, 1647, 1488, 1455, 1442, 1366 (O-SO_2), 1316, 1299, 1280, 1258, 1228, 1182 (O-SO_2), 1168, 1108, 1071, 1050, 1032 cm^{-1}; ^{1}H-NMR (400 MHz, $CDCl_3$): δ 2.27 (s, 6H, NMe_2), 4.35 (dd, *J* = 2.7, 11.3 Hz, 1H, 4-H), 4.50 (d, *J* = 11.3 Hz, 1H, 3-H), 5.90 (d, *J* = 2.7 Hz, 1H, 5-H), 7.35 - 7.42 (m, 3H, ArH), 7.44 - 7.45 (m, 3H, ArH), 7.51 - 7.53 (m, 4H, ArH); ^{13}C-NMR (100 MHz, $CDCl_3$): δ 41.28, 63.53, 64.85, 80.78, 91.69, 114.60, 120.93, 128.54, 128.87, 129.24, 129.68, 129.71, 129.84, 131.92, 135.18; HRMS: Found $[M+H]^+$ = 354.1157, $C_{20}H_{19}NO_3S$ requires $[M+H]^+$ = 354.1158.

6.2.2.5 Preparation of (*E*,*Z*)-1,2-diphenylethene 2.60a/b

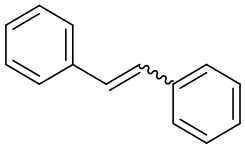

A solution of Et_3N (3.65 mL, 1 eq) in THF (10 mL) was cooled down to 0 °C and mixed dropwise with a solution of $PhCH_2SO_2Cl$ (5.00 g, 26.2 mmol, 1 eq) in THF (40 mL), while the temperature was maintained under 5 °C. The reaction mixture was allowed to reach room temperature for 4 h, before being filtered through alumina and the filtrate was condensed under reduced pressure. The crude mixture so obtained was triturated with hexane, affording a mixture of the two isomers as a pale yellow solid. Isomer separation by column chromatography (silica, dry loading, 10% EtOAc/ Hexane) yielded an aliquot of the (*E*)-isomer for characterisation:

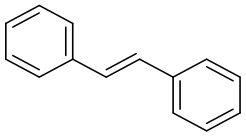

(*E*)-1,2-Diphenylethene **2.60a** as a white solid; R_f = 0.8 (10% EtOAc/ Hexane); m.p. = 125-127 °C (from EtOAc/ Hexane, lit. m.p. = 125 °C (from EtOAc/ Hexane))[255]; ν_{max} (neat): 3058, 3020, 1597, 1577, 1494, 1451, 1331, 1300, 1220, 1154, 1072, 1028 cm^{-1}; ^{1}H-NMR (400 MHz, $CDCl_3$): δ 7.13 (s, 2H, 2 × vinyl-H), 7.25 - 7.29 (m, 2H, ArH), 7.35 - 7.39 (m, 4H, ArH), 7.52 - 7.54 (m, 4H, ArH); ^{13}C-NMR (100 MHz, $CDCl_3$): δ 126.54, 127.65, 128.71, 137.34.

6.2.3 Preparation of 1,2-oxathiine 2,2-dioxides

6.2.3.1 Preparation of 3,5,6-trisubstituted 1,2-oxathiine 2,2-dioxides

3,5,6-(Triphenyl)-1,2-oxathiine 2,2-dioxide 2.63

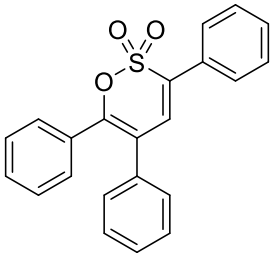

4-(Dimethylamino)-3,5,6-triphenyl-3,4-dihydro-1,2-oxatlhiine 2,2 dioxide **2.36** (5.54 g, 13.7 mmol) was dissolved in DCM (70 mL) and the solution was cooled down to 5 °C. To this, a solution of *m*-CPBA (4.18 g (75% corr.), 24.2 mmol, 1.7 eq) in DCM (40 mL) was added dropwise over 15 °C, while the temperature was maintained below 5°C. The reaction mixture was left to reach room temperature over 4 h and was subsequently washed with H_2O (75 mL), $Na_2SO_{3(aq)}$ (0.7 M, 110 mL), $NaOH_{(aq)}$ (1 M, 50 mL) and H_2O (60 mL). The organic layer so obtained was dried with Na_2SO_4 and the solvent was removed under reduced pressure. The crude product was purified by column chromatography (40% DCM in hexane) to afford the title product as yellow crystals (3.05 g, 62.0 %); R_f = 0.7 (20% EtOAc/Hexane); m.p. = 158 - 160 °C (from DCM/ Hexane); ν_{max} (neat): 3060, 3028, 2919, 1621, 1575, 1541, 1488, 1445, 1368 (O-SO_2), 1350, 1286, 1270, 1231, 1186 (O-SO_2), 1130, 1073, 1033, 1011, 1000 cm^{-1}; ^{1}H-NMR (400 MHz, $CDCl_3$): δ 7.01 (s, 1H, 4-H), 7.23 - 7.37 (m, 10H, ArH) 7.44 - 7.48 (m, 3H, ArH), 7.66 - 7.69 (m, 2H, ArH); ^{13}C-NMR (100 MHz, $CDCl_3$): δ 118.98, 127.74, 128.20, 128.34, 129.05, 129.12, 129.20, 129.28, 129.89, 129.95, 130.26, 131.10, 133.99, 134.10, 135,80, 152.14; HRMS: Found $[M+Na]^+$ = 383.0712, $C_{22}H_{16}O_3S$ requires $[M+Na]^+$ = 383.0712.

6-Benzyl-3,5-diphenyl-1,2-oxathiine 2,2-dioxide 2.62

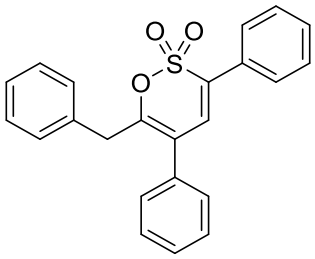

To a solution of 6-benzyl-4-(dimethylamino)-3,5-diphenyl-3,4-dihydro-1,2-oxathiine 2,2-dioxide **2.40a** (2.00 g, 4.8 mmol) in DCM at 0 °C was added a solution of *m*-CPBA (1.33 g (75 % corr.), 5.8 mmol, 1.2 eq) in DCM (25 mL) dropwise, with the temperature remaining below 5° C. The reaction mixture was left to reach room temperature over 4 h (an additional 0.3 eq of m-CPBA were added to achieve reaction completion). The resulting solution was washed with H_2O (25 mL), $Na_2SO_{3\,(aq)}$ (0.7 M, 2 × 25 mL), $NaOH_{(aq)}$ (1M, 25 mL) and H_2O (20 mL) again. The obtained organic layer was dried with Na_2SO_4 and DCM was removed through rotary evaporation to afford a crude mixture that was recrystallised from EtOAc/ Hexane to yield the product (1.21 g, 67.6 %) as a white solid; R_f = 0.9 (n. DCM); m.p. = 110- 111 °C (from DCM); ν_{max} (neat): 3062, 3026, 1634, 1601, 1576, 1557, 1493, 1454, 1444, 1421, 1365 (O-SO_2), 1349, 1286, 1264, 1224, 1175 (O-SO_2), 1155, 1105, 1072, 1031, 1002 cm^{-1}; ^{1}H-NMR (400 MHz, $CDCl_3$): δ 3.78 (s, 2H, PhCH_2), 6.85 (s, 1H, 4-H), 7.21 - 7.47 (m, 13H, ArH), 7.59 - 7.62 (m, 2H, ArH); ^{13}C-NMR (100 MHz, $CDCl_3$): δ 37.52, 119.73, 127.18, 127.74, 128.59, 128.59, 128.68, 128.82, 128.88, 129.00, 129.07, 129.07, 129.88,

129.91, 132.65, 133.89, 135.11, 135.32, 154.48; HRMS: Found $[M+NH_4]^+$ = 392.1315, $C_{23}H_{18}O_3S$ requires $[M+NH_4]^+$ = 392.1315;

6-(4-Trifluorophenyl)-3,4-diphenl-1,2-oxathiine 2,2 dioxide 2.65

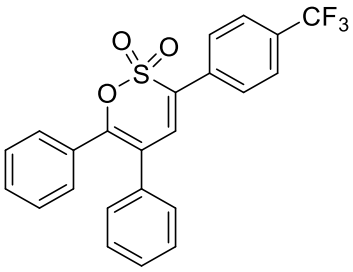

4-(Dimethylamino)-5,6-diphenyl-3-(4-(trifluoromethyl)phenyl)-3,4-dihydro-1,2-oxathiine 2,2 dioxide **2.37** (2.00 g, 4.2 mmol) was dissolved in DCM (25 mL) and cooled to 5 °C. A solution of *m*-CPBA (1.83 g (75% corr.), 10.6 mmol, 2.5 eq) in DCM (15 mL) was then added dropwise, while the temperature was kept near 5 °C, and the resulting reaction mixture was stirred for 4 hours after the addition. Upon reaction completion, the reaction mixture was washed with H_2O (25 mL), $Na_2SO_{3(aq)}$ (0.7 M, 40 mL), $NaOH_{(aq)}$ (1 M, 20 mL) and with H_2O (30 mL) again. The obtained organic layer was condensed under reduced pressure to afford a yellow solid that was purified by trituration with EtOH to yield the product (1.38 g, 77.0 %) as yellow crystals; R_f = 0.5 (10 % EtOAc/ Hexane); m.p. = 161 - 163 °C (from DCM); ν_{max} (neat): 3060, 1617, 1576, 1557, 1488, 1446, 1415, 1365 (O-SO_2), 1350, 1324, 1275, 1170 (O-SO_2), 1116, 1068, 1035, 1016, 1008 cm^{-1}; ^{1}H-NMR (400 MHz, d^6-AcMe): δ 7.32 - 7.44 (m, 10H, ArH), 7.54 (s, 1H, 4-H), 7.89 (m, 2H, ArH), 8.02 (m, 2H, ArH); ^{13}C-NMR (100 MHz, d^6-AcMe): δ 118.99, 123.74 (q, *J* = 270.0 Hz, CF_3), 126.02 (q, *J* = 3.7 Hz, *o*-Ar*C*-CF_3), 128.07, 128.30, 128.55, 129.08, 129.32, 129.34, 130.60, 130.82, 131.68 (q, *J* = 33 Hz, *C*-CF_3), 132.62, 133.44, 135.41, 135.61, 153.03; ^{19}F-NMR (376.5 MHz, d^6-AcMe): δ -63.34 (s, 3F); HRMS: Found $[M+NH_4]^+$ = 446.1042, $C_{23}H_{15}F_3O_3S$ requires $[M+NH_4]^+$ = 446.1032.

6.2.3.2 Preparation of (*E*)-*N'*-(2,2-dioxido-3,5-diphenyl-1,2-oxathiin-6-yl)-*N,N*-dimethylformimidamide 2.58

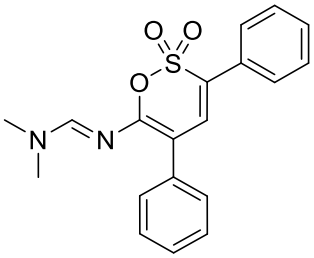

(*E*)-3-(dimethylamino)-N-(*E*)-dimethylamino) methylene)-2-phenylacrylamide **2.32** (3.00 g, 12.2 mmol) was dissolved in THF (35 mL), mixed with Et_3N (2.22 mL, 15.9 mmol, 1.3 eq) and cooled down to 0 °C. To that solution was added dropwise a solution of $PhCH_2SO_2Cl$ (3.03 g, 1.3 eq) in THF (30 mL) under a N_2 atmosphere, with the temperature maintained under °C (additional amounts of $PhCH_2SO_2Cl$ and Et_3N (0.3 eq) required to ensure reaction completion). The resulting mixture was filtered through a layer of alumina and THF was removed by rotary evaporation. The crude mixture was chromatographed in an alumina column (dry loading, 40% DCM/ Hexane) and the fractions containing the main component of the mixture were combined, washed with $Na_2CO_{3\,(aq)}$ (25 mL) and H_2O (2 × 25 mL), dried over Na_2SO_4 and condensed under reduced pressure. The resulting crude mixture was recrystallized from EtOAc/ P.E. to yield the title compound (0.38 g, 8.8 %) as yellow crystals; R_f = 0.3 (4% MeOH/ DCM); m.p. = 145 - 147 °C (from EtOAc/ P.E.); ν_{max} (neat): 3041, 2929, 1631, 1614, 1595, 1574, 1519, 1445, 1406, 1372, 1342 (O-SO_2), 1294, 1272,

1258, 1211, 1175 (O-SO_2), 1100, 1076, 1031 cm^{-1}; ^{1}H-NMR (300 MHz, $CDCl_3$): δ 3.04 (s, 3H, NMe), 3.15 (s, 3H, NMe), 7.15 (s, 1H, 4-H), 7.22-7.44 (m, 6H, ArH), 7.57-7.60 (m, 4H, ArH), 8.20 (s, 1H, vinyl-H); ^{13}C-NMR (100 MHz, $CDCl_3$): δ 35.44, 41.34, 104.76, 126.81, 127.17, 128.14, 128.59, 128.82, 129.12, 129.62, 131.49, 136.09, 136.80, 152.75, 153.42; HRMS: Found $[M+H]^+$ = 355.1111, $C_{19}H_{18}N_2O_3S$ requires $[M+H]^+$ = 355.1117.

6.2.3.3 Preparation of 5,6-disubstituted 1,2-oxathiine 2,2-dioxides

5,6-Diphenyl-1,2-oxathiine 2,2-dioxide 2.64

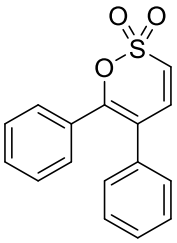

4-(Dimethylamino)-5,6-diphenyl-3,4-dihydro-1,2-oxathiine 2,2-dioxide **2.2** (3.00 g, 9.1 mmol) was dissolved in DCM (30 mL) and the solution was cooled down to 5 °C. *m*-CPBA (2.72 g (75% corr.), 11.8 mmol, 1.3 eq) was added dropwise as a DCM (35 mL) solution, with the temperature maintained under 5 °C. The reaction mixture was subsequently allowed to reach room temperature over 4.5 h, before being washed with H_2O (30 mL), $Na_2SO_{3(aq)}$ (0.7 M, 2 × 50 mL), $NaOH_{(aq)}$ (1M, 30 mL) and finally with H_2O (30 mL) again. The organic layer was dried over Na_2SO_4 and DCM was removed by rotary evaporation. The product was thus obtained (1.87 g, 72.3 %) as a pink-white solid; R_f = 0.8 (30% EtOAc/ Hexane); m.p. = 154 - 155 °C (from DCM); ν_{max} (neat): 3079, 1616, 1574, 1545, 1487, 1444, 1372, 1356 (O-SO_2), 1294, 1237, 1182 (O-SO_2), 1164, 1149, 1093, 1069, 1033, 1005 cm^{-1}; ^{1}H-NMR (400 MHz, $CDCl_3$): δ 6.73 (d, *J* = 10.2 Hz, 1H, 3-H), 7.03 (d, *J* = 10.2 Hz, 1H, 4-H), 7.18 - 7.34 (m, 10H, ArH); ^{13}C-NMR (100 MHz, $CDCl_3$): δ 117.49, 118.83, 128.20, 128.33, 129.00, 129.18, 129.46, 130.45, 131.10, 135.29, 139.32, 153.63; HRMS: Found $[M+H]^+$ = 285.0587, $C_{16}H_{12}O_3S$ requires $[M+H]^+$ = 285.058.

5,6-Bis-(4-methoxyphenyl)-1,2-oxathiine 2,2-dioxide 2.66

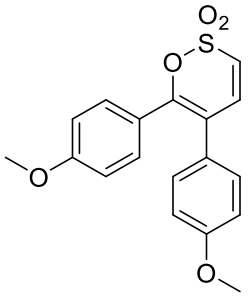

4-(Dimethylamino)-5,6-bis(4-methoxyphenyl)-3,4-dihydro-1,2-oxathiine 2,2-dioxide **2.42** (0.64 g, 1.6 mmol) was dissolved in DCM (25 mL) and cooled to 0 °C and subsequently mixed dropwise with a solution of *m*-CPBA (0.81 g (75% corr.), 3.3 mmol, 2 eq) in DCM (20 mL) at the same temperature. Upon complete addition, the reaction mixture was allowed to reach room temperature over 2h, before receiving consequent washes with H_2O (15 mL), $Na_2SO_{3(aq)}$ (0.7 M, 20 mL), $NaOH_{(aq)}$ (1 M, 15 mL) and again H_2O (10 mL). The obtained organic layer was dried over Na_2SO_4 and DCM was removed under reduced pressure to afford the title compound (0.47 g, 78.8 %) as an off-white solid; R_f = 0.7 (50% EtOAc/ Hexane); m.p. = 143 - 145 °C (from DCM); ν_{max} (neat): 3084, 3024, 2936, 2843, 1599, 1539, 1503, 1445, 1417, 1372, 1356

(O-SO_2), 1313, 1291, 1250, 1185, 1155 (O-SO_2), 1124, 1106, 1085, 1033, 1021 cm^{-1}; ^{1}H-NMR (300 MHz, $CDCl_3$): δ 3.79 (s, 3H, OMe), 3.81 (s, 3H, OMe), 6.65 (d, *J* = 10.2 Hz, 1H,4-H), 6.72 - 6.77 (m, 2H, ArH), 6.83 - 6.88 (m, 2H, ArH), 6.99 (d, *J* = 10.2 Hz, 1H, 3-H), 7.10 - 7.14 (m, 2H, ArH), 7.23 - 7.28 (m, 2H, ArH); ^{13}C-NMR (75 MHz, $CDCl_3$): δ 55.30, 55.33, 113.65, 114.64, 115.76, 117.81, 123.56, 127.69, 130.15, 131.09, 139.81, 153.26, 159.40, 161.03; HRMS: Found $[M+H]^+$ = 345.0789, $C_{18}H_{16}O_5S$ requires $[M+H]^+$ = 345.0794.

6.2.3.4 Preparation of 3,6-disubstituted 1,2-oxathiine 2,2-dioxides

3,6-Diphenyl-1,2-oxathiine 2,2-dioxide 2.67

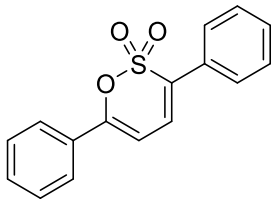

4-(Dimethylamino)-3,6-diphenyl-1,2-oxathiine 2,2-dioxide **2.43** (0.50 g, 1.5 mmol) was dissolved in DCM (15 mL) and cooled down to 5 °C. A solution of *m*-CPBA (0.50 g (75 % corr.), 2.4 mmol, 1.6 eq) in DCM (5 mL) was added dropwise at the same temperature. The resulting reaction mixture was allowed to reach room temperature overnight. Consequent washes with H_2O (35 mL), $Na_2SO_{3(aq)}$ (0.7 M, 55 mL), $NaOH_{(aq)}$ (1M, 25 mL) and again with H_2O (30 mL) yielded an organic layer which was condensed under reduced pressure to afford the product (0.34 g, 79 %) as pale yellow crystals; R_f = 0.8 (4% MeOH/ DCM); m.p. = 130 - 132 °C (from DCM); ν_{max} (neat): 3063, 1633, 1559, 1493, 1447, 1353 (O-SO_2), 1336, 1264, 1173 (O-SO_2), 1071, 1031, 1010 cm^{-1}; ^{1}H-NMR (400 MHz, $CDCl_3$): δ 6.58 (1H, d, *J* = 7.1 Hz, 5-H), 6.96 (1H, d, *J* = 7.1 Hz, 4-H), 7.47 - 7.50 (m, 6H, Ar-H), 7.64 - 7.67 (m, 2H, Ar-H), 7.77 - 7.83 (m, 2H, Ar-H); ^{13}C-NMR (100 MHz, $CDCl_3$): δ 101.60, 125.49, 127.66, 128.98, 129.01, 129.05, 129.87, 130.12, 130.65, 131.13, 134.48, 156.02; HRMS: Found $[M+H]^+$ = 285.0584, $C_{16}H_{12}O_3S$ requires $[M+H]^+$ = 285.0580.

3-Phenyl-6-(pyridine-4-yl)-1,2-oxathiine 2,2-dioxide 2.68

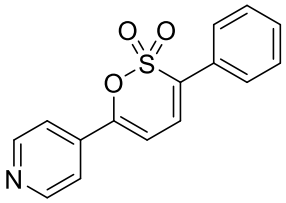

4-(Dimethylamino)-3-phenyl-6-(pyridin-4-yl)-3,4-dihydro-1,2-oxathiine 2,2-dioxide **2.44** (0.60 g, 1.8 mmol) was dissolved in DCM (10 mL) and cooled down to 5 °C. A solution of *m*-CPBA (1.08 g (75 % corr.), 4.5 mmol, 2.5 eq) in DCM (15 mL) was added dropwise, with the temperature maintained under 5 °C. Upon complete addition, the reaction mixture was allowed to reach room temperature over 4 h, before being washed with H_2O (15 mL), $Na_2SO_{3(aq)}$ (0.7 M, 2 × 13 mL), $NaOH_{(aq)}$ (1M, 15 mL) and H_2O (15 mL) again. The organic layer was dried over Na_2SO_4 and the solvent was removed by rotary evaporation. The crude mixture so obtained was recrystallised from EtOAc/ Hexane to afford the product (0.37 g, 72 %) as yellow crystals; R_f = 0.6 (10 % MeOH/ DCM); m.p. = 141 - 143 °C (from EtOAc/ Hexane); ν_{max} (neat): 3053, 1637, 1594, 1550, 1492, 1447, 1410, 1352 (SO_2-O), 1326, 1267, 1250, 1222, 1175 (SO_2-O), 1067, 1023 cm^{-1}; ^{1}H-NMR (400 MHz, $CDCl_3$): δ 6.74 (d, *J* = 7.0 Hz, 1H, 4-H), 6.95 (d, *J* = 6.9 Hz, 1H, 5-H), 7.48-7.63 (m, 7H, ArH/ PyH), 8.74-8.76 (m, 2H, PyH); ^{13}C-NMR (100 MHz, $CDCl_3$): δ 104.47, 118.63, 127.79, 127.91, 129.18, 129.59,

130.43, 136.99, 137.81, 150.74, 153.14; HRMS: Found $[M+H]^+$ = 286.0533, $C_{15}H_{11}NO_3S$ requires $[M+H]^+$ = 286.0532.

6-(Furan-2-yl)-3-phenyl-1,2-oxathiine 2,2-dioxide 2.74

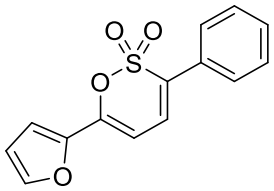

4-(Dimethylamino)-6-(furan-2-yl)-3-phenyl-3,4-dihydro-1,2-oxathiine 2,2-dioxide **2.50** (2.50 g, 7.8 mmol) was dissolved in DCM (60 mL) and cooled to -5 °C. At this temperature, a solution of *m*-CPBA (2.89 g (70 % corr.), 11.7 mmol, 1.5 eq) in DCM (50 mL) was added dropwise over 10 min. Upon complete addition, the reaction mixture was allowed to reach room temperature over 2.5 h, at which point reaction completion was confirmed by TLC. The mixture was washed with H_2O (60 mL), $Na_2SO_{3\,(aq)}$ (0.7 M, 2 × 50 mL), $NaOH_{\,(aq)}$ (1 M, 50 mL) and H_2O (50 mL) again. The resulting organic layer was dried over Na_2SO_4 and DCM was removed under reduced pressure to afford the title compound (1.95 g, 91.1 %) as a yellow solid. R_f = 0.4 (20 EtOAc/ Hexane); m.p. = 117 - 118 °C (from DCM); ν_{max} (neat): 3136, 2359, 2342, 1645, 1547, 1494, 1480, 1449, 1356 (O-SO_2), 1285, 1248, 1228, 1175 (O-SO_2), 1066, 1053, 1034, 1011 cm^{-1}; ^{1}H-NMR (400 MHz, $CDCl_3$): δ 6.46 (d, *J* = 7.2 Hz, 1H, 5-H), 6.56 - 6.67 (m, 1H, furyl-H), 6.92 (d, *J* = 7.2 Hz, 1H, 4-H), 6.93 - 6.94 (m, 1H, furyl-H), 7.44 - 7.47 (m, 3H, ArH), 7.55 - 7.56 (m, 1H, furyl-H), 7.59 - 7.61 (m, 2H, ArH); ^{13}C-NMR (100 MHz, $CDCl_3$): δ 100.00, 112.67, 112.77, 127.63, 127.64, 129.04, 129.82, 130.19, 134.29, 145.58, 145.77, 147.55; HRMS: Found $[M+Na]^+$ = 297.0190, $C_{14}H_{10}O_4S$ requires $[M+Na]^+$ = 297.0197.

(*E*)-3-Phenyl-6-styryl-1,2-oxathiine 2,2-dioxide 2.69

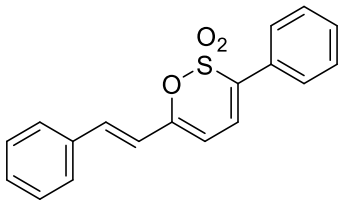

(*E*)-4-(Dimethylamino)-3-phenyl-6-styryl-3,4-dihydro-1,2-oxathiine 2,2-oxide **2.45** (0.70 g, 2.0 mmol) was dissolved in DCM (25 mL), cooled down to 0 °C and mixed with a solution of *m*-CPBA (0.69 g (75 % corr.), 2.8 mmol, 1.4 eq) in DCM (15 mL) dropwise, with the temperature remaining under 5 °C. Upon complete addition, the reaction mixture was allowed to reach room temperature over 2h, before receiving consecutive washes with H_2O (20 mL), $Na_2SO_{3\,(aq)}$ (0.7 M, 2 × 15 mL), $NaOH_{\,(aq)}$ (1 M, 15 mL) and H_2O (15 mL). The obtained organic layer was dried over Na_2SO_4 and DCM was removed under reduced pressure to yield the title compound as a yellow solid (0.54 g, 88.5 %); R_f = 0.75 (50 % EtOAc/ Hexane); m.p. = 155 - 158 °C (from DCM); ν_{max} (neat): 3025, 1627, 1602, 1540, 1494, 1448, 1356 (O-SO_2), 1291, 1263, 1199, 1169 (O-SO_2), 1069, 1032 cm^{-1}; ^{1}H-NMR (400 MHz, $CDCl_3$): δ 6.07 (d, *J* = 7.1 Hz, 1H, 5-H), 6.67 (d, *J* = 16.0 Hz, PhCH=C*H*), 6.88 (d, *J* = 7.1 Hz, 1H, 4-H), 7.33 - 7.42 (m, 4H, ArH/PhC*H*=CH), 7.43 - 7.47 (m, 3H, ArH), 7.50 - 7.53 (m, 2H, ArH), 7.60 - 7.63 (m, 2H, ArH); ^{13}C-NMR (100 MHz, $CDCl_3$): δ 105.45, 118.63, 127.57, 127.60, 128.98, 129.00, 129.04, 129.64, 129.84, 130.25, 134.85, 135.18, 135.65, 155.07; HRMS: Found $[M+Na]^+$ = 333.0562, $C_{18}H_{14}O_3S$ requires $[M+Na]^+$ = 333.0564.

(*E*)-6-(4-Methoxystyryl)-3-phenyl-1,2-oxathiine 2,2-dioxide 2.70

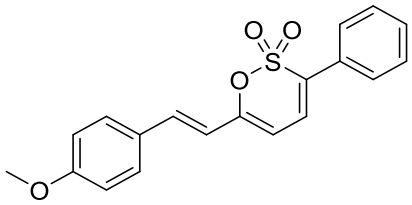

(*E*)-4-(Dimethylamino)-6-(4-methoxystyryl)-3-phenyl-3,4-dihydro-1,2-oxathiine 2,2-dioxide **2.46** (3.50 g, 9.1 mmol) was dissolved in DCM (75 mL) and cooled to 0 °C. To this, a solution of *m*-CPBA (3.14 g (70 % corr.), 12.7 mmol, 1.4 eq) in DCM (50 mL) was added dropwise, with the temperature maintained under 2 °C. Upon complete addition, the reaction mixture was allowed to reach room temperature overnight. Dilution to 200 mL allowed for subsequent washes with H_2O (75 mL), $Na_2SO_{3\,(aq)}$ (0.7 M, 2 × 75 mL), NaOH $_{(aq)}$ (1.0 M, 75 mL) and again H_2O (70 mL). The organic layer was dried over Na_2SO_4 and the solvent was evaporated under reduced pressure to afford the title compound (2.78 g, 89.7 %) as an orange solid; R_f = 0.7 (50 % EtOAc/ Hexane); m.p. = 205 - 207 °C (from DCM); ν_{max} (neat): 2962, 1631, 1598, 1571, 1540, 1509, 1444, 1361 (O-SO_2), 1311, 1298, 1251, 1171 (O-SO_2), 1151, 1070, 1026 cm^{-1}; ^{1}H-NMR (400 MHz, $CDCl_3$): δ 3.85 (s, 3H, OMe), 6.01 (d, *J* = 7.4 Hz, 1H, 5-H), 6.53 (d, *J* = 15.8 Hz, 1H, ArC*H*=CH), 6.87 (d, *J* = 7.4 Hz, 1H, 4-H), 6.91 - 6.93 (m, 2H, ArH), 7.31 (d, *J* = 15.8 Hz, 1H, ArCH=C*H*), 7.43 - 7.47 (m, 5H, ArH), 7.60 - 7.62 (m, 2H, ArH); ^{13}C-NMR (100 MHz, $CDCl_3$): δ 55.42, 104.48, 114.46, 116.35, 127.51, 128.01, 129.01, 129.18, 129.23, 129.67, 130.38, 134.11, 135.40, 155.52, 160.91; HRMS: Found $[M]^{+\cdot}$ = 340.0761, $C_{19}H_{16}O_4S$ requires $[M]^{+\cdot}$ = 340.0763.

(*E*)-6-(4-Nitrostyryl)-3-phenyl-1,2-oxathiine 2,2-dioxide 2.71

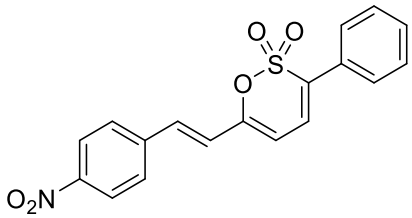

(*E*)-4-(Dimethylamino)-6-(4-nitrostyryl)-3-phenyl-3,4-dihydro-1,2-oxathiine 2,2-dioxide **2.47** (0.60 g, 1.5 mmol) was dissolved in DCM (25 mL) and cooled to -5 °C. At this temperature, a solution of *m*-CPBA (0.52 g (70 % corr.), 2.3 mmol, 1.5 eq) in DCM (25 mL) was added dropwise over 10 min. The resulting reaction mixture was allowed to reach room temperature overnight. Consecutive washes with H_2O (60 mL), Na_2SO_3 $_{(aq)}$ (0.7 M, 2 × 50 mL), NaOH $_{(aq)}$ (1M, 50 mL) and H_2O (50 mL) afforded an organic layer which was dried over Na_2SO_4 and had the solvent removed under reduced pressure. The title compound was thus obtained (0.49 g, 92.5 %) as yellow crystals; R_f = 0.7 (50 % EtOAc/ Hexane); m.p. = 230 - 232 °C (from DCM); ν_{max} (neat): 3060, 1607, 1590, 1514, 1446, 1339 (O-SO_2), 1259, 1168 (O-SO_2), 1104, 1060, 1034, 1009 cm^{-1}; ^{1}H-NMR (400 MHz, $CDCl_3$): δ 6.18 (d, *J* = 7.2 Hz, 1H, 5-H), 6.80 (d, *J* = 15.8 Hz, 1H, ArC*H*=CH), 6.90 (d, *J* = 7.2 Hz, 1H, 4-H), 7.37 (d, *J* = 15.8 Hz, 1H, ArCH=C*H*), 7.46 - 7.48 (m, 3H, ArH), 7.61 - 7.66 (m, 4H, ArH), 8.24 - 8.26 (m, 2H, ArH); ^{13}C-NMR (100 MHz, $CDCl_3$): δ 107.58, 122.69, 124.31, 127.66, 128.00, 128.41, 129.13, 129.91, 130.22, 132.52, 136.45, 141.36, 147.90, 153.88; HRMS: Found $[M]^{+\cdot}$ = 355.0504, $C_{18}H_{13}NO_5S$ requires $[M]^{+\cdot}$ = 355.0514.

(*E*)-3-Phenyl-6-(4-(trifluoromethyl)styryl)-1,2-oxathiine 2,2-dioxide 2.72

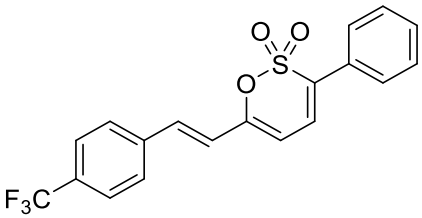

(*E*)-4-(Dimethylamino)-3-phenyl-6-(4-(trifluoromethyl)styryl)-3,4-dihydro-1,2-oxathiine 2,2-dioxide **2.48** (2.00 g, 4.7 mmol) was dissolved in DCM (50 mL) and cooled to -5 °C. A solution of *m*-CPBA (1.64 g (75 % corr.), 7.1 mmol, 1.5 eq) in DCM (50 mL) was then added dropwise at the same temperature. Upon complete addition, the reaction mixture was allowed to reach room temperature over 2 h. Subsequent washes of this mixture with H_2O (75 mL), $Na_2SO_{3\,(aq)}$ (0.7 M, 2 × 50 mL), $NaOH_{(aq)}$ (1 M, 60 mL) and H_2O (60 mL) afforded an organic layer which was dried Na_2SO_4 and had the solvent removed under reduced pressure. The title compound was thus obtained as yellow crystals (1.64 g, 92.1 %); R_f = 0.3 (20 % EtOAc/ Hexane); m.p. = 220 - 221 °C (from DCM); ν_{max} (neat): 3039, 1631, 1610, 1542, 1514, 1492, 1359 (O-SO_2), 1323, 1266, 1263, 1164 (O-SO_2), 1119, 1108, 1067, 1032, 1014 cm^{-1}; ^{1}H-NMR (400 MHz, $CDCl_3$): δ 6.12 (d, *J* = 7.1 Hz, 1H, 5-H), 6.73 (d, *J* = 15.6 Hz, 1H, ArC*H*=CH), 6.88 (d, *J* = 6.1 Hz, 1H, 4-H), 7.35 (d, *J* = 15.6 Hz, 1H, ArCH=C*H*), 7.45 - 7.47 (m, 3H, ArH), 7.59 - 7.65 (m, 6H, ArH); ^{13}C-NMR (100 MHz, $CDCl_3$): δ 106.65, 120.99, 123.92 (q, *J* = 271 Hz, CF_3), 125.92 (q, *J* = 3.2 Hz, *o*-Ar*C*-CF_3), 127.62, 127.63, 128.63, 129.09, 130.05, 130.06, 131.01 (q, *J* = 33 Hz, *C*-CF_3), 133.62, 135.80, 138.53, 154.31; ^{19}F-NMR (376.5 MHz, $CDCl_3$): δ -62.64 (s, 3F); HRMS: Found $[M]^{+\cdot}$ = 378.0532, $C_{19}H_{13}F_3O_3S$ requires $[M]^{+\cdot}$ = 378.0537.

(*E*)-6-(2-Bromostyryl)-3-phenyl-1,2-oxathiine 2,2-dioxide 2.73

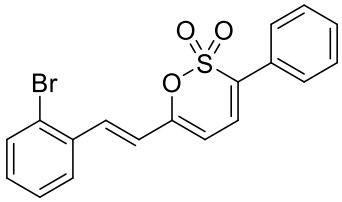

(*E*)-6-(2-Bromostyryl)-4-(dimethylamino)-3-phenyl-3,4-dihydro-1,2-oxathiine 2,2-dioxide **4.29** (3.00 g, 6.9 mmol) was dissolved in DCM (60 mL) and cooled to 0 °C. A solution of *m*-CPBA (2.39 g (75 % corr.), 10.4 mmol, 1.5 eq) in DCM (60 mL) was then added dropwise, while the temperature remained under 5 °C. The reaction mixture was allowed to reach room temperature over 2h, before being washed with H_2O (75 mL), $Na_2SO_{3\,(aq)}$ (0.7 M, 2 × 50 mL), $NaOH_{(aq)}$ (1 M, 75 mL) and H_2O (75 mL). The resulting organic layer was dried over Na_2SO_4 and the solvent was removed under removed pressure to yield the title compound (2.34 g, 87.0 %) as yellow crystals; R_f = 0.75 (50 % EtOAc/ Hexane); m.p. = 142 - 145 °C (from DCM); ν_{max} (neat): 1627, 1539, 1435, 1359 (O-SO_2), 1304, 1252, 1174 (O-SO_2), 1069, 1022 cm^{-1}; ^{1}H-NMR (400 MHz, $CDCl_3$): δ 6.10 (d, *J* = 6.6 Hz, 1H, 5-H), 6.61 (d, *J* = 15.6 Hz, 1H, ArC*H*=CH), 6.87 (d, *J* = 6.6 Hz, 1H, 4-H), 7.19 - 7.20 (m, 1H, ArH), 7.30 - 7.32 (m, 1H, ArH), 7.44 - 7.47 (m, 3H, ArH), 7.57 - 7.68 (m, 5H, ArH / ArCH=C*H*); ^{13}C-NMR (100 MHz, $CDCl_3$): δ 106.29, 121.38, 125.17, 127.16, 127.63, 127.65, 128.75, 129.05, 129.94, 130.19, 130.50, 133.59, 133.77, 135.18, 135.47, 154.65; HRMS: Found $[M]^{+\cdot}$ = 387.9768, $C_{18}H_{13}{}^{79}BrO_3S$ requires $[M]^{+\cdot}$ = 387.9769.

3-Phenyl-6-(phenylethynyl)-1,2-oxathiine 2,2-dioxide 2.75

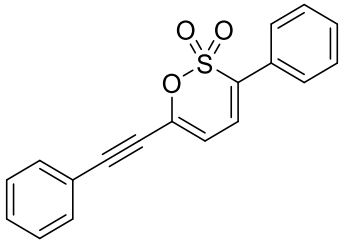

4-(Dimethylamino)-3-phenyl-6-(phenylethynyl)-3,4-dihydro-1,2-oxathiine 2,2-dioxide **2.51** (1.10 g, 3.1 mmol) was dissolved in DCM (15 mL) and cooled down to 0 °C. A solution of *m*-CPBA (1.00 g (75 % corr.), 4.4 mmol, 1.4 eq) in DCM (15 mL) was subsequently added dropwise at *circa* 5 °C. The resulting reaction mixture was allowed to reach room temperature overnight and was subsequently washed with H_2O (40 mL), $Na_2SO_{3\,(aq)}$ (0.7 M, 40 mL), $NaOH_{\,(aq)}$ (1 M, 30 mL) and H_2O (30 mL). The organic layer was dried over Na_2SO_4 and DCM was removed under reduced pressure. The crude solid so obtained was triturated with Et_2O to yield the title compound (0.81 g, 84.4 %) as a yellow solid; R_f = 0.4 (20 % EtOAc/ Hexane); m.p. = 133 - 135 °C (from DCM); ν_{max} (neat): 2203, 1622, 1546, 1488, 1441, 1361 (O-SO_2), 1280, 1270, 1251, 1177 (O-SO_2), 1155, 1126, 1063, 1031 cm^{-1}; ^{1}H-NMR (400 MHz, $CDCl_3$): δ 6.38 (d, *J* = 7.1 Hz, 1H, 5-H), 6.80 (d, *J* = 7.1 Hz, 1H, 4-H), 7.37 - 7.47 (m, 6H, ArH), 7.53 - 7.56 (m, 2H, ArH), 7.58 - 7.62 (m, 2H, ArH); ^{13}C-NMR (100 MHz, $CDCl_3$): δ 81.14, 98.52, 111.43, 120.50, 127.69, 128.02, 128.66, 129.09, 129.87, 130.23, 130.27, 132.05, 137.37, 139.80; HRMS: Found $[M]^{+\cdot}$ = 308.0491, $C_{18}H_{12}O_3S$ requires $[M]^{+\cdot}$ = 308.0502.

6.2.3.5 Preparation of 6-phenyl-1,2-oxathiine 2,2-dioxide 2.76

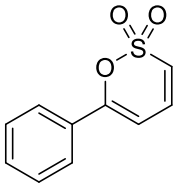

4-(Dimethylamino)-6-phenyl-3,4-dihydro-1,2-oxathiine 2,2-dioxide **2.52** (6.40 g, 25.3 mmol) was dissolved in a mixture of DCM (50 mL), THF (25 mL) and H_2O (5 mL). After being cooled down to 0 °C, the solution was mixed dropwise with a solution of *m*-CPBA (9.29 g (75 % corr.), 40.4 mmol, 1.6 eq) in DCM (75 mL), while the temperature was maintained below 5 °C. The resulting reaction mixture was stirred to room temperature over 3h, before being washed with H_2O (100 mL), $Na_2SO_{3\,(aq)}$ (0.7 M, 2 × 50 mL), $NaOH_{\,(aq)}$ (1 M, 75 mL) and H_2O (80 mL) again. The obtained organic layer was dried over Na_2SO_4 and DCM was removed under reduced pressure. The title compound was thus obtained (4.35 g, 82.7 %) as a white solid; R_f = 0.7 (50% EtOAc/ Hexane); m.p. = 86 – 87 °C (from DCM); ν_{max} (neat): 3109, 3080, 3040, 2358, 1638, 1623, 1548, 1493, 1450, 1346 (O-SO_2), 1315, 1273, 1178 (O-SO_2), 1135, 1048, 1034, 1001 cm^{-1}; ^{1}H-NMR (300 MHz, $CDCl_3$): δ 6.44 (d, *J* = 6.8 Hz, 1H, 5-H), 6.65 (d, *J* = 10.1 Hz, 1H, 3-H), 6.94 (dd, *J* = 6.8, 10.1 Hz, 1H, 4-H), 7.45 - 7.49 (m, 3H, ArH), 7.71 - 7.74 (m, 2H, ArH); ^{13}C-NMR (100 MHz, $CDCl_3$): δ 100.13, 118.88, 125.69, 129.01, 130.63, 131.40, 134.50, 157.49; HRMS: Found $[M+Na]^+$ = 231.0095, $C_{10}H_8O_3S$ requires $[M+Na]^+$ = 231.0086.

6.2.4 "One-pot"-synthesis route to 1,2-oxathiine 2,2-dioxides

6-Phenyl-1,2-oxathiine 2,2-dioxide 2.76

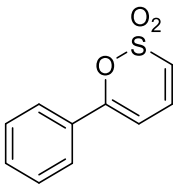

(*E*)-3-(Dimethylamino)-1-phenylprop-2-en-1-one **2.1** (2.00 g, 11.4 mmol) was dissolved in THF (40 mL), mixed with Et_3N (2.38 mL, 17.1 mmol, 1.5 eq) under a N_2 atmosphere and cooled to -5 °C. To this solution was added dropwise a solution of $MeSO_2Cl$ (1.33 mL, 17.1 mmol, 1.5 eq) in THF (20 mL), and the resulting reaction mixture was stirred at -2 °C for 1.5 h, then allowed to reach room temperature overnight. Upon reaction completion, the reaction mixture was filtered through alumina and the filtrate was condensed under reduced pressure. The crude intermediate was redissolved in DCM (35 mL), cooled to 0 °C and mixed with *m*-CPBA (3.41 g (75 % corr., 14.8 mmol, 1.3 eq) at the same temperature. This reaction mixture was also allowed to reach room temperature overnight, before being washed with H_2O (60 mL), $Na_2SO_{3\,(aq)}$ (0.7 M, 60 mL), $NaOH_{(aq)}$ (1 M, 40 mL) and H_2O (40 mL), dried over Na_2SO_4 and condensed under reduced pressure. The crude product so obtained was purified in a sinter column (silica, dry loading, n. DCM) to yield the product (1.51 g, 63.7 %, over 2 steps) as an off-white solid; ^{1}H-NMR signals were identical to those provided for **2.76** prepared by the two-step process.

6-(Pyridin-4-yl)-1,2-oxathiine 2,2-dioxide 2.78

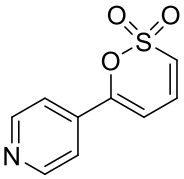

(*E*)-3-(Dimethylamino)-1-(4-pyridyl)-2-propen-1-one **2.6** (10.0 g, 56.7 mmol) was dissolved in DCM (150 mL), mixed with Et_3N (12.65 mL, 90.7 mmol, 1.6 eq) under a N_2 atmosphere and cooled to -5 °C. A solution of $MeSO_2Cl$ (7.05 mL, 90.7 mmol, 1.6 eq) in DCM (100 mL) was then added dropwise, with the temperature maintained at *circa* 0 °C. Upon complete addition, the reaction mixture was allowed to reach room temperature overnight. A further 0.4 eq of $MeSO_2Cl$ and Et_3N was required for complete starting material consumption, which was confirmed by TLC. A solution of *m*-CPBA (19.0 g (75 % corr.), 85.1 mmol, 1.5 eq) in DCM (150 mL) was subsequently added dropwise at *circa* 2 °C and the mixture was allowed to reach room temperature over 2 h. Reaction completion was confirmed *via* ^{1}H-NMR, so the final reaction mixture was washed with $NaOH_{(aq)}$ (1 M, 200 mL), $Na_2SO_{3\,(aq)}$ (0.667 M, 250 mL), $NaOH_{(aq)}$ (1 M, 200 mL) again, and H_2O (200 mL). The resulting organic layer was dried over Na_2SO_4 and the solvent was removed under reduced pressure. The crude product was purified by column chromatography (alumina, wet loading, 75% to 100% DCM in hexane) and the obtained solid was triturated with Et_2O to afford the title compound (4.14 g, 34.9 %, over 2 steps) as an off-white solid; R_f = 0.3 (4% MeOH/ $CHCl_3$); m.p. = 130 - 132 °C (from DCM/ Hexane); ν_{max} (neat): 3085, 1638, 1595, 1549, 1495, 1410, 1370, 1352 (O-SO_2), 1329, 1274, 1226, 1176 (O-SO_2), 1141, 1065, 1042, 1009 cm^{-1}; ^{1}H-NMR (400 MHz, $CDCl_3$): δ 6.61 (d, *J* = 6.7 Hz, 1H, 5-H), 6.77 (d, *J* = 10.2 Hz, 1H, 3-H), 6.97 (dd, *J* = 6.7, 10.1 Hz, 1H, 4-H), 7.55 - 7.57 (m, 2H, PyH), 8.74 - 8.75 (m, 2H, PyH); ^{13}C-NMR (100 MHz, $CDCl_3$): δ 102.79, 118.85, 121.31, 133.60, 137.78, 150.79, 154.81; HRMS: Found $[M+H]^+$ = 210.0221, $C_9H_7NO_3S$ requires $[M+H]^+$ = 210.0223.

6-(4-Methoxyphenyl)-1,2-oxathiine 2,2-dioxide 2.79

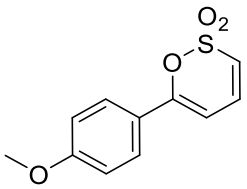

A solution of CH_3SO_2Cl (2.84 mL, 36.6 mmol, 1.5 eq) in THF (30 mL) was added dropwise to a solution of (*E*)-3-(dimethylamino)-1-(4-methoxyphenyl)prop-2-en-1-one (5.00 g, 24.4 mmol) and Et_3N (5.10 mL, 36.6 mmol, 1.5 eq) in THF (85 mL) under a N_2 atmosphere with the temperature maintained at *circa* -5 °C. The resulting mixture was stirred at 0 - 5 °C for 2 h and then at room temperature overnight. Reaction completion was ascertained by TLC and the reaction mixture was filtered through alumina and its solvent was removed under reduced pressure. The crude so obtained was re-dissolved in DCM (50 mL) and a solution of *m*-CPBA (7.29 g (75% corr.), 31.7 mmol, 1.3 eq) in DCM (50 mL) was added dropwise at *circa* 5 °C. This mixture was also allowed to reach room temperature overnight and was subsequently washed with H_2O (70 mL), $Na_2SO_{3\,(aq)}$ (0.7 M, 2 × 40 mL), $NaOH_{(aq)}$ (1 M, 50 mL) and H_2O (50 mL). Drying over Na_2SO_4 and removal of DCM under reduced pressure afforded a crude mixture which eluted through a sinter column (silica, wet loading, n. DCM) to afford the title compound (4.57 g, 78.7 % over 2 steps) as an off-white solid; R_f = 0.8 (n. DCM); m.p. = 83 - 86 °C (from DCM); ν_{max} (neat): 3077, 1626, 1604, 1547, 1508, 1467, 1423, 1371, 1346 (O-SO_2), 1314, 1272, 1250, 1190, 1174 (O-SO_2), 1139, 118, 1045, 1022 cm^{-1}; ^{1}H-NMR (400 MHz, $CDCl_3$): δ 3.86 (s, 3H, OMe), 6.31 (d, *J* = 6.8 Hz, 1H, 5-H), 6.58 (d, *J* = 10.2 Hz, 1H, 3-H), 6.91 (dd, *J* = 6.8, 10.2 Hz, 1H, 4-H), 6.94 - 6.97 (m, 2H, ArH), 7.66 - 7.68 (m, 2H, ArH); ^{13}C-NMR (100 MHz, $CDCl_3$): δ 55.52, 98.40, 114.44, 117.63, 123.13, 127.53, 134.81, 157.63, 162.19; HRMS: Found $[M+H]^+$ = 239.0371, $C_{11}H_{10}O_4S$ requires $[M+H]^+$ = 239.0376.

4-(2,2-Dioxido-1,2-oxathiin-6-yl)benzonitrile 2.80

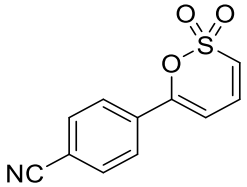

A solution of CH_3SO_2Cl (2.84 mL, 36.6 mmol, 1.5 eq) in THF (30 mL) was added dropwise to a solution of (*E*)-4-(3-(dimethylamino)acryloyl)benzonitrile (4.89 g, 24.4 mmol) and Et_3N (5.10 mL, 36.6 mmol, 1.5 eq) in THF (70 mL) under a N_2 atmosphere, with the temperature being maintained under 0 °C. After the addition, the reaction mixture was stirred at *circa* -5 °C for 2h, before being allowed to reach room temperature overnight. TLC showed that the starting material was present, so an extra 1 eq of CH_3SO_2Cl and Et_3N were added at -10 °C and the mixture was stirred at the same temperature for 30 min, before being allowed to reach room temperature over 2h. Monitoring by TLC showed reaction completion, so the formed precipitate was filtered through reaction completion and the filtrate had the solvent removed under reduced pressure. The crude intermediate was dissolved in DCM (40 mL), cooled to 5 °C and mixed with a solution of *m*-CPBA (7.29 g (75 % corr.), 31.7 mmol, 1.3 eq) in DCM (60 mL) dropwise at this temperature. This mixture was allowed to reach room temperature overnight, before being washed with H_2O (70 mL), $Na_2SO_{3\,(aq)}$ (0.7 M, 2 × 40 mL), $NaOH_{(aq)}$ (1 M, 50 mL) and H_2O (50 mL). The organic layer was dried over Na_2SO_4 and DCM was removed under reduced pressure. Purification of the crude product in a sinter column (silica, wet loading, n. DCM) yielded a solid which was triturated with Et_2O to afford the pure product (3.18 g, 55.9 % over 2 steps) as a white solid; R_f = 0.6 (n. DCM), m.p. = 203 - 205 °C (from DCM); ν_{max} (neat): 3083, 2230, 1626, 1550, 1503, 1414, 1351 (O-SO_2), 1276, 1184 (O-SO_2), 1136, 1046 cm^{-1}; ^{1}H-NMR (400 MHz, $CDCl_3$): δ 6.56 (d, *J* = 6.5 Hz, 1H, 5-H), 6.76 (d, *J* = 10.0 Hz, 1H, 3-H), 6.98 (dd, *J* = 6.5,

10.0 Hz, 1H, 4-H), 7.75 - 7.77 (m, 2H, ArH), 7.82 - 7.84 (m, 2H, ArH); ^{13}C-NMR (100 MHz, $CDCl_3$): δ 102.53, 114.62, 117.92, 120.73, 126.04, 132.76, 133.83, 134.61, 155.22; HRMS: Found $[M+H]^+$ = 234.0224, $C_{11}H_7NO_3S$ requires $[M+H]^+$ = 234.0223.

6-(2-Nitrophenyl)-1,2-oxathiine 2,2-dioxide 2.81

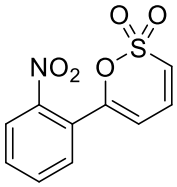

A solution of CH_3SO_2Cl (1.26 mL, 16.2 mmol, 1.5 eq) in DCM (15 mL) was added dropwise to a solution of (*E*)-3-(dimethylamino)-1-(2-nitrophenyl)prop-2-en-1-one (2.38 g, 10.8 mmol) and Et_3N (2.26 mL, 16.2 mmol, 1.5 eq) in DCM (40 mL) under a N_2 atmosphere with the temperature maintained at 5 °C. Upon complete addition, the reaction mixture was allowed to reach room temperature overnight, but reaction incompletion as observed by TLC prompted the addition of an extra 1 eq of CH_3SO_2Cl (0.84 mL, 10.8 mmol) and Et_3N (1.50 mL, 10.8 mmol) at *circa* 10 °C. The mixture was stirred at this temperature for 1h, before being allowed to reach room temperature for 2h. TLC examination showed full starting material consumption, thus a solution of *m*-CPBA (3.23 g (75 % corr.), 14.0 mmol, 1.3 eq) in DCM (10 mL) was added dropwise at *circa* 5 °C. The mixture was then allowed to reach room temperature over 72h, before being washed with H_2O (50 mL), $Na_2SO_{3\,(aq)}$ (0.7 M, 2 × 30 mL), $NaOH_{\,(aq)}$ (1 M, 40 mL) and H_2O (40 mL). Drying over Na_2SO_4 and removal of DCM under reduced pressure afforded a multicomponent crude mixture which was chromatographed in a silica column (dry loading, 20 % to 50 % EtOAc in P.E.). The fractions containing the product were recrystalised from EtOAc/P.E. produced the title compound (0.01 g, 3.7 %) as a brown solid; R_f = 0.4 (50 % EtOAc/ Hexane); m.p. = 144 - 146 °C (from EtOAc/ P.E.); ν_{max} (neat): 1652, 1605, 1563, 1530, 1442, 1345 (O-SO_2), 1290, 1245, 1180 (O-SO_2), 1137, 1089, 1043, 1032 cm $^{-1}$; ^{1}H-NMR (400 MHz, $CDCl_3$): δ 6.16 (d, *J* = 6.7 Hz, 1H, 5-H), 6.71 (d, *J* = 10.3 Hz, 1H, 3-H), 6.92 (dd, *J* = 6.7, 10.3 Hz, 1H, 4-H), 7.62 - 7.74 (m, 3H, ArH), 8.00 - 8.02 (m, 1H, ArH); ^{13}C-NMR (100 MHz, $CDCl_3$): δ 104.34, 120.02, 124.88, 126.24, 131.32, 131.93, 133.16, 133.66, 147.82, 154.58; HRMS: Found $[M+Na]^+$ = 275.9932, $C_{10}H_7NO_5S$ requires $[M+Na]^+$ = 275.9945.

6-(Thiophen-2-yl)-1,2-oxathiine 2,2-dioxide 2.82

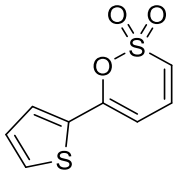

A solution of CH_3SO_2Cl (2.57 mL, 33.1 mmol, 1.5 eq) in THF (60 mL) was added dropwise at -5 °C to a solution of (*E*)-3-(dimethylamino)-1-(thiophen-2-yl)prop-2-en-1-one **2.8** (4.00 g, 22.1 mmol) and Et_3N (4.61 mL, 33.1 mmol, 1.5 eq) in THF (60 mL) under a N_2 atmosphere. The resulting reaction mixture was stirred at *circa* 0 °C for 1 h and then at room temperature overnight (additional 2 eq of CH_3SO_2Cl/Et_3N were required for reaction completion). Upon filtration of the salt precipitate through alumina, the mixture had the volatile components removed under reduced pressure before being re-dissolved in DCM (50 mL). After the temperature was lowered to -5 °C, a solution of *m*-CPBA (6.61 g (75% corr.), 28.7 mmol, 1.3 eq) in DCM (50 mL) was added dropwise at the same temperature, before being allowed to reach room temperature overnight. Upon reaction completion as monitored by H-NMR, the reaction mixture was washed with H_2O (100 mL), $Na_2SO_{3(aq)}$ (0.7 M, 2 × 50 mL), $NaOH_{(aq)}$ (1 M, 60 mL) and H_2O (70 mL). The

organic layer was dried over Na_2SO_4 and DCM was removed under reduced pressure to produce a crude mixture which eluted through a sinter column (silica, wet loading, 70 % DCM/ P.E.), affording a solid that was triturated with Et_2O to yield the title compound (1.60 g, 34.0 % over 2 steps) as a light brown solid; R_f = 0.8 (1 % MeOH/ DCM); m.p. = 80 - 83 °C (from DCM/P.E., decomposition after 60 °C); ν_{max} (neat): 1620, 1545, 1409, 1351 (O-SO_2), 1220, 1171 (O-SO_2), 1140, 1026 cm^{-1}; ^{1}H-NMR (400 MHz, $CDCl_3$): δ 6.27 (d, *J* = 6.7 Hz, 1H, 5-H), 6.60 (d, *J* = 9.8 Hz, 1H, 3-H), 6.89 (dd, *J* = 6.7, 9.8 Hz, 1H, 4-H), 7.11 - 7.13 (m, 1H, thienyl-H), 7.48 - 7.50 (m, 1H, thienyl-H), 7.53 - 7.55 (m, 1H, thienyl-H); ^{13}C-NMR (100 MHz, $CDCl_3$): δ 99.13, 118.39, 128.44, 128.53, 129.81, 134.23, 134.61, 152.89; HRMS: Found $[M]^{+\cdot}$ = 213.9752, $C_8H_6O_3S_2$ requires $[M]^{+\cdot}$ = 213.9758.

6-(4-Iodophenyl)-1,2-oxathiine 2,2-dioxide 2.83

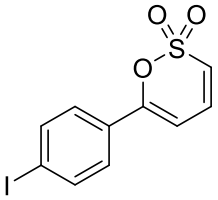

(*E*)-3-(dimethylamino)-1-(4-iodophenyl)prop-2-en-1-one **2.11** (2.00 g, 6.6 mmol) was dissolved in THF (25 mL), mixed with Et_3N (1.01 mL, 10.0 mmol, 1.5 eq) and cooled down to -10 °C, before being mixed dropwise with a solution of CH_3SO_2Cl (0.77 mL, 10.0 mmol, 1.5 eq) in THF (10 mL) under a N_2 atmosphere, with the temperature maintained under -5 °C. The resulting reaction mixture was stirred at -10 °C for 2 h and was then allowed to reach room temperature overnight. The precipitated salt was filtered through alumina and the filtrate was condensed under reduced pressure to yield the crude intermediate, which was dissolved in DCM (20 mL) and cooled down to 0 °C. Dropwise addition of a *m*-CPBA (1.97 g (75 % corr., 8.6 mmol, 1.3 eq) in DCM (25 mL) at 0 - 5 °C produced a second reaction mixture which was allowed to reach room temperature overnight. This mixture was subsequently washed with H_2O (40 mL), $Na_2SO_{3\,(aq)}$ (0.7 M, 40 mL), NaOH (1 M, 30 mL) and H_2O (30 mL), dried over Na_2SO_4 and condensed under reduced pressure to yield the title compound (0.99 g, 44.8 % over 2 steps) as an off-white solid; R_f = 0.8 (n. DCM); m.p. = 137 - 139 °C (from DCM); ν_{max} (neat): 3085, 2923, 1633, 1621, 1581, 1550, 1483, 1455, 1398, 1361, 1345 (O-SO_2), 1315, 1274, 1261, 1179 (O-SO_2), 1133, 1121, 1063, 1045, 1004 cm^{-1}; ^{1}H-NMR (400 MHz, $CDCl_3$): δ 6.44 (d, *J* = 6.8 Hz, 1H, 3-H), 6.67 (d, *J* = 10.1 Hz, 1H, 5-H), 6.92 (dd, *J* = 6.8, 10.1 Hz, 1H, 4-H), 7.42 - 7.44 (m, 2H, ArH), 7.79 - 7.81 (m, 2H, ArH); ^{13}C-NMR (100 MHz, $CDCl_3$): δ 98.19, 100.46, 119.39, 127.01, 130.12, 134.29, 138.25, 156.64; HRMS: Found $[M]^{+\cdot}$ = 333.9138, $C_{10}H_7IO_3S$ requires $[M]^{+\cdot}$ = 333.9142.

6-(Naphthalen-1-yl)-1,2-oxathiine 2,2-dioxide 2.84

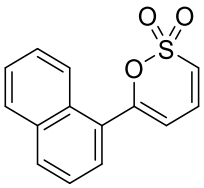

(*E*)-3-(dimethylamino)-1-(naphthalen-2-yl)prop-2-en-1-one **2.12** (0.5 g, 2.2 mmol) was dissolved in THF (10 mL), mixed with Et_3N (0.46 mL, 3.3 mmol, 1.5 eq) and cooled to -10 °C. To this solution was added dropwise a solution of $MeSO_2Cl$ (0.26 mL, 3.3 mmol, 1.5 eq) in THF (8 mL) under a N_2 atmosphere at *circa* -5 °C and the resulting reaction mixture was stirred at -5 °C for 2 h, before being allowed to reach room temperature over 72 h. Filtration of the precipitated salt through alumina and removal of THF under reduced pressure afforded the crude intermediate, which was dissolved in DCM (10 mL), cooled to 0 °C

and mixed dropwise with a solution of *m*-CPBA (0.67 g (75 % corr.), 2.9 mmol, 1.3 eq) in DCM (10 mL) at the same temperature. Upon complete addition, the reaction mixture was stirred to room temperature overnight, before being washed with H_2O (30 mL), $Na_2SO_{3\,(aq)}$ (0.7 M, 30 mL), $NaOH_{(aq)}$ 1 M, 25 mL) and H_2O (25 mL). The organic layer was dried over Na_2SO_4 and DCM was removed under reduced pressure. The crude mixture so obtained was purified by column chromatography (silica, dry loading, 20% to 30 % EtOAc/ P.E.) and the resulting solid was triturated with P.E. to yield the title compound as an off-white solid (0.09 g, 15.8 % over 2 steps); R_f = 0.3 (2 % MeOH/ DCM); m.p. = 89 - 92 °C (from EtOAc/ P.E.); ν_{max} (neat): 3086, 3051, 1631, 1561, 1508, 1366, 1353 (O-SO_2), 1276, 1249, 1176 (O-SO_2), 1145, 1107, 1059, 1032 cm^{-1}; ^{1}H-NMR (400 MHz, $CDCl_3$): δ 6.31 (d, *J* = 6.6 Hz, 1H, 5-H), 6.71 (d, *J* = 10.2 Hz, 1H, 3-H), 6.99 (dd, *J* = 6.6, 10.2 Hz, 1H, 4-H), 7.49 - 7.67 (m, 4H, ArH), 7.90 - 7.99 (m, 2H, ArH), 8.24 - 8.26 (m, 1H, ArH); ^{13}C-NMR (100 MHz, $CDCl_3$): δ 105.30, 118.98, 124.86, 124.89, 126.68, 127.69, 128.39, 128.63, 129.07, 130.86, 131.96, 133.67, 134.28, 158.97; HRMS: Found $[M]^{+\cdot}$ = 258.0343, $C_{14}H_{10}O_3S$ requires $[M]^{+\cdot}$ = 258.0345.

6.3 Chapter 3 compounds

6.3.1 α-Methylene ketone precursors and their precursors

1-(2,5-Dimethylthiophen-3-yl)-2-phenylethanone 3.52

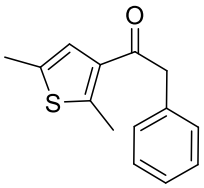

In a flame-dried flask, 2,5-dimethylthiophene (10.00 g, 89.1 mmol) was dissolved in DCM (30 mL) and mixed with phenylacetyl chloride (14.15 mL, 106.9 mmol, 1.2 eq). The mixture was cooled down to 0 - 5 °C and a solution of $AlCl_3$ (14.25 g, 106.9 mmol, 1.2 eq) in DCM (30 mL) and $MeNO_2$ (10 mL) was added dropwise, while the temperature was maintained below 5 °C. A $CaCl_2$ trap was used during the addition to create a dry atmosphere and allow for a smooth HCl release. Upon complete addition, the reaction mixture was allowed to reach room temperature over 2.5 h, before being poured into ice (*circa* 60 mL). The organic layer was separated and the aqueous phase was extracted with DCM (3 × 80 mL). The combined organic layers were washed with H_2O (2 × 100 mL), dried over Na_2SO_4 and the solvent was removed under reduced pressure. The crude mixture so obtained was purified by Kugelrohr distillation to yield the title compound (15.83 g, 77.1 %) as a dark red oil; R_f = 0.5 (10% EtOAc/ Hexane); b.p. = 130 - 135 °C (0.06 mbar); ν_{max} (neat): 3028, 2919, 1736, 1663 (C=O), 1602, 1548, 1477, 1452, 1358, 1307, 1247, 1222, 1186, 1162, 1125, 1073, 1030 cm^{-1}; ^{1}H-NMR (400 MHz, $CDCl_3$): δ 2.42 (s, 3H, thienyl-Me), 2.68 (s, 3H, thienyl-Me), 4.11 (s, 2H, α-CH_2), 7.09 (s, 1H, thienyl-H), 7.25-7.29 (m, 3H, ArH), 7.33-7.38 (m, 2H, ArH); ^{13}C-NMR (100 MHz, $CDCl_3$): δ 15.07, 16.19, 48.40, 126.15, 126.82, 128.61, 129.55, 134.79, 135.07, 135.19, 148.57, 193.57; HRMS: Found $[M+H]^+$ = 231.0840, $C_{14}H_{14}OS$ requires $[M+H]^+$ = 231.0838.

Ethyl 2,5-dimethylthiophene-3-glyoxylate 3.60

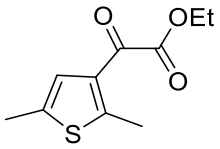

In a flame-dried flask, 2,5-dimethylthiophene (10.0 g, 89.0 mmol) was dissolved in $MeNO_2$ (40 mL), followed by the addition of ethyl oxalyl chloride (11.90 mL, 107.0 mmol, 1.2 eq). The mixture was cooled down to 0 - 5 and a solution of $AlCl_3$ (14.24 g, 106.8 mmol, 1.2 eq) in $MeNO_2$ (25 mL) was added dropwise with the temperature maintained under 5° C. A $CaCl_2$ trap was used during the addition to create a dry atmosphere and allow for a smooth HCl release. Upon complete addition, the reaction mixture reached room temperature over 2 h, before being into ice (*circa* 100 mL). The product was extracted with Et_2O (2 × 100 mL, 50 mL) and washed with H_2O (3 × 100 mL), $NaHCO_{3\ (aq)}$ (1M, 2 × 40 mL). The resulting organic layer was dried with Na_2SO_4, the solvent was removed under reduced pressure and the crude mixture was purified by Kugelrohr distillation to afford the title compound (13.22 g, 70.0 %) as a yellow liquid; R_f = 0.7 (10% EtOAc/ Hexane); b.p. = 140 - 145 °C, 0.07 bar, (lit. b.p. = 110 °C (0.001 bar))[256]; ν_{max} (neat): 2982, 2923, 1732 (OC=O), 1668 (C=O), 1549, 1477, 1446, 1378, 1284, 1207, 1116, 1013 cm^{-1}; ^{1}H-NMR (400 MHz, $CDCl_3$): δ 1.40 (t, *J* = 7 Hz, 3H, OCH_2CH_3), 2.41 (s, 3H, thienyl-Me), 2.70 (s, 3H, thienyl-Me), 4.39 (q, *J* = 7 Hz, 2H, OCH_2CH_3), 7.09 (s, 1H, thienyl-H); ^{13}C-NMR (100 MHz, $CDCl_3$): δ 14.02, 14.80, 15.90, 62.06, 126.81, 131.22, 135.90, 152.51, 164.04, 180.59.

2-(2,5-Dimethylthiophen-3-yl)acetic acid 3.61

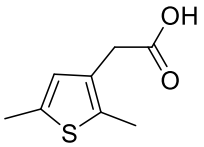

Ethyl 2,5-dimethylthiophene-3-glyoxylate **3.60** (12 g, 56.6 mmol) was slowly dissolved in $HO(CH_2)_2OH$ (50 mL). Upon complete dissolution, hydrazine monohydrate (4.87 mL, 62.3 mmol, 1.1 eq) was added. The reaction mixture was heated for 1 h at 70 °C, and then allowed to reach room temperature to allow the addition of KOH (8.07 g, 143.8 mmol, 2.5 eq), followed by further heating at reflux for 4.5 h, with forming H_2O being removed azeotropically. The reaction mixture was afterwards allowed to reach room temperature and poured into H_2O (50 mL). The pH was adjusted to *circa* 2 and the solid that formed was extracted with EtOAc (2 × 100 mL). After it was washed with brine (100 mL) and H_2O (100 mL), the organic layer was dried over Na_2SO_4 and the solvent was removed under reduced pressure to afford a brown-orange solid (8.88 g, 92.0 %); R_f = 0.5 (50% EtOAc/ Hexane), m.p. = 67 - 69 °C (from EtOAc, lit. m.p. = 67-68 °C)[257]; ν_{max} (neat): 2917, 2669, 2566, 2360, 1822, 1690 (C=O), 1573, 1496, 1437, 1409, 1303, 1276, 1213, 1198, 1144, 1122, 1075, 1037; ^{1}H-NMR (400 MHz, $CDCl_3$): δ 2.33 (s, 3H, thienyl-Me), 2.40 (s, 3H, thienyl-Me), 3.50 (s, 2H, α-CH_2), 6.55 (s, 1H, thienyl-H), 10.94 (br s, 1H, COOH); ^{13}C-NMR (100 MHz, $CDCl_3$): δ 12.95, 15.13, 33.79, 127.10, 127.98, 133.56, 135.83, 177.86.

1,2-Bis(2,5-dimethylthiophen-3-yl)ethan-1-one 3.53

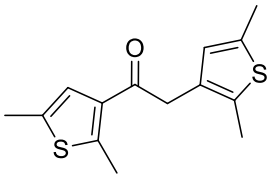

2-(2,5-Dimethylthiophen-3-yl)acetic acid **3.61** (10.00 g, 58.8 mmol) was dissolved in DCM (100 mL) and mixed with $SOCl_2$ (6.40 mL, 88.2 mmol, 1.5 eq). After the addition of DMF (10 drops), the reaction mixture was stirred at room temperature for 1 h. Upon evaporation of the volatile components, the resulting black-brown oil (12.06 g) was used for the next step without purification. In a flame-dried flask, 2,5-dimethylthiophene (5.60 mL, 48.9 mmol) was dissolved in $MeNO_2$ (50 mL) and mixed with the crude acid chloride (11.06 g (theor.), 58.8 mmol, 1.2 eq). The solution was cooled down to 0 - 5 °C and mixed with $AlCl_3$ (6.52 g, 48.9 mmol) in small portions, with the temperature remaining under 5 °C. The mixture was afterwards stirred at room temperature for 2 h, before being poured into ice (*circa* 80 mL). Addition of H_2O (70 mL) and extraction with DCM (2 × 200 mL, 50 mL) produced an organic layer that was washed with H_2O (2 × 100 mL), $Na_2CO_{3\,(aq)}$ (2 × 100 mL), dried over Na_2SO_4 and had the solvent removed under reduced pressure. The crude mixture was purified by column chromatography (silica, dry loading, 10% EtOAc/ Hexane) and the obtained solid was triturated with n-pentane to yield the product (5.97 g, 46.7 %) as an off-white solid; R_f = 0.5 (10 % EtOAc/ Hexane); m.p. = 48 - 50 °C (from EtOAc/ Hexane, lit. m.p. = 44 - 46 °C)[177]; ν_{max} (neat): 2949, 2915, 2872, 1666 (C=O), 1548, 1478, 1445, 1417, 1373, 1355, 1313, 1221, 1167, 1125, 1038 cm^{-1}; ^{1}H-NMR (400 MHz, $CDCl_3$): δ 2.31 (s, 3H, thienyl-Me), 2.38 (s, 3H, thienyl-Me), 2.42 (s, 3H, thienyl-Me), 2.66 (s, 3H, thienyl-Me), 3.92 (s, 2H, α-CH_2), 6.48 (s, 1H, thienyl-H), 7.05 (s, 1H, thienyl-H); ^{13}C-NMR (100 MHz, $CDCl_3$): δ 13.14, 15.07, 15.19, 16.13, 41.14, 125.94, 127.33, 129.62, 132.58, 135.03, 135.17, 135.48, 148.36, 193.24; HRMS: Found $[M+H]^+$ = 265.0729, $C_{14}H_{16}OS_2$ requires $[M+H]^+$ = 265.0715.

(*Z*)-4-((2,5-Dimethylthiophen-3-yl)methylene)-1,3-dimethyl-4*H*-thieno[3,4-*c*]pyran-6(7*H*)-one 3.62

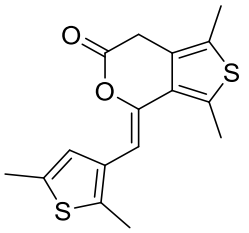

2-(2,5-Dimethylthiophen-3-yl)acetic acid **3.61** (4.00 g, 23.5 mmol) was dissolved in DCM (40 mL) and mixed with $SOCl_2$ (2.55 mL, 35.3 mmol, 1.5 eq). DMF (6 drops) was subsequently added and the mixture was stirred at room temperature for 1h. Upon evaporation of the volatile components, the crude chloride (4.57 g) was used in the next step without further purification. In a flame-dried flask, benzene (1.53 g, 19.6 mmol) was dissolved in $MeNO_2$ (30 mL), mixed with the chloride (4.57 g (theor.), 23.5 mmol, 1.2 eq) and cooled down to 5 °C. $AlCl_3$ (3.13 g, 23.5 mmol, 1.2 eq) was then added in small portions, while the temperature remained under 8 °C. Upon complete addition, the reaction mixture was allowed to reach room temperature over 2 h, before being poured into ice (*circa* 50 mL). Extraction with Et_2O (2 × 100 mL) and EtOAc (50 mL) afforded an organic layer that was washed with $NaHCO_{3\,(aq)}$ (3 × 50 mL) and H_2O (2 × 75 mL), dried over Na_2SO_4 and condensed under reduced pressure. Purification by column chromatography (silica, dry loading, 0% to 15% EtOAc in hexane) afforded a solid which was recrystallised from EtOAc/ Hexane to produce the title compound (0.32 g, 10.7 %) as light brown crystals; R_f = 0.6 (20% EtOAc/ Hexane); m.p. = 144 - 147 °C (from EtOAc/ Hexane); ν_{max} (neat): 2914, 2357, 1756 (OC=O), 1637, 1581, 1556, 1494, 1446, 1383, 1311, 1257, 1207, 1145, 1074, 1039 cm^{-1}; ^{1}H-NMR (400 MHz, $CDCl_3$): δ 2.30 (s, 3H, thienyl-Me), 2.42 (s, 3H, thienyl-Me), 2.44 (s, 3H, thienyl-Me), 2.56 (s, 3H, thienyl-Me), 3.67 (s, 2H,

α-CH_2), 5.85 (s, 1H, thienyl-H), 7.41 (s, 1H, vinyl-H); ^{13}C-NMR (100 MHz, $CDCl_3$): δ 12.14, 13.41, 15.05, 15.29, 31.87, 104.37, 126.05, 126.54, 126.74, 128.64, 130.64, 131.40, 134.88, 135.58, 140.95, 166.44; HRMS: Found $[M+H]^+$ = 305.0660, $C_{16}H_{16}O_2S_2$ requires $[M+H]^+$ = 305.0664.

2-(2,5-Dimethylthiophen-3-yl)-*N*-methoxy-*N*-methylacetamide 3.65

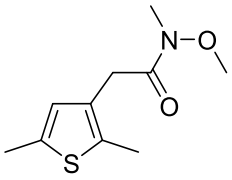

In a flame-dried flask, 2-(2,5-dimethylthiophen-3-yl)acetic acid **3.61** (7.00 g, 41.2 mmol) was dissolved in DCM (70 mL) and mixed with $SOCl_2$ (4.48 mL, 61.8 mmol, 1.5 eq). After DMF (10 drops) was added as well, the mixture was stirred at room temperature for 2 h under a dry atmosphere. The volatile components were removed by rotary evaporation and the crude chloride (7.93 g) was used on the next reaction without further purification. In a flame-dried flask and under a N_2 atmosphere, a solution of *N,O*-dimethylhydroxylamine hydrochloride (5.22 g, 45.3 mmol, 1.3 eq) in pyridine (7.33 mL, 90.6 mmol, 2.2 eq) was cooled down at 0-4 °C and mixed with a solution of the chloride (7.93 g, 41.2 mmol) in DCM (110 mL), while the temperature remained under 5 °C. Upon complete addition, the reaction mixture was allowed to reach room temperature, before being diluted with DCM (200 mL). After being washed with H_2O (3 × 100 mL), the isolated organic layer was further washed with a saturated aqueous $NaHCO_3$ solution (125 mL). Drying over Na_2SO_4 and removal of the solvent under reduced pressure afforded a crude mixture which was purified by column chromatography (silica, wet loading, 0 to 10% EtOAc/ DCM) to afford the product as a red-orange oil (5.69 g, 64.8 %); R_f = 0.5 (n. DCM); ν_{max} (neat): 2918, 2361, 1665 (C=O), 1576, 1413, 1378, 1285, 1176, 1144, 1097, 1002 cm^{-1}; ^{1}H-NMR (400 MHz, ($CDCl_3$): δ 2.32 (s, 3H, thienyl-Me), 2.37 (s, 3H, thienyl-Me), 3.18 (s, 3H, N Me), 3.59 (s, 2H, α-CH_2), 3.60 (s, 3H, OMe), 6.56 (s, 1H, thienyl-H); ^{13}C-NMR (100 MHz, $CDCl_3$): δ 12.99, 15.15, 32.26, 32.32 (2C), 61.15, 127.15, 129.57, 132.45, 135.40, 172.28; HRMS: Found $[M+H]^+$ = 214.0893, $C_{10}H_{15}NO_2S$ requires $[M+H]^+$ = 214.0896.

1-Phenyl-2-(2,5-dmethylthiophen-3-yl)-ethanone 3.54

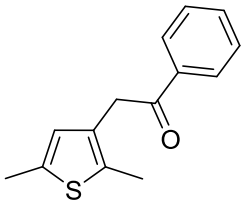

In a flame-dried flask and under a N_2 atmosphere, 2-(2,5-dimethylthiophen-3-yl)-*N*-methoxy-*N*-methylacetamide **3.65** (5.00 g, 23.5 mmol) was dissolved in dry THF (140 mL) and cooled down to -78 °C. A solution of phenyllithium in ^{n}Bu_2O (43.30 mL 1.9 M soln., 82.3 mmol, 3.5 eq) was then added dropwise with the temperature maintained under -70 °C. After the addition was completed, the reaction mixture was stirred at -70 °C for 1 h, before being quenched with saturated NH_4Cl aqueous solution (160 mL). The pH was adjusted to 7 - 8 and the product was extracted with DCM (200 mL, 100 mL). The resulting organic layer was washed with brine (300 mL), dried over Na_2SO_4 and the solvent was removed *under reduced pressure*. The crude mixture so obtained was purified by column chromatography (50 to 60% DCM/ P.E.) to yield the product as a pale green solid (3.56 g, 65.8 %); R_f = 0.6 (50% DCM/ Hexane); m.p. = 52 - 54 °C (from DCM/ P.E., lit. m.p. = 55 - 57 °C (from MeOH/ H_2O))[177]; ν_{max} (neat): 2916, 2875, 2356, 1683 (C=O), 1593, 1578, 1444, 1399, 1336, 1215, 1204, 1182, 1140, 1075, 1028 cm^{-1}; ^{1}H-NMR (400 MHz, $CDCl_3$): δ 2,34 (s, 3H, thienyl-Me), 2,37 (s, 3H, thienyl-Me), 4.12 (s, 2H, α-CH_2), 6.49 (s, 1H, thienyl-H), 7.46-7.49 (m, 2H,

ArH), 7.55-7.59 (m, 1H, ArH), 7.99-8.01 (m, 2H, ArH); ^{13}C-NMR (100 MHz, $CDCl_3$): δ 13.18, 15.18, 38.42, 127.22, 128.46, 128.66, 129.25, 132.73, 133.16, 135.69, 136.69, 197.31.

6.3.2 Enaminone precursors

(*E*)-(Dimethylamino)-1-(2,5-dimethylthiophen-3-yl)-2-phenylprop-2-en-1-one 3.66

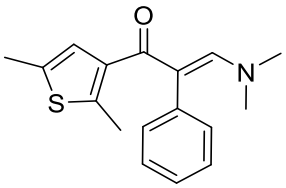

1-(2,5-Dimethylthiophen-3-yl)-2-phenylethanone **3.52** (10.00 g, 43.4 mmol) was dissolved in DMFDMA (14.91 mL, 108.5 mmol, 2.5 eq) under a N_2 atmosphere and the solution was stirred at reflux overnight. After removal of the volatile components by rotary evaporation, the orange-brown oil so obtained solidified after 1 h. Recrystallisation from EtOAc/ Hexane afforded the product (10.17 g, 82.1 %) as pale yellow crystals; R_f = 0.2 (50% EtOAc/ Hexane); m.p. = 85 - 87 °C (from EtOAc/ Hexane); ν_{max} (neat): 3048, 2911, 1620, 1563 (C=O), 1494, 1482, 1431, 1388, 1371, 1342, 1318, 1285, 1221, 1197, 1157, 1142, 1106, 1071, 1057, 1037, 1022 cm^{-1}; ^{1}H-NMR (400 MHz, $CDCl_3$): δ 2.32 (s, 3H, thienyl-Me), 2.41 (s, 3H, thienyl-Me), 2.72 (s, 6H, NMe_2); 6.49 (s, 1H, thienyl-H), 7.14-7.21 (m, 3H, ArH), 7.25-7.29 (m, 2H, ArH), 7.28 (s, 1H, vinyl-H); ^{13}C-NMR (100 MHz, $CDCl_3$): δ 14.42, 14.98, 43.56, 113.63, 126.30, 126.74, 127.55, 131.94, 134.96, 136.89, 137.48, 139.33, 153.56, 190.86; HRMS: Found $[M+H]^+$ = 286.1268, $C_{17}H_{19}NOS$ requires $[M+H]^+$ = 286.126.

(*E*)-3-(Dimethylamino)-1,2-bis(1,5-dimethylthiophen-3-yl)prop-2-en-1-one 3.67

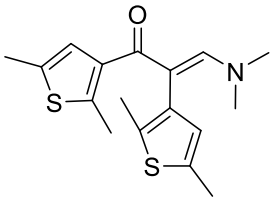

1,2-Bis(2,5-dimethylthiophen-3-yl)ethan-1-one **3.53** (5.00 g, 18.9 mmol) was dissolved in DMFDMA (6.29 mL, 47.3 mmol, 2.5 eq) under a N_2 atmosphere and stirred at reflux overnight. After removal of the volatile components by rotary evaporation, the reaction mixture was mixed with brine and extracted with EtOAc (3 × 50 mL). The extracts were washed with H_2O (40 mL), dried over Na_2SO_4 and the solvent was removed by rotary evaporation, producing a crude mixture that was purified by column chromatography (alumina, wet loading, n. DCM) to yield the product (3.62 g, 60.0 %) as a red-orange oil. R_f = 0.4 (50% EtOAc/ Hexane); ν_{max} (neat): 2914, 2858, 1628, 1578, 1553 (C=O), 1488, 1424, 1390, 1313, 1224, 1205, 1179, 1116, 1060, 1014 cm^{-1}; ^{1}H-NMR (400 MHz, $CDCl_3$): δ 2.12 (s, 3H, thienyl-Me), 2.33 (s, 3H, thienyl-Me), 2.37 (s, 3H, thienyl-Me), 2.42 (s, 3H, thienyl-Me), 2.77 (s, 6H, NMe_2), 6.43 (s, 1H, thienyl-H), 6.45 (s, 1H, thienyl-H), 7.30 (s, 1H, vinyl-H); ^{13}C-NMR (100 MHz, $CDCl_3$): δ 13.80, 14.44, 14.97, 15.34, 42.43, 107.24, 126.51, 129.66, 132.76, 133.81, 134.44, 134.74, 137.60, 139.39, 154.24, 190.37; HRMS: Found $[M+H]^+$ = 320.1149, $C_{17}H_{21}NOS_2$ requires $[M+H]^+$ = 320.1137.

(*E*)-3-(Dimethylamino)-2-(2,5-dimethylthiophen-3-yl)-1-phenylprop-2-en-1-one 3.68

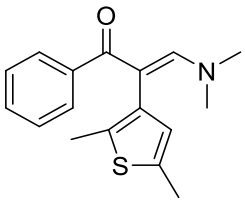

1-Phenyl-2-(2,5-dimethylthiophen-3-yl)-ethanone **3.54** (2.5 g, 10.9 mmol) was dissolved in PhMe (60 mL) and mixed with DMFDMA (1.6 mL, 12.0 mmol, 1.1 eq) under a N_2 atmosphere. The mixture was then stirred at reflux for 2.5 h, and afterwards poured into H_2O (10 mL). Extraction with EtOAc (2 × 25 mL) afforded an organic layer that was dried over Na_2SO_4 and condensed by rotary evaporation to yield the product (2.65 g, 85.5 %) as a pink solid; R_f = 0.3 (50% EtOAc/ Hexane); m.p. = 102- 105 °C (from EtOAc); ν_{max} (neat): 2913, 1599, 1581, 1557 (C=O), 1492, 1442, 1393, 1317, 1301, 1289, 1227, 1205, 1176, 1155, 1135, 1111m 1037, 1022 cm^{-1}; ^{1}H-NMR (400 MHz, ($CDCl_3$): δ 2.09 (s, 3H, thienyl-Me), 2.36 (s, 3H, thienyl-Me), 2.79 (s, 6H, NMe_2), 6.44 (s, 1H, thienyl-H), 7.26- 7.32 (m, 2H, ArH), 7.42- 7.43 (m, 3H, ArH); ^{13}C-NMR (100 MHz, $CDCl_3$): δ 13.77, 15.37, 42.82, 43.36, 105.30, 127.53, 128.36, 129.26, 129.76, 133.23, 133.81, 134.60, 141.91, 154.21, 194.35; HRMS: Found $[M+H]^+$ = 286.1266, $C_{17}H_{19}NOS$ requires $[M+H]^+$ = 286.126.

6.3.3 Preparation of 3,4-Dihydro 1,2-oxathiine 2,2-dioxide targets

6-(2,5-Dimethylthiophen-3-yl)-4-(dimethylamino)-3,4-dihydro-3,5-diphenyl-1,2-oxathiine 2,2 dioxide 3.43

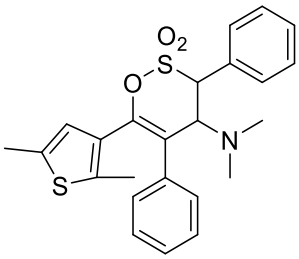

3-(Dimethylamino)-1-(2,5-dimethylthiophen-3-yl)-2-phenylprop-2-en-1-one **3.66** (6.00 g, 21.0 mmol) was dissolved in THF (70 mL) and mixed with Et_3N (3.51 mL, 25.2 mmol, 1.2 eq). The solution was then cooled down to 0 °C, before the dropwise addition of $PhCH_2SO_2Cl$ (4.80 g, 25.2 mmol, 1.2 eq) dissolved in THF (50 mL) under a N_2 atmosphere, while the temperature was maintained under 5 °C. Upon complete addition, the reaction mixture was allowed to reach room temperature overnight. Reaction completion was achieved with the addition of 0.4 eq of $PhCH_2SO_2Cl$ and Et_3N (at 5 °C) and 1 h of stirring. The reaction mixture was subsequently filtered through a thin layer of alumina and the filtrate was condensed under reduced pressure. The solid so obtained was dissolved in EtOAc (120 mL), washed with H_2O (2 × 60 mL), dried over Na_2SO_4 and the solvent was again removed by rotary evaporation. The crude mixture was recrystallized from EtOAc / Hexane to afford the product (6.57 g, 71.0 %) as an off-white solid; R_f = 0.9 (50% EtOAc/ Hexane); m.p. = 146 - 150 °C (from EtOAc/ Hexane); ν_{max} (neat): 2913, 2859, 2824, 2782, 1650, 1496, 1479, 1441, 1363 (O-SO_2), 1285, 1216, 1183 (O-SO_2), 1167, 1126, 1086, 1073, 1054, 1038, 1027 cm^{-1}; ^{1}H-NMR (400 MHz, $CDCl_3$): δ 2.02 (s, 3H, thienyl-Me), 2.20 (s, 6H, NMe_2), 2.31 (s, 3H, thienyl-Me), 4.56 (d, *J* = 7.9 Hz, 1H, 4-H), 4.89 (d, *J* = 7.9 Hz, 1H, 3-H), 6.50 (s, 1H, thienyl-H), 7.21- 7.28 (m, 5H, ArH), 7.42-7.44 (m, 2H, ArH), 7.58-7.61 (m, 3H, ArH); ^{13}C-NMR (100 MHz, $CDCl_3$): δ 14.20, 15.06, 40.55, 62.33, 70.99, 123.93, 126.09, 127.47, 127.95, 129.22, 129.26, 129.45, 129.52, 129.87, 131.90, 136.07, 137.16, 138.28, 144.90; HRMS: Found $[M+H]^+$ = 440.1345, $C_{24}H_{25}NO_3S_2$ requires $[M+H]^+$ = 440.1349.

4-(Dimethylamino)-5-(2,5-dimethylthiophen-3-yl)-3,6-diphenyl-1,2-oxathiine 2.2-dioxide 3.44

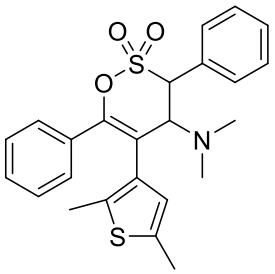

(*E*)-3-(Dimethylamino)-2-(2,5-dimethylthiophen-3-yl)-1-phenylprop-2-en-1-one **3.68** (2.00 g, 7.0 mmol) was dissolved in dry THF (25 mL), mixed with Et_3N (1.27 mL, 9.1 mmol, 1.3 eq) and cooled down to 0 °C. A solution of $PhCH_2SO_2Cl$ (1.73 g, 9.1 mmol, 1.3 eq) in THF (25 mL) was then added dropwise under a N_2 atmosphere, while the temperature remained under 5 °C. Upon complete addition, the reaction mixture was allowed to reach room temperature over 3 h (additional amounts of $PhCH_2SO_2Cl$ and Et_3N (0.3 eq) were required to ensure reaction completion). The reaction mixture was subsequently filtered through alumina and the solvent was evaporated under reduced pressure. The crude mixture was purified through column chromatography (alumina, dry loading, 50% to 75% DCM in hexane) and the obtained solid was recrystallized from EtOAc/ Hexane to afford the product (1.62 g, 52.6 %) as a white solid; R_f = 0.3 (50% DCM/ Hexane); m.p. = 133 - 135 °C (from EtOAc/ Hexane); ν_{max} (neat): 2941, 2832, 1495, 1446, 1369 (O-SO_2), 1339, 1317, 1266, 1240, 1225, 1178 (O-SO_2), 1152, 1134, 1099, 1061, 1050, 1037, 1025, 1000 cm^{-1}; ^{1}H-NMR (400 MHz, $CDCl_3$): δ 1.93 (s, 3H, thienyl-Me), 2.26 (s, 6H, NMe_2), 2.42 (s, 3H, thienyl-Me), 4.28 (d, *J* = 8.1 Hz, 1H, 4-H), 4.92 (d, *J* = 8.1 Hz, 1H, 3-H), 6.72 (s, 1H, thienyl-H), 7.22-7.26 (m, 5H, ArH), 7.42-7.45 (m, 3H, ArH), 7.56-7.58 (m, 2H, ArH); ^{13}C-NMR (100 MHz, $CDCl_3$): δ 13.47, 15.40, 40.80, 61.94, 71.26, 117.44, 127.40, 127.91, 128.25, 129.03, 129.24, 129.48, 129.88, 131.75, 132.39, 133.09, 134.50, 135.59, 148.59; HRMS: Found $[M+H]^+$ = 440.1335, $C_{24}H_{25}NO_3S_2$ requires $[M+H]^+$ = 440.1349.

4-(Dimethylamino)-5,6-bis-(2,5-dimethylthiophen-3-yl)-3-phenyl-3,4-dihydro-1,2-oxathiine 2,2-dioxide 3.45

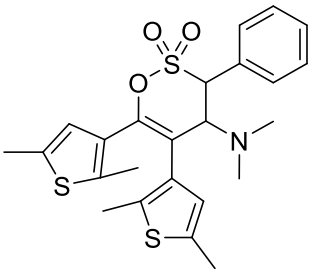

3-(Dimethylamino)-1,2-bis(1,5-dimethylthiophen-3-yl)prop-2-en-1-one **3.67** (2.00 g, 6.3 mmol) was dissolved in THF (25 mL), mixed with Et_3N (1.05 mL, 7.6 mmol, 1.2 eq) and cooled down to 0 °C. A solution of $PhCH_2SO_2Cl$ (1.44g, 7.56 mmol, 1.2 eq) in THF (20 mL) was then added dropwise Under a N_2 atmosphere, with the temperature maintained below 5 °C. Upon complete addition, the mixture was allowed to reach room temperature over 4h (reaction completion was achieved after the addition of an extra 0.3 eq of $PhCH_2SO_2Cl$ and Et_3N). After it was filtered through a thin layer of alumina, the reaction mixture was condensed under reduced pressure and the obtained oil was dissolved in EtOAc (50 mL), washed with H_2O (2 × 25 mL), dried over Na_2SO_4 and had its solvent removed under reduced pressure. Recrystallisation for the crude mixture from EtOAc/ Hexane afforded the product (1.57 g, 52.7 %) as an off-white solid; R_f = 0.8 (n. DCM); m.p. = 135 - 138 °C (from EtOAc/ Hexane); ν_{max} (neat): 2915, 2857, 2836, 2785, 1645, 1496, 1440, 1367 (O-SO_2), 1287, 1244, 1181, 1157 (O-SO_2), 1136, 1110, 1055, 1035 cm^{-1}; ^{1}H-NMR (400 MHz, $CDCl_3$): δ 2.01 (s, 3H, thienyl-Me), 2.21 (s, 3H, thienyl-Me), 2.23 (s, 6H, NMe_2), 2.28 (s, 3H, thienyl-Me),

2.38 (s, 3H, thienyl-Me), 4.32 (d, *J* = 7.9 Hz, 1H, 3-H), 4.85 (d, *J* = 7.9 Hz, 1H, 4-H), 6.32 (s, 1H, thienyl-H), 6.67 (s, 1H, thienyl-H), 7.42 - 7.43 (m, 3H, ArH), 7.55 - 7.57 (m, 2H, ArH); ^{13}C-NMR (100 MHz, $CDCl_3$): δ 13.85, 14.58, 15.02, 15.31, 40.71, 62.09, 70.97, 118.01, 125.96, 126.71, 129.21, 129.41, 129.55, 129.87, 131.92, 132.31, 134.89, 134.98, 135.29, 138.40, 145.35; HRMS: Found $[M+H]^+$ = 474.1236, $C_{24}H_{27}NO_3S_3$ requires $[M+H]^+$ = 474.1226.

4-(Dimethylamino)-5,6-bis(2,5-dimethylthiophen-3-yl)-3,4-dihydro-1,2-oxathiine 2,2-dioxide 3.46

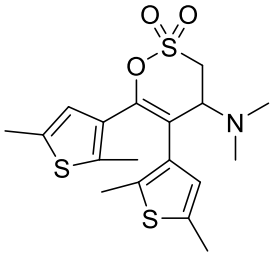

(*E*)-3-(dimethylamino)-1,2-bis(1,5-dimethylthiophen-3-yl)prop-2-en-1-one **3.67** (1.01 g, 3.2 mmol) was dissolved in THF (20 mL), mixed with Et_3N (0.57 mL, 4.1 mmol, 1.3 eq) and cooled down to *circa* 0°C. A solution of CH_3SO_2Cl (0.47 mL, 4.1 mmol, 1.3 eq) in THF (10 mL) was subsequently added dropwise under a N_2 atmosphere, with the temperature monitored under 5 °C. The reaction mixture was allowed to reach room temperature over 3 h (additional amounts of CH_3SO_2Cl/Et_3N (0.4 eq) required to achieve reaction completion). Filtration through a thin alumina layer and removal of the solvent by rotary evaporation afforded a solid that was triturated with EtOAc, dissolved in DCM and eluted through a sinter column (alumina, n. DCM). The title compound was thus obtained as a white solid (0.70 g, 55%); R_f = 0.5 (30% EtOAc/ Hexane); m.p. = 144 - 146 °C (from DCM); ν_{max} (neat): 2984, 2916, 2602, 2490, 2360, 1475, 1440, 1385 (O-SO_2), 1346, 1289, 1252, 1235, 1200, 1153 (O-SO_2), 1129, 1112, 1066, 1031, 1002 cm^{-1}; ^{1}H-NMR (300 MHz, $CDCl_3$): δ 1.92 (s, 3H, thienyl-Me), 2.17 (s, 3H, thienyl-Me), 2.26 (s, 3H, thienyl-Me), 2.30 (s, 6H, NMe_2), 2.38 (s, 3H, thienyl-Me), 3.54 (d, *J* = 9.0 Hz, 1H, 3-H), 3.55 (d, *J* = 7.7 Hz, 1H, 3-H), 4.17 (dd, *J* = 7.8, 9.1 Hz, 1H, 4-H), 6.23 (s, 1H, thienyl-H), 6.55 (s, 1H, thienyl-H); ^{13}C-NMR (100 MHz, $CDCl_3$): δ 13.71, 14.42, 14.98, 15.32, 40.25, 42.53, 63.26, 117.11, 125.88, 126.56, 129.64, 131.43, 134.77, 134.94, 135.27, 138.26, 145.50; HRMS: Found $[M+H]^+$ = 398.0910, $C_{18}H_{23}NO_3S_3$ requires $[M+H]^+$ = 398.0913.

6.3.4 1,2-Oxathiine 2,2-dioxide targets

6-(2,5-Dimethylthiophen-yl)-3,5-diphenyl-1,2-oxathiine 2,2-dioxide 3.48

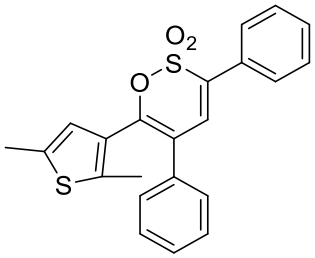

A solution of *m*-CPBA (1.12 g (75 % corr.), 6.5 mmol, 1.9 eq) in DCM (15 mL) was added dropwise to a solution of 6-(2,5-dimethylthiophen-3-yl)-4-(dimethylamino)-3,4-dihydro-3,5-diphenyl-1,2-oxathiine 2,2 dioxide **3.43** (1.00 g, 2.3 mmol) in DCM (25 mL), with the temperature maintained below 5 °C. Upon complete addition, the reaction mixture was allowed to reach room temperature overnight. Subsequent washes of the mixture with H_2O (15 mL), $Na_2SO_{3\,(aq)}$ (0.7 M, 2 × 15 mL), $NaOH_{\,(aq)}$ (1M, 15 mL) and H_2O (12

mL), followed by drying over Na_2SO_4 and removal of DCM under reduced pressure afforded a crude mixture that was recrystallised from EtOAc as yellow crystals (0.96 g, 71.1 %); R_f = 0.9 (n. DCM), m.p. = 143 - 145 °C (from EtOAc); ν_{max} (neat): 3062, 2961, 1613, 1537, 1494, 1442, 1359 (O-SO_2), 1284, 1270, 1228, 1178 (O-SO_2), 1146, 1113, 1075, 1035, 1003 cm^{-1}; ^{1}H-NMR (400 MHz, $CDCl_3$): δ 2.15 (s, 3H, thienyl-Me), 2.29 (s, 3H, thienyl-Me), 6.38 (s, 1H, thienyl-H), 7.04 (s, 1H, 4-H), 7.22 - 7.34 (m, 5H, ArH), 7.44 - 7.46 (m, 3H, ArH), 7.65-7.67 (m, 2H, ArH); ^{13}C-NMR (100 MHz, $CDCl_3$): δ 14.60, 15.03, 119.48, 125.94, 127.74, 127.87, 127.97, 128.66, 128.85, 129.02, 129.84, 130.08, 133.52, 133.90, 135.68, 136.39, 141.08, 149.48; HRMS: Found $[M+H]^+$ = 395.0777, $C_{22}H_{18}O_3S_2$ requires $[M+H]^+$ = 395.0770.

5-(2,5-Dimethylthiophen-3-yl)-3,6-diphenyl-1,2-oxathiine 2,2-dioxide 3.49

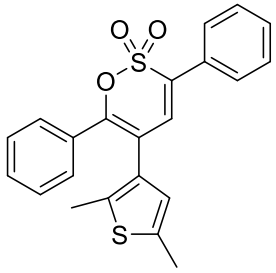

A solution of *m*-CPBA (0.68 g (75 % corr.), 3.0 mmol, 1.3 eq) in DCM (25 mL) was added dropwise to a solution of 4-(dimethylamino)-5-(2,5-dimethylthiophen-3-yl)-3,6-diphenyl-1,2-oxathiine 2.2-dioxide **3.44** (1.00 g, 2.3 mmol) in DCM (25 mL), with the temperature maintained below 5 °C. Upon complete addition, the mixture was allowed to reach room temperature over 2 h, before receiving subsequent washes with H_2O (15 mL), $Na_2SO_{3\,(aq)}$ (0.7 M, 2 × 15 mL), $NaOH_{\,(aq)}$ (1 M, 15 mL) and H_2O (10 mL) again. The organic layer so obtained was dried over Na_2SO_4 and the solvent was removed under reduced pressure, affording the product (0.71 g, 78.0 %) as a pale yellow solid; R_f = 0.8 (60% DCM/ Hexane), m.p. = 126 - 128 °C; ν_{max} (neat): 3025, 2914, 1625, 1577, 1552, 1488, 1446, 1363 (O-SO_2), 1321, 1264, 1223, 1182 (O-SO_2), 1170, 1153, 1139, 1086, 1067, 1035, 1009 cm^{-1}; ^{1}H-NMR (400 MHz, $CDCl_3$): δ 1.93 (s, 3H, thienyl-Me), 2.45 (s, 3H, thienyl-Me), 6.63 (s, 1H, thienyl-H), 6.89 (s, 1H, 4-H), 7.29- 7.37 (m, 3H, ArH), 7.40- 7.47 (m, 5H, ArH), 7.64-7.67 (m, 2H, ArH); ^{13}C-NMR (100 MHz, $CDCl_3$): δ 13.46, 15.34, 113.75, 125.31, 127.66, 128.26, 128.37, 129.01, 129.88, 129.89, 130.23, 130.87, 131.54, 133.68, 134.04, 134.81, 138.03, 152.10; HRMS: Found $[M+H]^+$ = 395.0768, $C_{22}H_{18}O_3S_2$ requires $[M+H]^+$ = 395.077.

5,6-Bis-(2,5-dimethylthiophen-3-yl)-3-phenyl-1,2-oxathiine 2,2-dioxide 3.50

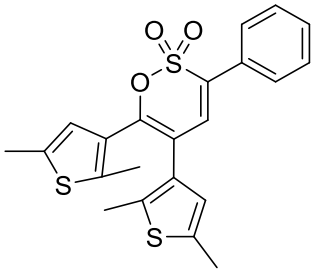

A solution of *m*-CPBA (0.68 g (75 % corr.), 3.0 mmol, 1.1 eq) in DCM (20 mL) was added dropwise to a solution of 4-(dimethylamino)-5,6-bis-(2,5-dimethylthiophen-3-yl)-3-phenyl-3,4-dihydro-1,2-oxathiine 2,2-dioxide **3.45** (1.30 g, 2.7 mmol) in DCM (20 mL), while the temperature remained under 5 °C. The mixture was then allowed to reach room temperature over 1.5 h (reaction completion was achieved after the addition of an extra 1.3 eq of m-CPBA). Subsequent washes of the reaction mixture with H_2O (15 mL), $Na_2SO_{3\,(aq)}$ (0.7 M, 2 × 15 mL), $NaOH_{\,(aq)}$ (1 M, 15 mL) and H_2O again (10 mL) yielded an organic layer that

was dried over Na_2SO_4 and condensed under reduced pressure. The crude mixture so obtained was purified in a sinter column (silica, dry loading, 10% EtOAc/ Hexane) and yielded the title product as brown crystals (0.96 g, 83.5 %); R_f = 0.4 (10% EtOAc/ Hexane); m.p. = 132-134 °C (from EtOAc/ Hexane); ν_{max} (neat): 2910, 2853, 1627, 1556, 1494, 1433, 1358 (O-SO_2), 1342, 1319, 1259, 1231, 1182, 1166 (O-SO_2), 1142, 1132, 1062, 1036 cm^{-1}; ^{1}H-NMR (400 MHz, ($CDCl_3$): δ 1.96 (s, 3H, thienyl-Me), 2.30 (s, 3H, thienyl-Me), 2.35 (s, 3H, thienyl-Me), 2.42 (s, 3H, thienyl-Me), 6.29 (s, 1H, thienyl-H), 6.56 (s, 1H, thienyl-H), 6.90 (s, 1H, 4-H), 7.43-7.46 (m, 3H, ArH), 7.62-7.65 (m, 2H, ArH); ^{13}C-NMR (100 MHz, $CDCl_3$): δ 13.65, 14.79, 15.05, 15.28, 114.08, 125.23, 125.52, 127.66, 128.25, 128.97, 129.73, 130.08, 130.90, 133.23, 133.64, 135.06, 135.97, 137.23, 141.42, 149.60; HRMS: Found $[M+Na]^+$ = 451.0467, $C_{22}H_{20}O_3S_3$ requires $[M+Na]^+$ = 451.0467.

5,6-Bis(2,5-dimethylthiophen-3-yl)-1,2-oxathiine 2,2-dioxide 3.51

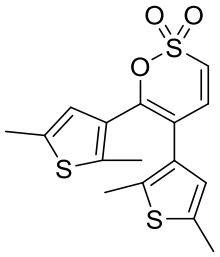

A solution of m-CPBA (0.30 g (75 % corr.), 1.3 mmol, 1.3 eq) in DCM (15 mL) was added dropwise to a solution of 4-(dimethylamino)-5,6-bis(2,5-dimethylthiophen-3-yl)-3,4-dihydro-1,2-oxathiine 2,2-dioxide **3.46** (0.40 g, 1.0 mmol) in DCM (10 mL), with the temperature remaining under 3 °C. The resulting reaction mixture was afterwards stirred to room temperature over 3 h (an additional amount of m-CPBA (0.6 eq) was required for reaction completion), before being washed with H_2O (10 mL), $Na_2SO_{3\,(aq)}$ (0.667 M, 15 mL), $NaOH_{(aq)}$ (1 M, 10 mL) and H_2O (10 mL) a second time. Upon drying the organic layer with Na_2SO_4 and removing DCM through rotary evaporation, the product was obtained as a pink solid (0.27 g, 77.7 %); R_f = 0.2 (30% EtOAc/ Hexane); m.p. = 145 - 146° C (from DCM); ν_{max} (neat): 3064, 2916, 1622, 1557, 1545, 1494, 1442, 1363 (O-SO_2), 1249, 1223, 1186, 1174 (O-SO_2), 1141, 1115, 1055 cm^{-1}; ^{1}H-NMR (300 MHz, $CDCl_3$): δ 1.90 (s, 3H, thienyl-Me), 2.28 (s, 3H, thienyl-Me), 2.32(s, 3H, thienyl-Me), 2.40 (s, 3H, thienyl-Me), 6.22 (s, 1H, thienyl-H), 6.48 (s, 1H, thienyl-H), 6.61 (d, *J* = 10.2 Hz, 1H, 4-H), 6.90 (d, *J* = 10.2 Hz, 1H, 3-H); ^{13}C-NMR (100 MHz, $CDCl_3$): δ 13.57, 14.68, 15.02, 15.26, 112.68, 118.06, 125.03, 125.46, 128.25, 130.36, 135.05, 136.01, 137.28, 138.98, 141.79, 150.84; HRMS: Found $[M+NH_4]^+$ = 370.0587, $C_{16}H_{16}O_3S_3$ requires $[M+NH_4]^+$ = 370.0600.

6.4 Chapter 4 compounds

6.4.1 Preparation of bromo-1,2-oxathiine 2,2-dioxides

3-Bromo-3,6-diphenyl-1,2-oxathiine 2,2-dioxide 4.9

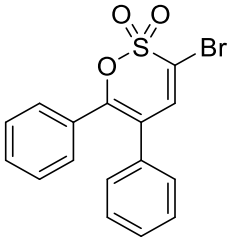

A solution of Br_2 (2.81 mL, 17.6 mmol) in $CHCl_3$ (50 mL) was added dropwise to a solution of 5,6-diphenyl-1,2-oxathiine 2,2-dioxide **4.5** (5.00 g, 17.6 mmol) in $CHCl_3$ (200 mL). The resulting reaction mixture was stirred at 70 °C for 72 h, before being diluted with $CHCl_3$ to 300 mL and washed with an aqueous $Na_2S_2O_3$ solution (250 mL) and H_2O (2 × 150 mL). Upon drying the organic layer with Na_2SO_4 and removal of the solvent by rotary evaporation, the product was triturated with 10 % EtOAc/ Et_2O as an off-white solid (4.68 g, 73.2 %); R_f = 0.6 (20% EtOAc/ Hexane); m.p. = 137 - 138 °C (from EtOAc/ Hexane); ν_{max} (neat): 3041, 1621, 1546, 1489, 1446, 1377 (O-SO_2), 1339, 1272, 1188 (O-SO_2), 1157, 1124, 1108, 1008, 1000 cm^{-1}; ^{1}H-NMR (400 MHz, d^6-AcMe): δ 7.30-7.43 (m, 10H, ArH), 7.62 (s, 1H, 4-H); ^{13}C-NMR (100 MHz, d^6-AcMe): δ 110.58, 119.64, 128.48, 128.56, 129.13, 129.19, 129.23, 130.68, 130.80, 134.54, 140.21, 152.09; HRMS: Found $[M+Na]^+$ = 384.9500, $C_{16}H_{11}{}^{79}BrO_3S$ requires $[M+Na]^+$ = 384.9504.

3-Bromo-6-phenyl-1,2-oxathiine 2,2-dioxide 4.10

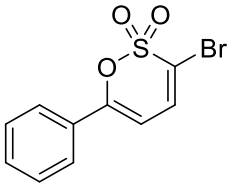

A solution of Br_2 (0.78 mL, 15.2 mmol, 1.1 eq) in $CHCl_3$ (50 mL) was added dropwise to a solution of 6-phenyl-1,2-oxathiine 2,2-dioxide **4.6** (2.87 g, 13.8 mmol) in $CHCl_3$ (100 mL). After the addition was complete, the reaction mixture was heated at reflux overnight. Due to reaction incompletion, pyridine (0.28 mL, 3.5 mmol, 0.25 eq) was added and the mixture was heated at reflux for 15 min. Subsequent dilution of the reaction mixture with $CHCl_3$ to 200 mL allowed for washing with an aqueous $Na_2S_2O_3$ solution (150 mL), a dilute aqueous HCl solution (1 M, 100 mL) and H_2O (100 mL). The obtained organic layer was dried with Na_2SO_4 and the solvent was removed under reduced pressure to yield a crude mixture, which was triturated with 20 % EtOAc/ P.E. to afford the title compound (3.43 g, 86.6 %) as an off-white solid; R_f = 0.4 (20 % EtOAc/ P.E.); m.p. = 130 - 132 °C (from $CHCl_3$); ν_{max} (neat): 3037, 2918, 2849, 1626, 1542, 1494, 1447, 1365 (O-SO_2), 1261, 1179 (O-SO_2), 1070, 1035, 1006 cm^{-1}; ^{1}H-NMR (400 MHz, $CDCl_3$): δ 6.33 (d, *J* = 7.3 Hz, 1H, 4-H), 7.10 (d, *J* = 7.3 Hz, 1H, 5-H), 7.44 - 7.52 (m, 3H, ArH), 7.69 - 7.71 (m, 2H, ArH); ^{13}C-NMR (100 MHz, $CDCl_3$): δ 101.57, 110.98, 125.55, 129.12, 130.07, 131.53, 135.09, 159.43; HRMS: Found $[M+Na]^+$ = 308.9186, $C_{10}H_7{}^{79}BrO_3S$ requires $[M+Na]^+$ = 308.9191.

5-Bromo-3,6-diphenyl-1,2-oxathiine 2,2-dioxide 4.11

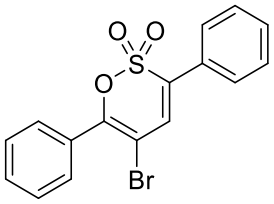

A solution of Br_2 (1.96 mL, 38.0 mmol, 2.7 eq) in 1,2-DCE (50 mL) was added dropwise to a solution of 3,6-diphenyl-1,2-oxathiine 2,2-dioxide **4.7** (4.00 g, 14.1 mmol) in 1,2-DCE (200 mL). The reaction mixture was then heated at reflux for 96 h and was subsequently washed with an aqueous $Na_2S_2O_3$ solution (2 × 150 mL) and H_2O (250 mL). The obtained organic layer was dried over Na_2SO_4 and the solvent was removed under reduced pressure. The crude product was purified by trituration with Et_2O yielding the product (2.35 g, 45.9 %) as a yellow solid; R_f = 0.5 (10% EtOAc/ P.E.), m.p. = 105 - 107 °C (from EtOAc/ P.E.); ν_{max} (neat): 3032, 2358, 1613, 1578, 1561, 1489, 1445, 1371 (O-SO_2), 1354, 1318, 1298, 1252, 1179 (O-SO_2), 1141, 1073, 1034, 1012 cm^{-1}; ^{1}H-NMR (400 MHz, $CDCl_3$): δ 7.02 (s, 1H, 4-H), 7.48-7.51 (m, 6H, ArH), 7.62-7.65 (m, 2H, ArH), 7.86-7.88 (m, 2H, ArH); ^{13}C-NMR (100 MHz, $CDCl_3$): δ 99.50, 127.79, 128.39, 128.87, 129.19, 129.21, 130.52, 130.66, 131.31, 133.62, 135.96, 151.85; HRMS: Found $[M+Na]^+$ = 384.9500, $C_{16}H_{11}{}^{79}BrO_3S$ requires $[M+Na]^+$ = 384.9504.

6.4.2 Suzuki Coupling/ Miyaura Borylation products

3,5,6-(Triphenyl)-1,2-oxathiine 2,2-dioxide 4.4 (2.63)

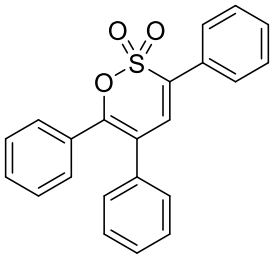

In a flame-fried flask, 3-bromo-3,6-diphenyl-1,2-oxathiine 2,2-dioxide **4.9** (0.40 g, 1.1 mmol), $PhB(OH)_2$ (0.20 g, 1.7 mmol, 1.5 eq), $Pd(OAc)_2$ (0.012 g, 0.06 mmol, 5 %-mol), PCy_3 (0.031 g, 0.11 mmol, 10%-mol) and $K_2HPO_4{\cdot}3H_2O$ (0.75 g, 3.3 mmol, 3.0 eq) were charged neat under N_2. Upon the addition of DMA (10 mL), the reaction mixture was heated to 75 °C for 48 h, at which point the reaction was completed, as monitored by TLC. The solvent was removed azeotropically using PhMe and the resulting crude mixture was purified in a sinter column (silica, wet loading, n. DCM), to afford the title compound (0.16 g, 40.0 %) as a yellow solid; the ^{1}H-NMR signals were identical to **2.63** prepared by the Cope elimination protocol described in section **6.2.3.1**.

3,6-Diphenyl-1,2-oxathiine 2,2-dioxide 4.7 (2.67)

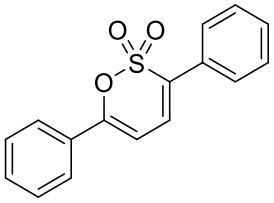

In a flame-dried flask, 3-bromo-6-phenyl-1,2-oxathiine 2,2-dioxide **4.10** (0.40 g, 1.4 mmol), $PhB(OH)_2$ (0.25 g, 2.1 mmol, 1.5 eq), $Pd(OAc)_2$ (0.015 g, 0.07 mmol, 5 %-mol), PCy_3 (0.039 g, 0.14 mmol, 10%-mol) and

$K_2HPO_4 \cdot 3H_2O$ (0.95 g, 4.2 mmol, 3.0 eq) were charged under N_2. DMA (10 mL) was added and the mixture was heated to 75 °C for 48 h. Upon reaction completion as monitored by TLC, the reaction mixture was poured into H_2O (40 mL) and extracted with EtOAc (5 × 20 mL). The extracts were washed with H_2O (100 mL), brine (100 mL) and dried with Na_2SO_4. Removal of the solvent under reduced pressure afforded a crude mixture containing two components, which were separated via column chromatography (silica, wet loading, 50% DCM/ P.E.):

Fraction 1: Title compound (0.11 g, 27.5 %) as a pale yellow solid; the ^{1}H-NMR signals were identical to **2.67** prepared by the Cope elimination protocol described in section **6.2.3.4**.

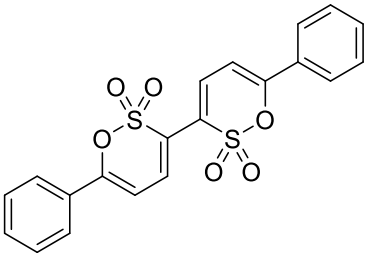

Fraction 2: (6,6'-Diphenyl-[3,3'-bi(1,2-oxathiine)] 2,2,2',2'-tetraoxide **4.29** (0.02 g, 10.0 %) as an orange solid; R_f = 0.3 (20% EtOAc/ Hexane); m.p. = 227 - 230 °C (decomposition after 230 °C, from DCM/ P.E.); ν_{max} (neat): 1614, 1537, 1490, 1445, 1376 (O-SO_2), 1340, 1309, 1266, 1237, 1183 (O-SO_2), 1064, 1032, 1004 cm^{-1}; ^{1}H-NMR (400 MHz, $CDCl_3$): δ 6.63 (d, *J* = 7.4 Hz, 2H, 2 × 5-H), 7.47 - 7.51 (m, 8H, ArH/ 2 × 4-H), 7.76 - 7.77 (m, 2H, ArH); ^{13}C-NMR (100 MHz, $CDCl_3$): δ 102.06, 124.24, 125.81, 129.18, 130.04, 131.61, 131.90, 157.17; HRMS: Found $[M+Na]^+$ = 437.0126, $C_{20}H_{14}O_6S_2$ requires $[M+Na]^+$ = 437.0132.

3-(4-Methoxyphenyl)-5,6-diphenyl-1,2-oxathiine 2,2-dioxide 4.26

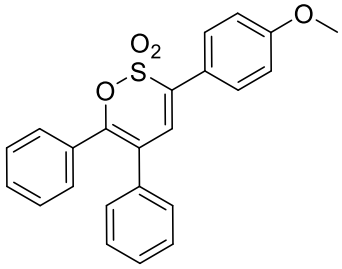

Under a N_2 atmosphere, 3-bromo-3,6-diphenyl-1,2-oxathiine 2,2-dioxide **4.9** (0.40 g, 1.1 mmol), $AnB(OH)_2$ (0.25 g, 1.7 mmol, 1.5 eq), PCy_3 (0.031 g, 0.11 mmol, 10 %-mol) and $K_2HPO_4 \cdot 3H_2O$ (0.75 g, 3.3 mmol, 3 eq) were charged neat. A suspension of $Pd(OAc)_2$ (0.012 g, 0.06 mmol, 5 %-mol) in DMA (7.5 mL) and MeOH (7.5 mL) was subsequently added and the reaction mixture was heated at 60 °C overnight. Upon reaction completion as monitored by TLC, the mixture was poured into H_2O (15 mL) and the product was extracted with EtOAc (4 × 20 mL). Extracts were washed with sat. $NaHCO_{3\,(aq)}$ (40 mL) and brine (40 mL), dried over Na_2SO_4 and the solvent was removed under removed pressure. The obtained crude was purified in a sinter column (silica, wet loading, n. DCM) and the obtained solid was triturated with Et_2O to afford the title compound (0.25 g, 58.1 %) as a pale yellow solid; R_f = 0.4 (20% EtOAc/ Hexane); m.p. = 147 - 148 °C (from DCM); ν_{max} (neat): 1604, 1510, 1444, 1364 (O-SO_2), 1305, 1272, 1254, 1228, 1180 (O-SO_2), 1127, 1035, 1007 cm^{-1}; ^{1}H-NMR (400 MHz, $CDCl_3$): δ 3.85 (s, 3H, OMe), 6.91 (s, 1H, 4-H), 6.96 - 6.98 (m, 2H, ArH), 7.22 - 7.34 (m, 10H, ArH), 7.60 - 7.62 (m, 2H, ArH); ^{13}C-NMR (100 MHz, $CDCl_3$): δ 55.46, 114.54, 119.06, 122.15, 128.16, 128.27, 129.13, 129.16, 129.22 (2C), 130.09, 131.21, 132.26, 133.87, 135.98, 151.50, 161.03; HRMS: Found $[M+Na]^+$ = 413.0813, $C_{23}H_{18}O_4S$ requires $[M+Na]^+$ = 413.0824.

6-(4-Trifluorophenyl)-3,4-diphenl-1,2-oxathiine 2,2 dioxide 4.27 (2.65)

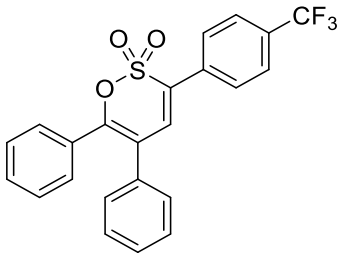

3-Bromo-3,6-diphenyl-1,2-oxathiine 2,2-dioxide **4.9** (0.40 g, 1.1 mmol), $CF_3C_6H_4B(OH)_2$ (0.31 g, 1.7 mmol, 1.5 eq), $Pd(OAc)_2$ (0.012 g, 0.06 mmol, 5 %-mol), PCy_3 (0.031 g, 0.11 mmol, 10 %-mol) and $K_2HPO_4{\cdot}3H_2O$ (0.75 g, 3.3 mmol, 3.0 eq) were mixed neat under a N_2 atmosphere, before the addition of a 1:1 mixture of DMA/MeOH. The reaction mixture was heated to 60 °C overnight. Upon reaction completion as monitored by TLC, the mixture was poured into H_2O (20 mL) and extracted with EtOAc (2 × 40 mL). The extracts were washed with sat. $NaHCO_{3\,(aq)}$ (40 mL) and brine (40 mL), dried over Na_2SO_4 and the solvent was removed under reduced pressure. The obtained crude mixture was triturated with Et_2O and the obtained solid eluted through a sinter column (silica, wet loading, n. DCM) to yield the product (0.17 g, 36.2 %) as yellow crystals; the ^{1}H-NMR signals were identical to **2.65** prepared by the Cope elimination protocol described in section **6.2.3.1**.

5,5',6,6'-Tetraphenyl-[3,3'-bi(1,2-oxathiine)] 2,2,2',2'-tetraoxide 4.32

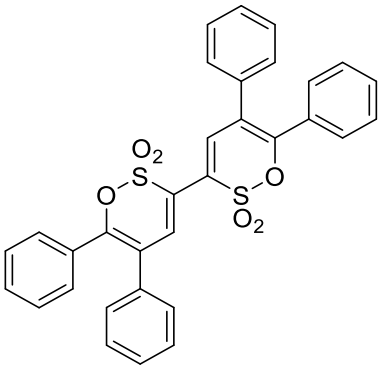

To a flame-dried flask, 3-bromo-3,6-diphenyl-1,2-oxathiine 2,2-dioxide **4.9** (0.5 g, 1.38 mmol), B_2pin_2 (0.16 g, 0.7 mmol, 0.5 eq), KOAc (0.34 g, 3.5 mmol, 2.5 eq), $Pd(dppf)_2Cl_2$ (0.12 g, 0.14 mmol, 10%-mol) were charged and dissolved in 1,4-dioxane (20 mL, separately degassed over N_2 for 30 min) under a N_2 atmosphere. The reaction mixture was stirred at 80 °C for 1.5 h and afterwards diluted with H_2O (30 mL). Extraction with EtOAc (5 × 50 mL) and DCM (50 mL) produced an organic layer that was washed with brine (150 mL), dried over Na_2SO_4 and condensed by rotary evaporation towards a crude mixture which was purified by column chromatography (silica, wet loading, n. DCM). The title compound was thus obtained (0.20 g, 51.3 %) as a yellow-orange solid; R_f = 0.5 (20% EtOAc/ Hexane); m.p.: Decomposition after 190 °C; ν_{max} (neat): 3062, 1609, 1533, 1486, 1442, 1364 (O-SO_2), 1329, 1317, 1284, 1191 (O-SO_2), 1154, 1126, 1102, 1073, 1035, 1008 cm^{-1}; ^{1}H-NMR (400 MHz, $CDCl_3$): δ 7.23 - 7.38 (m, 20H, ArH), 7.56 (s, 2H, 2 × vinyl-H); ^{13}C-NMR (100 MHz, $CDCl_3$): δ 119.69, 123.78, 128.33, 128.67, 129.10, 129.36, 129.45, 130.55, 130.89, 134.83, 136.75, 153.46; HRMS: Found $[M+Na]^+$ = 589.0749, $C_{32}H_{22}O_6S_2$ requires $[M+Na]^+$ = 589.0758.

6.4.3 C-H Activation Coupling Products

3,5,6-(Triphenyl)-1,2-oxathiine 2,2-dioxide 4.4 (2.63)

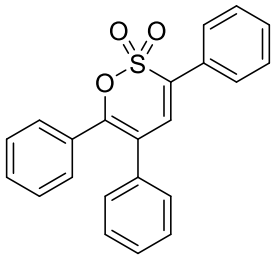

5,6-Diphenyl-1,2-oxathiine 2,2-dioxide **4.5** (0.40 g, 1.4 mmol), $Pd(PPh_3)_4$ (0.16 g, 0.14 mmol, 10 %-mol) and AcOAg (0.26 g, 1.6 mmol, 1,1 eq) were charged into a flame-dried flask under N_2. DMF (5 mL) was added, followed by PhI (0.47 mL, 4.22 mol, 3.0 eq) and the resulting suspension was heated to 80 °C overnight. Upon reaction completion as monitored by TLC, the reaction mixture was poured into H_2O (10 mL) and extracted with EtOAc (4 × 15 mL). The extracts were washed with H_2O (50 mL), dried over Na_2SO_4 and the solvent was removed under reduced pressure. The obtained crude product was processed through a sinter column (silica, wet loading, n. DCM), yielding a solid which was triturated with Et_2O to produce the title compound (0.20 g, 39.2 %) as a yellow solid; the ^{1}H-NMR signals were identical to **2.63** prepared by the Cope elimination protocol described in section **6.2.3.1**.

3,6-Diphenyl-1,2-oxathiine 2,2-dioxide 4.7 (2.67)

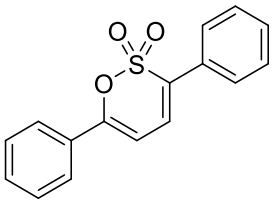

6-Phenyl-1,2-oxathiine 2,2-dioxide **4.6** (0.21 g, 1.0 mmol), AcOAg (0.18 g, 1.1 mmol, 1.1 eq) and PhI (0.33 mL, 3.0 mmol, 3.0 eq) were mixed as solids under a N_2 atmosphere. DMF (5 mL) and $Pd(PPh_3)_4$ (0.12 g, 0.1 mmol, 10 %-mol) were added and the reaction mixture was heated to 80 °C overnight. Upon reaction completion as observed by TLC, the reaction mixture was poured into H_2O (10 mL) and extracted with EtOAc (5 × 20 mL). The extracts were combined, washed with H_2O (80 mL), dried over Na_2SO_4 and the solvent was removed under reduced pressure. The crude mixture so obtained eluted through a sinter column (silica, wet loading (DCM), 20 % to 50 % EtOAc/ P.E.), yielding a solid that was recrystallised from EtOAc/P.E. to afford the title compound as a pale yellow solid (0.09 g, 32.1 %); the ^{1}H-NMR signals were identical to **2.67** prepared by the Cope elimination protocol described in section **6.2.3.4**.

3-(4-Methoxyphenyl)-5,6-diphenyl-1,2-oxathiine 2,2-dioxide 4.26

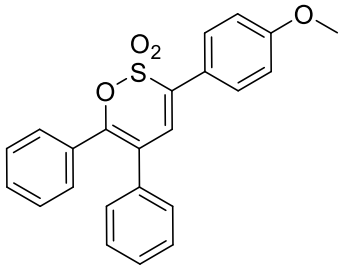

5,6-Diphenyl-1,2-oxathiine 2,2-dioxide **4.6** (0.20 g, 0.7 mmol), *p*-$MeOC_6H_4I$ (0.49 g, 2.1 mmol, 3.0 eq) and AcOAg (0.13 g, 0.8 mmol, 1.1 eq) were mixed in a flame-dried flask under a N_2 atmosphere. After the addition of DMF (5 mL), $Pd(PPh_3)_4$ (0.08 g, 0.07 mmol, 10 %-mol) was added portion-wise and the reaction mixture was heated to 80 °C overnight. Upon reaction completion as monitored by TLC, the reaction mixture was diluted with EtOAc (100 mL) and washed with H_2O (60 mL) and brine (60 mL). The organic layer was dried over Na_2SO_4 and the solvent was removed under reduced pressure. The crude mixture so obtained was purified by column chromatography (silica, dry loading, 20 % EtOAc/ P.E.) with the fractions containing the product being combined and condensed under reduced pressure. The resulting solid was recrystallised from EtOAc/ P.E. to produce the title compound (0.07 g, 25.9 %) as a yellow solid; the ^{1}H-NMR signals were identical to **4.26** prepared by the Suzuki coupling protocol described in section **6.4.2**.

6-(4-Trifluorophenyl)-3,4-diphenl-1,2-oxathiine 2,2 dioxide 4.27 (2.65)

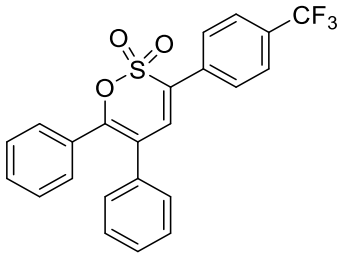

Under a N_2 atmosphere, 5,6-diphenyl-1,2-oxathiine 2,2-dioxide **4.6** (0.20 g, 0.7 mmol), $CF_3C_6H_4I$ (0.31 mL, 2.1 mmol, 3.0 eq) and AgOAc (0.13 g, 0.8 mmol, 1.1 eq) were charged into a flame-dried flask. DMF (5 mL) was added, followed by $Pd(PPh_3)_4$ (0.08 g, 0.07 mmol, 10 %-mol) in small portions, and the reaction mixture was heated to 80 °C for 2 h. Upon reaction completion, the reaction mixture was filtered through celite and the precipitate was washed with EtOAc. Removal of the solvents by rotary evaporation afforded a crude mixture which was triturated with Et_2O to afford the product (0.17 g, 56.7 %) as a pale yellow solid; the ^{1}H-NMR signals were identical to **2.65** prepared by the Suzuki coupling protocol described in section **6.4.2**.

5,6-Diphenyl-3-(pyridin-4-yl)-1,2-oxathiine 2,2-dioxide 4.28

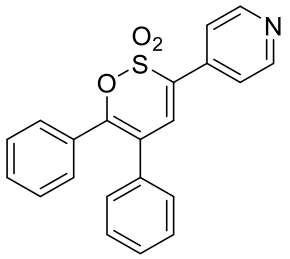

5,6-Diphenyl-1,2-oxathiine 2,2-dioxide **4.6** (0.20 g, 0.7 mmol), 4-iodopyridine (0.43 g, 2.1 mmol, 3.0 eq) and AgOAc (0.13 g, 0.8 mmol, 1.1 eq) were charged into a flame-dried flask under a N_2 atmosphere. DMF (10 mL) was added, followed by $Pd(PPh_3)_4$ (0.08 g, 0.07 mmol, 10 %-mol) in small portions, and the reaction mixture was heated to 80 °C for 1 h. Upon reaction completion, the reaction mixture was filtered through celite and the precipitate washed with EtOAc. Rotary evaporation of the solvents afforded a crude mixture that was purified by column chromatography (silica, dry loading, 40 % to 60 % EtOAc/ P.E.) to yield the title compound (0.17 g, 68.0 %) as a pale yellow solid; R_f = 0.3 (50 % EtOAc/ P.E.); m.p. = 144 - 146 °C (from EtOAc/ P.E.); ν_{max} (neat): 1592, 1558, 1540, 1371 (O-SO_2), 1181 (O-SO_2), 1133, 1073 cm^{-1}; ^{1}H-NMR (400 MHz, $CDCl_3$): δ 7.25 - 7.29 (m, 4H, ArH), 7.33 - 7.38 (m, 6H, ArH), 7.57 - 7.58 (m, 2H, PyH), 8.70 - 8.71 (m, 2H, PyH); ^{13}C-NMR (100 MHz, $CDCl_3$): δ 118.95, 121.25, 128.33, 128.64, 129.05, 129.37 (2C), 130.68, 130.78, 131.38, 135.24, 136.76, 137.47, 150.55, 153.70; HRMS: Found $[M+H]^+$ = 362.0843, $C_{21}H_{15}NO_3S$ requires $[M+H]^+$ = 362.0845.

5,6-Bis(4-methoxyphenyl)-3-(pyridin-4-yl)-1,2-oxathiine 2,2-dioxide 4.38

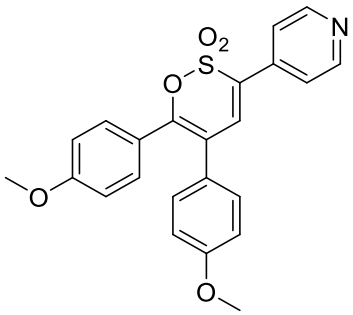

5,6-Bis(4-methoxyphenyl)-1,2-oxathiine 2,2-dioxide (0.50 g, 1.5 mmol), 4-iodopyridine (0.89 g, 4.4 mmol, 3.0 eq) and AgOAc (0.27 g, 1.6 mmol, 1.1 eq) were charged into a flame-dried flask under a N_2 atmosphere. DMF (5 mL) was added, followed by $Pd(PPh_3)_4$ (0.17 g, 0.15 mmol, 10 %-mol) in small portions, and the reaction mixture was heated to 80 °C for 0.5 h. Upon reaction completion, the reaction mixture was filtered through celite and the precipitated was washed with EtOAc, followed by rotary evaporation of the solvents. Chromatographic purification of the crude mixture (silica, dry loading, 0 % to 10 % MeOH/ EtOAc) yielded a solid that was triturated with EtOAc and the triturate was condensed under reduced pressure to afford the title compound (0.20 g, 32.8 %) as a red solid; R_f = 0.3 (50 % EtOAc/ P.E.); m.p. = 134 - 138 °C (from MeOH/ EtOAc); ν_{max} (neat): 1600, 1591, 1568, 1531, 1514, 1499, 1460, 1444, 1413, 1366 (O-SO_2), 1302, 1292, 1251, 1173 (O-SO_2), 1137, 1117, 1107, 1071, 1025, 1015 cm^{-1}; ^{1}H-NMR (400 MHz, $CDCl_3$): δ 3.80 (s, 3H, OMe), 3.83 (s, 3H, OMe), 6.76 - 6.78 (m, 2H, ArH), 6.89 - 6.91 (m, 2H, ArH), 7.19 (s, 1H, 4-H), 7.19 - 7.21 (m, 2H, ArH), 7.30 - 7.32 (m, 2H, ArH), 7.57 - 7.58 (m, 2H, PyH), 8.69 - 8.71 (m, 2H, PyH); ^{13}C-NMR (100 MHz, $CDCl_3$): δ 55.36, 55.40, 113.83, 114.83, 117.21, 121.19, 123.08, 127.59, 130.06, 130.24, 131.07, 137.24, 137.98, 150.21, 153.61, 159.66, 161.40; HRMS: Found $[M+H]^+$ = 422.1054, $C_{23}H_{19}NO_5S$ requires $[M+H]^+$ = 422.1060.

(*E*)-6-Styryl-3-(4-(trifluoromethyl)phenyl)-1,2-oxathiine 2,2-dioxide 4.40

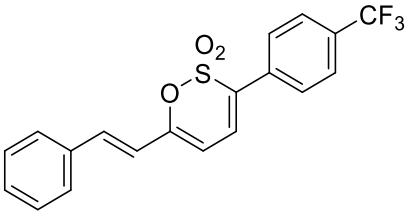

(*E*)-6-Styryl-1,2-oxathiine 2,2-dioxide (0.50 g, 2.1 mmol), 4-$CF_3C_6H_4I$ (0.94 mL, 6.4 mmol, 3.0 eq) and AgOAc (0.39 g, 2.3 mmol, 1.1 eq) were charged into a flame-dried flask under a N_2 atmosphere. DMF (15 mL) was added, followed by $Pd(PPh_3)_4$ (0.24 g, 0.2 mmol, 10 %-mol) in small portions, and the reaction mixture was heated to 80 °C for 2 h. Upon reaction completion, the reaction mixture was filtered through celite and the precipitate was washed with EtOAc. The solvents were removed under reduced pressure to produce a crude mixture that was triturated with Et_2O/ DCM (1:1) to yield the title compound (0.65 g, 82.3 %) as an orange solid; R_f = 0.3 (20 % EtOAc/ P.E.); m.p. = 192 - 195 °C (decomposition after 195 °C, from DMF/ EtOAc); ν_{max} (neat): 1631, 1616, 1543, 1353, 1326 (O-SO_2), 1263, 1195, 1170 (O-SO_2), 1153, 1111, 1064, 1017 cm^{-1}; ^{1}H-NMR (400 MHz, $CDCl_3$): δ 6.10 (d, *J* = 7.1 Hz, 1H, 5-H), 6.68 (d, *J* = 15.9 Hz, 1H, PhCH=C*H*), 6.96 (d, *J* = 7.1 Hz, 1H, 4-H), 7.36 - 7.42 (m, 4H, ArH/ PhC*H*=CH), 7.51 - 7.53 (m, 2H, ArH), 7.69 - 7.74 (m, 4H, ArH); ^{13}C-NMR (100 MHz, $CDCl_3$): δ 105.25, 118.38, 123.74 (q, *J* = 272 Hz, CF_3), 126.02 (q, *J* = 3.7 Hz, *o*-ArC-CF_3), 127.72, 127.84, 129.03, 129.92, 130.64, 131.54 (q, *J* = 33 Hz, C-CF_3), 133.23, 133.75, 134.97, 136.57, 155.93; ^{19}F-NMR (376.5 MHz, $CDCl_3$): δ -62.90 (s, 3F); HRMS: Found $[M]^{+\cdot}$ = 378.0530, $C_{19}H_{13}F_3O_3S$ requires $[M]^{+\cdot}$ = 378.0532.

6.4.4 Cycloaddition Products

6.4.4.1 PTAD addition reactions

2,5,9-Triphenyl-5,9-dihydro-1*H*-[1,2]oxathiino[5,6-*c*][1,2,4]triazolo[1,2-*a*]pyridazine-1,3(2*H*)-dione 8,8-dioxide 4.43b

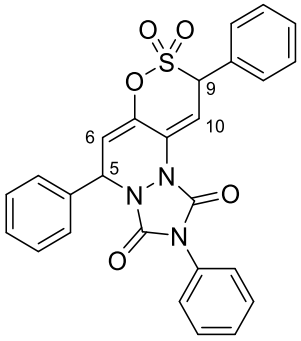

(*E*)-3-Phenyl-6-styryl-1,2-oxathiine 2,2-dioxide **4.45** (0.4 g, 1.3 mmol) was dissolved in 1,2-DCE (10 mL) and mixed dropwise with a solution of PTAD (0.32 g, 1.6 mmol, 1.2 eq) in 1,2-DCE (10 mL) and the reaction mixture was stirred overnight at room temperature. Upon monitoring of the reaction completion by ^{1}H-NMR, the solvent was removed under reduced pressure. The crude product was filtered through a short column (silica, wet loading, n. DCM) and the obtained pale yellow solid was triturated with Et_2O in room temperature to afford the product (0.38 g, 60.3 %) as an off-white solid; R_f = 0.8 (50% EtOAc/ Hexane), m.p. = 146 - 147 °C (from DCM); ν_{max} (neat): 3073, 1768, 1712 (NC=O), 1620, 1494, 1455, 1412, 1384 (O-SO_2), 1304, 1220, 1165 (O-SO_2), 1148, 1103, 1030 cm^{-1}; ^{1}H-NMR (400 MHz, $CDCl_3$): δ 5.48 (ddd, *J* = 0.8, 1.0, 3.6 Hz, 1H, 9-H), 5.96 (ddd, *J* = 0.5, 0.8, 6.1 Hz, 1H, 5-H), 6.14 (ddd, *J* = 1.0, 1.7, 6.1 Hz, 1H, 6-H), 7.11 (ddd,

J = 0.5, 1.7, 3.6 Hz, 1H, 10-H), 7.33 - 7.57 (m, 15H, ArH); ^{13}C-NMR (100 MHz, $CDCl_3$): δ 56.05, 63.07, 106.93, 112.26, 125.53, 126.60, 128.53, 128.75, 129.25, 129.35 (2 C), 129.39, 129.92, 130.01, 130.20, 130.28, 133.31, 142.17, 148.20, 148.95; HRMS: Found $[M+H]^+$ = 486.1121, $C_{26}H_{19}N_3O_5S$ requires $[M+H]^+$ = 486.1125.

5-(4-Methoxyphenyl)-2,9-diphenyl-5,9-dihydro-1*H*-[1,2]oxathiino[5,6-*c*][1,2,4]triazolo[1,2-*a*] pyridazine-1,3(2*H*)-dione 8,8-dioxide 4.64b

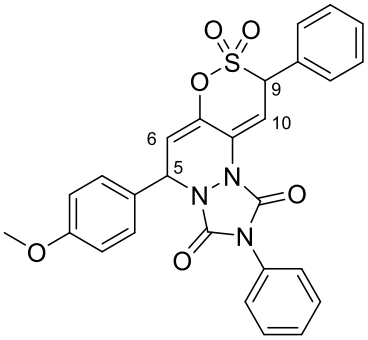

(*E*)-6-(4-Methoxystyryl)-3-phenyl-1,2-oxathiine 2,2-dioxide **4.46** (0.40 g, 1.2 mmol) was dissolved in 1,2-1,2-DCE (25 mL) and mixed with a solution of PTAD (0.33 g, 1.9 mmol, 1.6 eq) in 1,2-DCE (15 mL) dropwise at room temperature, with partial decolouration observed. The reaction mixture was stirred at room temperature overnight, but following reaction incompletion as monitored by TLC it was heated at reflux for 1.5 h. Upon full consumption of the starting material, the solvent was removed under removed pressure and the crude mixture was purified in a sinter column (silica, wet loading, n. DCM). The solid so obtained was triturated with Et_2O to afford the product (0.40 g, 66.7 %) as a pale pink solid; R_f = 0.3 (50 % EtOAc/ Hexane); m.p. = 158 - 160 °C (from DCM); ν_{max} (neat): 3063, 1770, 1712 (NC=O), 1608, 1512, 1504, 1491, 1442, 1401, 1381 (O-SO_2), 1307, 1262, 1240, 1170 (O-SO_2), 1144, 1103, 1089, 1020 cm^{-1}; ^{1}H-NMR (400 MHz, $CDCl_3$): δ 3.82 (s, 3H, OMe), 5.48 (dd, *J* = 1.1, 3.5 Hz, 1H, 9-H), 5.92 (dd, *J* = 0.5, 6.1 Hz, 1H, 5-H), 6.14 (ddd, *J* = 1.1, 1.6, 6.1 Hz, 1H, 6-H), 6.94 - 6.96 (m, 2H, ArH), 7.06 - 7.09 (ddd, *J* =0.5, 1.6, 3.5 Hz, 1H, 10-H), 7.34 - 7.55 (m, 12H, ArH); ^{13}C-NMR (100 MHz, $CDCl_3$): δ 55.37, 55.64, 63.09, 106.73, 112.53, 114.59, 114.60, 125.14, 125.52, 126.67, 128.70, 129.22, 129.33, 129.42, 129.92, 130.04, 130.25 (2C), 142.12, 148.20, 149.12, 160.76; HRMS: Found $[M]^{+\cdot}$ = 515.1148, $C_{27}H_{21}N_3O_6S$ requires $[M]^{+\cdot}$ = 515.1151.

2,9-diphenyl-5-(4-(trifluoromethyl)phenyl)-5,9-dihydro-1*H*-[1,2]oxathiino[5,6-*c*][1,2,4]triazolo[1,2-*a*]pyridazine-1,3(2*H*)-dione 8,8-dioxide 4.65b

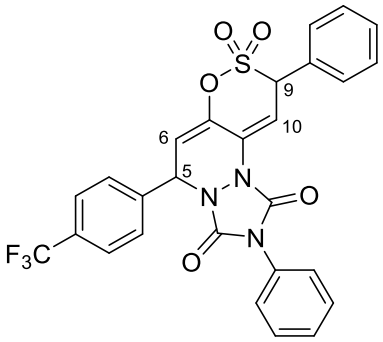

(*E*)-3-Phenyl-6-(4-(trifluoromethyl)styryl)-1,2-oxathiine 2,2-dioxide **4.47** (0.30 g, 0.8 mmol) was dissolved in 1,2-DCE (8 mL) and mixed dropwise with a solution of PTAD (0.28 g, 1.6 mmol, 2.0 eq) in 1,2-DCE (8 mL) at room temperature. The resulting mixture was heated at 50 °C overnight, whereupon the initial red colouration turned into yellow. The reaction mixture was subsequently condensed under reduced

pressure into a crude mixture, which was purified by column chromatography (silica, dry loading, 20 % to 30 % EtOAc/ P.E.). The obtained solid was triturated with Et_2O to afford the title compound (0.17 g, 38.6 %) as colourless crystals; R_f = 0.8 (50 % EtOAc/ Hexane); m.p. = 173 - 176 °C (decomposition after 150 °C, from EtOAc/ P.E.); ν_{max} (neat): 1776, 1709 (NC=O), 1620, 1599, 1495, 1405, 1388, 1323 (O-SO_2), 1166 (O-SO_2), 1115, 1067, 1018 cm^{-1}; ^{1}H-NMR (400 MHz, $CDCl_3$): δ 5.49 (dd, *J* = 1.0, 3.6 Hz, 1H, 9-H), 6.01 (dd, *J* = 0.5, 6.2 Hz, 1H, 5-H), 6.14 (ddd, *J* = 1.0, 1.5, 6.2 Hz, 1H, 6-H), 7.14 (ddd, *J* = 0.5, 1.5, 3.6 Hz, 1H, 10-H), 7.35 - 7.54 (m, 10H, ArH), 7.63 - 7.74 (m, 4H, ArH); ^{13}C-NMR (100 MHz, $CDCl_3$): δ 55.30, 63.11, 107.66, 111.34, 123.65 (q, *J* = 273 Hz), 125.46, 126.41 (q, *J* = 3.5 Hz), 127.93, 128.90, 128.98, 129.12, 129.32, 129.40, 129.90, 130.00, 130.38, 132.13 (q, *J* = 33 Hz), 137.18, 142.68, 148.07, 148.85; ^{19}F-NMR (376.5 MHz, $CDCl_3$) δ -62.89 (s, 3F); HRMS: Found $[M+Na]^+$ = 576.0815, $C_{27}H_{18}F_3N_3O_5S$ requires $[M+Na]^+$ = 576.0819.

2,5-Diphenyl-5,9-dihydro-1*H*-[1,2]oxathiino[5,6-*c*][1,2,4]triazolo[1,2-*a*]pyridazine-1,3(2*H*)-dione 8,8-dioxide 4.70

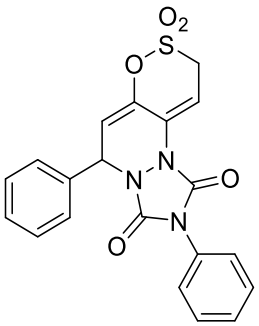

(*E*)-6-Styryl-1,2-oxathiine 2,2-dioxide (0.30 g, 1.3 mmol) was dissolved in 1,2-DCE (15 mL) and mixed dropwise with a solution of PTAD (0.25 g, 1.4 mmol, 1.1 eq) in 1,2-DCE (10 mL). The resulting reaction mixture was stirred at room temperature overnight (gradual decolouration) and the presence of starting material (monitored by TLC) prompted the addition of 1 eq of PTAD (0.23 g, 1.3 mmol). Stirring at room temperature continued for 3 h, before the temperature was increased to 50 °C for further 2 h. The solvent was removed under reduced pressure and the crude mixture was purified in a sinter column (silica, wet loading, 0 % to 10 % EtOAc/DCM) towards a solid that was triturated with Et_2O to yield the title compound (0.37 g, 69.8 %) as a white solid; R_f = 0.5 (n. DCM); m.p. = 196 - 198 °C (from EtOAc/ DCM); ν_{max} (neat): 1762, 1704 (NC=O), 1621, 1497, 1458, 1402, 1384 (O-SO_2), 1305, 1291, 1272, 1182, 1172 (O-SO_2), 1157, 1142, 1102, 1086, 1032 cm^{-1}; ^{1}H-NMR (400 MHz, $CDCl_3$): δ 4.24 (ddd, *J* = 0.7, 4.7, 17.6 Hz, 1H, *syn*-9-H), 4.28 (ddd, *J* = 0.7, 5.5, 17.6 Hz, 1H, *anti*-9-H), 5.93 (d, *J* = 6.0 Hz, 1H, 5-H), 6.10 (ddd, *J* = 0.7, 1.7, 6.0 Hz, 1H, 6-H), 6.98 (ddd, *J* = 1.7, 4.7, 5.5 Hz, 1H, 10-H), 7.36 - 7.46 (m, 10H, ArH); ^{13}C-NMR (100 MHz, $CDCl_3$): δ 46.92, 56.05, 101.24, 112.35, 125.58, 126.08, 128.42, 128.76, 129.26, 129.27, 129.94, 130.20, 133.37, 142.09, 148.26, 148.83; HRMS: Found $[M+H]^+$ = 410.0800, $C_{20}H_{15}N_3O_5S$ requires $[M+H]^+$ = 410.0802.

2,5-Diphenyl-9-(4-(trifluoromethyl)phenyl)-5,9-dihydro-1*H*-[1,2]oxathiino[5,6-*c*][1,2,4]triazolo[1,2-*a*]pyridazine-1,3(2*H*)-dione 8,8-dioxide 4.71

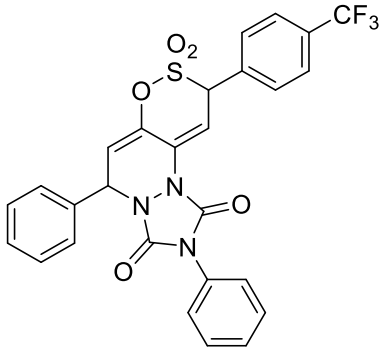

(*E*)-6-Styryl-3-(4-(trifluoromethyl)phenyl)-1,2-oxathiine 2,2-dioxide **4.40** (0.20 g, 0.5 mmol) was dissolved in 1,2-DCE (10 mL) and mixed dropwise with a solution of PTAD (0.11 g, 0.6 mmol, 1.1 eq) in 1,2-DCE (7 mL). After stirring at room temperature overnight, the presence of starting material prompted the addition of 0.5 eq of PTAD (0.05 g, 0.3 mmol) and the reaction mixture was heated at 50 °C for 72 h, before the solvent was removed under reduced pressure. The resulting crude mixture was purified by column chromatography (silica, dry loading, 20 % EtOAc/ P.E.) affording an off-white solid that was triturated with Et_2O to yield the product (0.09 g, 17.6 %) as a white solid; R_f = 0.2 (20 % EtOAc/ P.E.); m.p. = 156 - 157 °C (from EtOAc/ P.E.); ν_{max} (neat): 1770, 1715 (NC=O), 1410, 1388 (O-SO_2), 1328, 1184, 1167 (O-SO_2), 1133, 1103, 1069 cm^{-1}; ^{1}H-NMR (400 MHz, $CDCl_3$): δ 5.53 (dd, *J* = 1.0, 3.5 Hz, 1H, 9-H), 5.98 (dd, *J* = 0.5, 5.9 Hz, 1H, 5-H), 6.20 (ddd, *J* = 1.0, 1.5, 5.9 Hz, 1H, 6-H), 7.08 (ddd, *J* = 0.5, 1.5, 3.5 Hz, 1H, 10-H), 7.33 - 7.51 (m, 10H, ArH), 7.69 - 7.71 (m, 2H, ArH), 7.75 - 7.77 (m, 2H, ArH); ^{13}C-NMR (100 MHz, $CDCl_3$): δ 56.06, 62.56, 105.71, 112.91, 123.64 (q, *J* = 274 Hz), 125.50, 126.32 (q, *J* = 3.7 Hz), 126.98, 128.48, 128.82, 129.27, 129.39, 130.10, 130.13, 130.41, 132.62 (q, *J* = 33 Hz), 133.14, 133.47, 141.98, 148.20, 148.89; ^{19}F-NMR (376.5 MHz, $CDCl_3$): δ -62.94 (s, 3F); HRMS: Found $[M+H]^+$ = 554.0994, $C_{27}H_{18}F_3N_3O_5S$ requires $[M+H]^+$ = 554.0996.

6.4.4.2 PTAD addition reactions to 6-Styryl-1,2-oxathiine 2,2-dioxides for purpose of characterization of the silica sensitive initial adducts

Preparation of 5-(4-Methoxyphenyl)-2,9-diphenyl-5,10a-dihydro-1*H*-[1,2]oxathiino[5,6-*c*][1,2,4] triazolo[1,2-*a*]pyridazine-1,3(2*H*)-dione 8,8-dioxide 4.64a

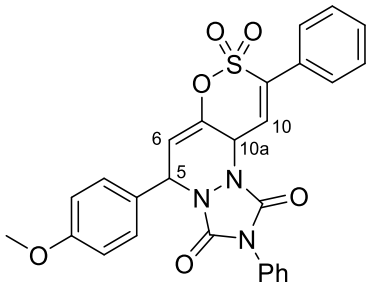

(*E*)-6-(4-Methoxystyryl)-3-phenyl-1,2-oxathiine 2,2-dioxide **2.70** (0.30 g, 0.9 mmol) was dissolved in 1,2-DCE (10 mL) and mixed with a solution of PTAD (0.19 g, 1.1 mmol, 1.2 eq) in 1,2-DCE (5 mL) dropwise at room temperature and the reaction mixture was stirred at room temperature overnight. Removal of the solvent was under reduced pressure and trituration of the resulting solid with AcMe afforded a white solid aliquot of the title compound for characterisation; (No R_f obtained on account of silica sensitivity); m.p. = 164 - 168 °C (from 1,2-DCE); ν_{max} (neat): 1717 (NC=O), 1599, 1503, 1409, 1372 (O-SO_2), 1256, 1180 (O-

SO_2), 1139, 1089, 1026 cm^{-1}; ^{1}H-NMR (300 MHz, $CDCl_3$): δ 5.36 (q, *J* = 2.3 Hz, 1H, 10a-H), 5.78 (dd, *J* = 2.2, 5.1 Hz, 1H, 5-H), 6.31 (dd, *J* = 2.2, 5.1 Hz, 1H, 6-H), 6.88 - 6.91 (m, 2H, ArH), 7.35 - 7.50 (m, 11H, ArH/ 10-H), 7.68 - 7.71 (m, 2H, ArH); ^{13}C-NMR (100 MHz, $CDCl_3$): δ 54.45, 54.86, 55.31, 114.35, 116.66, 125.24, 125.86, 126.96, 128.16, 128.55, 129.20, 129.21, 129.31, 130.39, 130.40, 130.81, 141.45, 141.85, 149.99, 154.64, 160.58; HRMS: Found $[M-H]^-$ = 514.1062, $C_{27}H_{21}N_3O_6S$ requires $[M-H]^-$ = 514.1067.

Preparation of 2,9-Diphenyl-5-(4-(trifluoromethyl)phenyl)-5,10*a*-dihydro-1*H*-[1,2]oxathiino [5,6-*c*][1,2,4]triazolo [1,2-*a*]pyridazine-1,3(2*H*)-dione 8,8-dioxide 4.65a

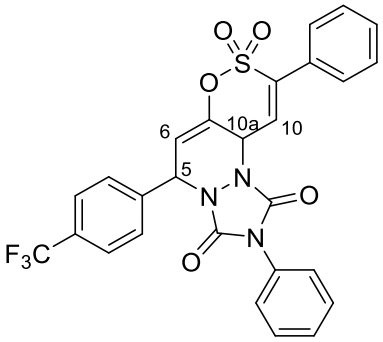

(*E*)-3-Phenyl-6-(4-(trifluoromethyl)styryl)-1,2-oxathiine 2,2-dioxide **4.46** (0.40 g, 1.1 mmol) was dissolved in 1,2-DCE (10 mL) and mixed dropwise with a solution of PTAD (0.20 g, 1.2 mmol, 1.1 eq) in 1,2-DCE (8 mL) at room temperature. The reaction mixture was stirred at room temperature overnight, before the solvent was removed under reduced pressure. The resulting solid was triturated with AcMe and *n*-pentane to afford a white solid aliquot of the product for characterisation; (No R_f obtained on account of silica sensitivity); m.p. = 169 - 172 °C (from 1,2-DCE); ν_{max} (neat): 1780, 1721 (NC=O), 1495, 1411, 1377, 1325 (O-SO_2), 1256, 1182, 1141 (O-SO_2), 1111, 1090, 1058, 1021 cm^{-1}; ^{1}H-NMR (400 MHz, $CDCl_3$): δ 5.40 (q, *J* = 2.3 Hz, 1H, 10a-H), 5.88 (dd, *J* = 5.0, 2.3 Hz, 1H, 5-H), 6.33 (dd, *J* = 5.0, 2.0 Hz, 1H, 6-H), 7.35 - 7.55 (m, 9H, ArH/ 10-H), 7.63 - 7.70 (m, 6H, ArH); ^{13}C-NMR (100 MHz, $CDCl_3$): δ 54.54, 54.59, 115.72, 123.72 (q, *J* = 272 Hz, CF_3), 125.18, 126.16 (q, *J* = 3.6 Hz, *o*-Ar*C*-CF_3), 126.55, 128.12, 128.75, 129.11, 129.27, 129.28, 129.40, 130.17, 130.95, 131.92 (q, *J* = 33 Hz, *C*-CF_3), 137.54, 141.76, 142.67, 149.85, 154.50; ^{19}F-NMR (376.5 MHz, $CDCl_3$) δ -62.90 (s, 3F); HRMS: Found $[M-H]^-$ = 552.0846, $C_{27}H_{18}F_3N_3O_5S$ requires $[M-H]^-$ = 552.0843.

6.4.5 DMAD addition reaction

Dimethyl 7-(4-methoxyphenyl)-3-phenylbenzo[*e*][1,2]oxathiine-5,6-dicarboxylate 2,2-dioxide 4.76

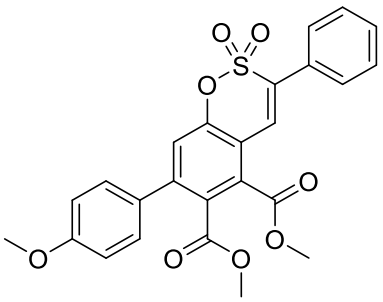

A mixture of DMAD (0.12 mL, 1.0 mmol, 1.1 eq) and (*E*)-6-(4-methoxystyryl)-3-phenyl-1,2-oxathiine 2,2-dioxide **4.46** (0.30 g, 0.9 mmol) was heated to reflux overnight. Upon reaction completion as monitored by H-NMR, the reaction mixture was separated to its components via column chromatography without solvent removal (silica, wet loading, n. DCM). The obtained solid was triturated from P.E./ Et_2O (8:2) to

yield the title compound (0.04 g, 9.5 %) as an off-white solid; R_f = 0.9 (10 % MeOH/ DCM); m.p. = 214 - 216 °C (from DCM); v_{max} (neat): 2953, 1747, 1728 (OC=O), 1719 (OC=O), 1609, 1516, 1491, 1438, 1387, 1373 (O-SO_2), 1329, 1275, 1247, 1217, 1180 (O-SO_2), 1152, 1112, 1021 cm^{-1}; ^{1}H-NMR (400 MHz, $CDCl_3$): δ 3.65 (s, 3H, OMe), 3.86 (s, 3H, CO_2Me), 3.93 (s, 3H, CO_2Me), 6.96 - 6.98 (m, 2H, ArH), 7.28 - 7.30 (m, 2H, ArH), 7.41 (s, 1H, 8-H), 7.50 - 7.51 (m, 3H, ArH), 7.63 (s, 1H, 4-H), 7.67 - 7.69 (m, 2H, ArH); ^{13}C-NMR (100 MHz, $CDCl_3$): δ 52.70, 53.38, 55.37, 114.23, 117.62, 122.12, 127.18, 129.15, 129.32, 129.91, 130.27, 130.53, 130.76, 131.58, 138.58, 144.08, 151.29, 160.18, 165.94, 167.71; HRMS: Found $[M+Na]^+$ = 503.0770, $C_{25}H_{20}O_8S$ requires $[M+Na]^+$ = 503.0777.

6.4.6 Benzyne addition products

1-(4-Methoxyphenyl)naphthalene 4.80

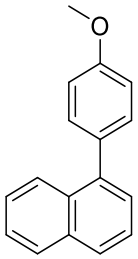

6-(4-Methoxyphenyl)-1,2-oxathiine 2,2-dioxide **4.74** (0.5 g, 2.1 mmol) was dissolved in MeCN (25 mL) in a flame dried flask and mixed with CsF (0.51 g, 3.4 mmol, 1.6 eq) at room temperature under a N_2 atmosphere. 2-(Trimethylsilyl)phenyl trifluoromethanesulfonate (0.56 mL, 2.3 mmol, 1.1 eq) was then added dropwise and the reaction was stirred at room temperature overnight. Mixing with H_2O (50 mL) and extraction with EtOAc (2 × 25 mL) afforded an organic layer which was washed with brine (30 mL), dried over Na_2SO_4 and condensed under reduced pressure. The resulting crude mixture was purified by column chromatography (silica, dry loading, 10 % EtOAc/ P.E.) and the obtained solid was triturated with n-pentane to yield the title compound (0.04 g, 8.2 %) as an off-white solid; R_f = 0.8 (20 % EtOAc/ Hexanes); m.p. = 111 - 114 °C (from EtOAc/ P.E., lit. m.p. = 112 - 113 °C)[258]; v_{max} (neat): 2991, 2954, 2831, 1607, 1513, 1504, 1461, 1451, 1437, 1422, 1393, 1282, 1239, 1207, 1173, 1143, 1107, 1057, 1030 cm^{-1}; ^{1}H-NMR (400 MHz, $CDCl_3$): δ 3.89 (s, 3H, OMe), 7.02 - 7.04 (m, 2H, ArH), 7.39 - 7.53 (m, 6H, ArH), 7.83 - 7.85 (m, 1H, ArH), 7.89 - 7.93 (m, 2H, ArH); ^{13}C-NMR (100 MHz, $CDCl_3$): δ 55.38, 113.72, 125.42, 125.72, 125.94, 126.08, 126.92, 127.35, 128.27, 131.13, 131.83, 133.13, 133.84, 139.91, 158.94.

1,2,4-Triphenylnaphthalene 4.85

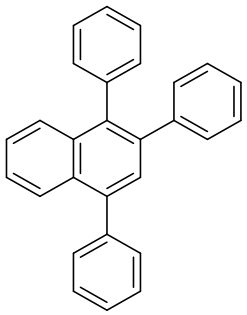

A solution of 3,5,6-(triphenyl)-1,2-oxathiine 2,2-dioxide **4.4** (0.50 g, 1.4 mmol) and 2-(trimethylsilyl)phenyl trifluoromethanesulfonate (0.36 mL, 1.5 mmol, 1.1 eq) in MeCN (10 mL) was added dropwise in a suspension of CsF (0.53 g, 3.5 mmol, 2.5 eq) in MeCN (15 mL) in a flame dried flask at room temperature

under a N_2 atmosphere. The resulting reaction mixture was stirred at room temperature for 3.5 h before being poured into H_2O (25 mL) and extracted with EtOAc (2 × 25 mL). The organic layer was washed with brine (30 mL) dried over Na_2SO_4 and the solvents were removed under reduced pressure. The crude product so obtained was purified by column chromatography (silica, dry loading, 10 % Et_2O/ P.E.), affording a solid that was washed with n-pentane to yield the product (0.16 g, 32.0 %) as an off-white solid; R_f = 0.8 (EtOAc/ P.E.); m.p. = 159 - 160 °C (from Et_2O/ P.E., lit. m.p. = 159 - 161 °C)[259]; ν_{max} (neat): 3053, 3019, 1599, 1573, 1491, 1439, 1419, 1379, 1251, 1209, 1141, 1070, 1056, 1032 cm^{-1}; ^{1}H-NMR (400 MHz, $CDCl_3$): δ 7.13 - 7.35 (m, 10H, ArH), 7.40 - 7.61 (m, 8H, ArH), 7.74 - 7.76 (m, 1H, ArH), 7.99 - 8.01 (m, 1H, ArH); ^{13}C-NMR (100 MHz, $CDCl_3$): δ 125.76, 126.04, 126.07, 126.26, 126.79, 127.20, 127.37, 127.61, 127.88, 128.33, 130.15, 130.20, 130.94, 131.56, 133.06, 137.14, 137.89, 139.06, 139.79, 140.61, 141.84.

1,4-Diphenylnaphthalene 4.86

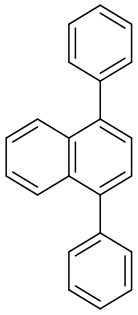

A solution of 2-(trimethylsilyl)phenyl trifluoromethanesulfonate (0.48 mL, 2.0 mmol, 1.1 eq) was added dropwise to a suspension of 3,6-diphenyl-1,2-oxathiine 2,2-dioxide **4.7** (0.5 g, 1.8 mmol) and CsF (0.68 g, 4.5 mmol, 2.5 eq) in MeCN (25 mL) in a flame dried flask at room temperature under a N_2 atmosphere. Upon complete addition, the reaction mixture was stirred at room temperature for 2 h and, upon reaction incompletion as monitored by TLC, it was heated to reflux for 1 h. Mixing with H_2O (50 mL) and extraction with EtOAc (2 × 25 mL) produced an organic layer that was washed with brine (30 mL), dried over Na_2SO_4 and condensed under reduced pressure. The resulting crude mixture was purified by column chromatography (silica, dry loading, 0 % to 3 % EtOAc/ P.E.), leading to a pale-yellow solid that was triturated with n-pentane to afford the title compound (0.11 g, 22.0 %) as an off-white solid; R_f = 0.9 (EtOAc/ Hexane); m.p. = 120 - 128 °C (from EtOAc/ P.E., lit. m.p. = 132 - 133 °C (from EtOH))[260]; ν_{max} (neat): 3052, 1598, 1573, 1512, 1488, 1469, 1446, 1384, 1238, 1154, 1071, 1028 cm^{-1}; ^{1}H-NMR (400 MHz, $CDCl_3$): δ 7.43 - 7.57 (m, 14H, ArH), 7.96 - 8.00 (m, 2H, ArH); ^{13}C-NMR (100 MHz, $CDCl_3$): δ 125.87, 126.41, 126.48, 127.29, 128.32, 130.17, 131.92, 139.84, 140.83.

REFERENCES

[1] P. Lue, J. V. Greenhill, *Enaminones in Heterocyclic Synthesis*; Elsevier, 1996, **67**, 207-343
[2] R. Olivera, R. SanMartin, E. Dominguez, X. Solans, M. K. Urtiaga, M. I. Arriortua, *J. Org. Chem.*, 2000, **65**, 6398-6411
[3] P.A. Stabnikov, G. I. Zharkova, I. A. Baidina, S. V. Tkachev, V.V. Krisyuk, I.K. Igumenov, *Polyhedron*, 2007, **26**, 4445-4450
[4] H. M. Al-Matar, A. Y. Adam, Kh. D. Khalil, M. H. Elnagdi, *ARKIVOC*, 2012, **6**, 1-15
[5] A. Golobic, J. Koller, *J. Mol. Struct.*, 2000, **532**, 109-126
[6] F. A. Abu-Shanab, S. M. Sherif, S. A. S. Mousa, *J. Heterocyclic Chem.*, 2009, **46**, 801-827
[7] Ch. Yongli (Henan Chemical Ind. Res. Inst. CO. LTD.), A kind of synthetic method of N, N Dimethylformamide dimethyl acetal, CN106083611A, 9 November 2016
[8] D. Kidjemet, *Synlett*, 2002, **10,** 1741-1742
[9] D. W. Boykin, A. Kumar, M. Bajic, G. Xiao, W. D. Wilson, B. C. Bender, D. R. McCurdy, J. E. Hall, R. R. Tidwell, *Eur. J. Med. Chem.*, 1997, **32**, 965-972
[10] M. N. Semenova, *ACS Comb. Sci.*, 2018, **20**, 700-721
[11] O. Bruno, S. Schenone, A. Ranise, F. Mazzeo, *Farmaco*, 1999, **54**, 95-100
[12] V. S. Moskvina, O. V. Shablykina, V. V. Ishchenko, V. P. Khilya, *Tetrahedron Lett.*, 2017, **58**, 245-247
[13] P. Belov, V. L. Campanella, A. W. Smith, R. Priefer, *Tetrahedron Lett*., 2011, **52**, 2776-2779
[14] A. N. Komogortsev, B. V. Lichitsky, A. D. Tretyakov, A. N. Fakhrutdinov, A. A. Dudinov, M. M. Krayushkin, *J. Heterocyclic Chem*. 2019, **56**, 3081-3087
[15] T. M. Abu Elmaati, S. B. Said, N. S. Abu Elenein, N. M. Khodeir, M. M. Sofan, *J. Heterocycl. Chem.*, 2003, **40**, 481-486
[16] C. Q. Huang, K. Wilcoxen, J. R. McCarthy, M. Haddach, D. Grigoriadis, C. Chen, *Bioorg. Med. Chem. Lett.*, 2003, **13**, 3371-3374
[17] A. S. Wagman, R. S. Boyce, S. P. Brown, E. Fang, D. Goff, J. M. Jansen, V. P. Le, B. H. Levine, S. C. Ng, Z. – J. Ni, J. M. Nuss, K. B. Pfister, S. Ramurthy, P. A. Renhowe, D. B. Ring, W. Shu, S. Subramanian, X. A. Zhou, C. M. Shafer, S. D. Harrison, K. W. Johnson, D. E. Bussiere, *J. Med. Chem.*, 2017, **60**, 8482-8514
[18] C. Chen, K. Wilcoxen, J. R. McCarthy, *Tetrahedron Lett.*, 1998, **39**, 8229-8232
[19] C. Chen, R. Dagnino, Jr., J. R. McCarthy, *J. Org. Chem.*, 1995, **60**, 8428-8430
[20] D. Kumar, D. N. Kommi, P. Chopra, M. I. Ansari, A. K. Chakraborti, *Eur. J. Org. Chem.*, 2012, 6407-6413
[21] S. B. Wakade, D. K. Tiwari, M. Phanindrudu, Pushpendra, D. K. Tiwari, *Tetrahedron,* 2019, **75**, 4024-4030
[22] M. M. Abdelkhalik, A. M. Eltoukhy, S. M. Agamy, M. H. Elnagdi, *J. Heterocyclic Chem.*, 2004, **41**, 431-434
[23] E. C. Taylor, J. S. Skotnicki, *Synth. Comm.*, 1983, **13**, 1137-1138
[24] J. M. Hook, L. N. Mander, *J. Org. Chem.*, 1980, **45**, 1724-1725
[25] J. Zhu, B. Qi, S. Guo, W. Zhang, X. Yu, C. Song, *Org. Lett.*, 2018, **20**, 3996-3999
[26] X. Liang, P. Guo, W. Yang, M. Li, C. Jiang, W. Sun, T. - P. Loh, Y. Jiang, *Chem. Commun.*, 2020, **56**, 2043-2046
[27] A. Hanzlowsky, B. Jelencic, S. Recnik, J. Svete, A. Golobic, B. Stanovnik, *J. Heterocycl. Chem.*, 2003, **40**, 487-498
[28] S. Youssif, *Monatsh. Chem.*, 1997, **128**, 493-501
[29] J. Popovici-Muller, G. W. Shipps Jr., K. E. Rosner, Y. Deng, T. Wang, P. J. Curran, M. A. Brown, M. A. Siddiqui, A. B. Cooper, J. Duca, M. Cable, V. Girijavallabhan, *Bioorg. Med. Chem. Lett.*, 2009, **19**, 6331-6336
[30] Gr. B. Bennett, R. B. Mason, *Org. Prep. Proced. Int.*, 1978, **10**, 67-72
[31] C. D. Gabbutt, J. D. Hepworth, B. M. Heron, S. J. Coles, M. B. Hursthouse, *J. Chem. Soc. Perkin Trans. 1*, 2000, 2930-2938
[32] L. Mosti, P. Schenone, G. Menozzi, S. Cafaggi, *J. Heterocyclic Chem.*, 1982, **19**, 1031-1034
[33] M. M. Gamal El-Din, M. El-Gamal, M. S. Abdel - Maksoud, K. Ho Yoo, C. - H. Oh, *J. Enzym. Inh. Med. Ch.*, 2019, **34**, 1534-1543
[34] J. T. Gupton, A. Shimozono, E. Crawford, J. Ortolani, E. Clark, M. Mahoney, C. Heese, J. Noble, C. P. Mandry, R. Kanters, R. N. Dominey, E. W. Goldman, J. A. Sikorski, D. C. Fisher, *Tetrahedron*, 2018, **74**, 2650-2663
[35] A. B. Sanchez Maya, C. Perez - Melero, N. Salvador, R. Pelaez, E. Caballero, M. Medarde, *Bioorg. Med. Chem.*, 2005, **13**, 2097-2107
[36] J. - P. Schülke, L. A. McAllister, K. F. Geoghegan, V. Parikh, T. A. Chappie, P. R. Verhoest, C. J. Schmidt, D. S. Johnson, N. J. Brandon*, A.C.S. Chem. Biol.*, 2014, **9**, 2823-2832
[37] A. Shahrisa, Z. Ghasemi, M. Saraei, *J. Heterocyclic Chem.*, 2009, **46**, 273-277
[38] L. Wang, J. A. Hubert, S. J. Lee, J. Pan, S. Qian, M. L. Reitman, A. M. Strack, D. T. Weingarth, D. J. MacNeil, A. E. Weber, S. D. Edmondson, *Bioorg. Med. Chem. Lett.*, 2011, **21**, 2911-2915

[39] L. C. Meurer, P. E. Finke, S. G. Mills, T. F. Walsh, R. B. Toupence, M. T. Goulet, J. Wang, X. Tong, T. M. Fong, J. Lao M. – T. Schaeffer, J. Chen, C. – P. Shen, D. S. Stribling, L. P. Shearman, A. M. Strack, L. H. T. Van der Ploeg, *Bioorg. Med. Chem. Lett.*, 2005, **15**, 645-651
[40] Z. Wu, R. G. Robinson, S. Fu, S. F. Barnett, D. Defeo - Jones, R. E. Jones, A. M. Kral, H. E. Huber, N. E. Kohl, G. D. Hartman, M. T. Bilodeau, *Bioorg. Med. Chem. Lett.*, 2008, **18**, 2211-2214
[41] F. Evangelisti, P. Schenone, Alb. Bargagna, *J. Heterocyclic Chem.*, 1979, **16**, 217-220
[42] Alb. Bargagna, P. Schenone, Fr. Bondavalli, M. Longobardi, *J. Heterocyclic Chem.*, 1980, **17**, 33-37
[43] Alb. Bargagna, F. Evangelisti, P. Schenone, *J. Heterocyclic Chem.*, 1981, **18**, 111-116
[44] Alb. Bargagna, P. Schenone, Fr. Bondavalli, M. Longobardi, *J. Heterocyclic Chem.*, 1980, **17**, 1201-1206
[45] B. Zwanenburg, *Sci. Synth.*, 2010, **27**, 123-134
[46] G. Opitz, *Angew. Chemie, Int. Ed.*, 1967, **6**, 107-123
[47] U. Hartwig, H. Pritzkow, W. Sundermeyer, J. Waldi, *Zeitschrift für Naturforschung B*, 1987, **43**, 271-274
[48] U. Burger, S. P. Schmidlin, J. Mareda, G. Bernardinelli, *Chimia*, 1992, **46**, 111-113
[49] St. Grossert, M. M. Bharadwaj, *J. Chem. Soc. Chem. Comm.*, 1974, **4**, 144-145
[50] E. Block, M. Aslam, *Tetrahedron Lett.*, 1982, **23**, 4203-4206
[51] J. L. Charlton, P. de Mayo, *Can. J. Chem.*, 1968, **46**, 55-60
[52] T. Durst, J. F. King, *Can. J. Chem.*, 1966, **44**, 1869-1872
[53] D. C. Dittmer, T. R. Nelsen, *J. Org. Chem.*, 1976, **41**, 3044-3046
[54] L. W. Christensen, *Synthesis*, 1973, **9**, 534-535
[55] M. Zarei, *Tetrahedron Lett.*, 2013, **54**, 1100-1102
[56] B. E. Smart, W. J. Middleton, *J. Am. Chem. Soc.*, 1987, **109**, 4982-4992
[57] W. E. Truce, D. J. Abraham, P. Son, *J. Org. Chem.*, 1967, **32**, 990-997
[58] I. J. Borowitz, *J. Am. Chem. Soc.*, 1964, **86**, 1146-1149
[59] L. A. Paquette, J. P. Freeman, S. Maiorana, *Tetrahedron*, 1971, **27**, 2599-2607
[60] Z. Yang, J. Xu, *J. Org. Chem.*, 2014, **79**, 10703-10708
[61] F. M. Koch, R. Peters, *Chem. Eur. J.*, 2011, **17**, 3679-3692
[62] Q. Wu Zh. Yang, J. Xu, *Org. Biomol. Chem.*, 2016, **14**, 7258-7267
[63] S. K. Borthakur, P. Boruah, B. N. Goswami, *J. Chem. Res.*, 2007, **2**, 127-128
[64] S. Mondal, *Chem. Rev.*, 2012, **112**, 5339-5355
[65] W. E. Barnett, M. G. Newton, J. A. McCormack, *J.C.S. Chem. Commun.*, 1972, 264-265
[66] J. Gaitzsch, V. O. Rogachev, P. Metz, M. S. Yusubov, V. D. Filimonov, O. Kataeva, *J. S. Chem.*, 2009, **30**, 4-9
[67] J. Gaitzsch, V. Rogachev, P. Metz, V. D. Filimonov, M. Zahel, O. Kataeva, *J. S. Chem.*, 2011, **32**, 3-16
[68] Th. Morel, P. E. Verkade, *Rec. Trav. Chim.*, 1949, **68**, 619-638
[69] R. H. Eastman, D. Gallup, *J. Am. Chem. Soc.*, 1948, **70**, 864-865
[70] K. Rad-Moghadam, S. T. Roudsari, M. Sheykhan, *Synlett*, 2014, **25**, 827-830
[71] K. Rad-Moghadam, S. A. R. M. Hassani, S. T. Roudsari, *J. Mol. Liq.*, 2016, **218**, 275-280
[72] S. T. Roudsari, K. Rad-Moghadam, *Tetrahedron*, 2018, **74**, 4047-4052
[73] St. M. Heilmann, J. K. Rasmussen, R. A. Newmark, H. K. Smith, *J. Org. Chem.*, 1979, **44**, 3987-3988
[74] D. C. Craig, J. D. Stevens, *Carbohydr. Res.*, 2011, **346**, 854-857
[75] I. Zeid, I. Ismail, *J. Prakt. Chem.*, 1972, **314**, 367-370
[76] I. Zeid, I. Ismail, B. Helferich, *Liebigs Ann. Chem.*, 1972, **761**, 115-117
[77] I. Zeid, M. Badawi, I. Ismail, *J. Prakt. Chem.*, 1973, **315**, 1166-1168
[78] E. Fanghänel, H. Bartossek, T. Lochter, U. Baumeister, H. Hartung, *J. Prakt. Chem.*, 1997, **339**, 277-283
[79] I. Zeid, I. Ismail B. Helferich, *Liebigs Ann. Chem.*, 1972, **761**, 118-120
[80] K. A. Ali, Ann. Jäger, P. Metz, *Arkivoc*, 2016, **3**, 15-22
[81] W. E. Barnett, J. McCormack, *Tetrahedron Lett.*, 1969, **8**, 651-654
[82] J. Gaitzsch, V. Rogachev, M. Zahel, P. Metz, *Synthesis*, 2014, **46**, 531-536
[83] J. Ancerewicz, P. Vogel, *Helv. Chim. Acta*, 1996, **79**, 1393-1414
[84] B. Gorewit, M. Rosenblum, *J. Org. Chem.*, 1973, **38**, 2257-2258
[85] J. F. King, P. de Mayo, E. Morkved, A. B. M. A. Sattar, A. Stoessl, *Can. J. Chem.*, 1963, **41**, 100-107
[86] S. Aiken, K. Anozie, O. D. C. C. de Azevedo, L. Cowen, R. J. L. Edgar, C. D. Gabbutt, B. M. Heron, P. A. Lawrence, A. J. Mills, C. R. Rice, M. W. J. Urquhart, D. Zonidis, *Org. Biomol. Chem*., 2019, **17**, 9585-9604
[87] B. Li, W. Yan, C. Zhang, Y. Zhang, M. Liang, F. Chu, Y. Gong, B. Xu, P. Wang, H. Lei, *Molecules*, 2015, **20**, 4307-4318
[88] A. Ungureanu, A. Levens, L. Candish, D. W. Lupton, *Angew. Chem. Int. Ed.*, 2015, **54**, 11780-11784
[89] Y. - M. Huang, S. - M. Wang, J. Leng, B. Moku, C. Zhao, N. S. Alharbi, H. - L. Qin, *Adv. Synth. Catal.*, 2017, **359**, 3254 - 3260

[90] H. Liu, B. Moku, F. Li, J. Ran, J. Han, S. Long, G. - F. Zha, H. - L. Qin, *Adv. Synth. Catal.*, 2019, **361**, 4596-4601
[91] X. Chen, G. - F. Zha, G. A. L. Bare, J. Leng, S.- M. Wang, H. - L. Qin, *Eur. J. Org. Chem.*, 2019, 4597-4603
[92] G. Menozzi, Alb. Bargagna, L. Mosti, P. Schenone, *J. Heterocyclic Chem.*, 1987, **24**, 633-635
[93] Alb. Bargagna, G. Bignardi, P. Schenone, M. Longobardi, *J. Heterocyclic Chem.*, 1983, **20**, 839-843
[94] P. Singh, K. Bisetty, M.P. Mahajan, *S. Afr. J. Chem.*, 2009, **62**, 47-55
[95] A. J. Ae, H. Y. Joon, K. J. Hwan, L. C. Haeng, L. Y. Min (LG CHEMICAL LTD), Non-Aqueous electrolyte and secondary battery comprising the same, KR 2009/0084547A, 5 August 2009
[96] K. C. Woo, K. J. Sung, L. K. Kuk, L. S. Il, O. S. Yon (SK INNOVATION CO LTD), Electrolyte for lithium secondary battery and lithium secondary battery containing the same, KR 2016/0032470 A, 24 March 2016
[97] H. Changlong, Z. Ming (NINGDE CONTEMPORARY AMPEREX TECH CO LTD), Positive electrode sheet and preparation method thereof, and lithium ion battery, CN 1089 87752 A, 11 December 2018
[98] A. Toshiaki, E. Akihiro (FUJI PHOTO FILM CO LTD), Infrared ray sensitive composition, JP 2004/144933 A, 20 May 2004
[99] F. Hirotoshi, N. Masaaki, O. Keiji, U. Fumiyoshi (WAKO JUNYAKU KOGYO LTD), Resist material, JPH03 223865 A, 2 October 1991
[100] G. R. Fulmer, A. J. M. Miller, N. H. Sherden, H. E. Gottlieb, A. Nudelman, B. M. Stoltz, J. E. Bercaw, K. I. Goldberg, *Organometallics*, 2010, **29**, 2176-2179
[101] E. Breitmaier, *Structure Elucidation by NMR in Organic Chemistry: A Practical Guide*, 3rd edn. (revised), John Wiley & Sons Ltd, West Sussex, England, 2002
[102] J. Sandstrom, *Dynamic NMR Spectroscopy*, Academic Press, New York, 1982
[103] H. Karlsen, P. Kolsaker, C. Romming, E. Uggerud, *Acta Chem. Scand.*, 1998, **52**, 391-398
[104] J. Clayden, N. Greeves, S. Warren, *Organic chemistry*, 2012, Oxford University Press, Oxford, 2001
[105] J. Llinares, J. Elguero, R. Faure, E. - J. Vincent, *Org. Magn. Res.*, 1980, **14**, 20-24
[106] M. J. Taylor, D. J. Calvert, C. M. Hobbis, *Magn. Res. Chem.*, 1988, **26**, 619-628
[107] G. Fairley, C. Hall, R. Greenwood, *Synlett*, 2013, **24**, 570 - 574
[108] M. Karplus, *J. Chem. Phys*., 1959, **30**, 11-15
[109] M. Karplus, *J. Am. Chem. Soc.*, 1963, **85**, 2870-2871
[110] Th. Morel, P. E. Verkade, *Recueil*, 1951, **70**, 35-49
[111] O. Arjona, M. L. León, J. Plumet, *J. Org. Chem.*, 1999, **64**, 272-275
[112] R. P. van Summeren, B. L. Feringa, A. J. Minnaard, *Org. Biomol. Chem.*, 2005, **3**, 2524-2533
[113] C. - L. Chang M.-K. Leung, M.-H. Yang, *Tetrahedron*, 2004, **60**, 9205-9212
[114] M. Edgar, B. C. Percival, M. Gibson, J. Masania, K. Beresford, P. B. Wilson, M. Grootveld, *J. Chem. Educ.*, 2019, **96**, 1938−1947
[115] R. B. Woodward, R. Hoffmann, *Angew. Chem. Int. Ed. Engl.*, 1969, **8**, 781-853
[116] A. C. Cope, T. T. Foster, P. H. Towle, *J. Am. Chem. Soc.*, 1949, **71**, 3929-3935
[117] A. C. Cope, P. H. Towle, *J. Am. Chem. Soc.*, 1949, **71**, 3423-3428
[118] A. C. Cope, E. R. Trumbull, *Org. React.*, 1960, **11**, 317-493
[119] C. H. DePuy, R. W. King, *Chem. Rev.*, 1960, **60**, 431-457
[120] A. G. Martinez, E. T. Vilar, A. G. Fraile, S. de la M. Cerero, B. L. Maroto, *Tetrahedron: Asymmetry*, 2002, **13**, 17-19
[121] Y. Shi, D. Frattarelli, N. Watanabe, A. Facchetti, E. Cariati, S. Righetto, E. Tordin, C. Zuccaccia, A. Macchioni, S. L. Wegener, C. L. Stern, M. A. Ratner, T. J. Marks, *J. Am. Chem. Soc.*, 2015, **137**, 12521 − 12538
[122] F. B. Mallory, C. W. Mallory, *Org. React.*, 1984, **30**, 1-456
[123] Fr. B. Mallory, Cl. S. Wood, J. T. Gordon, *J. Am. Chem. Soc.*, 1964, **86**, 3094-3102
[124] D. H. Waldeck, *Chem. Rev.*, 1991, **91**, 415-436
[125] G. H Brown, *Photochromism*, Wiley-Interscience, New York, 1971
[126] V. Balzani, M. Venturi, A. Credi, *Molecular Devices and Machines: A Journey into the Nanoworld*, Wiley-VCH Verlag GmbH & Co. KGaA, Weinheim, Germany, 2003
[127] H. Dürr, H. Bouas-Laurent, *Photochromism: Molecules and Systems*, 1st edn., Elsevier Science, 2003
[128] Eug. Hadjoudis, Ir. M. Mavridis, *Chem. Soc. Rev.*, 2004, **33**, 579-588
[129] J. Zhang, H. Tian, in *Photochromic Materials: Preparation, Properties and Applications*, 1st edn., ed. J. Zhang, H. Tian, Wiley-VCH Verlag GmbH & Co. KGaA, Weinheim, Germany, 2016, Ch. 10, 393-415
[130] C. - C. Ko, V. W. - W. Yam, *Acc. Chem. Res.,* 2018, **51**, 149-159
[131] J. C. Crano, R. J. Guglielmetti, in *Organic Photochromic and Thermochromic Compounds: Main Photochromic Families*, Springer US, 2002, vol. 1
[132] J. C. Crano, R. J. Guglielmetti, in *Organic Photochromic and Thermochromic Compounds: Physicochemical Studies, Biological Applications, and Thermochromism*, Springer US, 2002, vol. 2

[133] R. C. Bertelson, in *Techniques of Chemistry*, ed. G. H. Brown, Wiley-Interscience, New York, 1971, vol. 3 Ch. 3, 49-431
[134] L. Kortekaas, W. R. Browne, *Chem. Soc. Rev.*, 2019, **48**, 3406-3424
[135] E. Fischer, Y. Hirshberg, *J. Chem. Soc*, 1952, 4522-4524
[136] J. Hepworth, B. M. Heron, in *Functional Dyes*, ed. S. H. Kim, Elsevier, Amsterdam, 2008
[137] S. Ju, D. Kwon, S. Min, K. Ahn, K. Park, J. Kim, *J. Photochem. Photobiol. A*, 2003, **160**, 151-157
[138] G. Hartley, *Nature*, 1937, **140**, 281
[139] M. Irie, *Chemical Reviews*, 2000, **100**, 1685-1716
[140] L. Yongchao, A. S. Dvornikov, P. M. Rentzepis, *Macromolecules*, 2002, **35**, 9377-9382
[141] X. Qin, H. Sugimura, M. S. Boulineau, T. J. Moravec, D. Harris (Vision Ease LP), Photochromic lens, US 7858001 B2, 28 December 2010
[142] H. G. Heller, S. N. Oliver, J. Whittall, I. Tomlinson (Plessey Co. Plc.), Fotochrome Spiropyran-Verbindungen, EP 0246114 A2, 19 November 1987
[143] A. Kumar, B. van Gemert, D. B. Knowles (Transitions Optical, Inc.), Substituted naphthopyrans, US5458814A, 17 October 1995
[144] T. Tsujioka, F. Tatezono, T. Harada, K. Kuroki, M. Irie, *Jpn. J. Appl. Phys.*, 1994, **33**, 5788-5792
[145] S. Kawata, Y. Kawata, Chem. Rev., 2000, **100**, 1777-1788
[146] P. Samori, E. Orgiu, *Adv. Mater*. 2014, **26**, 1827-1845
[147] B. L. Feringa, W. R. Browne, in *Molecular Switches*, 2nd edn., Wiley-VCH Verlag GmbH & Co. KGaA, Weinheim, Germany, 2011, vol. 1
[148] B. L. Feringa, W. R. Browne, in *Molecular Switches*, 2nd edn., Wiley-VCH Verlag GmbH & Co. KGaA, Weinheim, Germany, 2011, vol. 2
[149] R. M. Kellogg, M. B. Groen, H. Wynberg, *J. Org. Chem.*, 1967, **32**, 3093-3100
[150] M. Irie, M. Mohri, *J. Org. Chem*. 1988, **53**, 803-808
[151] Nakamura, S., Irie, M. J., *Org. Chem.*, 1988, **53**, 6136-6138
[152] M. Irie, K. Sakemura, M. Okinaka, K. Uchida, *J. Org. Chem.*, 1995, **60**, 8305-8309
[153] S. Abe, K. Uchida, I. Yamazaki, M. Irie, *Langmuir*, 1997, **13**, 5504-5506
[154] J. Ch. - H. Chan, H. - L. Wong, W. - T. Wong, V. W. - W. Yam, *Chem. Eur. J.*, 2015, **21**, 6936-6948
[155] Q. Luo, F. Cao, C. Xiong, Q. Dou, D. - H. Qu, *J. Org. Chem.*, 2017, **82**, 10960-10967
[156] S. Pu, C. Fan, W. Miao, G. Liu, *Tetrahedron*, 2008, **64**, 9464-9470
[157] K. Uchida, Y. Nakayama, M. Irie, *Bull. Chem. Soc. Jpn.* 1990, **63**, 1311-1315
[158] A. G. Lvov, N. A. Milevsky, V. Z. Shirinian, M. M. Krayushkin, *Chem. Heterocycl. Compd.*, 2015, **51**, 933-935
[159] V. A. Shershnev, L. M. Bogdanova, N. D. Golubeva, E. A. Yuryeva, N. A. Sanina, V. Z. Shirinyan, S. M. Aldoshin, G. I. Dzhardimalieva, *J. Inorg. Organomet. Polym.*, 2016, **26**, 1320-1327
[160] D. - P. Gong, T. - B. Gao, D. - K. Cao, M. D. Ward, *R.S.C. Adv.*, 2016, **6**, 69677-69684
[161] D. - K. Cao, J. - S. Hu, M. - Q. Li, D. - P. Gong, X. - X. Li, M. D. Ward, *Dalton Trans.*, 2015, **44**, 21008-21015
[162] M. Y. Belikov, *Russ. J. Org. Chem.*, 2018, **54**, 785-788
[163] S. Li, J. Tang, Y. Zhao, R. Jiang, T. Wang, G. Gao, J. You, *Chem. Commun.*, 2017, **53**, 3489-3492
[164] C. - L. Wong, C. - T. Poon, V. W. - W. Yam, *Organometallics*, 2017, **36**, 2661-2669
[165] S. Pang, D. Jang, W. S. Lee, H. - M. Kang, S. - J. Hong, S. K. Hwang, K.-H. Ahn, *Photochem. Photobiol. Sci.*, 2015, **14**, 765-774
[166] F. Ortica, P. Smimmo, C. Zuccaccia, U. Mazzucato, G. Favaro, N. Impagnatiello, A. Heynderickx, C. Moustrou, *J. Photochem. Photobiol. A*, 2007, **188**, 90-97
[167] M. M. Krayushkin, B. V. Lichitskii, A. P. Mikhalev, B. V. Nabatov, A. A. Dudinov, S. N. Ivanov, *Russ. J. Org. Chem.*, 2006, **42**, 860-864
[168] M. M. Krayushkin, S. N. Ivanov, A. Yu. Martynkin, B. V. Lichitsky, A. A. Dudinov, B. M. Uzhinov, *Russ. Chem. Bull.*, 2001, **50**, 2424-2427
[169] L. Bougdid, A. Samat, C. Moustrou, *New J. Chem.*, 2009, **33**, 1357-1361
[170] N. M. - W. Wu, M. Ng, W. H. Lam, H. - L. Wong, V. W. - W. Yam, *J. Am. Chem. Soc.*, 2017, **139**, 15142-15150
[171] K. P. Schultz, D. W. Spivey, E. K. Loya, J. E. Kellon, L. M. Taylor, M. R. McConville, *Tetrahedron Lett.*, 2016, **57**, 1296-1299
[172] M. M. Krayushkin, D. V. Pashchenko, B. V. Lichitsky, B. V. Nabatov, A. M. Komogortsev, L. G. Vorontsova, Z. A. Starikova, *Russ. Chem. Bull. Int. Ed.*, 2008, **57**, 2168-2174
[173] S. N. Ivanov, B. V. Lichitskii, A. A. Dudinov, A. Y. Martynkin, M. M. Krayushkin, *Chem. Heterocycl. Compd.*, 2001, **37**, 85-90

[174] S. Kobatake, S. Kuma, M. Irie, *J. Phys. Org. Chem.*, 2007, **20**, 960-967
[175] N. P. Buu-Hoi, N. Hoan, *Rec. Trav. Chim. Pays Bas*, 1948, **67**, 309-327
[176] X. Wu, H. Neumann, M. Beller, *Adv. Synth. Catal.*, 2011, **353**, 788-792
[177] M. M. Krayushkin, B. V. Lichitskii, A. P. Mikhalev, A. A. Dudinov, S. N. Ivanov, *Russ. J. Org. Chem.*, 2005, **41**, 87-90
[178] Th. Mrozek, H. Görner, J. Daub, *Chem. Commun.*, 1999, **16**, 1487-1488
[179] V. F. Traven, A. Y. Bochkov, M. M. Krayushkin, V. N. Yarovenko, V. A. Barachevsky, I. P. Beletskaya, *Mendeleev Commun.*, 2010, **20**, 22-24
[180] Huang-Minlon, *J. Am. Chem. Soc.*, 1946, **68**, 2487-2488
[181] S. Maksymenko, K. N. Parida, G. K. Pathe, A. A. More, Y. B. Lipisa, A. M. Szpilman, *Org. Lett.*, 2017, **19**, 6312-6315
[182] M. P. Sibi, *Org. Prep. Proced. Int.*, 1993, **25**, 15-40
[183] M. Mentzel, H. M. R. Hoffmann, *J. Prakt. Chem.*, 1997, **339**, 517-524
[184] J. Singh, *J. Prakt. Chem.*, 2000, **342**, 340-347
[185] N. Duchemin, R. Buccafusca, M. Daumas, V. Ferey, S. Arseniyadis, *Org. Lett.*, 2019, **21**, 8205-8210
[186] L. C. Bouchez, C. Gerbeaux, M. Rusch, M. Patoor, M. Livendahl, N. J. Press, *Synlett*, 2017, **28**, 1219-1223
[187] M. Irie, T. Fukaminato, K. Matsuda, S. Kobatake, *Chem. Rev*., 2014, **114**, 12174-12277
[188] M. Irie, T. Lifka, K. Uchida, *Mol. Cryst. Liq. Cryst.*, 1997, **297**, 81-84
[189] M. Irie, K. Uchida, T. Eriguchi, H. Tsuzuki, *Chem. Lett.*, 1995, **24**, 899-900
[190] M. Munakata, L. P. Wu, T. Kuroda-Sowa, M. Maekawa, Y. Suenaga, K. Furuichi, *J. Am. Chem. Soc.*, 1996, **118**, 3305-3306
[191] O. D. C. C. de Azevedo, B. M. Heron, D. Zonidis, Synthesis, Reactivity and Applications of 1,2-Oxathiine 2,2-dioxides, in *Targets in Heterocyclic Systems*, Italian Society of Chemistry, Rome, 2020, vol. 24 (to be published)
[192] K. Kohler, K. Wussow, A. S. Wirth, in *Palladium-Catalyzed Coupling Reactions: Practical Aspects and Future Developments*, ed. A. Molnar, Wiley-VCH Verlag GmbH & Co. KGaA, 2013, Ch. 1
[193] S. S. Gujral, S. Khatri, P. Riyal, *Indo Glob. J. Pharm. Sci.*, 2012, **2**, 351-367
[194] I. Maluenda, O. Navarro, *Molecules*, 2015, **20**, 7528-7557
[195] G. A. Molander, S. L. J. Trice, S. M. Kennedy, S. D. Dreher, M. T. Tudge, *J. Am. Chem. Soc.*, 2012, **134**, 11667-11673
[196] Y. - l. Yun, J. Yang, Y. - h. Miao, J. Sun, X. - j. Wang, *J. Saudi Chem. Soc.*, 2020, **24**, 151-185
[197] B. Yang, S. Gao, *Chem. Soc. Rev.*, 2018, **47**, 7926-7953
[198] K. C. Nicolaou, S. A. Snyder, T. Montagnon, G. Vassilikogiannakis, *Angew. Chem. Int. Ed.*, 2002, **41**, 1668-1698
[199] M. M. Heravi, T. Ahmadi, M. Ghavidel, B. Heidari, H. Hamidi, *RSC Adv.*, 2015, **5**, 101999-102075
[200] A. C. Wright, B.. M. Stoltz, *Org. Synth.*, 2019, **96**, 80-97
[201] A. E. Goetz, T. K. Shaha, N. K. Garg, *Chem. Commun.*, 2015, **51**, 34-45
[202] J. - A. G. Lopez, M. F. Greaney, *Chem. Soc. Rev.*, 2016, **45**, 6766-6798
[203] A. V. Dubrovskiy, N. A. Markina, R. C. Larock, *Org. Biomol. Chem.*, 2013, **11**, 191-218
[204] S. M. Bronner, N. K. Garg, *J. Org. Chem.*, 2009, **74**, 8842-8843
[205] R. Sanz, *Org. Prep. Proced. Int.*, 2008, **40**, 215-291
[206] J. T. Watson, O. D. Sparkman, *Introduction to Mass Spectrometry*, John Wiley & Sons, Ltd, 2007
[207] L. Pauling, *J. Am. Chem. Soc.*, 1932, **54**, 3570-3582
[208] W. F. Bailey, P. J. Jeffrey, *J. Organomet. Chem.*, 1988, **352**, 1-46
[209] B. J. Wakefield, *Organolithium Methods,* Best Synthetic Methods Series, Academic Press, London, 1988
[210] C. D. Gabbutt, D. J. Hartley, J. D. Hepworth, B. M. Heron, M. Kanjia, M. M. Rahman, *Tetrahedron*, 1994, **50,** 2507-2522
[211] G. W. H. Cheeseman, S.G. Greenberg, *J. Organomet. Chem.*, 1979, **166**, 139-152
[212] M. G. Saulnier, G. W. Gribble, *J. Org. Chem.*, 1982, **47**, 757-761
[213] N. Miyaura, K. Yamada, A. Suzuki, *Tetrahedron Lett.*, 1979, **36**, 3437-3440
[214] R. Franzen, *Can. J. Chem.*, 2000, **78**, 957-962
[215] R. S. Varma, *Green Chem.*, 2019, **21**, 381-405
[216] X. Lei, L. Gao, Q. Ding, Y. Peng, J. Wu, *Org. Biomol. Chem.*, 2011, **9**, 6265-6270
[217] A. J. D. Koning, P. H. M. Budzelaar, J. Boersma, G. J. M. van der Kerk, *J. Organomet. Chem.*, 1980, **199**, 153-169
[218] T. Ishiyama, M. Murata, N. Miyaura, *J. Org. Chem.*, 1995, **60**, 7508-7510
[219] T. Ishiyama, K. Ishida, N. Miyaura, *Tetrahedron*, 2001, **57**, 9813-9816
[220] T. Yamada, H. Takiguchi, K. Ohmori, K. Suzuki, *Org. Lett.*, 2018, **20**, 3579-3582
[221] H. A. Duong, S. Chua, P. B. Huleatt, C. L. L. Chai, *J. Org. Chem.*, 2008, **73**, 9177-9180
[222] V. A Kallepalli, K. A. Gore, F. Shi, L. Sanchez, G. A. Chotana, S. L. Miller, R. E. Maleczka Jr., M. R. Smith III, *J. Org. Chem.*, 2015, **80**, 8341-8353

[223] H. M. L. Davies, D. Morton, *J. Org. Chem.*, 2016, **81**, 343-350
[224] D. Gallego, E. A. Baquero, *Open Chem.*, 2018, **16**, 1001-1058
[225] S. Martinsa, P. S. Branco, M. C. de la Torre, M. A. Sierra, A. Pereira, *Synlett*, 2010, **19**, 2918-2922
[226] K. D. Bruycker, S. Billiet, H. A. Houck, S. Chattopadhyay, J. M. Winne, F. E. D. Prez, *Chem. Rev.*, 2016, **116**, 3919-3974
[227] I.K. Korobitsyna, A.V. Khalikova, L. L. Rodina, N. P. Shusherina, *Chem. Heterocycl. Compd.*, 1983, **19**, 117-136
[228] R. M. Moriarty, I. Prakash, R. Penrnasta, *Synth. Commun.*, 1987, **17**, 409-413
[229] C. J. Moody, in *Advances in Heterocyclic Chemistry*, ed. A.R. Katritzky, Academic Press Inc., 1982, **30**, 1-45
[230] S. Radl, in *Advances in Heterocyclic Chemistry*, Academic Press Inc., 1997, **67**, 119-205
[231] B. Atasoy, M. Balci, O. Buyukgungor, *Tetrahedron Lett.*, 1987, **28**, 555-558
[232] R. C. Cookson, S. S. H. Gilani, D. R. Stevens, *J. Chem. Soc.*, 1967, 1905-1909
[233] D. Craig, S. R. J. Spreadbury, A. J. P. White, *Chem. Commun.*, 2020, **56**, 9803-9806
[234] D. H. R. Barton, X. Lusinchi, J. S. Ramirez, *Tetrahedron Lett.*, 1983, **24**, 2995-2998
[235] C. A. Seymour, F. D. Greene, *J. Am. Chem. Soc.*, 1980, **102**, 6384-6385
[236] V. D. Kiselev, D. A. Kornilov, O. V. Anikin, I. A. Sedov, A. I. Konovalov, Russ. J. Org. Chem., 2017, **53**, 1864-1869
[237] J. H. Hall M. L. Jones, *J. Org. Chem.*, 1983, **48**, 822-826
[238] C. D. Gabbutt, J. D. Hepworth, B. M. Heron, *Tetrahedron*, 1995, **51**, 13277-13290
[239] O. Acevedo, M. E. Squillacote, *J. Org. Chem.*, 2008, **73**, 912-922
[240] S. Ohashi, W. E. Ruch, G. B. Butler, *J. Org. Chem.*, 1981, **46**, 614-619
[241] W. H. Pirkle, J. C. Stickler, *Chem. Commun.*, 1967, 760-761
[242] Y. Himeshima, T. Sonada, H. Kobayashi, *Chem. Lett.*, 1983, 1211-1214
[243] W. M. Weber, L. A. Hunsaker, S. F. Abcouwer, L. M. Deck, D. L. Vander Jagt, *Bioorg. Med. Chem.*, 2005, **13**, 3811-3820
[244] S. Paul, M. Gupta, *Synth. Comm.*, 2005, **35**, 213-222
[245] S. Paul, T. Gorai, A. Koley, J. K. Ray, *Tetrahedron Lett.*, 2011, **52**, 4051-4055
[246] S. Hernandez, I. Moreno, R. SanMartin, G. Gómez, M. T. Herrero, E. Dominguez, *J. Org. Chem.*, 2010, **75**, 434-441
[247] J. K. Son, *Eur. J. Med. Chem.*, 2008, **43**, 675-682
[248] J. Bezensek, T. Kolesa, U. Groselj, J. Wagger, K. Stare, A. Meden, J. Svete, B. Stanovnik, *Tetrahedron Lett.*, 2010, **51**, 3392-3397
[249] M. A. Al-Shiekh, H. Y. Medrassi, M. H. Elnagdi, E. A. Hafez, *ARKIVOC*, 2008, **17**, 36-47
[250] Z. Arnold, *Collect. Czech. Chem. Commun.*, 1964, **29**, 645-51
[251] E. J. Breaux, K. E. Zwikelmaier, *J. Het. Chem.*, 1981, **18**, 183-184
[252] G. B. Bennett, R. B. Mason, L. J. Alden, J. B. Roach; *J. Med. Chem.*, 1978, **21**, 623-628
[253] F. Al-Qalaf, M. M. Abdelkhalik, A. Al-Enezi, *Heterocycles*, 2008, **75**, 145-156
[254] T. A. Dain, *Tetrahedron*, 2004, **60**, 5069-5076
[255] F. W. Lewis, T. C. McCabe, D. H. Grayson, *Tetrahedron*, 2011, **67**, 7517-7528
[256] B. Unterhalt, P. Gores, *Archiv der Pharmazie*, 1989, **322**, 839-840
[257] O. G. Karamov, *Russian Chemical Bulletin*, 2011, **60**, 168-174
[258] G. A. Molander, Fl. Beaumard, *Org. Lett.*, 2010, **12**, 4022-4025
[259] R. C. Larock, Q. Tian, *J. Org. Chem.*, 1998, **63**, 2002-2009
[260] J. G. Smith, R. B. McCall, *J. Org. Chem.*, 1980, **45**, 3982-3986

APPENDIX 1: Crystal structure information/ CIF files

checkCIF/PLATON report for compound 2.5

THIS REPORT IS FOR GUIDANCE ONLY. IF USED AS PART OF A REVIEW PROCEDURE FOR PUBLICATION, IT SHOULD NOT REPLACE THE EXPERTISE OF AN EXPERIENCED CRYSTALLOGRAPHIC REFEREE.

No syntax errors found. CIF dictionary Interpreting this report

Datablock: DZ017_0ma_a

Bond precision: C-C = 0.0021 A Wavelength=0.71073

Cell: a=11.8439(7) b=7.4115(5) c=23.3606(17)
alpha=90 beta=90 gamma=90
Temperature: 202 K

	Calculated	Reported
Volume	2050.6(2)	2050.6(2)
Space group	P b c a	P b c a
Hall group	: -P 2ac 2a	-P 2ac 2a
Moiety formula	C12 H12 N2 O	?
Sum formula	C12 H12 N2 O	C12 H12 N2 O
Mr	200.24	200.24
Dx,g cm-3	1.297	1.297
Z	8	8
Mu (mm-1)	0.085	0.085
F000	848.0	848.0
F000'	848.33	
h,k,lmax	16,10,33	16,10,33
Nref	3124	3116
Tmin,Tmax	0.983,0.992	0.780,0.960
Tmin'	0.983	

Correction method= # Reported T Limits: Tmin=0.780 Tmax=0.960
AbsCorr = MULTI-SCAN

Data completeness= 0.997 Theta(max)= 30.508

R(reflections)= 0.0669(2491) wR2(reflections)= 0.1925(3116)

S = 1.042 Npar= 138

The following ALERTS were generated. Each ALERT has the format
test-name_ALERT_alert-type_alert-level.
Click on the hyperlinks for more details of the test.

Alert level C

PLAT905_ALERT_3_C	Negative K value in the Analysis of Variance ...	-0.889 Report
PLAT911_ALERT_3_C	Missing FCF Refl Between Thmin & STh/L= 0.600	5 Report

Alert level G

PLAT072_ALERT_2_G	SHELXL First Parameter in WGHT Unusually Large	0.11 Report
PLAT432_ALERT_2_G	Short Inter X...Y Contact O1 ..C11	2.98 Ang.
	-1/2+x,3/2-y,1-z =	4_466 Check
PLAT910_ALERT_3_G	Missing # of FCF Reflection(s) Below Theta(Min).	1 Note
PLAT912_ALERT_4_G	Missing # of FCF Reflections Above STh/L= 0.600	2 Note
PLAT913_ALERT_3_G	Missing # of Very Strong Reflections in FCF	1 Note
PLAT978_ALERT_2_G	Number C-C Bonds with Positive Residual Density.	5 Info

0 **ALERT level A** = Most likely a serious problem - resolve or explain
0 **ALERT level B** = A potentially serious problem, consider carefully
2 **ALERT level C** = Check. Ensure it is not caused by an omission or oversight
6 **ALERT level G** = General information/check it is not something unexpected

0 ALERT type 1 CIF construction/syntax error, inconsistent or missing data
3 ALERT type 2 Indicator that the structure model may be wrong or deficient
4 ALERT type 3 Indicator that the structure quality may be low
1 ALERT type 4 Improvement, methodology, query or suggestion
0 ALERT type 5 Informative message, check

PLATON version of 26/09/2018; check.def file version of 13/09/2018

Datablock DZ017_0ma_a - ellipsoid plot

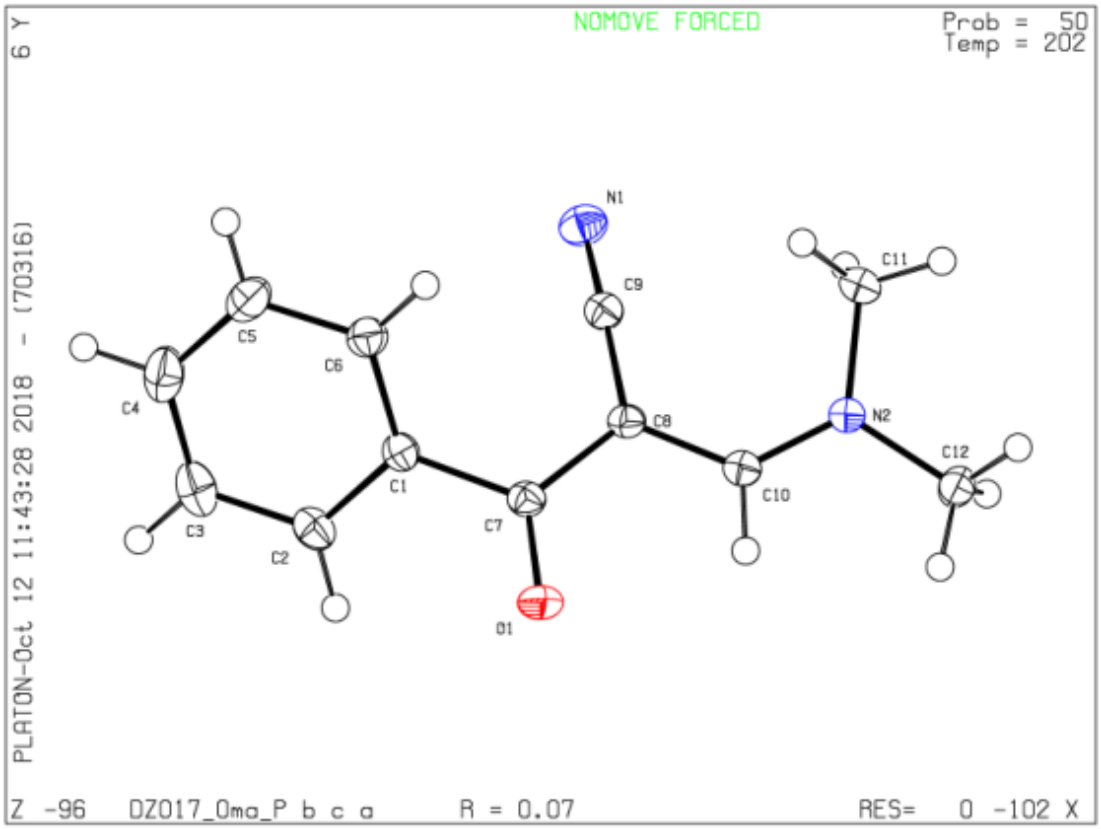

checkCIF/PLATON report for compound 2.5a

Structure factors have been supplied for datablock(s) cu_ColourChem_ID0176_0m_a

THIS REPORT IS FOR GUIDANCE ONLY. IF USED AS PART OF A REVIEW PROCEDURE FOR PUBLICATION, IT SHOULD NOT REPLACE THE EXPERTISE OF AN EXPERIENCED CRYSTALLOGRAPHIC REFEREE.

No syntax errors found. CIF dictionary Interpreting this report

Datablock: cu_ColourChem_ID0176_0m_a

```
Bond precision:  C-C = 0.0025 A          Wavelength=1.54178

Cell:            a=38.3150(15)     b=38.3150(15)     c=5.5470(8)
                 alpha=90          beta=90           gamma=90
Temperature:     150 K

                 Calculated                Reported
Volume           8143.2(13)                8143.4(16)
Space group      I 41/a                    I 41/a
Hall group       -I 4ad                    -I 4ad
Moiety formula   C19 H11 N2 O2, C4 H12 N   ?
Sum formula      C23 H23 N3 O2             C23 H23 N3 O2
Mr               373.44                    373.44
Dx,g cm-3        1.218                     1.218
Z                16                        16
Mu (mm-1)        0.631                     0.631
F000             3168.0                    3168.0
F000'            3177.14
h,k,lmax         47,47,6                   46,47,6
Nref             4139                      4122
Tmin,Tmax        0.963,0.969               0.690,0.890
Tmin'            0.881

Correction method= # Reported T Limits: Tmin=0.690 Tmax=0.890
AbsCorr = MULTI-SCAN

Data completeness= 0.996          Theta(max)= 74.521

R(reflections)= 0.0502( 3134)     wR2(reflections)= 0.1205( 4122)

S = 1.055                 Npar= 257
```

The following ALERTS were generated. Each ALERT has the format
test-name_ALERT_alert-type_alert-level.
Click on the hyperlinks for more details of the test.

Alert level C

PLAT906_ALERT_3_C	Large K Value in the Analysis of Variance	5.263 Check
PLAT911_ALERT_3_C	Missing FCF Refl Between Thmin & STh/L= 0.600	15 Report

Alert level G

PLAT083_ALERT_2_G	SHELXL Second Parameter in WGHT Unusually Large	5.93 Why ?
PLAT152_ALERT_1_G	The Supplied and Calc. Volume s.u. Differ by ...	-3 Units
PLAT180_ALERT_4_G	Check Cell Rounding: # of Values Ending with 0 =	3 Note
PLAT912_ALERT_4_G	Missing # of FCF Reflections Above STh/L= 0.600	6 Note
PLAT978_ALERT_2_G	Number C-C Bonds with Positive Residual Density.	1 Info

0 **ALERT level A** = Most likely a serious problem - resolve or explain
0 **ALERT level B** = A potentially serious problem, consider carefully
2 **ALERT level C** = Check. Ensure it is not caused by an omission or oversight
5 **ALERT level G** = General information/check it is not something unexpected

1 ALERT type 1 CIF construction/syntax error, inconsistent or missing data
2 ALERT type 2 Indicator that the structure model may be wrong or deficient
2 ALERT type 3 Indicator that the structure quality may be low
2 ALERT type 4 Improvement, methodology, query or suggestion
0 ALERT type 5 Informative message, check

Datablock cu_ColourChem_ID0176_0m_a - ellipsoid plot

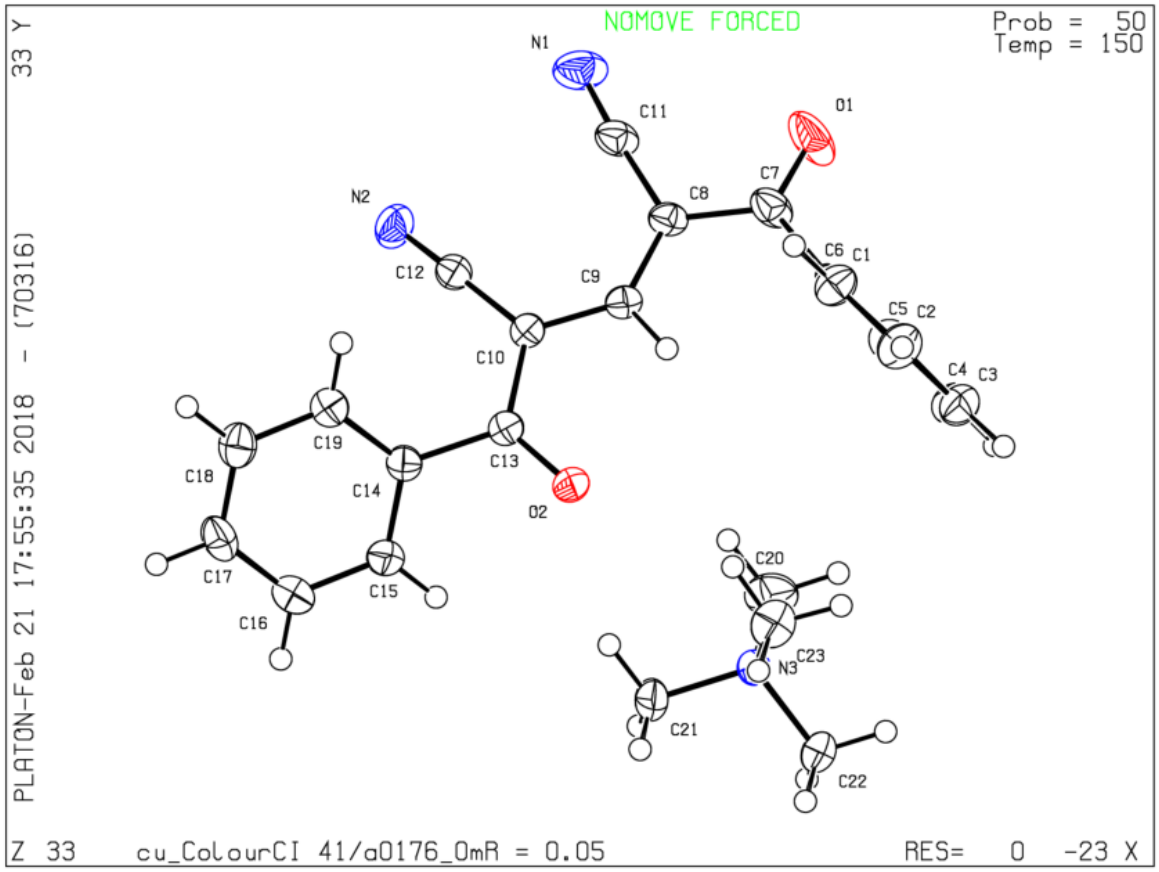

checkCIF/PLATON report for compound 2.5b

Structure factors have been supplied for datablock(s) mo_ColourChem_DZ025b_0m_a

THIS REPORT IS FOR GUIDANCE ONLY. IF USED AS PART OF A REVIEW PROCEDURE FOR PUBLICATION, IT SHOULD NOT REPLACE THE EXPERTISE OF AN EXPERIENCED CRYSTALLOGRAPHIC REFEREE.

No syntax errors found. CIF dictionary Interpreting this report

Datablock: mo_ColourChem_DZ025b_0m_a

```
Bond precision:  C-C = 0.0026 A          Wavelength=0.71073

Cell:           a=9.145(6)         b=11.501(7)      c=11.649(8)
                alpha=117.55(2)    beta=94.48(3)    gamma=91.05(2)
Temperature:    150 K

                Calculated                Reported
Volume          1080.9(12)                1080.9(12)
Space group     P -1                      P -1
Hall group      -P 1                      -P 1
Moiety formula  C19 H11 N2 O2, C5 H13 N2  ?
Sum formula     C24 H24 N4 O2             C24 H24 N4 O2
Mr              400.47                    400.47
Dx,g cm-3       1.230                     1.230
Z               2                         2
Mu (mm-1)       0.080                     0.080
F000            424.0                     424.0
F000'           424.16
h,k,lmax        12,16,16                  12,16,16
Nref            6292                      6260
Tmin,Tmax       0.980,0.985               0.580,0.890
Tmin'           0.978

Correction method= # Reported T Limits: Tmin=0.580 Tmax=0.890
AbsCorr = MULTI-SCAN

Data completeness= 0.995          Theta(max)= 29.984

R(reflections)= 0.0610( 4483)     wR2(reflections)= 0.1621( 6260)

S = 1.024                 Npar= 275
```

The following ALERTS were generated. Each ALERT has the format
test-name_ALERT_alert-type_alert-level.
Click on the hyperlinks for more details of the test.

Alert level C

PLAT906_ALERT_3_C	Large K Value in the Analysis of Variance	5.974	Check
PLAT911_ALERT_3_C	Missing FCF Refl Between Thmin & STh/L= 0.600	2	Report
PLAT918_ALERT_3_C	Reflection(s) with I(obs) much Smaller I(calc) .	1	Check

Alert level G

PLAT230_ALERT_2_G	Hirshfeld Test Diff for C8 --C9 .	5.5	s.u.
PLAT230_ALERT_2_G	Hirshfeld Test Diff for C11 --C24 .	5.6	s.u.
PLAT380_ALERT_4_G	Incorrectly? Oriented X(sp2)-Methyl Moiety	C19	Check
PLAT912_ALERT_4_G	Missing # of FCF Reflections Above STh/L= 0.600	32	Note
PLAT978_ALERT_2_G	Number C-C Bonds with Positive Residual Density.	11	Info

0 **ALERT level A** = Most likely a serious problem - resolve or explain
0 **ALERT level B** = A potentially serious problem, consider carefully
3 **ALERT level C** = Check. Ensure it is not caused by an omission or oversight
5 **ALERT level G** = General information/check it is not something unexpected

0 ALERT type 1 CIF construction/syntax error, inconsistent or missing data
3 ALERT type 2 Indicator that the structure model may be wrong or deficient
3 ALERT type 3 Indicator that the structure quality may be low
2 ALERT type 4 Improvement, methodology, query or suggestion
0 ALERT type 5 Informative message, check

Datablock mo_ColourChem_DZ025b_0m_a - ellipsoid plot

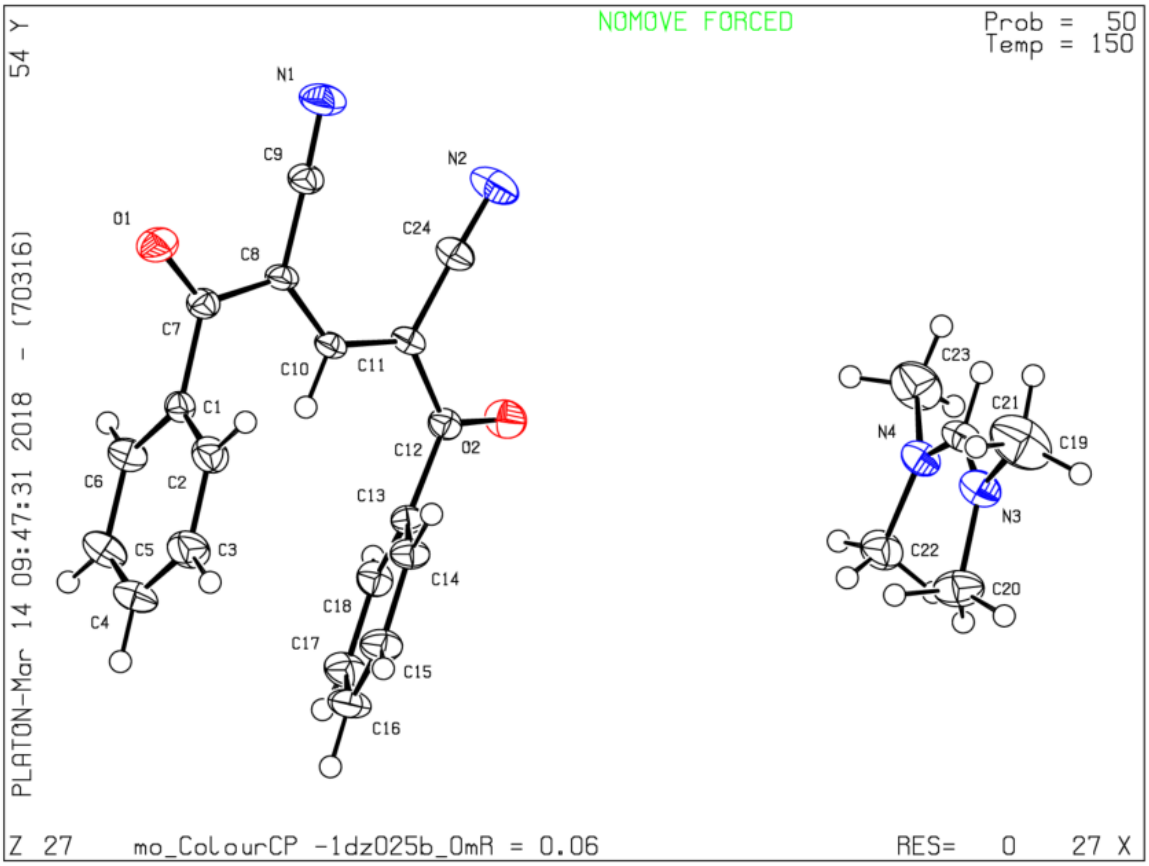

checkCIF/PLATON report for compound 2.63

Structure factors have been supplied for datablock(s) mo_CC_KAA9R_0m_a

THIS REPORT IS FOR GUIDANCE ONLY. IF USED AS PART OF A REVIEW PROCEDURE FOR PUBLICATION, IT SHOULD NOT REPLACE THE EXPERTISE OF AN EXPERIENCED CRYSTALLOGRAPHIC REFEREE.

No syntax errors found. CIF dictionary Interpreting this report

Datablock: mo_CC_KAA9R_0m_a

```
Bond precision: C-C = 0.0033 A           Wavelength=0.71073

Cell:            a=8.8058(9)     b=20.394(2)          c=9.6437(10)
            alpha=90             beta=99.794(4)      gamma=90
Temperature:     150 K

Calculated                       Reported
Volume           1706.6(3)       1706.7(3)
Space group      P 21/n                    P 1 21/n 1
Hall group       -P 2yn                    -P 2ybc (x-
Moiety formula C22 H16 O3 S                C22 H16 O3 S
Sum formula      C22 H16 O3 S              C22 H16 O3 S
Mr               360.41          360.44
Dx,g cm-3        1.403           1.403
Z                4               4
Mu (mm-1)        0.209           0.209
F000             752.0           752.9
F000'            752.83
h,k,lmax         12,29,13        12,29,13
Nref             5220            5218
Tmin,Tmax        0.959,0.975
Tmin'            0.959

Correction method= Not given

Data completeness= 1.000         Theta(max)= 30.510

R(reflections)= 0.0686( 3595)      wR2(reflections)= 0.1417( 5218)
S = 1.056                  Npar= 235
```

The following ALERTS were generated. Each ALERT has the format **test-name_ALERT_alert-type_alert-level.**
Click on the hyperlinks for more details of the test.

Alert level C

```
PLAT126_ALERT_1_C Error in or Uninterpretable Hall Symbol  .......    -P 2YBC (X-
Z,Y
PLAT906_ALERT_3_C Large K value in the Analysis of Variance ......      7.438 Check
```

```
PLAT906_ALERT_3_C Large K value in the Analysis of Variance ......      2.097 Check
```

Alert level G

```
PLAT073_ALERT_1_G H-atoms ref, but _hydrogen_treatment reported as     constr Check
PLAT395_ALERT_2_G Deviating  X-O-Y  Angle from 120 Deg for  O1          120.2
Degree
PLAT910_ALERT_3_G Missing # of FCF Reflection(s) Below Theta(Min)           1 Note
PLAT933_ALERT_2_G Number of OMIT Records in Embedded .res File ...          1 Note
PLAT960_ALERT_3_G Number of Intensities with I  <   - 2*sig(I) ...          8 Check
PLAT978_ALERT_2_G Number C-C Bonds with Positive Residual Density.         11 Note
```

```
   0 ALERT level A = Most likely a serious problem - resolve or explain
   0 ALERT level B = A potentially serious problem, consider carefully
   3 ALERT level C = Check. Ensure it is not caused by an omission or oversight
   6 ALERT level G = General information/check it is not something unexpected

  2    ALERT type 1 CIF construction/syntax error, inconsistent or missing data
  3    ALERT type 2 Indicator that the structure model may be wrong or deficient
  4    ALERT type 3 Indicator that the structure quality may be low
  0 ALERT type 4 Improvement, methodology, query or suggestion
  0 ALERT type 5 Informative message, check
```

PLATON version of 26/02/2017; check.def file version of 21/02/2017

Datablock mo_CC_KAA9R_0m_a - ellipsoid plot

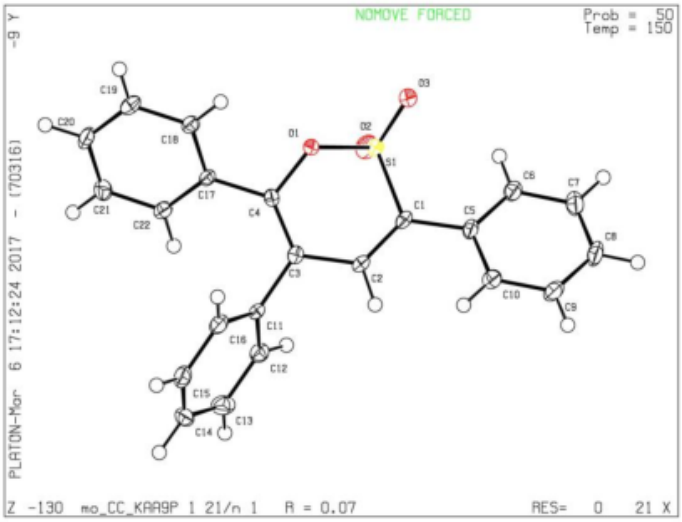

checkCIF/PLATON report for compound 3.45

Structure factors have been supplied for datablock(s) ColourChem_DZ050_0m_a

THIS REPORT IS FOR GUIDANCE ONLY. IF USED AS PART OF A REVIEW PROCEDURE FOR PUBLICATION, IT SHOULD NOT REPLACE THE EXPERTISE OF AN EXPERIENCED CRYSTALLOGRAPHIC REFEREE.

No syntax errors found. CIF dictionary Interpreting this report

Datablock: ColourChem_DZ050_0m_a

Bond precision: C-C = 0.0033 A Wavelength=0.71073

Cell: a=9.869(5) b=11.897(5) c=13.181(5)
alpha=113.322(17) beta=109.14(2) gamma=90.79(2)
Temperature: 150 K

	Calculated	Reported
Volume	1324.1(10)	1324.1(10)
Space group	P -1	P -1
Hall group	-P 1	-P 1
Moiety formula	2(C24 H27 N O3 S3), C4 H10 O	?
Sum formula	C52 H64 N2 O7 S6	C26 H32 N O3.50 S3
Mr	1021.41	510.70
Dx,g cm-3	1.281	1.281
Z	1	2
Mu (mm-1)	0.309	0.309
F000	542.0	542.0
F000'	542.95	
h,k,lmax	14,16,18	14,16,18
Nref	8086	8011
Tmin,Tmax	0.939,0.988	0.710,0.890
Tmin'	0.937	

Correction method= # Reported T Limits: Tmin=0.710 Tmax=0.890
AbsCorr = MULTI-SCAN

Data completeness= 0.991 Theta(max)= 30.533

R(reflections)= 0.0519(5853) wR2(reflections)= 0.1481(8011)

S = 1.027 Npar= 331

The following ALERTS were generated. Each ALERT has the format
test-name_ALERT_alert-type_alert-level.
Click on the hyperlinks for more details of the test.

Alert level C

PLAT243_ALERT_4_C	High	'Solvent' Ueq as Compared to Neighbors of	O4 Check

---

Alert level G

PLAT003_ALERT_2_G	Number of Uiso or Uij Restrained non-H Atoms ...		5 Report
PLAT045_ALERT_1_G	Calculated and Reported Z Differ by a Factor ...		0.50 Check
PLAT177_ALERT_4_G	The CIF-Embedded .res File Contains DELU Records		1 Report
PLAT178_ALERT_4_G	The CIF-Embedded .res File Contains SIMU Records		1 Report
PLAT302_ALERT_4_G	Anion/Solvent/Minor-Residue Disorder (Resd 2)		80% Note
PLAT395_ALERT_2_G	Deviating X-O-Y Angle From 120 for O3		115.6 Degree
PLAT398_ALERT_2_G	Deviating C-O-C Angle From 120 for O4		51.9 Degree
PLAT793_ALERT_4_G	Model has Chirality at C3	(Centro SPGR)	R Verify
PLAT793_ALERT_4_G	Model has Chirality at C4	(Centro SPGR)	S Verify
PLAT860_ALERT_3_G	Number of Least-Squares Restraints		54 Note
PLAT883_ALERT_1_G	No Info for _atom_sites_solution_primary		Please Do !

---

0 **ALERT level A** = Most likely a serious problem - resolve or explain
0 **ALERT level B** = A potentially serious problem, consider carefully
1 **ALERT level C** = Check. Ensure it is not caused by an omission or oversight
11 **ALERT level G** = General information/check it is not something unexpected

2 ALERT type 1 CIF construction/syntax error, inconsistent or missing data
3 ALERT type 2 Indicator that the structure model may be wrong or deficient
1 ALERT type 3 Indicator that the structure quality may be low
6 ALERT type 4 Improvement, methodology, query or suggestion
0 ALERT type 5 Informative message, check

Datablock ColourChem_DZ050_0m_a - ellipsoid plot

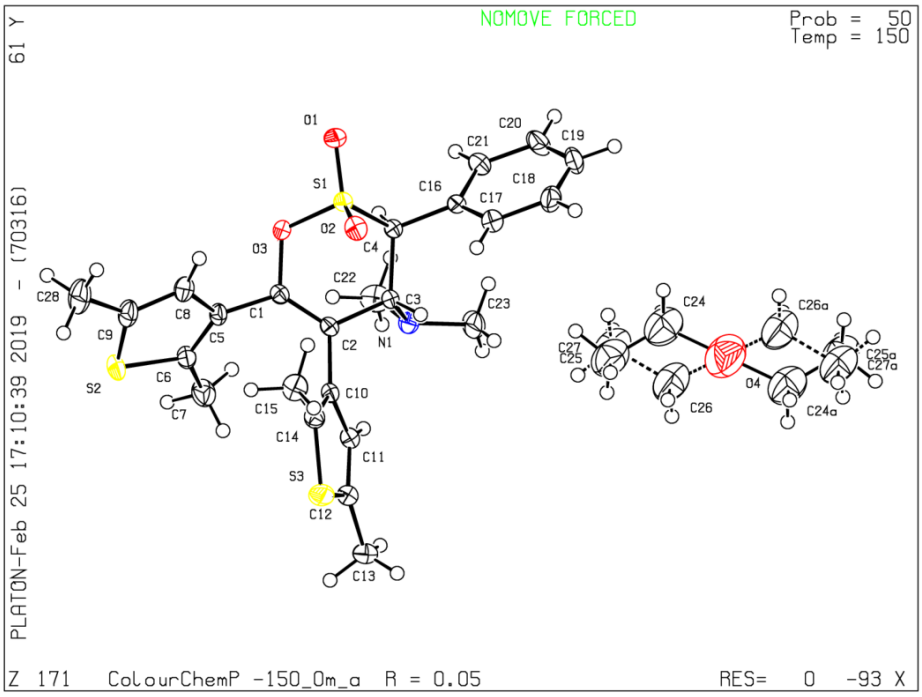

APPENDIX 2: Publications arising from work contained within this thesis

To date, two published research articles and one invited review article (manuscript accepted but not yet published) have resulted from the investigations presented in this thesis.

Article 1: Invited Review

Title: Synthesis, Reactivity and Applications of 1,2-Oxathiine 2,2-dioxides

Authors: Orlando D. C. C. de Azevedo*, B. Mark Heron*, Dimitrios Zonidis*

Book: Targets in Heterocyclic Systems - Chemistry and Properties; Publisher: Italian Chemical Society

Citation: *Targets in Heterocyclic Systems*, **2020**, volume *24*, pending;

DOI: http://dx.medra.org/10.17374/targets.2021.24.33

Date of Publication: manuscript accepted; publication estimated February / March 2021

Author contribution: For this review article I performed extensive background literature searching and selected and abstracted manuscripts for the following subsections: Synthesis section 2.2.1 (3,4-Dihydro-1,2-oxathiine 2,2-dioxides: Synthesis), Synthesis section 2.3 (1,2-Oxathiine 2,2-dioxides), Reactivity and Applications section 3.2 (Dihydro-1,2-oxathiine 2,2-dioxides), Reactivity and Applications section 3.3 (1,2-Oxathiine 2,2-dioxides). I drafted the original discussion for the foregoing sections based upon my selections and made appropriate revisions in accord with Professor Heron's suggestions. Revised and updated content from this review article features in parts of this thesis introduction chapter (Chapter 1).

SYNTHESIS, REACTIVITY AND APPLICATIONS OF 1,2-OXATHIINE 2,2-DIOXIDES

DOI: http://dx.medra.org/10.17374/targets.2021.24.33

Orlando D. C. C. de Azevedo, B. Mark Heron, Dimitrios Zonidis

Department of Chemical Sciences, School of Applied Sciences, University of Huddersfield, Queensgate, HD1 3DH Huddersfield, UK

(e-mail: orlando.deazevedo@hud.ac.uk; m.heron@hud.ac.uk; dimitrios.zonidis@hud.ac.uk)

Abstract. *The structure, synthesis, reactivity and applications of the 1,2-oxathiine 2,2-dioxide ring system are reviewed. This relatively scarcely studied heterocycle can be accessed by a variety of traditional and modern synthetic chemistry strategies and offers great potential as a building block for the construction of acyclic and heterocyclic compounds. Furthermore, the δ-sultone ring is an invaluable reagent for imparting water solubility into a variety of materials including colorants and polymers.*

Contents

1. Introduction
2. Synthesis
  2.1. 1,2-Oxathiane 2,2-dioxides
  2.2. Dihydro-1,2-oxathiine 2,2-dioxides
    2.2.1. 3,4-Dihydro-1,2-oxathiine 2,2-dioxides
    2.2.2. 3,6-Dihydro-1,2-oxathiine 2,2-dioxides
    2.2.3. 5,6-Dihydro-1,2-oxathiine 2,2-dioxides
  2.3. 1,2-Oxathiine 2,2-dioxides
3. Reactivity and applications
  3.1. 1,2-Oxathiane 2,2-dioxides
  3.2. Dihydro-1,2-oxathiine 2,2-dioxides
  3.3. 1,2-Oxathiine 2,2-dioxides
4. Concluding remarks
References

1. Introduction

1,2-Oxathiine 2,2-dioxides, historically described as either 1,4-sultones, 1,4-butanesultone or δ-sultones, are the relatively scarcely studied isomers in the homologous series of sultones.[1,2,3] Indeed the 1,2-oxathiine ring is the lesser explored isomer of the six-membered heterocyclic systems which contain one sulfur and one oxygen atom.[4] The objective of this review is to present the structure, synthesis, chemistry and applications of this interesting class of heterocycle and will encompass the tetrahydro- **1** (1,2-oxathiane 2,2-dioxide), the three isomeric dihydro- **2**, **3**, **4** and the fully unsaturated **5** 1,2-oxathiine 2,2-dioxide systems which can be considered as SO_2 isosteres of the extensively studied, biologically significant, pyran-2-one system **6** (Figure 1).

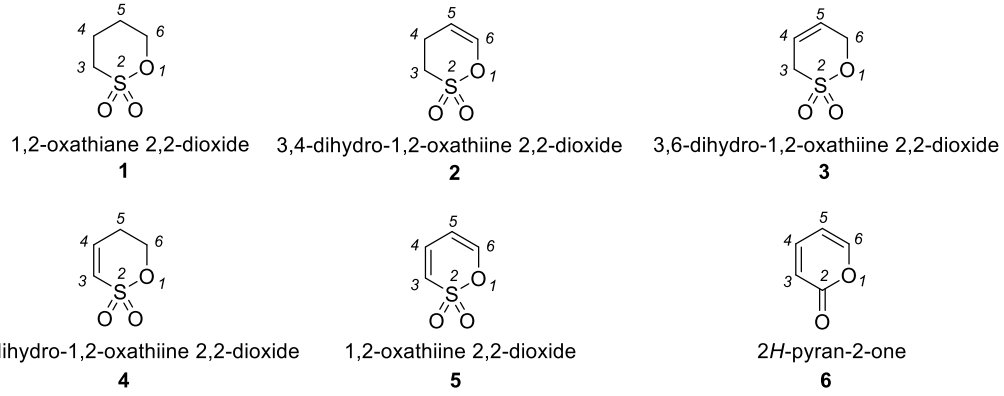

Figure 1. Structure and nomenclature.

2. Synthesis

In this section, the synthesis of monocyclic ring systems is organised by degree of saturation, commencing with the fully saturated 1,2-oxathiane 2,2-dioxides and progressing through the three isomeric dihydro derivatives leading to the fully unsaturated 1,2-oxathiine 2,2-dioxides. It should be noted that for organisational purposes the transformation of, for example, a dihydro isomer into the fully unsaturated analogue, is included in the synthesis section rather than in the discussion of reactivity.

2.1. 1,2-Oxathiane 2,2-dioxides

Historical routes to 1,2-oxathiane 2,2-dioxides (saturated δ-sultones) **1**, which have been reviewed in the mid-1950s[5] and late 1980s,[2] include the vacuum distillation of δ-halogeno and δ-hydroxy sulfonic acids.[6] The process has been extended to the thermal cyclisation of δ-acyloxysulfonic acids[7] and of 4,4'-oxybis(butane-1-sulfonic acid) (Scheme 1).[8] The sulfonation, dimerization of simple terminal alkenes with dioxane:sulfur trioxide complex, was extensively studied by Bordwell *et al.*, and several examples of 4,6-disubstituted 1,2-oxathiane 2,2-dioxides were described (Scheme 2).[9] Barium 2,4-diphenylbut-3-ene-1-sulfonate, derived from the ring-opening and thermolysis of 4,6-diphenyl-1,2-oxathiane 2,2-dioxide, underwent halosultonisation upon treatment with either bromine or chlorine (Scheme 3).[10] The electrophilic cyclisation of 2-allylphenol to 3-ethyl-6-(2-hydroxyphenyl)-1,2-oxathiane 2,2-dioxide was accomplished in 61% yield upon reaction with butyl sulfurochloridate generated *in situ* from SO_3 and butyl chloride at low temperature in CCl_4.[11] Sulfonation of internal olefins such as 9-octadecene using SO_3 and a falling film reactor afforded low yields of *trans*-3,6-dialkyl δ-sultones.[12] Progress on the synthesis of δ-sultones was reviewed by Gaunersdorfer *et al.*, in 2018.[13]

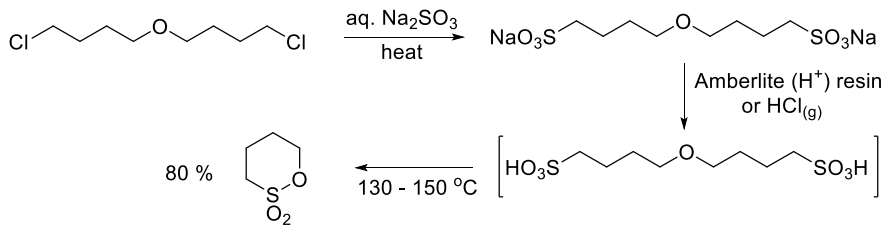

Scheme 1. Thermal cyclisation of 4,4'-oxybis(butane-1-sulfonic acid).

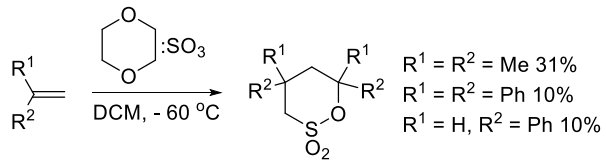

Scheme 2. Sulfonation, dimerization of simple alkenes.

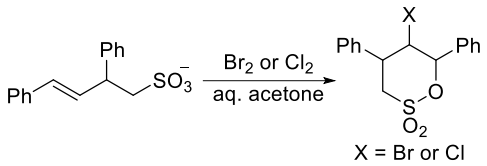

Scheme 3. Halosultonisation reaction.

Fumaronitrile reacts with SO_3 in dichloromethane (DCM) at -40 °C to afford the tetra-SO_3 adduct, (*E*)-6,6'-(ethene-1,2-diyl)bis(1,3,2,4,5-dioxadithiazine 2,2,4,4-tetraoxide), in 87% yield. Subsequent sulfonation of styrene in pyridine at low temperature forms an initial β-sultone which reacts with further styrene upon warming to afford 4,6-diphenyl-1,2-oxathiane 2,2-dioxide (Scheme 4).[14]

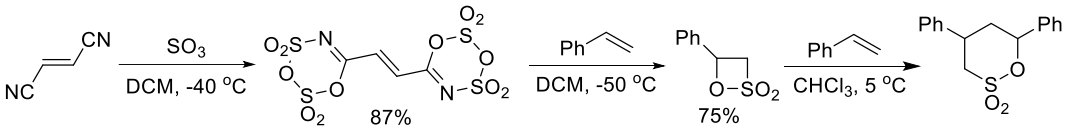

Scheme 4. Sulfonation of styrene with fumaronitrile tetra-SO_3 adduct.

Following from the initial study by Durst and Tin, who described the anion-mediated cyclisation of 1,3-alkanedisulfonate esters in good to excellent yields,[15] this strategy has been employed to obtain 5,5-diethyl-1,2-oxathiane 2,2-dioxide **7** in 72% yield. Reaction of **7** with ^{n}BuLi at low temperature and quenching with either methyl iodide or acetone gave 3-substituted derivatives in good yield (Scheme 5).[16] Intramolecular cyclisation of the sulfur stabilised carbanion from 2,2-dimethyl-3-oxobutyl methanesulfonate afforded 4-hydroxy-4,5,5-trimethyl-1,2-oxathiane 2,2-dioxide in 49% yield; X-ray crystallography was employed to firmly establish the structure.[17]

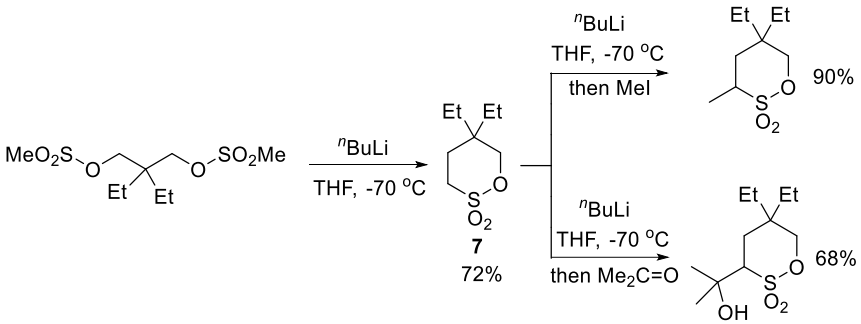

Scheme 5. Anion mediated cyclisation of 1,3-methanedisulfonate esters.

The ytterbium triflate-mediated aldol condensation between trifluoromethyltrimethylsilane and isobutyraldehyde afforded the difluoroaldol precursor **8** in 49% yield. *O*-Mesylation was readily accomplished in 74% with MsCl and Et_3N and subsequent deprotonation of the $MeSO_2$ function with ^{t}BuOK in THF effected the smooth cyclisation to the 1,2-oxathiane 2,2-dioxide **9** (Scheme 6).[18]

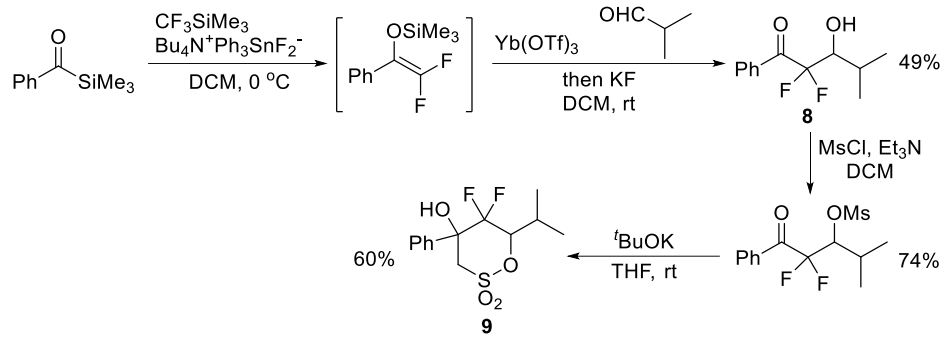

Scheme 6. Formation of difluorinated 1,2-oxathiane 2,2-dioxide.

During an enantioselective synthesis of Oasomycin A, the tetrasubstituted 1,2-oxathiane 2,2-dioxide **10** was isolated as a significant by-product in up to 25% yield from the attempted Kocienski-Julia olefination. The formation of **10** was rationalised by a Brook rearrangement of the Julia intermediate followed by alkoxide attack on the sulfur atom (Scheme 7).[19]

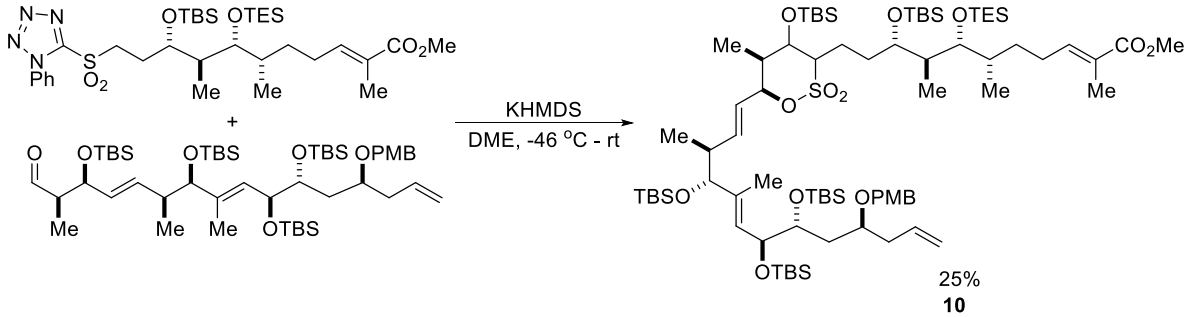

Scheme 7. Serendipitous formation of tetrasubstituted 1,2-oxathiane 2,2-dioxide **10**.

Michael addition of methyl phenylacetate anion to phenyl vinyl sulfonate provided a mixture of the mono- and bis-adducts from which the former was isolated in 48% yield. Reduction of the ester to the primary alcohol was accomplished using DIBAL in 93% yield. Generation of the alkoxide anion with NaH resulted in cyclisation to the 5-phenyl-1,2-oxathiane 2,2-dioxide **11** in 86% yield with elimination of phenoxide. The scope of the reaction was extended to include the 4-bromo- and 4-hydroxy-phenyl analogues (Scheme 8).[20]

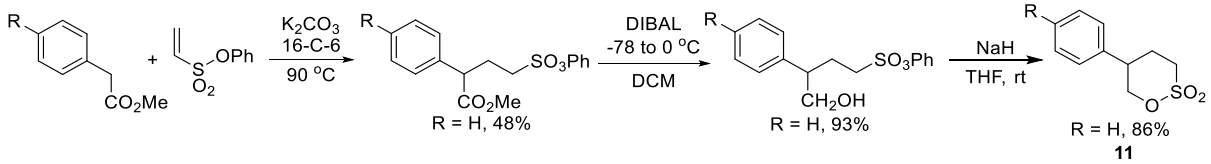

Scheme 8. Alkoxide mediated cyclisation to form a δ-sultone.

Tributyltin hydride-promoted free radical reaction of homopropargyl benzosulfonates resulted in an unexpected rearrangement to afford 3-tributylstannyl-4-aryl substituted 1,2-oxathiane 2,2-dioxides **12** in moderate yields. Crystal structures of **12** revealed a *cis*-orientation of the ring substituents which suggested that the tin hydride reduction of the intermediate radical occurred stereoselectively in a *trans* fashion (Scheme 9).[21]

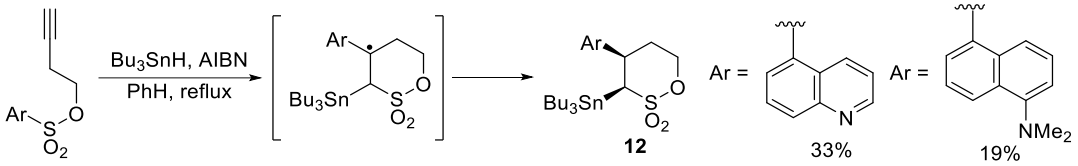

Scheme 9. Free radical reaction of homopropargyl benzosulfonates.

Both primary and tertiary α,ω-alkenols have been cyclised by a photo-redox-catalysed procedure to afford a diverse range of trifluoromethylated δ-sultones in excellent yields. A single-electron transfer process, mediated by the photoexcited copper catalyst, affords the trifluoromethyl radical which adds to the alkenol to generate a second radical that captures SO_2Cl from an intermediate Cu(II) complex and subsequently cyclises to the product (Scheme 10).[22]

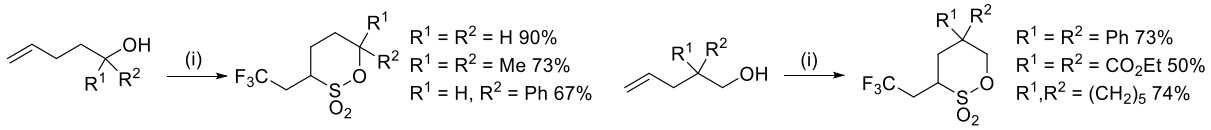

Reagents and conditions: (i) alkenol (1.0 eq.), CF_3SO_2Cl (2.0 eq.), K_2HPO_4 (2.0 eq.), $[Cu(dap)_2]Cl$ (1 mol%), MeCN, 530 nm irradiation, *ca*. 17 h. (dap = 2,9-di(*p*-anisyl)-1,10-phenanthroline)

Scheme 10. Photo-redox-catalysed synthesis of trifluoromethyl substituted δ-sultones.

Perhaps the most recently and widely exploited approach to variously substituted 1,2-oxathiane 2,2-dioxides employs the intramolecular C-H insertion reactions of carbenoids derived from α-diazosulfonates (ethyl 2-diazo-2-(alkoxysulfonyl)acetates) **13** which were conveniently obtained from the requisite ethyl 2-(alkoxysulfonyl)acetates *via* established diazo transfer protocols. Novikov *et al*., effected the cyclisation of a series of Rh-carbenoids to afford substituted -sultones in good yields (Scheme 11).[23]

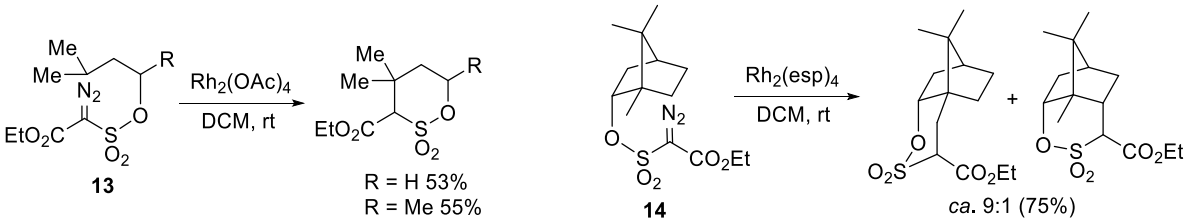

Scheme 11. Rh-carbenoid approach to substituted δ-sultones.

Extension of the foregoing methodology to the ethyl 2-(alkoxysulfonyl)acetate derived from citronellol enabled a quaternary stereocentre to be installed at C-4.[24] Application to the borneol derived diazosulfonate **14** afforded two fused δ-sultones resulting from insertion into the C-H bond of the methyl group and the methylene bridge (Scheme 11).[25]

The foregoing rhodium carbenoid cyclisation methodology was complemented by Du Bois *et al*., who also simplified the protocol by obviating the requirement to isolate the ethyl 2-diazo-2-(alkoxysulfonyl)acetates and instead cyclised the precursor ethyl 2-(alkoxysulfonyl)acetates directly employing iodosobenzene and $Rh_2(OAc)_4$ to generate aryliodonium ylides as surrogate diazo intermediates. Interestingly, in addition to simple di-, tri- and tetra- substituted δ-sultones, strained bicyclic [4.1.0] δ-sultones were constructed by this methodology (Scheme 12).[26]

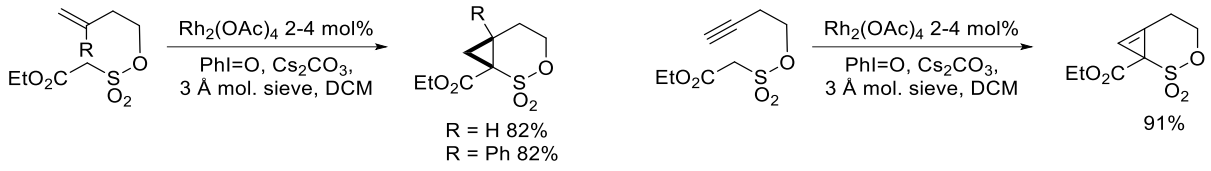

Scheme 12. Synthesis of strained bicyclic δ-sultones by $Rh_2(OAc)_4$-mediated cyclisation of *in situ* generated aryliodonium ylides.

An extensive series of 3,4-disubstituted 1,2-oxathiane 2,2-dioxides has been generated through an iron phthalocyanine-catalysed alkylation of allylic and benzylic C(sp^3)-H bonds. An electrophilic iron carbene is purported to mediate the homolytic C-H bond cleavage and subsequent C3-C4 bond formation (Scheme 13).[27]

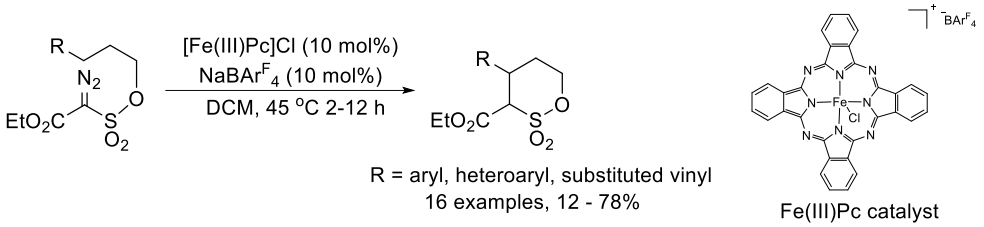

Scheme 13. Iron phthalocyanine-mediated formation of 3,4-disubstituted 1,2-oxathiane 2,2-dioxides.

The oxidation of 4-chloro-4-methyl-1,2-oxathiane 1-oxide, derived from the reaction of 3-methylbut-3-en-1-ol with $SOCl_2$, using H_2O_2 gave 4-chloro-4-methyl-1,2-oxathiane 2,2-dioxide; the route constitutes a unique heteroatom oxidation approach to the δ-sultone unit.[28]

2.2. Dihydro-1,2-Oxathiine 2,2-dioxides

2.2.1. 3,4-Dihydro-1,2-oxathiine 2,2-dioxides

Lupton *et al.*, have reported the *N*-heterocyclic carbene (NHC)-catalysed annulation of multiple trimethylsilyl enol ethers **15** with various α,β-unsaturated sulfonyl fluorides **16** to afford the corresponding 3,4-dihydro-1,2-oxathiine 2,2-dioxides **17** in moderate to very good yields (40-88%) (Scheme 14).[29]

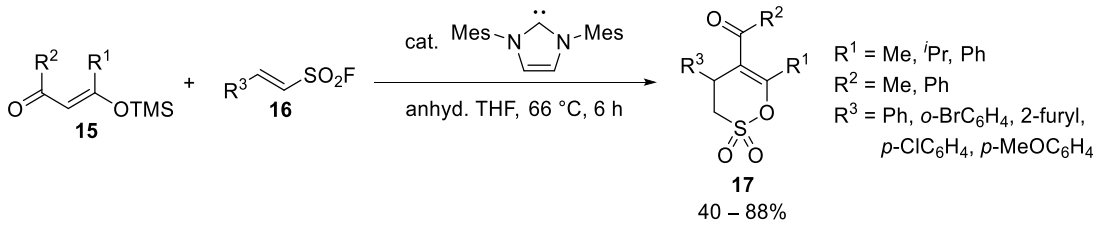

Scheme 14. NHC-catalysed annulation of trimethylsilyl enol ethers with various α,β-unsaturated sulfonylfluorides to afford 3,4-dihydro-1,2-oxathiine 2,2-dioxides.

The authors propose that the reaction progresses by the addition of the NHC to the α,β-unsaturated sulfonyl fluoride with simultaneous loss of the fluoride and desilylation of the trimethylsilyl enol ether generating a sulfonyl azolium and a desilylated enolate, respectively. The latter then undergoes a conjugate addition to the sulfonyl azolium generating a sulfonyl azolium enolate that, after proton transfer and loss of the NHC, formed the δ-sultone. The reaction conditions were sensitive to the electronic nature of the substrates as electron-deficient sulfonyl

fluorides generated the corresponding 3,4-dihydro-1,2-oxathiine 2,2-dioxides in higher yields than the electron-rich analogues.

Qin *et al.*, have reported the DBU-catalysed annulation of (*E*)-2-(4-nitrophenyl)ethene-1-sulfonyl fluoride with 1,3-diketones to afford the condensed monocyclic 3,4-dihydro-1,2-oxathiine 2,2-dioxides **18** (Scheme 15) as part of a screening project for treatments for Alzheimer's disease.[30] The reactions were performed under mild conditions of DBU catalysis and $NaHCO_3$ in DCM at rt. The authors postulate that the reaction progressed by the conjugate addition of the enolizable 1,3-diketone to the α,β-unsaturated sulfonyl fluoride promoted by $NaHCO_3$, followed by fluoride activation by DBU and subsequent cyclisation to afford the δ-sultone.

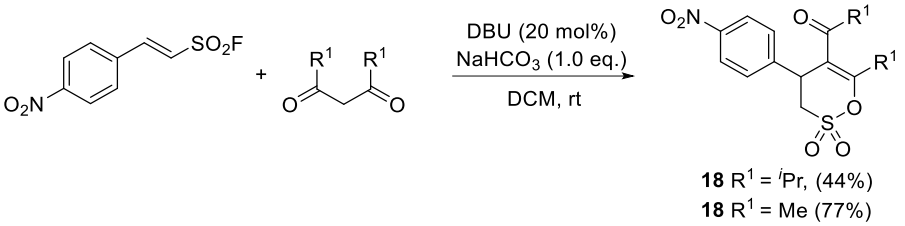

Scheme 15. DBU-catalysed annulation of a styrylsulfonyl fluoride with 1,3-diketones to afford 3,4-dihydro-1,2-oxathiine 2,2-dioxides.

The same group has reported the DBU-catalysed annulation between (*E*)-2-([1,1'-biphenyl]-4-yl)ethenesulfonyl fluoride and the enolizable ketones affording the 3,4-dihydro-1,2-oxathiine 2,2-dioxides **19** in good yields (Scheme 16).[31] Once again a catalytic amount of DBU was employed, but with a weaker base (K_2HPO_4) at a higher temperature (50 °C) in DMF. Qin *et al.*, have also prepared an extensive series of 4-(hetero)aryl-6-heteroaryl-3,4-dihydro-1,2-oxathiine 2,2-dioxides **20** from the treatment of (*E*)-(hetero)arylethenesulfonyl fluorides with a range of acyl aza-heterocycles (Scheme 17).[32] In a similar way, a $Ni(acac)_2$-catalysed annulation of 2-(*Z*)-phenylethenesulfonyl fluoride with 2-acetyl pyridine afforded 4-phenyl-6-(pyridin-2-yl)-3,4-dihydro-1,2-oxathiine 2,2-dioxide in 69% yield. (Scheme 17).[33]

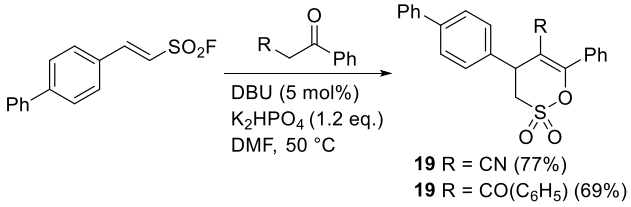

Scheme 16. DBU-catalysed annulation of a styrylsulfonyl fluoride with enolizable ketones to afford 3,4-dihydro-1,2-oxathiine 2,2-dioxides.

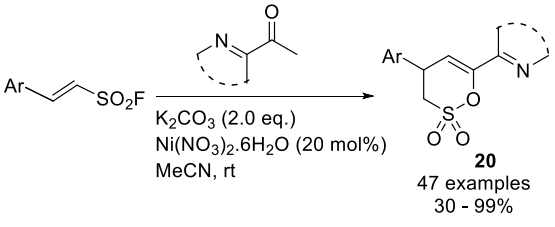

Scheme 17. Ni-mediated synthesis of 3,4-dihydro-1,2-oxathiine 2,2-dioxides from styrylsulfonyl fluorides and acyl substituted heterocycles.

Building upon early work concerning the addition of sulfenes to enaminoketones[34-36] Schenone *et al.*, have reported the synthesis of 3,4-dihydro-1,2-oxathiine 2,2-dioxides **21** by the cycloaddition of sulfene, generated *in situ* from the action of Et_3N upon methanesulfonyl chloride, to a series of enaminoketones, derived from acetophenone, in fair to good yield (45-77%) (Scheme 18).[37] The foregoing sulfene methodology was exploited by Schenone and co-workers to afford an extensive series of condensed ring systems incorporating the 3,4-dihydro-1,2-oxathiine 2,2-dioxide moiety.[38-46] Mahajan *et al*., have prepared 6-styryl substituted 3,4-dihydro-1,2-oxathiine 2,2-dioxides **22** in excellent yield (85-91%) by reaction between enaminoketones, derived from

(*E*)-4-arylbut-3-en-2-ones, and methanesulfonyl chloride in the presence of Et_3N in DCM (Scheme 19).[47]

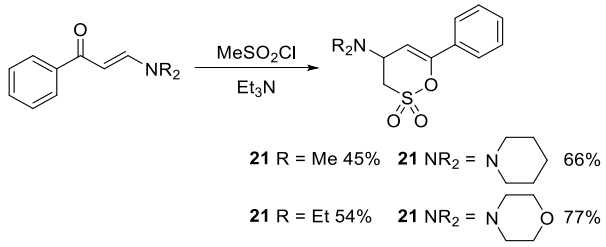

Scheme 18. Synthesis of 3,4-dihydro-1,2-oxathiines from the addition of sulfenes to aryl enaminoketones.

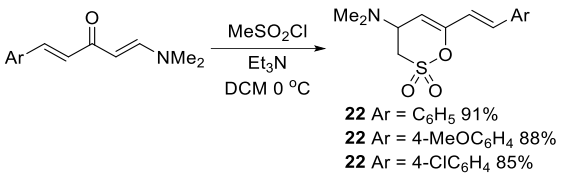

Scheme 19. Synthesis of 3,4-dihydro-1,2-oxathiines from the addition of sulfenes to styryl enaminoketones

The addition of sulfenes, generated by the action of base on a series of alkanesulfonyl chlorides, to enaminoketones has been revisited in two studies by Zonidis *et al.*, with the reported synthesis of a series of 3-thienyl substituted 3,4-dihydro-1,2-oxathiine 2,2-dioxides **23** which exhibited P-type photochromism (Scheme 20).[48] By employing an identical sulfene addition protocol diverse examples of poly-substituted 3,4-dihydro-1,2-oxathiine 2,2-dioxides **24** with different substituents at C-3, C-5 and C-6 were obtained in generally good yields (Table 1). The authors noted that the reaction progressed stereoselectively as the major products adopted a half-chair like conformation with a *trans*-diaxial arrangement of R^3 and NMe_2 as established by X-ray crystallography.[49]

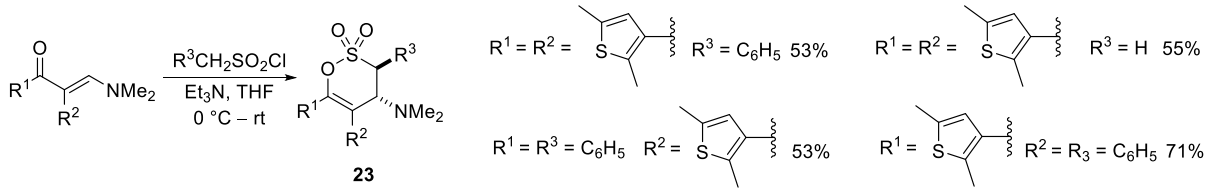

Scheme 20. Application of the sulfene route to the synthesis of photochromic 3,4-dihydro-1,2-oxathiine 2,2-dioxides.

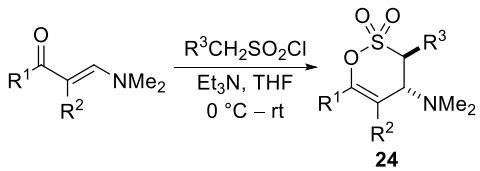

R^1	**R^2**	**R^3**	**Yield (%)**
C_6H_5	C_6H_5	C_6H_5	92
C_6H_5	C_6H_5	4-$CF_3C_6H_5$	60
4-$MeOC_6H_4$	4-$MeOC_6H_4$	C_6H_5	68
Bn	C_6H_5	C_6H_5	48 (*trans*), 25 (*cis*)
C_6H_5	Bz	C_6H_5	96
C_6H_5	H	C_6H_5	52
4-$MeOC_6H_4$	H	C_6H_5	83

4-$CF_3C_6H_4$	H	C_6H_5	64
4-C_5H_5N	H	C_6H_5	10
2-$NO_2C_6H_4$	H	C_6H_5	75
C_6H_5	C_6H_5	H	53
4-$MeOC_6H_4$	H	H	40
Me	2-FC_6H_5	C_6H_5	79

Table 1. Structural diversity of 3,4-dihydro-1,2-oxathiine 2,2-dioxides obtained from the addition of sulfenes to enaminoketones.

Lei *et al.*, describe an alternative synthesis of a styryl substituted 3,4-dihydro-1,2-oxathiine 2,2-dioxide **25** in 36% yield by sulfonation-mediated ring-closure of cinnamic acid derived ketoester using acetic anhydride and concentrated sulfuric acid (Scheme 21).[50]

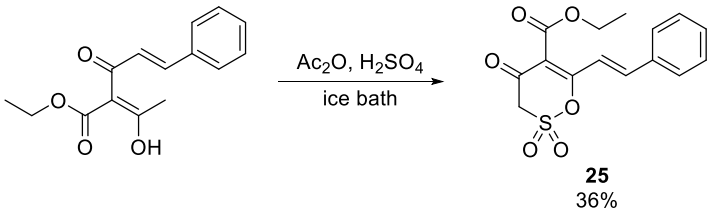

Scheme 21. Sulfonation-mediated ring closure of an enolisable ketoester.

2.2.2. 3,6-Dihydro-1,2-oxathiine 2,2-dioxides

The use of dienes features prominently in the synthesis of 3,6-dihydro-1,2-oxathiine 2,2-dioxides. Bordwell *et al.*, in 1958, examined the sulfonation (dioxane-SO_3 in 1,2-DCE) of 2,3-dimethyl-1,3-butadiene and obtained a 16% yield of 4,5-dimethyl-3,6-dihydro-1,2-oxathiine 2,2-dioxide.[51] Comparative data for the sulfonation of various 1,3-dienes with either SO_3-dioxane or SO_3-DMF has been summarised.[2] Cerfontain and co-workers studied the sulfonation of a series of 1,3-dienes using dioxane-SO_3 at -30 °C -rt in DCM and obtained the requisite 3,6-dihydro-1,2-oxathiine 2,2-dioxides in low to moderate yields. Of note was the reaction of (2*Z*,4*E*)- and (2*E*,4*E*)-hexa-2,4-dienes which led to the same oxathiine **26** (Scheme 22).[52] Mechanistically the reaction was thought to proceed *via* a fast [2+2]-cycloaddition to the diene to afford an initial β-sultone followed by a rapid ring cleavage-recyclisation process to the δ-sultone. In the same work, sulfonation of substituted allenes afforded oxathiine sulfonic acids **27** (Scheme 23). Further examples of diene sulfonation with SO_3-dioxane have been reported by Semenovskii *et al*.[53]

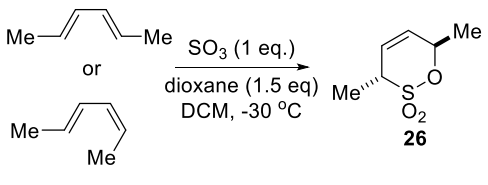

Scheme 22. Sulfonation of 1,3-dienes to afford 3,6-dihydro-1,2-oxathiine 2,2-dioxides.

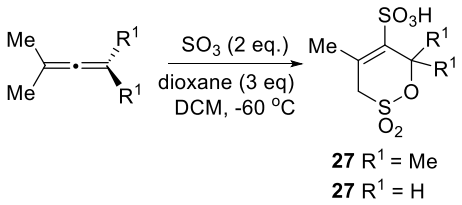

Scheme 23. Sulfonation of allenes to afford 3,6-dihydro-1,2-oxathiine

Kawanisi *et al.*, have reported the synthesis of 3,6-dihydro-1,2-oxathiine 2,2-dioxide in 48% yield by reaction of isoprene with SO_3-DMF complex.[54] The reaction of hexafluorobutadiene with SO_3 in a sealed ampule at 80 °C for 20 h gave a complex mixture of adducts which contained

between 15-25 mol% of 3,3,4,5,6,6-hexafluoro-3,6-dihydro-1,2-oxathiine 2,2-dioxide which was characterized by ^{19}F NMR spectroscopy.[55]

Treatment of the tetrasubstituted cyclopropane **28** with dimethylchloronium ion in liquid SO_2 at -78 °C affords the iminium ion **29**, which when warmed to 35 °C in fluorosulfonic acid undergoes ring-opening, sulfonation and cyclisation to the 3,6-dihydro-1,2-oxathiine 2,2-dioxide **30** (Scheme 24).[56]

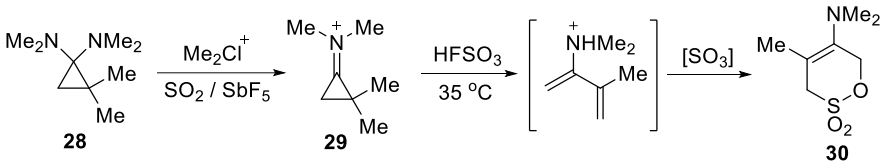

Scheme 24. Ring-opening of a *N*-cyclopropylidene-*N*-methylmethanaminium to afford a 3,6-dihydro-1,2-oxathiine 2,2-dioxide upon sulfonation.

Ring-closing metathesis of vinyl sulfonates, constructed by the base-mediated esterification of allylsulfonyl chloride with vinyl alcohols, was accomplished employing Grubbs' ruthenium catalysts and has proved to be an efficient and convenient strategy to access 3,6-dihydro-1,2-oxathiine 2,2-dioxides.[57, 58] Metz *et al.*, demonstrated the concept with the synthesis of δ-sultone **31** in good yield using Grubbs' generation I and II catalysts (Scheme 25).[59]

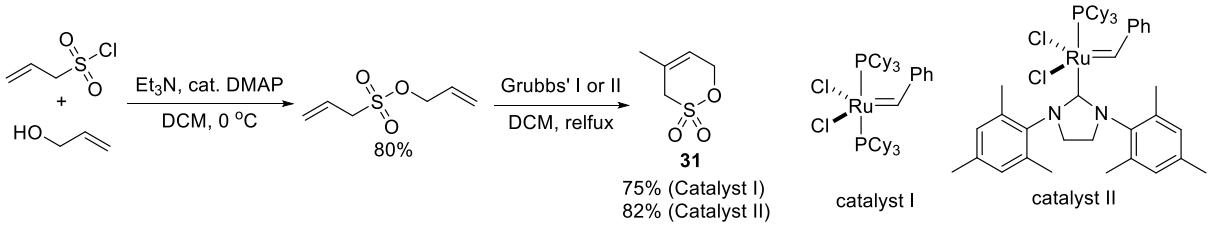

Scheme 25. Tethered diene metathesis route to a 3,6-dihydro-1,2-oxathiine 2,2-dioxide.

Later, Cossy *et al.*, expanded this strategy and prepared multiple 3,6-dihydro-1,2-oxathiine 2,2-dioxides **33** in good to quantitative yields (65-100%) from the olefin metathesis of sulfonates **32**, derived from the condensation reaction between the vinyl sulfonyl chlorides and primary alkenols (Scheme 26). In this same work, the metathesis protocol was extended to encompass the synthesis of the 3,6-dihydro-1,2-oxathiine 2,2-dioxides **34** from the ring-closing metathesis of but-2-yn-1-yl prop-2-ene-1-sulfonates (Scheme 26).[60]

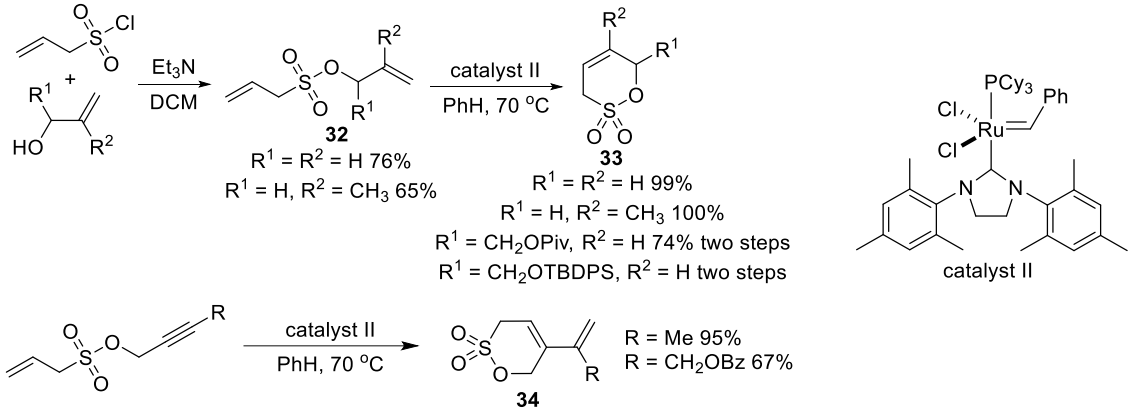

Scheme 26. Ring-closing metathesis approach to 3,6-dihydro-1,2-oxathiine 2,2-dioxides.

2.2.3. 5,6-Dihydro-1,2-oxathiine 2,2-dioxides

Ring-closing metathesis utilizing Grubbs' catalyst II has also been employed to access the unsubstituted 5,6-dihydro-1,2-oxathiine 2,2-dioxide ring by cyclisation of sulfonate **35** which was derived by the esterification of ethenesulfonyl chloride with but-3-en-1-ol (Scheme 27).[59] Two 6-substituted 5,6-dihydro-1,2-oxathiine 2,2-dioxides **36** have been obtained by a similar protocol albeit in lower yield (Scheme 28).[60]

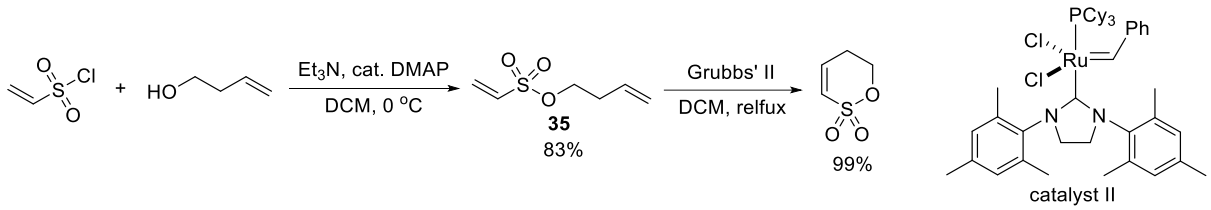

Scheme 27. Synthesis of 5,6-dihydro-1,2-oxathiine 2,2-dioxide by an RCM reaction.

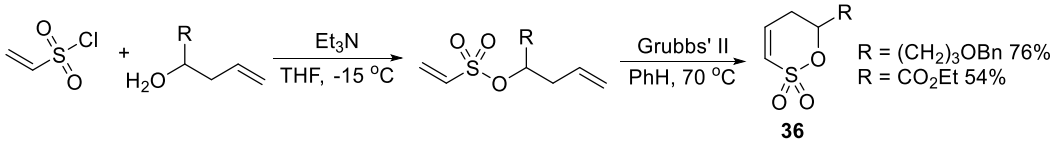

Scheme 28. Extension of the RCM approach to substituted 5,6-dihydro-1,2-oxathiine 2,2-dioxides.

A ring-closing metathesis reaction has been used to simultaneously construct both pyran-2-one and 5,6-dihydro-1,2-oxathiine 2,2-dioxide rings **37** in high yield. The oxathiine ring served as a homoallyic alcohol protecting group through the Cu-promoted 1,4-addition of $PhMe_2SiCl$ which was subsequently removed by fluoride ion with concomitant cleavage of the oxathiine ring regenerating the homoallylic alcohol. The protection strategy formed a key step in the synthesis of fragments of the unnatural enantiomers of the polyene polyol antibiotics Filipin III and Pentamycin (Scheme 29).[61]

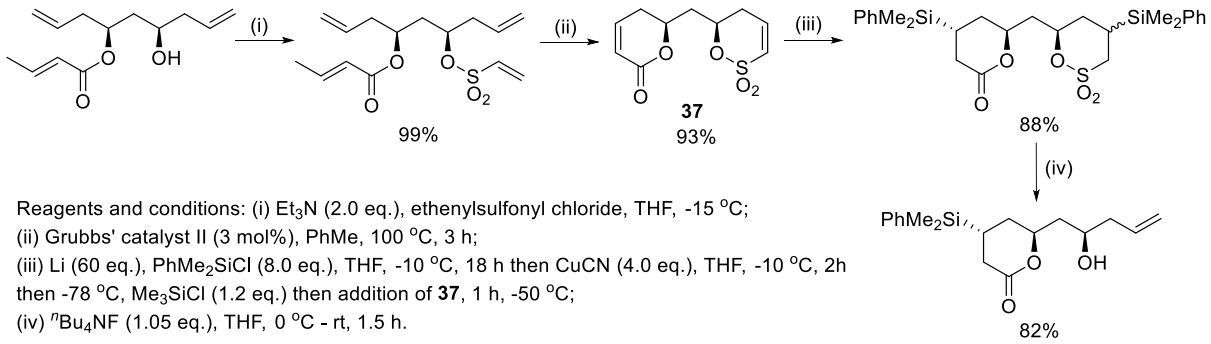

Scheme 29. Simultaneous RCM to construct a pyran-2-one ring and a 5,6-dihydro-1,2-oxathiine 2,2-dioxide ring.

A series of novel 4-aryl-5,6-dihydro-1,2-oxathiine 2,2-dioxides were obtained by Motherwell *et al.*, from the addition of a tri-^{n}butylstannyl radical to arenesulfonate esters of the homopropargyl alcohol **38**. The reaction proceeds *via ipso*-substitution and a subsequent 6-*endo* addition-elimination protocol (Scheme 30).[62] Further examples from this route were reported by Zhang *et al.*, who also isolated 3-tributylstannyl substituted δ-sultones.[21]

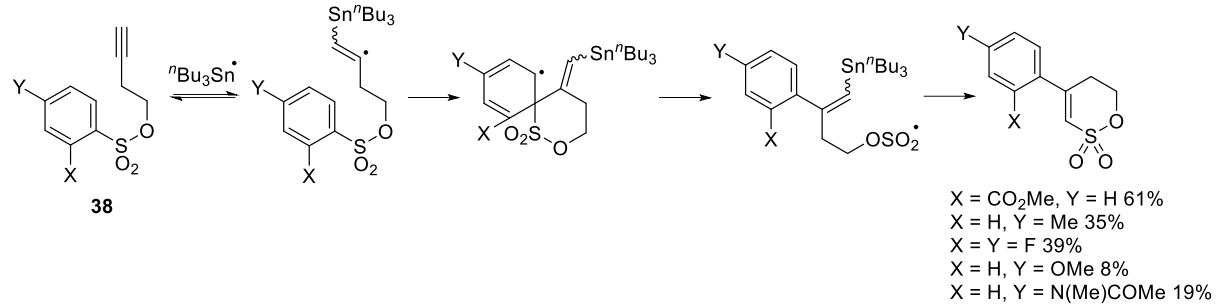

Scheme 30. Radical-mediated cyclisation route to 5,6-dihydro-1,2-oxathiine 2,2-dioxides.

The bromination of 4-methyl-3,6-dihydro-1,2-oxathiine 2,2-dioxide with molecular bromine in chloroform generated the expected dibromo adduct **39** in 91% yield. Base-promoted dehydrohalogenation afforded the 5-bromo-4-methyl-5,6-dihydro-1,2-oxathiine 2,2-dioxide in excellent yield (95%) (Scheme 31).[54] The bicyclic δ-sultone **40** was transformed into the diacetate **41** upon ozonolysis and trapping of the intermediate with a large excess of Et_3N in acetic anhydride (Scheme 32).[63]

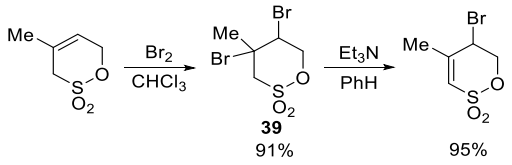

Scheme 31. Double bond migration to afford a 5,6-dihydro-1,2-oxathiine 2,2-dioxide.

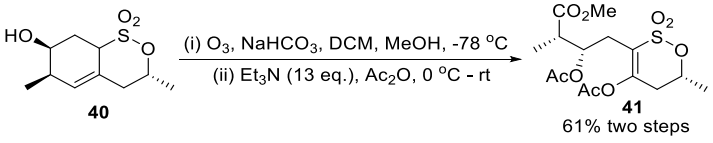

Scheme 32. Ozonolysis induced ring cleavage to afford monocyclic dihydro oxathiine **41**.

The oxidation of 3,4-di-*t*butylthiophene 1,1-dioxide with H_2O_2 in TFA induced a ring expansion to afford the penta-substituted 5,6-dihydro-1,2-oxathiine 2,2-dioxide **43** in low yield (18%). The initial step of the transformation is thought to involve epoxidation of the 2,3-bond and acid-catalysed ring-opening to afford the carbocation **42**. Methyl group migration and capture of the new tertiary carbocationic centre affords the six-membered ring and *S*-oxidation completes the sequence (Scheme 33).[64]

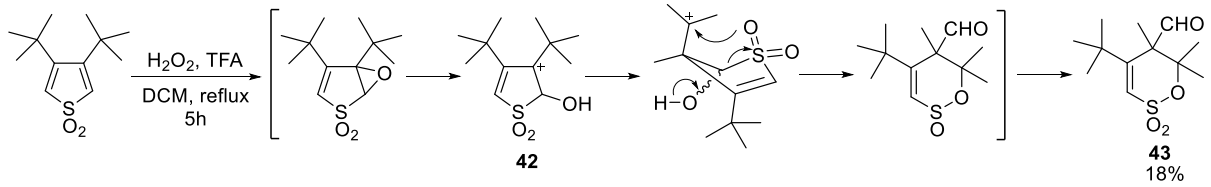

Scheme 33. Oxidative ring-expansion of a thiophene 1,1-dioxide to generate a 5,6-dihydro-1,2-oxathiine 2,2-dioxide.

2.3. 1,2-Oxathiine 2,2-dioxides

Structural studies of the 1,2-oxathiine 2,2-dioxide ring are rare and are typically confined to articles concerning synthesis and reactivity studies. However, Barnett *et al.*, reported the X-ray crystal structure of 6-(4-bromophenyl)-1,2-oxathiine 2,2-dioxide and concluded that the ring was a non-aromatic 6π-electron system. Whilst the O1-C6=C5-C4=C3 unit is essentially planar the sulfur function escapes this plane by 0.58 Å. Furthermore, there is bond alternation with C4-C5 exhibiting appreciable single bond character (1.443 Å) with the C5-C6 (1.320 Å) and C3-C4 (1.341 Å) showing only minor deviation from the typical C=C bondlength.[65] The bond alternation and deviation from planarity was also noted for the crystal structure of 3,5,6-triaryl-1,2-oxathiine 2,2-dioxide which was obtained in a recent study by Zonidis *et al.*, concerning the synthesis of an

extensive series of 3,5,6-triaryl-, 3,6-diaryl-, 3,5-diaryl- and 5,6-diaryl- 1,2-oxathiine 2,2-dioxides.[48,49] In the latter study, a facile Cope elimination of the 4-dimethylamino unit from the 3,4-dihydro-1,2-oxathiine 2,2-dioxide precursor was essential to introduce the 3,4-double bond into **44** as a consequence of the *anti-peri*-planar orientation of the dimethylamino group and the C-3 substituent (Scheme 34). Additional evidence from this study which is suggestive of the bond alternation of the diene unit of **44** was garnered from coupling constants $J_{3,4}$=10.2 Hz and $J_{4,5}$=7.1 Hz for the 5,6-diphenyl- **45** and 3,6-diphenyl **46** substituted 1,2-oxathiine 2,2-dioxides.

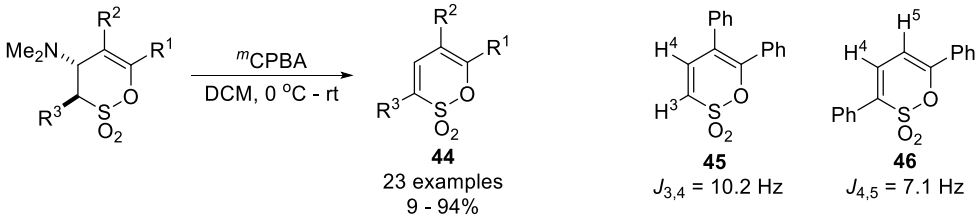

Scheme 34. Facile Cope elimination route to afford oxathiine 2,2-dioxides.

The unsaturated 1,2-oxathiine 2,2-dioxide system was first prepared by Morel and Verkade by the sulfonation of α,β- or β,γ- unsaturated ketones with concd. H_2SO_4 in Ac_2O; moderate to good yields were noted for this first small library of 1,2-oxathiine 2,2-dioxide derivatives **47** (Scheme 35).[66] Additional examples of this sulfonation-cyclisation methodology using concd. H_2SO_4 in Ac_2O were reported by Klebert *et al*.[67] In a variation of this protocol, the reaction of mesityl oxide with chlorosulfonic acid in Ac_2O gave 4,6-dimethyl-1,2-oxathiine 2,2-dioxide in 41% yield.[68]

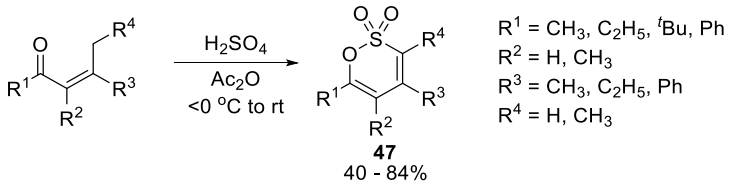

Scheme 35. Sulfonation-mediated ring-closure of γ-methylene ketones.

Further variations of the foregoing strategy include the use of the active ionic liquids such as methylsulfonylimidazolium triflate hydrochloride [(MSIm)TfO HCl] to effect the efficient condensation and sulfonation-cyclisation of acetophenones to afford 4,6-diaryl-1,2-oxathiine 2,2-dioxides **48** in excellent yield (Scheme 36).[69] Comparable results were obtained using *N*-methyl-2-pyrrolidonium chlorosulfonate, [NMP-$ClSO_3H$] albeit at higher reaction temperatures.[70] Unfortunately, the scope of the foregoing protocol is limited to the introduction of identical aryl groups, derived from the acetophenone, at the 4- and 6-positions of the oxathiine moiety.

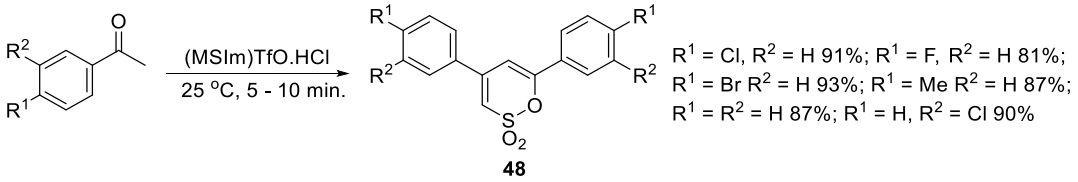

Scheme 36. Condensation and sulfonation-cyclisation of acetophenones to afford 4,6-diaryl-1,2-oxathiine 2,2-dioxides.

Methylsulfonylimidazolium chlorosulfonate hydrochloride [(MSIm)$ClSO_3$ HCl] in conjunction with TFAA effected the smooth conversion of a series of 4-substituted acetophenones into 3-chlorosulfonyl substituted oxathiines **49** (Scheme 37).[71]

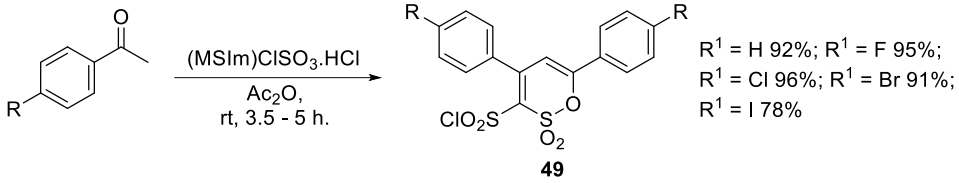

Scheme 37. Condensation and sulfonation-cyclisation of acetophenones to afford 3-chlorosulfonylated 4,6-diaryl-1,2-oxathiine 2,2-dioxides.

The sulfonation of a series of ethynylbenzenes with either SO_3-dioxane or trimethylsilylchlorosulfonate ($TMSOSO_2Cl$) provides a useful, if low yielding, alternative to the sulfonation-cyclisation of acetophenones, to afford **50**. However, this protocol also suffers from the same disadvantage of affording identical 4,6-diaryl substituents in the oxathiine ring (Scheme 38).[72]

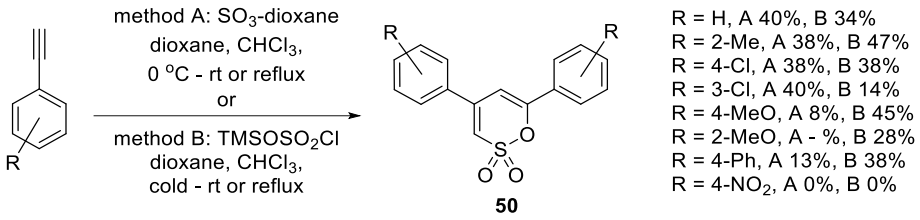

Scheme 38. Tandem sulfonylation-condensation of ethynylbenzenes.

A serendipitous formation of an oxathiine 2,2-dioxide in 8-10% yield was noted by Craig and co-worker during the H_2SO_4-Ac_2O mediated deprotection of the acetonide function on the furanose ring **51** (Scheme 39).[73] Heating a solution of 2-acrylamido-2-methylpropane sulfonic acid **52** in Ac_2O also unexpectedly afforded an oxathiine 2,2-dioxide (Scheme 40).[74]

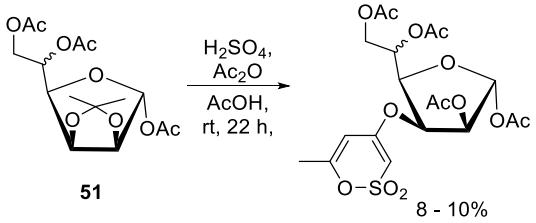

Scheme 39. Serendipitous formation of an oxathiine 2,2-dioxide.

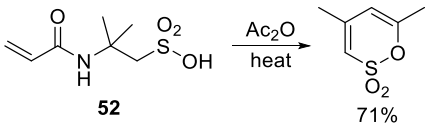

Scheme 40. Ac_2O-mediated cyclisation of **52** to afford an oxathiine 2,2-dioxide.

Phenylsulfene, generated *in situ* from the action of Et_3N on phenylmethanesulfonyl chloride, underwent a hetero Diels-Alder cycloaddition with the benzoyl ketene acetal to afford the 3,4,6-trisubstituted oxathiine 2,2-dioxide **53** directly as a consequence of the facile elimination of ethanol from the initial adduct (Scheme 41).[35]

Kawanisi *et al.*, have demonstrated that a fully unsaturated 1,2-oxathiine derivative can be obtained, albeit in a low yield, *via* an $AgBF_4$-assisted dehydrobromination reaction of the 5,6-dihydro precursor **54** (Scheme 42).[54]

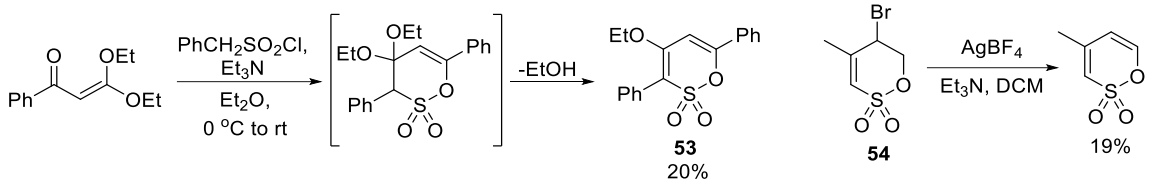

Scheme 41. Sulfene addition to a benzoyl ketene acetal.

Scheme 42. 1,3-Oxathiine 2,2-dioxide by elimination of HBr using $AgBF_4$.

3. Reactivity and applications

In this section, the reactivity of the various 1,2-oxathiine 2,2-dioxide rings is presented wherein a reaction is a transformation that does not lead to another 1,2-oxathiine ring. Where there is an application associated with the target product this has been discussed.

3.1. 1,2-Oxathiane 2,2-dioxides

The chemistry of the 1,2-oxathiane 2,2-dioxide unit is dominated by its propensity to undergo ring-opening upon the addition of nucleophiles to C-6 to afford new entities bearing a sulfobutyl chain (Scheme 43). The foregoing chemistry is particularly attractive as it enables water solubility to be imparted into a wide variety of molecules and polymers under relatively mild conditions.

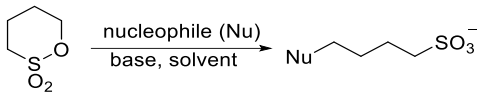

Scheme 43. Generic nucleophilic ring-opening of the 1,2-oxathiane 2,2-dioxide unit.

The reaction of δ-sultone with carbon-based nucleophiles, derived from acidic methylene compounds, has been widely applied to fluorene derivatives *e.g.* **55**[75,76] and 'heterocyclic fluorenes', such as **56**, for the formation of conjugated polymers for modern material applications (Scheme 44).[77-79]

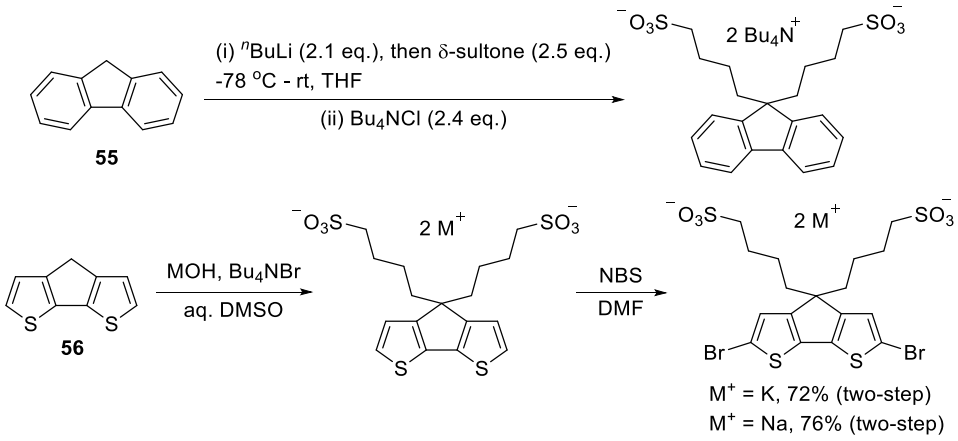

Scheme 44. Sulfobutylation of fluorene derivatives.

The living anionic polymerisation of styrene was terminated through the addition of δ-sultone to afford a poly(styrene) which was end modified with a sulfonic acid residue and which possessed a polydispersity index of 1.03 and a M_n of 1.9×10^4 (Scheme 45).[80]

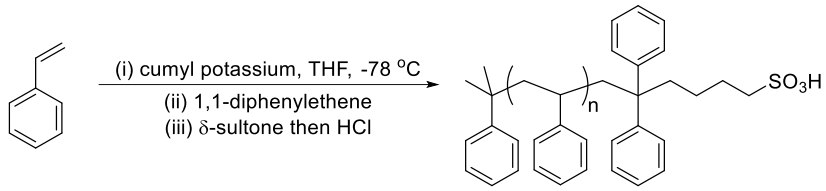

Scheme 45. δ-Sultone termination of a living anionic polymerisation.

The C-2 alkylation of ethyl 2-methyl-3-oxobutanoate has been extensively studied as the derived 5-(ethoxycarbonyl)-5-methyl-6-oxoheptane-1-sulfonic acid is essential for the preparation of water soluble 3*H*-indoles *e.g.* **57**,[81] that are key intermediates for the preparation of water soluble cyanine dyes which are extensively used in biomedical imaging applications (Scheme 46).[82-84]

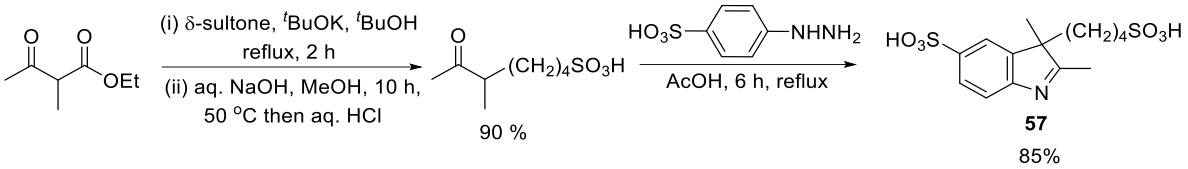

Scheme 46. Preparation of 5-(ethoxycarbonyl)-5-methyl-6-oxoheptane-1-sulfonic acid.

Moving to nitrogen-based nucleophiles, the sp^2 hybridised *N*-atom of a variety of nitrogen containing heterocycles have been sulfoalkylated upon reaction with δ-sultone. Of great significance is the reaction of 3*H*-indoles to afford derivatives such as **58**, which are required for NIR absorbing and emitting cyanine colourants (Scheme 47).[85] Perhaps the best known of these colorants is indocyanine green **59** and together with a significant number of derivatives.[86]

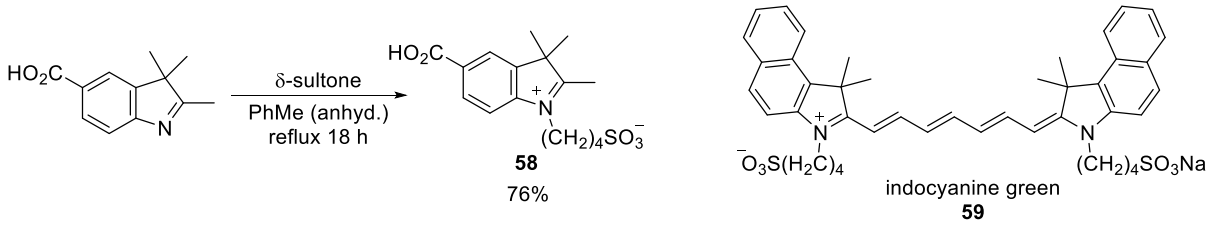

Scheme 47. Synthesis of *N*-sulfoalkylated 3*H*-indole **58**.

Extensive use has been made of δ-sultone to *N*-sulfoalkylate azoles (imidazoles and 1,2,3-triazoles) for the preparation of task specific ionic liquids. Typically, the synthesis involves heating the *N*-alkyl imidazole in either neat δ-sultone or in an inert solvent with δ-sultone often followed by a subsequent acidification step. Examples of representative structures of the azoles are presented in Figure 2.[87-93]

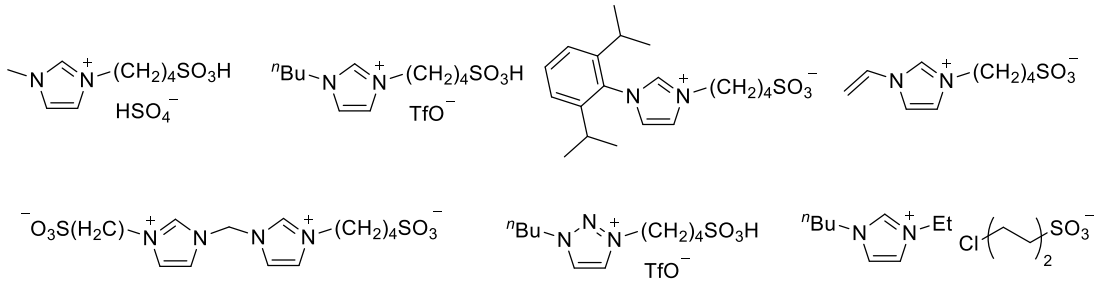

Figure 2. Representative ionic liquids prepared from δ-sultone.

Of note in Figure 2 is the example 1-butyl-3-ethyl-1*H*-imidazol-3-ium 4-chlorobutylsulfonate which was obtained by the nucleophilic ring-opening of δ-sultone by the chloride counter ion of the imidazolium ionic liquid upon stirring at 40 °C.[94]

In a similar manner to azoles, substituted pyridine,[95] bipyridine[96] and quinoline[97], *N*-atoms also effect nucleophilic ring-opening of the δ-sultone unit upon heating either neat or in a solvent to afford water soluble zwitterions (Figure 3).

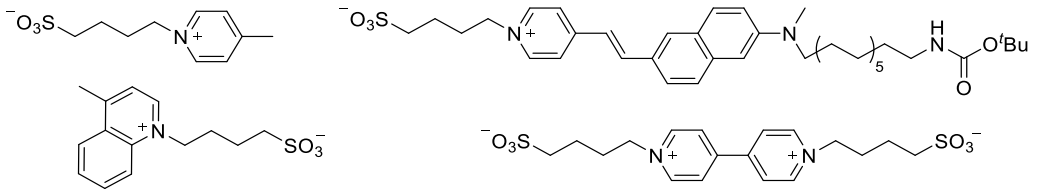

Figure 3. Selected sulfobutylated pyridinium salts.

The water solubility of the organic azo-pigment (C.I. Pigment Yellow 150) for ink-jet applications has been improved by reaction of the amide like *N*-atoms of the pyrimidinone rings with δ-sultone (Scheme 48).[98] 5-Methyl-2-phenyl-1,2-dihydro-3*H*-pyrazol-3-one afforded the sulfobutyl derivative **60** upon reaction with δ-sultone.[99]

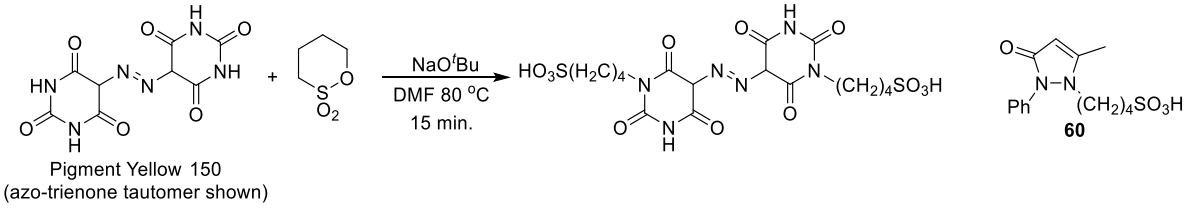

Scheme 48. Modification of C.I. Pigment Yellow 150 with δ-sultone.

The nucleophilicity of terminal trialkylamine functions in a wide range of polymers, co-polymers and dendrimer-like hyperbranched polymers has been exploited in order to ring-open δ-sultone in a post polymerisation modification to impart either water solubility, surfactant or gelation properties into the resulting zwitterionic materials (Scheme 49).[100-103]

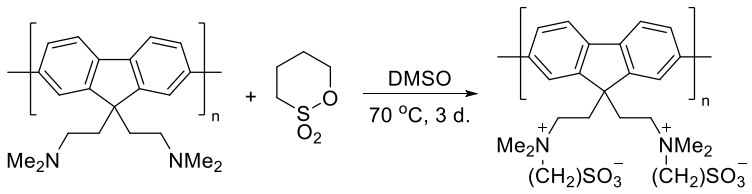

Scheme 49. Preparation of a zwitterionic, conjugated polymeric fluorescent hydrogel.[100]

In a similar manner to the modification of polymers containing pendant trialkylamine functions, polymers comprising of phenolic units [substituted poly(aryl ether sulfones)[104] and poly(aryl ether ketones)[105]] or aliphatic hydroxyl functions *e.g.* poly(cyclodextrins)[106] have been successfully modified upon reaction with δ-sultone in the presence of a base.

Nanospheres have been obtained from sulfobutylated poly(vinyl alcohol)-graft-poly(lactide-co-glycolide)s[107] and proton-conducting composite membranes incorporating surface-modified sulfobutylated montmorillonite have been described.[108] Hyperbranched poly(glycerol) functionalised graphene oxide has been prepared *via* an acid-catalysed sulfobutylation process (Scheme 50) and employed as a catalyst for the synthesis of a variety of condensed heterocycles.[109]

In addition to the ionic liquid-mediated chloride induced ring-opening of δ-sultone[94], the nucleophilic ring-opening of 3-benzyl-1,2-oxathiane 2,2-dioxides with [^{18}F]fluoride afforded the [^{18}F]-labelled fluorosolfonates **61**, in good radiochemical yields, which were developed for PET imaging (Scheme 51).[110] The direct fluorination of δ-sultone itself has been accomplished with elemental fluorine at low temperature and affords a mixture of the perfluoro-δ-sultone and the ring-opened perfluorobutane sulfonyl fluoride (Scheme 51).[111]

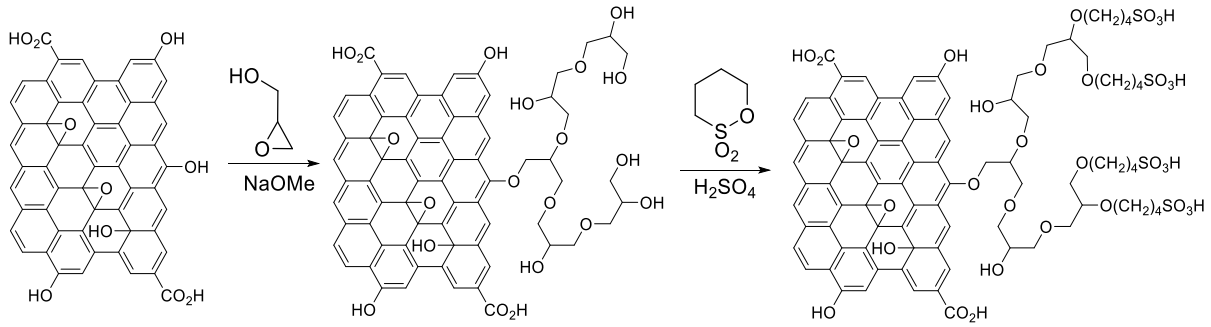

Scheme 50. Modification of functionalised graphene oxide with δ-sultone.

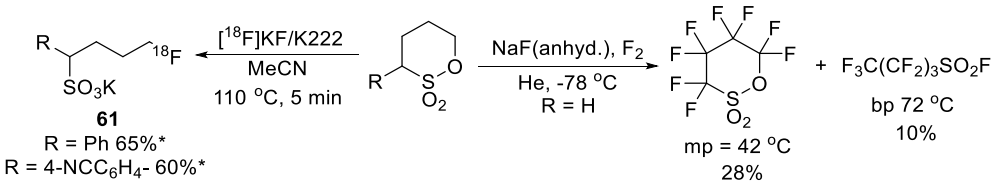

Scheme 51. Fluorination reactions of 1,2-oxathiane 2,2-dioxides.

Cyanide ion-induced ring-opening of the trisubstituted 1,2-oxathiane 2,2-dioxide **62** with subsequent Zn(Cu) couple removal of the sulfonyl chloride gave the δ-cyano ester in 55% over three-steps. In the same study, treatment of the enolate derived from **63** with Davis' oxaziridine in THF gave the lactol in 85% yield (Scheme 52).[26]

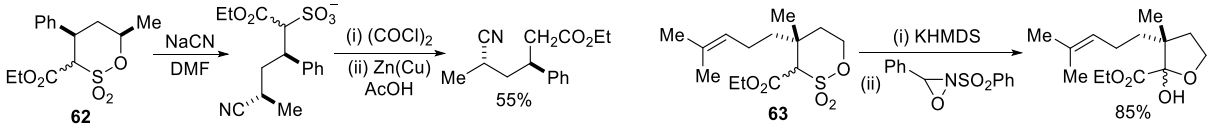

Scheme 52. Versatility of substituted 1,2-oxathiane 2,2-dioxides in synthesis.

The oxathiane **63** proved to be a useful starting material for the synthesis of Bakuchiol. Reduction and elimination provided the exomethylene derivative **64** which was desulfonated using ^{n}Bu$_3$SnLi to afford the dienol intermediate *en-route* to Bakuchiol (Scheme 53).[112]

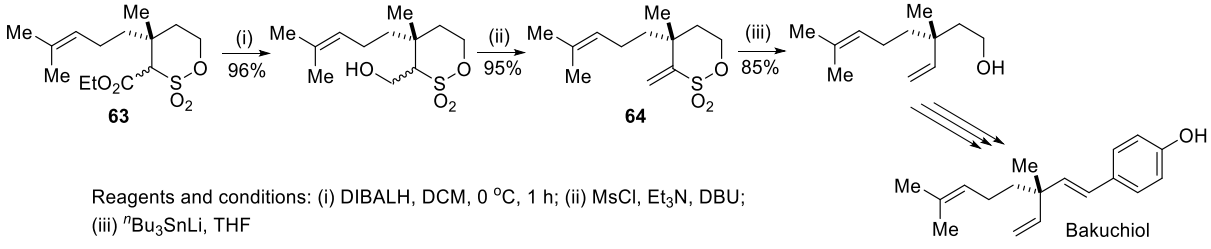

Scheme 53. Synthesis of Bakuchiol.

The acidity of the 3-proton in 4,4-dimethyl-3-ethoxycarbonyl-1,2-oxathiane 2,2-dioxide has also been employed to introduce a 3-allyl substituent in 85% yield by classical anion chemistry. Additionally, in this work, a short series of δ-lactones **65** were obtained from substituted 3-ethoxycarbonyl-1,2-oxathiane 2,2-dioxides upon treatment with SmI_2 in the presence of DMPU (Scheme 54).[113] A related series of γ-lactones **66** were constructed in good to excellent yields by treatment of the anion derived from substituted 3-ethoxycarbonyl-1,2-oxathiane 2,2-dioxides with ^{t}BuOOH (Scheme 54). The route provided straightforward access to a key lactone intermediate **67** for the preparation of (-)-eburnamonin.[114]

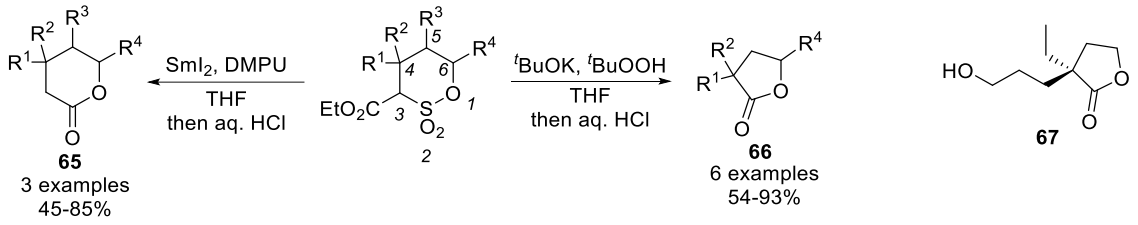

Scheme 54. Conversion of 3-ethoxycarbonyl-1,2-oxathiane 2,2-dioxides into lactones.

Reduction of substituted 1,2-oxathiane 2,2-dioxides with $LiAlH_4$ in either refluxing Et_2O or refluxing 1,4-dioxane effected ring cleavage to afford moderate to low yields of 4-mercaptobutanols often together with 1,4-dihydroxybutanes.[16] Treatment of 4,6-dimethyl-1,2-oxathiine 2,2-dioxide with $NaBH_4$ in aq. NaOH and subsequent hydrogenation over PtO_2 with acidification and recyclisation upon heating under vacuum gave the 4,6-dimethyl-1,2-oxathiane 2,2-dioxide.[115]

In addition to the foregoing reactions and applications of 1,2-oxathiane 2,2-dioxides, a significant number of patents have claimed variously substituted δ-sultones as non-aqueous solvents, electrolytes and additives in Li-ion batteries.[116-123]

3.2. Dihydro-1,2-oxathiine 2,2-dioxides

In comparison to the 1,2-oxathiane 2,2-dioxides (δ-sultones) there is relatively little published on the reactivity of the three isomeric dihydro-1,2-oxathiine 2,2-dioxides.

Qin *et al.*, have shown that by employing a stoichiometric amount of DBU, decomposition of 3,4-dihydro-1,2-oxathiine 2,2-dioxide takes place, *via* loss of SO_2, generating the β-hydroxyketone **68** in 42% yield (Scheme 55).[30] The hydrolysis of the sulfonic acid with aq. KOH solution affords the dipotassium 4-methyl-2-(sulfomethyl)-1,3-pentadiene-3-sulfonate **69** in quantitative fashion (Scheme 56).[52]

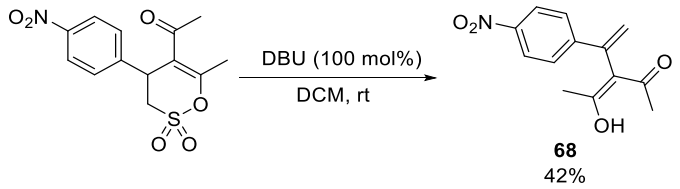

Scheme 55. Base-mediated ring-opening of an acyl-3,4-dihydro 1,2-oxathiine 2,2-dioxide.

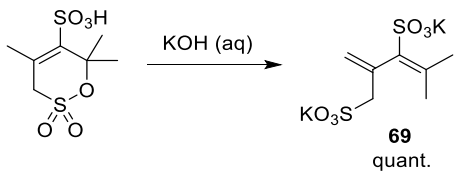

Scheme 56. Preparation of the disulfonic acid **69**.

Semenovsky *et al.*, have also explored the base-mediated ring-opening of 3,6-dihydro-1,2-oxathiine 2,2-dioxides; the (*Z*)-4-hydroxy-2-methylbut-2-ene-1-sulfonate potassium salt **70** was isolated in 80% yield upon treatment of the requisite δ-sultone with a 0.1 N aq. KOH solution (Scheme 57).[124]

The electron deficient double bond of the 5,6-dihydro-1,2-oxathiine 2,2-dioxide unit has been utilised as a dienophile in Diels-Alder cycloadditions. Metz *et al.*, have shown that cyclohexa-1,3-diene undergoes a [4+2]-cycloaddition to **71** (n=1) in good yield using 2,6-di-^{t}butyl-4-methylphenol (BHT) as a catalyst, albeit under forced conditions (Scheme 58).[57] Interestingly, the reaction was found to selectively afford the *endo* product, which may indicate strong secondary orbital interactions between the diene and the 1,2-oxathiine system. Considering the increased reaction time as compared with the corresponding 5-membered sultone **71** (n=0) (6 d versus 27 h), it can be suggested that the conformation and bond angles of the 5,6-dihydro-1,2-oxathiine 2,2-dioxide ring have a detrimental effect on the rate of the reaction (Scheme 58).

The 4-hydroxy-5,5-dimethyl derivative **72** has been employed in a three-component one-pot reaction to afford podophyllotoxin-based heterolignans, which are examples of condensed [1,2]oxathiino[4,3-*b*]quinoline 1,1-dioxides, **73** (Scheme 59).[125] The tetracycles **73** exhibited mild insecticidal activity against mustard beetle pest (*Phaedon cochleariae*) during a broad SAR study of potential insecticidal agents through inhibition of tubulin polymerization.

Several simple alkyl substituted 5,6-dihydro-1,2-oxathiine 2,2-dioxides[126-128] have been incorporated in electrolytes in lithium batteries as have (poly)fluorinated derivatives[129] and substituted 5,6-dihydro-1,2-oxathiin-6-one 1,1-dioxides.[130,131] 3,6-Dihydro-1,2-oxathiine 2,2-dioxides have also been employed as additives in the positive electrode film in energy storage devices.[132]

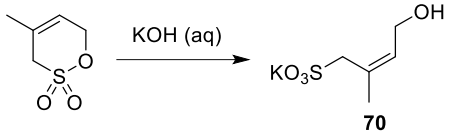

Scheme 57. Hydrolysis of 4-methyl-3,6-dihydro-1,2-oxathiine 2,2-dioxide.

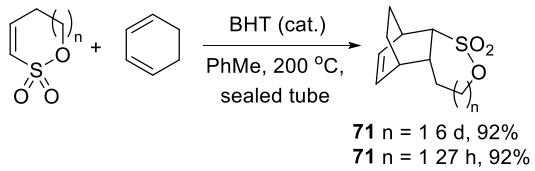

Scheme 58. 5,6-Dihydro-1,2-oxathiine 2,2-dioxide unit as a dienophile.

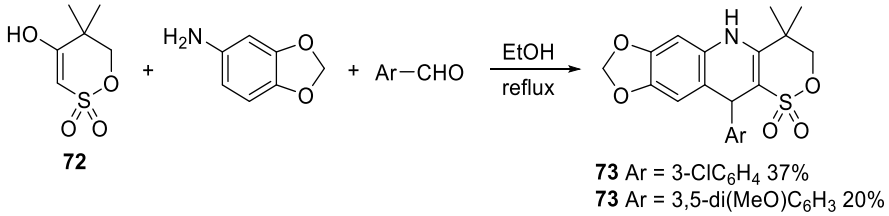

Scheme 59. Assembly of condensed [1,2]oxathiino[4,3-*b*]quinoline 1,1-dioxides *via* a multi-component reaction.

3.3. 1,2-Oxathiine 2,2-dioxides

Among the reactions that have been reported for the unsaturated 1,2-oxathiine 2,2-dioxides, the most exhaustively explored is the substitution of the *O*-atom of the 6-membered ring with a substituted *N*-atom, *via* an ANRORC (Addition of Nucleophile-Ring-Opening-Ring-Closing) reaction to afford a sultam. An extensive range of substituted anilines, benzidines and benzylamine have been employed to afford sultams **74** and the reaction typically requires heating over 100 °C either neat[133-134] or in a solvent *e.g.* anisole at reflux[135] to effect completion in moderate to good yields (Scheme 60). The presence of a 3-bromine atom on the oxathiine ring is tolerated and bromo sultams have been isolated.[136] Interestingly, the use of ^{n}BuOH as the solvent resulted in the formation of δ-aminosulfonic acids **75** with hydrazine, benzamide, urea, thiourea and electron deficient amino-substituted heterocycles (Scheme 61).[137]

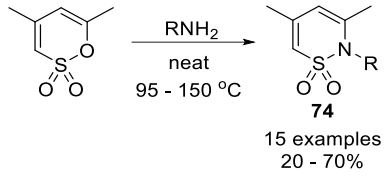

Scheme 60. Transformation of a δ-sultone into a sultam.

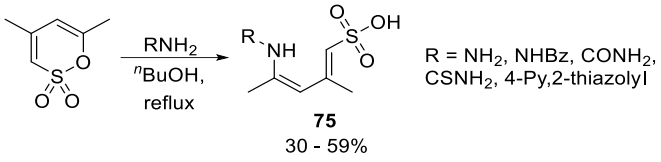

Scheme 61. Nucleophilic ring-opening of 1,2-oxathiine 2,2-dioxides.

Elaborating on the reactivity of 4,6-substituted 1,2-oxathiine 2,2-dioxides with amines and hydrazines (Scheme 60 and 61), Ali, Jäger and Metz presented a range of different addition reactions where reaction with *N*-containing bi-nucleophiles led to new heterocyclic products in moderate yields from 4,6-diphenyl oxathiine **76** (Scheme 62).[138]

The bromination of unsaturated 1,2-oxathiines is also of significant interest, as it provides brominated precursors for further manipulation. Eastman and Gallup first attempted the bromination of the 4,6-dimethyl 1,2-oxathiine 2,2-dioxide using Br_2 in CCl_4 and claimed that the product was the 5-bromo analogue **77**.[68] The latter finding was disputed by Barnett and McCormack, who repeated the reaction and showed that the product was in fact the 3-bromo-4,6-dimethyl-1,2-oxathiine 2,2-dioxide isomer **78** (63%) by both NMR spectroscopy and the unequivocal synthesis of the 5-bromo isomer by cyclisation of 3-bromomesityl oxide (Scheme 63).[139]

Bromination of a series of 4,6-diaryl substituted 1,2-oxathiine 2,2-dioxides was unequivocally established by X-ray crystallography to afford the 3-bromo derivatives **79** in excellent yields. The bromine atom was subsequently replaced in a high yielding Sonogashira reaction with ethynylbenzene to afford **80** (Scheme 64).[72]

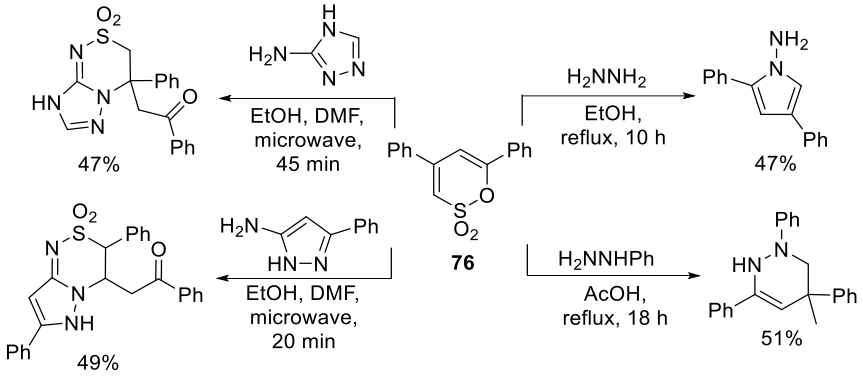

Scheme 62. Transformation of oxathiine **76** into other heterocyclic ring systems.

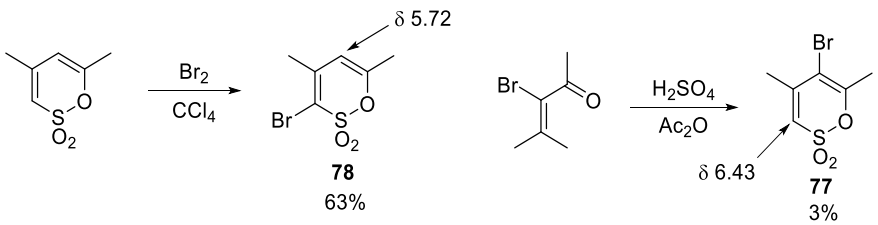

Scheme 63. Synthesis of 3- and 5- bromo-1,2-oxathiine 2,2-dioxides.

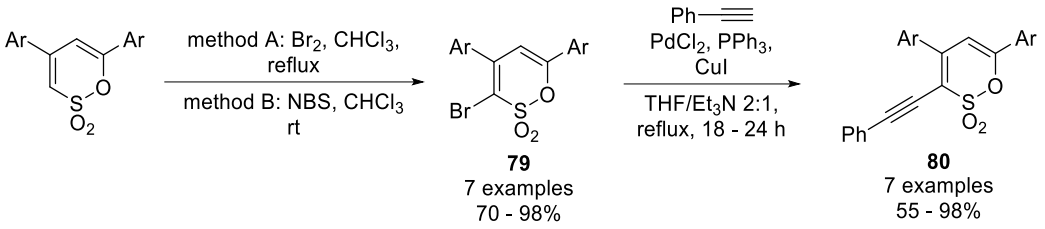

Scheme 64. Preparation of 3-phenylethynyl-1,2-oxathiine 2,2-dioxides.

The exploration of 4,6-diphenyl-1,2-oxathiine 2,2-dioxide as the diene in cycloaddition reactions with DMAD met with success to afford a mixture of terphenylene **81** and anhydride **82** through a Diels-Alder–retro Diels-Alder sequence with additional cyclisation of the proximal ester groups to afford the anhydride unit of **82** (Scheme 65).[140] This methodology was subsequently extended by the same group to encompass symmetrical 4,6-diaryl-1,2-oxathiine 2,2-dioxides and a selection of dienophiles to afford an extended series of substituted 1,3-terphenyls.[141]

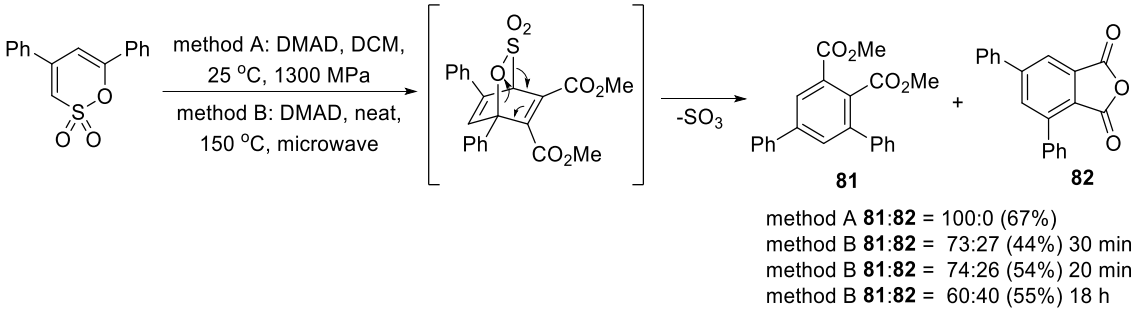

Scheme 65. Synthesis of terphenyls by a Diels-Alder–retro Diels-Alder reaction sequence.

Reflecting on the reactivity of the sulfonyl moiety of the sultone ring, ring contraction reactions have been attempted under either thermal or photochemical conditions. Morel and Verkade have shown that heating various 4,6-disubstituted-1,2-oxathiine 2,2-dioxides in quinoline in the presence of CaO, 2,4-disubstituted furans **83** can be obtained in moderate to good yields (Scheme 66).[142] The thermal SO_2 extrusion process constitutes a useful approach to these relatively inaccessible substituted furans of which 2,4-dimethylfuran is a useful building block for long chain polypropionates[143] and the A and C ring subunits of taxol.[144]

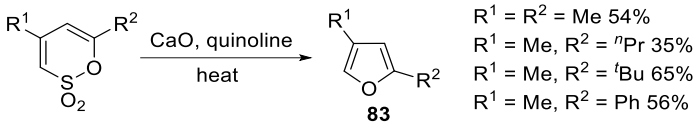

Scheme 66. Thermal extrusion of SO_2 from oxathiines to afford substituted furans.

Ether solutions of 4,6-di-substituted 1,2-oxathiine 2,2-dioxides can lose a sulfur monoxide fragment to afford the corresponding furanones **84** upon irradiation. Interestingly, when the photochemical reaction was sensitized by the addition of benzophenone, [2+2]-dimers **85** of the starting oxathiines were isolated (Scheme 67).[145]

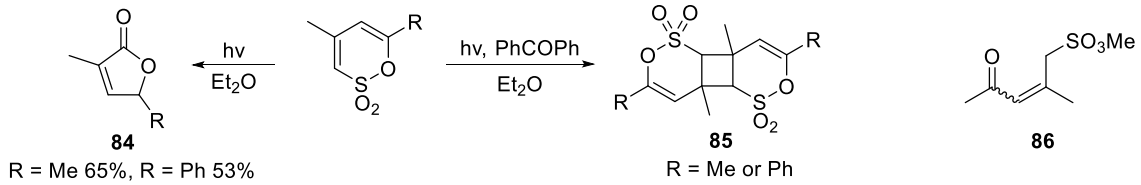

Scheme 67. Photolysis of 1,2-oxathiine 2,2-dioxides.

Photolysis of 2,4-dimethyl-1,2-oxathiine 2,2-dioxide in the presence of MeOH results in the formation of the acyclic sulfone ester **86** in an unspecified yield through interception of an intermediate resulting from an electrocyclic ring-opening of the oxathiine moiety.[146] The propensity of 1,2-oxathiine 2,2-dioxides to ring open upon irradiation has been utilised in the development commercial photoresists (photo-acid generators) by Masaaki *et al.*, (Scheme 68).[147] 1,2-Oxathiine 2,2-dioxides have also been incorporated in lithographic printing systems, as key components in the IR photosensitive mixtures that are applied to the printing plate.[148]

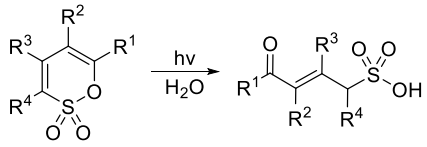

Scheme 68. 1,2-Oxathiine 2,2-dioxide photoresists.

Similar to their perhydro and dihydro counterparts, the unsaturated 1,2-oxathiine 2,2-dioxide analogues have found use in lithium secondary battery technologies.[149-151]

4. Concluding remarks

The various 1,2-oxathiine 2,2-dioxides are readily accessible by employing established chemistry in generally good to excellent yields from commercially available starting materials. Their varied reactivity, which can be harnessed to obtain a multitude of interesting compounds including sulfonic acids, carbocycles and numerous heterocycles should ensure sustained interest in the years to come. Moreover, their appearance in modern technological applications such as printing, energy storage and photochromism continues to grow.

References

1. Mondal, S. *Chem. Rev*. **2012**, *112*, 5339-5355.
2. Roberts, D. W.; Williams, D. L. *Tetrahedron* **1987**, *43*, 1027-1062.
3. Metz, P. J. *Prakt. Chem.* **1998**, *340*, 1-10.
4. (a) Cook, M. J. *Comp. Heterocycl. Chem.* **1984**, *3*, 943-995. (b) Kleinpeter, E. *Comp. Heterocycl. Chem. III.* **2008**, 8, 677-738.
5. (a) Mustafa, A. *Chem. Rev*. **1954**, *54*, 195-223. (b) Willems, J. *Bull. Soc. Chim. Belg*. **1955**, *64*, 747-771.
6. (a) Truce, W. E.; Hoerger, F. D. *J. Am. Chem. Soc*. **1954**, *76*, 5357-5360; (b) Truce, W. E.; Burdge, D. N.; Steltenkamp, R. J. *J. Org. Chem.* **1962**, *27*, 3913-3916.
7. Hieronymus, E.; Quadflieg, T. Wirtz, R. (Hoechst AG), *Netherland Pat. Appl*., 6407653, **1965**.
8. Snoddy, A. O. *Org. Synth, Coll. Vol. 4* **1963**, 529-531.
9. (a) Bordwell, F. G.; Rondestvedt Jr. C. S. *J. Am. Chem. Soc*. **1948**, *70*, 2429-2433. (b) Bordwell, F. G.; Peterson, M. L. *J. Am. Chem. Soc.* **1959**, *81*, 2000-2002.
10. Bordwell, F. G.; Colton, F. B.; Knell, M. *J. Am. Chem. Soc*. **1954**, *76*, 3950-3952.
11. Magerramov, A. M.; Bairamov, M. P.; Mamedov, I. G.; Dzhavadov, M. A. *Russ. J. Org. Chem.* **2002**, *38*, 1210-1211.
12. Roberts, D. W.; Williams, D. L. *J. Am. Oil Chem. Soc*. **1990**, *67*, 1020-1027.
13. Gaunersdorfer, C.; Waser, M. *Monatsh. Chem*. **2018**, *149*, 701-714.
14. Matsulevich, Zh. V.; Borisov, A. V.; Bodrikov, I. V. *Zh. Org. Khim*. **1994**, *30*, 948-949.
15. Durst, T; Tin, K.-C. *Can. J. Chem.* **1970**, *48*, 845-851.
16. Smith, M. B.; Wolinsky, J. *J. Org. Chem*. **1981**, *46*, 101-106.

17. De Kimpe, N.; Boeykens, M.; Lazar, L.; Szakonyi, Z.; Kemme, A.; Duburs, G. *Bull. Chem. Soc. Belg*. **1994**, *103*, 299-302.
18. LeFebvre, O.; Brigaud, T.; Portella, C. *J. Org. Chem*. **2001**, *66*, 1941-1946.
19. Evans, D. A.; Nagorny, P.; McRae, K. J.; Sonntag, L-S.; Reynolds, D. J.; Vounatsos, F. *Angew. Chem. Int. Ed*. **2007**, *46*, 545-548.
20. Morris, J.; Wishka, D. G. *J. Org. Chem*. **1991**, *56*, 3549-3556.
21. Zhang, W.; Pugh, G. *Synlett* **2002**, 778-780.
22. Rawner, T.; Knorn, M.; Lutsker, E.; Hossain, A.; Reiser, O. *J. Org. Chem*. **2016**, *81*, 7139-7147.
23. John, J. P.; Novikov, A. V. *Org. Lett.* **2007**, *9*, 61-63.
24. Bequette, J. P.; Jungong, C. S.; Novikov, A. V. *Tetrahedron Lett*. **2009**, *50*, 6963-6964.
25. Liyanage, D. S.; Jungong, C. S.; Novikov, A. V. *Synth. Commun*. **2015**, *45*, 226-231.
26. Wolckenhauer, S. A.; Devlin A. S.; Du Bois J. *Org. Lett*. **2007**, *9*, 4363-4366.
27. Griffin, J. R.; Wendell, C. I.; Garwin, J. A.; White, M. C. *J. Am. Chem. Soc*. **2017**, *139*, 13624-13627.
28. Dhami, K. S. *Chem. Ind. (London)* **1968**, *30*, 1004-1005.
29. Ungureanu, A.; Levens, A.; Candish, L.; Lupton, D. W. *Angew. Chem. Int. Ed.* **2015**, *54*, 11780-11784.
30. (a) Chen, X.; Zha, G.-F.; Bare, G. A. L.; Leng, J.; Wang, S.-M.; Qin, H.-L. *Adv. Synth. Catal.* **2017**, *359*, 3254-3260. (b) Xu, Y.; Zhang, Z.; Jiang, X.; Chen. X.; Wang, Z.; Alsulami, H.; Qin, H.-L.; Tang, W. *Eur. J. Med. Chem*. **2019**, *181*, 111598 (1)-111598 (14).
31. Liu, H.; Moku, B.; Li, F.; Ran, J.; Han, J.; Long, S.; Zha, G.-F.; Qin H.-L. *Adv. Synth. Catal.* **2019**, *361*, 4596-4601.
32. Chen, X.; Zha, G.-F.; Fang, W.-Y.; Rakesh, K. P.; Qin, H.-L. *Chem. Commun*. **2018**, *54*, 9011-9014.
33. Huang, Y.-M.; Wang, S.-M.; Leng, J.; Moku, B.; Zhao, C.; Alharbi, N.S.; Qin, H.-L. *Eur. J. Org. Chem.* **2019**, *2019*, 4597-4603.
34. Opitz, G.; Tempel, E. *Angew. Chem. Int. Ed.* **1964**, *3*, 754-755.
35. Truce, W. E.; Abraham, D. J.; Son, P. *J. Org. Chem*. **1967**, *32*, 990-997.
36. Gandini, A.; Schenone, P.; Bignardi, G. *Monatsh. Chem.* **1967**, *98*, 1518-1531.
37. Evangelisti, F.; Schenone, P.; Bargagna, A. *J. Heterocyclic Chem.* **1979**, *16*, 217-220.
38. Schenone, P.; Bignardi, G.; Morasso, S. *J. Heterocycl. Chem.* **1972**, *9*, 1341-1346.
39. Schenone, P.; Mosti, L.; Bignardi, G. *J. Heterocycl. Chem.* **1976**, *13*, 225-230.
40. Bargagna A.; Schenone, P.; Bondavalli, F.; Longobardi, M. *J. Heterocycl. Chem.* **1980**, *17*, 1201-1206.
41. Menozzi, G.; Bargagna A.; Mosti, L.; Schenone, P. *J. Heterocycl. Chem.* **1986**, *23*, 455-458.
42. Mosti, L.; Schenone, P.; Menozzi, G.; Cafaggi, S. *J. Heterocycl. Chem.* **1982**, *19*, 1031-1034.
43. Mosti, L.; Schenone, P.; Menozzi, G.; Romussi, G.; Baccichetti, F. *J. Heterocycl. Chem.* **1982**, *19*, 1227-1229.
44. Menozzi, G.; Bargagna A.; Mosti, L.; Schenone, P. *J. Heterocycl. Chem.* **1987**, *24*, 633-635.
45. Bargagna A.; Schenone, P.; Bondavalli, F.; Longobardi, M. *J. Heterocycl. Chem.* **1980**, *17*, 33-37.
46. Bargagna A.; Evangelisti, F.; Schenone, P. *J. Heterocycl. Chem.* **1981**, *18*, 111-116.
47. Singha, P.; Bisettya, K.; Mahajan, M. P. *S. Afr. J. Chem.* **2009**, *62*, 47-55.
48. Aiken, S.; Gabbutt, C. D.; Heron, B. M.; Rice, C. R.; Zonidis, D. *Org. Biomol. Chem*. **2019**, *17*, 9578-9584.
49. Aiken, S.; Anozie, K., de Azevedo, O. D. C. C.; Cowen, L.; Edgar, R. J. L.; Gabbutt, C. D.; Heron, B. M.; Lawrence, P. A.; Mills, A. J.; Rice, C. R.; Urquhart, M. W. J.; Zonidis, D. *Org. Biomol. Chem*. **2019**, *17*, 9585-9604.

50. Li, B.; Yan, W.; Zhang, C.; Zhang, Y.; Liang, M.; Chu, F.; Gong, Y.; Xu, B.; Wang, P.; Lei, H. *Molecules* **2015**, *20*, 4307-4318.
51. Bordwell, F. G.; Chapman, R. D.; Osborne, C. E. *J. Am. Chem. Soc*. **1959**, *81*, 2002-2007.
52. Schonk, R. M.; Bakker, B. H.; Cerfontain, H. *Rec. Trav. Chim. Pay-Bas* **1993**, *112*, 201-209.
53. Semenovskii, A. V.; Polunin, E. V.; Zaks, I. M.; Moiseenkov, A. M. *Izvestiya Akad. Nauk SSSR, Ser. Khim., Engl. Transl.* **1979**, 1240-1244.
54. Akiyama, T.; Sugihara, M.; Imagawa, T.; Kawanisi, M. *Bull. Chem. Soc. Jpn.* **1978**, *51*, 1251-1252.
55. Lebedev, N. V.; Emel'yanov, G. A.; Makhmutov, F. A.; Moldavskii, D. D.; Berenblit, V. V. *Russ. J. Appl. Chem*. **2007**, *80*, 424-427.
56. Jongejan, E.; Steinberg, H.; de Beer, Th. J. *Tetrahedron Lett.* **1976**, 397-400.
57. Karsch, S.; Freitag, D.; Schwab, P.; Metz, P. *Synthesis* **2004**, 1696-1712.
58. Le Flohic, A.; Meyer, C.; Cossy, J. *Tetrahedron* **2006**, *62*, 9017-9037.
59. Karsch, S.; Schwab, P.; Metz, P. *Synlett* **2002**, 2019-2022.
60. Le Flohic, A.; Meyer, C.; Cossy, J.; Desmurs, J-R.; Galland, J-C. *Synlett* **2003**, 667-670.
61. Walleser, P.; Brückner, R. *Eur. J. Org. Chem.* **2014**, 3210-3224.
62. (a) Motherwell, W. B.; Pennell, A. M. K.; Ujjainwalla, F. *J. Chem. Soc., Chem. Commun*. **1992**, 1067-1068. (b) Bonfand, E.; Motherwell, W. B.; Andrew M. K. Pennell, A. M. K.; Uddin, M. K.; Ujjainwalla, F. *Heterocycles* **1997**, *46*, 523-534.
63. Meiners, U.; Cramer, E.; Fröhlich, R.; Wibbeling, B.; Metz, P. *Eur. J. Org. Chem*. **1998**, 2073-2078.
64. Nakayama, J.; Sugihara, Y. *J. Org. Chem*. **1991**, *56*, 4001-4005.
65. Barnett, W. E.; Newton, M. G.; McCormack, J. A. *J. Chem. Soc., Chem. Commun*. **1972**, 264-265.
66. Morel, Th.; Verkade, P. E. *Rec. Trav. Chim. Pays-Bas* **1949**, *68*, 619-638.
67. Helferlich, B.; Klebert, W. *Liebigs. Ann. Chem*. **1962**, *657*, 79-86.
68. Eastman, R. H.; Gallup, D. *J. Am. Chem. Soc.* **1948**, *70*, 864-865.
69. Rad-Moghadam, K.; Roudsari, S. T.; Sheykhan, M. *Synlett* **2014**, 0827-0830.
70. Rad-Moghadam, K.; Hassani, S. A. R. M.; Roudsari, S. T. *J. Mol. Liq.* **2016**, *218*, 275-280.
71. Rad-Moghadam, K.; Roudsari, S. T. *Tetrahedron* **2018**, *74*, 4047-4052.
72. Gaitzsch, J.; Rogachev V.; Metz, P.; Filimonov. V. D.; Zahel, M.; Kataeva, O. *J. Sulfur Chem*. **2011**, *32*, 3-16.
73. Craig, D. C.; Stevens, J. D. *Carbohydr. Res.* **2011**, *346*, 854-857.
74. Heilmann, S. M.; Rasmussen, J. K.; Newmark, R. A.; Smith II, H. K. *J. Org. Chem*. **1979**, *44*, 3987-3988.
75. Voortman, T. P.; Chiechi, R. C. *ACS Appl. Mater. Interfaces* **2015**, *7*, 28006-28012.
76. Lee, J-H.; Kwon, S.; Jeong, S. Y.; Park, B.; Hong, S.; Kim, J.; Jang, S-Y.; Lee, K. *ACS Appl. Electron. Mater.* **2019**, *1*, 2566-2573.
77. Mai, C-K.; Schlitz, R. A.; Su, G. M.; Spitzer, D.; Wang, X.; Fronk, S. L.; Cahill, D. G.; Chabinyc, M. L.; Bazan, G. C. *J. Am. Chem. Soc.* **2014**, *136*, 13478-13481.
78. Moon, S.; Khadtare, S.; Wong, M.; Han, S-H.; Bazan, G. C.; Choi, H. *J. Coll. Int. Sci*. **2018**, *518*, 21-26.
79. Danielson, S. P. O.; Sanoja, G. E.; McCuskey, S. R.; Hammouda, B.; Bazan, G. C.; Fredrickson, G. H.; Segalman, R. A. *Chem. Mater*. **2018**, *30*, 1417-1426.
80. Noro, A.; Tamura, A.; Wakao, S.; Takano, A.; Matsushita, Y. *Macromolecules* **2008**, *41*. 9277-9283.
81. Markova, L. I.; Fedyunyaeva, I. A.; Povrozin, Y. A.; Semenova, O. M.; Khabuseva, S. U.; Terpetschnig, E. A.; Patsenker, L. D. *Dyes Pigm*. **2013**, *96*, 535-546.
82. Terpetschnig, E. A.; Patsenker, L. D.; Markova, L. I.; Fedyunyaeva, I. A.; Kolosova, O. S.; Starko, S.; Tatarets, A. *PCT WO 2010/083471*, **2010**.

83. Mokkapati, U. P. *PCT WO 2012/001063*, **2012**.
84. Cooper, M. E. *PCT WO 2008/015415*, **2008**.
85. Pham, W.; Lai, W-F.; Weissleder, R.; Tung, C-H. *Bioconjugate Chem*. **2003**, *14*, 1048-1051.
86. (a) Heterocyclic Polymethine Dyes. Ed. L. Strekowski, Springer-Verlag, Berlin, **2008**. (b) Shuai, T.; Zhou, Y.; Shao, G.; Yang, R.; Wang, L.; Wang, J.; Sun, J.; Ren, L.; Wang, J.; Liao, Y.; Wei, M.; Xu, Q.; Li, Y.; Zhao, L. *Anal. Chem*. **2020**, *92*, 1138-1146.
87. Turgis, R.; Estager, J.; Draye, M.; Ragaini, V., Bonrath, W., Lévêque, J-M. *ChemSusChem*. **2010**, *3*, 1403-1408.
88. Jeong, Y.; Kim, D-Y.; Choi, Y.; Ryu, J-S. *Org. Biomol. Chem*. **2011**, *9*, 374-378.
89. Yoshida, M.; Katagiri, Y.; Zhu, W-B.; Shishido, K. *Org. Biomol. Chem*. **2009**, *7*, 4062-4066.
90. Liu, X.; Xiao, L.; Wu, H.; Li, Z.; Chen, J.; Xia, C. *Catal. Commun*. **2009**, *10*, 424-427.
91. Braga, T. C.; Silva, T. F.; Maciel, T. M. S.; da Silva, E. C. D.; da Silva Jr., E. F.; Modolo, L. V.; Figueiredo, I. M.; Santos, J. C. C.; de Aquino, T. M.; de Fátima, Â. *New. J. Chem*. **2019**, *43*, 15187-15200.
92. Basaiahgari, A.; Yadav, S. K.; Gardas, R. L. *Pure Appl. Chem.* **2018**, *91*, 1279-1294.
93. Cole, A. C.; Jensen, J. L.; Ntai, I.; Tran, K. L. T.; Weaver, K. J.; Forbes, D. C.; Davis Jr, J. H. *J. Am. Chem. Soc*. **2002**, *124*, 5962-5963.
94. Paape, N.; Wei, W.; Bösmann, A.; Kolbeck, C.; Maier, F.; Steinrück, H-P.; Wasserscheid, P.; Schulz, P. S. *Chem. Commun*. **2008**, 3867-3869.
95. (a) Bisso, P. W.; Tai, M.; Katepalli, H.; Bertrand, N.; Blankschtein, D; Langer, R. *Nano Lett*. **2018**, *18*, 618-628. (b) Yan, P.; Acker, C. D.; Loew, L. M. *ACS Sens*. **2018**, *3*, 2621-2628.
96. Wang, Y.; Zhou, J.; Liu, K.; Dai, L. *RSC Adv*. **2013**, *3*, 9965-9972.
97. Patrick, M. J.; Ernst, L. A.; Waggoner, A. S.; Thai, D.; Tai, D.; Salama, G. *Org. Biomol. Chem*. **2007**, *5*, 3347-3353.
98. Jeong, Y.; Jung, H.; Lee, H.; Kang, S.; Kim, B.; Park, J. *Mol. Cryst. Liq. Cryst*. **2018**, *662*, 109-113.
99. Helberger, J. H.; Sproviero, J. F. *Justus Liebigs. Ann. Chem*. **1963**, *666*, 78-80.
100. Elmalem, E.; Biedermann, F.; Scherer, M. R.; Koutsioubas, A.; Toprakcioglu, C.; Biffi, G.; Huck, W. T. S. *Chem. Commun*. **2014**, *50*, 8930-8933.
101. Costa, T.; de Azevedo, D.; Stewart, B.; Knaapila, M.; Valente, A. J. M.; Kraft, M.; Scherf, U.; Burrows, H. D. *Polym. Chem*. **2015**, *6*, 8036-8046.
102. Ingverud, T.; Malkoch, M. *ACS Appl. Polym. Mater*. **2019**, *1*, 1845-1853.
103. Zhu, Y.; Noy, J-M.; Lowe, A. B.; Roth, P. J. *Polym. Chem*. **2015**, *6*, 5705-5718.
104. (a) Li, G.; Zhao, C.; Li, X.; Qi, D.; Liu, C.; Bu, F.; Na, H. *Polym. Chem*. **2015**, *6*, 5911-5920; (b) Wang, C.; Li, N.; Shin, D. W.; Li, S. Y.; Kang, N. R.; Lee, Y. M.; Guiver, M. D. *Macromolecules* **2011**, *44*, 7296-7306; (c) Xie, H.; Tao, D.; Ni, J.; Xiang, X.; Gao, C.; Wang, L. *J. Membrane Sci.* **2016**, *497*, 55-60.
105. (a) Zhang, L.; Qi, D.; Zhang, G.; Zhao, C.; Na, H. *RSC Adv*. **2014**, *4*, 51916-51925. (b) Hu, H.; Dong, T.; Sui, Y.; Li, N.; Ueda, M.; Wang, L.; Zhang, X. *J. Mater. Chem. A* **2018**, *6*, 3560-3570. (c) Zhang, Y.; Wan, Y.; Zhao, C.; Shao, K.; Zhang, G.; Li, H.; Lin, H.; Na, H. *Polymer* **2009**, *50*, 4471-4478.
106. (a) Thomsen, H.; Benkovics, G.; Fenyvesi, É.; Farewell, A.; Malanga, M.; Ericson, M. B. *Int. J. Pharm*. **2017**, *531*, 650-657. (b) Ma, D-Y.; Zhang, Y-M.; Xu, J-N. *Tetrahedron* **2016**, *72*, 3105-3112. (c) Munavalli, B. B.; Naik, S. R.; Kariduraganavar, M. Y. *Electrochim. Acta* **2018**, *286*, 350-364.
107. Jung, T.; Breitenbach, A.; Kissel, T. *J. Control. Rel*. **2000**, *67*, 157-169.
108. Kim, Y.; Lee, J. S.; Rhee, C. H.; Kim, H. K.; Chang, H. *J. Power Sources* **2006**, *162*, 180-185.
109. Naeimi, H.; Zarabi, M. F. *RSC Adv*. **2019**, *9*, 7400-7410.
110. Schmitt, S.; Bouteiller, C.; Barré, L.; Perrio, C. *Chem. Commun*. **2011**, *47*, 11465-11467.

111. Huang, H-N.; Roesky, H.; Lagow, R. J. *Inorg. Chem*. **1991**, *30*, 789-794.
112. Bequette, J. P.; Jungong, C. S.; Novikov, A. V. *Tetrahedron Lett.* **2009**, *50*, 6963-6964.
113. Jungong, C. S.; John, J. P.; Bequette, J. P.; Novikov, A. V. *Heterocycles* **2009**, *78*, 2531-2539.
114. Liyanage, D. S.; Jungong, C. S.; Novikov, A. N. *Tetrahedron Lett*. **2015**, *56*, 2269-2271.
115. Scott Jr., R. B.; Heller, M. S. *J. Org. Chem.* **1966**, *31*, 1999-2000.
116. Park, D. I.; Kwak, H. S.; Kim, M. L.; Cho, I. H. *U.S. Pat. Appl., US 20200044279*, **2020**.
117. Zhang, C.; Han, C.; Zhang, M.; Zhang, H.; Zou, H. *Eur. Pat. Appl., EP 3576207*, **2019**.
118. Zhang, M.; Han, C.; Zhang, H.; Zhang, C. *Eur. Pat. Appl., EP 3570350*, **2019**.
119. Won, J.-H.; Choi, M.-H.; Oh, M.-S.; Lee, H.-C.; Hough, L. A.; Kim, H.-Y. *PCT WO 2019211353*, **2019**.
120. Kim, J.-R.; Lee, J.-J.; Bridel, J.-S.; Won, J.-H.; Choi, M.-H.; Oh, M.-S.; Lee, H.; Hough, L. A.; Kim, H.-Y. *PCT WO 2019211366*, **2019**.
121. Park, D. I.; Kim, J. S.; Kim, C. W.; Lee, K. K. *U.S. Pat. Appl., US 20180233778*, **2018**.
122. Cheng, G.; Zhu, Y.; Strand, D.; Hallac, B.; Metz, B. M. *PCT Int. Appl., WO 2016209839*, **2016**.
123. Wolf, J. F.; Savner, S. M.; Maxfield, M.; Shacklette, L. W. *U.S. Pat. Appl., US 4528254*, **1985**.
124. Moiseenkov, A. W.; Polunin, E. V.; Semenovsky, A. V. *Tetrahedron Lett.* **1976**, 20, 4759-4760.
125. Frackenpohl, J.; Adelt, I.; Antonicek, H.; Arnold, C.; Behrmann, P.; Blaha, N.; Böhmer, J.; Gutbrod, O.; Hanke, R.; Hohmann, S.; van Houtdreve, M.; Lösel, P.; Malsam, O.; Melchers, M.; Neufert, V.; Peschel, E.; Reckmann, U.; Schenke, T.; Thiesen, H-P., Velten, R.; Vogelsang, K.; Weiss, H-C. *Bioorg. Med. Chem.* **2009**, *17*, 4160-4184.
126. Cho, J.-J.; Lee, H. C.; Yoon, S.-J.; Park, S.-M. *PCT WO2008050971*, **2008**.
127. Park, S.-Y.; Kang, H.-G.; Bae, J.-S. *PCT WO2009131419*, **2009**.
128. Cho, J.-J.; Lee, H. C.; Yoon, S.-J.; Park, S.-M. *US Pat. Appl. US8895195*, **2014**.
129. Park, S.-Y.; Kang, H.-G.; Bae, J.-S. *US Pat. Appl. US8697293*, **2014**.
130. Ihara, M.; Tanaka, T.; Kubota, T. *US Pat. Appl. US20120058401*, **2012**.
131. Ihara, M.; Wakita, S.; Kubota, T. *Eur. Pat. Appl. EP2211402*, **2010**.
132. Zhang, M.; Han, C. *US Pat. Appl. US20180294483*, **2018**.
133. Zeid, I.; Ismail, I. *J. Prakt. Chem.* **1972**, *314*, 367-370.
134. Zeid, I.; Ismail, I.; Helferich, B. *Liebigs Ann. Chem.* **1972**, *761*, 115-117.
135. Fanghänel, E.; Bartossek, H.; Lochter, T.; Baumeister, U.; Hartung, H. *J. Prakt. Chem*. **1997**, *339*, 277-283.
136. Zeid, I.; Badawi, M.; Ismail, I. *J. Prakt. Chem*. **1973**, *315*, 1166-1168.
137. Zeid, I.; Ismail, I.; Helferich, B. *Liebigs Ann. Chem*. **1972**, *761*, 118-120.
138. Ali, K. A.; Jäger, A.; Metz, P. *Arkivoc* **2016**, *3*, 15-22.
139. Barnett, W. E.; McCormack, J. *Tetrahedron Lett.* **1969**, *8*, 651-654.
140. Gaitzsch, J.; Rogachev, V. O.; Metz, P.; Yusubov, M. S.; Filimonov, V. D.; Kataeva, O. *J. Sulfur Chem*. **2009**, *30*, 4-9.
141. Gaitzsch, J.; Rogachev, V. O.; Zahel, M.; Metz, P. *Synthesis* **2014**, *46*, 0531-0536.
142. Morel, Th.; Verkade, P. E. *Recueil* **1951**, *70*, 35-49.
143. Ancerewicz, J.; Vogel, P. *Helv. Chim. Acta* **1996**, *79*, 1393-1414.
144. Arjona, O.; León, M. L.; Plumet, J. *J. Org. Chem*. **1999**, *64*, 272-275.
145. Gorewit, B.; Rosenblum, M. *J. Org. Chem.* **1973**, *38*, 2257-2258.
146. King, J. F.; De Mayo, P.; Morkved, E.; Sattar, A. B. M. A.; Stoessl, A. *Can. J. Chem*. **1963**, *41*, 100-107.
147. (a) Fujie, H.; Nakahata, M.; Ono, K.; Urano, F. *JPH03223865A*, **1990**. (b) Fujie, H.; Nakahata, M.; Ono, K.; Urano, F. *JPH0488348A*, **1990**.

148. Toshiaki, A.; Akihiro, E. *JP2004144933A*, **2004**.
149. An, J. H.; Ae, J.; Haeng, L.C. *KR2009/0084547A*, **2008**.
150. Sung-Sung, K.; Cheol-woo, K.; Seung-yeon, O.; Gwang-guk, L.; Sung-il, L. *KR20160032470A*, **2014**.
151. Ming, Z.; Changlong, H. *CN108987752A*, **2017**.

Article 2: Full Paper

Title: 'Expedient synthesis of highly substituted 3,4-dihydro-1,2-oxathiine 2,2-dioxides and 1,2-oxathiine 2,2-dioxides: revisiting sulfene additions to enaminoketones'

Authors: Stuart Aiken, Kelechi Anozie, Orlando D. C. C. de Azevedo, Lewis Cowen, Ross J. L. Edgar, Christopher D. Gabbutt, B. Mark Heron*, Philippa A. Lawrence, Abby J. Mills, Craig R. Rice, Mike W. J. Urquhart and Dimitrios Zonidis*

Journal: Organic & Biomolecular Chemistry; Publisher: Royal Society of Chemistry

Citation: *Org. Biomol. Chem*., **2019**, *17*, 9585-9604; DOI: https://doi.org/10.1039/C9OB01657K

Date of Publication: 31st October 2019

Author Contribution: This full paper contains examples of novel 1,2-oxathiine 2,2-dioxides and intermediates which I synthesised under the supervision of Professor Heron and which feature in Chapters 2 and 3 of this thesis. The specific compounds are compound numbers **9a**, **9c**, **9e**, **9f**, **9f'**, **9f''**, **9g**, **9j**, **36**, **39**, **10a**, **10b**, **10d1**, **10d2**, **10f**, **10i**, **12a**, **12b**, **40**, **11a**, **11b**, **11d**, **11f**, **11i**, **13a**, **13b** and **42** (compound numbers used as presented in the publication). In addition to their synthesis I undertook their spectroscopic and purity characterization and also that of their precursors. I drafted the experimental section of the manuscript, which relates to the foregoing compounds. In the draft manuscript my interpretation of their synthesis and NMR characterization data was used alongside data with that of the other examples contained within the manuscript to produce a comprehensive overview of the synthesis, structural and spectroscopic features of this class of compounds. I made revisions to the draft manuscript in accord with Professor Heron's suggestions.

Organic & Biomolecular Chemistry

PAPER

View Article Online
View Journal | View Issue

Cite this: Org. Biomol. Chem., 2019, 17, 9585

Expedient synthesis of highly substituted 3,4-dihydro-1,2-oxathiine 2,2-dioxides and 1,2-oxathiine 2,2-dioxides: revisiting sulfene additions to enaminoketones†

Stuart Aiken, [a] Kelechi Anozie, [a] Orlando D. C. C. de Azevedo, [a] Lewis Cowen, [a] Ross J. L. Edgar, [a] Christopher D. Gabbutt, [a] B. Mark Heron, *[a] Philippa A. Lawrence, [a] Abby J. Mills, [a] Craig R. Rice, [a] Mike W. J. Urquhart [b] and Dimitrios Zonidis *[a]

Received 26th July 2019,
Accepted 31st October 2019

DOI: 10.1039/c9ob01657k

rsc.li/obc

Diversely substituted 1,2-oxathiine 2,2-dioxides, including 3,5,6-triaryl-, 3,6-diaryl-, 3,5-diaryl-, 5,6-diaryl- and selected fused heterocyclic analogues, have been efficiently obtained by the application of a mild Cope elimination of a 4-amino moiety from the requisite 4-amino-3,4-dihydro-1,2-oxathiine 2,2-dioxides, which themselves were readily obtained by the addition of sulfenes to enaminoketones.

Introduction

1,2-Oxathiine 2,2-dioxides (Fig. 1), historically referred to as δ-sultones, are the relatively scarcely studied isomers in the homologous series of sultones.[1] Indeed the 1,2-oxathiine ring is the lesser explored isomer of the six-membered heterocyclic systems which contain one sulfur and one oxygen atom.[2] However, there has been recent interest in the 1,2-oxathiine 2,2-dioxide unit in energy storage/battery technology[3] and as photoresists for high resolution lithography.[4]

There are relatively few synthetic routes to this fully unsaturated ring system, simple alkyl substituted analogues can be obtained by sulfonation of either α,β- or β,γ-unsaturated ketones.[5] 4,6-Diaryl substituted compounds result from either sulfonation of acetophenones[6] or arylacetylenes[7] though one drawback of this sulfonation approach is that the 4- and 6-aryl substituents are identical. Unexpected syntheses of the 1,2-oxathiine 2,2-dioxide ring have been noted from the sulfuric acid mediated acetolysis of methyl 5,6-di-*O*-acetyl-2,3-*O*-isopropylidene-β-L-gulofuranoside,[8] from the oxidative ring expansion of 2,5,9,12-tetra(*tert*-butyl)diacenaphtho[1,2-*b*:1′,2′-*d*]thiophene[9] and *via* tri-*n*-butylstannyl radical rearrangement of but-3-ynyl arenesulfonates.[10] Recent interest in the synthesis of benzofused δ-sultones has been stimulated by the Rh(III)-catalyzed oxidative coupling of arylsulfonic acids with internal alkynes.[11] In spite of the lack of general and versatile synthetic routes to 1,2-oxathiine 2,2-dioxides their chemistry offers potential with photolysis affording ketosulfonic esters[12] and thermolysis providing an efficient and frequently exploited route to 2,4-dimethylfuran[13] which serves as a useful building block for the A and C ring subunits of taxol[14] and the complex side chain of mycolactones A and B.[15] The addition of hydrazines to 1,2-oxathiine 2,2-dioxides affords both pyrroles and pyrazoles[16] and cycloaddition with acetylenes under forcing conditions results in overall expulsion of SO_3 to afford a useful array of terphenylene derivatives.[17]

A relatively scarcely explored route to the 1,2-oxathiine system involves the addition of sulfenes to enaminoketones.[18,19] Examination of the literature revealed that Schenone and co-workers had exploited the addition of sulfenes[20–24] to a selection of enaminoketones to afford 3,4-dihydro-1,2-oxathiine 2,2-dioxides. Interestingly, the amino function was retained in each of these sulfene addition reactions affording 3,4-dihydro-1,2-oxathiine 2,2-dioxide rather than undergoing a facile elimination to produce the conjugated 1,2-oxathiine 2,2-dioxide

3,4-dihydro-1,2-oxathiine 2,2-dioxide

1,2-oxathiine 2,2-dioxide

Fig. 1 Structure and numbering for the 1,2-oxathiine 2,2-dioxide ring system.

[a]Department of Chemical Sciences, School of Applied Sciences, University of Huddersfield, Queensgate, Huddersfield, HD1 3DH, UK. E-mail: m.heron@hud.ac.uk, dimitrios.zonidis@hud.ac.uk
[b]GlaxoSmithKline Research and Development Limited, Medicines Research Centre, Gunnels Wood Road, Stevenage, Hertfordshire, SG1 2NY, UK

† Electronic supplementary information (ESI) available. CCDC 1913653–1913658. For ESI and crystallographic data in CIF or other electronic format see DOI: 10.1039/c9ob01657k

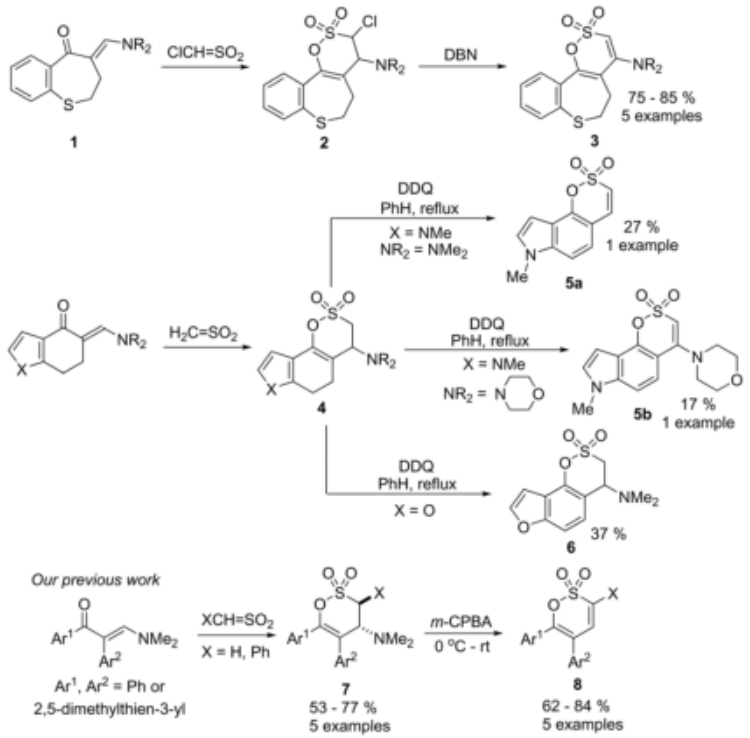

Fig. 2 Previous attempts to obtain the 1,2-oxathiine 2,2-dioxide from substituted dihydro-1,2-oxathiine 2,2-dioxides.

system.[21–23] Notably, when chlorosulfene was added to a series of enaminoketones **1** the elimination of HCl was accomplished from the adducts **2** upon subsequent treatment with DBN to afford the substituted amino-1,2-oxathiine 2,2-dioxides **3**, but not the unsubstituted alkene, in good yield (Fig. 2).[24] In a related study the dehydrogenation of sulfene adduct **4** (NR_2 = NMe_2) with DDQ in refluxing benzene for 10 h gave the oxathiine **5a** in 27% yield and a similar treatment of **4** (NR_2 = morpholine) with a 24 h reflux gave **5b** in 17% yield (Fig. 2).[25] In the foregoing study the authors noted the variably of their DDQ aromatization protocol which failed to dehydrogenate the 1,2-oxathiine ring of the furan analogue **4** X = O and instead gave **6**.[26] We have previously examined the synthesis of a novel dithienylethene photochromic system in which the ethene bridge forms part of a 1,2-oxathiine 2,2-dioxide ring.[27] In the latter work the oxathiine unit was introduced by (phenyl) sulfene addition to a series of thienyl substituted enaminoketones with the intermediate 3,4-dihydro-1,2-oxathiine 2,2-dioxides **7** undergoing a facile, room temperature Cope elimination of the dimethylamine function to afford the unsaturated 1,2-oxathiine 2,2-dioxide moiety **8** in good yield (Fig. 2).

Given the success of our Cope elimination protocol coupled with the limited literature reports for the formation of 1,2-oxathiine 2,2-dioxides from preformed 3,4-dihydro analogues (Fig. 2) we commenced our exploration of the addition of arylsulfenes to a diverse series of enaminoketones with a view to widening access to 3,4-dihydro-1,2-oxathiine 2,2-dioxides and examining their transformation into new unsaturated 1,2-oxathiine 2,2-dioxides.

Results and discussion

A range of enaminoketones **9a–k** were efficiently prepared by treatment of the requisite α-methylene ketones in *N*,*N*-dimethylformamide dimethylacetal (DMFDMA) according to literature procedures. Of note was the influence of the reaction medium and conditions on the outcome of the reaction of 3-oxo-3-phenylpropanenitrile (benzoylacetonitrile) with DMFDMA to afford **9f**; here crystalline salts **9f′** and **9f″** were isolated as minor by-products and have been characterised by X-ray crystallography (see ESI Fig. 1–3†).

Arylsulfenes, readily generated *in situ* from the base mediated elimination of HCl from the requisite arylmethanesulfonyl chlorides, underwent efficient addition to the acyclic enaminoketones **9a–d** to afford the 3,5,6-triaryl-4-amino-3,4-

dihydro-1,2-oxathiines 2,2-dioxides **10a–e** in generally high yield (48–96%). Enaminoketone **9d** which possesses an additional electron withdrawing group (X = Bz) required an extended reaction time in order to afford the desired oxathiine adduct **10e**. However, no oxathiines could be observed from the prolonged reaction of either **9e** or **9f** and the enaminoketone precursors were recovered (Scheme 1). The enaminoketones **9g–9k**, derived from 'acetophenones', similarly underwent smooth arylsulfene addition to afford 3,6-diaryl-4-amino-3,4-dihydro-1,2-oxathiines 2,2-dioxides **10f–j** in generally good yield (52–83%) with the exception of the pyridyl example **10i** (10%) where work-up was protracted due to the presence of the basic pyridyl function.

In a limited number of instances, the isolated crude 3,5,6-trisubstituted 4-dimethylamino-3,4-dihydro-1,2-oxathiines **10** were obtained as an unequal mixture of diastereoisomers as indicted from their NMR spectra. For example, the ^{1}H NMR spectrum of crude **10a** revealed doublets at δ 4.96 (4-H) and δ 4.49 (3-H) with $J_{3,4}$ = 8.0 Hz for the major isomer and doublets at δ 4.89 (4-H) and δ 4.73 (3-H) with $J_{3,4}$ = 5.9 Hz for the minor isomer (Fig. 4), with the isomer ratio determined as 4 : 1. Similarly, crude **10d** displayed doublets at δ 4.76 (4-H) and δ 4.51 (3-H) with $J_{3,4}$ = 9.4 Hz for the major isomer (**10d1**) and doublets at δ 4.81 (4-H) and δ 4.69 (3-H) with $J_{3,4}$ = 6.3 Hz for the minor isomer (**10d2**), with an isomer ratio of 1.6 : 1. The major diastereoisomer **10d1** could be obtained in 48% yield by flash chromatography and crystallization. Additionally, a small amount of the minor isomer **10d2** was isolated (25%) and fully characterized. Interestingly, recording the ^{1}H NMR spectrum of a $CDCl_3$ solution of **10d2** over 6 days revealed the gradual epimerisation of **10d2** into the original major isomer **10d1** (Fig. 3). We suspect that this epimerisation of **10d2** may be facilitated by protonation of the enol moiety (at C-5) which enables the 4-NMe_2 group to adopt a less hindered orientation that leads to a proposed *transoid* equatorial–equatorial arrangement of the 4-NMe_2 and 3-Ph substituents in the major isomer **10d1** (Scheme 5 insert).

The geometry of **10a** was established by X-ray crystallography (CCDC 1913655†), (Fig. 5 and ESI†) which revealed a *trans*-diaxial arrangement of 3-H and 4-H (H_3–C_3–C_4–H_4 torsion angle = 153°) in a half-chair conformation. The magnitude of ^{1}H NMR coupling constant, $J_{3,4}$ = 8.0 Hz, in **10a** is somewhat diminished for such an arrangement *viz.* the typically larger *trans*-diaxial coupling in cyclohexane rings,[28] though in this instance the O–C_6–C_5–C_4–C_3 unit of the oxathiine ring is near planar. The $J_{3,4}$ coupling constants for the other 3,5,6-triaryl substituted dihydro-1,2-oxathiines are comparable with that of **10a** with **10b**, $J_{3,4}$ = 8.8 Hz and **10c**, $J_{3,4}$ = 7.6 Hz. Interestingly, the $J_{3,4}$ coupling constants for the remaining 3,5,6-trisubstituted oxathiines were larger with **10d1**, $J_{3,4}$ = 9.4 Hz and **10e**, $J_{3,4}$ = 10.3 Hz. For the minor isomer **10d2** the smaller $J_{3,4}$ coupling of 6.3 Hz results from the interaction between axial and equatorial disposed protons.

In contrast, $J_{3,4}$ for the 3,6-diaryl substituted oxathiines (unsubstituted at C-5) (**10f–10j**) were again larger for those of **10a–e** typically of the order of 11.2 Hz. Clearly the presence of an aryl ring at C-5 in **10a–e** modifies the conformation of the dihydro-1,2-oxathiine ring and thus the coupling constants (Fig. 4).

Examination of the ^{1}H NMR spectra of the adducts **12a, b** which resulted from the addition of sulfene to enaminoketones **9a, b** (Scheme 3) revealed $J_{3,4}$ coupling constants of 7.4 Hz and 9.1 Hz (**12a**) and 6.3 Hz and 11.4 Hz (**12b**), respectively and which are indicative of the 4-dimethylamino substituent occupying an equatorial site of the half-chair conformer. Of note in the ^{1}H NMR spectrum of **12b** was a long-range coupling of 1.0 Hz between 5-H and the equatorially disposed 3-H. Interestingly, a second component was isolated from the reaction between sulfene and **9b** which was characterized as the oxathiine-2,2-dioxide **13b** (50%) on the basis of the chemical shift of 3-H (δ 6.57, d, J = 10.0 Hz), 4-H (δ 6.91, dd, J = 10.0, 6.8 Hz) and 5-H (δ 6.30, d, J = 6.8 Hz) and which presumably forms by the facile elimination of dimethylamine from the isomer in which the dimethylamine group and a 3-H are *trans*-disposed (*anti-peri*-planar arrangement). Selected ^{1}H NMR data is presented in Fig. 4 for a series of 3,5,6-triphenyl-, 3,6-diphenyl- and 5,6-diphenyl-1,2-oxathiine 2,2-dioxides.

In order to extend the structural diversity of the dihydro-1,2-oxathiines, by substrate variation, sulfene additions to enaminoketones **15** and **18**, derived from arylmethyleneketone

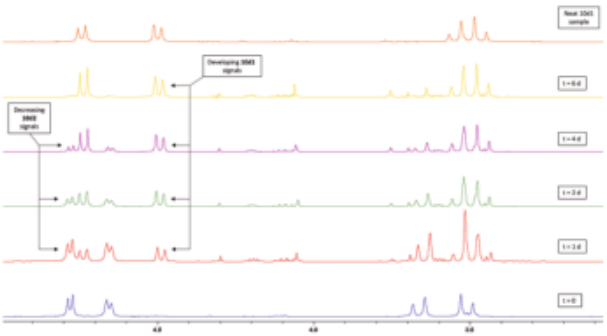

Fig. 3 Time resolved ^{1}H NMR spectra (δ 3.0–5.0) showing epimerisation of **10d2** into **10d1** over 6 days in $CDCl_3$ solution.

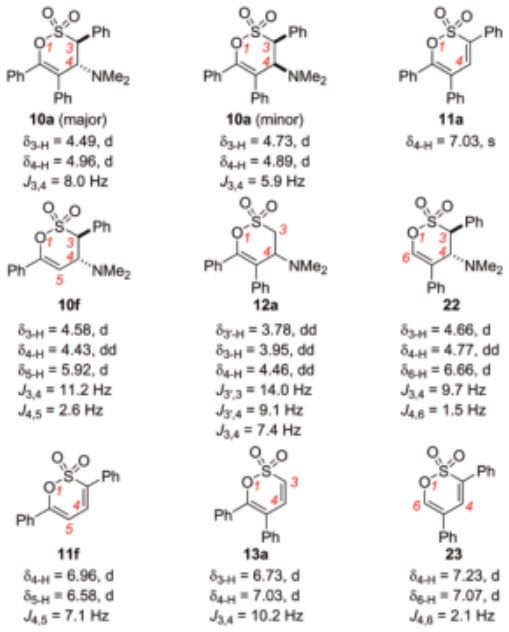

Fig. 4 Selected ^{1}H NMR data ($CDCl_3$) for 3,5,6-triphenyl-, 3,6-diphenyl-, 3,5-diphenyl- and 5,6-diphenyl- (3,4-dihydro) 1,2-oxathiine 2,2-dioxides.

14 and 2-tetralone, respectively and sulfene addition to the enaminoaldehyde **21** were explored (Scheme 4). Phenylsulfene addition to **15** proceeded smoothly to afford **16** in 79% yield. As a consequence of restricted rotation of the *o*-fluorophenyl unit due to steric congestion with the adjacent methyl and dimethylamino groups the ^{1}H NMR spectrum of **16** was complex. Indeed recording the spectrum at 233 K revealed a mixture of two rotamers (ESI) which coalesce upon recording the spectrum at 323 K. A small variation in $J_{3,4}$ was observed with the rotamers affording couplings of 9.7 and 9.9 Hz (233 K) and the thermally averaged compound giving $J_{3,4}$ = 9.5 Hz (323 K). The 1,2,5,6-tetrahydronaphtho[1,2-*e*][1,2]oxathiine 3,3-dioxide **19** (from **18**) was isolated in 65% yield and exhibited $J_{3,4}$ = 8.9 Hz. In contrast to the foregoing reactions of enaminoketones, the enaminoaldehyde derivative **21** afforded a complex crude product from which two new pure components **22** (5%) and **23** (2.9%) were isolated. The dihydro-1,2-oxathiine **22** exhibited a doublet with allylic coupling of 1.5 Hz, at δ 6.66 for 6-H and a doublet at δ 4.66 for 3-H with the typical $J_{3,4}$ value of 9.7 Hz. The introduction of the C=C bond in **23** resulted in the presence of a pair of doublets (δ 7.07, 7.03) in the ^{1}H NMR spectrum with a coupling constant of 2.1 Hz (Fig. 4).

With a series of 4-dimethylamino-3,4-dihydro-1,2-oxathiine 2,2-dioxides to hand (**10a–j**, **12a**, **12b**, **16** and **19**) the introduction of the C-3–C-4 oxathiine ring double bond by the elimination of dimethylamine was examined. From our earlier observations it is clear that the elimination of dimethylamine can be facile *e.g.* **12b** → **13b** and **22** → **23**, presumably from an isomer where 3-H is suitably disposed to the 4-dimethylamino function. Thus, treatment of a PhMe solution of **10a** with a catalytic amount of 4-TsOH and stirring at either room temperature or under reflux failed to afford any **11a**. Indeed, increasing the amount of 4-TsOH up to a 10-fold molar excess of **10a** and heating the solution under reflux overnight resulted in darkening of the reaction mixture together with the formation of decomposition products as indicated by the presence of several very minor components observed by TLC together with some unchanged major component. Given the conformation depicted in Fig. 5, a Cope elimination protocol[29] was explored. Treatment of a cooled CH_2Cl_2 solution of **10a** with a slight excess of *m*-CPBA and stirring at room temperature for 18 h resulted in the efficient elimination of the dimethylamine unit to afford **11a** in 71% isolated yield. A singlet

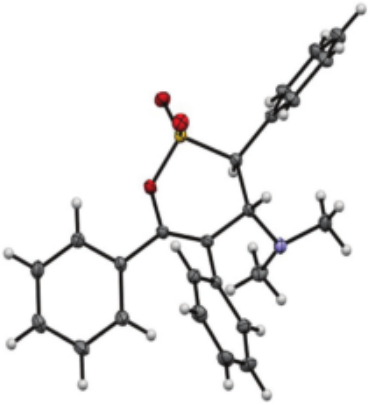

Fig. 5 Crystal structure of **10a** (thermal ellipsoids shown at 50% probability level).

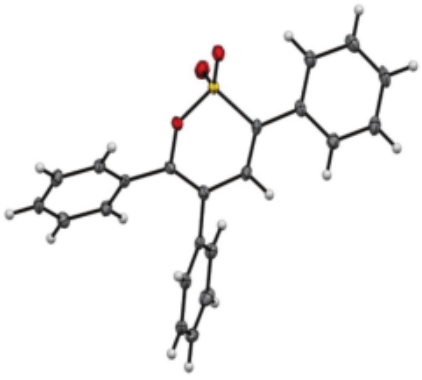

Fig. 6 Crystal structure of **11a** (thermal ellipsoids shown at 50% probability level).

was observed at δ 7.03 for 4-H confirming the elimination of the amine and a single crystal structure (CCDC 1913656†), (Fig. 6) confirmed the successful elimination protocol. The Cope reaction sequence was then carried out on the remaining 4-dimethylamino substituted 1,2-oxathiine 2,2-dioxides to afford **11b–j**, **13a**, **13b**, **17** and **20** in good to excellent yields (68–96%) (Schemes 1 and 2). Interestingly for the 3,6-diaryl substituted 1,2-oxathiines (**11f–j**) $J_{4,5}$ was *ca.* 6.8–7.2 Hz, whereas $J_{3,4}$ = 10.2 Hz was typical of *cis*-alkene coupling for the 5,6-disubstituted analogue **13a** (Fig. 4). The foregoing trend in the magnitude of the coupling constants was consistent for the mono-aryl substituted oxathiine **13b** with $J_{3,4}$ = 10.0 Hz and $J_{4,5}$ = 6.8 Hz.

In an extension of the foregoing elimination study, we examined the acid-catalysed elimination of dimethylamine from the isolated minor isomer **10d2** in which 4-NMe_2 group is in an *anti-peri*-planar arrangement with 3-H. Thus, heating **10d2** in toluene containing 4-TsOH (20 mol%) gave a multi-

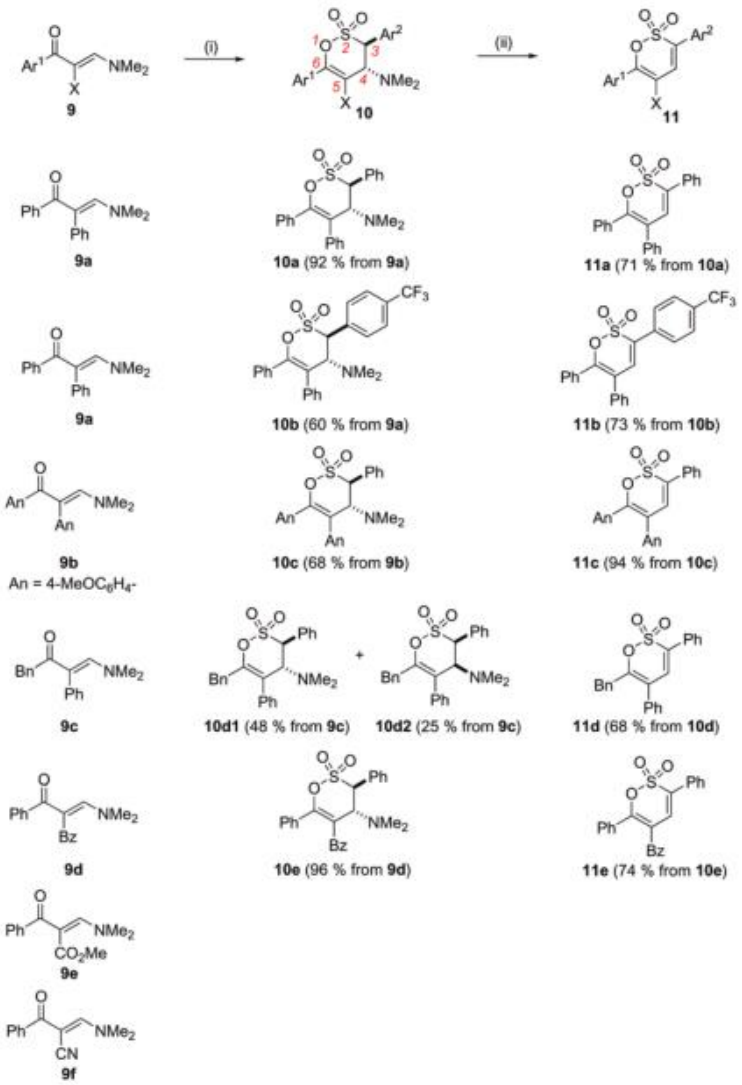

Scheme 1 Synthesis of 3,5,6-trisubstituted 1,2-oxathiines 2,2-dioxides **11**. Reagents and conditions: (i) $Ar^2CH_2SO_2Cl$, Et_3N, THF 0 °C–rt; (ii) *m*-CPBA (1.2 eq), CH_2Cl_2, 0 °C–rt.

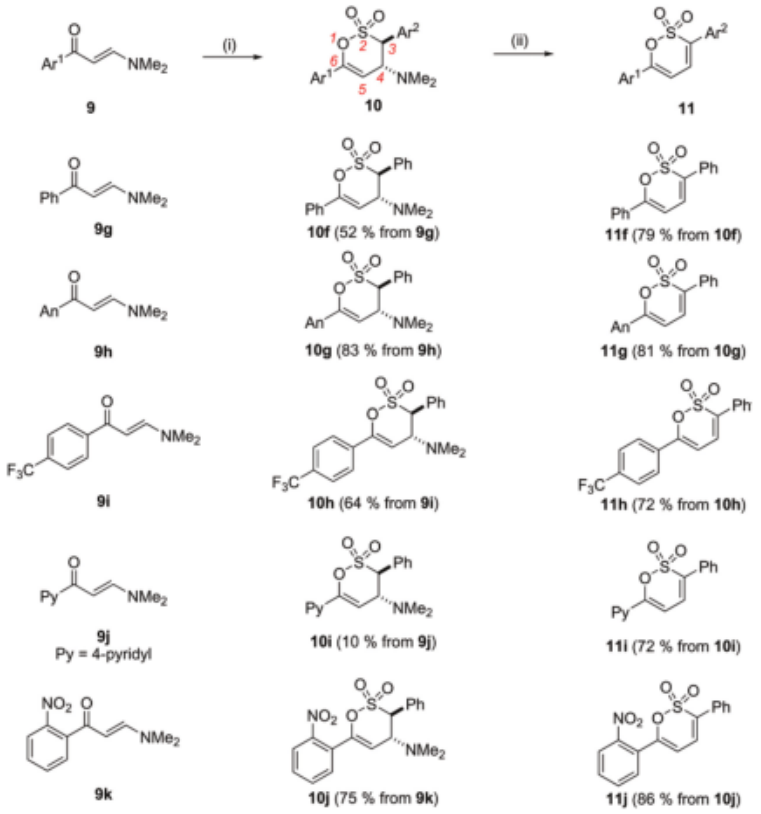

Scheme 2 Synthesis of 3,6-disubstituted 1,2-oxathiine 2,2-dioxides **11**. Reagents and conditons: (i) $Ar^2CH_2SO_2Cl$, Et_3N, THF 0 °C–rt; (ii) *m*-CPBA (1.2 eq), CH_2Cl_2, 0 °C–rt.

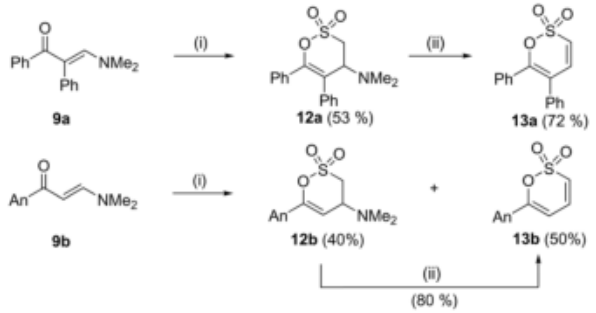

Scheme 3 Synthesis of 5,6-diaryl- and 6-aryl-1,2-oxathiine 2,2-dioxides. Reagents and conditions: (i) $MeSO_2Cl$, Et_3N, THF 0 °C–rt; (ii) *m*-CPBA (1.2 eq.), CH_2Cl_2, 0 °C–rt.

component reaction mixture from which the major component, the 1,2-oxathiine 2,2-dioxide **11d**, was isolated in low yield (15%) (Scheme 5).

With efficient methodology developed for the addition of sulfenes to the series of enaminoketones and the subsequent elimination of the dimethylamino function from the 3,4-

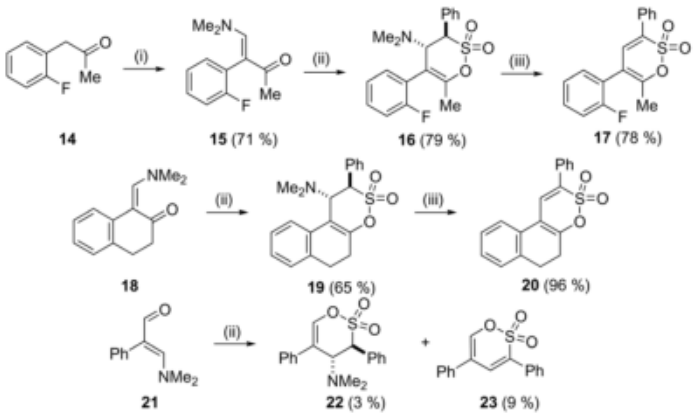

Scheme 4 Synthesis of substituted 1,2-oxathiine 2,2-dioxides **17**, **20** and **23**. Reagents and conditions: (i) DMFDMA, reflux; (ii) $PhCH_2SO_2Cl$, Et_3N, THF 0 °C–rt; (iii) *m*-CPBA, CH_2Cl_2, 0 °C–rt.

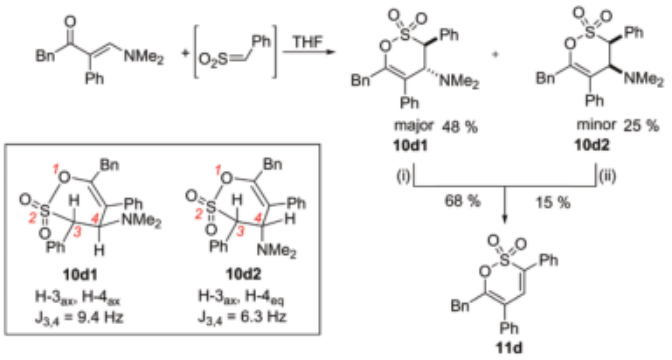

Scheme 5 Elimination reactions to afford **11d**. Reagents and conditions: (i) *m*-CPBA (1.2 eq.), CH_2Cl_2, 0 °C–rt; (ii) 4-TsOH (20 mol%), PhMe, reflux.

dihydro-1,2-oxathine 2,2-dioxides to afford a diverse series of novel 1,2-oxathine 2,2-dioxides the synthesis of some condensed heterocyclic ring systems was examined. 3-Hydroxymethylene substituted chroman-**24** and thiochroman-4-ones **25** were readily obtained by literature protocols.[30,31] Allowing a dry PhMe solution of either **24** or **25** containing pyrrolidine to stand overnight over anhyd. Na_2SO_4 resulted in the efficient formation of the enaminoketones **26** (82%) and **27** (95%), respectively. Using our standard procedure, the reaction of phenylsulfene, generated *in situ*, with **26** and **27** was undertaken and afforded the fused dihydro-1,2-oxathiines **28** (54%) and **29** (43%) (Scheme 6). The ^{1}H NMR spectrum of crude **28** indicated the presence of a minor isomer (ratio minor : major = 3 : 20) with $J_{3,4}$ = 5.1 Hz ($\delta_{3\text{-H}}$ 4.65, $\delta_{4\text{-H}}$ 4.25) which was readily removed upon recrystallization to leave the major diastereoisomer which exhibited $\delta_{3\text{-H}}$ 4.94 and $\delta_{4\text{-H}}$ 4.61 with $J_{3,4}$ = 7.6 Hz. The X-ray crystal structure of **28** (CCDC 1913658†), (Fig. 7) revealed that the C_3–C_4–C_5–C_6–O is near planar with the SO_2 unit out of plane and that H-3 and H-4 are in a *trans*-diaxial arrangement with a H_3–C_3–C_4–H_4 torsion angle of *ca.* 162°. The ^{1}H NMR spectrum of crude **29** also indicated the presence of a minor isomer (ratio minor : major = 3 : 50 with $J_{3,4}$ = 4.5 Hz). The ^{1}H NMR spectrum of the major isomer showed similar features to that of **28** with $\delta_{3\text{-H}}$ 4.91 and $\delta_{4\text{-H}}$ 4.61, however $J_{3,4}$ is now smaller at 5.2 Hz which suggests that the presence of the larger sulfur atom exerts an influence on the geometry of the fused oxathiine dioxide ring.

The Cope elimination reaction proceeded smoothly with **28** to afford **30** in 49% yield. An excess of *m*-CPBA was used for the Cope reaction of **29**, as a consequence of the possibility of oxidation of the thiochroman ring heteroatom, and resulted in a mixture of the *S*-oxidised analogues **31a** (32%) and **31b** (50%) (Scheme 6). The chemical shift of the oxathiine ring proton (4-H) for the series **30**, **31a** and **31b** appeared in the narrow range δ 6.75–6.97 and the *gem*-methyl groups (C-5) are

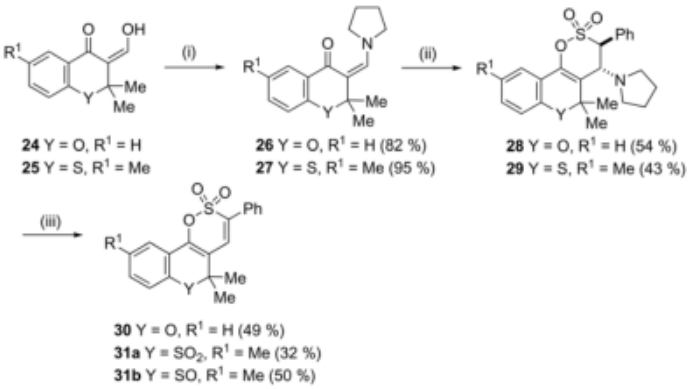

Scheme 6 Synthesis of fused benzo(thio)pyrano 1,2-oxathiines **30** and **31**. Reagents and conditions: (i) pyrrolidine, PhMe (anhyd.), rt; (ii) $PhCH_2SO_2Cl$, Et_3N, THF 0 °C–rt; (iii) *m*-CPBA (1.2–3.0 eq.), CH_2Cl_2, 0 °C–rt.

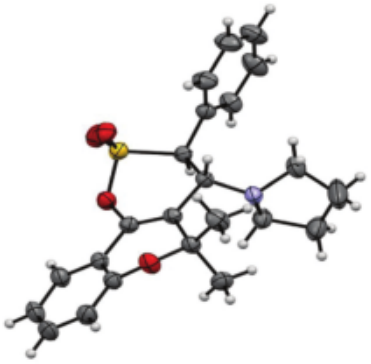

Fig. 7 Crystal structure of **28** (thermal ellipsoids shown at 50% probability level).

non-equivalent in **31b** (δ_{Me} = 1.46, 1.71) and equivalent in **30** (δ_{Me} = 1.65) and **31a** (δ_{Me} = 1.68).

Isothiochromanone **32** was readily prepared by the Friedel–Crafts cyclisation of commercial *S*-benzylthioacetic acid according to the procedure described by Aiken *et al.*[32] Reaction of **32** with DMFDMA afforded the enaminoketone **33** ($\delta_{1\text{-H}}$ 3.75; $\delta_{\text{—CH}}$ 7.99) in 86% yield after crystallisation. Phenylsulfene addition proceeded smoothly to afford **34** in 74% yield, after routine flash column chromatography. Compound **34** was isolated as an inseparable mixture of diastereoisomers in a ratio 1.7 : 1.0 based on relative integrals of the ^{1}H NMR signals for 3-H and for 4-H in each isomer which appear at (major)$\delta_{3\text{-H}}$ 4.79 ($J_{3,4}$ = 10.5 Hz) and (minor)$\delta_{3\text{-H}}$ 4.88 ($J_{3,4}$ = 6.4 Hz) and (major)$\delta_{4\text{-H}}$ 4.59 and (minor)$\delta_{4\text{-H}}$ 4.65. Cope elimination of the NMe_2 function using a 7.25-fold excess of *m*-CPBA afforded the tricyclic tetraoxide **35** in 76% yield (Scheme 7). In the ^{1}H NMR spectrum of **35** 4-H and the 6-CH_2 unit appear as singlets at δ 7.54 and δ 5.00, respectively. Notably the signal for the equivalent 6-CH_2 protons in **35** is shifted downfield relative to that in **34**, in which the non-equivalent protons resonate as doublets [major diastereoisomer δ 3.56, δ 4.15 (J = 14.2 Hz) and minor diastereoisomer δ 3.75, δ 4.07 (J = 14.2 Hz)] as a consequence of the oxidation of the S atom during the Cope elimination protocol. The structure of **35** (Fig. 8) was confirmed by X-ray crystallography (CCDC 1913657†) which revealed that the SO_2 unit of each hetero-ring lies out of the main ring plane.

Given the preliminary success concerning the synthesis of the oxathiines **11a–j**, **13a**, **13b**, **17**, **20**, **23** and fused oxathiines **30**, **31a,b** and **35** we briefly examined the reaction of (*E*)-*N*-[(dimethylamino)methylene]-4-methylbenzamide **36**, derived from

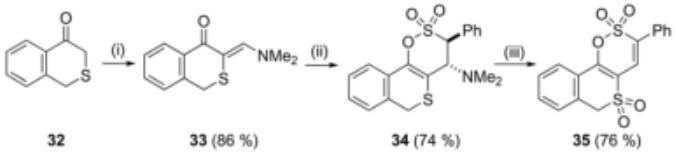

Scheme 7 Preparation of 3-phenyl-6*H*-isothiochromeno[3,4-*e*][1,2]oxathiine 2,2,5,5-tetraoxide **35**. Reagents and conditions: (i) DMFDMA, reflux; (ii) $PhCH_2SO_2Cl$, Et_3N, THF 0 °C–rt; (iii) *m*-CPBA (7.25 eq.), CH_2Cl_2, 0 °C–rt.

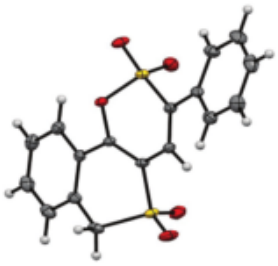

Fig. 8 Crystal structure of **35** (thermal ellipsoids shown at 50% probability level).

p-toluamide and DMFDMA, with a view to obtaining the 3,4-dihydro-1,2,5-oxathiazine 2,2-dioxide **37** (Scheme 8). Unfortunately, **37** could not be detected from the reaction of **36** with phenylsulfene and instead the *N*-formylbenzamide **38** (62%) was the major product isolated after aqueous work-up. The hydrolysis of *N*-[(dimethylamino)methylene]benzamides has been previously reported as a useful route to *N*-formylbenzamides.[33]

We sought to capitalise on the foregoing observation and examined the reaction of the unsymmetrical bis-dimethylaminomethylene **39** with phenylsulfene in order to obtain the *N*-formyl protected 6-amino substituted 3,4-dihydrooxathiine dioxide **33** (Scheme 9). Our initial attempt to prepare precursor **39** upon refluxing a solution of 2-phenylacetamide was unsuccessful with the ^{1}H NMR spectrum of the crude reaction product indicating two singlets at δ 3.02 and δ 2.95 each accounting for 6H and lower field singlet at δ 3.74 accounting for 3H. Column chromatography of the mixture gave the pure formimidate **41** (39%) as a consequence of adventitious addition of *in situ* produced MeOH to the formed **39**. Repeating the reaction with DMFDMA but with removal of the produced methanol from the reaction by distillation resulted in the smooth formation of **39**. Bis-dimethylaminomethylene **39** has been previously obtained in 90% yield by the reaction of bis(dimethylamino)-*t*-butoxymethane (Bredereck's reagent) with 2-phenylacetamide[34] though the present method affording **39** in 63% yield is advantageous as a consequence of the readily available and inexpensive DMFDMA. The generation of phenylsulfene in the presence of **39** unexpectedly afforded the oxathiine dioxide **42** directly in 9% yield after aqueous washings, column chromatography and recrystallizations; the anticipated 3,4-dihydro adduct **40** was not observed.

Conclusions

(*E*)-2,4-Dicyano-1,5-dioxo-1,5-diphenylpent-3-en-2-ide, a new extensively delocalised carbanion, has been isolated and structurally characterised from the preparation of (*E*)-2-benzoyl-3-(dimethylamino)acrylonitrile from benzoylacetonitrile. The nature of the accompanying cation was dictated by the reaction conditions; with DMFDMA diluted with PhMe at RT the *N*-[(dimethylamino)methylene]-*N*-methylmethanaminium counterion was preferred whereas neat DMFDMA favoured the formation of the tetramethylammonium counterion.

The addition of various sulfenes, generated *in situ* from the (aryl)alkylsulfonyl chlorides and Et_3N, to an extensive series of enaminoketones proceeded smoothly to afford diversely substituted 4-amino-3,4-dihydro-1,2-oxathiine 2,2-dioxides, including 3,5,6-triaryl-, 3,6-diaryl-, 3,5-diaryl- and 5,6-diaryl- analogues, in good yield. A *transoid* (di-equatorial) relationship between the 3-aryl substituent and the 4-amino function for the isolated major isomers was established by X-ray crystallo-

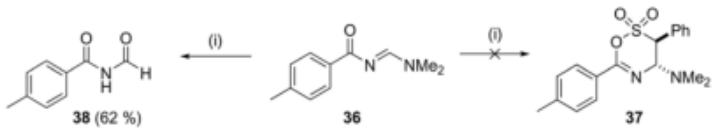

Scheme 8 Formation of *N*-formylbenzamide **38**. Reagents and conditions: (i) $PhCH_2SO_2Cl$, Et_3N, THF 0 °C–rt.

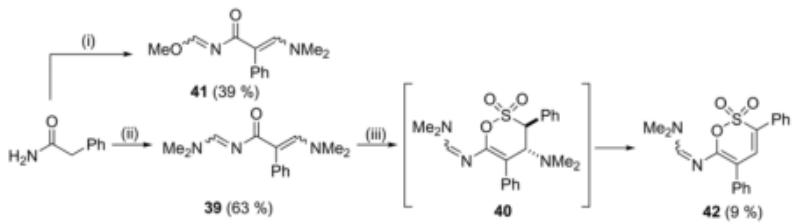

Scheme 9 Formation of *N*-protected 6-amino 1,2-oxathine **42**. Reagents and conditions: (i) DMFDMA, reflux; (ii) DMFDMA, reflux, MeOH removal; (iii) $PhCH_2SO_2Cl$, Et_3N, THF 0 °C–rt.

graphy and NMR spectroscopy for the adducts derived from an aryl methanesulfonyl chloride. In $CDCl_3$ solution, a sample of an isolated pure minor isomer (**10d2**) was observed by ^{1}H NMR spectroscopy to epimerise to afford the major isomer in *ca.* 6 days.

The 4-amino-3-aryl-3,4-dihydro-1,2-oxathiine 2,2-dioxide (**10a**) resisted attempts to effect an acid-catalysed elimination of the 4-amino function. However, the isolated minor isomer (**10d2**) underwent a reluctant acid acid-catalysed elimination to afford the 1,2-oxathiine 2,2-dioxide **11d**. Application of Cope methodology resulted in the efficient, smooth elimination of the 4-amino function from **10a–j** and **10d1** to afford the unsaturated 1,2-oxathiine 2,2-dioxides series **11** in high yield. This simple protocol constitutes an efficient route to a series of novel, structurally diverse 1,2-oxathiine 2,2-dioxides and in particular describes a new condensed heterocyclic ring system, the 6*H*-isothiochromeno[3,4-*e*][1,2]oxathiine. It is noteworthy that previously reported direct routes to 1,2-oxathiine 2,2-dioxides cannot provide the structural diversity afforded by the two-step protocol described herein. Attempts to extend our sulfene addition–elimination protocol to *N*-((dimethylamino) methylene)benzamides to obtain 1,2,5-oxathiazine 2,2-dioxides was unsuccessful and resulted in a new route to *N*-formylbenzamides.

Our studies concerning both the reactivity and the application of the 1,2-oxathiine 2,2-dioxide moiety as a scaffold for materials applications are ongoing.

Equipment and materials

Unless otherwise stated, reagents and solvents were purchased from major chemical catalogue companies and were used as supplied. Routine ^{1}H NMR (400 MHz) and ^{13}C NMR (100 MHz) spectra were recorded on a Bruker Avance DPX400 instrument in $CDCl_3$. Variable Temperature ^{1}H NMR (500 MHz) and ^{13}C NMR (125 MHz) spectra were recorded on a Bruker Avance I 500 MHz NMR instrument in $CDCl_3$. Chemical shifts are provided in parts per million (ppm) using either the residual solvent peak or TMS as the internal reference. Coupling constants (J) are provided in Hz and where applicable, in order to resolve close signals and extract valuable coupling information, the raw FID data was processed using a Gaussian multiplication in place of the more usual exponential multiplication. All FT-IR spectra were recorded on a Nicolet 380 FTIR spectrophotometer equipped with a diamond ATR attachment (neat sample). Flash column chromatography was performed on chromatography silica gel (Fluorochem, 40–63 micron particle size distribution). All final compounds were homogeneous by TLC using a range of eluent systems of differing polarity (Merck TLC aluminium sheets silica gel 60 F254 (Cat. No. 105554)) when visualised with a dual lamp (254 and 365 nm) Spectroline 8 W hand held TLC inspection lamp. High resolution mass spectra were recorded on an Agilent 6210 1200 SL TOF spectrometer within the IPOS centre at the University of Huddersfield. Single crystal X-ray diffraction data was collected on a Bruker Venture diffractometer equipped with a graphite monochromated Cu(Kα) radiation source and a cold stream of N_2 gas.

The following enamino-carbonyl compounds: (*E*)-3-(dimethylamino)-1,2-diphenylprop-2-en-1-one[35] (**9a**), (*E*)-3-(dimethylamino)-1,2-bis(4-methoxyphenyl)prop-2-en-1-one[36] (**9b**), (*E*)-3-(dimethylamino)-1-(4-methoxyphenyl)prop-2-en-1-one[37] (**9h**), (*E*)-3-(dimethylamino)-1-(2-nitrophenyl)prop-2-en-1-one[38] (**9k**), (*E*)-3-(dimethylamino)-1-(4-(trifluoromethyl)phenyl)-prop-2-en-1-one[39] (**9i**), 2-((dimethylamino)methylene)-1,3-diphenylpropane-1,3-dione[40] (**9d**), methyl 2-benzoyl-3-(dimethylamino) acrylate[41] (**9e**), 1-((dimethylamino)methylene)-3,4-dihydronaphthalen-2(1*H*)-one[42] (**18**), 3-(dimethylamino)-2-phenylacrylaldehyde[43] (**21**), (*E*)-3-(dimethylamino)-1-phenylprop-2-en-1-one[44] (**9g**) and (*E*)-*N*-((dimethylamino)methylene)-4-methylbenzamide[45] (**36**) were obtained by refluxing the requisite α-methylene carbonyl compound or amide in neat *N*,*N*-dimethylformamide dimethylacetal (DMFDMA) (2.5 equivalents) until TLC examination of the reaction mixture indicated that no starting α-methylene carbonyl compound remained. (*Z*)-3-(Hydroxymethylene)-2,2-dimethylchroman-4-one[30] (**24**) and (*Z*)-3-(hydroxymethylene)-2,2,6-trimethylthiochroman-4-one[31] (**25**) and isothiochromanone[32] (**32**) were prepared according to previously reported procedures. 4-(Dimethylamino)-3-(2-fluorophenyl)but-3-en-2-one (**15**) was prepared according to the procedure described by Kozmin *et al.*, for the preparation of 4-(dimethylamino)-3-phenylbut-3-en-2-one.[46] (*E*)-4-(Dimethylamino)-1,3-diphenylbut-3-en-2-one[47] (**9c**) was prepared by heating 1,3-diphenylacetone in toluene containing DMFDMA. 3-(Dimethylamino)-1-(4-pyridyl)-2-propen-1-one (**9j**) was obtained by heating 4-acetylpyridine in DMFDMA containing 10 mol% L-proline.[44]

Preparation of enaminoketones

Preparation of (*E*)-2-benzoyl-3-(dimethylamino)acrylonitrile 9f

A solution of benzoylacetonitrile (12.0 g, 82.7 mmol) in *N*,*N*-dimethylformamide dimethylacetal (27.4 mL, 207 mmol, 2.5 eq.) under nitrogen was heated under reflux overnight. Upon cooling the excess *N*,*N*-dimethylformamide dimethylacetal and other volatiles were removed and the resulting crude product was eluted from silica using 4% to 10% MeOH in DCM to afford two fractions:

Fraction 1, (*E*)-2-Benzoyl-3-(dimethylamino)acrylonitrile **9f** as an off-white solid (9.36 g, 57%); mp 111–113 °C (lit. mp 113–114 °C (ref. 48)); ν_{max} (neat) 2924, 2191, 1640, 1586, 1568, 1444, 1426, 1412, 1318, 1300, 1229, 1180, 1135, 1095, 1070, 1056, 1027 cm^{-1}; δ_H ($CDCl_3$, 400 MHz) 3.38 (3H, s, NMe), 3.47 (3H, s, NMe), 7.45–7.41 (2H, m, Ar–H), 7.52–7.48 (1H, m, Ar–H), 7.69–7.67 (2H, m, Ar–H), 7.88 (s, 1H, alkene-H); δ_C ($CDCl_3$, 100 MHz) 39.0, 48.3, 79.7, 120.3, 128.1, 128.2, 131.5, 138.5, 159.4, 190.3; found $[M + H]^+$ = 201.1027, $C_{12}H_{12}N_2O$ requires $[M + H]^+$ = 201.1022.

Fraction 2, Tetramethylammonium (*E*)-2,4-dicyano-1,5-dioxo-1,5-diphenylpent-3-en-2-ide **9f′** as yellow crystals (2.15 g, 14%); mp 250 °C (decomp.); ν_{max} (neat) 3031, 2199, 2186, 1612, 1596,

1574, 1483, 1448, 1316, 1295, 1241, 1176, 1109, 1074, 1026, 1002 cm^{-1}; δ_H (DMSO-d_6, 400 MHz) 3.09 (12H, s, N^+Me_4), 7.51–7.39 (10H, m, Ar–H), 8.02 (1H, s, alkene-H); δ_C (DMSO-d_6, 100 MHz) 54.38 (t, J = 4.0 Hz), 86.68, 118.62, 127.75, 127.96, 130.21, 139.76, 152.52, 190.04; found $[M - NMe_4]^-$ = 299.0825, $C_{23}H_{23}N_3O_2$ requires $[M - NMe_4]^-$ = 299.0821.

Alternative preparation of (*E*)-2-benzoyl-3-(dimethylamino) acrylonitrile 9f

A solution of benzoylacetonitrile (2.00 g, 13.8 mmol) in PhMe (50 mL) containing *N*,*N*-dimethylformamide dimethylacetal (2.02 mL, 15.2 mmol, 1.1 eq.) was stirred overnight at room temperature whereupon the volatiles were removed *in vacuo*. Recrystallization from EtOH gave two fractions:

Fraction 1, (*E*)-2-Benzoyl-3-(dimethylamino)acrylonitrile **9f** from the room temperature crystallization as yellow filaments (2.34 g, 85%) mp 110–112 °C (lit. mp 113–114 °C (ref. 48)) with spectroscopic data identical to that obtained previously.

Fraction 2, *N*-((Dimethylamino)methylene)-*N*-methylmethanaminium (*E*)-2,4-dicyano-1,5-dioxo-1,5-diphenylpent-3-en-2-ide **9f″** from cooling the filtrate as an off-white solid (0.090 g, 3.5%); mp 146–147 °C; ν_{max} (neat) 3044, 2203, 2195, 1698, 1605, 1574, 1495, 1442, 1423, 1413, 1369, 1337, 1250, 1168, 1114, 1066, 1025, 1001 cm^{-1}; δ_H ($CDCl_3$, 400 MHz) 3.29 (6H, s, NMe_2), 3.32 (6H, s, NMe_2), 7.26–7.40 (6H, m, Ar–H), 7.56–7.58 (4H, m, Ar–H), 8.04 (1H, s, alkene-H), 8.16 (1H, s, Me_2NCH=); δ_C ($CDCl_3$, 100 MHz) 39.35, 46.51, 87.86, 120.09, 128.12, 128.32, 130.51, 139.77, 154.69, 157.49, 192.16; found $[M - Me_2N{=}CHNMe_2]^-$ = 299.0824, $C_{24}H_{24}N_4O_2$ requires $[M - Me_2N{=}CHNMe_2]^-$ = 299.0826.

Preparation of 4-(dimethylamino)-3-(2-fluorophenyl)but-3-en-2-one 15

A solution of 1-(2-fluorophenyl)propan-2-one (5.0 g, 33 mmol) in *N*,*N*-dimethylformamide dimethylacetal (10.9 mL, 82.1 mmol) was heated under reflux for 48 h. Upon cooling the excess *N*,*N*-dimethylformamide dimethylacetal and other volatiles were removed by vacuum distillation to leave 4-(dimethylamino)-3-(2-fluorophenyl)but-3-en-2-one **15** as a pale brown viscous oil (4.80 g, 71%) which was used directly; ν_{max} (neat) 3034, 2923, 1651, 1614, 1557, 1492, 1423, 1384, 1351, 1288, 1213, 1087, 956, 754, 635 cm^{-1}; δ_H ($CDCl_3$, 400 MHz) 1.87 (3H, s, Me), 2.62 (6H, vbs, NMe_2), 6.92–6.97 (1H, m, Ar–H), 6.99–7.03 (1H, m, Ar–H), 7.06–7.10 (1H, m, Ar–H), 7.15–7.20 (1H, m, Ar–H), 7.58 (1H, s, alkene-H); δ_C ($CDCl_3$, 100 MHz) 26.89, 42.50 (broad), 103.34, 115.11 (d, J = 22.8 Hz), 123.56 (d, J = 3.6 Hz), 125.59 (d, J = 17.3 Hz), 129.01 (d, J = 7.9 Hz), 134.25 (d, J = 2.8 Hz), 150.29, 161.02 (d, J = 241.5 Hz), 195.33; found $[M + H]^+$ = 208.1132, $C_{12}H_{14}FNO$ requires $[M + H]^+$ = 208.1138. A sample of **15** was used directly for the preparation of the dihydro-1,2-oxathiine 2,2-dioxide **16**.

Preparation of (*Z*)-2,2-dimethyl-3-(pyrrolidin-1-ylmethylene) chroman-4-one 26

Pyrrolidine (4.22 mL, 51.4 mmol) was added dropwise over 5 minutes to a stirred solution of (*Z*)-3-(hydroxymethylene)-2,2-dimethylchroman-4-one **24** (10.0 g, 49 mmol) in anhydrous toluene (150 mL) at room temperature. The resulting yellow solution was stirred at room temperature overnight and the resulting mixture was dried with anhydrous sodium sulphate and the toluene and excess pyrrolidine were removed by rotary evaporation to afford the crude product as a bright orange/yellow solid which was recrystallized from EtOAc/hexane to afford the pure pyrrolidinomethylene compound **26** as a bright yellow solid (10.40 g, 82%); mp 105–108 °C; ν_{max} (neat) 2976, 2844, 1652, 1589, 1538, 1455, 1250, 1212, 1177, 985, 837, 823, 758, 536 cm^{-1}; δ_H ($CDCl_3$, 400 MHz) 1.58 (6H, s, 2-Me), 1.90–1.93 (4H, m, $(CH_2)_2$), 3.36 (4H, bs, $N(CH_2)_2$), 6.82, (1H, s, alkene-H), 6.83 (1H, d, J = 8.3 Hz, 8-H), 6.93 (1H, app. t, J = 7.5 Hz, 6-H), 7.31–7.36 (1H, m, 7-H), 7.89 (1H, dd, J = 7.8, 1.6 Hz, 5-H); δ_C ($CDCl_3$, 100 MHz) 25.5, 28.9, 53.7, 81.5, 107.0, 117.4, 120.3, 123.5, 126.2, 133.7, 144.3, 158.1, 179.1; found $[M + H]^+$ = 258.1485, $C_{16}H_{19}NO_2$ requires $[M + H]^+$ = 258.1489.

Preparation of (*Z*)-2,2,6-trimethyl-3-(pyrrolidin-1-ylmethylene) thiochroman-4-one 27

Pyrrolidine (1.36 mL, 16.6 mmol) was added dropwise over 5 minutes to a stirred solution of (*Z*)-3-(hydroxymethylene)-2,2,6-trimethylthiochroman-4-one **25** (3.70 g, 16 mmol) in anhydrous toluene (70 mL) at room temperature. The resulting yellow solution was stirred at room temperature for 48 h and then the mixture was dried with anhydrous sodium sulfate and the toluene and excess pyrrolidine were removed by rotary evaporation to afford the crude product as a bright orange/yellow solid which was recrystallized from EtOAc/hexane to afford the pure pyrrolidinomethylene **27** as a bright yellow solid (4.38 g, 95%); mp 128–131 °C; ν_{max} (neat) 2944, 2866, 1625, 1598, 1538, 1463, 1372, 1335, 1266, 1215, 1159, 1133, 928, 827, 782, 671, 523 cm^{-1}; δ_H ($CDCl_3$, 400 MHz) 1.63 (6H, s, 2-Me), 1.89–1.92 (4H, m, $(CH_2)_2$), 2.35 (3H, s, 6-Me), 3.20 (4H, bs, $N(CH_2)_2$), 6.89 (1H, s, alkene-H), 7.09–7.16 (2H, m, 7-H, 8-H), 8.04 (1H, bs, 5-H); δ_C ($CDCl_3$, 100 MHz) 21.0, 25.5, 29.7, 47.5, 53.4, 109.7, 127.4, 128.6, 132.2, 132.7, 134.3, 135.9, 142.7, 182.4; found $[M + H]^+$ = 288.1412, $C_{17}H_{21}NOS$ requires $[M + H]^+$ = 288.1417.

Preparation of (*Z*)-3-((dimethylamino)methylene) isothiochroman-4-one 33

A solution of isothiochroman-4-one **32** (5.0 g, 30 mmol) in *N*,*N*-dimethylformamide dimethylacetal (10.5 mL, 76 mmol) was heated under reflux for 18 h. Upon cooling the excess *N*,*N*-dimethylformamide dimethylacetal and other volatiles were removed by rotary evaporation to afford an orange-brown solid which was recrystallized from hexane/EtOAc to afford the title compound **33** as orange needles (5.75 g, 86%); mp 107–109 °C; ν_{max} (neat) 1633, 1595, 1539, 1402, 1319, 1293, 1255, 1131, 1092, 1051, 1031, 963, 946, 913, 896, 867, 780, 760, 728, 707, 685, 646, 573, 533, 484, 416 cm^{-1}; δ_H ($CDCl_3$, 400 MHz) 3.25 (6H, s, $N(CH_2)_2$), 3.75 (2H, s, 1-H), 7.10–7.12 (1H, m, 8-H), 7.32–7.39 (2H, m, 6-H, 7-H), 7.99 (1H, s, alkene-H), 8.00–8.02 (1H, m, 5-H); δ_C ($CDCl_3$, 100 MHz) 31.8, 43.6, 94.6, 125.8,

127.5, 128.8, 131.1, 134.7, 139.8, 149.7, 183.9; found $[M + H]^+$ = 220.0792, $C_{12}H_{13}NOS$ requires $[M + H]^+$ = 220.0791.

Preparation of 1,2-oxathiine 2,2-dioxides

General method for the preparation of dihydro-1,2-oxathiine 2,2-dioxides from arylmethanesulfonyl chlorides

A solution of the arylmethanesulfonyl chloride (1.1 eq.) [phenylmethanesulfonyl chloride unless otherwise indicated] in anhydrous THF (50 mL) under a nitrogen atmosphere was added dropwise over 15 minutes to an ice cold (0–5 °C) vigorously stirred solution of the enaminoketone (1.0 eq.) and triethylamine (1.125 eq.) in anhydrous THF (60 mL for a typical 20 mmol scale reaction) under nitrogen. Upon completion of the addition the ice-water bath was removed and the resulting solution was stirred until TLC examination of the reaction mixture indicated that no starting enaminoketone remained (typically stirred overnight). The reaction mixture was filtered through a sinter containing chromatography silica (*ca.* 20 mm depth) with further THF (*ca.* 200 mL) used to wash any remaining product from the silica. The THF and excess triethylamine were removed from the filtrate by rotary evaporation to afford the crude product which was then suspended in EtOAc (*ca.* 100 mL) and washed with water (3 × 50 mL) and brine (50 mL). The EtOAc layer was dried (anhyd. Na_2SO_4) and then evaporated to give the crude product which was purified by either column chromatography or crystallization. The following 3,4-dihydro-1,2-oxathiine 2,2-dioxides were obtained in this manner:

4-(Dimethylamino)-3,5,6-triphenyl-3,4-dihydro-1,2-oxathiine 2,2-dioxide 10a from **9a** (19.9 mmol) as off-white microcrystals (7.40 g, 92%) from EtOAc/hexane; mp = 152–154 °C; ν_{max} (neat) 3063, 2938, 1644, 1455, 1365 (SO_2–O), 1182 (SO_2–O), 1036, 925, 692, 508 cm^{-1}; δ_H ($CDCl_3$, 400 MHz)‡ 2.23 (6H, s, NMe_2), 4.49 (1H, d, J = 8.0 Hz, 4-H), 4.96 (1H, d, J = 8.0 Hz, 3-H), 7.15–7.32 (10H, m, Ar–H), 7.42–7.47 (3H, m, Ar–H), 7.60–7.62 (2H, m, Ar–H); δ_C ($CDCl_3$, 100 MHz) 40.64, 62.36, 71.75, 122.78, 127.72, 127.85, 128.22, 129.02, 129.14, 129.24, 129.49, 129.88, 129.95, 131.75, 132.84, 137.27, 148.30; found $[M + H]^+$ = 406.1471, $C_{24}H_{23}NO_3S$ requires $[M + H]^+$ = 406.1471. ‡The ^1H NMR spectrum of the crude isolated product indicated a mixture of diastereoisomers in a *ca.* 4 : 1 ratio (see ESI for spectrum†).

4-(Dimethylamino)-5,6-diphenyl-3-(4-(trifluoromethyl) phenyl)-3,4-dihydro-1,2-oxathiine 2,2 dioxide 10b from **9a** (15.5 mmol) and 4-trifluoromethylphenylmethanesulfonyl chloride (4.50 g, 17.4 mmol) as colourless microcrystals (4.40 g, 60%) from EtOAc/hexane; mp = 125–128 °C; ν_{max} (neat) 2833, 2794, 2248, 2222, 2179, 2159, 2041, 2028, 2005, 1978, 1955, 1662, 1620, 1491, 1446, 1421, 1371, 1364 (SO_2–O), 1323, 1223, 1186, 1162 (SO_2–O), 1114, 1098, 1069, 1049, 1035, 1018, 1000 cm^{-1}; δ_H ($(CD_3)_2CO$, 400 MHz) 2.22 (6H, s, NMe_2), 4.79 (1H, d, J = 8.8 Hz, 4-H), 5.42 (1H, d, J = 8.8 Hz, 3-H), 7.22–7.27 (8H, m, Ar–H), 7.35–7.38 (2H, m, Ar–H), 7.86 (2H, app. d, J = 8.2 Hz, Ar–H), 8.06 (2H, app. d, J = 8.2 Hz, (Ar–H); δ_C ($(CD_3)_2CO$, 100 MHz) 40.13, 61.90, 70.88, 124.2 (q, J = 270.0 Hz, CF_3), 123.58, 125.84 (q, J = 4.0 Hz, o-Ar*C*-CF_3), 127.65, 127.97, 128.07, 129.04, 130.06, 130.76 (q, J = 32.0 Hz, Ar*C*-CF_3), 131.05, 133.29, 136.66, 137.03, 147.83; δ_F ($(CD_3)_2CO$, 376 MHz) −63.13; found $[M + H]^+$ = 473.1260, $C_{25}H_{22}F_3NO_3S$ requires $[M + H]^+$ = 473.1272.

4-(Dimethylamino)-5,6-bis(4-methoxyphenyl)-3-phenyl-3,4-dihydro-1,2-oxathiine 2,2-dioxide 10c from **9b** (16.1 mmol) as off-white microcrystals (5.10 g, 68%) from EtOAc/hexane; mp = 120–121 °C; ν_{max} (neat) 2945, 2836, 2793, 1604, 1509, 1371, 1354 (SO_2–O), 1240, 1171 (SO_2–O), 1063, 965, 839, 728 cm^{-1}; δ_H ($CDCl_3$, 400 MHz)‡ 2.23 (6H, s, NMe_2), 3.76 (3H, s, OMe), 3.79 (3H, s, OMe), 4.39 (1H, d, J = 7.6 Hz, 4-H), 4.92 (1H, d, J = 7.6 Hz, 3-H), 6.67–6.72 (2H, m, Ar–H), 6.77–6.80 (2H, m, Ar–H), 7.14–7.17 (2H, m, Ar–H), 7.21–7.25 (2H, m, Ar–H), 7.40–7.45 (3H, m, Ar–H), 7.57–7.59 (2H, m, Ar–H); δ_C ($CDCl_3$, 100 MHz) 40.59, 55.16, 55.26, 62.23, 71.93, 113.29, 113.70, 120.79, 125.31, 127.10, 128.06, 129.20, 129.39, 129.76, 129.89, 130.57, 130.82, 131.14, 132.03, 148.01, 158.98, 159.84; found $[M + H]^+$ = 466.1684, $C_{26}H_{27}NO_5S$ requires $[M + H]^+$ = 466.1688. ‡The ^1H NMR spectrum of the crude isolated product indicated a mixture of diastereoisomers in a *ca.* 5 : 1 ratio.

6-Benzyl-4-(dimethylamino)-3,5-diphenyl-3,4-dihydro-1,2-oxathiine 2,2-dioxide 10d1 and **10d2** from **9c** (18.8 mmol) after elution from silica using 10% to 30% EtOAc/hexane and crystallization from EtOAc/hexane. Fraction 1: **10d1** as colourless microcrystals (3.78 g, 48%), mp = 133–136 °C; ν_{max} (neat) 2935, 2834, 2788, 2010, 1667, 1600, 1495, 1454, 1442, 1428, 1361 (SO_2–O), 1313, 1223, 1182 (SO_2–O), 1119, 1091, 1067, 1031 cm^{-1}; δ_H ($CDCl_3$, 400 MHz)‡ 2.07 (6H, s, NMe_2), 3.48 (1H, d, J = 15.3 Hz, PhCH), 3.56 (1H, d, J = 15.3 Hz, PhCH), 4.51 (1H, d, J = 9.4 Hz, 4-H), 4.76 (1H, d, J = 9.4 Hz, 3-H), 7.18–7.45 (13H, m, Ar–H), 7.57–7.60 (2H, m, Ar–H); δ_C ($CDCl_3$, 100 MHz) 30.97, 37.89, 40.82, 62.59, 70.51, 122.86, 126.84, 127.88, 128.42, 128.57, 128.69, 129.06, 129.18, 129.53, 129.80, 131.03, 135.84, 137.10, 148.67; found $[M + H]^+$ = 420.1627, $C_{25}H_{25}NO_3S$ requires $[M + H]^+$ = 420.1628.

Fraction 2: **10d2** as a white solid (1.94 g, 25%), mp = 101–102 °C; ν_{max} (neat) 2863, 2796, 1657, 1600, 1493, 1453, 1362 (O–SO_2), 1290, 1247, 1187, 1163 (O–SO_2), 1102, 1071, 1041 cm^{-1}; δ_H ($CDCl_3$, 400 MHz) 2.06 (6H, s, N(CH_3)$_2$), 3.52 (1H, d, J = 15.3 Hz, PhC*H*), 3.68 (1H, d, J = 15.3 Hz, PhC*H*), 4.67 (1H, d, J = 6.3 Hz, 4-H), 4.79 (1H, d, J = 6.3 Hz, 3-H), 7.21–7.41 (13H, m, ArH), 7.55–7.57 (2H, m, ArH); δ_C ($CDCl_3$, 100 MHz) 37.80, 42.03, 64.76, 68.09, 120.74, 126.88, 127.89, 128.29, 128.61, 128.64, 128.78, 129.33, 129.44, 129.79, 130.58, 136.18, 136.90, 148.37; found $[M + H]^+$ = 420.1627, $C_{25}H_{25}NO_3S$ requires $[M + H]^+$ = 420.1631.

‡The ^1H NMR spectrum of the crude isolated product indicated a mixture of diastereoisomers in a *ca.* 1.6 : 1 ratio.

(4-(Dimethylamino)-2,2-dioxido-3,6-diphenyl-3,4-dihydro-1,2-oxathiin-5-yl)(phenyl)methanone 10e from **9d** (17.9 mmol) as a waxy solid (7.40 g, 96%) after filtration through silica using CH_2Cl_2 as eluent. Crystallization of a small sample from

EtOAc/hexane gave off-white microcrystals; mp = 146–148 °C; ν_{max} (neat) 1655, 1613, 1596, 1448, 1371 (SO_2–O), 1242, 1185, 1160 (SO_2–O), 1072, 883, 711, 670, 684, 513 cm^{-1}; δ_H ($CDCl_3$, 400 MHz) 2.06 (6H, s, NMe_2), 4.83 (1H, d, J = 10.3 Hz, 4-H), 4.87 (1H, d, J = 10.3 Hz, 3-H), 7.27–7.31 (3H, m, Ar–H), 7.43–7.48 (5H, m, Ar–H), 7.52–7.56 (3H, m, Ar–H), 7.60–7.62 (2H, m, Ar–H), 7.94 (2H, app. d, J = 7.3 Hz, Bz–H); δ_C ($CDCl_3$, 100 MHz) 40.68, 62.14, 69.03, 123.01, 128.29, 128.65, 128.83, 128.87, 129.41, 129.65, 129.74, 130.01, 130.35, 131.39, 133.29, 136.45, 149.84, 193.25; found $[M + H]^+$ = 434.1428, $C_{25}H_{23}NO_4S$ requires $[M + H]^+$ = 434.1421.

4-(Dimethylamino)-3,6-diphenyl-3,4-dihydro-1,2-oxathiine 2,2 dioxide 10f from **9g** (28.5 mmol) as colourless microcrystals (4.96 g, 52%) from EtOH; mp = 144–146 °C; ν_{max} (neat) 3388, 2831, 2783, 1659, 1575, 1494, 1469, 1452, 1367 (SO_2–O), 1313, 1272, 1222, 1178 (SO_2–O), 1117, 1105, 1072, 1039 cm^{-1}; δ_H ($CDCl_3$, 400 MHz) 2.29 (6H, s, NMe_2), 4.43 (1H, dd, J = 11.2, 2.6 Hz, 4-H), 4.58 (1H, d, J = 11.2 Hz, 3-H), 5.92 (1H, d, J = 2.6 Hz, 5-H), 7.51–7.37 (6H, m, Ar–H), 7.60–7.51 (2H, m, Ar–H), 7.69–7.60 (2H, m, Ar–H); δ_C ($(CD_3)_2CO$, 100 MHz) 41.27, 63.08, 64.60, 104.38, 125.02, 128.69, 129.24, 129.36, 129.76 (×2), 129.86, 131.81, 150.51; found $[M + H]^+$ = 330.1140, $C_{18}H_{19}NO_3S$ requires $[M + H]^+$ = 330.1158.

4-(Dimethylamino)-6-(4-methoxyphenyl)-3-phenyl-3,4-dihydro-1,2-oxathiine 2,2-dioxide 10g from **9h** (24.4 mmol) as off-white microcrystals (7.30 g, 83%) from EtOAc/hexane; mp = 123–124 °C; ν_{max} (neat) 2943, 2798, 1662, 1606, 1509, 1359 (SO_2–O), 1250, 1172 (SO_2–O), 1045, 984, 903, 818, 790, 698, 592 cm^{-1}; δ_H ($CDCl_3$, 400 MHz) 2.28 (6H, s, NMe_2), 3.85 (3H, s, OMe), 4.41 (1H, dd, J = 11.1, 2.6 Hz, 4-H), 4.55 (1H, d, J = 11.1 Hz, 3-H), 5.79 (1H, d, J = 2.5 Hz, 5-H), 6.92 (2H, app. d, J = 8.9 Hz, Ar–H), 7.44–7.46 (3H, m, Ar–H), 7.54–7.57 (4H, m, Ar–H); δ_C ($CDCl_3$, 100 MHz) 41.24, 55.42, 63.04, 64.60, 102.36, 114.04, 124.36, 126.54, 129.21, 129.49, 129.70, 129.76, 150.37, 160.86; found $[M + H]^+$ = 360.1264, $C_{19}H_{21}NO_4S$ requires $[M + H]^+$ = 360.1264.

4-(Dimethylamino)-6-(4-trifluoromethylphenyl)-3-phenyl-3,4-dihydro-1,2-oxathiine 2,2-dioxide 10h from **9i** (14.4 mmol) as off-white microcrystals (3.67 g, 64%) from EtOAc/hexane; mp = 125–127 °C; ν_{max} (neat) 2981, 1615, 1497, 1455, 1375 (SO_2–O), 1322, 1167 (SO_2–O), 1114, 1066, 990, 903, 785, 733, 698, 566, 500 cm^{-1}; δ_H ($CDCl_3$, 400 MHz) 2.29 (6H, s, NMe_2), 4.46 (1H, dd, J = 11.2, 2.4 Hz, 4-H), 4.62 (1H, d, J = 11.2 Hz, 3-H), 6.06 (1H, d, J = 2.4 Hz, 5-H), 7.45–7.47 (3H, Ar–H), 7.54–7.57 (2H, m, Ar–H), 7.67 (2H, app d, J = 8.4 Hz, Ar–H), 7.75 (2H, app d, J = 8.4 Hz, Ar–H); δ_C ($CDCl_3$, 100 MHz) 41.29, 63.05, 64.67, 106.77, 123.77 (q, J = 272 Hz), 125.31, 125.74 (q, J = 3.8 Hz), 128.99, 129.33, 129.73, 129.94, 131.66 (q, J = 32.9 Hz), 135.09, 149.23; δ_F ($CDCl_3$, 376 MHz) −62.80; found $[M + H]^+$ = 398.1033, $C_{19}H_{18}F_3NO_3S$ requires $[M + H]^+$ = 398.1032.

4-(Dimethylamino)-3-phenyl-6-(pyridin-4-yl)-3,4-dihydro-1,2-oxathiine 2,2-dioxide 10i from **9j** (29 mmol) as orange-yellow microcrystals (0.95 g, 10%) from 2 × EtOAc; mp = 124–126 °C; ν_{max} (neat) 3046, 2979, 2942, 2800, 2359, 1651, 1594, 1548, 1495, 1474, 1454, 1410, 1368 (SO_2–O), 1315, 1278, 1220, 1178 (SO_2–O), 1117, 1099, 1072, 1056, 1040 cm^{-1}; δ_H ($CDCl_3$, 400 MHz) 2.29 (6H, s, NMe_2), 4.45 (1H, dd, J = 11.2, 2.6 Hz, 4-H), 4.61 (1H, d, J = 11.2 Hz, 3-H), 6.17 (1H, d, J = 2.6 Hz, 5-H), 7.46–7.51 (5H, m, Ar–H), 7.54–7.56 (2H, m, Py–H), 8.68–8.70 (2H, m, Py–H); δ_C ($CDCl_3$, 100 MHz) 41.35, 63.20, 64.62, 108.46, 118.70, 128.82, 129.34, 129.71, 129.97, 138.99, 148.14, 150.49; found $[M + H]^+$ = 331.1117, $C_{17}H_{18}N_2O_3S$ requires $[M + H]^+$ = 331.1111.

4-(Dimethylamino)-6-(2-nitrophenyl)-3-phenyl-3,4-dihydro-1,2-oxathiine 2,2-dioxide 10j from **9k** (22.7 mmol) as off-white microcrystals (6.40 g, 75%) from EtOAc/hexane; mp = 125–127 °C; ν_{max} (neat) 2950, 2835, 2778, 1530, 1471, 1356 (SO_2–O), 1182 (SO_2–O), 1109, 1034, 985, 902, 848, 805, 705, 569 cm^{-1}; δ_H ($CDCl_3$, 400 MHz) 2.28 (6H, s, NMe_2), 4.40 (1H, dd, J = 11.3, 2.1 Hz, 4-H), 4.63 (1H, d, J = 11.3 Hz, 3-H), 5.63 (1H, d, J = 2.1 Hz, 5-H), 7.45–7.47 (3H, m, Ar–H), 7.55–7.57 (2H, m, Ar–H), 7.60–7.63 (2H, m, Ar–H), 7.67–7.70 (1H, m, Ar–H), 7.98 (1H, d, J = 7.9 Hz, Ar–H); δ_C ($CDCl_3$, 100 MHz) 41.24, 63.29, 64.54, 109.08, 124.55, 127.68, 128.90, 129.27, 129.77, 129.85, 130.94, 131.39, 133.13, 147.39, 148.04; found $[M + H]^+$ = 375.1008, $C_{18}H_{18}N_2O_5S$ requires $[M + H]^+$ = 375.1015.

4-(Dimethylamino)-5-(2-fluorophenyl)-6-methyl-3-phenyl-3,4-dihydro-1,2-oxathiine 2,2-dioxide 16 from **15** (23.1 mmol) as off-white microcrystals (6.62 g, 79%) from EtOAc/hexane; mp = 130–132 °C; ν_{max} (neat) 2919, 2833, 2785, 1612, 1487, 1359 (SO_2–O), 1230, 1159 (SO_2–O), 1143, 1106, 1037, 934, 853, 829, 742, 618, 553 cm^{-1}; δ_H ($CDCl_3$, 400 MHz, 295 K) 1.92 (3H, s, 6-Me), 2.04 (6H, s, NMe_2), 4.61 (1H, bs, 4-H), 4.78 (1H, d, J = 9.5 Hz, 3-H), 7.10–7.20 (2H, m, Ar–H), 7.28–7.36 (2H, m, Ar–H), 7.44–7.49 (3H, m, Ar–H), 7.62–7.64 (2H, m, Ar–H); δ_F ($CDCl_3$, 376 MHz) −114.5 to −112.7; δ_C ($CDCl_3$, 100 MHz) 18.58, 40.69, 62.47, 68.93, 69.59, 115.66, 115.89, 116.19,† 123.99, 124.66, 124.81, 127.26, 128.14, 129.30, 129.35, 129.43, 129.58, 129.89, 130.08, 130.57, 130.80, 131.04,† 133.75, 148.32, 158.94, 161.38.

1-(Dimethylamino)-2-phenyl-1,2,5,6-tetrahydronaphtho[1,2-*e*][1,2]oxathiine 3,3-dioxide 19 from **18** (61.4 mmol) as off-white microcrystals (14.18 g, 65%) from EtOAc/hexane; mp = 154–156 °C; ν_{max} (neat) 2946, 2832, 2788, 1666, 1467, 1363 (SO_2–O), 1169 (SO_2–O), 1139, 1026, 937, 829, 805, 765, 698, 571 cm^{-1}; δ_H ($CDCl_3$, 400 MHz) 2.14 (6H, s, NMe_2), 2.48 (1H, ddd, J = 2.4, 7.0, 17.1, 5-H), 2.65–2.75 (1H, m, 5-H), 2.86 (1H, ddd, J = 2.5, 6.3, 17.1 Hz, 6-H), 3.00–3.09 (1H, m, 6-H), 4.80 (1H, dd, J = 3.0, 8.9 Hz, 1-H), 4.90 (1H, d, J = 8.9 Hz, 2-H), 7.16–7.27 (4H, m, Ar–H), 7.43–7.50 (3H, m, Ar–H), 7.62–7.65 (2H, m, Ar–H); δ_C ($CDCl_3$, 100 MHz) 27.71, 28.26, 40.10, 61.34, 65.47, 115.60, 125.17, 126.34, 126.80, 127.34, 129.35, 129.71, 129.98, 131.32, 132.00, 133.88, 151.02; found $[M + H]^+$ = 356.1314, $C_{20}H_{21}NO_3S$ requires $[M + H]^+$ = 356.1320.

δ_H ($CDCl_3$, 500 MHz, 233 K)* 1.89 (3H, app. t, J = 1.5 Hz, 6-Me), 1.97 (3H, d, J = 1.7 Hz, 6-Me), 2.01 (12H, bs, NMe_2), 4.52 (1H, ddd, J = 1.5, 3.5, 9.7 Hz, 4-H), 4.76 (1H, ddd, J = 1.7, 3.5, 9.9 Hz, 4-H), 4.80 (1H, d, J = 9.7 Hz, 3-H), 4.87 (1H, d, J = 9.9 Hz, 3-H), 7.07–7.39 (8H, m, Ar–H), 7.43–7.52 (6H, m, Ar–H), 7.60–7.68 (4H, m, Ar–H); δ_C ($CDCl_3$, 126 MHz) 18.84, 19.07, 40.62, 61.55, 61.84, 67.69, 69.73, 114.63, 115.71, 115.88,

115.98, 116.16, 117.39, 124.03, 124.05, 124.30, 124.33, 124.45, 124.65, 124.78, 129.46, 129.52, 129.61, 129.67, 129.90, 129.97, 130.33, 131.92, 148.24, 148.53, 158.77, 159.32, 160.71, 161.28.

δ_H ($CDCl_3$, 500 MHz, 323 K) 1.89 (3H, dd, J = 0.8, 1.8 Hz, 6-Me), 2.04 (6H, s, NMe_2), 4.55 (1H, app. d, J = 9.5 Hz, 4-H), 4.73 (1H, d, J = 9.5 Hz, 3-H), 7.05–7.17 (2H, m, Ar–H), 7.22–7.32 (2H, m, Ar–H), 7.37–7.45 (3H, m, Ar–H), 7.56–7.63 (2H, m, Ar–H); δ_C ($CDCl_3$, 126 MHz) 18.43, 40.58, 62.80, 69.30, 115.64, 115.82, 123.91, 123.94, 124.78, 124.90, 129.08, 129.46, 129.50, 129.56, 129.87, 131.01, 148.35, 159.25, 161.21; found $[M + H]^+$ = 362.1215, $C_{19}H_{20}FNO_3S$ requires $[M + H]^+$ = 362.1226.

*At this temperature there are two rotamers present in solution. †Very broad signal and approximate position is given.

General method for the preparation of dihydro-1,2-oxathiine 2,2-dioxides from methanesulfonyl chloride

A solution of methanesulfonyl chloride (1.1 eq.) in anhydrous THF (50 mL) under a nitrogen atmosphere was added dropwise over 15 minutes to an ice cold (0–5 °C) vigorously stirred solution of the enaminoketone (1.0 eq.) and triethylamine (1.125 eq.) in anhydrous THF (60 mL for a typical 20 mmol scale reaction) under nitrogen. Upon completion of the addition the ice-water bath was removed and the resulting solution was stirred until TLC examination of the reaction mixture indicated that no starting enaminoketone remained (typically stirred overnight). The reaction mixture was filtered through a sinter containing chromatography silica (*ca.* 20 mm depth) with further THF (*ca.* 200 mL) used to wash any remaining product from the silica. The THF and excess triethylamine were removed from the filtrate by rotary evaporation to afford the crude product which was then suspended in EtOAc (*ca.* 100 mL) and washed with water (3 × 50 mL) and brine (50 mL). The EtOAc layer was dried (anhyd. Na_2SO_4) and then evaporated to give the crude product which was purified by either column chromatography or crystallization. The following dihydro-1,2-oxathiine 2,2-dioxides were obtained in this manner:

4-(Dimethylamino)-5,6-diphenyl-3,4-dihydro-1,2-oxathiine 2,2-dioxide 12a from **9a** (27.4 mmol) as off-white microcrystals (10.03 g, 53%) from EtOAc/hexane; mp = 157–159 °C; ν_{max} (neat) 3398, 2830, 2781, 1658, 1493, 1443, 1370 (SO_2–O), 1339, 1280, 1260, 1225, 1192, 1173 (SO_2–O), 1149, 1114, 1101, 1072, 1045, 1004 cm^{-1}; δ_H ($(CD_3)_2CO$, 400 MHz) 2.30 (6H, s, NMe_2), 3.78 (1H, dd, J = 9.1, 14.0 Hz, 3-H), 3.95 (1H, dd, J = 7.4, 14.0 Hz, 3-H), 4.46 (1H, dd, J = 7.4, 9.1 Hz, 4-H), 7.14–7.23 (10H, m, ArH); δ_C ($CDCl_3$, 100 MHz) 40.13, 42.63, 63.92, 121.71, 127.66, 127.82, 128.14, 128.99, 129.15, 129.90, 132.94, 136.38, 148.47; found $[M + H]^+$ = 330.1155, $C_{18}H_{19}NO_3S$ requires $[M + H]^+$ = 330.1158.

6-(4-Methoxyphenyl)-1,2-oxathiine 2,2-dioxide 13b and 4-(dimethylamino)-6-(4-methoxyphenyl)-3,4-dihydro-1,2-oxathiine 2,2-dioxide 12b from **9b** (19.9 mmol) after elution from silica with 50% EtOAc in hexanes increasing to 80% EtOAc in hexanes after elution of fraction 1.

Fraction 1: **6-(4-Methoxyphenyl)-1,2-oxathiine 2,2-dioxide 13b** as off-white microneedles (2.38 g, 50%) from EtOAc/hexane, mp = 86–88 °C; ν_{max} (neat) 1603, 1547, 1507, 1345 (SO_2–O), 1173 (SO_2–O), 1022, 920, 759, 708, 646, 530 cm^{-1}; δ_H ($CDCl_3$, 400 MHz) 3.86 (3H, s, MeO), 6.31 (1H, d, J = 6.8 Hz, 5-H), 6.58 (1H, d, J = 10.0 Hz, 3-H), 6.91 (1H, dd, J = 10.0, 6.8 Hz, 4-H), 6.93–6.96 (2H, m, Ar–H), 7.64–7.67 (2H, m, Ar–H); δ_C ($CDCl_3$, 100 MHz) 55.52, 98.43, 114.45, 117.60, 123.11, 127.52, 134.87, 157.58, 162.18; found $[M + H]^+$ = 239.0375, $C_{11}H_{10}O_4S$ requires $[M + H]^+$ = 239.0373.

Fraction 2: **4-(dimethylamino)-6-(4-methoxyphenyl)-3,4-dihydro-1,2-oxathiine 2,2-dioxide 12b** as off-white microcrystals (2.28 g, 40%) from EtOAc/hexane, mp = 104–105 °C; ν_{max} (neat) 2928, 2831, 2780, 1613, 1486, 1355 (SO_2–O), 1317, 1259, 1246, 1171 (SO_2–O), 1110, 1028, 989, 967, 843, 831, 818, 766, 570, 549 cm^{-1}; δ_H ($CDCl_3$, 400 MHz) 2.37 (6H, s, NMe_2), 3.25 (1H, dd, J = 13.3, 11.4 Hz, 3-H), 3.50 (1H, ddd, J = 13.3, 6.3, 1.0 Hz, 3-H), 3.83 (3H, s, OMe), 4.15 (1H, ddd, J = 11.4, 6.3, 2.6 Hz, 4-H), 5.65 (1H, dd, J = 2.6, 1.0 Hz, 5-H), 6.88–6.92 (2H, m, Ar–H), 7.48–7.52 (2H, m, Ar–H); δ_C ($CDCl_3$, 100 MHz) 40.64, 42.75, 55.40, 59.46, 103.00, 114.02, 124.30, 126.45, 150.45, 160.85; found $[M + H]^+$ = 284.0956, $C_{13}H_{17}NO_4S$ requires $[M + H]^+$ = 284.0951.

Method for the addition of phenylsulfene to 3-(dimethylamino)-2-phenylacrylaldehyde 21

A solution of phenylmethanesulfonyl chloride (7.07 g, 37.1 mmol) in anhydrous THF (70 mL) under a nitrogen atmosphere was added dropwise over 15 minutes to an ice cold (0–5 °C) vigorously stirred solution of the crude 3-(dimethylamino)-2-phenylacrylaldehyde **21** (5.0 g, 28 mmol) and triethylamine (5.4 mL, 38 mmol) in anhydrous THF (100 mL) under nitrogen. Upon completion of the addition the ice-water bath was removed and the resulting solution was stirred until TLC examination of the reaction mixture indicated that no starting enaminoketone remained (30 h). The reaction mixture was filtered through a sinter containing chromatography silica (*ca.* 20 mm depth) with further THF (*ca.* 100 mL) used to wash any remaining product from the silica. The THF and excess triethylamine were removed from the filtrate by rotary evaporation to give the crude product as a multicomponent viscous brown sludge which was chromatographed on silica using CH_2Cl_2 (5–100% in hexanes) to MeOH (2% in CH_2Cl_2) gradient as eluent. The fractions eluting at R_f values of 0.15 and 0.38 (TLC eluent CH_2Cl_2 40% in hexanes) were collected. The band with R_f = 0.38 was further chromatographed on silica using CH_2Cl_2 (40% in hexanes) as eluent and the solvent removed under reduced pressure. The residue was crystallised from hot toluene/hexanes to give **3,5-diphenyl-1,2-oxathiine 2,2-dioxide 23** (0.71 g, 9%) as a cream powder. The solvent was reduced to give a second crop (0.24 g, 3%) as a pale-yellow powder; mp = 90–91 °C; ν_{max} (neat) 2989, 2932, 2850, 1634, 1496, 1454, 1362 (SO_2–O), 1174 (SO_2–O), 1108, 1082, 1048, 955, 841, 765, 759, 732, 697, 620, 570, 540, 474 cm^{-1}; δ_H ($CDCl_3$, 400 MHz) 7.07 (1H, d, J = 2.1 Hz, 6-H‡), 7.23 (1H, d, J = 2.1 Hz, 4-H‡), 7.54–7.40 (8H, m, Ar–H), 7.70–7.63 (2H, m, Ar–H); δ_C ($CDCl_3$, 100 MHz) 122.37, 126.43, 127.95, 128.89, 129.11, 129.26, 129.95, 130.25, 130.34, 133.45, 136.07, 142.11; found

$[M + NH_4]^+$ = 302.0850, $C_{16}H_{12}O_3S$ requires $[M + NH_4]^+$ = 302.0845.

‡ ^1H NMR assignments may be reversed.

The fraction with R_f = 0.15 was crystallised from chloroform/hexanes to give **4-(dimethylamino)-3,5-diphenyl-3,4-dihydro-1,2-oxathiine 2,2-dioxide 22** (0.27 g, 3%) as a cream powder. The solvent was reduced to give a second crop (0.20 g, 2%) as a pale orange powder; mp = 145–150 °C (dec.); ν_{max} (neat) 2953, 2839, 1556, 1494, 1449, 1359 (SO_2–O), 1285, 1175 (SO_2–O), 1131, 1002, 974, 688, 664, 643, 622, 595, 582, 560, 512, 459 cm^{-1}; δ_H ($CDCl_3$, 400 MHz) 2.08 (6H, s, NMe_2), 4.77 (1H, dd, J = 9.7, 1.5 Hz, 4-H), 4.66 (1H, d, J = 9.7 Hz, 3-H), 6.66 (1H, d, J = 1.5 Hz, 6-H), 7.32–7.42 (5H, m, Ar–H), 7.45–7.52 (3H, m, Ar–H), 7.62–7.69 (2H, m, Ar–H); δ_C ($CDCl_3$, 100 MHz) 40.55, 62.52, 67.44, 127.11, 127.52, 128.09, 128.38, 129.30, 129.76, 129.90, 130.63, 135.48, 138.12; found $[M + H]^+$ = 330.1178, $C_{18}H_{19}NO_3S$ requires $[M + H]^+$ = 330.1158.

General method for the preparation of 1,2-oxathiine 2,2-dioxides

A solution of 3-chloroperoxybenzoic acid (1.2 eq., *ca.* 77%) in dichloromethane (40 mL) was added dropwise over 15 minutes to an ice cold (*ca.* 0–5 °C) vigorously stirred solution of the 3,4-dihydro-1,2-oxathiine 2,2-dioxide (1.0 eq.) in dichloromethane (70 mL for a typical 12 mmol scale reaction). Upon completion of the addition the cooling bath was removed and the resulting solution was stirred until TLC indicated that no starting 3,4-dihydro-1,2-oxathiine 2,2-dioxide remained (*ca.* 24 h). The mixture was transferred into a separating funnel and diluted with dichloromethane (50 mL). The mixture was washed with aq. sodium thiosulfate solution (5 × 100 mL, 10% aq.) followed by washing with dilute NaOH (3 × 50 mL, 1 M aq.) solution and finally with water (100 mL). The dichloromethane solution was dried with anhydrous Na_2SO_4 and then the solvent was removed by rotary evaporation to afford the crude product which was further purified by crystallization from EtOAc/hexane. The following compounds were obtained by this protocol:

3,5,6-Triphenyl-1,2-oxathiine 2,2-dioxide 11a from **10a** (12.3 mmol) as pale yellow microcrystals (3.15 g, 71%) from EtOAc/hexane; mp = 159–160 °C; ν_{max} (neat) 3060, 1621, 1540, 1444, 1368 (SO_2–O), 1349, 1186 (SO_2–O), 1130, 1011, 972, 851, 771, 697, 605, 524 cm^{-1}; δ_H ($CDCl_3$, 400 MHz) 7.03 (1H, s, 4-H), 7.25–7.39 (10H, m, Ar–H), 7.46–7.50 (3H, m, Ar–H), 7.67–7.71 (2H, m, Ar–H); δ_C ($CDCl_3$, 100 MHz) 118.99, 127.74, 128.21, 128.35, 129.05, 129.13, 129.20, 129.28, 129.90, 129.95, 130.27, 131.11, 133.99, 134.11, 135.80, 152.14; found $[M + NH_4]^+$ = 378.1158, $C_{22}H_{16}O_3S$ requires $[M + NH_4]^+$ = 378.1158.

5,6-Diphenyl-3-(4-(trifluoromethyl)phenyl)-1,2-oxathiine 2,2-dioxide 11b from **10b** (4.2 mmol) as pale yellow microcrystals (1.38 g, 73%) from EtOH; mp = 161–163 °C; ν_{max} (neat) 3060, 1617, 1576, 1557, 1488, 1446, 1415, 1365 (SO_2–O), 1350, 1324, 1275, 1170 (SO_2–O), 1116, 1068, 1035, 1016, 1008 cm^{-1}; δ_H ($(CD_3)_2CO$, 400 MHz) 7.32–7.44 (10H, m, Ar–H), 7.54 (1H, s, 4-H), 7.89 (2H, app. d, J = 8 Hz, Ar–H), 8.02 (2H, app. d, J = 8 Hz, Ar–H); δ_C ($(CD_3)_2CO$, 100 MHz) 118.99, 123.74 (q, J = 270.0 Hz), 126.02 (q, J = 3.7 Hz), 128.07, 128.30, 128.55, 129.08, 129.32, 130.60, 130.82, 131.68 (q, J = 33 Hz), 132.62, 133.44, 135.41, 135.61, 153.03; δ_F ($CDCl_3$, 376 MHz) −63.32; found $[M + NH_4]^+$ = 428.0707, $C_{23}H_{15}F_3O_3S$ requires $[M + NH_4]^+$ = 428.0694.

5,6-Bis(4-methoxyphenyl)-3-phenyl-1,2-oxathiine 2,2-dioxide 11c from **10c** (9.13 mmol) as bright yellow microcrystals (3.60 g, 94%) from EtOAc/hexane; mp = 129–131 °C; ν_{max} (neat) 3006, 2935, 2838, 1604, 1506, 1462, 1354 (SO_2–O), 1256, 1243, 1171 (SO_2–O), 1130, 1106, 1032, 972, 835, 788, 697, 589 cm^{-1}; δ_H ($CDCl_3$, 400 MHz) 3.80 (3H, s, OMe), 3.82 (3H, s, OMe), 6.75–6.77 (2H, m, Ar–H), 6.87–6.89 (2H, m, Ar–H), 6.98 (1H, s, 4-H), 7.18–7.21 (2H, m, Ar–H), 7.29–7.31 (2H, s, Ar–H), 7.43–7.46 (3H, m, Ar–H), 7.64–7.67 (2H, m, Ar–H); δ_C ($CDCl_3$, 100 MHz) 55.32, 55.34, 113.68, 114.65, 117.22, 123.60, 127.64, 128.21, 129.00, 129.71, 130.11, 130.28, 130.57, 130.88, 133.08, 134.56, 151.92, 159.45, 160.94; found $[M + NH_4]^+$ = 438.1370, $C_{24}H_{20}O_5S$ requires $[M + NH_4]^+$ = 438.1370.

(6-Benzyl-3,5-diphenyl-1,2-oxathiine 2,2-dioxide 11d from **10d1** (4.8 mmol) as colourless microcrystals (1.21 g, 68%) from EtOAc/hexane; mp = 110–111 °C; ν_{max} (neat) 3062, 3026, 1634, 1601, 1576, 1557, 1493, 1454, 1444, 1421, 1365 (SO_2–O), 1349, 1286, 1264, 1224, 1175 (SO_2–O), 1155, 1105, 1072, 1031, 1002 cm^{-1}; δ_H ($CDCl_3$, 400 MHz) 3.78 (2H, s, CH_2), 6.85 (1H, s, 4-H), 7.21–7.47 (13H, m, Ar–H), 7.59–7.62 (2H, m, Ar–H); δ_C ($CDCl_3$, 100 MHz) 37.52, 119.73, 127.18, 127.74, 128.59, 128.68, 128.82, 128.88, 129.00, 129.07, 129.88, 129.91, 132.65, 133.89, 135.11, 135.32, 154.48; found $[M + NH_4]^+$ = 392.1315, $C_{23}H_{18}O_3S$ requires $[M + NH_4]^+$ = 392.1315.

(2,2-Dioxido-3,6-diphenyl-1,2-oxathiin-5-yl)(phenyl)methanone 11e from **10e** (9.2 mmol) as pale yellow microcrystals (2.64 g, 74%) after elution from silica CH_2Cl_2 (60–100% gradient) in hexanes and crystallization from EtOAc/hexanes; mp = 129–130 °C; ν_{max} (neat) 1655, 1612, 1558, 1369 (SO_2–O), 1256, 1242, 1175 (SO_2–O), 1090, 922, 882, 711, 684, 544 cm^{-1}; δ_H ($CDCl_3$, 400 MHz) 7.21–7.31 (6H, m, Ar–H, s, 4-H), 7.35–7.39 (1H, m, Ar–H), 7.48–7.49 (5H, m, Ar–H), 7.68–7.71 (2H, m, Ar–H), 7.73–7.76 (2H, m, Ar–H); δ_C ($CDCl_3$, 100 MHz) 117.60, 127.88, 128.51, 128.54, 129.13, 129.42, 129.64, 129.68, 130.23, 130.44, 132.03, 133.75, 134.78, 136.03, 157.77, 193.27; found $[M + NH_4]^+$ = 406.1112, $C_{23}H_{16}O_4S$ requires $[M + NH_4]^+$ = 406.1108.

3,6-Diphenyl-1,2-oxathiine 2,2-dioxide 11f from **10f** (1.52 mmol) as pale yellow microcrystals (0.34 g, 79%) from CH_2Cl_2; mp = 130–132 °C; ν_{max} (neat) 3063, 1633, 1559, 1493, 1447, 1353 (SO_2–O), 1336, 1264, 1173 (SO_2–O), 1071, 1031, 1010 cm^{-1}; δ_H ($CDCl_3$, 400 MHz) 6.58 (1H, d, J = 7.1 Hz, 5-H), 6.96 (1H, d, J = 7.1 Hz, 4-H), 7.50–7.47 (6H, m, Ar–H), 7.67–7.64 (2H, m, Ar–H), 7.83–7.77 (2H, m, Ar–H); δ_C ($CDCl_3$, 100 MHz) 101.60, 125.49, 127.66, 128.98, 129.01, 129.05, 129.87, 130.12, 130.65, 131.13, 134.48, 156.02; found $[M + H]^+$ = 284.0511, $C_{16}H_{12}O_3S$ requires $[M + H]^+$ = 284.0507.

6-(4-Methoxyphenyl)-3-phenyl-1,2-oxathiine 2,2-dioxide 11g from **10g** (11.8 mmol) as yellow microcrystals (3.00 g, 81%) from EtOAc/hexane; mp = 173–174 °C; ν_{max} (neat) 2984, 2939, 2842, 1626, 1604, 1547, 1507, 1456, 1361 (SO_2–O), 1253, 1182,

1168 (SO_2–O), 1117, 999, 815, 787, 695, 569 cm^{-1}; δ_H ($CDCl_3$, 400 MHz) 3.89 (3H, s, OMe), 6.44 (1H, d, J = 7.2 Hz, 5-H), 6.93 (1H, d, J = 7.2 Hz, 4-H), 6.97–7.01 (2H, m, Ar–H), 7.44–7.50 (3H, m, Ar–H), 7.652–7.65 (2H, m, Ar–H), 7.71–7.74 (2H, m, Ar–H); δ_C ($CDCl_3$, 100 MHz) 55.52, 99.88, 114.47, 123.17, 127.31, 127.56, 129.00, 129.41, 129.62, 130.31, 133.21, 156.19, 162.03; found $[M + NH_4]^+$ = 332.0953, $C_{17}H_{14}O_4S$ requires $[M + NH_4]^+$ = 332.0951.

6-(4-Trifluoromethylphenyl)-3-phenyl-1,2-oxathiine 2,2-dioxide 11h from **10h** (4.3 mmol) as yellow microcrystals (1.09 g, 72%) from EtOAc/hexane; mp = 139–140 °C; ν_{max} (neat) 3049, 1629, 1615, 1366 (SO_2–O), 1328, 1301, 1177 (SO_2–O), 1116, 1065, 957, 870, 757, 690, 581 cm^{-1}; δ_H ($CDCl_3$, 400 MHz) 6.64 (1H, d, J = 7.1 Hz, 5-H), 6.95 (1H, d, J = 7.1 Hz, 4-H), 7.46–7.49 (3H, m, Ar–H), 7.61–7.66 (2H, m, Ar–H), 7.72 (2H, app d, J = 8.3 Hz, Ar–H), 7.87 (2H, app d, J = 8.3 Hz, Ar–H); δ_C ($CDCl_3$, 100 MHz) 103.36, 123.61 (q, J = 272 Hz), 125.65, 126.02 (q, J = 3.8 Hz), 127.72, 128.40, 129.13, 129.76, 130.21, 132.54 (q, J = 33 Hz), 133.93 (q, J = 1.4 Hz), 135.82, 154.23; δ_F ($CDCl_3$, 376 MHz) −62.96; found $[M + NH_4]^+$ = 370.0723, $C_{17}H_{11}F_3O_3S$ requires $[M + NH_4]^+$ = 370.0719.

3-Phenyl-6-(pyridin-4-yl)-1,2-oxathiine 2,2-dioxide 11i from **10i** (1.82 mmol) as pale-yellow microcrystals (0.37 g, 72%) from EtOAc/hexane; mp = 141–143 °C; ν_{max} (neat) 3053, 1637, 1594, 1550, 1492, 1447, 1410, 1352 (SO_2–O), 1326, 1267, 1250, 1222, 1175 (SO_2–O), 1067, 1023 cm^{-1}; δ_H ($CDCl_3$, 400 MHz) 6.74 (1H, d, J = 6.9 Hz, 4-H), 6.95 (1H, d, J = 6.9 Hz, 5-H), 7.48–7.63 (7H, m, Ar–H, Py–H), 8.74–8.76 (2H, m, Py–H); δ_C ($CDCl_3$, 100 MHz) 104.47, 118.63, 127.79, 127.91, 129.18, 129.59, 130.43, 136.99, 137.81, 150.74, 153.14; found $[M + H]^+$ = 286.0533, $C_{15}H_{11}NO_3S$ requires $[M + H]^+$ = 286.0532.

6-(2-Nitrophenyl)-3-phenyl-1,2-oxathiine 2,2-dioxide 11j from **10j** (2.67 mmol) as pale-yellow microcrystals (0.76 g, 86%) from EtOAc/hexane; mp = 208–210 °C; ν_{max} (neat) 2914, 2842, 1642, 1568, 1519, 1368 (SO_2–O), 1178 (SO_2–O), 1061, 1030, 788, 550 cm^{-1}; δ_H (DMSO-d_6, 400 MHz) 6.86 (1H, d, J = 7.2 Hz, 5-H), 7.41 (1H, d, J = 7.2 Hz, 4-H), 7.51–7.55 (3H, m, Ar–H), 7.62–7.67 (2H, m, Ar–H), 7.80–7.90 (3H, m, Ar–H), 8.10 (1H, d, J = 7.9 Hz, Ar–H); δ_C (DMSO-d_6, 100 MHz) 106.99, 125.02, 128.00, 129.67, 129.71, 130.64, 131.83, 133.07, 134.11, 134.14, 147.86, 152.65; found $[M + NH_4]^+$ = 347.0693, $C_{16}H_{11}NO_5S$ requires $[M + NH_4]^+$ = 347.0696.

5-(2-Fluorophenyl)-6-methyl-3-phenyl-1,2-oxathiine 2,2-dioxide 17 from **16** (5.1 mmol†) as colourless needles (1.25 g, 78%) from EtOAc/hexane; mp = 98–99 °C; ν_{max} (neat) 1651, 1579, 1491, 1359 (SO_2–O), 1264, 1155 (SO_2–O), 971, 782, 719, 568 cm^{-1}; δ_H ($CDCl_3$, 400 MHz) 2.15 (3H, s, 6-Me), 6.76 (1H, s, 4-H), 7.15–7.31 (3H, m, Ar–H), 7.37–7.43 (4H, m, Ar–H), 7.59–7.62 (2H, m, Ar–H); δ_C ($CDCl_3$, 100 MHz) 18.65, 112.69, 116.30 (d, J = 21.7 Hz), 122.82 (d, J = 15.2 Hz), 124.63 (d, J = 3.7 Hz), 127.73, 128.99, 129.83, 129.87, 130.68 (d, J = 8.1 Hz), 131.25 (d, J = 2.6 Hz), 132.21, 133.26, 155.18, 159.67 (d, J = 246.6 Hz); found $[M + NH_4]^+$ = 334.0911, $C_{17}H_{13}FO_3S$ requires $[M + NH_4]^+$ = 334.0908. †An additional 0.2 eq. of *m*-CPBA with an additional 24 h reaction time was required.

2-Phenyl-5,6-dihydronaphtho[1,2-*e*][1,2]oxathiine 3,3-dioxide 20 from **19** (14.1 mmol) as off-white microcrystals (4.20 g, 96%) from EtOAc/hexane; mp = 126–128 °C; ν_{max} (neat) 2889, 1634, 1583, 1364 (SO_2–O), 1184, 1171 (SO_2–O), 1158, 1090, 973, 925, 778, 755, 734, 690, 557 cm^{-1}; δ_H ($CDCl_3$, 400 MHz) 2.81 (2H, t, J = 8.0 Hz, 6-H), 3.06 (2H, t, J = 8.0 Hz, 5-H), 7.21–7.34 (5H, m, Ar–H, 1-H), 7.45–7.48 (3H, m, Ar–H), 7.63–7.65 (2H, m, Ar–H); δ_C ($CDCl_3$, 100 MHz) 26.82, 27.88, 113.35, 122.87, 127.34, 127.75, 127.86, 127.89, 128.25, 129.07, 129.91, 130.37, 130.49, 132.99, 135.00, 155.91; found $[M + NH_4]^+$ = 328.1002, $C_{18}H_{14}O_3S$ requires $[M + NH_4]^+$ = 328.1002.

5,6-Diphenyl-1,2-oxathiine 2,2-dioxide 13a from **12a** (6.6 mmol) as off-white microcrystals (1.87 g, 72%) from EtOAc/hexane; mp = 154–155 °C; ν_{max} (neat) 3079, 1616, 1574, 1545, 1487, 1444, 1372, 1356 (SO_2–O), 1294, 1237, 1182 (SO_2–O), 1164, 1149, 1093, 1069, 1033, 1005 cm^{-1}; δ_H ($CDCl_3$, 400 MHz) 6.73 (1H, d, J = 10.2 Hz, 3-H), 7.03 (1H, d, J = 10.2 Hz, 1H, 4-H), 7.18–7.34 (10H, m, Ar–H); δ_C ($CDCl_3$, 100 MHz) 117.49, 118.83, 128.20, 128.33, 129.00, 129.18, 129.46, 130.45, 131.10, 135.29, 139.32, 153.63; found $[M + H]^+$ = 285.0587, $C_{16}H_{12}O_3S$ requires $[M + H]^+$ = 285.0580.

6-(4-Methoxyphenyl)-1,2-oxathiine 2,2-dioxide 13b from **12b** (10.6 mmol) as pale fawn microneedles (2.02 g, 80%) by trituration from Et_2O; mp = 86–88 °C; ν_{max} (neat) 1603, 1547, 1507, 1345 (SO_2–O), 1173 (SO_2–O), 1022, 920, 759, 708, 646, 530 cm^{-1}; δ_H ($CDCl_3$, 400 MHz) 3.86 (3H, s, MeO), 6.31 (1H, d, J = 6.8 Hz, 5-H), 6.58 (1H, d, J = 10.0 Hz, 3-H), 6.91 (1H, dd, J = 10.0, 6.8 Hz, 4-H), 6.93–6.96 (2H, m, Ar–H), 7.64–7.67 (2H, m, Ar–H); δ_C ($CDCl_3$, 100 MHz) 55.52, 98.43, 114.45, 117.60, 123.11, 127.52, 134.87, 157.58, 162.18; found $[M + H]^+$ = 239.0375 $C_{11}H_{10}O_4S$ requires $[M + H]^+$ = 239.0373.

Acid-catalysed dehydration of 10d2: alternative preparation of (6-benzyl-3,5-diphenyl-1,2-oxathiine 2,2-dioxide 11d

4-(Dimethylamino)-3,5,6-triphenyl-3,4-dihydro-1,2-oxathiine 2,2 dioxide **10d2** (0.50 g, 1.2 mmol) was dissolved in PhMe (60 mL) and mixed with 4-TsOH (0.046 g, 0.24 mmol, 20 mol%) at room temperature. The reaction mixture was heated under reflux overnight, with the colour of the mixture gradually turning orange. Upon full consumption of the starting material, as confirmed by TLC, the solvent was removed under reduced pressure. Purification of the crude product by column chromatography (neutral alumina, dry loading, 10% EtOAc in petroleum ether (bp 60–80 °C)) gave 6-benzyl-3,5-diphenyl-1,2-oxathiine 2,2-dioxide **11d** as colourless microcrystals in 15% yield which was identical to material previously obtained by the Cope elimination reaction on **10d1**.

Addition of phenylsulfene to (*Z*)-2,2-dimethyl-3-(pyrrolidin-1-ylmethylene)chroman-4-one 26

A solution of phenylmethanesulfonyl chloride (1.17 g, 6.12 mmol) in anhydrous THF (15 mL) under a nitrogen atmosphere was added dropwise over 10 minutes to an ice cold (−10 to 0 °C) vigorously stirred solution of the pyrrolidinomethylenechromanone **26** (1.5 g, 5.8 mmol) and triethylamine (0.90 mL, 6.4 mmol) in anhydrous THF (25 mL) under nitrogen. The resulting solution was stirred and allowed to warm room temperature over *ca.* 4 hours. The mixture was filtered

through a sinter containing a little chromatography silica (1 cm depth) and then the THF and excess Et_3N were removed by rotary evaporation to afford the crude product which was further purified by recrystallization from ethyl acetate and hexane to afford 5,5-dimethyl-3-phenyl-4-(pyrrolidin-1-yl)-4,5-dihydro-3*H*-[1,2]oxathiino[5,6-*c*]chromene 2,2-dioxide **28** as a yellow solid (1.29 g, 54%); mp 134–136 °C; ν_{max} (neat) 2980, 2932, 2823, 1660, 1485, 1456, 1372 (SO_2–O), 1184 (SO_2–O), 1034, 935, 880, 830, 768, 702, 516, 508 cm^{-1}; δ_H ($CDCl_3$, 400 MHz)‡ 1.46 (3H, s, 5-Me), 1.56–1.70 (7H, m, $(CH_2)_2$, s, 5-Me), 2.47 (2H, bs, NCH_2), 2.59–2.64 (2H, m, NCH_2), 4.61 (1H, d, J = 7.6 Hz, 4-H), 4.94 (1H, d, J = 7.6 Hz, 3-H), 6.86 (1H, d, J = 8.1 Hz, 7-H), 6.95–6.99 (1H, m, 9-H), 7.22–7.27 (1H, m, 8-H), 7.40 (1H, dd, J = 7.7, 1.4 Hz, 10-H), 7.42–7.48 (3H, m, Ar–H), 7.53–7.56 (2H, m, Ar–H); δ_C ($CDCl_3$, 100 MHz) 23.6, 25.4, 26.4, 47.6, 61.9, 62.0, 79.8, 116.6, 117.9, 121.2, 122.3, 129.4, 129.69, 129.73, 131.0, 131.7, 153.4; found $[M + H]^+$ 412.1575, $C_{23}H_{25}NO_4S$ requires $[M + H]^+$ 412.1577. ‡The ^1H NMR spectrum of the crude isolated product indicated a mixture of diastereoisomers in a *ca.* 20 : 3 ratio.

Addition of phenylsulfene to (*Z*)-2,2,6-trimethyl-3-(pyrrolidin-1-ylmethylene)thiochroman-4-one 27

A solution of phenylmethanesulfonyl chloride (1.14 g, 5.98 mmol) in anhydrous THF (15 mL) under a nitrogen atmosphere was added dropwise over 10 minutes to an ice cold (−10 to 0 °C) vigorously stirred solution of the pyrrolidinomethylenethiochromanone **27** (1.53 g, 5.32 mmol) and excess Et_3N (0.87 mL, 6.2 mmol) in anhydrous THF (25 mL) under nitrogen. The resulting yellow solution was then allowed to warm to room temperature and stirred. After the reaction was judged to be complete by TLC examination (5 h) the mixture was filtered through a sinter containing chromatography silica (1 cm depth) and the THF and triethylamine were removed by rotary evaporation to afford the crude product which was further purified by elution from silica with 20% EtOAc in *n*-hexanes to afford the 5,5,9-trimethyl-3-phenyl-4-(pyrrolidin-1-yl)-4,5-dihydro-3*H*-thiochromeno[3,4-*e*][1,2]oxathiine 2,2-dioxide **29** as a yellow solid (1.00 g, 43%); mp 146–148 °C; ν_{max} (neat) 2939, 2865, 1626, 1598, 1537, 1462, 1372 (SO_2–O), 1266, 1160 (SO_2–O), 1133, 827, 782, 403 cm^{-1}; δ_H ($CDCl_3$, 400 MHz) 1.55 (3H, s, 5-Me), 1.62 (3H, s, 5-Me), 1.68–1.75 (4H, m, $(CH_2)_2$), 2.35 (3H, s, 9-Me), 2.61–2.65 (4H, m, $N(CH_2)_2$), 4.61 (1H, d, J = 5.2 Hz, 4-H), 4.91 (1H, d, J = 5.2 Hz, 3-H), 7.08 (1H, dd, J = 7.9, 1.0 Hz, 8-H), 7.19 (1H, d, J = 7.9 Hz, 7-H), 7.42–7.47 (4H, m, Ar–H, 10-H), 7.52–7.54 (2H, m, Ar–H); δ_C ($CDCl_3$, 100 MHz) 21.2, 23.8, 26.9, 27.5, 43.9, 47.0, 62.4, 63.2, 122.2, 124.9, 126.9, 127.4, 129.37, 129.39, 129.8, 130.4, 133.2, 135.4, 145.6; found $[M + H]^+$ 442.1500, $C_{24}H_{27}NO_3S_2$ requires $[M + H]^+$ 442.1505.

Addition of phenylsulfene to (*Z*)-3-((dimethylamino)methylene)isothiochroman-4-one 33

A solution of phenylmethanesulfonyl chloride (2.80 g, 14.7 mmol) in anhydrous THF (50 mL) under a nitrogen atmosphere was added dropwise over 10 minutes to a cold (~0 °C) vigorously stirred solution of (*Z*)-3-((dimethylamino)methylene)isothiochroman-4-one **33** (2.80 g, 12.8 mmol) and excess Et_3N (2.14 mL, 15.3 mmol) in anhydrous THF (50 mL) under nitrogen. The resulting yellow suspension was then allowed to warm to room temperature and stirred. After the reaction was judged to be complete by TLC examination (7 h) the mixture was filtered through a sinter containing chromatography silica (30 mm depth) and the volatiles were removed by rotary evaporation to afford the crude product as a yellow solid which was recrystallized from EtOAc/hexanes to afford the 4-(dimethylamino)-3-phenyl-4,6-dihydro-3*H*-isothiochromeno[3,4-*e*][1,2]oxathiine 2,2-dioxide **34** as yellow microcrystals (3.55 g, 74.4%); mp 173–176 °C; ν_{max} (neat) 2981, 2875, 2796, 1490, 1448, 1364 (SO_2–O), 1183 (SO_2–O), 1161, 1008, 983, 947, 839, 792, 776, 697, 573, 533 cm^{-1}; δ_H ($CDCl_3$, 400 MHz)† 2.16 (6H, s, NMe_2(maj)), 2.18 (6H, s, NMe_2(min)), 3.56 (1H, d, J = 14.2 Hz, 6-H (maj)), 3.75 (1H, d, J = 14.2 Hz, 6-H(min)), 4.07 (1H, d, J = 14.2 Hz, 6-H(min)), 4.15 (1H, d, J = 14.2 Hz, 6-H(maj)), 4.59 (1H, d, J = 10.5 Hz, 4-H(maj)), 4.65 (1H, d, J = 6.4, 4-H(min)), 4.79 (1H, d, J = 10.5 Hz, 3-H(maj)), 4.88 (1H, d, J = 6.4, 3-H (min)), 7.15–7.21 (2H, m, Ar–H), 7.29–7.49 (11H, m, Ar–H), 7.57–7.63 (4H, m, Ar–H), 7.64–7.69 (1H, m, Ar–H(min)); δ_C ($CDCl_3$, 100 MHz) 30.71, 30.85, 40.99, 41.57, 62.67, 63.49, 66.53, 68.74, 118.74, 120.18, 122.51, 122.58, 126.56, 126.58, 127.52, 127.79, 128.33, 128.53, 129.17, 129.41, 129.75, 129.79, 129.89, 129.98, 130.01, 130.44, 130.65, 131.11, 140.60, 141.28; found $[M + H]^+$ 374.0876, $C_{19}H_{19}NO_3S_2$ requires $[M + H]^+$ 374.0879. †Sample present as an inseparable mixture of diastereoisomers by routine flash chromatography (ratio 1.7 : 1.0 based on relative integrals of ^1H NMR signals) where possible signals from the major (maj) and minor (min) isomer have been identified.

Preparation of 5,5-dimethyl-3-phenyl-5*H*-[1,2]oxathiino[5,6-*c*] chromene 2,2-dioxide 30

A solution of 3-chloroperoxybenzoic acid (*ca.* 77%, 1.64 g, 6.69 mmol) in dichloromethane (20 mL) was added dropwise over 15 minutes to an ice cold vigorously stirred solution of 5,5-dimethyl-3-phenyl-4-(pyrrolidin-1-yl)-4,5-dihydro-3*H*-[1,2]oxathiino[5,6-*c*]chromene 2,2-dioxide **20** (2.5 g, 6.1 mmol) in dichloromethane (50 mL). The orange solution was allowed to warm to room temperature and stirred for 48 hours. The mixture was then diluted with water and the CH_2Cl_2 layer was separated. The CH_2Cl_2 layer was washed with aqueous sodium thiosulfate (2 × 50 mL), washed with dilute aqueous sodium bicarbonate (4 × 50 mL) and then with water (50 mL). The orange solution was then dried with anhydrous sodium sulphate and the solvent was removed by rotary evaporation to afford the crude product which was further purified by column chromatography with 25% EtOAc in *n*-hexanes to afford the title product **30** as a pale yellow solid (1.02 g, 49%); mp 98–100 °C; ν_{max} (neat) 2976, 1633, 1549, 1482, 1362 (SO_2–O), 1352, 1170 (SO_2–O), 1053, 950, 833, 778, 695, 682, 563, 525 cm^{-1}; δ_H ($CDCl_3$, 400 MHz) 1.65 (6H, s, 5-Me), 6.75 (1H, s, 4-H), 6.88 (1H, dd, J = 8.2, 0.4 Hz, 7-H), 7.00–7.04 (1H, m, 9-H), 7.30–7.35 (1H, m, 8-H), 7.44–7.48 (3H, m, Ar–H), 7.55 (1H, dd,

J = 7.7, 1.5 Hz, 10-H), 7.62–7.64 (2H, m, Ar–H); δ_C ($CDCl_3$, 100 MHz) 27.3, 78.6, 114.7, 115.8, 117.1, 121.8, 122.9, 127.3, 127.7, 129.1, 130.0, 130.3, 132.9, 134.8, 146.9, 154.0; found $[M + H]^+$ 341.0843, $C_{19}H_{16}O_4S$ requires $[M + H]^+$ 341.0842.

Oxidation of 5,5,9-trimethyl-3-phenyl-4-(pyrrolidin-1-yl)-4,5-dihydro-3*H*-thiochromeno[3,4-*e*][1,2]oxathiine 2,2-dioxide 29

A solution of 3-chloroperoxybenzoic acid (*ca.* 77%, 4.59 g, 18.7 mmol) in dichloromethane (35 mL) was added dropwise over 15 minutes to an ice cold vigorously stirred solution of 5,5,9-trimethyl-3-phenyl-4-(pyrrolidin-1-yl)-4,5-dihydro-3*H*-thiochromeno[3,4-*e*][1,2]oxathiine 2,2-dioxide **29** (2.5 g, 5.7 mmol) in dichloromethane (50 mL). The cloudy orange/yellow solution was allowed to warm to room temperature and stirred until TLC examination of the reaction mixture indicated that no starting material remained (*ca.* 48 hours). The mixture was then diluted with water (200 mL) and the dichloromethane layer was separated. The CH_2Cl_2 layer was washed with aqueous sodium thiosulfate solution (2 × 50 mL), washed with dilute aqueous sodium bicarbonate solution (3 × 50 mL) and finally with water (100 mL). The orange/yellow solution was then dried with anhydrous sodium sulfate and solvent was removed by rotary evaporation to afford the crude product which was further purified by column chromatography using 40% EtOAc in *n*-hexanes to afford two fractions. Fraction 1, 5,5,9-trimethyl-3-phenyl-5*H*-thiochromeno[3,4-*e*][1,2]oxathiine 2,2,6,6-tetraoxide **31a** as a yellow solid (0.79 g, 32%); mp 161–163 °C; ν_{max} (neat) 2973, 1633, 1549, 1481, 1455, 1362 (SO_2–O), 1267 (SO_2), 1168 (SO_2–O), 1138 (SO_2), 946, 760, 697, 562 cm^{-1}; δ_H ($CDCl_3$, 400 MHz) 1.68 (6H, s, 5-Me), 2.53 (3H, s, 9-Me), 6.95 (1H, s, 4-H), 7.48–7.50 (4H, m, Ar–H, 8-H), 7.61–7.64 (2H, m, Ar–H), 7.76 (1H, s, 10-H), 7.96 (1H, d, J = 7.9 Hz, 7-H); δ_C ($CDCl_3$, 100 MHz) 20.1, 21.8, 58.1, 119.8, 125.5, 126.6, 126.7, 127.0, 127.8, 129.3, 129.5, 130.4, 130.7, 132.6, 137.3, 145.2, 146.5; found $[M + H]^+$ 403.0669, $C_{20}H_{18}O_5S_2$ requires $[M + H]^+$ 403.0668.

Fraction 2, 5,5,9-trimethyl-3-phenyl-5*H*-thiochromeno[3,4-*e*][1,2]oxathiine 2,2,6-trioxide **31b** as a yellow solid (1.19 g, 50%); mp 70–73 °C; ν_{max} (neat) 2976, 1633, 1548, 1455, 1363 (SO_2–O), 1172 (SO_2–O), 1298, 1267, 1124, 1083, 1036 (SO), 953, 901, 759, 734, 696, 564 cm^{-1}; δ_H ($CDCl_3$, 400 MHz) 1.46 (3H, s, 5-Me), 1.71 (3H, s, 5-Me), 2.49 (3H, s, 9-Me), 6.97 (1H, s, 4-H), 7.44 (1H, d, J = 7.9 Hz, 8-H), 7.48–7.51 (3H, m, Ar–H), 7.61–7.64 (2H, m, Ar–H), 7.70–7.72 (2H, app. d, J = 7.6 Hz, 7-H, 10-H); δ_C ($CDCl_3$, 100 MHz) 20.03, 21.62, 22.49, 55.27, 116.07, 124.53, 126.51, 127.78, 127.91, 129.20, 129.77, 129.81, 130.40, 132.74, 132.91, 136.61, 143.51, 148.28; found $[M + H]^+$ 387.0716, $C_{20}H_{18}O_4S_2$ requires $[M + H]^+$ 387.0719.

Preparation of 3-phenyl-6*H*-isothiochromeno[3,4-*e*][1,2]oxathiine 2,2,5,5-tetraoxide 35

A solution of 3-chloroperoxybenzoic acid (*ca.* 77%, 13.05 g, 58.23 mmol) was added portionwise over 15 minutes to an ice cold vigorously stirred solution of 4-(dimethylamino)-3-phenyl-4,6-dihydro-3*H*-isothiochromeno[3,4-*e*][1,2]oxathiine 2,2-dioxide **34** (3.0 g, 8.0 mmol) in dichloromethane (150 mL). The yellow suspension was allowed to warm to room temperature and stirred for 6 days. The mixture was then diluted with water (200 mL) and the CH_2Cl_2 layer was separated. The CH_2Cl_2 layer was washed with aqueous sodium sulfite solution (6 × 50 mL), washed with dilute aqueous sodium bicarbonate (5 × 50 mL) and then with water (100 mL). The yellow solution was then dried with anhydrous sodium sulphate and the solvent was removed by rotary evaporation to afford the crude product which was recrystallized from acetone/MeOH to afford the title product **35** as a pale yellow solid (2.21 g, 76%); mp 215–216 °C; ν_{max} (neat) 1610, 1381 (SO_2–O), 1307, 1155 (SO_2–O), 1053, 752, 684, 612, 543, 442 cm^{-1}; ^1H NMR ($(CD_3)_2CO$, 400 MHz) 5.00 (2H, s, 6-H), 7.54 (1H, s, 4-H), 7.61–7.63 (3H, m, Ar–H), 7.70–7.77 (3H, m, Ar–H), 7.79–7.83 (2H, m, Ar–H), 8.03–8.07 (1H, m, 10-H); ^{13}C NMR ($(CD_3)_2CO$, 100 MHz) 54.3, 118.7, 122.4, 124.8, 126.3, 128.0, 129.1, 129.3, 129.7, 130.2, 130.6, 130.8, 133.4, 136.0, 154.6; found $[M + K]^+$ = 398.9771 $C_{17}H_{12}O_5S_2$ requires $[M + K]^+$ = 398.9758.

Attempted preparation of 4-(dimethylamino)-3-phenyl-6-(*p*-tolyl)-3,4-dihydro-1,2,5-oxathiazine 2,2-dioxide 37 (Preparation of *N*-formyl-4-methylbenzamide 38)

A solution of phenylmethanesulfonyl chloride (3.98 g, 20.9 mmol) in anhydrous THF (40 mL) was added dropwise to a cold (−5 °C) stirred solution of (*E*)-*N*-((dimethylamino) methylene)-4-methylbenzamide (3.79 g, 19.9 mmol) and triethylamine (3.05 mL, 21.9 mmol) in anhydrous THF (50 mL) under nitrogen. The solution was allowed to warm to room temperature and stirred for 24 hours. Following TLC analysis, further triethylamine (3.05 mL, 21.9 mmol) was added to the reaction mixture which was cooled to −5 °C and a solution of phenylmethanesulfonyl chloride (3.98 g, 20.9 mL) in anhydrous THF (40 mL) was added dropwise to the reaction mixture. The reaction mixture was allowed to warm to room temperature stirred for 6 days. The reaction mixture was filtered through Celite and the solvent removed under vacuum. The resulting residue was purified by column chromatography (1% methanol in dichloromethane) to afford *N*-formyl-4-methylbenzamide **38** as the major fraction (2.00 g, 62%) as colourless needles; mp = 128–130 °C (lit. mp = 130–132 °C[49]); ν_{max} 1668, 1609, 1443, 1363, 1204, 1182, 11223, 1067, 1036, 834, 726, 677, 640, 608, 563, 471 cm^{-1}; ^1H NMR (400 MHz, $CDCl_3$) δ_H 10.1 (1H, bd, J = 8.2 Hz, NH), 9.38 (1H, d, J = 9.7 Hz, CHO), 7.89–7.87 (2H, m, Ar–H), 7.35–7.26 (2H, m Ar–H), 2.44 (3H, s, Ar–Me).

Preparation of (*E*)-3-(dimethylamino)-*N*-((*E*)-(dimethylamino) methylene)-2-phenylacrylamide 39

A stirred solution of 2-phenylacetamide (2.0 g, 15 mmol) in DMF·DMA (10 mL, 83 mmol) was heated in a distillation set up such that the produced MeOH was removed. After 4 h the reaction mixture was cooled to room temperature and the volume reduced under pressure. The crude yellow product was washed with hexane containing a little EtOAc and filtered to yield the title compound **39** (2.3 g, 63%) as pale yellow crystals;

mp 115–116 °C (lit. mp 112 °C[37]); ν_{max} (neat) 1601, 1553, 1495, 1435, 1421, 1384, 1328, 1283, 1266, 1204, 1172, 1087, 1063, 981, 947, 920, 890, 798, 738, 728, 700, 634, 568, 546 cm^{-1}; δ_H ($CDCl_3$, 400 MHz) 2.69 (6H, s, =CH-NMe_2), 3.02 (3H, s, NMe), 3.05 (3H, s, NMe), 7.15–7.28 (5H, m, Ar–H), 8.13 (1H, s, =CH-NMe_2), 8.42 (1H, s, N=CH-NMe_2); δ_C ($CDCl_3$, 100 MHz) 34.77, 40.90, 43.22, 107.60, 125.69, 127.12, 132.17, 138.28, 150.28, 158.39, 179.26; found $[M + H]^+$ = 246.1604 $C_{14}H_{19}N_3O$ requires $[M + H]^+$ = 246.1601.

Preparation of methyl *N*-((*E*)-3-(dimethylamino)-2-phenylacryloyl)formimidate 41

A stirred solution of 2-phenylacetamide (10.1 g, 75 mmol) in DMF-DMA (35 mL, 262 mmol) was heated at reflux for 24 h. The reaction mixture was cooled to room temperature and the volatiles removed under reduced under pressure. The resulting dark red oil was purified by column chromatography (1% methanol in dichloromethane) to afford the title compound **41** (6.8 g, 39%) as a pale-yellow powder; mp 65–66 °C; ν_{max} (neat) 1537, 1414, 1395, 1221, 1185, 1118, 1046, 1024, 770, 695 cm^{-1}; δ_H ($CDCl_3$, 400 MHz) 2.96 (3H, s, NMe), 3.02 (3H, s, NMe), 3.74 (3H, s, OMe), 7.22–7.18 (1H, m, Ar–H), 7.33–7.29 (2H, m, Ar–H), 7.48–7.45 (2H, m, Ar–H), 7.70 (1H, s, =CH-NMe_2), 8.04 (1H, s, N=CH-OMe); δ_C ($CDCl_3$, 100 MHz) 169.72, 160.72, 152.78, 135.43, 130.97, 127.14, 126.14, 117.16, 51.41, 40.48, 35.08; found $[M + H]^+$ = 233.1287 $C_{13}H_{16}N_2O_2$ requires $[M + H]^+$ = 233.1290.

Preparation of (*E*)-*N*′-(2,2-dioxido-3,5-diphenyl-1,2-oxathiin-6-yl)-*N*,*N*-dimethylformimidamide 42

A solution of phenylmethanesulfonyl chloride (3.03 g, 1.3 eq.) in THF (30 mL) was added dropwise over 10 min to a cold (0–5 °C) stirred solution of (*E*)-3-(dimethylamino)-*N*-((*E*)-(dimethylamino)methylene)-2-phenylacrylamide **39** (3.00 g, 12.2 mmol) in THF (35 mL) containing Et_3N (2.22 mL, 15.9 mmol, 1.3 eq.) under N_2. Additional amounts of phenylmethanesulfonyl chloride (0.3 eq.) and Et_3N (0.3 eq.) were added as required to ensure reaction completion. The resulting mixture was filtered through a layer of alumina (5 mm) and the THF was removed by rotary evaporation. The crude mixture was chromatographed on an alumina column (40% DCM in hexane) and the fractions containing the main component of the mixture were combined, washed with aq. sat. Na_2CO_3 (25 mL) and H_2O (2 × 25 mL) and dried over anhyd. Na_2SO_4. Recrystallization of the obtained solid from EtOAc/petroleum spirit (bp 40–60 °C) gave the title compound **42** (0.38 g, 9%) as yellow crystals; mp 145–147 °C; ν_{max} (neat) 3041, 2929, 1631, 1614, 1595, 1574, 1519, 1445, 1406, 1372, 1342 (O–SO_2), 1294, 1272, 1258, 1211, 1175 (O–SO_2), 1100, 1076, 1031 cm^{-1}; δ_H ($CDCl_3$, 400 MHz) 3.04 (3H, s, NCH_3), 3.15 (3H, s, NCH_3), 7.15 (1H, s, 4-H), 7.22–7.44 (6H, m, Ar–H), 7.57–7.60 (4H, m, Ar–H), 8.20 (1H, s, HC=N); δ_C ($CDCl_3$, 100 MHz) 35.44, 41.34, 104.76, 126.81, 127.17, 128.14, 128.59, 128.82, 129.12, 129.62, 131.49, 136.09, 136.80, 152.75, 153.42; found $[M + H]^+$ = 355.1111, $C_{19}H_{18}N_2O_3S$ requires $[M + H]^+$ = 355.1117.

Conflicts of interest

There are no conflicts to declare.

References

1 S. Mondal, *Chem. Rev.*, 2012, **112**, 5339–5355.
2 M. Sainsbury, Chapter 40: Compounds containing a Six-membered Ring having two Hetero-atoms from Group VIB of the Periodic Table: Dioxanes, Oxathianes and Dithianes, in *Rodd's Chemistry of Carbon Compounds*, 2nd edn, 1964, vol. IV, pp. 375–426; M. J. Cook, Chapter 2.26: Six-membered Rings with More than One Oxygen or Sulfur Atom, in *Comprehensive Heterocyclic Chemistry*, ed. A. J. Boulton and A. McKillop, 1984, vol. 3, pp. 943–994; E. Kleinpeter, Chapter 8.10: 1,2-Dioxins, Oxathiins, Dithiins, and their Benzo Derivatives, in *Comprehensive Heterocyclic Chemistry III*, ed. A. Aitken, 2008, vol. 8, pp. 677–738.
3 M. Zhang and C. Han, *US Patent*, US20180294483A1, 2018; K. Hatta, N. Shimosaka, M. Machida, M. Aoki and M. Miyamoto, *PCT Int. Appl*, WO2015107910A1, 2015.
4 J. H. Ko, Y. J. Ha, C. H. Lee, Y. M. Lim and J. A. Ahn, *Republic of Korea Patent*, KR2009084547 A, 2009; T. Aoai and A. Endo, *Japanese Patent*, JP2004144933A, 2004; F. Urano, M. Nakahata, H. Fujie and K. Ono, *Japanese Patent*, JP03223865A, 1991.
5 R. H. Eastman and D. Gallup, *J. Am. Chem. Soc.*, 1948, **70**, 864–865.
6 K. Rad-Moghadam, S. T. Roudsari and M. Sheykhan, *Synlett*, 2014, 0827–0830; S. T. Roudsari and K. Rad-Moghadam, *Tetrahedron*, 2018, **74**, 4047–4052.
7 J. Gaitzsch, V. Rogachev, P. Metz, V. D. Filimonov, M. Zahel and O. Kataeva, *J. Sulfur Chem.*, 2011, **32**, 3–16.
8 D. C. Craig and J. D. Stevens, *Carbohydr. Res.*, 2011, **346**, 854–857.
9 K. V. Kilway, K. A. Lindgren, J. W. Vincent, J. A. Watson Jr., R. B. Clevenger, R. D. Ingalls, D. M. Ho and R. A. Pascal Jr., *Tetrahedron*, 2004, **60**, 2433–2438.
10 E. Bonfand, W. B. Motherwell, A. M. K. Pennell, M. K. Uddin and F. Ujjainwalla, *Heterocycles*, 1997, **46**, 523–534.
11 Z. Qi, M. Wang and X. Li, *Chem. Commun.*, 2014, **50**, 9776–9778.
12 J. L. Charlton and G. N. Lypka, *Can. J. Chem.*, 1980, **58**, 1059–1060.
13 Th. Morel and P. E. Verkade, *Recueil*, 1951, **70**, 35–49.
14 O. Arjona, M. L. León and J. Plumet, *J. Org. Chem.*, 1999, **64**, 272–275.
15 R. P. van Summeren, B. L. Feringa and A. J. Minnaard, *Org. Biomol. Chem.*, 2005, **3**, 2524–2533.
16 K. A. Ali, A. Jäger and P. Metz, *ARKIVOC*, 2016, **iii**, 15–22.
17 J. Gaitzsch, V. Rogachev, P. Metz, M. S. Yusubov, V. D. Filimonov and O. Kataeva, *J. Sulfur Chem.*, 2009, **30**, 4–9; J. Gaitzsch, V. Rogachev and P. Metz, *Synthesis*, 2014, **46**, 0531–0536.

18 G. Opitz and E. Tempel, *Angew. Chem., Int. Ed. Engl.*, 1964, **3**, 754–755.
19 W. E. Truce, D. J. Abraham and P. Son, *J. Org. Chem.*, 1967, **32**, 990–997.
20 B. Zwanenburg, *Product class 3: thioaldehyde and thioketone S,S-dioxides and oxyimides (sulfenes and derivatives), Science of Synthesis*, 2004, vol. 27, pp. 123–134.
21 P. Schenone, G. Bignardi and S. Morasso, *J. Heterocycl. Chem.*, 1972, **9**, 1341–1346.
22 P. Schenone, L. Mosti and G. Bignardi, *J. Heterocycl. Chem.*, 1976, **13**, 225–230.
23 A. Bargagna, P. Schenone, F. Bondavalli and M. Longobardi, *J. Heterocycl. Chem.*, 1980, **17**, 1201–1206.
24 G. Menozzi, A. Bargagna, L. Mosti and P. Schenone, *J. Heterocycl. Chem.*, 1986, **23**, 455–458.
25 L. Mosti, P. Schenone, G. Menozzi and S. Cafaggi, *J. Heterocycl. Chem.*, 1982, **19**, 1031–1034.
26 L. Mosti, P. Schenone, G. Menozzi, G. Romussi and F. Baccichetti, *J. Heterocycl. Chem.*, 1982, **19**, 1227–1229.
27 S. Aiken, C. D. Gabbutt, B. M. Heron, C. R. Rice and D. Zonidis, *Org. Biomol. Chem.*, 2019, DOI: 10.1039/C9OB02128K.
28 A. C. Huitric, J. B. Carr, W. F. Trager and B. J. Nist, *Tetrahedron*, 1963, **19**, 2145–2151.
29 M. J. Fuchter, in *Name Reactions for Functional Group Transformations*, ed. J. Li and E. J. Corey, John Wiley & Sons, New York, 2007, pp. 343–353.
30 C. D. Gabbutt, J. D. Hepworth, B. M. Heron and S. L. Pugh, *J. Chem. Soc., Perkin Trans. 1*, 2002, 2799–2808.
31 C. D. Gabbutt, J. D. Hepworth, B. M. Heron, S. J. Coles and M. B. Hursthouse, *J. Chem. Soc., Perkin Trans. 1*, 2000, 2930–2938.
32 R. A. Aiken, C. Hauduc, M. S. Hossain, E. McHale, A. L. Schwan, A. M. Z. Slawin and C. A. Stewart, *Aust. J. Chem.*, 2014, **67**, 1288–1295.
33 Y.-i. Lin and S. A. Lang Jr., *Synthesis*, 1980, 119–121.
34 H. Bredereck, G. Simchen and B. Funke, *Chem. Ber.*, 1971, **104**, 2709–2726.
35 J. T. Gupton, K. E. Krumpe, B. S. Burnham, K. A. Dwornik, S. A. Petrich, K. X. Du, M. A. Bruce, P. Vu, M. Vargas, K. M. Keertikar, K. N. Hosein, C. R. Jones and J. A. Sikorski, *Tetrahedron*, 1998, **54**, 5075–5088.
36 A. Tanaka, Y. Motoyama and H. Takasugi, *Chem. Pharm. Bull.*, 1994, **42**, 1828–1834.
37 J. T. Gupton, N. Telang, E. J. Banner, E. J. Kluball, K. E. Hall, K. L. Finzel, X. Jia, S. R. Bates, R. S. Welden, B. C. Giglio, J. E. Eaton, P. J. Barelli, L. T. Firich, J. A. Stafford, M. B. Coppock, E. F. Worrall, R. P. F. Kanters, K. Keertikar and R. Osterman, *Tetrahedron*, 2010, **66**, 9113–9122.
38 J. Tois, M. Vahermo and A. Koskinen, *Tetrahedron Lett.*, 2005, **46**, 735–737.
39 Y. Li, X. Cao, Y. Liua and J.-P. Wan, *Org. Biomol. Chem.*, 2017, **15**, 9585–9589.
40 P. Schenone, L. Mosti and G. Menozzi, *J. Heterocycl. Chem.*, 1982, **19**, 1355–1361.
41 J. T. Gupton, E. J. Banner, A. B. Scharf, B. K. Norwood, R. P. F. Kanters, R. N. Dominey, J. E. Hempel, A. Kharlamova, I. Bluhn-Chertudi, C. R. Hickenboth, B. A. Little, M. D. Sartin, M. B. Coppock, K. E. Krumpe, B. S. Burnham, H. Holt, K. X. Du, K. M. Keertikar, A. Diebes, S. Ghassemi and J. A. Sikorski, *Tetrahedron*, 2006, **62**, 8243–8255.
42 J.-C. Zhuo, *Magn. Reson. Chem.*, 1996, **34**, 595–602.
43 S. Takano, Y. Imamura and K. Ogasawara, *Heterocycles*, 1982, **19**, 1223–1225.
44 D. Kumar, D. N. Kommi, P. Chopra, Md. I. Ansari and A. K. Chakraborti, *Eur. J. Org. Chem.*, 2012, 6407–6413.
45 W. Zhao, R. Wang, M. J. Mosey and A. Petitjean, *Org. Lett.*, 2011, **13**, 5160–5163.
46 S. A. Kozmin, T. Iwama, Y. Huang and V. H. Rawal, *J. Am. Chem. Soc.*, 2002, **124**, 4628–4641.
47 M. M. Abdelkhalik, A. M. Eltoukhy, S. M. Agamy and M. H. Elnagdi, *J. Heterocycl. Chem.*, 2004, **41**, 431–434.
48 S. Morimura, *Heterocycles*, 1980, **14**, 1449–1454.
49 Z. Niu, S. Lin, Z. Dong, H. Sun, F. Liang and J. Zhang, *Org. Biomol. Chem.*, 2013, **11**, 2460–2465.

Article 1: Short Communication

Title: 'Synthesis and photochromism of some mono and bis (thienyl) substituted oxathiine 2,2-dioxides'

Authors: Stuart Aiken, Christopher D. Gabbutt, B. Mark Heron*, Craig R. Rice and Dimitrios Zonidis*

Journal: Organic & Biomolecular Chemistry; Publisher: Royal Society of Chemistry

Citation: *Org. Biomol. Chem*., **2019**, *17*, 9578-9584; DOI: https://doi.org/10.1039/C9OB02128K

Date of Publication: 11th October 2019

Author contribution: This communication describes my investigations concerning the synthesis of novel photochromic 1,2-oxathiine 2,2-dioxides which features in Chapter 3 of this thesis. Under the guidance of Professor Heron, I completed the synthesis of all of the series of novel photochromic 1,2-oxathiine 2,2-dioxides, their precursors and their spectroscopic / purity characterization. I additionally characterized their photochromic response. I drafted the whole of the experimental section of the manuscript and contributed to the discussion sections and made revisions in accord with Professor Heron's suggestions.

Organic & Biomolecular Chemistry

COMMUNICATION

View Article Online
View Journal | View Issue

Cite this: Org. Biomol. Chem., 2019, 17, 9578

Received 1st October 2019,
Accepted 9th October 2019

DOI: 10.1039/c9ob02128k

rsc.li/obc

Synthesis and photochromism of some mono and bis (thienyl) substituted oxathiine 2,2-dioxides†

Stuart Aiken, Christopher D. Gabbutt, B. Mark Heron,* Craig R. Rice and Dimitrios Zonidis*

1,2-Oxathiine 2,2-dioxides have been obtained from their respective 3,4-dihydro-4-dimethylamino precursors, for the first time, by a mild Cope elimination of the 4-dimethylamino function. The application of the 1,2-oxathiine 2,2-dioxide scaffold in materials chemistry is exemplified by the efficient P-type photochromism of the 5,6-bis(2,5-dimethyl-3-thienyl) substituted oxathiine 2,2-dioxides.

P-type photochromic dithienylethenes such as **1-open**, which readily undergoes reversible conversion to the coloured isomer **1-closed**, (Scheme 1) are fundamental switching units which have been used to modulate a variety of physical and optical properties.[1] Structural variation of the essential 1,2-bis(2,5-dimethylthiophen-3-yl)ethene core has been frequently explored by modification of the 2,5-dimethylthiophene moiety[1,2] and to a somewhat lesser extent by variation of the perfluorocycle, particularly replacement of the latter with a 5-membered heterocyclic unit to afford **2**, wherein the heterocycle has been selected from imidazole,[3,4] imidazolium,[5] pyrrole,[6] thienophosphole,[7] phosphindolothiophene,[8] thiophene,[9–11] thiopyranothiophene,[12] silole,[13,14] 1,3-dithiole[15] and thiazole[16] and less commonly with a six-membered unit leading to **2** where the heterocyclic unit includes quinoxaline,[17] triazoloquinoline,[18] pyridazine,[19] thiazine,[20] 1,2-oxazine[21] and 1,2,4-triazine.[22]

We have previously studied the synthesis and performance of various T-type photochromic systems, *e.g.* naphthopyrans[23–25] and naphthoxazines,[26,27] and we have recently explored negatively photochromic systems.[28] In this study we describe the preliminary examples of an efficient synthetic route to the relatively little studied 1,2-oxathiine 2,2-dioxide unit and in doing so define a route to new photochromic dithienylethenes with a central 1,2-oxathiine 2,2-dioxide core.

Department of Chemical Sciences, School of Applied Sciences, University of Huddersfield, Queensgate, Huddersfield, HD1 3DH, UK. E-mail: m.heron@hud.ac.uk, dimitrios.zonidis@hud.ac.uk

† Electronic supplementary information (ESI) available: Experimental details and characterization data. CCDC 1905437. For ESI and crystallographic data in CIF or other electronic format see DOI: 10.1039/c9ob02128k

This work constitutes part of our ongoing programme of heterocyclic synthesis concerning strategies to 1,2-oxathiine 2,2-dioxides in which we are exploring the versatility of sulfene additions to enaminoketones to afford relatively inaccessible substitution patterns on the 4-dimethylamino-3,4-dihydro-1,2-oxathiine 2,2-dioxide core and subsequent mechanistic investigations concerning the elimination of the 4-dimethylamino function to access diversely substituted unsaturated 1,2-oxathiine 2,2-dioxides.[29]

The addition of sulfenes to enaminoketones to afford 4-amino-3,4-dihydro-1,2-oxathiine 2,2-dioxides has been explored by Schenone *et al.*[30] Interestingly, the formation of the unsaturated 1,2-oxathiine 2,2-dioxides was a relatively scarcely observed feature in these initial studies.[31] Indeed when chlorosulfene was added to an enaminoketone a subsequent facile base-promoted elimination of HCl was observed and the unsaturated 4-amino-1,2-oxathiine 2,2-dioxide resulted[32] and attempts to effect dehydrogenation of 4-amino-3,4-dihydro-1,2-oxathiine 2,2-dioxides using excess DDQ met with variable results.[33] We elected to utilise the foregoing sulfene addition chemistry[30,34] and explore the subsequent elimination step required to obtain the unsaturated 1,2-oxathiine 2,2-dioxides. Fundamental to the present study was access to a series of methylene ketones and whilst deoxybenzoin **11** is widely commercially available the isomeric thienylketones **9** and **10** and the 1,2-bis(2,5-dimethylthiophen-3-yl)ethan-1-one **6** required preparation (Scheme 2). Examination of the literature revealed that the 2,5-dimethylthienyl-3-acetic acid **4** has been prepared from 2,5-dimethylthiophene in three steps, acylation,

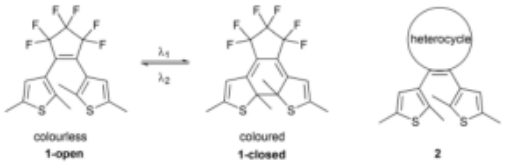

Scheme 1 Representative photochromic response of a dithienylethene system.

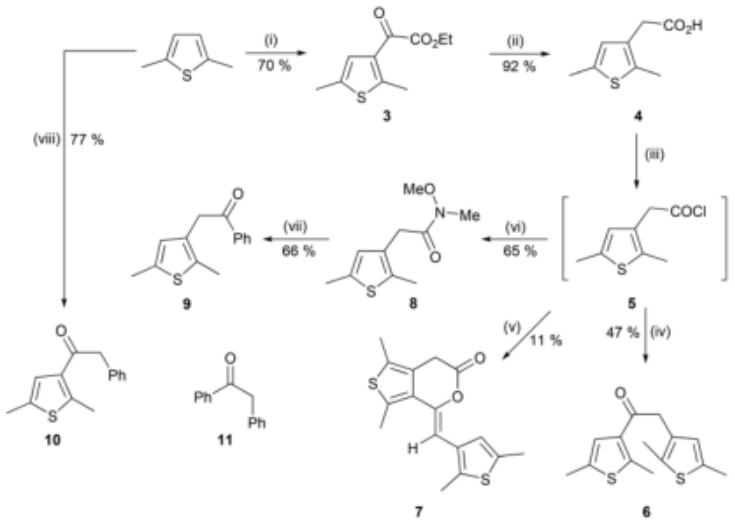

Scheme 2 Synthesis of thienyl ketones **6**, **9** and **10**. Reagents and conditions: (i) Ethyl oxalyl chloride, $AlCl_3$, anyhd., $MeNO_2$, 5 °C–RT; (ii) NH_2NH_2-H_2O, $HOCH_2CH_2OH$, then KOH, 70 °C – reflux; (iii) $SOCl_2$, cat. DMF, CH_2Cl_2; (iv) 2,5-dimethylthiophene, $AlCl_3$, anyhd., $MeNO_2$, 5 °C–RT; (v) PhH, $AlCl_3$, anyhd., $MeNO_2$, 5 °C–RT; (vi) MeNHOMe·HCl, pyridine, CH_2Cl_2, 0–5 °C–RT; (vii) PhLi in Bu_2O, anhyd., THF, N_2, –78 °C–RT; (viii) $PhCH_2COCl$, $AlCl_3$, anyhd., CH_2Cl_2, $MeNO_2$, 5 °C–RT.

Willgerodt–Kindler reaction and hydrolysis, in moderate overall yield.[35] Given the unappealing nature of this sequence we elected to examine an alternative protocol. Friedel–Crafts acylation of 2,5-dimethylthiophene with ethyl oxalyl chloride gave the glyoxalate **3** which underwent a smooth Wolff–Kishner reduction with concomitant hydrolysis to afford **4** in 64% yield (two-steps). The acid chloride **5** was prepared and used directly in a Friedel–Crafts acylation with 2,5-dimethylthiophene to afford **6** (47%) which displayed a characteristic singlet in its ^{1}H NMR spectrum at δ 3.92 assigned to the methylene unit. Interestingly, applying this Friedel–Crafts strategy to benzene failed to afford **9** and instead **5** underwent a 'homo Friedel–Crafts' reaction followed by cyclisation to afford the novel thieno[3,4-*c*]pyranone **7** (δ_{CH} 7.41; $\delta_{methylene}$ 3.67; $\delta_{C=O}$ 166.44); the geometry of which was established as the *Z*-isomer by a NOESY experiment. Evidently the thiophene moiety of **5** is more electron rich than benzene and is thus the favoured substrate in the foregoing acylation reaction. Undeterred by this setback, the Weinreb amide **8** (δ_{OMe} 3.60; δ_{NMe} 3.18; $\delta_{methylene}$ 3.59) was obtained (65%) from **5** by standard methodology.[36] The addition of PhLi to **8** proceeded without complication to afford target ketone **9** ($\delta_{methylene}$ 4.12) in 66% yield (Scheme 2).

Ketone **10** was readily prepared by the Friedel–Crafts reaction of phenylacetyl chloride with 2,5-dimethylthiophene in 77% yield. Here the characteristic methylene singlet appeared at δ 4.11 in the ^{1}H NMR spectrum.

Ketones **6**, **9–11** were transformed into their respective enaminoketones **12a–d** (60–86% yield) upon reaction with *N*,*N*-dimethylformamide dimethylacetal (DMFDMA) (Scheme 3). Phenylsulfene, generated *in situ* by the action of Et_3N on phenylmethanesulfonyl chloride, added cleanly to the foregoing enaminoketones to afford the 3,4-dihydro-1,2-oxathiine 2,2-dioxides **13a-open–d-open** (53–77%) after either chromatography or recrystallization. Oxathiine 2,2-dioxide **13e-open** was obtained in a similar manner in 55% yield from the addition of sulfene to **12a**. The ^{1}H NMR spectrum of **13e-open** revealed an AA′B spin pattern for the C-3 and C-4 hydrogens with $J_{3,4(trans)}$ = 9.1 Hz, $J_{3',4(cis)}$ = 7.8 Hz and $^2J_{3,3'}$ = 13.8 Hz.

Attempts to effect the acid elimination of dimethylamine from **13d-open** using increasing amounts of 4-TsOH (0.05–5 eq.) at either RT or reflux in PhMe were unsuccessful and at elevated temperature some yellowing of the reaction mixture was observed together the formation of minor amounts of polar 'degradation' material as indicated by TLC. The magnitude of the coupling constants between 3-H and 4-H ($^3J_{3,4}$ = 7.8–8.1 Hz) of the 3-phenyl substituted series **13a-open–13d-open** suggest that these protons occupy an *anti-peri*-planar arrangement.

A crystal of **13a-open** was obtained from Et_2O and hexane (stored at −20 °C for 24 h) and an X-ray crystal structure (Fig. 1) confirmed the arrangement of 3-H and 4-H which have a torsion angle of *ca.* 39.5° with the torsion angle between the 3-Ph and 4-NMe_2 moieties as 78.9°. The SO_2 unit of the oxathiine 2,2-dioxide ring protruded out of the main oxathiine ring plane (O1–C3–C4–C5–C6) with C3–S2–O1 angle of *ca.* 110°. The thiophene rings adopt an *anti*-parallel conformation which favours the reversible photocyclistion process.[1,2,37]

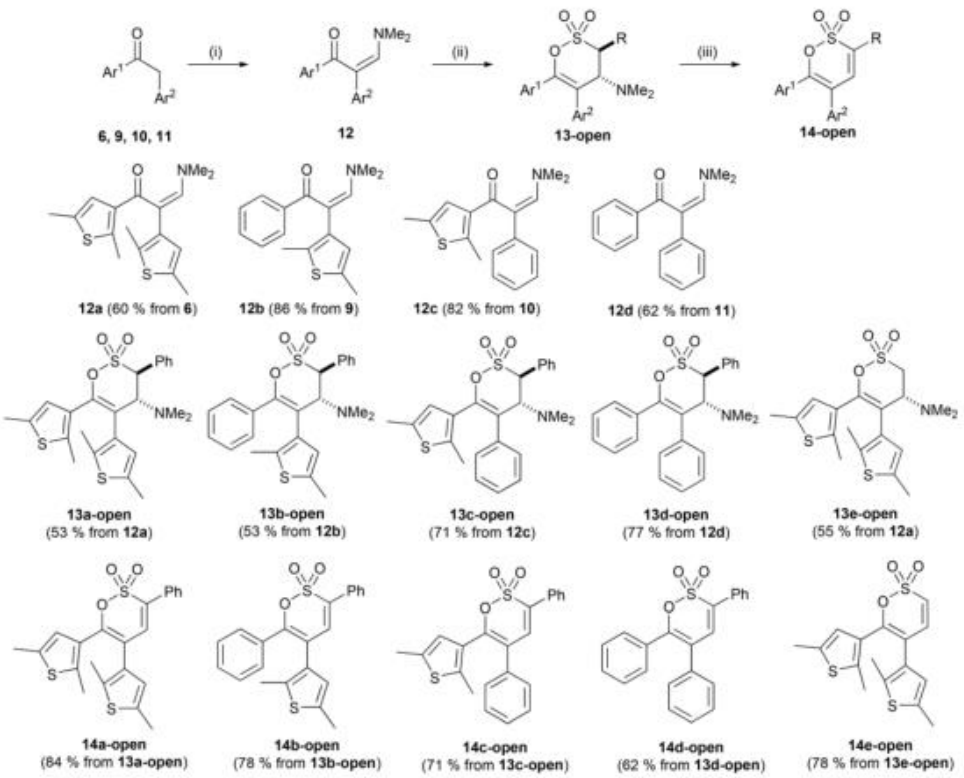

Scheme 3 Synthesis of thienyl substituted 1,2-oxathiine 2,2-dioxides. Reagents and conditions: (i) DMFDMA, reflux; (ii) either phenylmethanesulfonyl chloride (for **13a–d**) or methanesulfonyl chloride (for **13e**), Et_3N, anhyd. THF, 0 °C–RT; (iii) *m*-CPBA, CH_2Cl_2, 0 °C–RT.

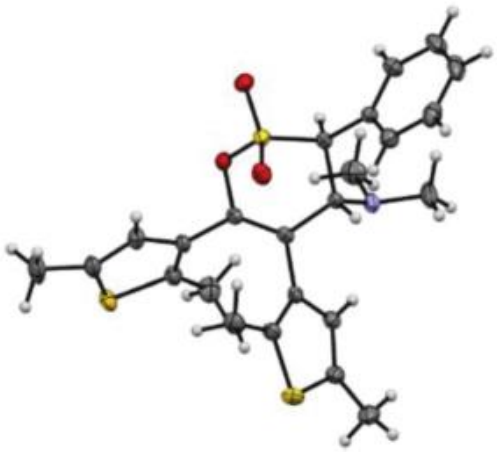

Fig. 1 Crystal structure of **13a-open** (thermal ellipsoids shown at 50% probability level and disordered Et_2O solvent molecule omitted for clarity).[38]

Given the *syn*-relationship between 3-H and the 4-NMe_2 moiety a Cope elimination protocol was adopted to affect the *syn*-elimination of the dimethylamine unit.[39] Pleasingly, treating a DCM solution of **13d-open** with an excess of *m*-CPBA (0–5 °C → RT, 4 h) afforded **14d-open** ($\delta_{4\text{-H}}$ 7.01) as pale-yellow crystals in 62% yield. Repeating this procedure enabled the isolation of **14a-open** (84%, $\delta_{4\text{-H}}$ 6.89), **14b-open** (78%, $\delta_{4\text{-H}}$ 6.89), **14c-open** (71%, $\delta_{4\text{-H}}$ 7.04) and **14e-open** (78%, $\delta_{3\text{-H}}$ 6.61, $\delta_{4\text{-H}}$ 6.90 ($J_{3,4}$ = 10.2 Hz)) without the detection of any S oxidised products (Scheme 3). This facile elimination protocol provides an efficient strategy to form unsaturated 1,2-oxathiine 2,2-dioxides from the 4-dialkylamino substituted 3,4-dihydro-1,2-oxathiine 2,2-dioxides which are easily obtained from sulfene additions to enaminoketones.

With the series of oxathiine 2,2-dioxides **13-open** and **14-open** to hand their photochromic response was examined. Irradiating hexane solutions of **13a-open**, **b-open**, **c-open** and **e-open** revealed very weak to moderate yellow – orange colour development (Table 1) due to photoinduced ring closure (Scheme 4) with λ_{max} in the range 413 to 441 nm after prolonged irradiation to a steady state (*ca.* 145 min, λ_{irr} =

Table 1 Photochromic response of series **13-open** and series **14-open**

	λ_{max}[a] (nm) Hexane	Absorbance at λ_{max}[b]			
		A_0	A_{PSS}	ε_m at PSS[c] (mol^{-1} dm^3 cm^{-1})	% closed form[d]
13a-open/13a-closed	414	0.01	0.55	1300	2
14a-open/14a-closed	503	0.03	0.82	1708	38
13b-open/13b-closed	413	0.01	0.23	489	5
14b-open/14b-closed	481	0.01	0.07	125	0.5
13c-open/13c-closed	474	0	0.03	61	2
14c-open/14c-closed	513	0	0.01	25	2
13e-open/13e-closed	441	0.01	0.38	1524	8
14e-open/14e-closed	494	0.01	0.94	1541	9

[a] Wavelength of maximum absorption of the closed species. [b] Absorbance A_0 before UV irradiation and absorbance A_{PSS} at photostationary state (PSS) for hexane solution of *ca.* 0.5 mmol dm^{-3}. [c] Molar extinction coefficient of closed form at photostationary state as calculated using the Beer–Lambert Law. [d] % closed form determined by comparison of the relative integrals of the signals for the thiophene ring methyl group protons in the original open forms and the closed forms at PSS.

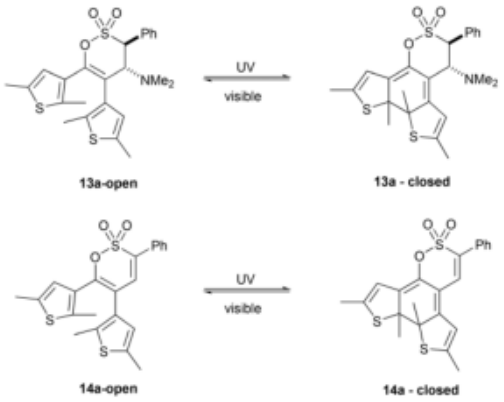

Scheme 4 Structures of **13a-open/14a-open** before and after irradiation.

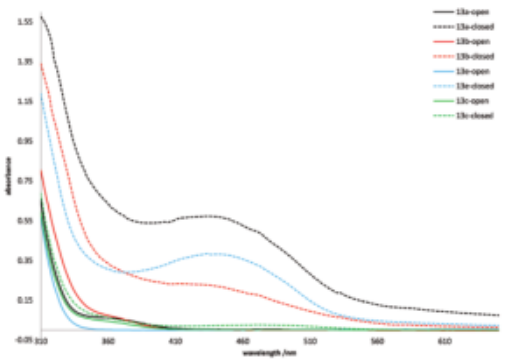

Fig. 2 Absorption spectra (in hexane) of 3,4-dihydro-1,2-oxathiine 2,2-dioxides **13a-open**, **b-open**, **c-open**, **e-open** before irradiation and at photostationary state.

260–380 nm, 150 W) (Fig. 2). ^{1}H NMR spectra for **13a-open** before and after irradiation are provided in the ESI.† The remaining 5,6-diphenyl analogue **13d-open** showed no photochromic response.

The photochromic behaviour of the unsaturated series **14a-open–e-open** was next examined in hexane solution. Irradiation of a hexane solution of **14a-open** resulted in the generation of an intense red hue (λ_{max} = 503 nm, PSS 45 min) (Fig. 3 and insert 1, Table 1) which is assigned to the ring-closed isomer **14a-closed** (Scheme 4). Visible light bleaching (455–650 nm) of the foregoing red solution of **14a-closed** was efficiently accomplished after 25 min. The colouration and bleaching of **14a-open** (PhMe solution) was repeated 10 times to illustrate the reversibility of the system (insert 2 on Fig. 3).

Repeating the irradiation experiment of **14a-open** in $CDCl_3$ and recording the ^{1}H NMR spectra over time revealed the presence of new signals attributed to **14a-closed** at δ 2.05 (Th-Me), 2.11 (Th-Me), 2.12 (Th-Me), 2.22 (Th-Me), 5.96 (Th-H) 6.07 (Th-H) and 6.83 (4-H) (Fig. 4). Comparison of the integrals for

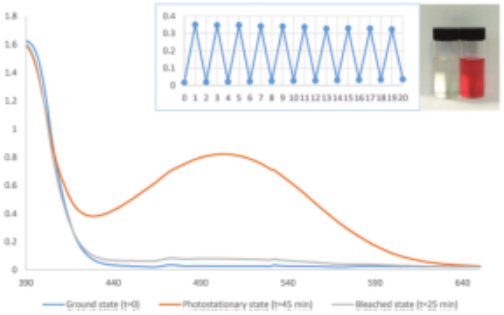

Fig. 3 Absorption spectra of **14a-open** (initial, after UV activation and after visible light bleaching); inset shows recyclability with UV activation and visible light bleaching cycles.

4-H in **14a-open** (δ = 6.89) and **14a-closed** (δ = 6.83) of the $CDCl_3$ solution revealed a ratio of *ca.* 5 : 3 (**14a-open**/**14a-closed**) at the photostationary state (Fig. 4, Table 1).

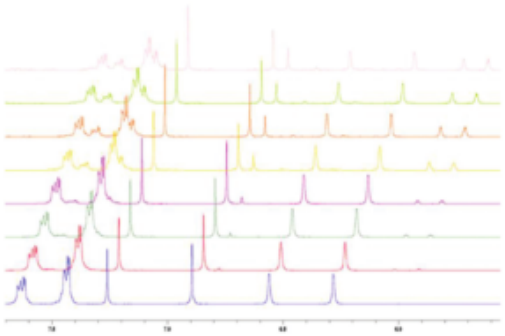

Fig. 4 ^{1}H NMR spectra (δ 5.5–7.7, $CDCl_3$) showing evolution of signals for photochemical ring-closure of **14a-open**.

Irradiation of **14e-open**, similarly substituted with 2,5-dimethylthiophen-3-yl units, offered inferior performance to **14a-open** with λ_{max} at 494 nm (50 min irradiation, ratio **14e-open** : **14e-closed** *ca.* 10 : 1 based on the relative integrals of the doublets for 3-H at δ 6.61 (open) and δ 6.38 (closed) (see ESI† for ^{1}H NMR spectra for **14e-open** before and after irradiation). In the ^{1}H NMR spectrum of **14e-closed** signals were observed at δ 2.18, 2.31, 2.39 and 2.64 for the methyl groups, at *ca.* δ 5.95 for the thiophene ring protons and at δ 6.82 (d, J = 10.3 Hz) for 4-H. Unfortunately, **14b-open** and **14c-open** only showed an exceptionally weak red hue upon irradiation to generate their ring-closed forms (Fig. 5) and the diphenyl analogue **14d** showed no photochromism, emphasising the requirement for at least one 2,5-dimethylthiophene unit on the central ethene bond.

Interestingly, the introduction of the C-3–C-4 double bond induced a bathochromic shift in λ_{max} of **14a-closed** (503 nm) and **14e-closed** (494 nm) relative to their dihydro precursors [**13a-closed** (414 nm), **13e-closed** (441 nm)] presumably as a result of the extended lateral conjugation. It should be noted that the conjugation with the C-3 phenyl group (**14a-open**)

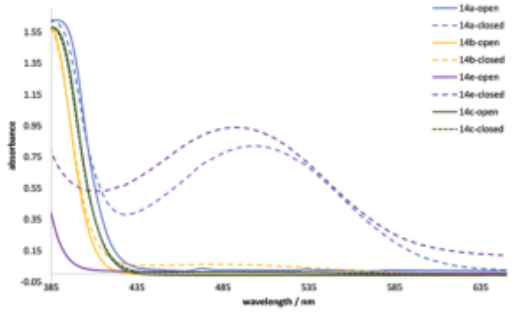

Fig. 5 Absorption spectra (in hexane) of oxathiine 2,2-dioxides **14a-open**, **b-open**, **c-open**, **e-open** before irradiation and at photostationary state.

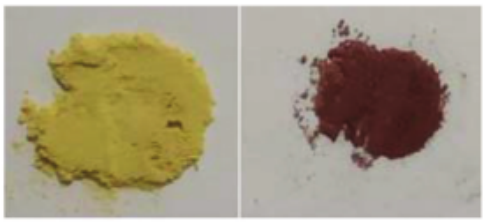

Fig. 6 Photograph of **14a-open** powdered sample on white paper background (LHS pre-irradiated, RHS post-irradiation).

resulted in the largest (89 nm) shift. The photochromic response of the series **13-open** and **14-open** is summarised in Table 1.

The solid-state photochromism of **14a-open** was also briefly examined; with a powdered sample irradiated for 30 s with a TLC inspection lamp (Spectroline E Series 365 nm, 8 Watt). The change in appearance of the sample is clearly visible from the photograph presented in Fig. 6 with the unirradiated sample appearing pale yellow and a post-irradiated sample developing a red/brown hue.

In summary, 1,2-oxathiine 2,2-dioxides with combinations of aryl and heteroaryl substituents have been efficiently obtained for the first time by a Cope elimination protocol from their respective 4-dimethylamino-3,4-dihydro precursors which were derived from sulfene additions to enaminoketones. The 3,4-dihydro-1,2-oxathiine 2,2-dioxide series **13** exhibited very weak photo-colouration (low percentage ring closed form and hence weak molar extinction coefficients), perhaps due to limited activation as a consequence of a relatively low degree of unsaturation resulting in a low absorption in the activating UV region. Of the series **13** the 5,6-bis(2,5-dimethylthien-3-yl) analogues **13a-open** and **13e-open** exhibited the best photochromism with UV irradiation generating their closed ring isomers which exhibited a weak yellow – orange hue. The series of unsaturated oxathiines **14** typically exhibited better photochromism then the dihydro precursors **13**. The oxathiine 2,2-dioxides **14a-open** and **14e-open** offered the best photochromism with λ_{max} of their closed ring forms bathochromically shifted relative to their dihydro-precursors, leading to moderately intense red-brown hues as a consequence of the extended lateral conjugation. The presence of a phenyl substituent on the oxathiine ring lead to a further small bathochromic shift in λ_{max} *viz.* **14a-open** (503 nm) and **14e-open** (494 nm). The photochromic response of **14a-open** and **14e-open** of this preliminary series of novel dithienylethenes containing a 1,2-oxathiine 2,2-dioxide core offered comparable performance to other heterocyclic bridged dithienylethenes.[17–22] However, it is clear from this study that for good photochromic performance the presence of two substituted thiophene units at the termini of the central ethene bond combined with further unsaturation in the central oxathiine moiety is essential.[1,2] Our exploration of the appli-

cation of the oxathiine moiety as the central core in photochromic systems continues and is presently focussed on both further extending the lateral conjugation using substituted (hetero)aromatic systems and enhancing the photocolouration process.

Conflicts of interest

There are no conflicts to declare.

Acknowledgements

DZ thanks the University of Huddersfield for funding for his PhD studies.

Notes and references

1 M. Irie, *Chem. Rev.*, 2000, **100**, 1685–1716.
2 M. Irie, T. Fukaminato, K. S. Matsuda and S. Kobatake, *Chem. Rev.*, 2014, **114**, 12174–12277.
3 D.-K. Cao, J.-S. Hu, M.-Q. Li, D.-P. Gong, X.-X. Li and M. D. Ward, *Dalton Trans.*, 2015, **44**, 21008–21015.
4 D.-P. Gong, T.-B. Gao, D.-K. Cao and M. D. Ward, *RSC Adv.*, 2016, **6**, 69677–69684.
5 S. Li, J. Tang, Y. Zhao, R. Jiang, T. Wang, G. Gao and J. You, *Chem. Commun.*, 2017, **53**, 3489–3492.
6 M. Yu. Belikov, *Russ. J. Org. Chem.*, 2018, **54**, 785–788.
7 N. M.-W. Wu, M. Ng, W. H. Lam, H.-L. Wong and V. W.-W. Yam, *J. Am. Chem. Soc.*, 2017, **139**, 15142–15150.
8 J. C.-H. Chan, H.-L. Wong, W.-T. Wong and V. W.-W. Yam, *Chem. – Eur. J.*, 2015, **21**, 6936–6948.
9 C.-L. Wong, C.-T. Poon and V. W.-W. Yam, *Organometallics*, 2017, **36**, 2661–2669.
10 C.-T. Poon, W. H. Lam, H.-L. Wong and V. W.-W. Yam, *Chem. – Eur. J.*, 2015, **21**, 2182–2192.
11 J. C.-H. Chan, W. H. Lam, H.-L. Wong, N. Zhu, W.-T. Wong and V. W.-W. Yam, *J. Am. Chem. Soc.*, 2011, **133**, 12690–12705.
12 S. Pang, D. Jang, W. S. Lee, H.-M. Kang, S.-J. Hong, S. K. Hwang and K.-H. Ahn, *Photochem. Photobiol. Sci.*, 2015, **14**, 765–774.
13 L. Bougdid, A. Samat and C. Moustrou, *New J. Chem.*, 2009, **33**, 1375–1361.
14 M. Cipolloni, F. Ortica, L. Bougdid, C. Moustrou, U. Mazzucato and G. Favaro, *J. Phys. Chem. A*, 2008, **112**, 4765–4771.
15 F. Ortica, P. Smimmo, C. Zuccaccia, U. Mazzucato, G. Favaro, N. Impagnatiello, A. Heyndericks and C. Moustrou, *J. Photochem. Photobiol., A*, 2007, **188**, 90–97.
16 M. M. Krayushkin, B. V. Lichitskii, A. P. Mikhalev, B. V. Nabatov, A. A. Dudinov and S. N. Ivanov, *Russ. J. Org. Chem.*, 2006, **42**, 860–864.
17 J. S. Park, T. T. Tran, J. Kim and J. L. Sessler, *Chem. Commun.*, 2018, **54**, 4553–4556.
18 M. M. Krayushkin, B. V. Lichitskii, D. V. Pashchenko, I. A. Antonov, B. V. Nabatov and A. A. Dudinov, *Russ. J. Org. Chem.*, 2007, **43**, 1357–1363.
19 M. M. Krayushkin, D. V. Pashchenko, B. V. Lichitsky, B. V. Nabatov, A. M. Komogortsev, L. G. Vorontsova and Z. A. Starikova, *Russ. Chem. Bull. Int. Ed.*, 2008, **57**, 2168–2174.
20 L. I. Belen'kii, A. V. Kolotaev, V. Z. Shirinyan, M. M. Krayushkin, Yu. P. Strokach, T. M. Valova, Z. O. Golotyuk and V. A. Barachevskii, *Chem. Heterocycl. Compd.*, 2005, **41**, 86–92.
21 K. P. Schultz, D. W. Spivey, E. K. Loya, J. E. Kellon, L. M. Taylor and M. R. McConville, *Tetrahedron Lett.*, 2016, **57**, 1296–1299.
22 S. N. Ivanov, B. V. Lichitskii, A. A. Dudinov, A. Yu. Martynkin and M. M. Krayushkin, *Chem. Heterocycl. Compd.*, 2001, **37**, 85–90.
23 J. D. Hepworth and B. M. Heron, in *Functional Dyes*, ed. S.-H. Kim, Elsevier, Amsterdam, 2006, pp. 85–135; J. D. Hepworth and B. M. Heron, *Prog. Heterocycl. Chem.*, 2007, **17**, 33–62.
24 S. Aiken, C. D. Gabbutt, B. M. Heron, C. S. Kershaw, N. J. Smith and J.-P. Cano, *US Patent*, US8703978B2, 2014.
25 S. Aiken, K. Booth, C. D. Gabbutt, B. M. Heron, C. R. Rice, A. Charaf-Eddin and D. Jacquemin, *Chem. Commun.*, 2014, **50**, 7900–7903.
26 D. A. Clarke, B. M. Heron, C. D. Gabbutt, J. D. Hepworth, S. M. Partington and S. N. Corns, *PCT Int. Appl*, WO9920630A1, 1999.
27 M. Rickwood, J. D. Hepworth, C. D. Gabbutt and S. D. Marsden, *Eur. Pat. Appl*, EP600669A1, 1994.
28 S. Aiken, R. J. L. Edgar, C. D. Gabbutt, B. M. Heron and P. A. Hobson, *Dyes Pigm.*, 2018, **149**, 92–121.
29 S. Aiken, K. Anozie, O. D. C. C. de Azevedo, L. Cowan, R. J. Edgar, C. D. Gabbutt, B. M. Heron, P. A. Lawrence, A. J. Mills, C. R. Rice, M. W. J. Urquhart and D. Zonidis, *Org. Biomol. Chem.*, 2019, DOI: 10.1039/C9OB01657K.
30 A. Bargagna, P. Schenone, F. Bondavalli and M. Longobardi, *J. Heterocycl. Chem.*, 1980, **17**, 1201–1206.
31 A. Bargagna, F. Evangelisti and P. Schenone, *J. Heterocycl. Chem.*, 1981, **18**, 111–116; F. Evangelisti, P. Schenone and A. Bargagna, *J. Heterocycl. Chem.*, 1979, **16**, 217–220.
32 A. Bargagna, P. Schenone, G. Bignardi and M. Longobardi, *J. Heterocycl. Chem.*, 1983, **20**, 1549–1552; G. Menozzi, A. Bargagna, L. Mosti and P. Schenone, *J. Heterocycl. Chem.*, 1987, **24**, 633–635.
33 L. Mosti, P. Scheneone, G. Menozzi and S. Cafaggi, *J. Heterocycl. Chem.*, 1982, **19**, 1031–1034.
34 B. Zwanenburg, in *'Science of Synthesis', Volume 27: Heteroatom Analogues of Aldehydes and Ketones, 27.3: Product Class 3: Thioaldehyde and Thioketone S,S-Dioxides and Oxyimides (Sulfenes and Derivatives)*, ed. A. Padwa, Georg Thieme, Stuttgart, 2004, pp. 123–134.
35 J. B. Press and J. J. Mcnally, *J. Heterocycl. Chem.*, 1988, **25**, 1571–1581; O. G. Karamov, V. P. Rybalkin, N. I. Makarova, A. V. Metelitsa, V. S. Kozyrev, G. S. Borodkin, L. L. Popova,

V. A. Breń and V. I. Minkin, *Russ. Chem. Bull., Int. Ed.*, 2011, **60**, 168–174.

36 M. Nowak, *Synlett*, 2015, **26**, 561–562.

37 M. Irie, K. Sakemura, M. Okinaka and K. Uchida, *J. Org. Chem.*, 1995, **60**, 8305–8309.

38 Crystal for **13a**. Crystal data for $C_{26}H_{32}NO_{3.50}S_3$, M = 510.70, triclinic, a = 9.869 (5), b = 11.897 (5), c = 13.181 (5) Å, α = 113.322 (17), β = 109.14 (2), γ = 90.79 (2)°, V = 1324.1 (10) Å^3, T = 150 K, space group $P\bar{1}$, Z = 2, 19 176 reflections measured, 8011 independent reflections (R_{int} = 0.0392). The final R_1 values were 0.0519 ($I > 2\sigma(I)$). The final w$R(F^2)$ values were 0.1309 ($I > 2\sigma(I)$). The final R_1 values were 0.0778 (all data). The final w$R(F^2)$ = 0.1481 (all data). The goodness of fit on F^2 was 1.027. Peak and hole = 0.823/−1.120. CCDC 1905437† contains the supplementary crystallographic data for this paper. The structure contained a disordered diethyl ether solvent molecule which was modelled in two positions using the *PART* instruction in the refinement. The anisotropic displacement parameters were restrained using the *DELU* and *SIMU* instructions.

39 P. C. Astles, S. V. Mortlock and E. J. Thomas, in *Comprehensive Organic Synthesis*, Elsevier, Amsterdam, 1991, vol. 6, ch. 5.3, pp. 1011–1039.